KANSAS GEOLOGICAL SURVEY
OPEN-FILE REPORT 75-1

A Computer Analysis of the Geochemistry and Mineralogy
Together with the Petrology of the Upper Pennsylvanian
and Lower Permian Shales of Kansas, U.S.A.

by

John M. Cubitt

Disclaimer

The Kansas Geological Survey does not guarantee this document to be free from errors or inaccuracies and disclaims any responsibility or liability for interpretations based on data used in the production of this document or decisions based thereon. This report is intended to make results of research available at the earliest possible data, but is not intended to constitute final or formal publications.

KANSAS GEOLOGICAL SURVEY
1930 Constant Avenue
University of Kansas
Lawrence, KS 66047

Missing Page #73

A Thesis Entitled

A COMPUTER ANALYSIS OF THE GEOCHEMISTRY AND MINERALOGY TOGETHER WITH THE PETROLOGY OF THE UPPER PENNSYLVANIAN AND LOWER PERMIAN SHALES OF KANSAS, U.S.A.

Submitted for the degree of

DOCTOR OF PHILOSOPHY

in the

FACULTY OF SCIENCE

of the

UNIVERSITY OF LEICESTER

by

JOHN M. CUBITT

B.Sc. (Leicester)

June, 1975

ABSTRACT

The objectives of this thesis are twofold; firstly, to conduct a detailed geochemical, mineralogical and petrological survey of the Upper Pennsylvanian and Lower Permian Shales of Kansas, U.S.A., and to relate the variation observed in the stratigraphic and tectonic framework of the Mid-Continent during this period. Secondly, it was necessary to study the instrumental techniques applied to fine-grained rocks, to develop standardized procedures and where appropriate to implement new techniques.

Six facies are developed in Kansas Shales - a sand and siltstone facies and a brown clayey shale facies, corresponding to deltaic sands and silts and prodeltaic marine muds respectively, a calcareous grey shale facies and a black shale facies, deposited in normal marine and restricted marine environments respectively, and two minor facies, a purple and red shale facies and shale partings in Limestones. The first two facies normally constitute the thick shale Formations (outside shales) separating Limestone Formations in which the second facies pair develop (inside shales). The facies distributions subdivide the stratigraphic section into five zones - the Pleasanton and Lower Kansas City Groups (with cycles of marine and deltaic shales) the Upper Kansas City, Lansing and Douglas Groups, the Shawnee Group (containing cycles), the Wabaunsee Group and the Admire, Chase and Council Grove Groups.

A combined standards regression technique was implemented for quantitative X-ray diffraction analysis of shale mineralogy. The smear technique of XRD sample preparation was shown to be superior for distinguishing between shale samples although the pressed pellet and membrane filter techniques (developed in this thesis) were considered more appropriate to this study. Major oxide and trace element concentrations were determined by emission spectroscopy. Structural sites of ions in shales were estimated by electron spin resonance. Fabrics of shales were examined by scanning electron microscopy and micromorphological techniques.

DECLARATION

This thesis is the result of original research conducted by the candidate during the period of registration. No part of this thesis has been submitted for another degree.

John M. Cubitt

June 1975

CONTENTS

INTRODUCTION

The Upper Carboniferous (Pennsylvanian) and Permian stratigraphy of Kansas, U.S.A. has been extensively studied in the past 100 years culminating in the development of the revolutionary concept of cyclic sedimentation by R.C. Moore in the 1930's. From a detailed examination of the lithology and palaeontology of limestones in eastern Kansas, the repetitive sequence of characteristic fossiliferous limestones was accounted for by cyclic changes in sedimentary environments. This concept has developed dramatically in the past fifteen years with applications to many different stratigraphical horizons and areas. For example cyclic sediments have been described from North America and Europe by Weller (1956, 1958, 1964), Read (1961, 1965, 1967, 1969), Merriam (1964), Duff, Hallam and Walton (1967), Read and Dean (1967, 1968, 1972), Reyment and Collinson (1971), Read and Merriam (1972), Mayers and Worsley (1973), and from Australia by Johnson and Cook (1973). It is notable that although the concept has been widely accepted by geologists as a true representation of sedimentary processes, the original "ideal cyclic sequence" (Moore, 1936) is still being questioned.

Moore's ideal cyclothem, representative of much of the Upper Pennsylvanian and Lower Permian succession of Kansas (Moore, 1936, 1949, 1950, 1959), contains ten lithological and palaeontological units including six or more clastic units. Moore based this cyclothem on the occurrence of characteristic limestones - a molluscan limestone, a fusilinid limestone and an algal limestone. However, the intervening poorly exposed shales have been studied only superficially and their mineralogy and petrology is largely unknown. It is on this point that the two serious alternatives to Moore's hypothesis seem to dwell (Davis and Cocke, 1972; Schwarzacher, 1967, 1969). These concepts are based on a three-state depositional system (limestone, thick, coarse, sandy and silty shales, and

thin calcareous shales) which were developed from computer-orientated statistical analyses of detailed lithological and stratigraphical investigations.

As a further possibility, tectonic features of the Mid-Continent, U.S.A., suggest the presence of four possible shale facies - a clastic wedge lithology similar to Ferm's Appalachian facies (Ferm, 1973) derived from the Ouachita Mountains of Arkansas and Texas; a deltaic sandstone and siltstone facies derived from the lowlands to the east, northeast and southeast of Kansas; a normal marine shale associated with fossiliferous marine limestones; and a restricted marine black shale lithology.

In the light of the recent revival of interest in cyclic sedimentation, it is most important that the confusion surrounding the "classic" cyclic sequences of the Upper Pennsylvanian and Lower Permian of Kansas be removed and an hypothesis based on the regional tectonic framework of the U.S. Mid-Continent established to account for the stratigraphic record during this period.

The poor exposure and monotonous nature of Carboniferous and Permian shales in Kansas has hindered previous attempts to differentiate shale types in the field. The fine-grained nature of the shales has also precluded optical microscopic investigations of mineralogy and petrology. Instrumental techniques have, however, provided considerable information about the geochemistry and mineralogy of fine-grained clastics (Van Moort, 1972, 1973; Reimer, 1972) and their use has proved to be especially illuminating in the study of shales (Davis, 1967). Three techniques, in particular, X-ray diffraction, providing details of the mineral composition of shales (Chapter 3), emission spectroscopy providing trace element concentrations (Chapter 4) and electron spin resonance revealing the structural positions of certain trace ionic constituents (Chapter 6), can be used to examine the mineralogy and geochemistry of the Carboniferous and Permian shales of Kansas.

From raw geochemical and mineralogical data, it may be impossible to differentiate shale types manually. However, with the aid of a computer, statistical analyses of the geochemical and mineralogical data can reveal major variations between rock samples (Joyce, 1973) and consequently a classification of the shales can be prepared (Chapters 3, 5 and 7). To relate this classification to field identifications, it is also necessary to develop petrological and lithological classification by careful examination of thin sections and hand specimens (Chapter 8). Fabric analysis using scanning electron microscopy can also provide additional information for distinguishing shale types (Gillott, 1969).

The three classifications of the Upper Pennsylvanian and Lower Permian shales of Kansas currently under examination can be compared with the combined geochemical, mineralogical and petrological classification. Any repetition of shale types based on the classification derived within this thesis, can then be explained in terms of the stratigraphy, tectonics and palaeogeography of the Mid-Continent, U.S.A.

PURPOSE OF THE PRESENT RESEARCH

This research project has a two-fold objective. The primary aim is to make a detailed geochemical, mineralogical and petrological study of the Upper Pennsylvanian and Lower Permian shales of Kansas and to relate the variations observed to the stratigraphical and tectonic setting of Kansas at that time. Secondly, in obtaining this information, it is necessary to study the methods of instrumental analysis commonly used in the study of fine-grained shales, to improve the techniques by standardisation of analytical procedures and, where necessary, to develop new techniques.

Mineralogical data on shales is readily obtained by X-ray diffraction from whole rock samples. This technique has proved most effective in previous studies of shale mineralogy and there is an extensive literature on the advantages of the technique. Quantitative analysis of shales has,

however, proved unreliable because of irregularities in laboratory conditions and equipment. Therefore, standardization of techniques, instruments and conditions is necessary before detailed quantitative analysis can be performed (Chapter 2).

Emission spectroscopy is relatively unknown to the sedimentologist yet geochemists have used it widely (Celenk, 1972) to calculate major and minor element geochemistry of rock samples. Although rather low accuracy estimates of shale geochemistry are produced, the information is sufficiently definitive to statistically distinguish shale types (Chapter 4).

Electron spin resonance, a technique new to sedimentology and relatively unknown in geology, was introduced to aid the classification and geochemical interpretation of shales. The distribution of certain ions in shale samples can be determined by ESR and related to their environment of deposition.

The combination of complex instrumental methods and microscopic techniques was designed to establish the nature of the shales with the Upper Pennsylvanian and Lower Permian of Kansas, U.S.A. Hypotheses could then be built to relate the geochemical, mineralogical and petrological parameters to the regional setting and to provide an explanation for any variations these parameters have within the stratigraphical section studied.

ACKNOWLEDGEMENTS

The author would like to thank:

The Kansas Geological Survey for financial support for 18 months, field expenses, laboratory equipment, secretarial and photographic services,

The Department of Geology at the University of Leicester for typing Appendix 2 and providing laboratory equipment and assistance,

Dr. J.C. Davis, without whose supervision, encouragment, advise and friendship this thesis could never have been completed,

Dr. A. Khan, who supervised this work, for his suggestions during the course of this project, and for critically reading this manuscript,

Professor D.F. Merriam, who initiated the project, provided invaluable assistance with fieldwork and supervision and produced the final stimulus for completion of this thesis,

Dr. J.G. Wilkinson, for his assistance and most helpful discussions about electron spin resonance,

Dr. O. Celenk, for advice about statistical programs and discussion of Appendix 5,

Dr. P. Bulluck, who introduced the author to fabric analysis in fine-grained clastic rocks,

Dr. W. Read, for useful discussions about the tectonics of the Mid-Continent,

Dr. C.H. James and Miss V. Rutherford, for providing assistance with the Emission Spectrometer,

Dr. R.J. King for providing a selection of mineral samples for analysis by Electron Spin Resonance,

Drs. Ford, Heckel and Conley for encouragment, initial discussion of the manuscript and for their constructive advice,

Professor Symmons, for the use of the electron spin resonance spectrometer,

The Leicester Computer Laboratory, for their assistance to the author during the tenure of his research,

Mr. M. Sackin and the Medical Research Council Unit for use of the computer programs: ITBNTOMT and ITBNCLST,

Miss J. Westerman and Mrs. N. Minchin for preparing figures and diagrams,

Mrs. N. Corby for typing this thesis,

His parents and parents-in-law for their constant encouragment and help,

and lastly to his wife, Cynthia, who advised and assisted the author with laboratory work, with typing the first drafts of the thesis, in the preparation of diagrams and to whose endless enthusiasm and encouragement the work is indebted.

CHAPTER ONE

STRATIGRAPHY AND TECTONIC FRAMEWORK OF KANSAS DURING THE UPPER PENNSYLVANIAN AND LOWER PERMIAN

INTRODUCTION

The primary objective of this thesis, as previously stated, was to examine in detail the Upper Pennsylvanian and Lower Permian clastic deposits and relate the mineralogical, geochemical and petrological variation observed to the stratigraphic and tectonic framework of the period. This chapter essentially provides the background information upon which the later chapters are based.

A summary of the stratigraphy is presented, emphasising current ideas about the clastic sediments, in order to elucidate description of stratigraphic variation in later chapters and to provide the basis for the next section in this chapter, cyclicity of the sediments. Interpreted by Moore (1936) in terms of oscillating environmental conditions, sedimentary cycles are recognised in the Upper Pennsylvanian and Lower Permian by the occurrence of distinctive limestone lithologies. However, a number of alternatives to Moore's original interpretation have been proposed, based on recognition of both characteristic clastic and non-clastic lithologies (Schwarzacher, 1969; Davis and Cocke, 1972). Therefore, the discussion of cyclic sedimentation presented, emphasises the problems associated with Moore's concepts and the current alternative hypotheses.

In recent years, a revival of interest in tectonic control of sedimentary cycles has been enhanced by modern theories of plate tectonics and sea-floor spreading. The introduction of this new aspect of sedimentology has produced another interpretation of the stratigraphic column in Kansas. A full description of this application to Kansas geology and the implications to this project are presented.

As this chapter provides essential, but also previously documented information, it is considered unnecessary to present any conclusions herein.

STRATIGRAPHY

The Upper Pennsylvanian

The Upper Pennsylvanian outcrops in Mid-Continent North America from Iowa through Nebraska, Missouri and Eastern Kansas to Oklahoma and consists of approximately 650m. (2200 ft.) of alternating limestone and shale Formations. The limestone Formations with included thin shales, average 5-15m. in thickness and generally contain abundant marine fossils whereas the intervening shale Formations averaging 15-30 m., are generally poorly fossiliferous.

The Upper Pennsylvanian stratigraphical section (Fig. 1.1) consists of 2 Stages - the Missourian and Virgilian. The Missourian Stage lies unconformably on the Desmoinesian Stage of the Middle Pennsylvanian, and is subdivided into the Pleasanton, Kansas City and Lansing Groups. Conformably overlying the Lansing are the Douglas, Shawnee and Wabaunsee Groups of the Virgilian Stage.

At the base of the Missourian series of the Upper Pennsylvanian is the Pleasanton Group, which is composed of 10-45 m. of shale with some sandstone, limestone and coal (Jewett et al., 1965). The irregular basal Hepler Sandstone Member rests in channels and is overlain by the South Mound Shale Member, the Checkerboard Limestone Formation and the Tacket Formation. Shales are often rich in phosphate nodules (Runnels, 1949; Runnels et al., 1953; Rose and Hardy, 1967) and organic material (Jewett, 1940). Some lenticular sandstones are present in the Tacket Formation and are locally known as the Knobtown Sandstone and Charlton Conglomerate (Branson, 1962b; Jewett et al., 1965).

The Kansas City Group lying above the Pleasanton Group is characterised by six relatively thick, persistent limestone Formations separated by six shale Formations of variable thickness. Sandstones form a minor lithology in Northern Kansas but thicken considerably towards

Fig.1-1. STRATIGRAPHIC SUCCESSION IN KANSAS (After Zeller, 1968)

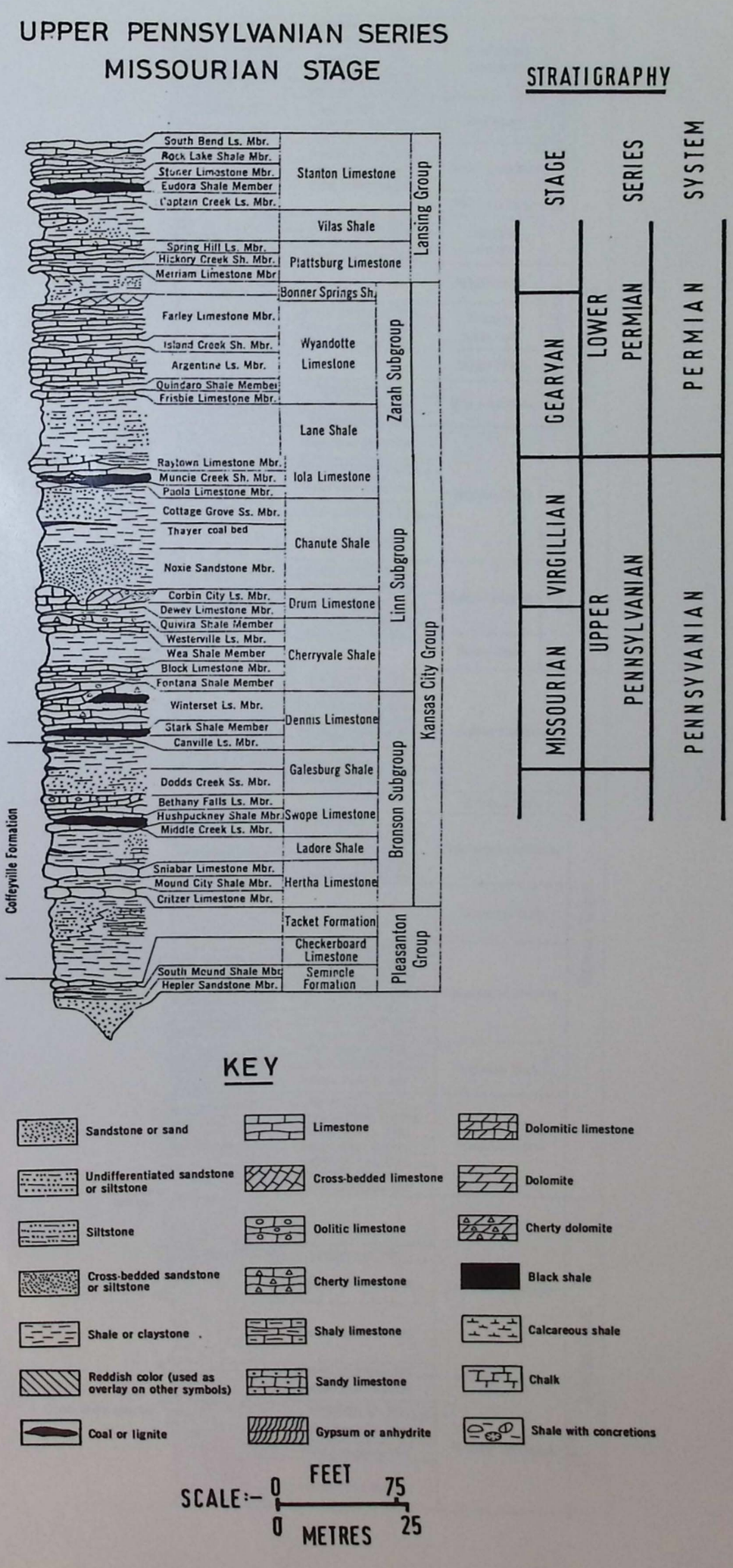

UPPER PENNSYLVANIAN SERIES
VIRGILIAN STAGE

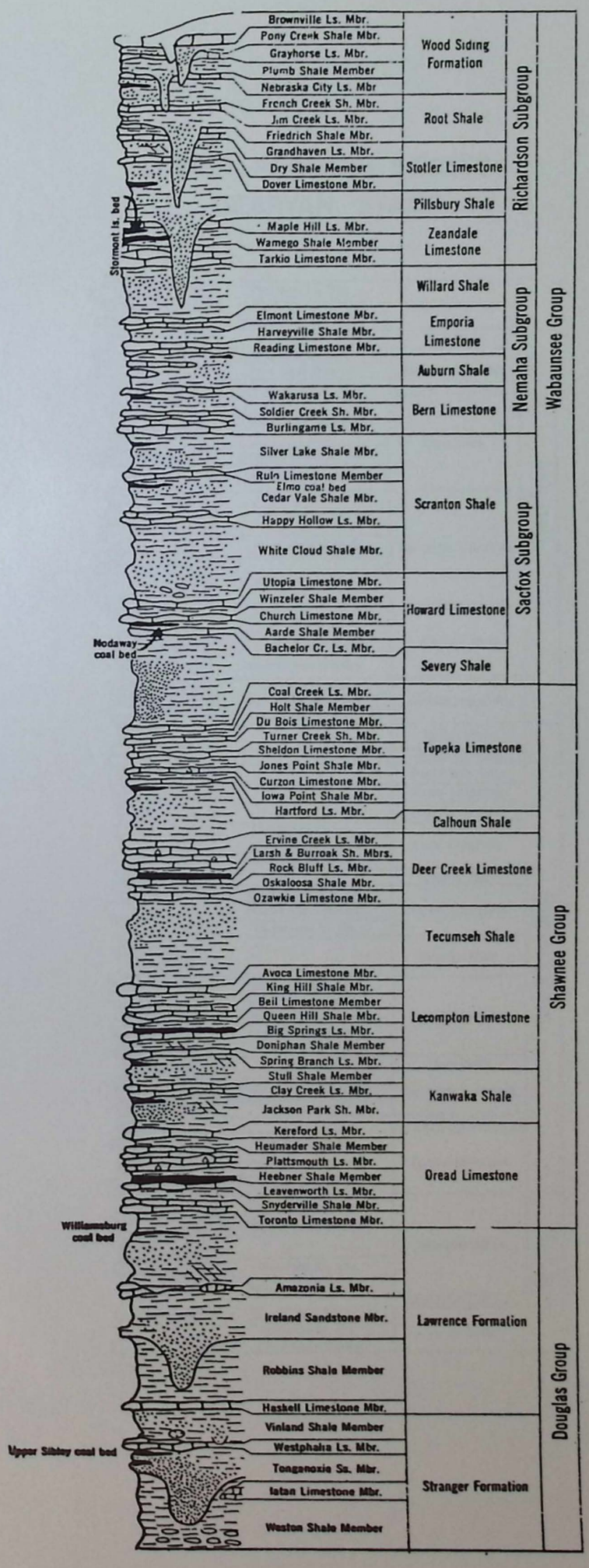

LOWER PERMIAN SERIES
GEARYAN STAGE

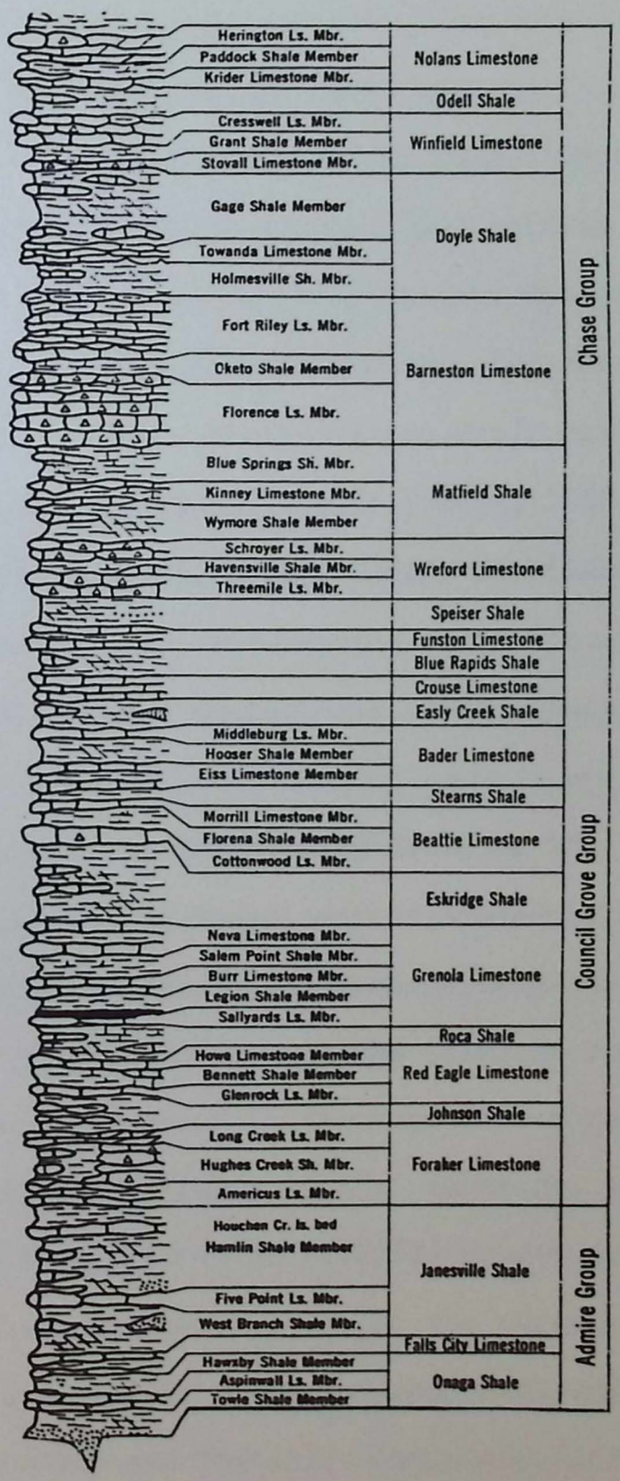

Oklahoma (Schutze, 1959). Many of the limestones are algal, oolitic and cross bedded, locally thickening to form carbonate buildups (Hall, 1961; Merriam, 1963; Crowley, 1969; Hamblin, 1969; Heckel, 1972a, 1974). Thin discontinuous coal beds occur in the middle of the Kansas City Group and several "paper-thin" black shales act as marker horizons. This Group contains a number of limestones that wedge out in Southern Kansas e.g. In Southern Allen County the Wyandotte Limestone pinches out bringing the Bonner Springs Shale in contact with the Lane Shale to form a single inseparable unit termed the Lane-Bonner Springs Shale (Merriam, 1963). The Lane Shale has therefore been interpreted as a deltaic platform upon which the Wyandotte Limestone algal banks of Eastern Kansas were formed (Crowley, 1968). Another deltaic clastic complex, the Bonner Springs Shale, then covered this buildup. Similar algal reefs have been reported in the underlying Iola (Heckel, 1969), Dennis (Frost, 1968, 1975), Swope (Mossler, 1970, 1971, 1973; Scott, 1970), Cherryvale (Heckel, 1969) and Hertha (Heckel, 1969) Formations. Information on the intervening beds, with the exception of the Chanute Shale (Hall, 1961; Schutze, 1969) is minimal.

Conformably overlying the Kansas City Group is the Lansing Group consisting of two thick limestone Formations separated by one shale Formation. At the base, the Plattsburg Limestone consists of 7 to 28 m. of limestone and shale, thickening towards the Oklahoma border. Algal buildups in the Plattsburg Limestone of Southern Kansas has attracted much attention as possible oil traps (Davis, 1959; Harbaugh, 1959, 1960, 1964, 1965). The Vilas Shale Formation (Kinell, 1962) varies in thickness and lithology southwards, directly attributable to the surrounding marine banks (Harbaugh, 1959). It is generally a monotonous, unferruginous marine shale but locally beds of sandstone and fossiliferous sandy limestones are found (Zeller, 1968). The Lansing culminates with the Stanton Limestone Formation consisting of three limestone and two shale Members. The

Formation's most distinct features are the algal buildups in the limestone Members (Wilson, 1957a, 1957b, 1962; Heckel, 1972a, 1972b, 1974) and the Eudora black Shale Member comprising approximately 1 m. of greyish-black fissile shale with phosphate nodules overlain by 1 m. to 2 m. of calcareous green-grey and dark grey shale and is recognised both in subsurface and outcrop.

The Douglas Group (O'Connor, 1963) consists largely of coarse shales and siltstones with occasional inpersistent thin limestones and local sandstone channels. A few thin coals make suitable marker horizons (e.g. Sibley coalbeds). Beds in the group thicken from 80 m. (260 ft.) in Northern Kansas to 130 m. (420 ft.) on the Kansas/Oklahoma border but precise identification of horizons is problematic as distinguishing gross lithological characteristics are generally lacking and the Lower boundary with the Lansing Group is often obscure (Ball, 1964). However, deltaic sandstone channels have been mapped in this Group by Winchell (1957), Sanders (1959) and Bower, (1961). The Lawrence Shale Formation (Upper Douglas Group) was thought by Moore (1936, 1950) to represent a transgressive phase of sediment deposition. Faunal evidence now indicates that a restricted, marine environment existed and that no change from marine to non-marine can be inferred (Hakes, 1973). The Douglas Group is therefore considered to be a non-marine phase separating the generally marine phases of the Lansing and Shawnee Groups.

The Shawnee Group consists of four Limestone Formations - Topeka, Deer Creek, Lecompton and Oread Limestones - separated by thick shales and siltstones. Coals and sandstones are thin and of local occurrence only, e.g. the Elgin Sandstone (Brown, 1966, 1967) is a deltaic distributary complex that only outcrops in South-Central Kansas. The thick limestone Formations have been extensively described by Brown (1956), Perkins et al. (1962), Toomey (1964), Troell (1965, 1969), Galle and Waugh (1966) and Griesemer (1972) in terms of marine depositional environments, but the

intervening Kanwaka, Tecumseh and Calhoun Shale Formations are almost unknown. Thin shales found in the limestone Formations (Rowell, 1973; Von Bitter, 1973; Brondos, 1974) are also poorly described with the exception of the Heebner Shale (Evans, 1967), a paper thin black shale lying between the Leavenworth and Plattsburg Limestone Members. This is a very distinctive horizon and is consistently recognised both in outcrop and boreholes (Merriam, 1963). Evans (1967) and Heckel (1972a) have related this characteristic black shale lithology to a restricted marine basin environment with anoxic bottom conditions. Shales of this type are recurrent features of the Kansas City, Shawnee and Wabaunsee Groups and find extensive use as marker horizons (Moore, 1936, 1949, 1950, 1957).

The Wabaunsee Group conformably overlies the Shawnee Group and consists predominantly of shales and limestones with local sandstone lenses and several thin but persistent coal beds - the Nodaway and Elma coals. The limestones are normally indistinguishable but the Dover, Zeandale and Howard Limestones can be recognised by their lithology (Merriam, 1963). Channel sandstones occur in the Richardson Subgroup and often confuse the normal shale-limestone sequence (Mudge, 1956). A number of important underclays occur in association with the coals, e.g. Nodaway Underclay (McMillan, 1956). The total group thickness is 165 m. (540 ft.).

The Permian-Pennsylvanian boundary has been placed at the base of the Indian Care Sandstone of the Towle Shale Member (Zeller, 1968). This is unfortunately a poor choice of boundary as it is a channel sandstone of local importance only and is often difficult to recognise in the field. The Wellington Formation (Cimarronian Stage of the Lower Permian) has been suggested as an alternative by Branson (1960a, 1960b), and there has been recent palynological evidence for a Pennsylvanian-Permian boundary above the Eskridge Shale (Wilson, 1973). However, there is general agreement that little is to be gained by moving a boundary that has only reached reasonable stability in the past three decades.

The Lower Permian

The Lower Permian rocks of Kansas have been subdivided into two Stages, Gearyan (below) and Cimarronian (above). The Admire Group forms the lowest division of the Permian and consists of shale deposits with some thin limestones and coal beds. The sequence is similar to that of the underlying Wabaunsee Group and is difficult to differentiate on lithology alone. Conformably overlying the Admire Group is the Council Grove Group comprising approximately 100 m. (325 ft.) of limestones and shales in fourteen Formations. The limestones are generally thinner and less massive than those in the overlying Chase Group, but they form a greater proportion of the total thickness than in the underlying Groups. Another indication of changing sedimentary conditions is provided by the sudden increase in red and varicoloured shales (Merriam, 1963). Together with cherty limestones, these characteristic sediments are interpreted by Moore and Merriam (1959) in terms of oscillating transgressions and regressions. This repetition is well developed in the Beattie Limestone (Walker, 1951; Imbrie, 1955; Imbrie et al. 1959, 1964; Laporte, 1962; Elias, 1964; Laporte and Imbrie, 1964). The palaeoecology of the Red Eagle Limestone has been interpreted in similar terms (McCrone, 1963) and the Eskridge Shale has been examined in connection with the Pennsylvanian-Permian boundary problem (Brookins and Chaudhuri, 1973) and depositionsl environments (Wells, 1950; Moore, 1957, 1959; Mudge and Yochelson, 1962). Red shales, green shales, cherty and dolomitic limestones characterise and divide the Chase Group into seven alternating predominantly shale-and-limestone Formations. There is a noticeable increase in the number of evaporite horizons suggesting some restriction of the Kansas sea at this time. Little information is available, however, on horizons in the Chase Group, except those in the Wreford Limestone Formation, which have been examined palaeontologically by Cuffey (1967), Newton (1970, 1971), Warner

and Cuffey (1973), Bifano et al. (1974) and Lutz-Garihan (1974) and sedimentologically by Hattin (1957) and Lutz-Garihan and Cuffey (1973).

CYCLICITY OF THE SEDIMENTS

R.C. Moore (1936, 1949, 1950, 1959) has recognised repetitive associations of sediments in the Pennsylvanian and Permian stratigraphy of Kansas which he termed cyclotherms and interpreted as recurrent transgression/regression sequences. The typical or "ideal" cyclothem (Fig. 1.2) consists of ten beds symmetrically developing from a non-marine sandstone or shale (0, 1a) up to a fusilinid limestone (5), representing the culmination of normal marine transgression, and then back to a non-marine shale and sandstone bed (9), representing the regressive marine phase. This "ideal" cycle is characteristic of Wabaunsee Group sediments (Moore, 1949).

However, this is not a common occurrence in Kansas and a number of different cyclic sequences have now been recognised. In the Shawnee Group, for example, the most distinct cycle consists of a black shale followed by thick limestones separated occasionally by thin calcareous shales (Fig. 1.3). Frequently a thick, coarse, non-marine shale occurs between each group of thick limestones. The Lansing and Kansas City beds also contain cyclothems that bear no resemblance to the "ideal" cyclothem and Abernathy (1937) noted little correlation between Cherokee cyclothems (Desmoinesian Stage) and the "ideal" cycle. In the Permian beds, cycles were recognised by Moore and Merriam (1959) and Elias (1937, 1964) and are diagrammatically summarised in Fig. 1.3. The variation in Kansas cyclothems is summarised in Table 1.1 and it is clear that the "ideal" cyclothem is certainly not the typical cycle developed in Kansas. Merriam (1963) has pointed out that this variation is a result of the non-development of particular beds or their development and subsequent destruction. However,

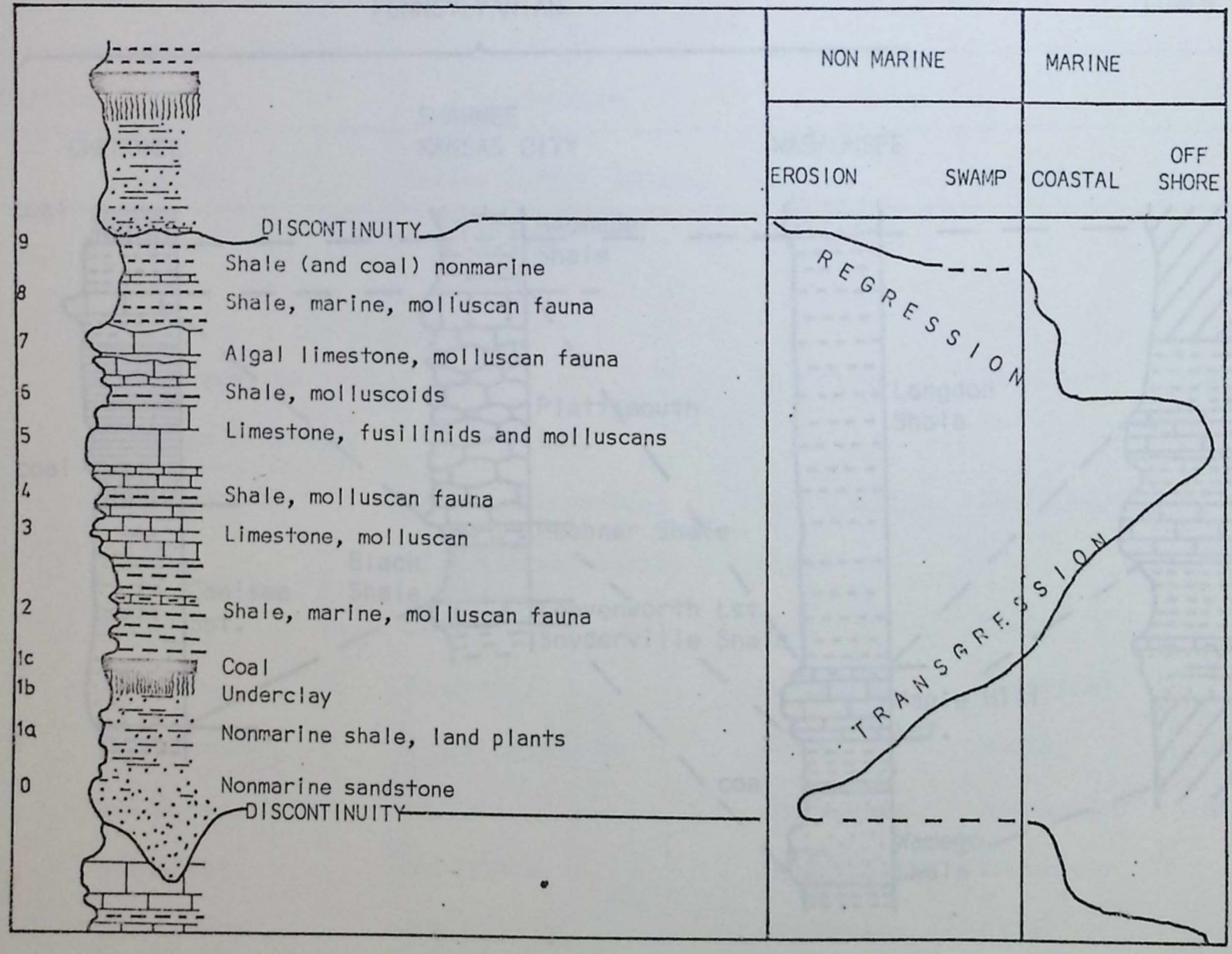

Fig. 1.2 Diagrammatic section of Pennsylvanian rocks in Kansas showing the "ideal cyclothem" (after Moore and Merriam, 1959).

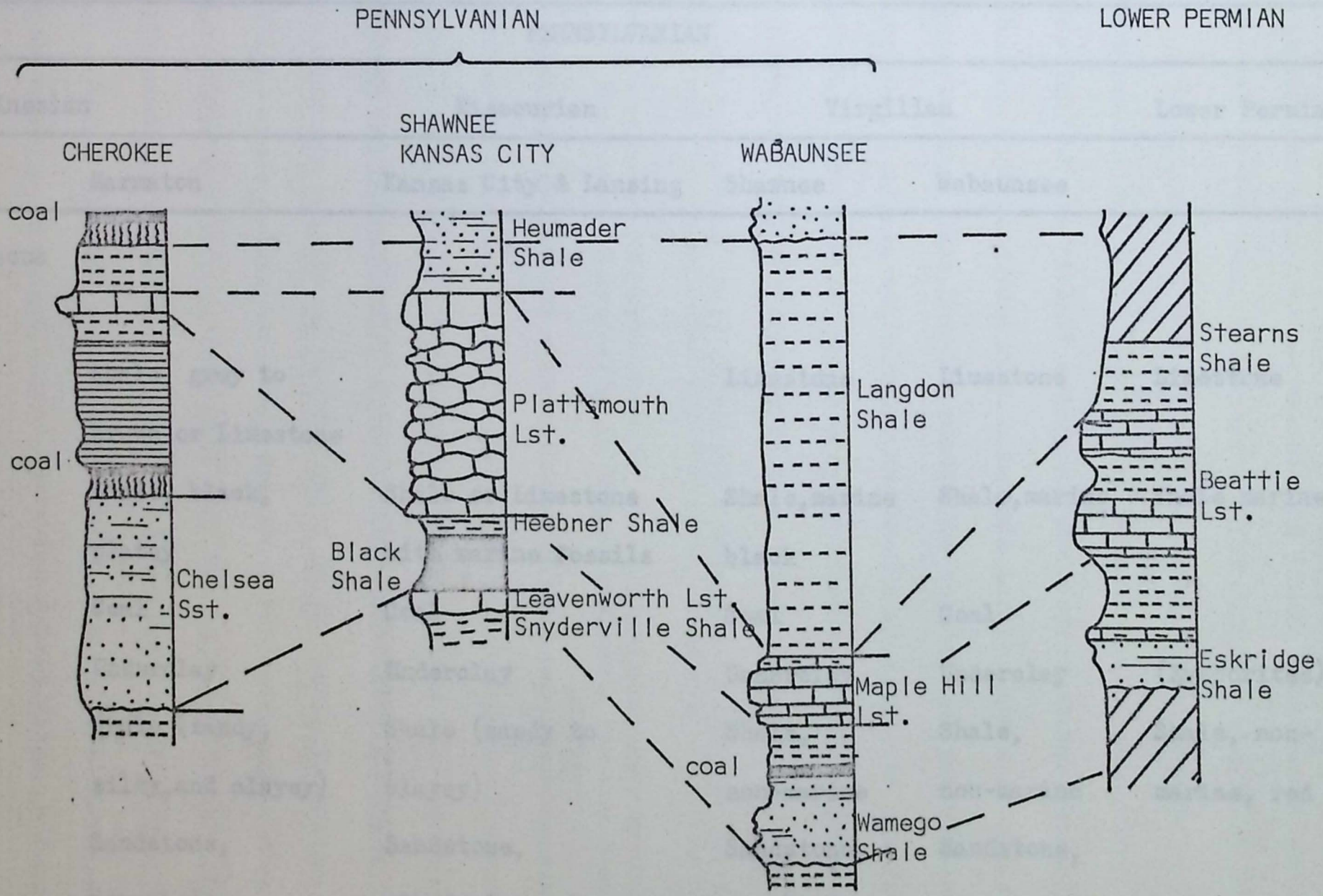

Fig. 1.3 Generalised sections depicting cyclothems found in the Pennsylvanian and Permian Systems of Kansas, U.S.A. (adapted from Moore, 1949 and 1950; Moore and Merriam, 1950).

TABLE 1.1 VARIATION IN KANSAS CYCLOTHEMS

PENNSYLVANIAN					
Desmoinesian		Missourian	Virgilian		Lower Permian
Cherokee	Marmaton	Kansas City & Lansing	Shawnee	Wabaunsee	
Shale, calcareous					
Limestone					
Shale, grey	Shale, grey to brown or Limestone		Limestone	Limestone	Limestone
Shale, black	Shale, black, platey	Shale or Limestone with marine fossils	Shale, marine black	Shale, marine	Shale marine
Coal	Coal	Coal	Coal	Coal	
Underclay	Underclay	Underclay	Underclay	Underclay	(Evaporites)
Shale (sandy)	Shale (sandy, silty, and clayey)	Shale (sandy to clayey)	Shale, non-marine	Shale, non-marine	Shale, non-marine, red
Sandstone	Sandstone, non-marine	Sandstone, non-marine	Sandstone, non-marine	Sandstone, fine micaceous	
Moore, 1949	Moore, 1949	Moore, 1949	Moore, 1936	Moore, 1950	Moore & Merriam, 1959

Branson (1962b) describes the situation more forcefully:

"A general misconception of the nature of cyclical sediments has been widely held. An ideal cyclothem has not been found and in the Mid-Continent, no cyclothem approaches the ideal. The normal well-developed cyclothem of the area, and there are few such, is shown" in Fig. 1.4.

In comparison, Moore (1959) considered that the different Upper Pennsylvanian and Lower Permian sedimentary cycles recognised were minor variations of the "ideal" sequence. Repetitive occurrences of these cyclothem varieties were also noted and termed "cycle of cyclothems" or megacyclothems. The Shawnee succession consists of two distinct cyclic sequences, a simple shale sequence which corresponds to one Wabaunsee cyclothem and the more common complex limestone-shale sequence which, with some imagination, corresponds to 1 or 3 Wabaunsee cycles. As a result the Shawnee succession could represent a sequence of complex and simple cycles or megacyclothems.

The scale of cyclicity in Kansas sediments has now been extended to include hypercyclothems - repetitions of four megacyclothems with intervening detrital units (Weller, 1958), and magnacyclothems - repetition of major stratigraphic units, genetically related and systematic in size although not corresponding to systematic boundaries (Merriam, 1963). This extension can only be of dubious value as the basic cyclothem unit is still so inadequately defined. Branson (1962) added that megacycles and hypercycles are so imperfect that they can be regarded only as hypothetical units possibly indicating some sort of recurrent condition.

Megacyclothems have been reported from many different stratigraphic levels (Fig. 1.5) but it should be realised that although Pennsylvanian and Permian successions in Kansas consist of alternating clastics and carbonates, neither cyclothems nor megacyclothems have been reported from all divisions. The Douglas Group for example is carefully avoided by all advocates of cyclic sedimentation.

9) Shale, dark, unfossiliferous, with clay-ironstone concretions

8) Limestone, locally rich in fusilinids

7) Shale, grey, containing myalinid fossils

6) Limestone or clay-ironstone, margiferids abundant

5) Shale, black, fissile, phosphatic

4) Coal

3) Underclay

2) Shale, silty, fossil plants

1) Sandstone, non-marine, locally conglomeratic

Fig. 1.4 The "normal" cyclothem (Branson, 1962b, p.449).

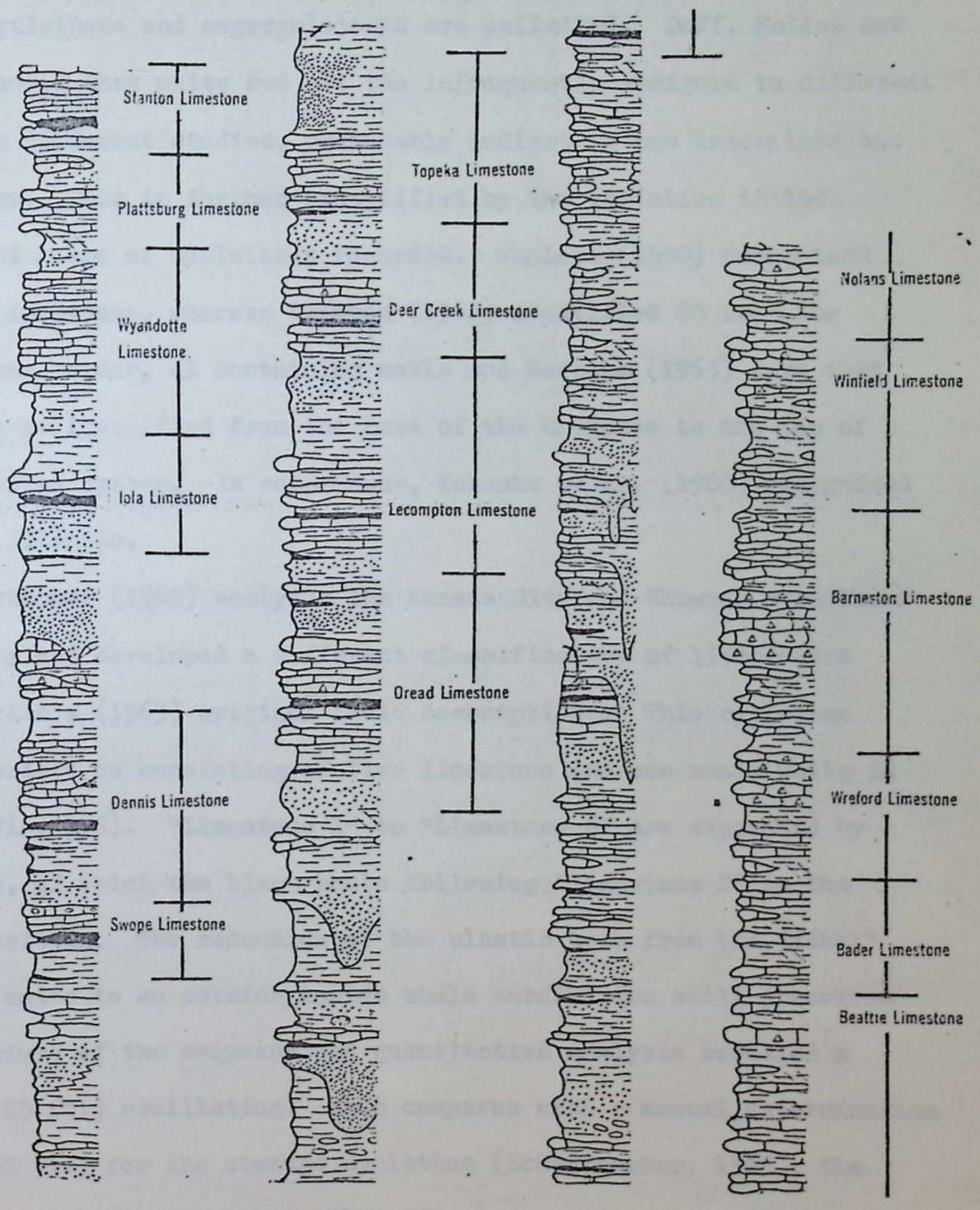

Fig. 1.5 Megacyclothems recorded in the Upper Pennsylvanian and Lower Permian of Kansas. Major formations are named in each cycle. (Information from Moore, 1949, 1964)

Although some units, particularly limestones, can be traced from Oklahoma to Pennsylvania (Moore, 1959) and cover areas as large as 80,000 sq. ml. (Duff, Hallam and Walton, 1967), it is not easy to see how individual cyclothems and megacyclothems are delimited. Duff, Hallam and Walton have noted that units are not too infrequently assigned to different cyclothems in different studies, presumably indicating how incomplete the cyclothems are. This is further examplified by the variation in the number and thickness of cyclothems recorded. Wanless (1950) recognised 25-30 cycles in Kansas, whereas Branson (1962) identified 60 from the Oklahoma/Kansas border, 41 containing coals and Merriam (1963) says that 85 cycles can be identified from the base of the Cherokee to the top of the Pennsylvanian system. In comparison, Kosanke et al. (1960) recognised only 37 from Illinois.

Schwarzacher (1969) analysed the Kansas City and Shawnee cyclothems mathematically and developed a different classification of lithologies based on Merriam's (1963) original field descriptions. This cyclothem could be described as consisting of five limestone and one shale units in each cycle (Fig. 1.6). "Limestone 1" to "Limestone 4" are separated by inside shales, of which the black shale following "Limestone 2" is the most characteristic. The reduction of the clastic beds from the "ideal" six or seven units to an outside/inside shale subdivision still preserves the cyclic nature of the sequence and quantitative analysis revealed a 13-20 m. (42-65 ft.) oscillation. This compares with a manual determination of 24.5 m. (80 ft.) for the average cyclothem (Schwarzacher, 1969), the difference being attributed to the classification of the Douglas Group as an outside shale. Schwarzacher admits that this classification may be a mistake geologically but states there is no evidence for a missing cycle and it is obvious that the Douglas Group represents abnormal sedimentary conditions. Such irregularities are eliminated to an extent using the method of recurrent probabilities and it is for this reason that the

	EXAMPLE
LIMESTONE 5	Clay Creek
OUTSIDE SHALE	
LIMESTONE 4	Kereford
LIMESTONE 3	Ervine Creek
LIMESTONE 2	Leavanworth
LIMESTONE 1	Toronto
OUTSIDE SHALE	

Fig. 1.6 Example of simplified cyclothem (after Schwarzacher, 1969).

reconstructed cyclothem is a valuable aid to interpreting the nature of the succession.

Moore's cyclothem phases would be ideal lithological states if one were able to recognise the phases by its lithology and faunal characteristics. However, available descriptions did not allow such an identification, nor to the author's knowledge has such an attempt been successful. A less detailed classification is possible. By combining lithologies described as "yellowish shale, shales with plant fragments, silts, sands and sandstones" into one group and "grey fossiliferous shales, shales with predominantly molluscan fauna", and "black fissile shales" into a second group, two states can be obtained which closely resembled outside and inside shales. Thus a three state system could be adopted consisting of limestone, outside shale and inside shale.

Pearn (1964) distinguished only five lithologies in Pennsylvanian sediments which constituted a revised form of Moore's "ideal" cycle (Fig. 1.7). Certain problems were recognised in classification by these five lithologies, yet it was noted that the average cyclothem observed in Kansas would be similar to that proposed by Moore (1959).

Davis and Cocke (1972), on the other hand, recognised seventeen lithologies including nine clastic units in a study of Kansas City and Lansing Group cycles. Using a technique known as substitutability analysis, a classification procedure that groups states on the basis of their context in a sequence, it was concluded that lithologies must be grouped into fewer than eight states before any cyclic pattern emerges from the Upper Pennsylvanian succession.

Further analysis revealed that the stratigraphical succession contains a pattern of alternating calcilutites, calcarenites and marine shales. Sporadic incursions of coarser sediment may interrupt this pattern at any point. It may, therefore, be inferred that the various limestones and inside shale facies are interrelated and the occurrence of

5. Limestone with fusillnids and molluscoids

4. Shale, molluscoids dominant

3. Limestone with molluscans

2. Shale non-marine with coals, shale with molluscan fauna

1. Sandstone

Fig. 1.7 Transgressive hemicycle (after Pearn, 1964).

a specific lithological type at certain points within the sequence seems to have no great significance. In contrast, the coarser outside shales and siltstones seem to represent a clastic influx independent of the basic depositional pattern. Thus, Davis and Cocke infer that the limestone-inside shale depositional environment constitutes the normal sedimentation pattern with an occasional influx of coarser outside shales. Megacyclothems are not recognised in detailed examination of the rocks and, in fact, cyclothems and megacyclothems may be characteristic only of idealised successions. Alternatively, cyclothems may depend upon characteristics not expressed in the lithological nature of the rocks themselves.

Moore's "ideal" cyclothem and megacyclothem have, therefore, been questioned by detailed analysis of reportedly cyclic sequences. Yet there are many notable geologists who accept cyclic sedimentation without doubt. Zhemchuzhnikow (1958) wrote:

"Those who accept rhythem in nature will find it when it is rather indistinct, and they will arrive at proper conclusions. Those who do not want to, will not find it even when it is obvious."

It is necessary to resolve this conflict of opinion and geologists (Pearn, 1964) have suggested that detailed lithological, palaeontological, geochemical and mineralogical studies of the Pennsylvanian and Permian deposits in Kansas may provide a solution. This research hopes to shed some light on the mineralogical and geochemical nature of the fine-grained clastics within the succession and to relate this to the possible repetitive nature of the sediments.

TECTONIC HISTORY OF MID-CONTINENT U.S.A. DURING THE UPPER PENNSYLVANIAN AND LOWER PERMIAN

Throughout the Pennsylvanian and Permian, Kansas was covered by a shallow epeiric sea (Heckel, 1972a, 1972b) and sediment was continually

deposited in a number of broad, north-south trending anticlinal and synclinal structures (Fig. 1.8). Local and external tectonic events affected the sedimentary succession throughout Kansas and Weller (1956) went as far as to propose that cyclic patterns in Kansas sediments are a product of tectonism alone. Therefore, to present a complete picture of phenomena that may be responsible for cyclic sedimentation, it is necessary to summarise the structural and tectonic features of Kansas and its neighbouring states.

Structurally, Kansas is split into five regions (Merriam, 1963) that were active during the Pennsylvanian and Permian eras. Firstly, the Forest City Basin, occupying the north-east and eastern edge of the state, is a remnant of the earlier North Kansas Basin and has been a depositional area since the Arbuckle period (Lower Ordivician). It contains approximately 1300 m. (4000 ft.) of Palaeozoic sediments lying on Precambrian metamorphics with the greatest thicknesses of sediments recorded on the basin's western flank. The basinal axis, the Brownville Syncline (Condra, 1927) trends slightly east of north and lies close to the axis of the Nemaha Anticline producing an asymmetrical basin profile.

The Nemaha structural zone was active during the Mississippian (Branson, 1962b; Merriam, 1963) and was in part block faulted down the east side. Some sediments were eroded from the northern end and deposited along the eastern flank. The anticline separates the Forest City Basin from the Salina Basin (Reed, 1954), a post-Mississippian syncline trending northwestwards and plunging northwards with the greatest thicknesses of sediment recorded in North-Central Kansas. To the southwest of the Salina Basin lies an indistinct unnamed saddle (Merriam, 1963), delimiting the edge of the Sedgewick Basin. This shelf-like, northerly-plunging area in Southern Kansas is a major pre-Desmoinesian, post-Mississippian structural feature. Southwards, sedimentary facies change and thicknesses increase as the Sedgewick Basin passes into the Anadarko geosynclinal basin.

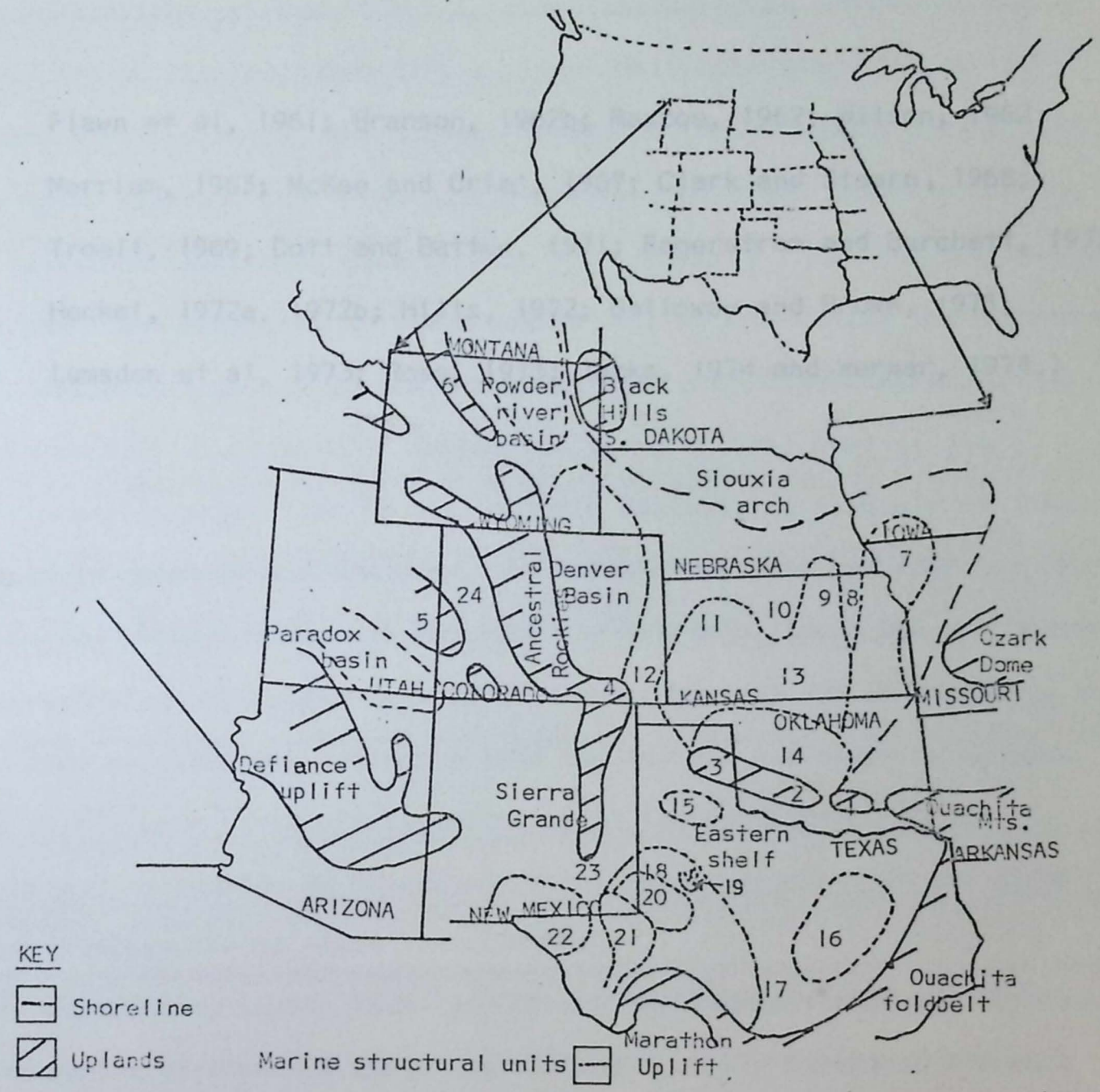

KEY

Shoreline

Uplands

Marine structural units

1. Arbuckle Mts.
2. Wichita Mts.
3. Amarillo uplift
4. Apishapa uplift
5. Uncompahgre uplift
6. Bighorn Mts.
7. Forest City Basin
8. Nemaha Anticline
9. Salina Basin
10. Central Kansas uplift
11. Hugoton embayment
12. Dalhart basin
13. Sedgewick basin
14. Anadarko basin
15. Plainview basin
16. Fort Worth basin
17. Llano uplift
18. Midland basin
19. Scurry platform
20. Central basin platform
21. Delaware basin
22. Diablo platform
23. Northwestern shelf
24. Central Colorado trough

Fig. 1.8 Tectonic features of the Mid-Continent U.S.A. during the Upper Pennsylvanian and Lower Permian (Information obtained from:-

Flawn et al, 1961; Branson, 1962b; Rascoe, 1962; Wilson, 1962; Merriam, 1963; McKee and Oriel, 1967; Clark and Stearn, 1968; Troell, 1969; Dott and Batten, 1971; Fagerstrom and Burchett, 1972; Heckel, 1972a, 1972b; Hills, 1972; Galloway and Brown, 1973; Lumsden et al, 1973; Ross, 1973; Jacka, 1974 and Werner, 1974.)

The extent of the Mississippian beds in Kansas outlines the northern-trending pre-Desmoinesian, post-Mississippian Central Kansas Uplift, and in the southwest lies a large shelf-like extension of the Oklahoma Anadarko Basin, the Hugoton Embayment (Maher and Collines, 1956). These areas separate the tectonically active Denver and Anadarko Basins, with sediments thickening considerably off the shelf. The Hugoton Embayment development was completed by the Mesozoic with a peak during the Desmoinesian.

Tectonic activity in these regions made a distinct impression on the sedimentary succession of Kansas but these effects were of minor significance in comparison to the tectonic activity in Kansas's neighbouring states: in Oklahoma and Arkansas, the Ouachita orogeny was reaching its peak in the Pennsylvanian and Permian; in Colorado, Idaho and New Mexico, the ancestral Rocky Mountains were developing rapidly and in Missouri, the Ozark Dome was shedding sediments into the epeiric sea covering Kansas. These events were particularly important in the development of the sedimentary succession in Kansas and should be re-examined in the light of recent developments in plate tectonic theory.

Surrounding Kansas therefore during the Pennsylvanian and Permian, were a series of mountain ranges stretching from the Ozarks of Missouri to the Black Hills of South Dakota (Fig. 1.8). These were the major sources of sediment for the Kansas basins and tectonic events within the mountain regions produced dramatic changes in sediment deposition in the shelf seas of Kansas and Colorado (Fig. 1.9).

Considering firstly the Ozark Dome of East Central Missouri, we find that the area remained a complex uplifted block of PreCambrian and Cambrian igneous and sedimentary rocks from the early Palaeozoic. Although channel sandstones are revealed in many Pennsylvanian deposits including Wabaunsee and Lower Permian sediments (Hinds and Greene, 1915; Mudge, 1956; Mudge and Yochelson,1962), the Dome is considered to be stable during this period (Elias, 1964) and sediments deposited in the Forest City

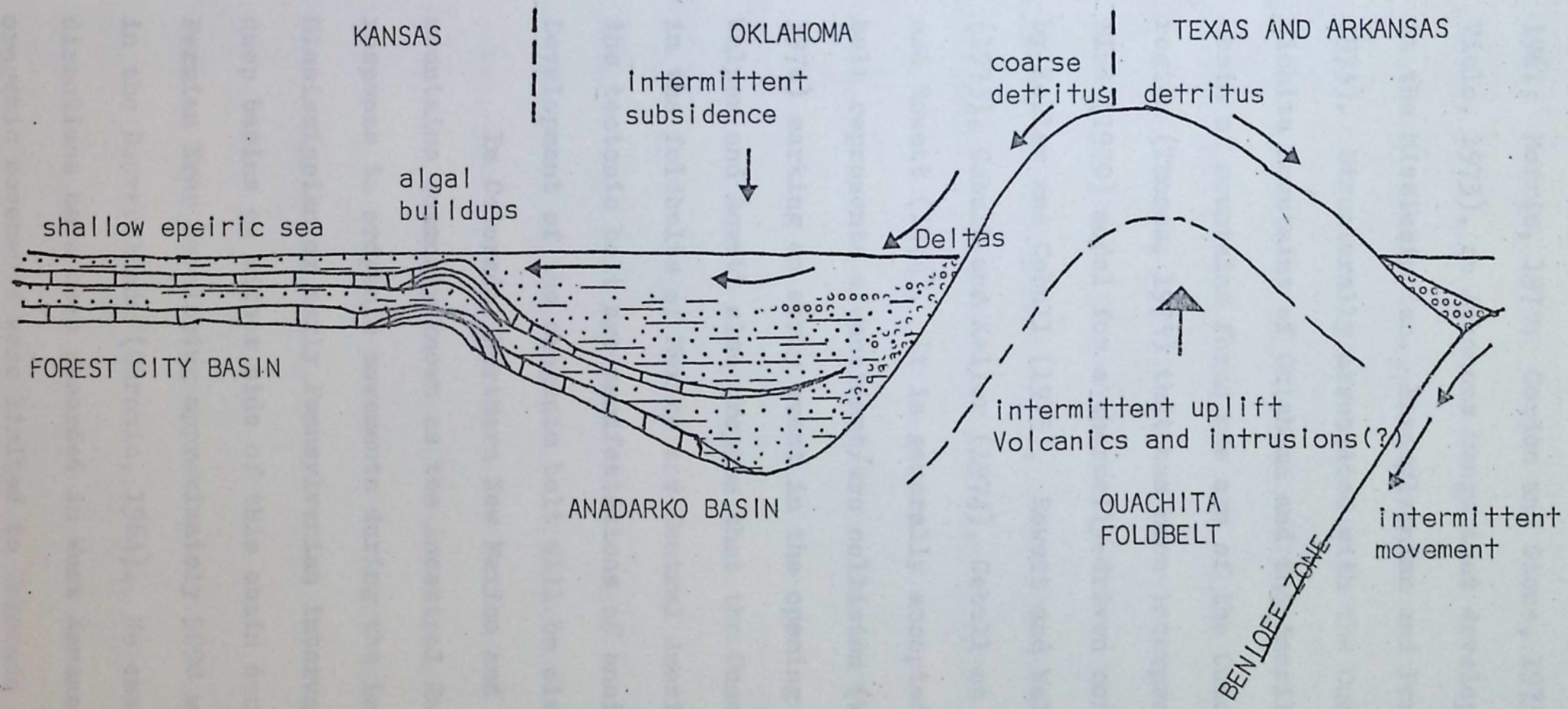

Fig. 1.9 A schematic section illustrating detrital sediment buildup in Kansas with the orogenic development of the Ouachita foldbelt.

Basin were predominantly silts and clays.

To the south of the Ozark Dome lies the Ouachita Mountains (King, 1961; Morris, 1973; Gordon and Stone, 1973; Haley and Charles, 1973; Viele, 1973), an Arkansas range that developed during orogenic movements in the Mississippian. Pennsylvanian and Permian Eras (Keller and Cebull, 1973). Structurally associated with the Ouachitas, are the Arbuckle and Wichita Mountains of Oklahoma and the Amarillo uplift of Texas. This chain of mountains forms one arm of the Ouachita - Appalachian tectonic region (Thomas, 1973) that has been interpreted in terms of the Dewey and Bird (1970) model for a thermally-driven cordilleran-type mountain belt by Keller and Cebull (1973), Rowett and Walper (1973), Walper and Rowett (1973), Cebull and Keller (1974), Cebull et al. (1974), Griffin (1974) and Rowett (1974). It is generally accepted that the Ouachita orogenic belt represents a continent/arc collision (Walper and Rowett, 1973; Hatcher, 1974) marking an early event in the opening of a Proto-Atlantic ocean. Walper and Rowett also propose that the Ouachita orogenic belt is continued in the foldbelts of Mexico and Central America and that apparent offsets in the tectonic belt are manifestations of ancient transform faults. Development of the orogenic belt will be discussed in detail subsequently.

In Colorado, Northern New Mexico and Southern Idaho, a chain of mountains commonly known as the Ancestral Rocky Mountains developed in response to orogenic movements during the Late Devonian to early Mississippian or early Pennsylvanian interval. Sediments were shed into deep basins on either side of this chain during the Pennsylvanian and Permian Eras developing approximately 5000 m. (16250 ft.) of coarse clastics in the Denver Basin (Chronic, 1964). No easterly sediment transport directions have been recorded in West Kansas as the effects of the orogenic movements were limited to Colorado and little sediment reached Kansas.

The Ancestral Rockies are continued in Idaho by the Bighorn

Mountains, a long sinuous mountain chain marking the western boundary of the Powder River Basin. Undulating deltaic lowlands persist from North Dakota to the Ozark Dome and form the boundary for the Power River Basin, Denver Basin and Kansas shelf sea. The lowlands were not tectonically active during the Pennsylvanian and Permian and supplied limited quantities of sediments to the basins.

It would appear therefore that the Kansas shelf sea was surrounded by lowlands and orogenic mountain belts. However, one narrow channel to the open marine seas in North-West Texas existed. The Dalhart Basin, separating the Amarillo Uplift and the Apishapa Uplift (part of the Ancestral Rockies), formed a shallow barrier bar during the Pennsylvanian and Permian and produced in extreme conditions, a stratification of the seas in the Kansas area, anaerobic bottom waters and the development of a black shale lithology (cf. Black Sea sediments (Heckel, 1972a, 1972b)).

To illustrate the tectonic development of the Mid-Continent during the Pennsylvanian and Permian, three palaeogeographic maps are presented (Figs. 1.10; 1.11; 1.12). Initially, in the early Palaeozoic, a Benioff zone was instigated in the Gulf Coast region of Texas and slow movement of the oceanic plate down the Benioff zone resulted in the development of an orogenic zone in Arkansas, Texas and Oklahoma. A shallow shelf sea extended northwards from the orogenic belt onto the stable cratonic continental crust of Kansas, with a deep subsiding basin, the Anadarko Basin, separating them. During the early Pennsylvanian, development of the orogenic belt reached its peak, as an "orogenic welt" rose and great thicknesses of flysch were deposited on the collapsing shelf (McBride, 1969). Some of these "clastic wedges" (Ferm, 1973) spread over the shelf, thinning rapidly northwards, and in the Forest Hills Basin, the thicker, coarser shales may represent the finer fraction of the "clastic wedge" lithologies. The flysch deposits were followed in the late Pennsylvanian/early Permian periods by a mollasse facies marking the

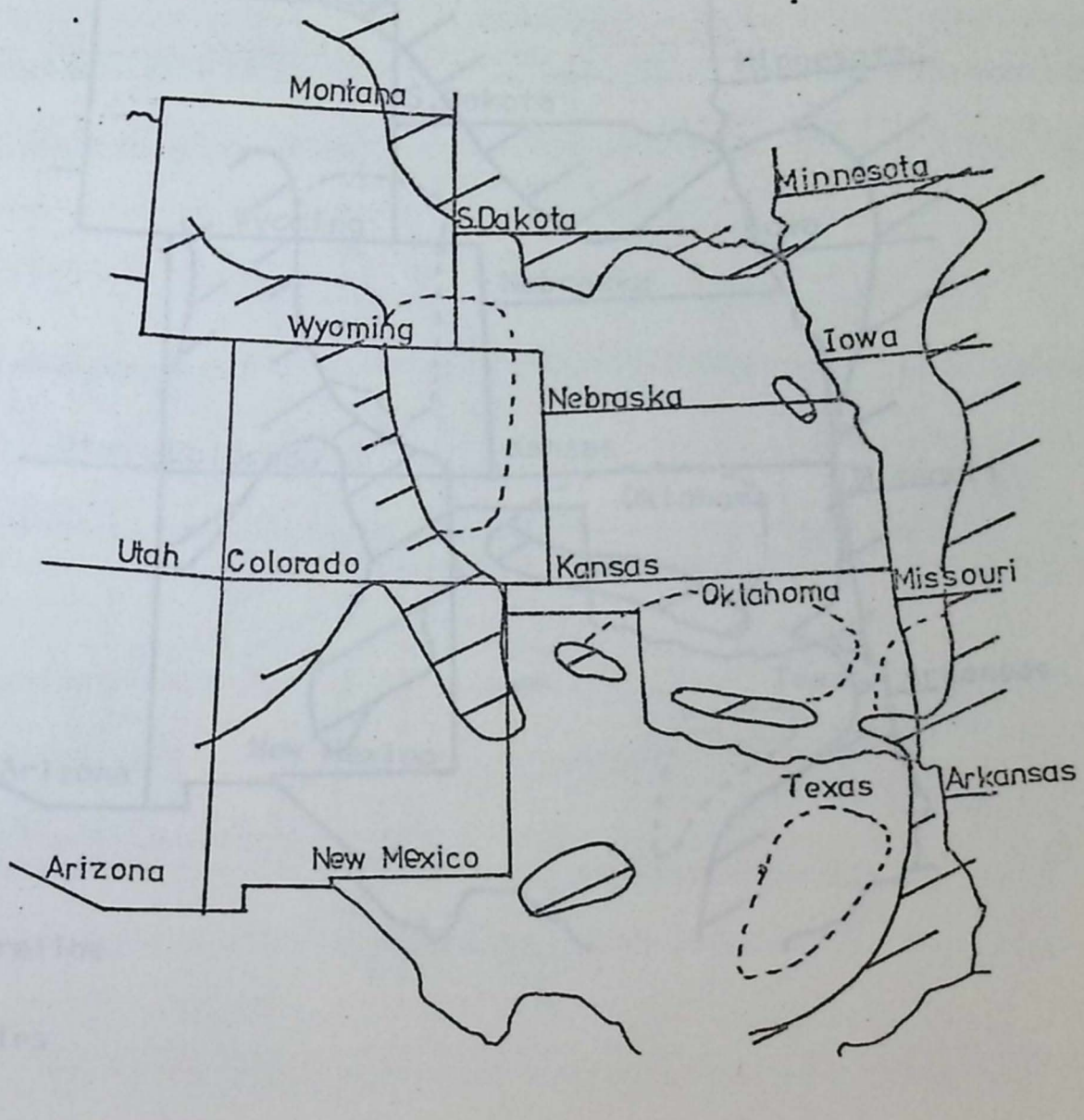

Fig. 1.10 Upper Pennsylvanian (Missourian Stage) paleogeography of Mid-Continent, U.S.A. (Adapted from Sloss et al, 1960; Rascoe, 1962: Wanless et al, 1970 and Moore and Nelson, 1974).

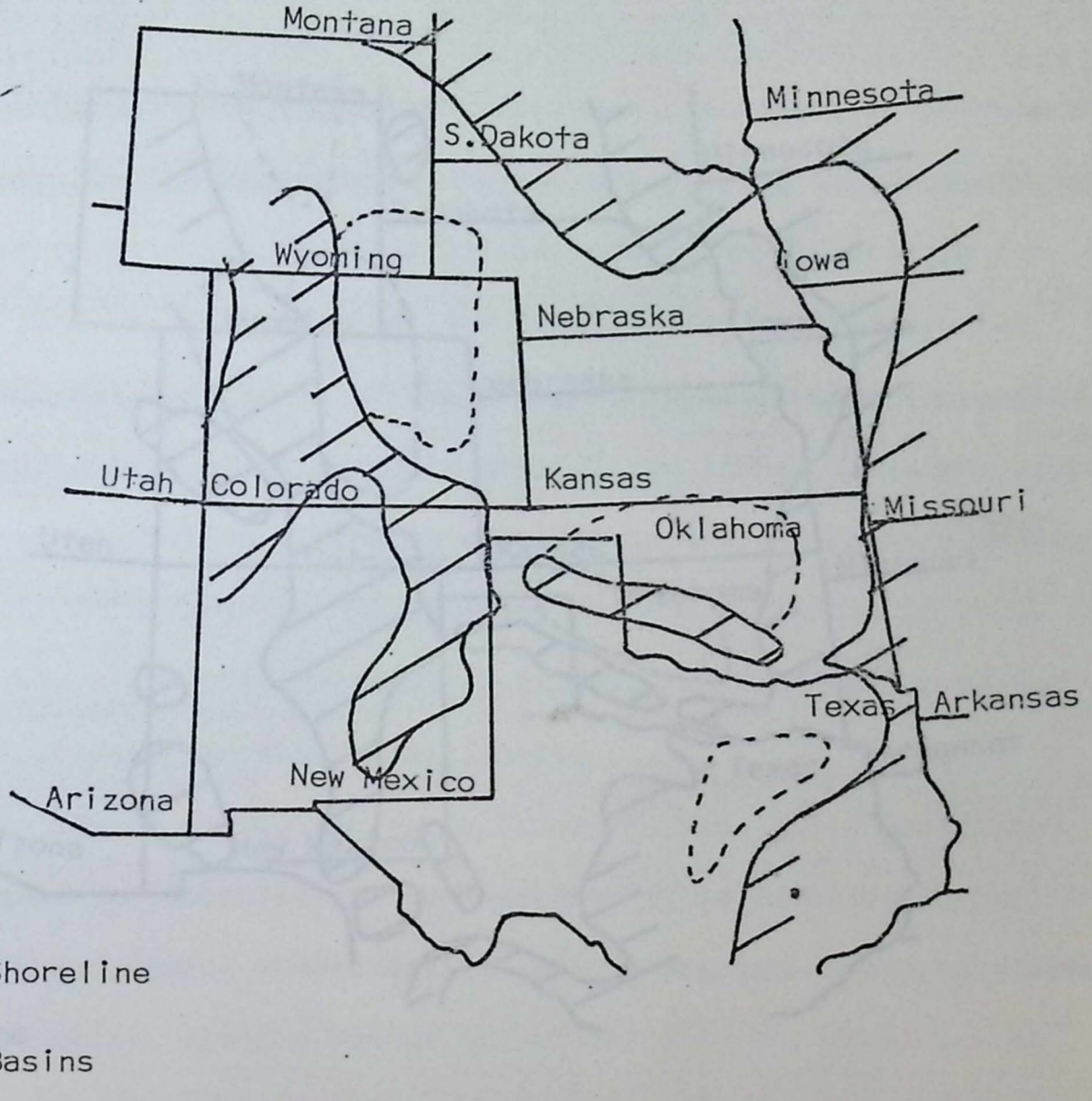

Fig. I.11 Upper Pennsylvanian (Virgilian Stage) paleogeography of Mid-Continent U.S.A.(adapted from Sloss et al., 1960; Rascoe, 1962; Schuchert, 1963; Clark and Stearn, 1968; Troell, 1969; Bott and Batten, 1971; Heckel, 1972b and Moore and Nelson, 1974).

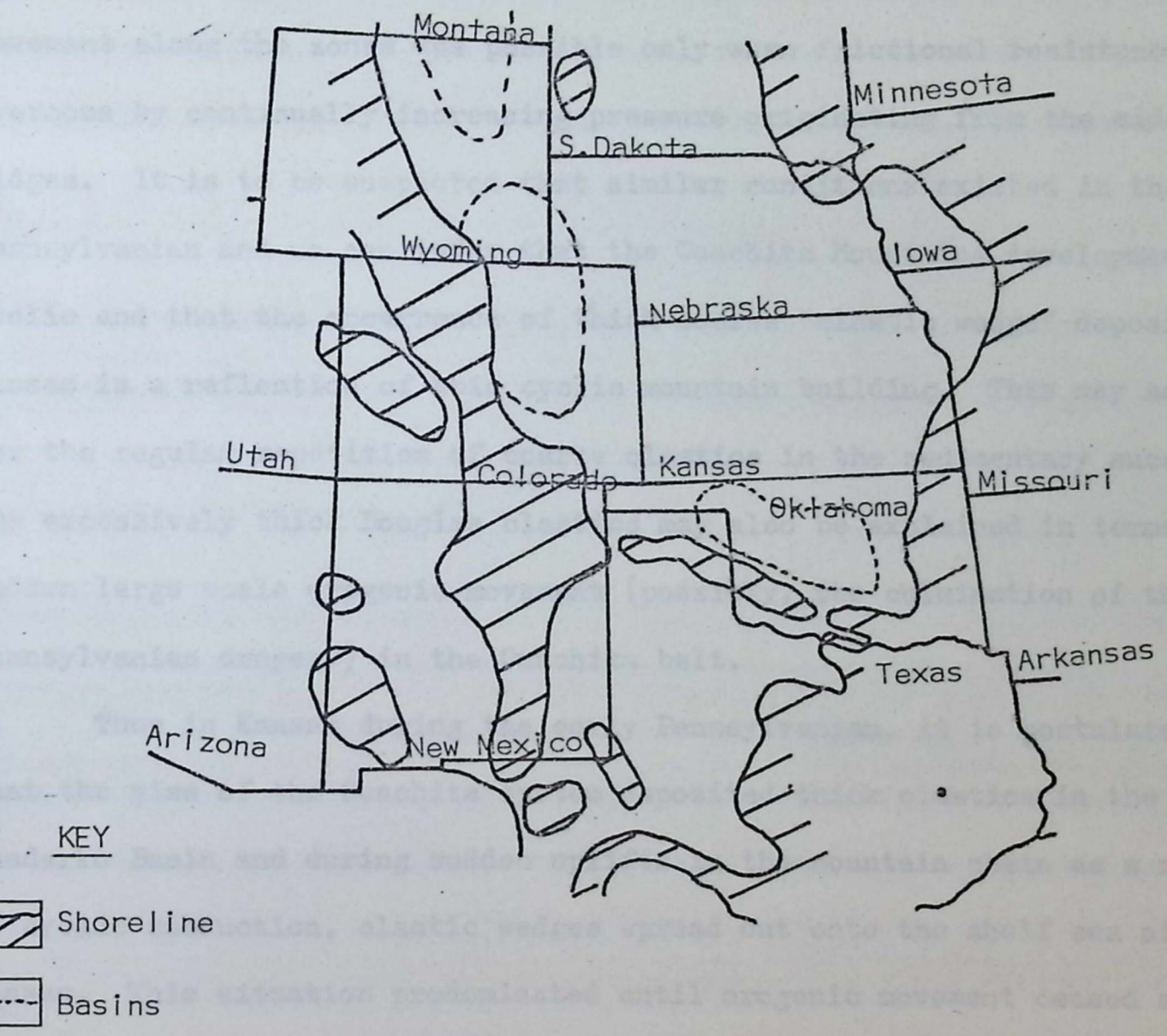

Fig. I.12 Lower Permian (Gearyan Stage) paleogeography of the Mid-Contient, U.S.A. (adapted from Sloss et al, 1960; Rascoe, 1962; Schuchert, 1963; Elias, 1964; McKee and Oriel, 1967; Hills, 1972; Ross, 1973; Seyfert and Sirkin, 1973; and Moore and Nelson, 1974).

cessation of subduction and orogenic activity. Subsequently, stabilization of the orogenic belt resulted in the disappearance of "clastic wedges" from Kansas and the development of evaporite/carbonate sedimentary sequences.

Bott and Deans (1973) studied stress diffusion at plate boundaries and noted that movement along subduction zones was of cyclic nature, i.e. movement along the zones was possible only when frictional resistance was overcome by continually increasing pressure originating from the mid-ocean ridges. It is to be suspected that similar conditions existed in the Pennsylvanian and we can infer that the Ouachita Mountains development was cyclic and that the occurrence of thick coarse "clastic wedge" deposits in Kansas is a reflection of this cyclic mountain building. This may account for the regular repetition of coarse clastics in the sedimentary succession. The excessively thick Douglas clastics may also be explained in terms of sudden large scale orogenic movement (possibly, the culmination of the Pennsylvanian orogeny) in the Ouachita belt.

Thus in Kansas during the early Pennsylvanian, it is postulated that the rise of the Ouachita system deposited thick clastics in the Anadarko Basin and during sudden uplifts in the mountain chain as a result of cyclic subduction, clastic wedges spread out onto the shelf sea of Kansas. This situation predominated until orogenic movement ceased at the end of the Permian era.

The normal sedimentary deposits formed in the Kansas epeiric sea during the Pennsylvanian consisted of limestones alternating with thin, calcareous shales (Heckel, 1972a). Algal buildups of Southern Kansas developed in response to subsidence in the Anadarko Basin and consequently, tectonism in the Ouachita belt. In comparison, the intervening clastics were deposited from deltas on the lowlands to the east and north of Kansas.

The orogenic belt of Colorado, New Mexico and Idaho was throughout this period providing coarse clastic sediments for the Denver and Powder

River Basins but had little direct effect on the sedimentary succession of Kansas. It did, however, complete a ring of land around Kansas providing a classic epeiric sea setting for the Kansas shelf. The narrow Dalhart Basin separated the Ouachita and Rocky Mountains and formed a barred entrance to the Kansas sea. As a result, stratification of the epeiric sea occurred at a number of times during the Pennsylvanian (Heckel, 1972a) encouraging anaerobic conditions to prevail in the bottom waters and sediments of the sea. Black shales, a distinct lithology used as a marker horizon in the "ideal" cyclic sequences (Moore, 1950), are a product of these anaerobic conditions and are normally enriched in trace elements.

With the cessation of orogenic development in the Ouachitas at the beginning of the Permian (Fig. 1.12), the palaeogeographic conditions of the Mid-Continent changed dramatically. Carbonate deposition increased and towards the end of the Council Grove Group, evaporite sediments develop substantial thicknesses. The Amarillo Uplift-Wichita Mountains-Arbuckle Mountains belt became a series of islands (Rascoe,1962) separating the Ouachita and Rocky Mountains and the Kansas epeiric sea became a partially barred carbonate/evaporite basin similar to that of the Mediterranean during the Miocene (Hsu et al., 1973). The tear-drop distribution of carbonate and evaporite sediments (McKee and Oriel, 1967, Fig. 4) reflects the partially barred nature of the Kansas Permian sea.

The overall tectonic environment of Kansas during the Upper Pennsylvanian and Lower Permian has a close analogy in the modern tectonic environment of the Arafaru epeiric sea off northern Australia (Fig. 1.13). Here, New Guinea is part of a complex orogenic belt of comparable size to the Amarillo Uplift-Wichita Mountains-Arbuckle Mountains arm of the Ouachita foldbelt. Clastic sediments are carried from the mountains and deposited at the margins of an epeiric sea covering the edge of the stable Australian craton. Carbonate sediments and active reefs also cover much of the area. Differences in the two regimes are noticeable however, and

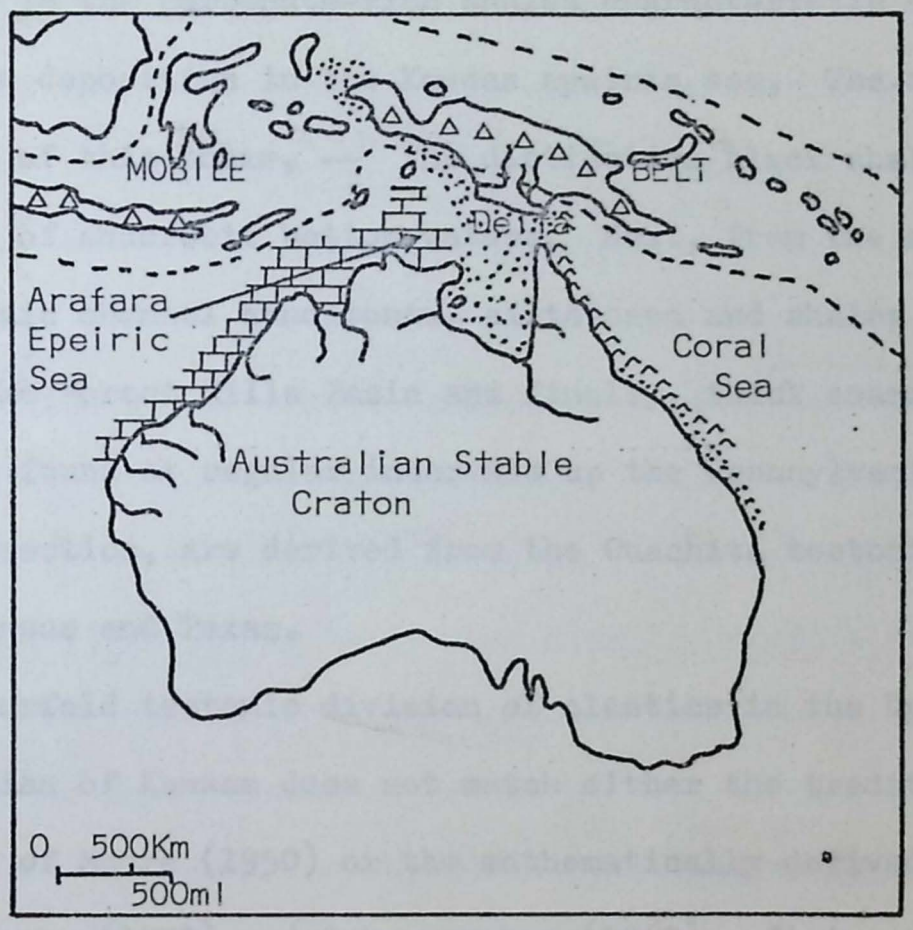

Fig. 1.13 Relationship of the modern orogenic islands of New Guinea and Indonesia to the stable Australian craton - an analogy to Upper Pennsylvanian and Lower Permian conditions in the Mid Continent, U.S.A. (After Dott and Batten, 1971).

Heckel (1972a) has suggested the Yellow Sea as an alternative for the restricted marine basin environment. A similar environment has been reported in the Tasman Sea by Hayes and Ringis (1973).

To summarise, therefore, tectonic events in Oklahoma, Texas and Arkansas have affected the Pennsylvanian and Permian sedimentary succession in Kansas and produced a fourfold division of the clastic sediments. Firstly, there is the carbonate-rich shales characteristic of "normal" carbonate/shale deposition in the Kansas epeiric sea. The second division is a variation of this theme, — the distinctive black shale lithology characteristic of anaerobic bottom waters. Next, from the east came a number of deltaic channel sandstones, siltstones and shales that were deposited in the Forest Hills Basin and finally, thick coarse clastic units that are found at regular intervals up the Pennsylvanian stratigraphic section, are derived from the Ouachita tectonic belt of Oklahoma, Arkansas and Texas.

This fourfold tectonic division of clastics in the Upper Pennsylvanian and Lower Permian of Kansas does not match either the traditional classification of Moore (1950) or the mathematically-derived classifications of Davis and Cocke (1972) and Schwarzacher (1969). It is necessary therefore to resolve these differences by studying the clastics in detail and testing the various classifications.

SAMPLING PATTERN

Stratigraphically, it was realised that each clastic horizon in the Upper Pennsylvanian and Lower Permian was not necessarily restricted to a unique lithology. In fact in Moore's classification, two or even three lithological divisions of a cyclothem could be found in one clastic bed. As Moore based his conclusions on field and hand specimen evidence, it was concluded that lithologies, recognisably different in the field, should be sampled for mineralogical, petrological and geochemical analysis. Samples

were collected from horizons in the Tacket Formation (Pleasanton Group) and all clastic units up to the Paddock shale member of the Nolans Limestone (Chase Group) and the distribution can be seen in Fig. 1.14. The only exceptions to this pattern were the Auburn and Winzeller Shales (Wabaunsee Group) where lack of surface exposure prevented adequate collection.

Samples collected for each horizon are considered representative of that horizon for many hundreds of miles along the outcrop strike. Merriam (1963) for example, has commented on how it is possible to recognise single lithologies over remarkable distances in Kansas and how stable bed thicknesses are.

The distribution of sample collecting stations in eastern Kansas (Fig. 1.15) is restricted to the Forest Hill Basin. However, adequate exposures could in some cases only be found in southern Kansas. In the later situation, it should be noted that clastic deposits do coarsen and thicken southwards from South Kansas into the Anadarko Basin of Oklahoma inferring that the South Kansas outcrops will not necessarily be representative of the normal Pennsylvanian and Permian sediments in the Forest City Basin. Interpretation of analytical results in succeeding chapters will take this into consideration.

Outcrops of Pennsylvanian and Permian deposits are found along all major motorways cutting east-west across the state (Figs. 1.16 and 1.17). Samples collected from such exposures were extracted at a depth of six inches from the surface to obtain relatively unweathered sediments. Suitable samples were then thin-sectioned and analysed by X-ray diffraction, emission spectroscopy and electron spin resonance. Appendix 6 summarises the sampling information in tabular form, recording sample number code, collecting station and analyses performed on each sample.

Analyses were performed on a representative selection of sediments extracted from the total sample collection. This was considered necessary

Fig.1-14 STRATIGRAPHIC DISTRIBUTION OF SAMPLES.

UPPER PENNSYLVANIAN SERIES
MISSOURIAN STAGE

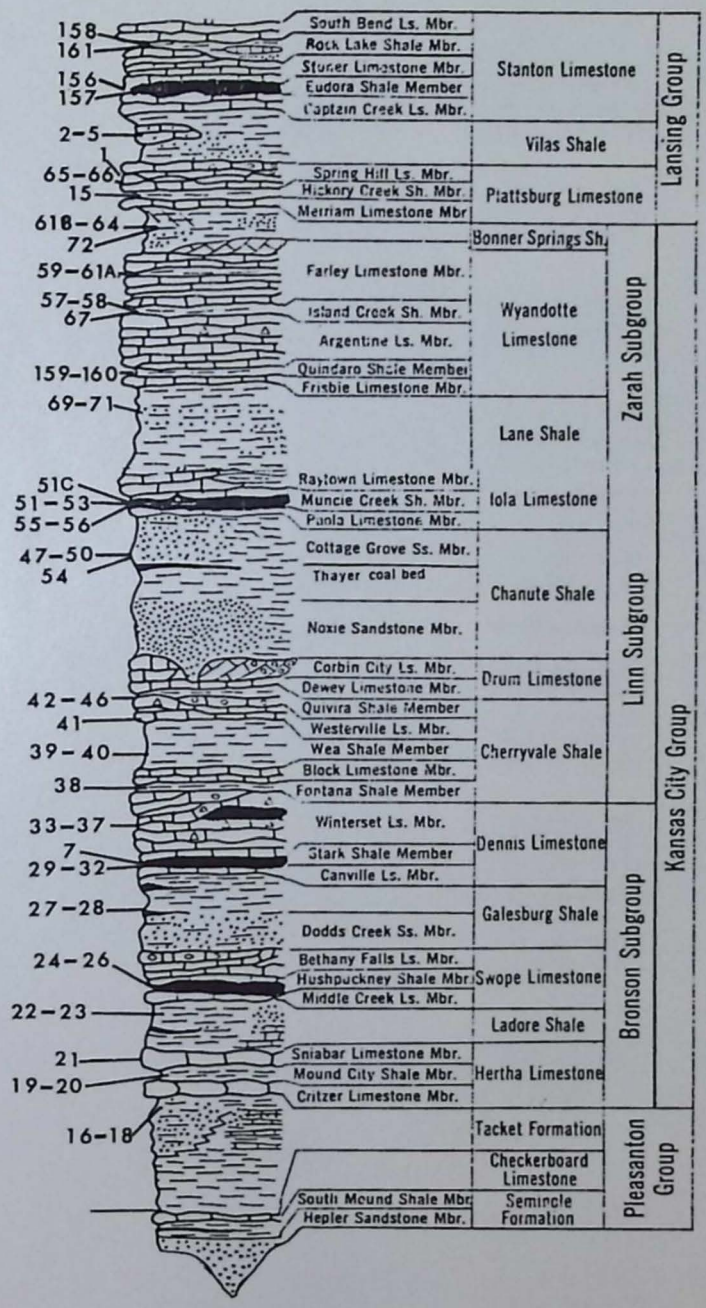

STRATIGRAPHY

SYSTEM	SERIES	STAGE
PERMIAN	LOWER PERMIAN	GEARYAN
PENNSYVANIAN	UPPER PENNSYLVANIAN	VIRGILLIAN
		MISSOURIAN

KEY

- Sandstone or sand
- Undifferentiated sandstone or siltstone
- Siltstone
- Cross-bedded sandstone or siltstone
- Shale or claystone
- Reddish color (used as overlay on other symbols)
- Coal or lignite
- Limestone
- Cross-bedded limestone
- Oolitic limestone
- Cherty limestone
- Shaly limestone
- Sandy limestone
- Gypsum or anhydrite
- Dolomitic limestone
- Dolomite
- Cherty dolomite
- Black shale
- Calcareous shale
- Chalk
- Shale with concretions

SCALE:- 0 FEET 75
0 METRES 25

UPPER PENNSYLVANIAN SERIES
VIRGILIAN STAGE

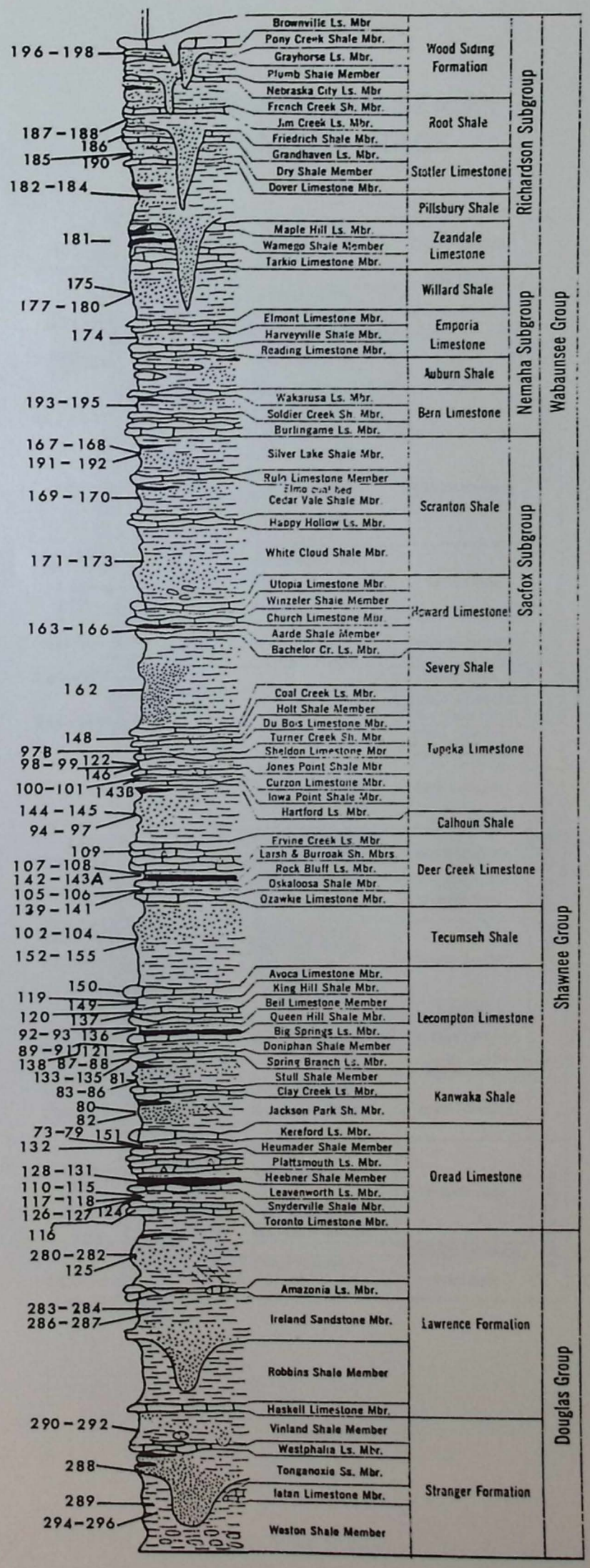

LOWER PERMIAN SERIES
GEARYAN STAGE

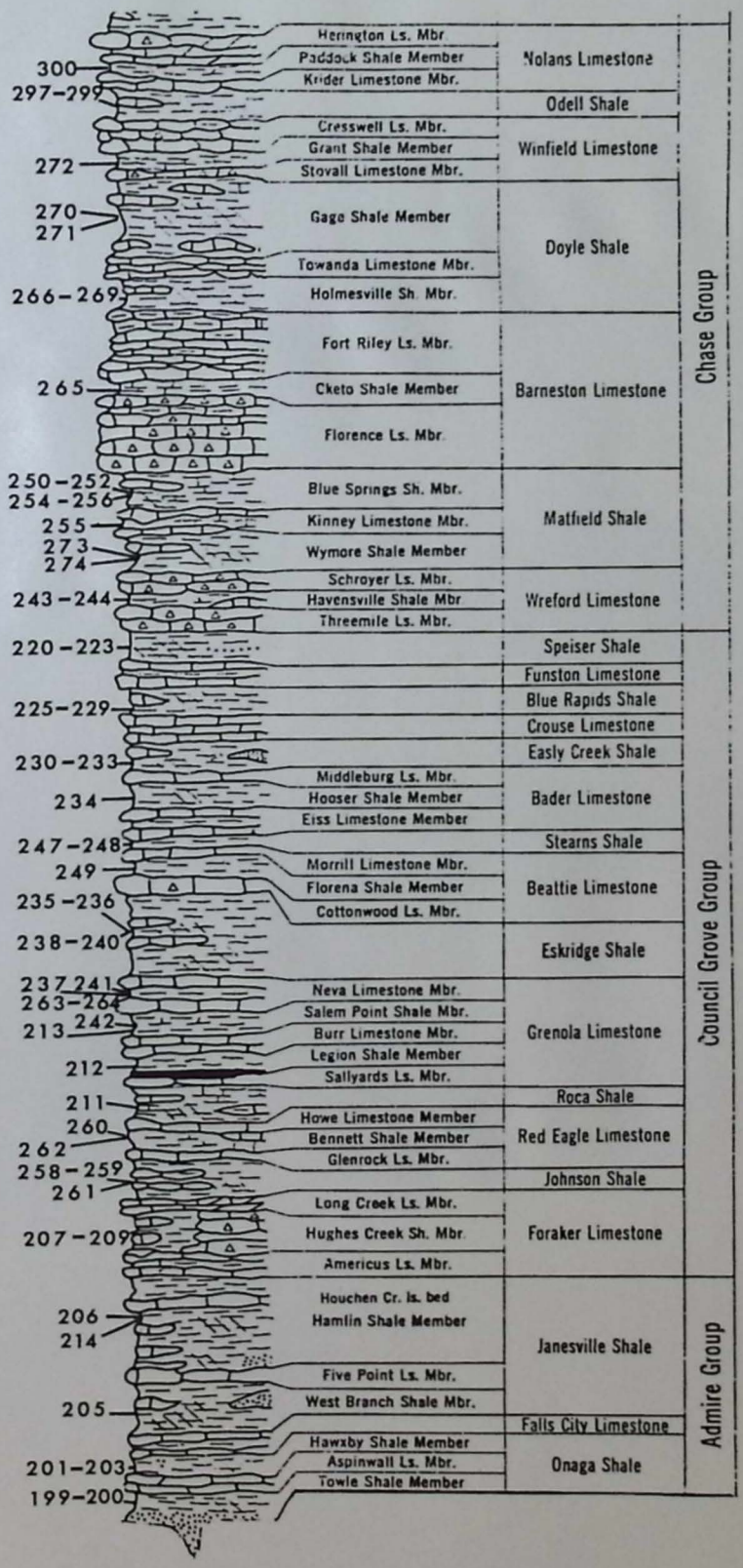

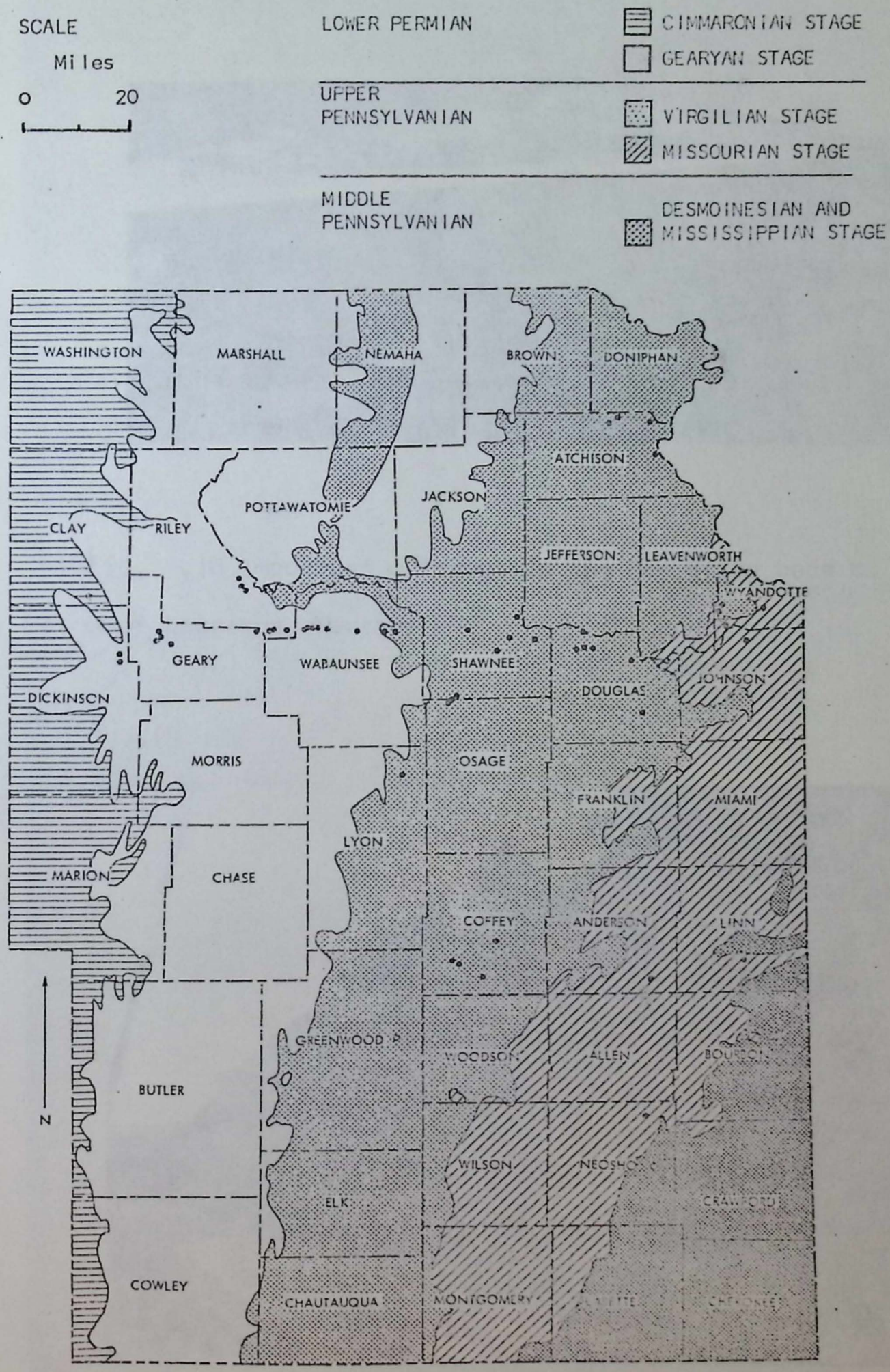

Fig. 1.15 Distribution of sample collecting stations in eastern Kansas.

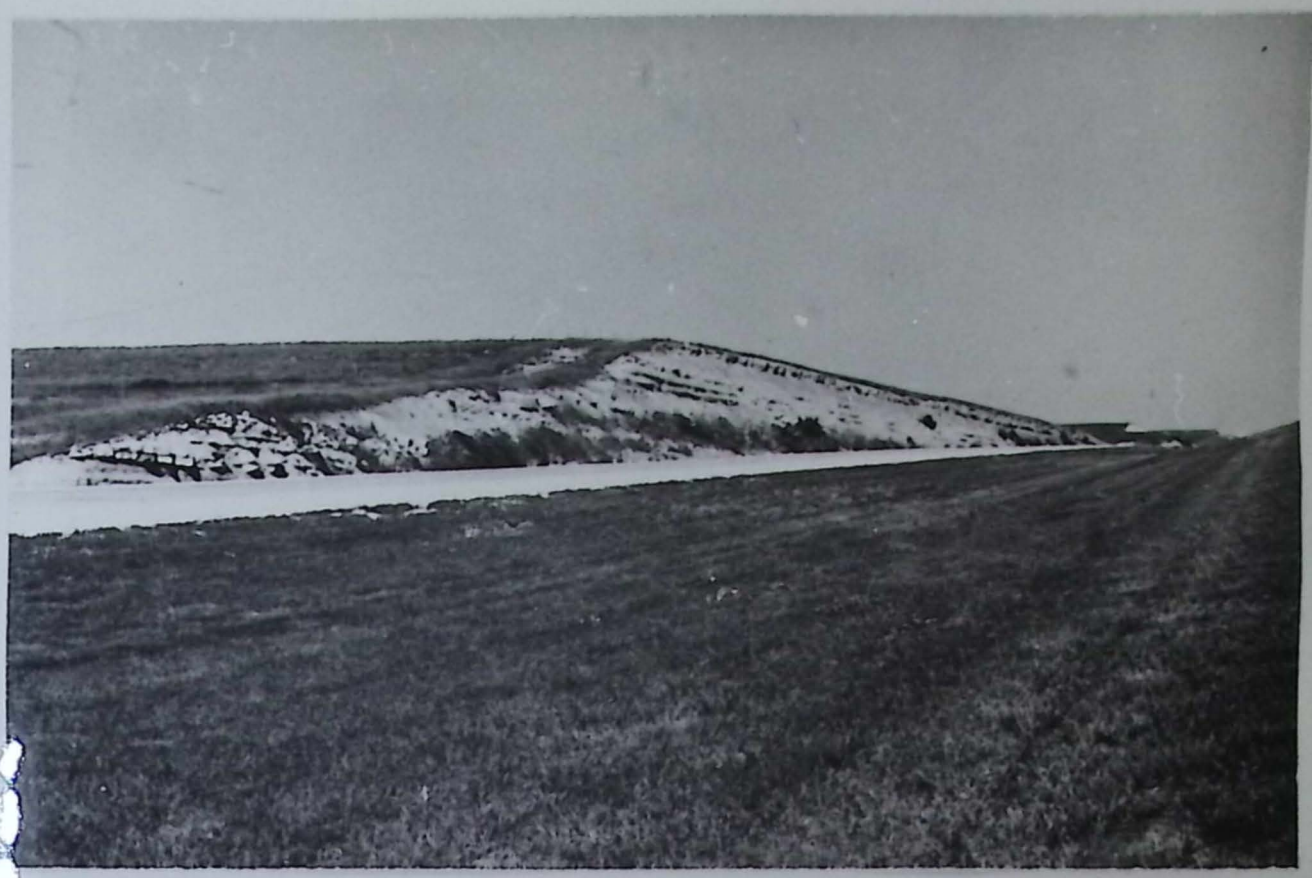

Fig. I.16 Important outcrops of Shawnee Group beds on Interstate 70, W of Lawrence, Kansas.

Fig. I.17 Road cutting exposure of Vilas Shale near Altoona, Wilson County in Southern Kansas.

to establish overall trends and cycles throughout the stratigraphical section and avoid unnecessary noise caused by minor lithological variations. Therefore, only gross lithologies were analysed for mineralogical and geochemical variations.

CHAPTER TWO

A REGRESSION TECHNIQUE FOR THE ANALYSIS OF SHALES BY X-RAY DIFFRACTOMETRY

INTRODUCTION

The mineralogy of fine-grained clastics is normally obtained using X-ray diffraction. Quantitative determinations involve the measurement of intensity of X-rays diffracted from minerals and comparison with a calibrated standard. Although simple in principle, experimental results are highly variable; consequently, a number of alternative preparation techniques have been proposed to assess the mineralogy of sediments by quantitative X-ray diffraction.

Various reasons for inconsistency in results have been suggested, with most emphasis on the relative magnitudes of errors produced by sample preparation techniques (Gibbs, 1967). Other sources of errors including instrument fluctuations, operator error, and structural and chemical variations between minerals have also been described.

To establish a system which minimizes these errors and consequently maximizes analytical accuracy, it is necessary to have complete knowledge of the effects of the errors. In this chapter, the primary sources of error in quantitative X-ray diffraction analysis of fine-grained sediments are described and studied. By statistically designing an error-analysis experiment, it is possible to establish standardized preparation procedures and analytical conditions which minimize the controllable errors. Under these conditions, calibration charts for a number of minerals can be produced, using regression analysis, which will act as external standards for the analysis of Upper Pennsylvanian and Lower Permian shales of Kansas, U.S.A.

PREVIOUS WORK

The basic principles of quantitative X-ray diffractometry were developed and discussed by Klug and Alexander (1954); many workers have used variations of their methods for determining mineral percentages,

especially quartz and calcite (Levy, 1964; Gorbunova, 1969; Till and Spears, 1969). More rarely whole rock samples have been analysed by X-ray diffraction techniques. Schultz (1964) described methods devised for analysis of the Cretaceous Pierre Shale and concluded that an overall accuracy of ± 10 percent could be achieved by (1) controlling the uniformity of grinding procedures, (2) careful homogenization of samples, (3) consistent interpretation, and (4) standardization of sampling and sample preparation.

Other quantitative studies include those of Tatlock (1966), Baker (1968), Bristol (1968), and Hausen (1973). Nelson and Cochrane (1970) determined mineral percentages in calcareous mudstones, sandstones, and hydrothermally altered andesites. Accuracy was obtained by initial standardization of procedure and equipment, yet differences in crystallization remained as a major source of error.

Gibbs (1967, 1968) has studied the errors involved in different sample preparation techniques for clay mineral studies and concludes that the smear-on-glass slide technique, suction-on-ceramic tile, and dry powder press technique were the only acceptable preparation methods. Errors due to segregation are partially responsible for the inaccuracy and lack of precision of alternative methods.

The factors affecting peak intensity and thus the accuracy of diffraction analysis were studied statistically by Griffiths (personal communication). It was concluded that factorial designs were a powerful tool for exploring the magnitude of variation in performing a simple analysis by X-ray diffraction.

VARIANCE IN QUANTITATIVE X-RAY DIFFRACTION

Different samples of the same pure mineral will produce X-ray peaks of the same intensity. Theoretically, the relationship for a pure mineral will be expressed as

$$\theta \approx k$$

where θ is the peak intensity and k is a constant unique for each mineral. However, for mixtures of minerals in a sedimentary rock, the peak intensity of a mineral becomes

$$\theta \approx k\left(\frac{a}{100}\right) - m$$

where a is the percentage of the mineral in the sample. So-called "matrix effects", m, are produced by absorption and reemission of X-rays by certain elements in the mixture.

In practice, intensity is affected by many factors other than abundance and matrix effects, as shown in Fig. 2.1. These other factors can be divided into two general categories of within-sample variation. One source is inherent; that is, variation within the crystalline mixture itself resulting from differences in the degree and nature of crystallinity of the particles (Grim, 1968). This is termed compositional variation and is beyond the control of the investigator.

Compositional variation contributes only a small proportion of the total variance for most non-clay minerals and may be ignored. The primary source of within-sample variation is induced, or independent of the samples themselves. This external variation is termed experimental variation and can be ascribed to three sources: (1) inhomogeneity within a prepared replicate, (2) differences between prepared replicates of samples, and (3) instrument fluctuation.

External variation generally results from inconsistencies in preparation and analysis, incomplete grinding or disaggregation, inconsistent mounting of samples, variations in line voltage to the X-ray unit, non-uniform maintenance of laboratory conditions, and fluctuations in detection and recording circuits. Many of these variances can be reduced by use of quality-control methods and statistical analyses. Variation resulting from prepared sample inhomogeneity and differences

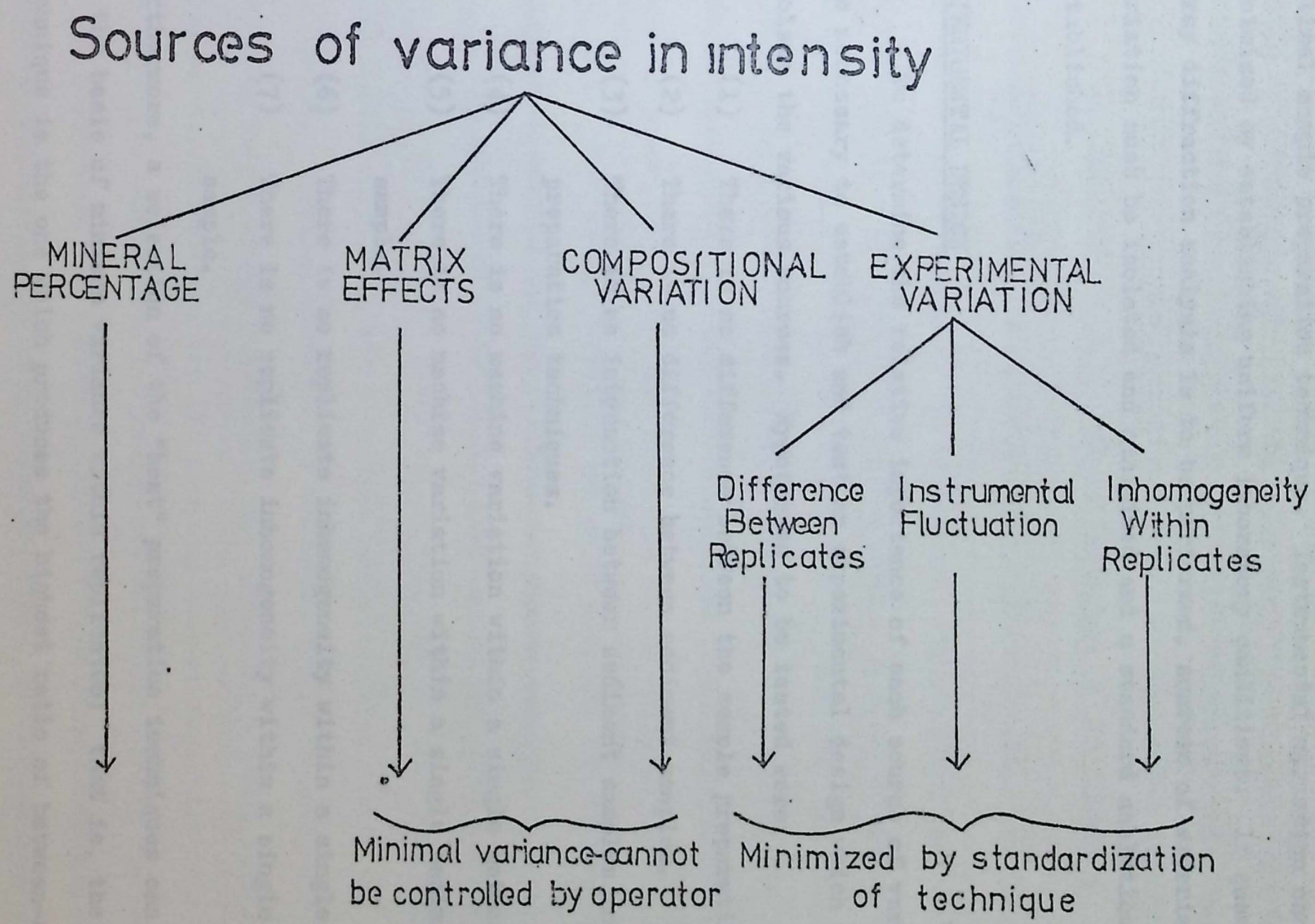

Fig. 2.1. Sources of variation in the quantitative mineralogical analysis of sediments by X-ray diffraction.

between replicates can be minimized by experimentation and selection of an optimal sample preparation technique. Instrumental variation can be minimized by establishing uniform laboratory conditions. If quantitative X-ray diffraction analysis is to be performed, sources of experimental variation must be isolated and minimized and a standard analytical technique established.

EXPERIMENTAL DESIGN

To determine the relative importance of each source of variance it was necessary to establish and test an experimental design which would isolate the various sources. Hypotheses to be tested were:

(1) There is no difference between the sample preparation methods.

(2) There is no difference between sediment samples.

(3) There is no interaction between sediment samples and preparation techniques.

(4) There is no machine variation within a single method.

(5) There is no machine variation within a single sediment sample.

(6) There is no replicate inhomogeneity within a single method.

(7) There is no replicate inhomogeneity within a single sediment sample.

Furthermore, a selection of the "best" preparation techniques can be made on the basis of minimum variance within replicates; that is, the superior technique is the one which produces the highest ratio of between-sample to within-sample variance. In order to assess the effects of machine variation (an independent source of error) and inhomogeneities within prepared replicates, their variance must be measured as well. The entire analysis was performed for both peak height and peak area methods of measurement. Because all currently employed sample preparation techniques are analysed, the number of possible treatments is fixed. However, samples

selected for analysis are chosen randomly from an essentially infinite population of sedimentary rock samples. The resulting pattern of a fixed number of treatments and a random selection of samples is termed a mixed effects model (Bennett and Franklin, 1954). The experimental design used is a classic two-way analysis of variance with replicates (Griffiths, 1967). Each analytical result X_{ijk} can be described by the equation

$$X_{ijk} = \mu + \alpha_i + \beta_j + \gamma_{ij} + (\delta_{k(ij)} + \epsilon_{(ijk)}) ,$$

expressing the structure of the experiment. This states that an observation is composed of a constant (the overall mean μ), a contribution from the preparation technique α_i, from the sample β_j, and from "discrepancy" or differential effect of samples over techniques γ_{ij}, plus final contributions from replicates $\delta_{k(ij)}$ and from unspecified (unassigned) sources, otherwise known as error, $\epsilon_{(ijk)}$. The structure of the analysis is shown in Fig. 2.2. This design describes two major effects, the differences between preparation methods and the differences between samples.

Two sources of variation contributing to the error term $\epsilon_{(ijk)}$ in the two-way ANOVA are not described by this design, that resulting from instrumental variation, and that from inhomogeneities within the prepared replicates. However, these can be estimated by (1) choosing one replicate from each method/sample combination for re-running without changes in the experimental conditions, and (2) choosing another replicate from each method/sample combination for re-running but repositioning the replicate in the X-ray beam. To assess the relative importance of instrumental variation and within-replicate inhomogeneities, it is necessary to run a one-way ANOVA test for each of these variances. It should be noted that a single experiment could be designed to assess these sources at the same time as the primary sources, but this would require either an inordinate number of levels of replication or a complex, unbalanced design.

The ANOVA for the two-way design is shown in Table 2.1. The significance of the variance contributions is tested by an F-test of the

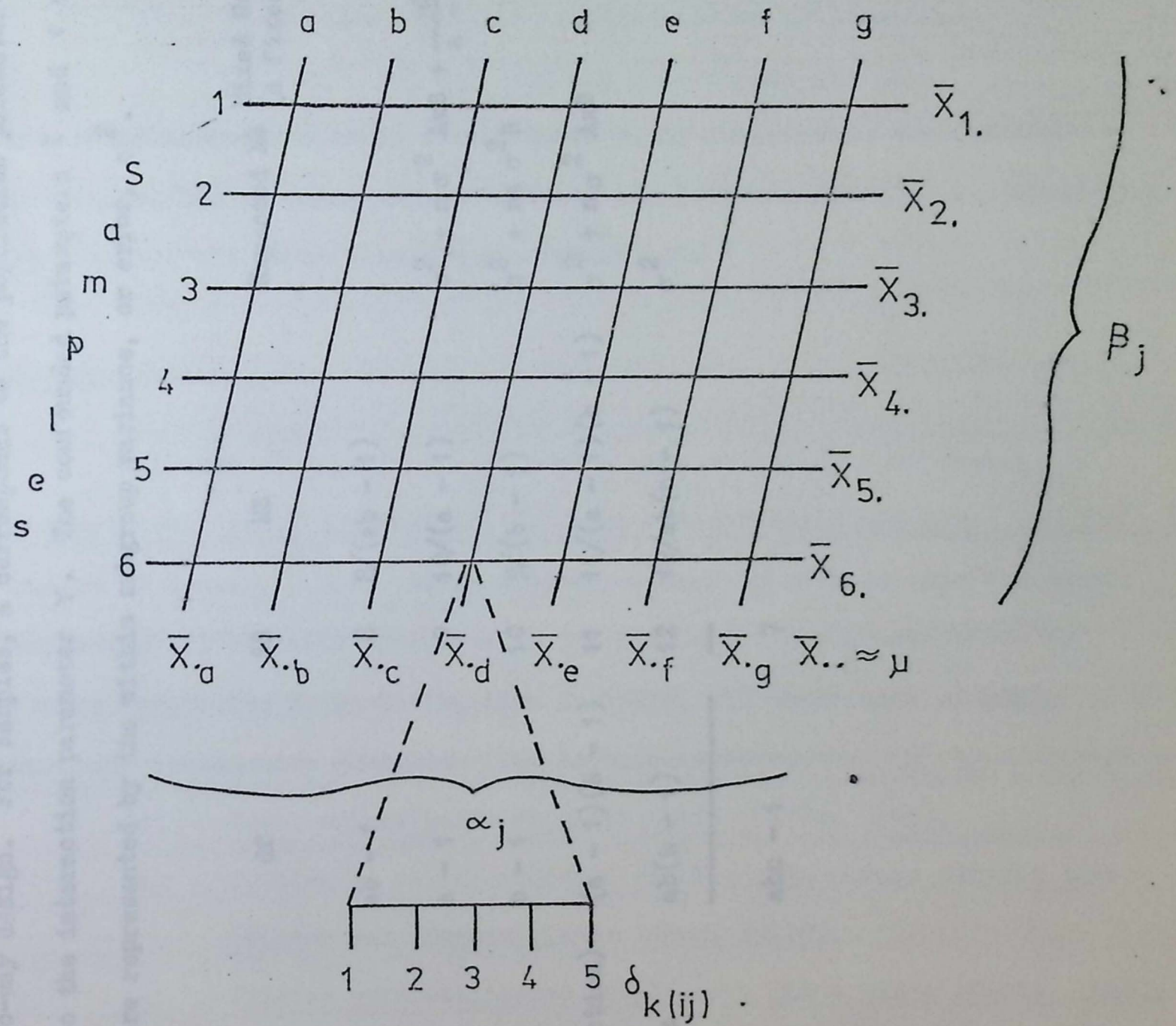

Fig. 2.2 Experimental design with replication (after Griffiths, 1967)

TABLE 2.1 ANOVA table for a two-way design. For samples, A corresponds to the population parameter α, B to β, and A x B to the interaction parameter γ. The confounded parameters δ and ϵ of the model equation are represented by the within subgroup variance, or error, σ^2.

Source of variation		df	SS	MS	Expected MS Mixed Model (A fixed, B random)
$\bar{Y} - \bar{\bar{Y}}$	Subgroups	ab - 1	8	8/(ab - 1)	
$\bar{Y}_A - \bar{\bar{Y}}$	A (columns)	a - 1	9	10/(a - 1)	$\sigma^2 + n\sigma^2_{AxB} + \frac{nb}{a-1}\Sigma\alpha^2$
$\bar{Y}_B - \bar{\bar{Y}}$	B (rows)	b - 1	10	9/(b - 1)	$\sigma^2 + na\sigma^2_B$
$\bar{Y} - \bar{Y}_A - \bar{Y}_B + \bar{\bar{Y}}$	A x B (interaction)	(a - 1)(b - 1)	11	11/(a - 1)(b - 1)	$\sigma^2 + n\sigma^2_{AxB}$
$Y - \bar{Y}$	Within subgroups	ab(n - 1)	12	12/ab(n - 1)	σ^2
$Y - \bar{\bar{Y}}$	Total	abn - 1	7		

mean-squares ratio. Three assumptions are necessary for the F-test.

(1) The observations X_{ijk} are random variables.

(2) The variables are the sums of the contributions of the component variables α_i and β_j; i.e. $\alpha_i = \beta_j = \alpha_i\beta_j = 0$.

(3) The random variables are distributed with variances σ_α^2, σ_β^2, and σ_σ^2 and all covariances are zero.

The third assumption implies that there is no interaction between the variables, but by using the ANOVA test, any interactions that may exist can be assessed and their significance determined.

METHOD

For this study, six shale samples were selected to represent the compositional range apparent in the Upper Pennsylvanian and Lower Permian shales of Kansas, U.S.A. Seven sample preparation methods were evaluated, including all of those advocated in the literature for quantitative or semi-quantitative X-ray diffraction analysis, and those most commonly used for qualitative analysis. The techniques were:

(1) Smear of wet paste on glass slide (Gibbs, 1965),

(2) Suction of water-dispersed samples onto porous ceramic tile (Kinter and Diamond, 1956; Shaw, 1972),

(3) Pipette water-dispersed sample onto glass slide (Gibbs, 1965),

(4) Water-dispersed sample sedimented onto glass slide (Gipson, 1966),

(5) Ground dry sample moulded into pellet using a high-pressure press (Hidalgo and Renton, 1970),

(6) Ground dry sample packed in a Norelco aluminium sample holder (Gibbs, 1965), and

(7) Suction of water-dispersed sample onto membrane filter (Appendix 5).

The centrifuge-on-glass slide and centrifuge-through-ceramic tile methods have been shown to be inaccurate and subject to great variation in results (Gibbs, 1965) and were not considered in this study. Detailed descriptions of the various methods of preparation can be found in Gibbs (1965, 1967, 1968, 1969), Quakernaat (1970), Shaw (1972), and Kittrick (1961). It should be noted that techniques 3 and 4 will be affected by orientation and segregation of minerals due to differential settling of certain mineral groups. This enhances the intensity of certain X-ray peaks, especially those of the clay minerals, and may produce a biased estimate of shale mineralogy. However, both techniques have proved useful in qualitative assessment of shale mineralogy.

The shale samples were dried in air and then ground in a shatterbox to less than 60μ. No additional treatment was applied to the ground material. Each shale sample was divided into seven parts and randomly assigned to a sample preparation technique. Individual runs were grouped into classes representing all possible different combinations of shales and preparation methods. Each run was replicated five times, resulting in 210 X-ray analyses for the assessment of preparation methods.

As discussed previously, one replicate from each method/sample combination was run five times without change in experimental conditions. Another replicate from each method/sample combination was run five times changing the position of the sample within the X-ray beam after each run. Thus instrumental variation and inhomogeneity of the prepared replicate could be assessed. Peak area and peak height measurements were recorded for all analyses.

RESULTS

The completed ANOVAs are shown in Table 2.2 and indicate significant differences between methods of sample preparation and between the shales analysed. They also indicate significant interactions between

TABLE 2.2 ANOVA for two-way design, comparing sample preparation methods, shale samples, and interaction. Table A is for peak height measurements, Table B for peak area measurements.

A. ANOVA for Peak Heights

Source	Sum of Squares	Degrees of Freedom	Mean Squares	F-ratio
Between Methods	3,668	6	611.3	36.1**
Between Shales	10,178	5	2035.5	120.1**
Method x Shale Interaction	2,998	30	99.9	5.9**
Error (replicates)	2,765	168	17.0	
Total	19,609	209		

B. ANOVA for Peak Areas

Source	Sum of Squares	Degrees of Freedom	Mean Squares	F-ratio
Between Methods	53,231,684	6	8,871,947	26.4**
Between Shales	288,497,404	5	57,699,481	172.0**
Method x Shale Interaction	115,233,135	30	3,841,105	11.4**
Error (replicates)	65,001,239	168	335,533	
Total	521,963,462	209		

**Highly significant

preparation methods and samples. The first ANOVA in Table 2.2 uses peak height as the variable, and the second uses peak area. The ratio of between-shale variance/within-shale variance ("error") can be regarded as an index of efficiency of distinction between shale samples, i.e. a measure of separation between means of replicates compared to dispersion of replicates. This ratio is 120 using peak heights and 172 using peak areas indicating that peak area measurements are more effective than peak height for distinguishing between samples. Note, however, that there is significantly more interaction using peak area measurements.

Having established that different sample preparation methods do produce significantly different results, it is necessary to rank them in order to select the optimum procedure. This can be done by computing the ratio of the between-shale variance, within a method, to the within-shale variance, within a method. These ratios are shown in Table 2.3 for both peak height and peak area measurements.

Peak area is superior to peak height for all preparation methods except (6) hand packing of powdered sample into holder. All methods allow discrimination between shales except method (3) pipetting a dispersed sample onto a slide. Even this method allows the distinguishing of samples if peak area measurements are used.

Clearly the most effective preparation technique, judged by the peak area criterion, is the smear method (Table 2.3). The second most effective procedure is pressing a powdered sample into a pellet. Interestingly, both of these procedures tend to produce oriented samples. The filter-mounting method and that of sedimenting a sample onto a glass slide in a beaker are approximately equal in their effectiveness. Other techniques are significantly less effective for discrimination between shales. This presumably results from the low counting rates produced by these methods, which result from increased contributions by the X-ray background level.

TABLE 2.3 Ratios of between-shale variance to within-shale variance for seven sample preparation techniques.

	1 Smear	2 Suction on tile	3 Pipette onto slide	4 Settling onto slide	5 Pressed pellet	6 Sample holder	7 Filter mount
Peak Height	89	13	2	35	43	51	15
Rank	1	6	7	4	3	2	5
Peak Area	166	16	7	52	109	35	52
Rank	1	6	7	3	2	5	3

TABLE 2.4 Variances of homogeneity runs, averaged across shale samples. Rank indicates smallest to largest within-mount variances. Only data for peak area measurements given.

	1 Smear	2 Suction on tile	3 Pipette onto slide	4 Settling onto slide	5 Pressed pellet	6 Sample holder	7 Filter mount
Variance	165,363	308,168	21,216	361,158	130,561	212,228	141,075
Rank	4	6	1	7	2	5	3

Sample homogeneity, or the tendency for a sample to vary in composition across a prepared mount, is a major factor which affects reproducibility. Table 2.4 contains the average variances of replicates repositioned in the X-ray beam to measure sample homogeneity, calculated across samples. Their ranking indicates relative tendency for specific preparation methods to create inhomogeneous mounts.

The small variance of the pipette method (3) results from the small area of the prepared sample which insures that almost all of a sample is in the X-ray beam regardless of its orientation in the machine. Unfortunately, this method is the poorest for distinguishing between shale samples. The second most uniform method is the pressed pellet; the third most effective, the filter mount. The smear technique, which produces the highest between-shale variance, ranks fourth for uniformity.

At this stage of the analysis, three sample preparation techniques can be selected as superior. These are the smear method, the pressed-pellet method, and the filter-mount method. However, as the technique to be applied to this project involved analysis of several hundred samples, each replicated a number of times, practical considerations of sample preparation time were important, and an assessment of the physical procedure became necessary. In this regard, the smear method is decidedly inferior to either the pellet method or the filter mount. Therefore the smear method was not considered further and the filter-mount and pellet methods were adopted for this study. However, if time is not an important consideration in a quantitative X-ray diffraction study of sediments, the smear method is the most suitable sample-preparation technique.

INTERNAL AND EXTERNAL STANDARDS

Having established a standard preparation procedure, the next problem is determination of the mineralogical content of the samples. Many

techniques have been used for prediction, most of them derived from the work of Alexander and Klug (1948). Two methods receiving great attention, especially in clay mineralogy, are external and internal standard techniques.

Klug and Alexander derived the basic equation for the external standard technique in 1948 and 1954. The method involves use of absorption coefficients, as expressed in the basic equation

$$\frac{I_p}{I_{o,p}} = w_p \frac{\mu_p^*}{\bar{\mu}^*}$$

where

I_p = reflected intensity of mineral P in the multi-component system,

$I_{o,p}$ = reflected intensity of the pure mineral P,

μ_p^* = mean absorption coefficient of mineral P,

$\bar{\mu}^*$ = mean absorption coefficient of the mixture, and

w_p = weight proportion of P in the mixture.

By adding a known weight of a pure component (a "spike") to a sample containing this component and measuring the reflected intensities before and after this addition, the weight proportion of the component in the original sample can be approximately determined. Leroux, Lennox and Kay (1953) studied this relation for a series of mixtures containing quartz and their results demonstrated the feasibility of the method. Gordon and Harris (1956) concluded that the combination of external standard method and measurement of mass absorption coefficient occupies less time than the preparation of an internal standard mixture and its examination, and that the two methods are comparable in accuracy.

Internal standards were first employed by Clark and Reynolds (1936). In this method, which is essentially a dilutation technique, a known weight of a substance S is added to a set amount of the mixture and convenient reflections from S and from the components P, Q, R, ... S of the mixture

are compared. The internal standard is added in a known weight proportion. Let w_s be the weight of the standard added to 1 gm of the mixture. The weight proportion of S in the resulting mixture will be $w_s/(1 + w_s)$ and similarly for P will be $w_p/(1 + w_p)$. Klug and Alexander (1954) derived the following equations

$$I_p = K_p \frac{W_p}{1 + W_s} \cdot \frac{1}{\mu^*}$$

and

$$I_s = K_s \frac{W_s}{1 + W_s} \cdot \frac{1}{\mu^*}$$

so that

$$\frac{I_p}{I_s} = \frac{K_p}{K_s} \cdot \frac{W_p}{W_s}$$

where

I_p is the reflection intensity of the determined mineral,

I_s is the reflection intensity of the internal standard,

K_p and K are coefficients of proportionality,

W_p is the weight % of the determined mineral, and

W_s is the weight % of the internal standard.

Molybdenite (Quakernaat, 1970), boehemite (Griffin, 1954; Gibbs, 1967), calcium fluoride (Gorbunova, 1969), aluminium oxide (Calvert, 1966), aluminium powder, lithium fluoride (Brindley, 1961), and corundum (Mitchell, 1960) have been used with varying degrees of success as internal standards. The main difficulty with this technique is that mixtures containing two, three, or four mineral components and several minor components will give so many reflections that it may be nearly impossible to choose an internal standard whose reflections do not interact with existing reflections.

The procedure used in this investigation is a combination technique that retains desirable features of both external and internal standard methods. A preliminary series of samples are run until a group is assembled that represents the range of variability of minerals encountered

in the sample suite. Each of these samples is analysed by internal standard methods. Results are plotted as total counts against mineral content and a regression on total counts computed. This establishes a calibration curve that can be used as an external standard to analyse the remainder of the samples.

To prepare internally standardized samples, five replicates were made of $< 60\mu$ ground material, and analysed by the methods selected in the investigation of preparation techniques. Approximately 1 gm of sample and 0.02 gm of spike were weighed in an analytical balance and thoroughly mixed by agitation with an ultrasonic probe. Five replicate mounts of the spiked sample were then prepared and analysed. Mean values of original intensity (I_o) and intensity of the spiked sample (I_n) were compared and the original mineral content computed by the relationship

$$P = \left(\frac{I_o}{I_n}\right) \cdot \left(\frac{S}{O + S - \left(\frac{I_o}{I_n} \cdot O\right)}\right)$$

where O is the original weight of the sample,

S is the weight of the spike, and

P is % of mineral in the sample.

This equation was used to calculate the percentages of quartz, calcite, and dolomite in a number of samples. Approximately 0.02 gm of pure quartz spike were added to a known weight of sample and the increase in X-ray intensity was observed. This was repeated using calcite and dolomite spikes for all replicates of the seven shale samples. The results were then used to establish calibration curves of the three minerals, shown in Figures 2.3, 2.4 and 2.5, by regression peak area against percentage composition. These curves were used to estimate the composition of several hundred shale samples from the Upper Pennsylvanian and Lower Permian of Kansas.

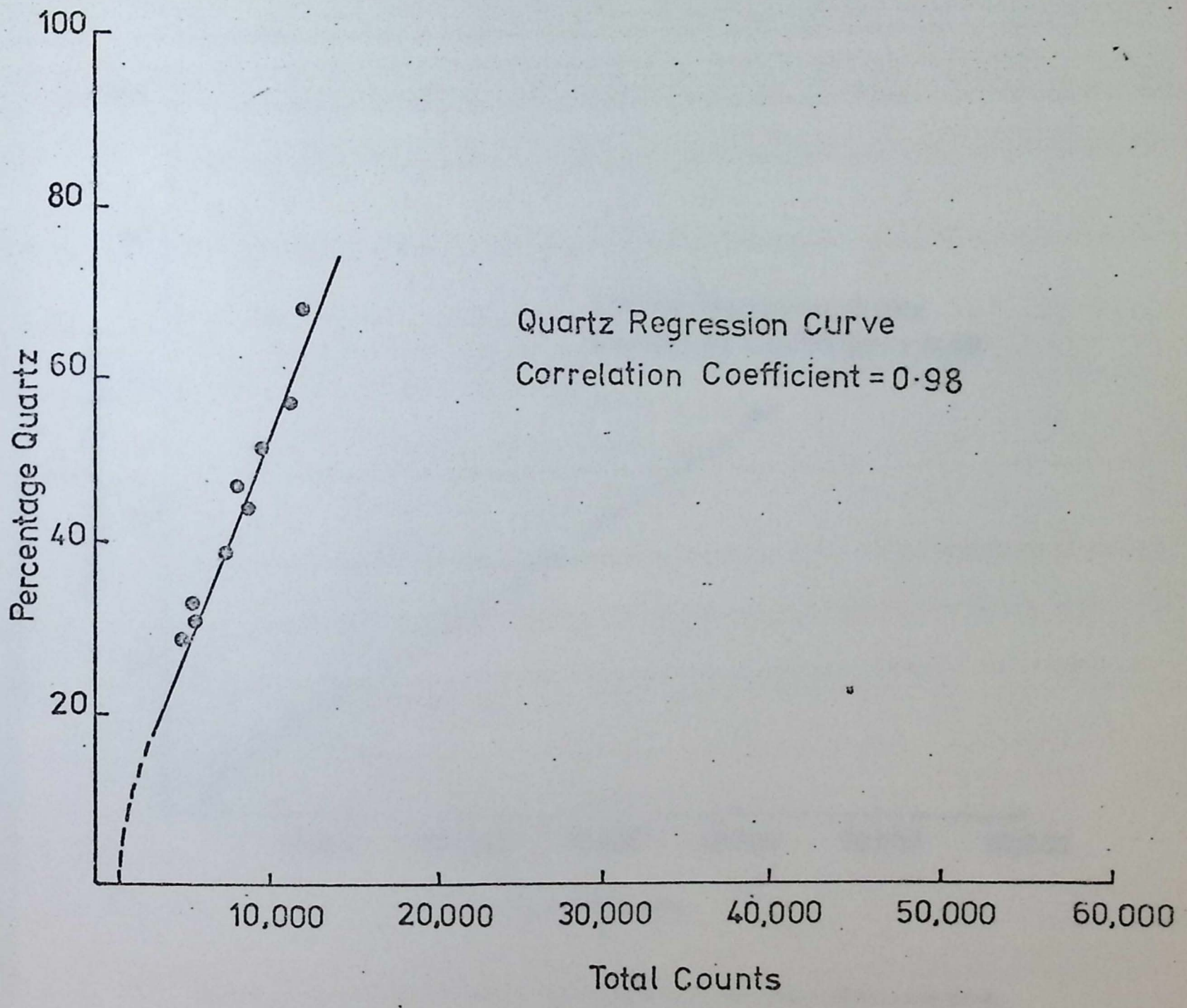

Fig. 2.3 Regression curve for quartz % on integrated areas of diffraction peak.

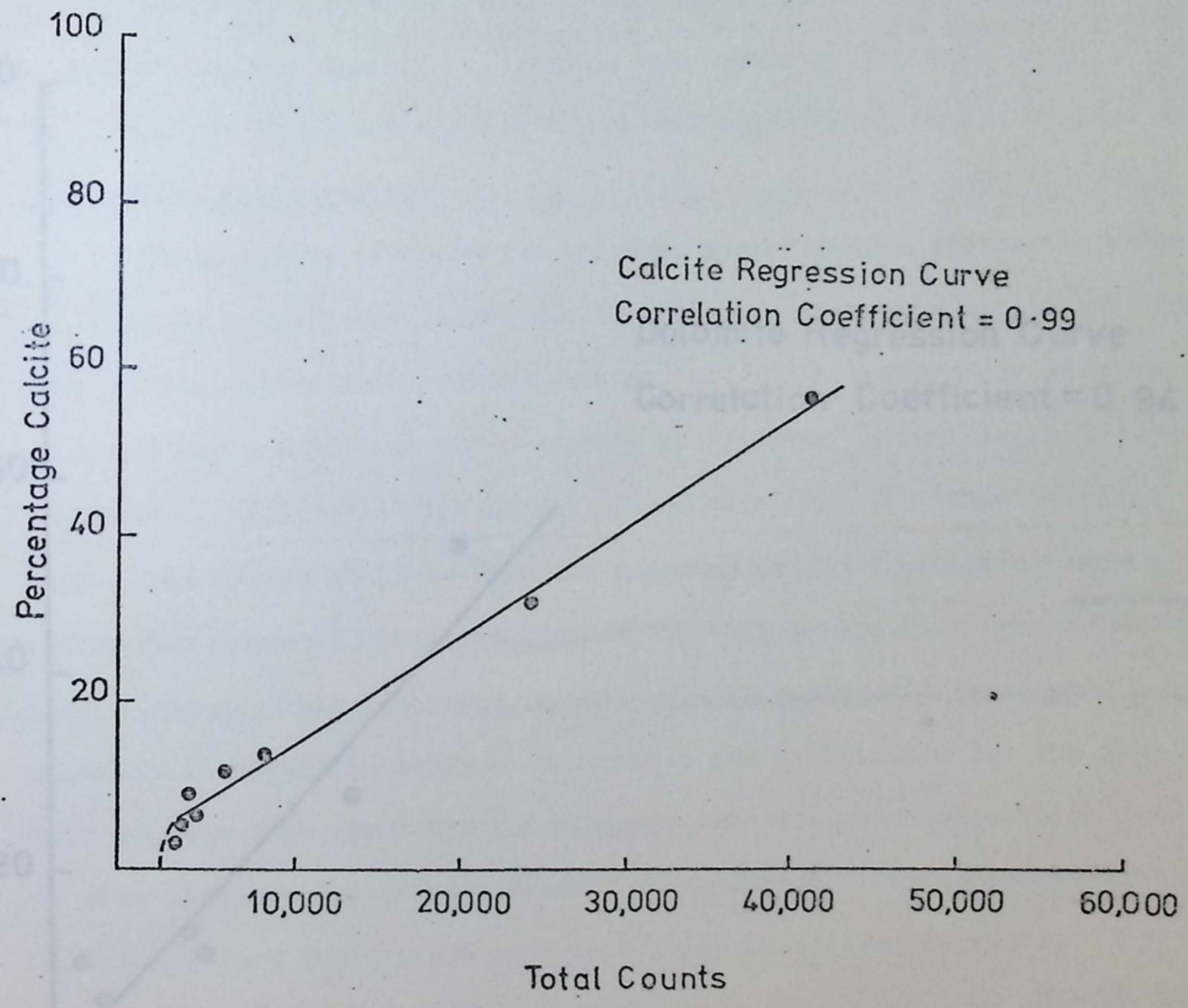

Fig. 2.4 Regression curve for calcite % on integrated area of diffraction peak.

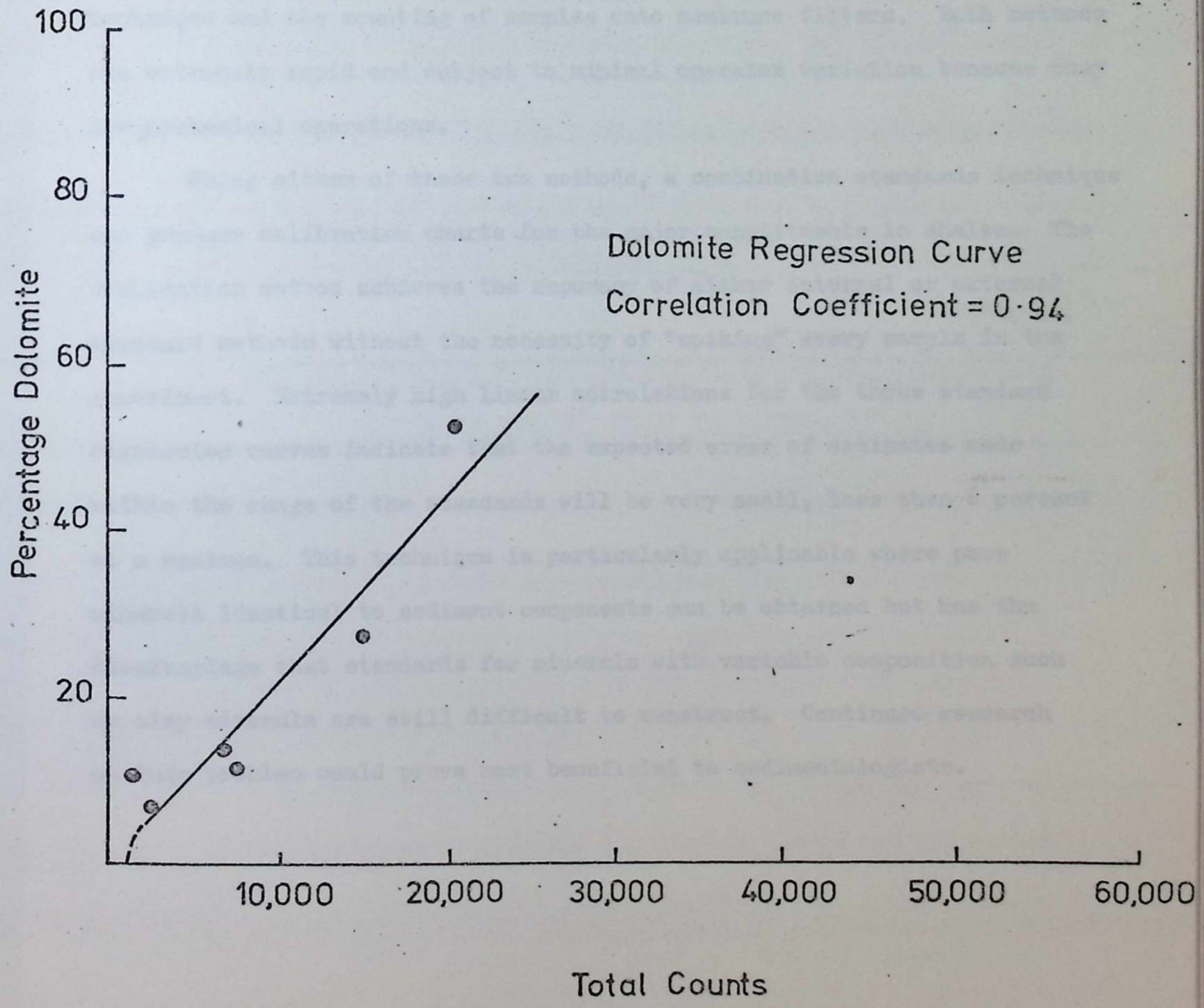

Fig. 2.5 Regression curve for dolomite % on integrated area of diffraction peak.

CONCLUSIONS

Detailed statistical tests of competing sample preparation methods show that the commonly used smear technique is superior for distinguishing between shales on the basis of quantitative assessment of mineral content. However, practical considerations make this method inapplicable for large experiments. The next most effective methods are the pressed-pellet technique and the mounting of samples onto membrane filters. Both methods are extremely rapid and subject to minimal operator variation because they are mechanical operations.

Using either of these two methods, a combination standards technique can produce calibration charts for the major constituents in shales. The combination method achieves the accuracy of either internal or external standard methods without the necessity of "spiking" every sample in the experiment. Extremely high linear correlations for the three standard regression curves indicate that the expected error of estimates made within the range of the standards will be very small, less than 6 percent at a maximum. This technique is particularly applicable where pure minerals identical to sediment components can be obtained but has the disadvantage that standards for minerals with variable composition such as clay minerals are still difficult to construct. Continued research on this problem could prove most beneficial to sedimentologists.

CHAPTER THREE

FACTORS AFFECTING THE MINERALOGY OF THE UPPER PENNSYLVANIAN AND LOWER PERMIAN SHALES OF KANSAS, U.S.A.

INTRODUCTION

The objectives of this chapter are twofold -- to determine the mineralogical nature of the Upper Pennsylvanian and Lower Permian shales of Kansas and to observe and account for the stratigraphic distribution of the major mineral components. Using the X-ray diffraction techniques developed in Chapter 2 and Appendix 4, it is possible both to identify the minerals and quantify the major components present in the shales. The resulting stratigraphic distribution of minerals throughout the Upper Pennsylvanian and Lower Permian shales can be plotted, analysed and interpreted in terms of changing tectonic and sedimentary environments. Similarly any periodic elements detected in the mineral distributions can be examined and tested by statistical analysis.

ANALYTICAL EQUIPMENT AND TECHNIQUE

The equipment employed in the X-ray diffraction analysis, consists of a Norelco X-ray Diffractometer, wide-range goniometer, AMR3 - 202 LiF curved crystal monochromator, proportional counter and pulse-height analyser.

All shale samples were ground to less than sixty microns and prepared for X-ray diffraction analysis using the sample mounting procedure described in Appendix 4. Individuals were then placed in the sample cavity of the Norelco Diffractometer and examined at $2^{\circ}2\theta$/min. over a period of 30 mins. under standard conditions (Table 3.1). All major peaks were recorded within the range $2^{\circ}2\theta$ to $60^{\circ}2\theta$ and minerals present were identified.

X-RAY IDENTIFICATION AND CHARACTERISTICS OF MINERALS

The identification of minerals in the X-ray diffraction traces was primarily achieved by examining standard d-spacings in the A.S.T.M. Powder

TABLE 3.1 NORELCO DIFFRACTOMETER: X-RAY CONDITIONS AND SETTINGS

Generator and general information:

Kilovolts - 35

Milliamperes - 18

Water pressure - 50 lbs/sq. in.

Slits - $1^{\circ}/1^{\circ}$(antiscatter) / 4°(receiver)

CuK α radiation

Ni. head.

Recorder:

Proportional counter input

Linear amplifier with attentuation setting of 1

Detector 1 voltage - 40 kv

Detector 2 voltage - 40 kv

Baseline - 82 pha - manual

Window - 22 pha - internal

Scale counts - 10^2, multiplier - 2

Time constant - 2

Chart recorder rate - 60 ins/hr.

Data File. However, several clay minerals are not easily identified using this method and tests on the shale samples were required to establish the species present. The standard identification procedure for clay minerals (Carroll, 1970; Griffin, 1971) was therefore adopted:

1. Position of main peaks. This is of primary importance in the identification of minerals as each has a unique and characteristic set of peak positions. However, for a number of clay minerals, the most intense peaks overlap and it may be necessary to examine —

2. Effects of glycolation on peak positions. Normally montmorillonite, illite and the interstratified clay minerals are indistinguishable as major peak positions overlap, and minor peaks are inevitably lost in background noise. However, they may be differentiated by their swelling reactions in an atmosphere of ethylene glycol; illite does not respond to the organic reagent but swelling clays such as montmorillonite absorb the molecules, producing an expansion of the crystal lattice and a characteristic shift in major peak positions on the diffraction trace. One pair of non-swelling clay minerals, kaolinite and chlorite are indistinguishable by either of these methods thereby necessitating the introduction of one further test —

3. Effects of heating on peak positions. Heating clay minerals results in an initial loss of water from the crystal lattice, especially in the case of illite, and at higher temperatures, volatilization of organic molecules from the interlayer sites. Other notable features include the breakdown of kaolinite to an amorphous state at 500-600°C and chlorite at 800°C. Each of these events is marked by a drop in height of the X-ray peaks on the diffraction trace. Table 3.2 illustrates the important role these effects play in the identification of clay minerals in shale samples and Fig. 3.1 shows the changes that may occur in peak positions during heating and glycolation of chlorite (at 6°2θ), kaolinite (at 12°2θ) and illite (at 9°2θ).

The major mineral constituents of the shales were, therefore,

TABLE 3.2 EFFECTS OF TEST TREATMENTS ON PEAK POSITION OF MAJOR MINERALS IN THE SHALE SAMPLES

Mineral	Basal Spacings (001 Unless Stated Otherwise)	2θ Transformation on Main Peak	Effect of Glycolation on Peak Position	Effect of Heating on Peak Position
Quartz	3.34Å (101); 4.26Å (100)	26.66 20.85	none	none
Feldspar	3.30Å	27.70	none	none
Calcite	3.03Å (104)	29.47	none	none
Dolomite	2.88Å (104)	30.05	none	none
Chlorite	14.1Å + integral series of basal spacings	6.27	none	(001) increases in intensity; at 800°C shows wt. loss (Mg form)/ collapse (Fe form)
Kaolinite	7.15Å; 3.75Å (002)	12.56	none	Becomes amorphous at 550-600°C
Illite	10Å (002) broad	8.70	none	(001) more intense as H_2O removed from structure

N.B. Disordered kaolinite shows broadening of X-ray peaks.

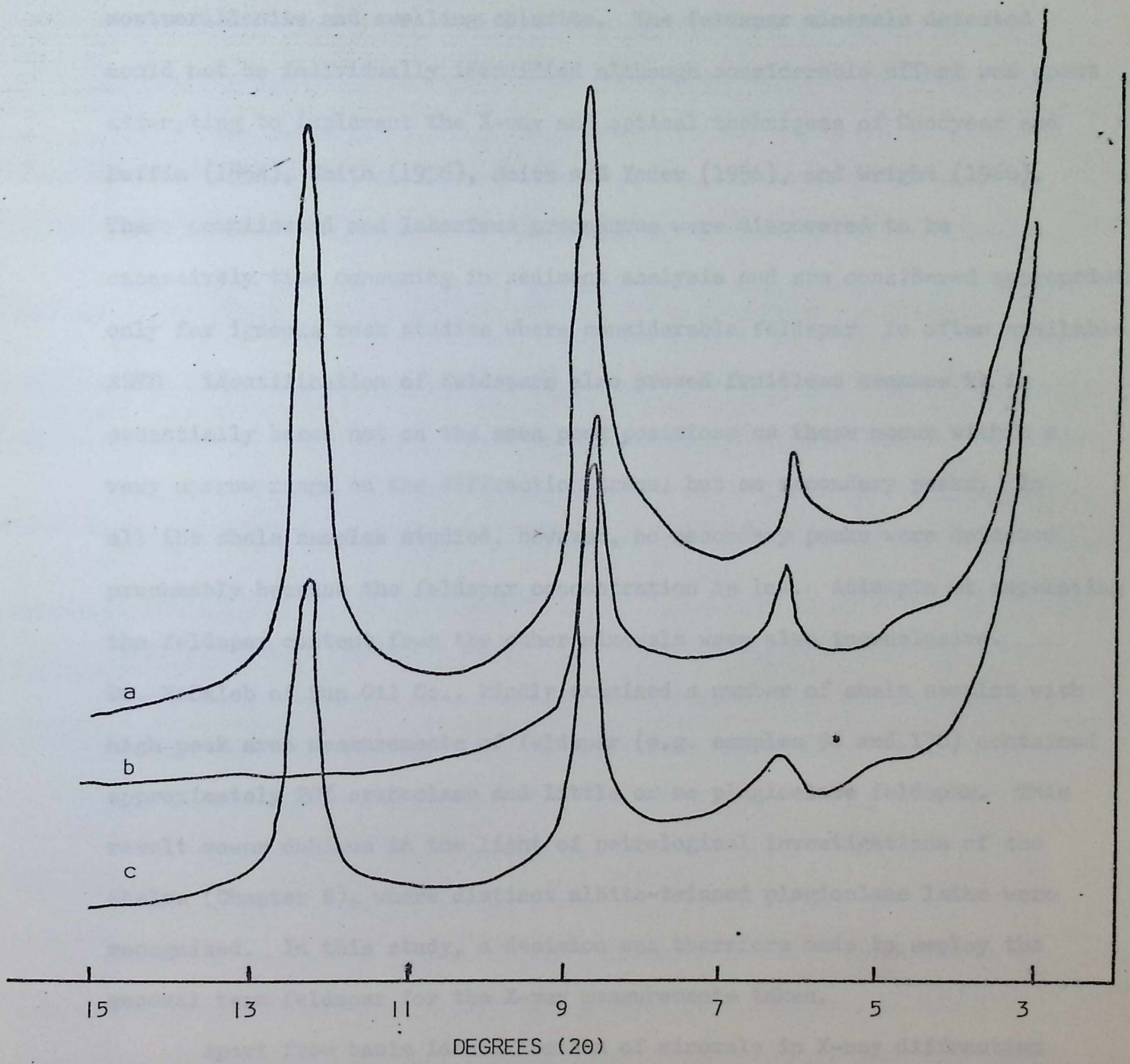

Fig. 3.1. X-ray diffraction traces of shale sample no.5. (a) normal temperature and humidity, (b) heated to 500°C for one hour, (c) glycolated.

identified as quartz, calcite, dolomite, feldspar, illite, chlorite and kaolinite, although the following secondary minerals were also recorded: gypsum, jarosite, pyrite, mixed layered illite--montmorillonite, montmorillonite and swelling chlorite. The feldspar minerals detected could not be individually identified although considerable effort was spent attempting to implement the X-ray and optical techniques of Goodyear and Duffin (1954), Smith (1956), Smith and Yoder (1956), and Wright (1968). These complicated and laborious procedures were discovered to be excessively time consuming in sediment analysis and are considered appropriate only for igneous rock studies where considerable feldspar is often available. ASTM identification of feldspars also proved fruitless because it is essentially based not on the mean peak positions as these occur within a very narrow range on the diffraction trace, but on secondary peaks. In all the shale samples studied, however, no secondary peaks were detected presumably because the feldspar concentration is low. Attempts at separating the feldspar content from the other minerals were also inconclusive. Dr. McCaleb of Sun Oil Co., kindly examined a number of shale samples with high peak area measurements of feldspar (e.g. samples 96 and 170) contained approximately 20% orthoclase and little or no plagioclase feldspar. This result seems dubious in the light of petrological investigations of the shales (Chapter 8), where distinct albite-twinned plagioclase laths were recognised. In this study, a decision was therefore made to employ the general term feldspar for the X-ray measurements taken.

Apart from basic identification of minerals in X-ray diffraction traces, it was possible to interpret shapes of X-ray peaks and examine order-disorder phenomena, mixed-layering and detrital versus secondary origins for some of the minerals.

Eslinger et al. (1973) studied X-ray diffraction patterns of fine-grained quartz and on the basis of relative intensities of the X-ray diffraction peaks from the (100) and (101) crystallographic planes, were

able to distinguish detrital and secondary forms of quartz. Fig. 3.2 illustrates the differences in the X-ray patterns of detrital quartz (a) and secondary quartz (b) and for comparison, a typical Kansas shale pattern is presented (Fig. 3.3). All samples from the Upper Pennsylvanian and Lower Permian, in fact, revealed the presence of detrital quartz.

Kaolinite X-ray diffraction traces show two intense peaks, one at approximately $12^{\circ}2\theta$ and another at $25^{\circ}2\theta$. The second of these peaks is indicative of the degree of disorder present in the crystal structure (Hinckley, 1963; Noble, 1971), and also of the environment of sedimentary deposition. A well crystallized kaolinite ('hard' kaolinite) is associated with the marine environment, whereas poorly crystallized ('soft') kaolinite is formed in fresh water. Both are often recrystallized, leached and form detrital kaolinite but the two types still record differing X-ray patterns. Multiple peaks in the region of $28^{\circ}2\theta$ are characteristic of well crystallized kaolinite whereas one simple peak at $24^{\circ}2\theta$ is common in poorly crystallized samples. Kansas kaolinite patterns show similarity to well-crystallized kaolinite indicating a marine environment of deposition for Kansas shales but the degree of crystallinity is lower than expected and is probably the result of diagenetic activity.

Mixed-layered clay minerals are commonly found in argillaceous sediments and may be identified using the glycolation and heating effects described previously. However, their presence is often indicated by the form of the illite peak at $8.7^{\circ}2\theta$. A sharp peak indicates no mixed-layering whereas asymmetry towards lower 2θ values shows that some mixed-layer minerals are present. Most Kansas shales exhibited slight asymmetry in the illite peak indicating the presence of mixed-layered minerals.

X-RAY MEASUREMENTS MADE ON SHALE SAMPLES

The following X-ray measurements were taken on samples prepared

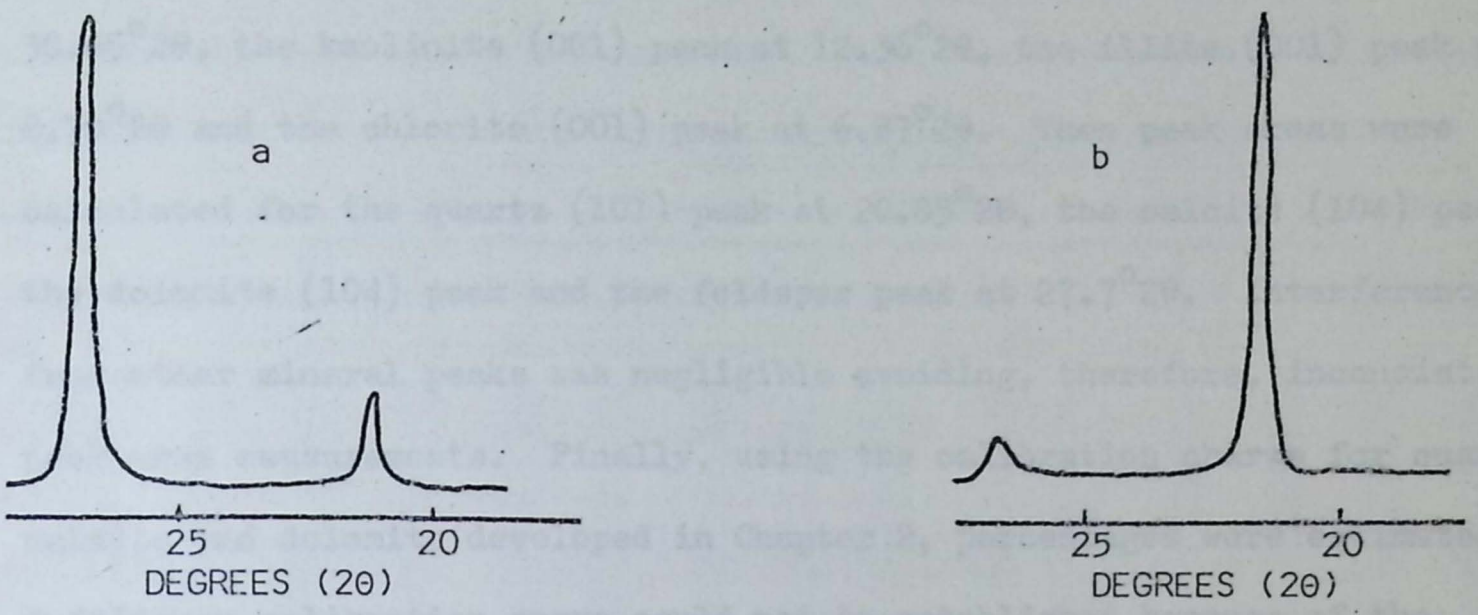

Fig.3.2 X-ray diffracrograms of fine-grained quartzes showing the relative intensities of the diffraction peaks from the (100) and (101) crystallographic planes. (a) crushed quartz, (b) Brassfield Limestone, insoluable residue, (After Eslinger et al (1973)).

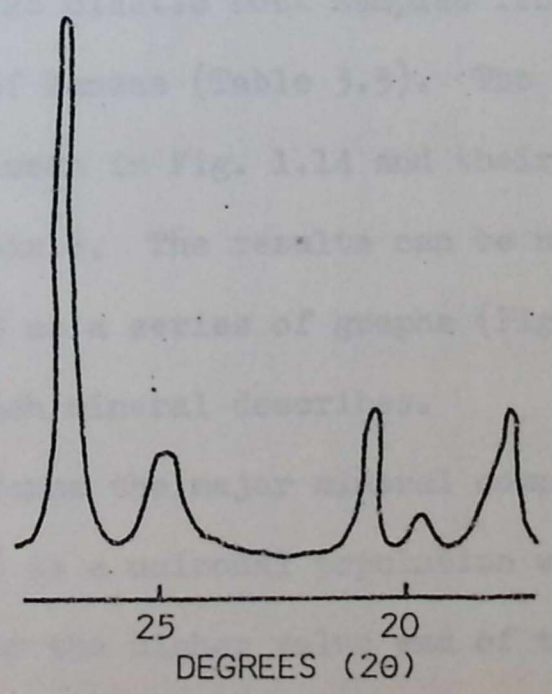

Fig. 3.3 X-ray diffractogram of shale sample no.3. within range 17.5-27.5°2θ. The quartz peak distribution matches that in Fig. 3.2a above and indicates a detrital origin for the quartz in Kansas shales.

were taken of the quartz (100) peak at 26.66°2θ, the calcite (104) peak at 29.47°2θ, the feldspar peak at 27.7°2θ, the dolomite (104) peak at 30.05°2θ, the kaolinite (001) peak at 12.36°2θ, the illite (001) peak at 8.70°2θ and the chlorite (001) peak at 6.87°2θ. Then peak areas were calculated for the quartz (101) peak at 20.85°2θ, the calcite (104) peak, the dolomite (104) peak and the feldspar peak at 27.7°2θ. Interference from other mineral peaks was negligible avoiding, therefore, inconsistent peak area measurements. Finally, using the calibration charts for quartz, calcite and dolomite developed in Chapter 2, percentages were estimated. A feldspar calibration curve could not be established because of the identification problem mentioned previously and no curves could be set up for clay minerals as variable crystallinity prevented exact matching of sample clay minerals and "spikes". The results of the X-ray diffraction analyses are presented in Table 3.3.

STRATIGRAPHIC DISTRIBUTION OF MINERALS

X-ray measurements described previously were taken on the major components of 128 clastic rock samples from the Upper Pennsylvanian and Lower Permian of Kansas (Table 3.3). The stratigraphic positions of these samples can be seen in Fig. 1.14 and their geographic position will be found in Appendix 6. The results can be summarised as a statistical table (Table 3.4) and as a series of graphs (Fig. 3.4), showing the mathematical distribution each mineral describes.

Quartz forms the major mineral component of most shales and varies from 14% to 96% as a unimodal population with a slightly skewed distribution. The tail towards the higher value end of the histogram is produced by a number of sandstones and siltstones with high quartz values.

Stratigraphically, the distribution of quartz in Upper Pennsylvanian

Table. 3-3 Results of X-Ray diffraction analyses of Pennsylvanian and Lower Permian shales of Kansas, U.S.A.

X-RAY DIFFRACTION MEASUREMENTS

Sample Number	Quartz PEAK AREA	Quartz PEAK HEIGHT	Quartz PERCENT	Calcite PEAK AREA	Calcite PEAK HEIGHT	Calcite PERCENT	Fieldspar PEAK AREA	Fieldspar PEAK HEIGHT	Dolomite PEAK AREA	Dolomite PEAK HEIGHT	Dolomite PERCENT	KAOLINITE PEAK HEIGHT	ILLITE PEAK HEIGHT	CHLORITE PEAK HEIGHT
16	10833.00	100.00	57.00	2387.00	7.00	3.00	6119.00	23.00	2547.00	7.00	5.00	21.00	32.00	22.00
19	7393.00	100.00	41.00	2941.00	7.00	4.00	4310.00	15.00	2311.00	5.00	6.00	28.00	33.00	21.00
20	8684.00	100.00	47.00	5475.00	21.00	8.00	4962.00	21.00	5135.00	18.00	11.00	15.00	22.00	18.00
21	4227.00	53.00	24.00	16629.00	64.00	23.00	2792.00	9.00	7786.00	36.00	17.00	10.00	14.00	15.00
23	4019.00	44.00	22.00	15358.00	48.00	21.00	2979.00	8.00	7551.00	28.00	16.00	7.00	13.00	14.00
24	7208.00	76.00	40.00	4043.00	7.00	6.00	4306.00	12.00	3405.00	11.00	7.00	10.00	18.00	15.00
25	6806.00	96.00	38.00	3387.00	7.00	5.00	4534.00	17.00	3248.00	7.00	7.00	17.00	33.00	16.00
26	8200.00	130.00	46.00	4036.00	12.00	6.00	5377.00	19.00	2758.00	5.00	6.00	12.00	31.00	21.00
27	4273.00	53.00	24.00	23557.00	85.00	28.00	2355.00	9.00	1532.00	4.00	2.00	7.00	11.00	15.00
28	7445.00	87.00	42.00	3743.00	9.00	6.00	5866.00	10.00	3391.00	8.00	7.00	6.00	30.00	24.00
7	9564.00	100.00	50.00	3965.00	8.00	6.00	4127.00	10.00	4113.00	7.00	9.00	7.00	17.00	16.00
31	6152.00	91.00	35.00	3371.00	8.00	5.00	4652.00	16.00	3402.00	7.00	7.00	20.00	32.00	18.00
32	6754.00	90.00	37.00	3692.00	8.00	6.00	6291.00	18.00	4371.00	8.00	8.00	14.00	27.00	17.00
34	6456.00	86.00	36.00	7012.00	10.00	13.00	4938.00	15.00	5283.00	7.00	11.00	16.00	28.00	17.00
36	5688.00	66.00	32.00	15487.00	65.00	21.00	4015.00	12.00	2194.00	4.00	4.00	14.00	17.00	13.00
35	2709.00	31.00	17.00	21779.00	89.00	29.00	1983.00	8.00	15958.00	85.00	35.00	4.00	9.00	11.00
38	6003.00	97.00	34.00	3956.00	10.00	6.00	4872.00	14.00	2889.00	7.00	6.00	17.00	32.00	20.00
40	6543.00	97.00	37.00	3156.00	7.00	4.00	4583.00	15.00	2984.00	5.00	6.00	25.00	44.00	27.00
41	4176.00	68.00	23.00	13700.00	71.00	19.00	3494.00	18.00	4197.00	10.00	9.00	18.00	24.00	17.00
43	5875.00	74.00	33.00	3498.00	6.00	5.00	4951.00	14.00	3544.00	6.00	7.00	12.00	26.00	18.00
46	6240.00	86.00	35.00	4619.00	11.00	7.00	5399.00	14.00	3564.00	10.00	8.00	19.00	30.00	19.00
47	6659.00	99.00	37.00	4771.00	13.00	7.00	4662.00	15.00	3572.00	6.00	8.00	19.00	33.00	20.00
48	7402.00	100.00	42.00	4319.00	12.00	7.00	4650.00	15.00	4707.00	12.00	10.00	17.00	42.00	19.00
54	7465.00	130.00	42.00	12815.00	65.00	18.00	3862.00	34.00	2314.00	5.00	5.00	11.00	23.00	11.00
50	4998.00	69.00	28.00	7128.00	25.00	11.00	4687.00	16.00	2892.00	4.00	6.00	6.00	16.00	19.00
53	4087.00	46.00	21.00	2408.00	7.00	3.00	6119.00	7.00	2337.00	4.00	4.00	8.00	15.00	16.00
69	6721.00	100.00	38.00	3097.00	8.00	4.00	3457.00	16.00	3402.00	7.00	7.00	36.00	37.00	20.00
70	8113.00	130.00	44.00	3856.00	7.00	6.00	6071.00	17.00	3383.00	5.00	6.00	36.00	32.00	20.00
71	8926.00	130.00	48.00	3547.00	12.00	6.00	6044.00	29.00	2544.00	7.00	5.00	23.00	36.00	25.00
160	5971.00	82.00	33.00	6066.00	28.00	9.00	4956.00	13.00	3098.00	7.00	6.00	17.00	24.00	22.00
67	6915.00	100.00	38.00	2528.00	6.00	4.00	4807.00	19.00	7465.00	8.00	5.00	49.00	63.00	28.00
61A	6259.00	96.00	35.00	7250.00	21.00	11.00	3201.00	15.00	2533.00	5.00	5.00	28.00	45.00	20.00
63	7075.00	100.00	39.00	2646.00	8.00	4.00	5382.00	12.00	2698.00	5.00	5.00	45.00	50.00	24.00
12	8009.00	126.00	44.00	3449.00	9.00	5.00	6142.00	31.00	3564.00	9.00	7.00	25.00	22.00	19.00
66	3043.00	27.00	18.00	3611.00	13.00	5.00	3411.00	4.00	21340.00	100.00	48.00	4.00	7.00	10.00
15	5257.00	66.00	29.00	13254.00	54.00	18.00	3201.00	10.00	2258.00	5.00	4.00	13.00	20.00	27.00
3	5598.00	83.00	31.00	2967.00	7.00	4.00	4098.00	10.00	2796.00	6.00	6.00	30.00	36.00	17.00
157	7387.00	88.00	41.00	2878.00	6.00	4.00	5273.00	15.00	2533.00	5.00	5.00	25.00	34.00	21.00
161	7398.00	92.00	41.00	4687.00	12.00	7.00	4773.00	16.00	2387.00	7.00	6.00	8.00	24.00	16.00
296	7748.00	99.00	43.00	4754.00	15.00	7.00	4754.00	15.00	2764.00	7.00	6.00	24.00	23.00	18.00
294	14173.00	100.00	79.00	2362.00	3.00	3.00	4047.00	21.00	2565.00	3.00	5.00	9.00	11.00	11.00
290	16877.00	130.00	85.00	2554.00	6.00	4.00	4648.00	17.00	2309.00	4.00	5.00	16.00	21.00	13.00
284	6662.00	100.00	37.00	3894.00	7.00	6.00	4884.00	11.00	2553.00	6.00	5.00	25.00	27.00	18.00
287	7243.00	100.00	40.00	5447.00	16.00	8.00	7716.00	13.00	2378.00	5.00	5.00	20.00	28.00	15.00
281	10365.00	100.00	54.00	4128.00	14.00	7.00	5638.00	15.00	7719.00	22.00	17.00	17.00	21.00	13.00
125	13387.00	100.00	72.00	2521.00	5.00	4.00	5297.00	18.00	2312.00	4.00	5.00	25.00	33.00	20.00
116	6296.00	83.00	35.00	8079.00	20.00	12.00	4709.00	12.00	3378.00	8.00	7.00	22.00	28.00	21.00
110	6531.00	89.00	37.00	7709.00	23.00	11.00	2569.00	13.00	2906.00	4.00	6.00	9.00	12.00	17.00
112	11034.00	100.00	58.00	2449.00	6.00	4.00	4132.00	15.00	2300.00	5.00	5.00	27.00	29.00	19.00
128	6916.00	87.00	39.00	4201.00	8.00	7.00	4201.00	11.00	4522.00	10.00	9.00	15.00	27.00	20.00
130	4689.00	53.00	25.00	7536.00	23.00	11.00	2275.00	6.00	21333.00	100.00	46.00	7.00	15.00	12.00
79	4584.00	62.00	25.00	11418.00	47.00	16.00	4847.00	9.00	4767.00	13.00	10.00	15.00	24.00	18.00
151	6428.00	98.00	37.00	3359.00	7.00	5.00	4684.00	19.00	3713.00	7.00	8.00	38.00	48.00	23.00
82	6738.00	98.00	39.00	3691.00	7.00	6.00	4396.00	11.00	2558.00	6.00	5.00	20.00	23.00	22.00
80	6497.00	85.00	36.00	3675.00	7.00	6.00	4204.00	13.00	3744.00	6.00	8.00	24.00	36.00	27.00
81	5811.00	77.00	33.00	3252.00	7.00	9.00	4124.00	11.00	2976.00	8.00	6.00	22.00	31.00	28.00
85	11761.00	100.00	63.00	2265.00	6.00	3.00	9967.00	35.00	3224.00	4.00	7.00	13.00	29.00	12.00
135	3041.00	30.00	18.00	11092.00	42.00	16.00	2598.00	4.00	15374.00	57.00	33.00	7.00	12.00	13.00
121	18913.00	130.00	96.00	1982.00	6.00	3.00	1884.00	9.00	2225.00	4.00	4.00	9.00	10.00	16.00
138	5141.00	57.00	28.00	8705.00	26.00	12.00	4314.00	10.00	3965.00	8.00	8.00	8.00	24.00	17.00
136	6398.00	100.00	36.00	6201.00	20.00	9.00	4535.00	16.00	6232.00	24.00	13.00	14.00	29.00	20.00
137	4293.00	50.00	24.00	22244.00	74.00	30.00	4962.00	8.00	2253.00	7.00	4.00	9.00	16.00	14.00
149	8659.00	100.00	48.00	6228.00	17.00	9.00	5475.00	17.00	2939.00	6.00	6.00	13.00	21.00	14.00
150	8987.00	130.00	48.00	3375.00	7.00	5.00	4272.00	17.00	3236.00	7.00	7.00	9.00	20.00	25.00
152	7697.00	100.00	42.00	3417.00	7.00	5.00	4664.00	17.00	2546.00	6.00	6.00	12.00	28.00	20.00
153	7165.00	100.00	40.00	2686.00	7.00	4.00	5417.00	19.00	2525.00	7.00	5.00	34.00	62.00	26.00
155	9676.00	100.00	51.00	3356.00	5.00	5.00	5765.00	19.00	2539.00	5.00	5.00	17.00	33.00	20.00
105	7453.00	92.00	41.00	12790.00	61.00	18.00	1383.00	11.00	2268.00	4.00	4.00	15.00	14.00	13.00
107	7152.00	81.00	40.00	2988.00	7.00	4.00	4354.00	13.00	2761.00	12.00	6.00	20.00	25.00	15.00
109	2872.00	28.00	16.00	25017.00	94.00	34.00	1383.00	8.00	1564.00	4.00	2.00	7.00	12.00	11.00
94	4640.00	17.00	25.00	14627.00	100.00	20.00	2586.00	4.00	3332.00	21.00	7.00	6.00	10.00	9.00
96	9900.00	130.00	52.00	2218.00	6.00	3.00	8381.00	39.00	2431.00	7.00	5.00	19.00	40.00	20.00
97	6347.00	77.00	34.00	4265.00	8.00	7.00	4576.00	11.00	3337.00	7.00	6.00	25.00	33.00	28.00
144	8097.00	96.00	45.00	2903.00	5.00	4.00	5758.00	18.00	6617.00	20.00	14.00	33.00	39.00	22.00
101	7558.00	100.00	42.00	3851.00	13.00	6.00	4687.00	18.00	2734.00	7.00	5.00	33.00	43.00	33.00
122	4013.00	47.00	22.00	22978.00	89.00	28.00	5010.00	8.00	2023.00	4.00	4.00	10.00	18.00	14.00
978	9859.00	100.00	51.00	5601.00	18.00	8.00	6164.00	23.00	2738.00	5.00	5.00	11.00	19.00	18.00
148	6906.00	76.00	38.00	3546.00	6.00	5.00	4534.00	15.00	3637.00	7.00	7.00	18.00	24.00	20.00
162	8976.00	100.00	44.00	2439.00	7.00	4.00	5974.00	27.00	2369.00	6.00	5.00	14.00	30.00	21.00
163	6131.00	39.00	35.00	3194.00	15.00	4.00	3022.00	6.00	2250.00	5.00	4.00	29.00	15.00	10.00
171	6364.00	100.00	34.00	2613.00	7.00	4.00	5244.00	16.00	2754.00	6.00	6.00	26.00	38.00	20.00
173	6566.00	99.00	37.00	3471.00	6.00	5.00	4875.00	14.00	2589.00	7.00	5.00	25.00	38.00	22.00
168	9848.00	130.00	52.00	2142.00	5.00	3.00	5976.00	38.00	2225.00	4.00	4.00	19.00	29.00	15.00
192	5964.00	77.00	34.00	6966.00	27.00	10.00	3543.00	18.00	17802.00	82.00	39.00	11.00	17.00	15.00
194	6576.00	95.00	37.00	5106.00	6.00	9.00	5073.00	22.00	3146.00	4.00	6.00	13.00	15.00	15.00
176	4883.00	69.00	26.00	3093.00	7.00	4.00	4171.00	11.00	3315.00	6.00	7.00	31.00	31.00	23.00
180	7337.00	100.00	41.00	2865.00	7.00	4.00	4289.00	18.00	2531.00	7.00	5.00	28.00	41.00	20.00
181	8449.00	130.00	46.00	4470.00	14.00	7.00	5387.00	14.00	2320.00	6.00	6.00	15.00	18.00	22.00
184	9291.00	100.00	49.00	2378.00	8.00	3.00	7654.00	31.00	3303.00	6.00	6.00	28.00	32.00	18.00
185	8818.00	130.00	48.00	4376.00	21.00	7.00	6303.00	16.00	3350.00	7.00	7.00	14.00	16.00	14.00
186	6206.00	74.00	35.00	5102.00	14.00	8.00	6725.00	11.00	3308.00	5.00	7.00	9.00	13.00	22.00
187	3862.00	44.00	21.00	13433.00	44.00	19.00	2831.00	9.00	3925.00	10.00	8.00	7.00	19.00	14.00
197	5161.00	69.00	29.00	8779.00	29.00	12.00	3179.00	12.00	9916.00	38.00	22.00	11.00	19.00	15.00
200	6768.00	86.00	37.00	5293.00	12.00	8.00	5013.00	17.00	3134.00	5.00	6.00	13.00	22.00	20.00
205	7287.00	98.00	40.00	3470.00	8.00	5.00	5037.00	15.00	2923.00	7.00	6.00	24.00	35.00	22.00
206	3550.00	39.00	20.00	23486.00	88.00	32.00	1692.00	4.00	2319.00	4.00	4.00	7.00	11.00	11.00
208	2676.00	40.00	17.00	23180.00	96.00	31.00	6044.00	6.00	1771.00	4.00	3.00	8.00	13.00	13.00
209	3100.00	34.00	19.00	23596.00	88.00	29.00	2231.00	6.00	3592.00	14.00	8.00	9.00	16.00	14.00
261	3032.00	41.00	18.00	18205.00	66.00	25.00	2032.00	6.00	2503.00	8.00	5.00	10.00	13.00	14.00
262	4686.00	46.00	25.00	13612.00	56.00	19.00	3002.00	9.00	2537.00	6.00	5.00	8.00	13.00	14.00
212	4594.00	61.00	25.00	18711.00	100.00	25.00	2569.00	8.00	1776.00	4.00	3.00	7.00	22.00	15.00
213	3079.00	34.00	18.00	22979.00	98.00	31.00	5382.00	6.00	1581.00	4.00	2.00	7.00	13.00	12.00
264	4779.00	46.00	26.00	13649.00	35.00	15.00	3438.00	10.00	6009.00	17.00	13.00	8.00	13.00	14.00
237	2888.00	30.00	17.00	33646.00	100.00	41.00	1572.00	5.00	1546.00	5.00	2.00	5.00	11.00	11.00
235	3929.00	41.00	22.00	12965.00	43.00	18.00	2406.00	7.00	2110.00	4.00	4.00	6.00	15.00	13.00
238	7137.00	77.00	40.00	5783.00	19.00	9.00	4511.00	13.00	2808.00	4.00	6.00	6.00	21.00	17.00
249	3528.00	43.00	20.00	7206.00	29.00	11.00	1888.00	6.00	20220.00	100.00	44.00	6.00	12.00	13.00
248	5169.00	49.00	29.00	6163.00	24.00	9.00	3089.00	8.00	14905.00	94.00	33.00	6.00	12.00	14.00
234	2874.00	20.00	17.00	15325.00	70.00	21.00	1987.00	6.00	2148.00	4.00	4.00	9.00	11.00	20.00
230	5727.00	65.00	33.00	6515.00	18.00	13.00	4620.00	10.00	3077.00	6.00	6.00	5.00	29.00	18.00
226	5685.00	69.00	31.00	8599.00	32.00	12.00	3233.00	9.00	2426.00	5.00	5.00	5.00	16.00	13.00
227	8007.00	97.00	44.00	3179.00	8.00	6.00	3975.00	11.00	3013.00	5.00	5.00	6.00	20.00	17.00
221	6599.00	67.00	37.00	11286.00	40.00	16.00	3842.00	8.00	3363.00	7.00	7.00	5.00	16.00	13.00
222	2107.00	19.00	14.00	27611.00	100.00	37.00	1368.00	3.00	1341.00	4.00	3.00	4.00	8.00	10.00
243	5292.00	61.00	29.00	5564.00	22.00	10.00	3910.00	9.00	2999.00	6.00	6.00	8.00	23.00	21.00
244	5249.00	87.00	29.00	4849.00	9.00	7.00	6824.00	11.00	3907.00	8.00	8.00	6.00	36.00	22.00
273	4549.00	51.00	25.00	3597.00	8.00	6.00	2616.00	10.00	14851.00	62.00	32.00	7.00	12.00	16.00
253	3100.00	38.00	18.00	19456.00	73.00	26.00	1763.00	7.00	2795.00	10.00	6.00	8.00	15.00	12.00
251	4106.00	41.00	24.00	11884.00	37.00	17.00	2633.00	6.00	7677.00	21.00	16.00	8.00	16.00	13.00
256	7697.00	92.00	42.00	7854.00	24.00	11.00	3449.00	13.00	6091.00	26.00	13.00	9.00	15.00	12.00
265	3545.00	39.00	20.00	19237.00	66.00	17.00	2227.00	7.00	3521.00	11.00	7.00	10.00	16.00	14.00
268	6293.00	78.00	35.00	2830.00	7.00	4.00	3381.00	13.00	3895.00	14.00	8.00	11.00	29.00	17.00
270	7606.00	96.00	42.00	3524.00	11.00	6.00	4006.00	12.00	5358.00	21.00	11.00	9.00	19.00	15.00
272	4152.00	49.00	23.00	16211.00	59.00	22.00	2948.00	7.00	2192.00	4.00	4.00	7.00	15.00	19.00
298	8917.00	130.00	48.00	3439.00	7.00	5.00	4528.00	16.00	7104.00	28.00	15.00	9.00	15.00	16.00
300	4844.00	68.00	27.00	2465.00	5.00	5.00	3039.00	9.00	23333.00	100.00	52.00	6.00	16.00	16.00

TABLE 3.4 Summary Statistics of X-ray Diffraction Measurements

PH = peak height; PA = peak area; % = percent

X-RAY MEASUREMENTS

MINERALS	QUARTZ			CALCITE			FELDSPAR		DOLOMITE			KAOLINITE	ILLITE	CHLORITE
STATISTICS	PH	PA	%	PH	PA	%	PH	PA	PH	PA	%	PH	PH	PH
Mean	76.8	6611.0	36.2	26.9	7648.0	10.9	13.6	4332.0	13.7	4351.0	9.1	15.5	28.8	17.6
Standard Deviation	25.1	2673.0	13.4	28.5	6546.0	8.6	6.8	1537.0	20.7	4148.0	9.4	10.0	10.9	4.7
Median	86.0	6476.5	36.5	12.5	5694.0	7.0	13.0	4251.0	7.0	3067.0	6.0	16.0	21.5	17.0
Minimum	17.0	2107.0	14.0	3.0	1982.0	3.0	3.0	1368.0	3.0	1341.0	0.0	4.0	7.0	9.0
Maximum	100.0	18913.0	96.0	100.0	30646.0	41.0	39.0	9967.0	100.0	23333.0	52.0	54.0	62.0	33.0

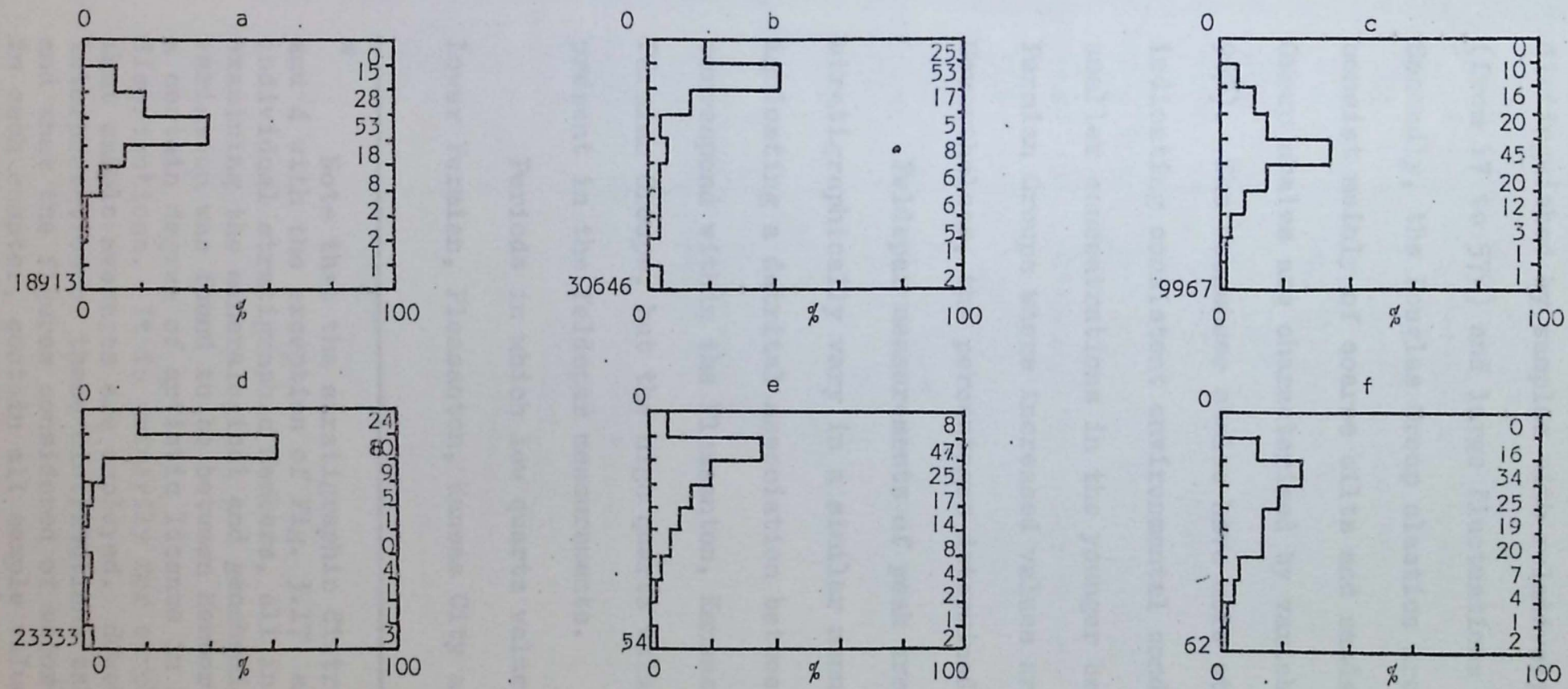

Fig. 3.4 Histograms showing the variation and distribution of the major mineral components measured by X-ray diffraction; peak areas for (a) quartz, (b) calcite, (c) feldspar, (d) dolomite; peak heights for (e)kaolinite, (f) illite, and (g) chlorite. Vertical scale is 0 to maximum value in 10 divisions. Numbers on the right of each histogram are the total number of samples contributing to each division.

and Lower Permian shales (Fig. 3.5)* can be interpreted in terms of five zones. Firstly the Pleasanton, Kansas City and Lansing Groups are distinguished by samples with relatively low concentrations of quartz (from 17 to 57%) and large fluctuations in concentration between samples. Secondly, the Douglas Group clastics are rich in quartz (up to 85%) as they consist mainly of coarse silts and sands, whereas the succeeding Shawnee Group shales are characterised by variable quartz concentrations (16 to 96%). The Wabaunsee shales have more stable quartz values (21 to 52%) indicating consistent environmental conditions, and a general tendency for smaller concentrations in the younger beds. This is reversed in the Lower Permian Groups where increased values are recorded in Chase Group samples. Nevertheless, the percentages determined are still low (14 to 48%).

Feldspar measurements of peak area (Fig. 3.5) and peak height stratigraphically vary in a similar manner to the quartz distribution indicating a detrital association between the minerals. The graphs correspond within the Pleasanton, Kansas City, Lansing, Shawnee and Lower Permian Groups, but the high quartz values in the Douglas samples are not present in the feldspar measurements.

Periods in which low quartz values are recorded such as the Shawnee, Lower Permian, Pleasanton, Kansas City and Lansing Groups are marked by

---

* Note that the stratigraphic distributions illustrated in Chapters 3 and 4 with the exception of Fig. 3.17 are calculated by averaging, for individual stratigraphic Members, all included sample values. By carefully examining the mineralogical and geochemical results, most of the data variation was found to be between Members rather than within Members, allowing a certain degree of artistic licence in illustrating the stratigraphic distributions. It is primarily for simplicity of illustration therefore that sample averages are employed. However, it should also be noted that interpretation of these distributions takes the generalisation into account and that the figures considered of major importance to the conclusions drawn in each chapter, contain all sample values (Figs. 3.17, 5.8, 6.19, 6.24 and all distributions in Chapter 7).

To ease the interpretation of stratigraphic distributions produced in Chapters 3, 4, 5, 6 and 7, a summary succession is presented in Fig. 3.5. A fold-out copy of this section can be found at the end of the thesis.

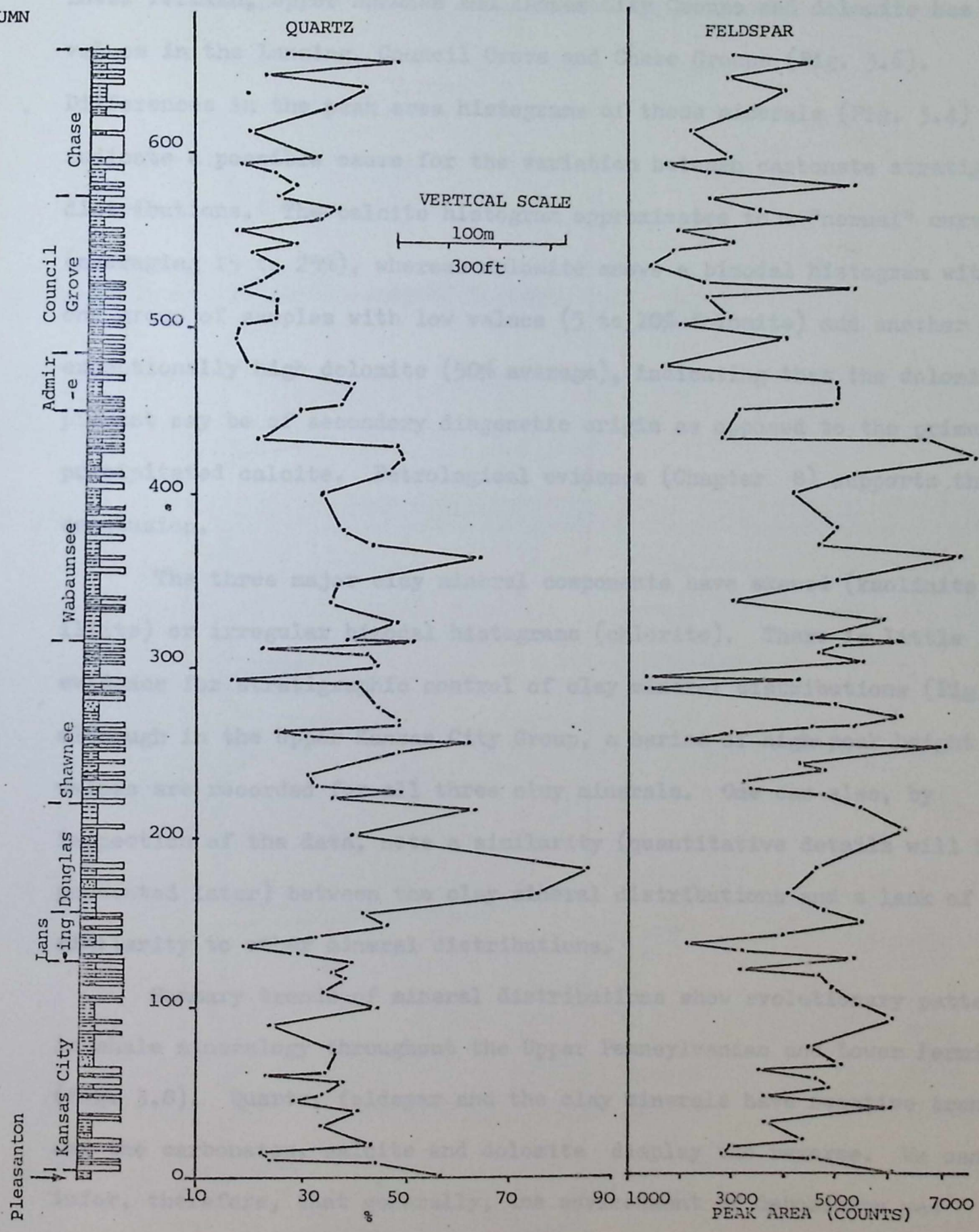

Fig. 3.5 Distribution of quartz(%) and feldspar (peak area) in shales from the Upper Pennsylvanian and Lower Permian of Kansas, U.S.A.

intensive carbonate generation. Both calcite and dolomite distributions (Fig. 3.6) show low values in the Douglas and Wabaunsee Groups (averaging 5 to 10% carbonate) whereas calcite shows high concentrations in the Lower Permian, Upper Shawnee and Kansas City Groups and dolomite has high values in the Lansing, Council Grove and Chase Groups (Fig. 3.6). Differences in the peak area histograms of these minerals (Fig. 3.4) indicate a possible cause for the variation between carbonate stratigraphic distributions. The calcite histogram approximates to a "normal" curve (averaging 15 to 25%), whereas dolomite shows a bimodal histogram with one group of samples with low values (5 to 10% dolomite) and another with exceptionally high dolomite (50% average), indicating that the dolomite present may be of secondary diagenetic origin as opposed to the primary precipitated calcite. Petrological evidence (Chapter 8) supports this conclusion.

The three major clay mineral components have skewed (kaolinite and illite) or irregular bimodal histograms (chlorite). There is little evidence for stratigraphic control of clay mineral distributions (Fig. 3.7), although in the Upper Kansas City Group, a series of high peak height values are recorded for all three clay minerals. One can also, by inspection of the data, note a similarity (quantitative details will be presented later) between the clay mineral distributions and a lack of similarity to other mineral distributions.

Summary trends of mineral distributions show evolutionary patterns in shale mineralogy throughout the Upper Pennsylvanian and Lower Permian (Fig. 3.8). Quartz, feldspar and the clay minerals have negative trends, and the carbonates, calcite and dolomite display the reverse. We can infer, therefore, that generally, the environment of deposition was conducive to carbonate precipitation in the Lower Permian and to the development of detrital clastics in the Upper Pennsylvanian.

This environmental association of minerals is supported statistically,

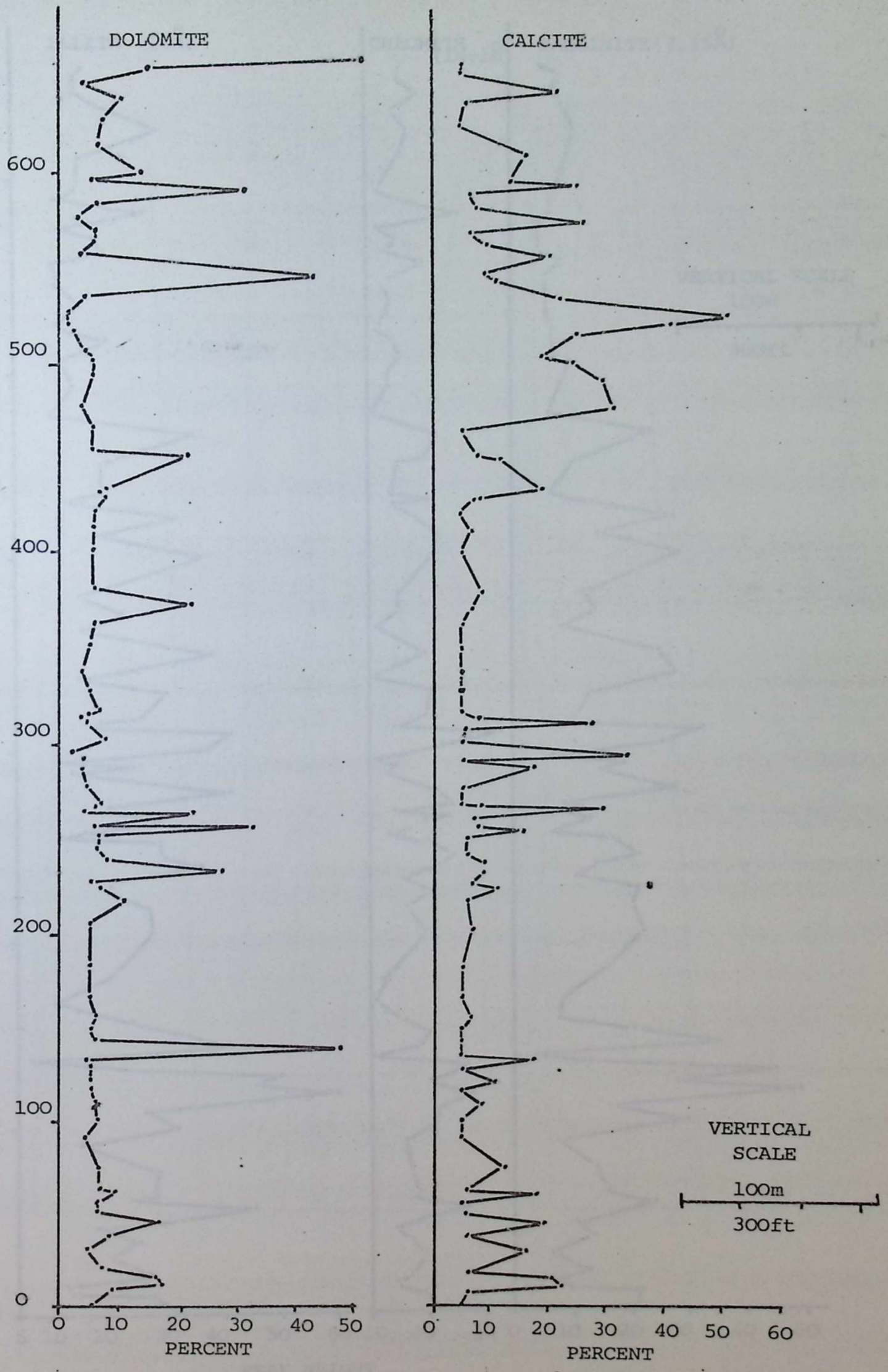

Fig. 3.6 Variation of calcite and dolomite in Upper Pennsylvanian and Lower Permian shales of Kansas. Vertical scale matches that in Fig. 3.5 and stratigraphic comparisons can be made.

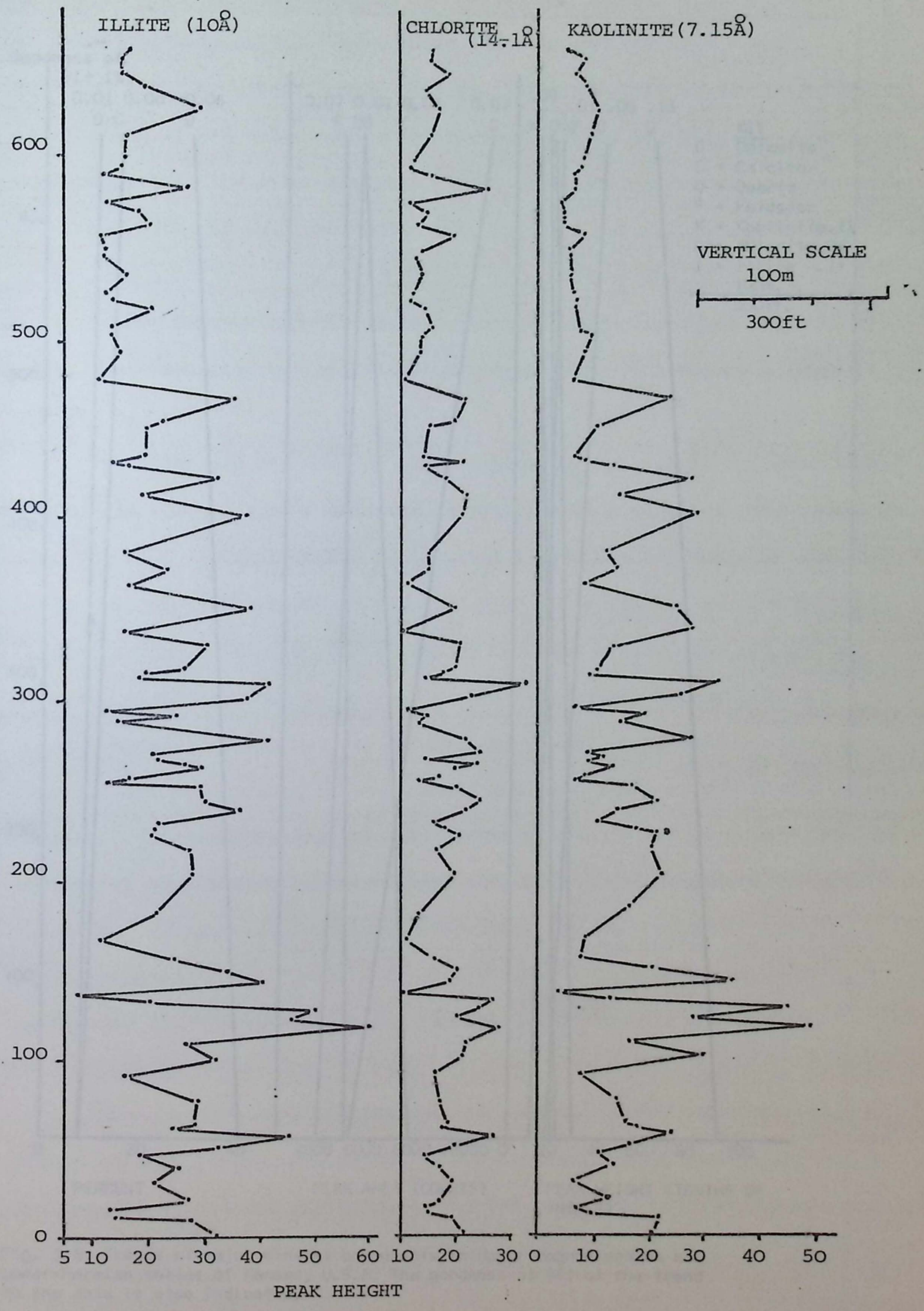

Fig. 3.7 Variation in illite, chlorite and kaolinite clay mineral peak heights from Upper Pennsylvanian and Lower Permian shales of Kansas, U.S.A. Vertical scale is identical to Fig. 3.5 and 3.6 and stratigraphic comparisons can be made.

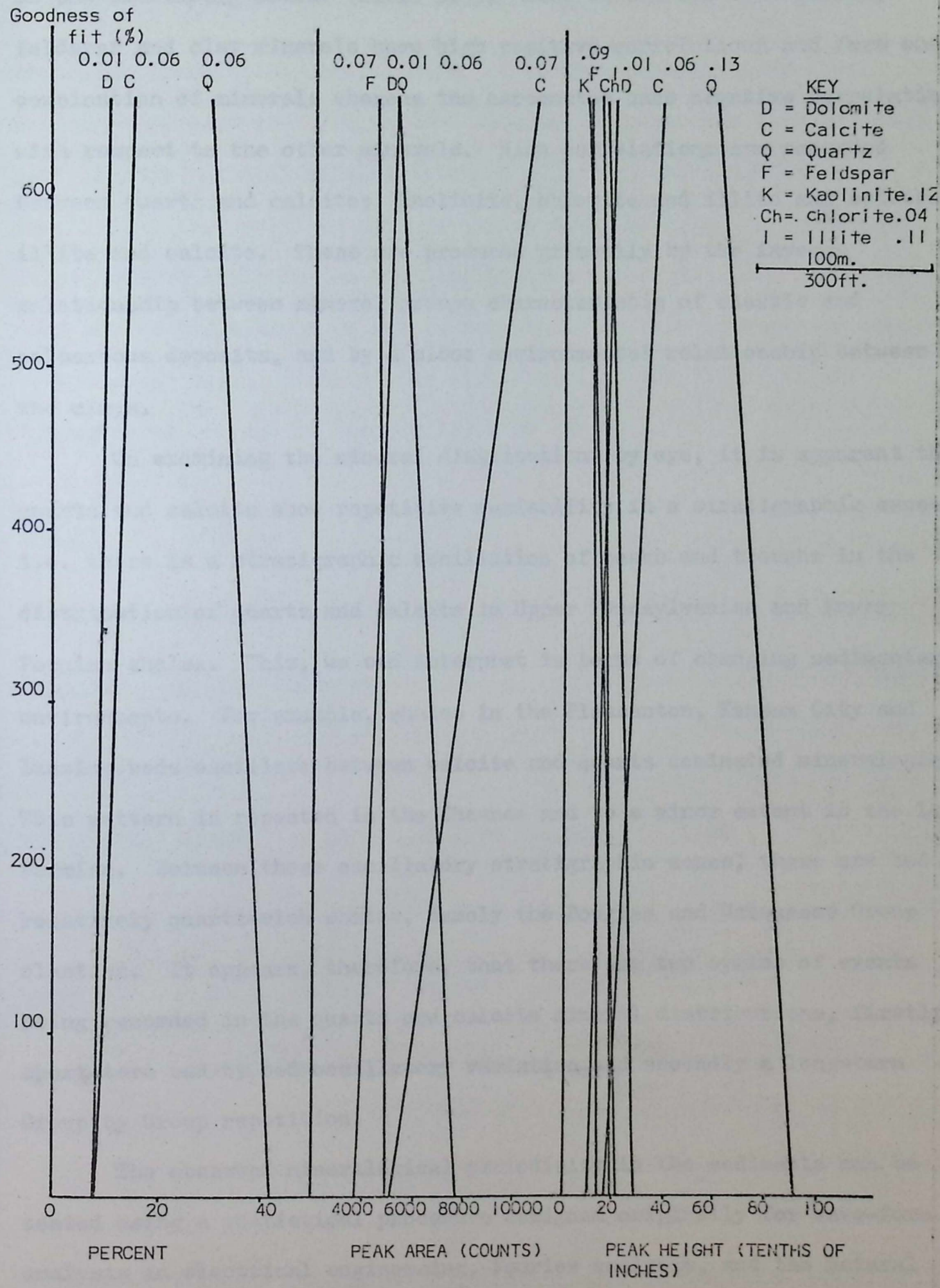

Fig. 3.8. Trends of major mineral components in Upper Pennsylvanian and Lower Permian shales of Kansas, U.S.A. The goodness of fit of the trend to the data is also indicated.

in the similarity matrix (Table 3.5). Here we can see that quartz, feldspar and clay minerals have high positive correlations and form one combination of minerals whereas the carbonates have negative correlations with respect to the other minerals. High correlations are recorded between quartz and calcite; kaolinite, chlorite and illite and between illite and calcite. These are produced primarily by the inverse relationship between mineral groups characteristic of clastic and calcareous deposits, and by a close environmental relationship between the clays.

On examining the mineral distributions by eye, it is apparent that quartz and calcite show repetitive variability in a stratigraphic sense, i.e. there is a stratigraphic oscillation of peaks and troughs in the distribution of quartz and calcite in Upper Pennsylvanian and Lower Permian shales. This, we can interpret in terms of changing sedimentary environments. For example, shales in the Pleasanton, Kansas City and Lansing beds oscillate between calcite and quartz dominated mineralogies. This pattern is repeated in the Shawnee and to a minor extent in the Lower Permian. Between these oscillatory stratigraphic zones, there are beds of relatively quartz-rich shales, namely the Douglas and Wabaunsee Group clastics. It appears, therefore, that there are two cycles of events being recorded in the quartz and calcite mineral distributions, firstly a short-term bed by bed oscillatory variation and secondly a long-term Group by Group repetition.

The observed mineralogical periodicity in the sediments can be tested using a statistical procedure designed originally for wave-form analysis in electrical engineering, Fourier analysis, and the natural cycles recognised. A series of computations have to be performed prior to the Fourier analysis, however, to transform the data into a suitable form for entry into the computer program. Initially, using a linear interpolation procedure (Appendix 1) the data is changed from sample

TABLE 3.5 SIMILARITY MATRIX FOR THE MINERAL DISTRIBUTIONS

employing correlation coefficients. Note that although peak area measurements were used for quartz, calcite, feldspar and dolomite, and peak heights for kaolinite, illite and chlorite, the correlation coefficient is a unitless measure and as such the original measurement units have no influence on the similarities recorded. Only the lower half of the correlation matrix is reproduced as this is a mirror image of the upper half. Correlations significant at the 95% level are indicated by * and at the 99% level by **.

QUARTZ	1.00						
FELDSPAR	0.26**	1.00					
CALCITE	-0.62**	-0.43**	1.00				
DOLOMITE	-0.20*	-0.21*	-0.03	1.00			
KAOLINITE	0.20*	0.10	-0.32**	-0.24**	1.00		
ILLITE	0.26**	0.23**	-0.52**	-0.24**	0.73**	1.00	
CHLORITE	0.16	0.14	-0.45**	-0.25**	0.48**	0.69**	1.00
MINERAL	QUARTZ	FELDSPAR	CALCITE	DOLOMITE	KAOLINITE	ILLITE	CHLORITE

values with irregular depth intervals to a pattern of values taken at a constant depth interval. An interval of 10 feet (3.05 m)* was chosen as the most practical equal spacing interval as Schwarzacher (1967) has shown that the smallest lithological cycle occur at intervals of 45 feet, and any larger equal distance would obscure these cycles. The total number of data points is, in this way, increased from 128 to 218. In the case of the quartz distribution shown in Fig. 3.9a, it was noted that although major peaks correspond to those in the raw data plot (Fig. 3.5), it was possible that through this interpolation process, there may have been a significant alteration to the raw data variability and trend. A linear regression analysis however, showed that although the trend and goodness of fit measures had changed, the differences were acceptable, i.e. goodness of fit increased from .06 to .13 and the correlation coefficient from .26 to .37. The equal spaced data was then run through a Fourier analysis and the raw power spectrum calculated, is shown in Fig. 3.10. It can be seen that the two main peaks corresponding to the 3rd and 7th harmonics (multiples of the fundamental wavelength chosen i.e. 10 foot) are indistinguishable from surrounding points. Noise in the equal spaced data may have produced this power spectrum fuzziness. An 11-term smoothing operation on the raw data, however, removed the short-term noise and revealed the power spectrum shown in Fig. 3.10 (dashed lines). Features retained in the smoothed power spectrum include two main peaks at the 3rd and 7th harmonics and subsidiary peaks at the 5th, 11th, 13th and 14th. These indicate fundamental periodic elements in the quartz distribution with 30, 50, 70, 110, 130 and 140 foot intervals, that may be

---

* Note that it is now a normal policy in geology theses to quote distances in metric terms. Certain portions of this research were, however, performed before metrication was an accepted practice and some results will therefore be quoted in feet. This particularly applies to Fourier analysis results. However, in most sections of this thesis, adjustments have been made and distances are quoted in metres with feet in brackets.

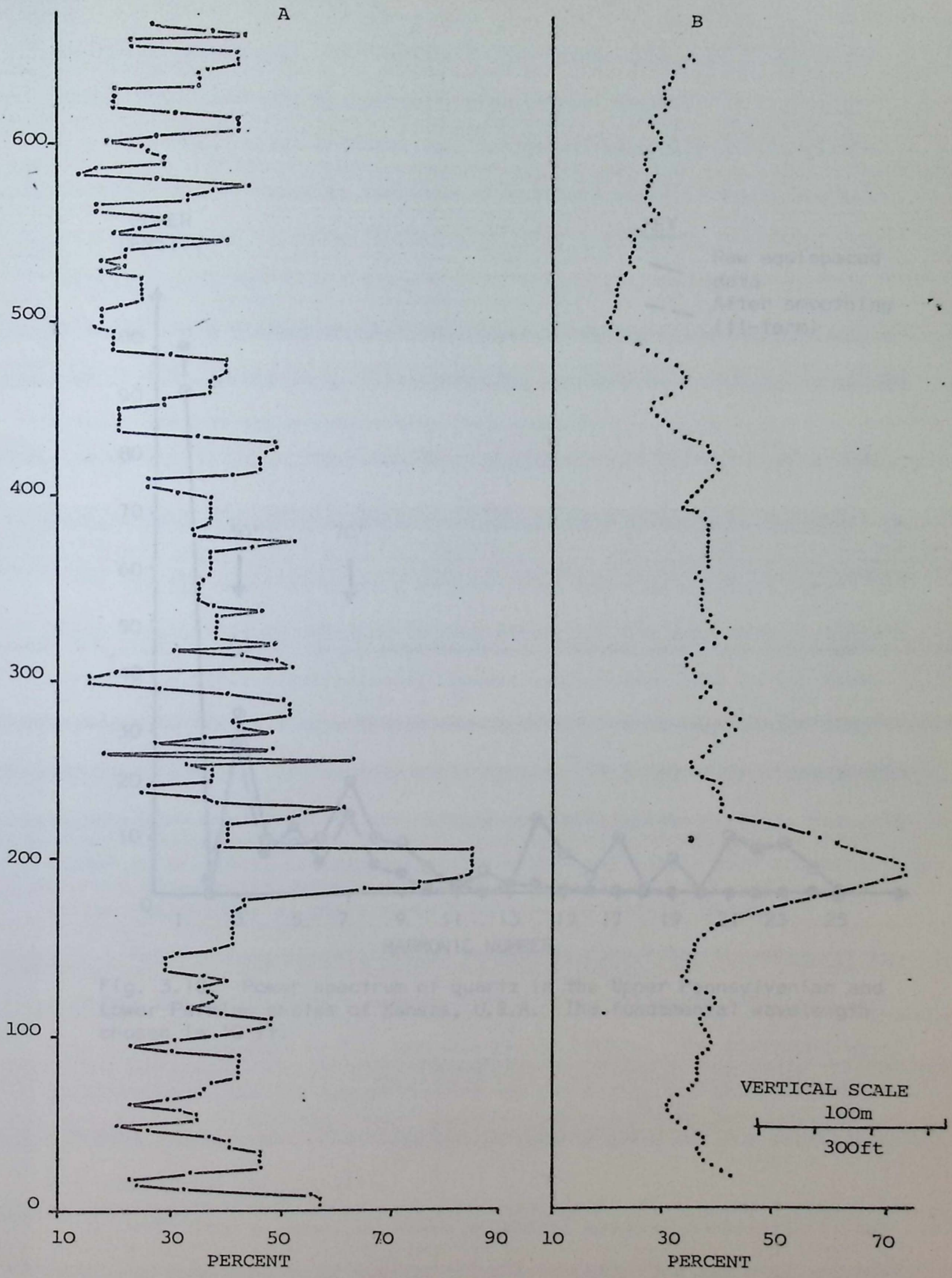

Fig. 3.9 Distribution of quartz (in percent) after (A) equal spacing by a linear interpolation procedure, (B) equal spacing and smoothing (using an 11-term moving average equation. For a stratigraphical comparison see Fig. 3.5.

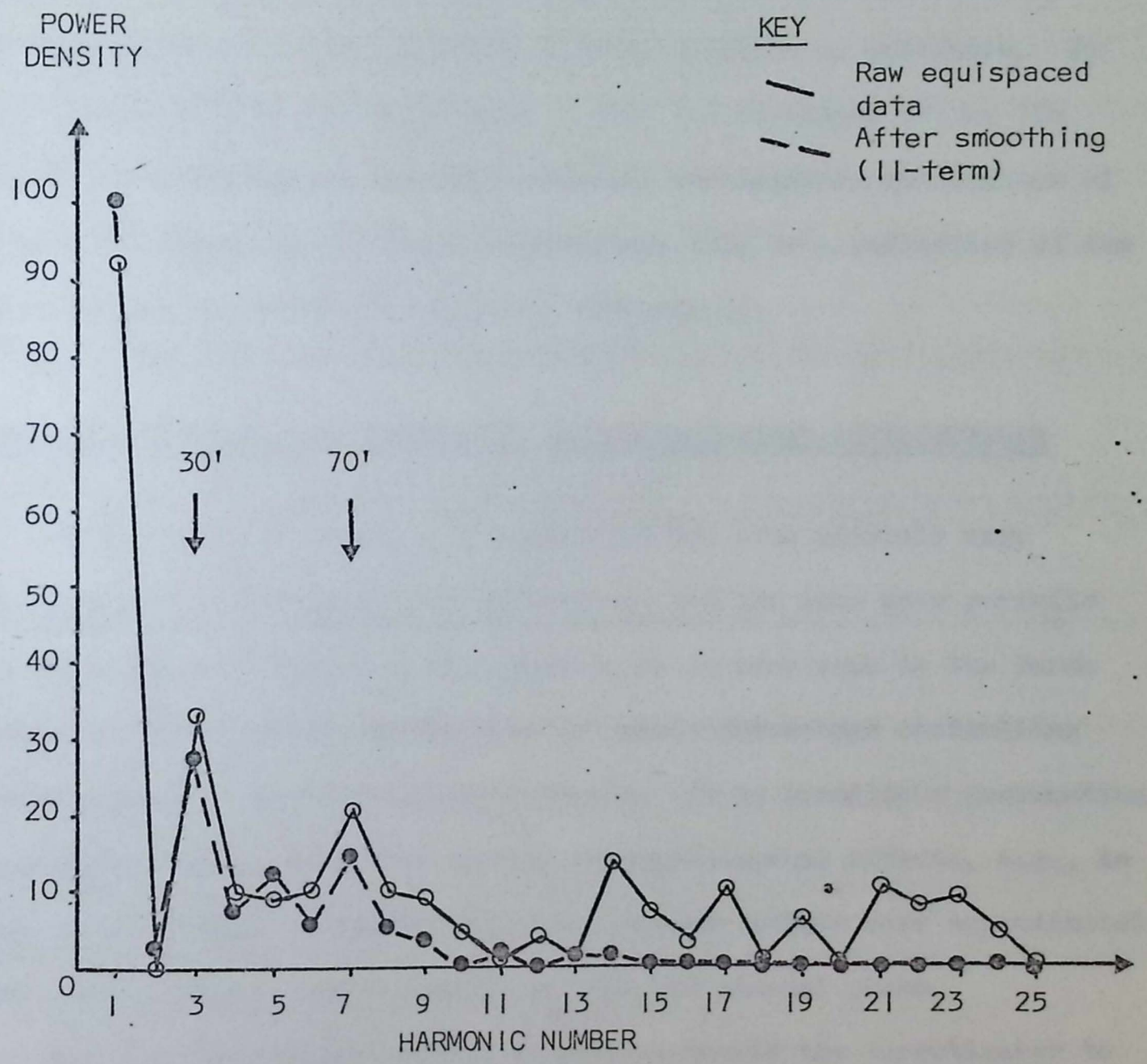

Fig. 3.10. Power spectrum of quartz in the Upper Pennsylvanian and Lower Permian shales of Kansas, U.S.A. The fundamental wavelength chosen is 10 ft.

explained in terms of oscillations in the quartz values of Pleasanton, Kansas City, Lansing, Shawnee and Lower Permian shales.

Although these features were recognised initially in the quartz distribution, no evidence for these conclusions could be found in the power spectra of dolomite, feldspar, illite, chlorite or kaolinite. In calcite's spectrum on the other hand, a peak was developed at the 7th harmonic and a plateau at the 3rd. However, the negative association of calcite with quartz in all these results, may only be a reflection of the closed data set under examination (see Appendix 1).

MULTIVARIATE STATISTICAL ANALYSIS OF THE MINERALOGICAL DISTRIBUTIONS

In the previous section we have noted how some minerals vary stratigraphically in relation to each other, and how some show periodic elements in their distributions. However, it is very rare in the Earth Sciences to find a single factor such as quartz percentage controlling the development of sedimentary environments. It is normally a combination of variables that produces the overall sedimentological effects, e.g., in Kansas an assemblage of mineral distributions may relate more approximately to the periodicity of shale deposition than one mineral phase.

Multivariate classification techniques enable the investigator to quantify the relationships between variables and classify shale samples into groups dependent on the variable relationships. The distribution of individuals within the groups matched against depth, can then be used to indicate stratigraphic divisions not previously noted and any repetition in the shale group associations.

With this in mind, an R-mode principal components analysis of the peak area measurements of quartz, calcite, feldspar and dolomite and the peak heights of kaolinite, illite and chlorite was performed. Three components were found to be significant (i.e. eigenvalues greater than one).

The principal axis component loadings (Fig. 3.11 and 3.12a) reveal similar relationships to the simple correlation coefficients. On the first component, the carbonate minerals have high positive loadings whereas illite, chlorite, kaolinite, quartz and feldspar have high negative loadings. This component can therefore be considered as an indicator of clastic or carbonate conditions of sedimentary deposition. Similarly, the second component's high positive loadings for quartz and feldspar and high negative loadings of calcite and clay minerals reflect the detrital versus non-detrital origin of most of the shales. Quartz and feldspar are commonly associated with detrital sediments and calcite is normally a non-detrital mineral. It would seem at first glance, unusual to note a connection of clay minerals with calcite, but it must be remembered that many of the thin shales occurring between limestones in the Kansas City and Shawnee Groups have high values for both calcite and clay minerals. Alternatively, this component may reflect the high quartz and feldspar content of some coarse shales, silts and sandstones and corresponding lack of calcite and clay minerals in these samples. The high negative loading of dolomite on the final significant component represents the influence of the irregular dolomite distribution and may be an indicator of primary or secondary mineral origin. As noted previously, the irregular distribution of dolomitic shales indicates a diagenetic origin for the dolomitic shale samples. We can now express the variation of mineralogy in the Kansas shales in terms of three geologically interpretable components. An attempt can, however, be made to clarify the geological interpretation of the components by emphasising the loadings of the influential variables using the varimax and promax rotation procedure (see Appendix 1). With the component loadings matrix, we find that on varimax rotation there is an accentuation of the clay mineral loadings (Fig. 3.12b) on Factor 1 and the quartz/calcite antipathy is weighted more strongly on Factor 2. The highlighting of known information has proved valuable but with promax

COMPONENT NO. 1.

Eigenvalue = 3.05
Variance =43.52%

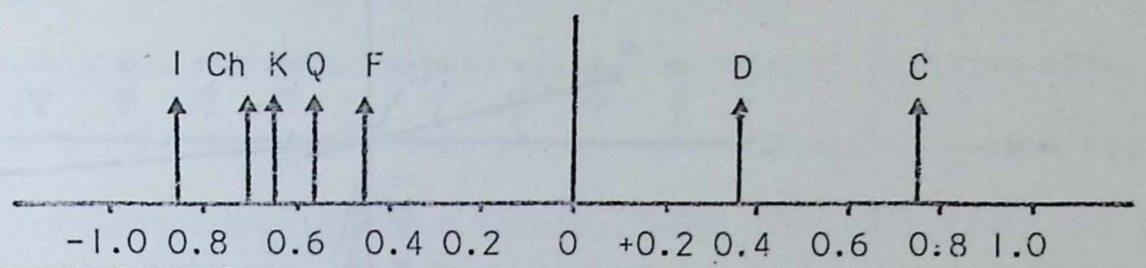

COMPONENT NO.2.

Eigenvalue = 1.29
Variance =18.39%

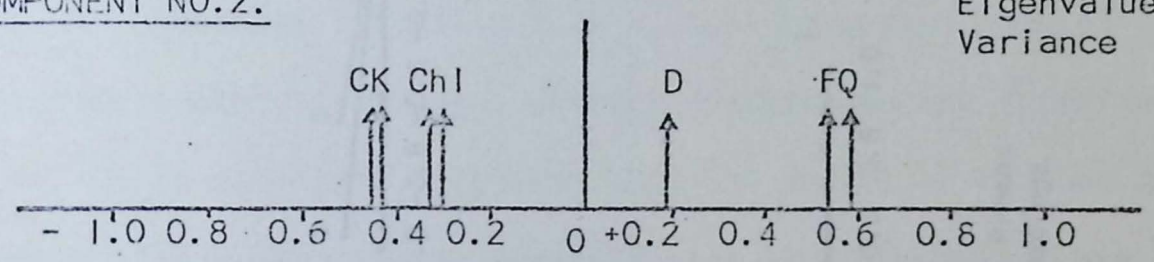

COMPONENT NO.3.

Eigenvalue = 1.0i
Variance =14.48%

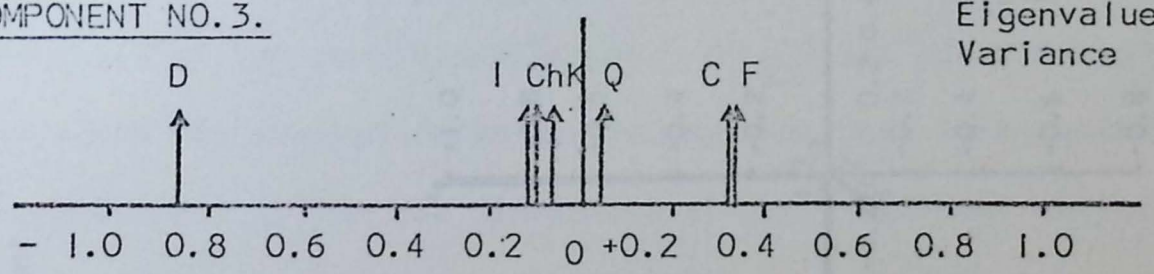

KEY

D = Dolomite
C = Calcite
F = Feldspar
Q = Quartz
K = Kaolinite
Ch= Chlorite
I = Illite

Fig. 3.11 Principal Axis Loadings of the significant components (i.e. components with eigenvalues > 1.0)

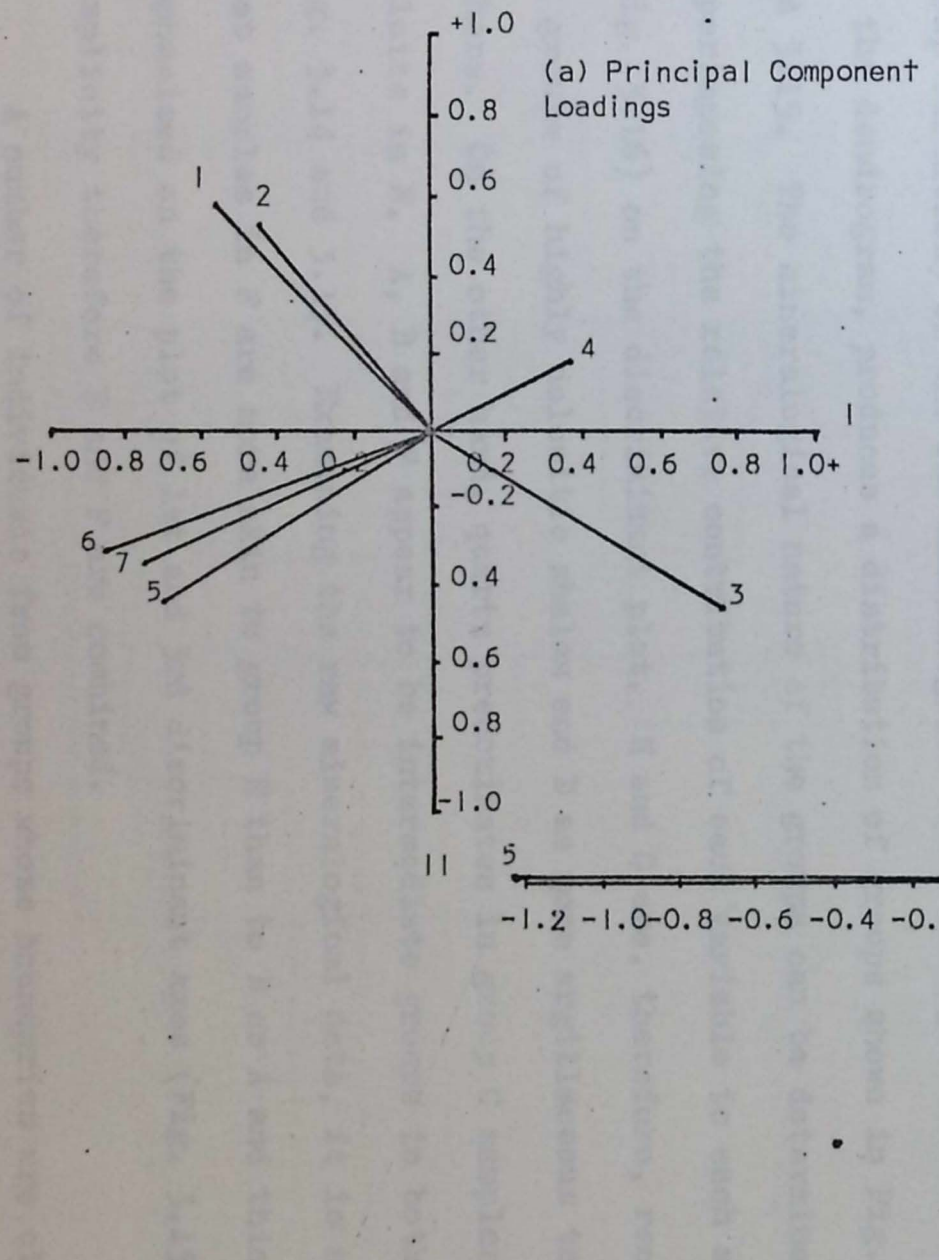

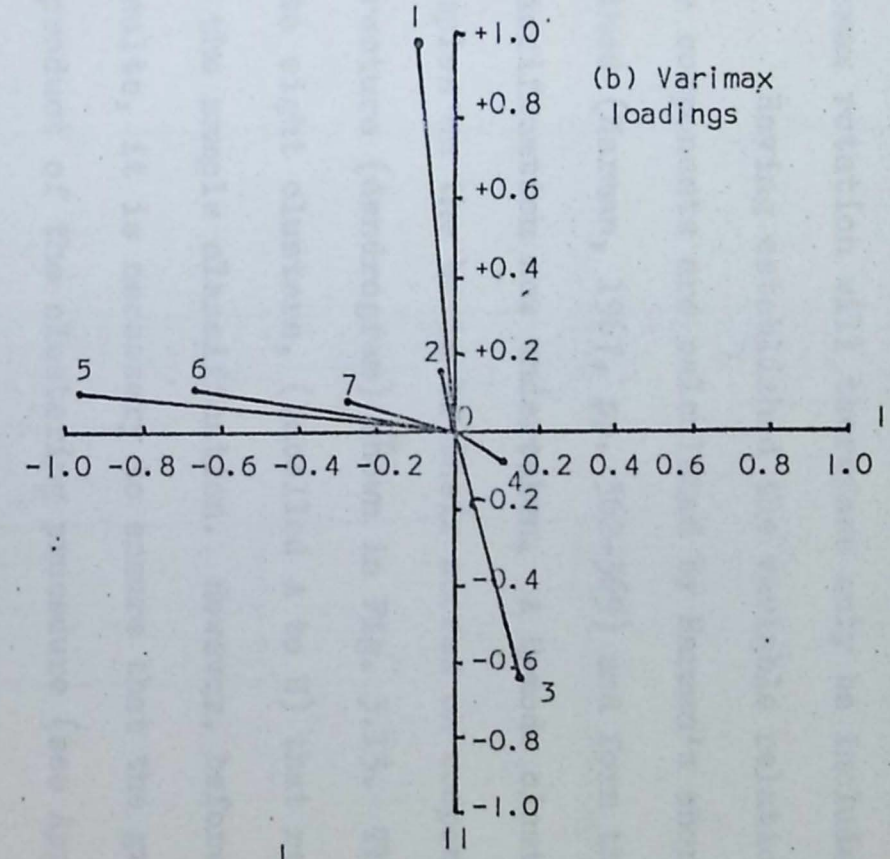

Fig. 3.12. Plot of loadings on two components extracted from raw mineralogy data. Variables plotted are (1) quartz, (2) feldspars, (3) calcite, (4) dolomite, (5) kaolinite, (6) illite, (7) chlorite. Note that Promax factors I and II are not orthogonal, (Correlation = -0.0308) but for simplicity, are drawn so.

rotation (an oblique factor rotation -- see Appendix 1) of the mineralogical data, (Fig. 3.12c) interpretation becomes a major problem. The results of promax rotation will therefore only be included for comparative purposes.

Having established the variable relationships, scores of samples on the components are calculated by Harman's short regression and square root method (Harman, 1967, pp. 362-369) and form the basis of the sample classification now undertaken. A Q-mode cluster analysis arranges the samples on the basis of their scores on component axes into the hierarchical structure (dendrogram) shown in Fig. 3.13. The dendrogram can be divided into eight clusters, (labelled A to H) that represent natural subdivisions of the sample classification. However, before placing faith in these results, it is necessary to ensure that the groups of samples are not just a product of the clustering procedure (see Appendix 1) but are unique subdivisions of the sample population. A multiple discriminant analysis (a procedure for statistically developing functions that maximize between-group variation) of the raw mineralogical data, arranged in the same manner as the dendrogram, produces a distribution of groups shown in Fig. 3.14 and 3.15. The mineralogical nature of the groups can be determined by superimposing the relative contribution of each variable to each axis (Fig. 3.16) on the discriminant plot. H and G are, therefore, recognised as groups of highly dolomitic shales and D as more argillaceous than the others. On the other hand, quartz predominates in group C samples and calcite in E. A, B and F appear to be intermediate groups in both Fig. 3.14 and 3.15. Examining the raw mineralogical data, it is noticeable that samples in F are more akin to group E than to B or A and this is emphasised on the plot of 1st and 3rd discriminant axes (Fig. 3.15). For simplicity therefore E and F are combined.

A number of individuals from groups whose boundaries are closely related (i.e. A, B and E) are also misplaced by the clustering algorithm. Manual examination of sample scores on the first three discriminant axes

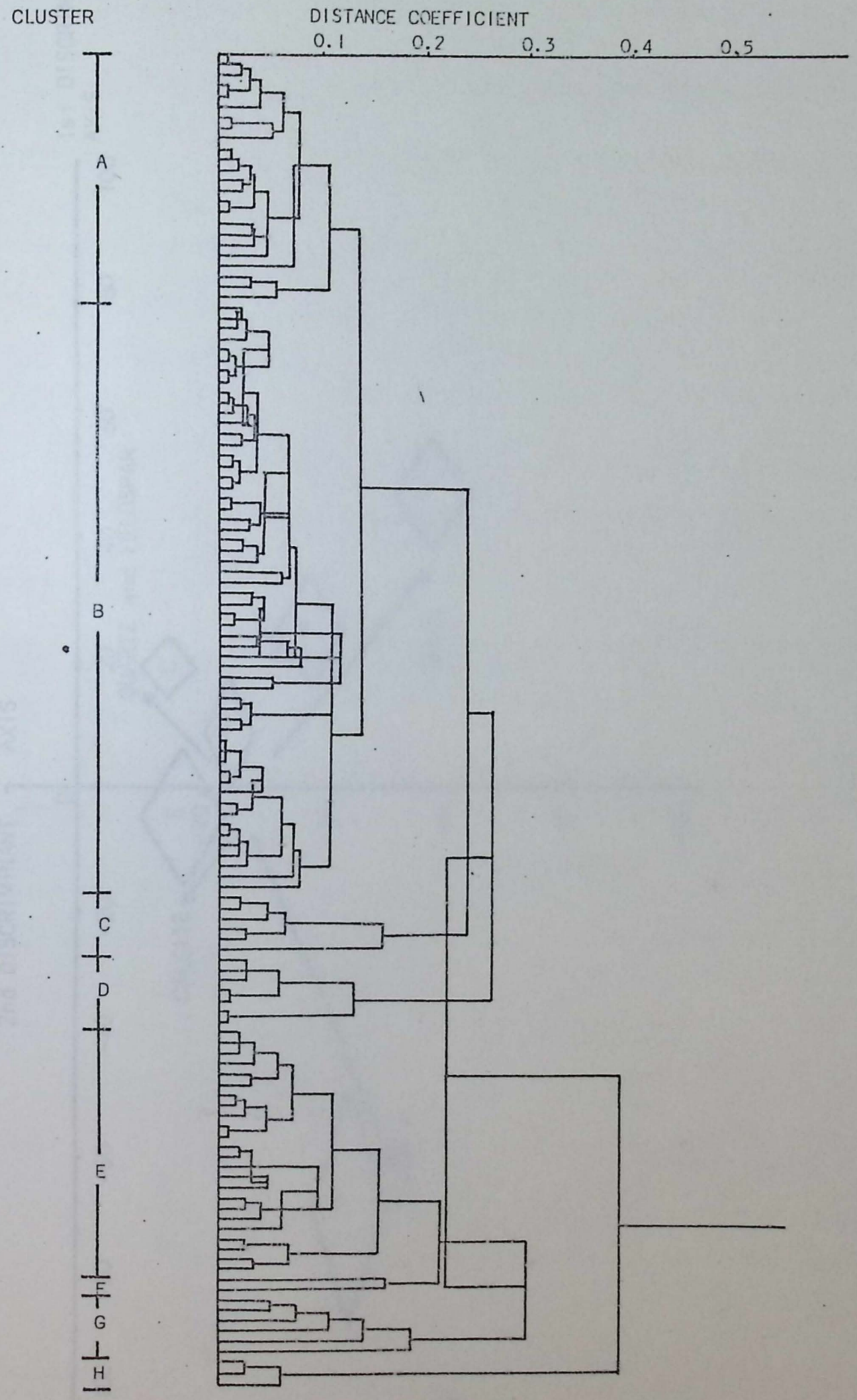

Fig. 3.13. A dendrogram produced by a Q-mode cluster analysis of mineralogical data. Clusters produced are outlined on the left of the diagram.

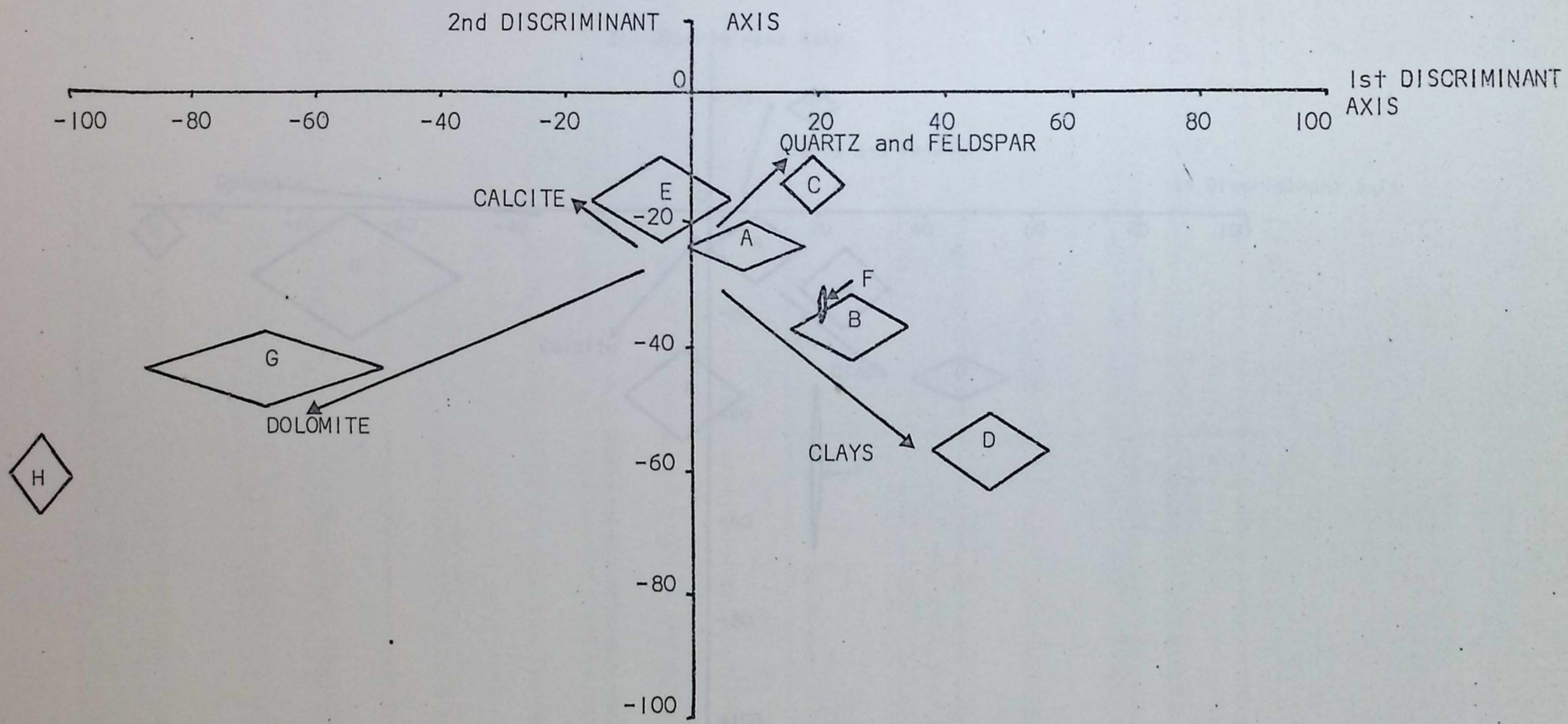

Fig. 3.14. Distribution of cluster analysis groups on the first two discriminant axes. Primary mineralogical variation is superimposed for reference. Diamonds represent the mean of each group ±1 standard deviation of each axis.

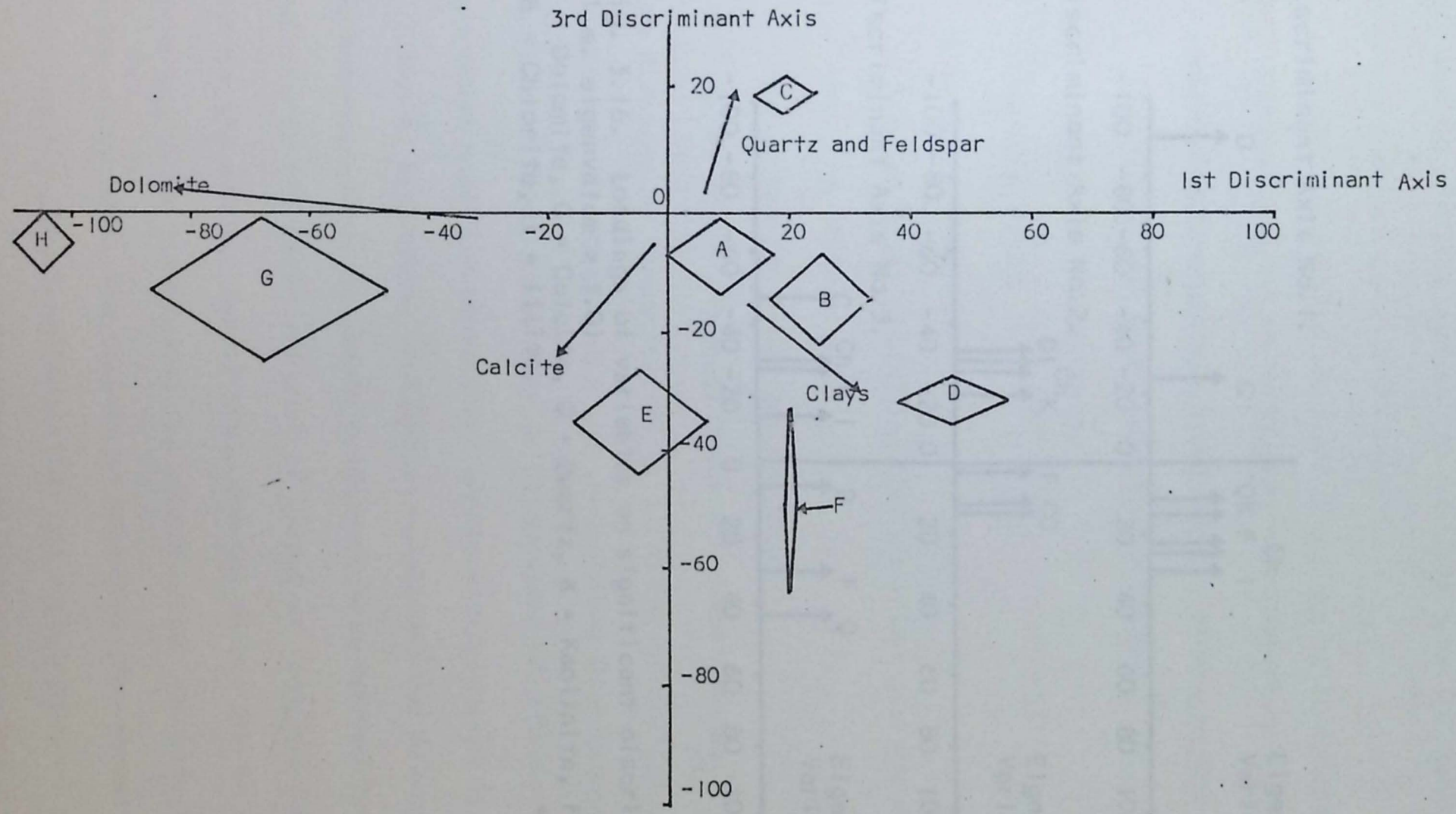

Fig.3.15 Distribution of cluster analysis groups on the first and third discriminant axes. Primary mineralogical variation is superimposed for reference. Diamonds represent the mean of each group ± 1 standard deviation on each axis.

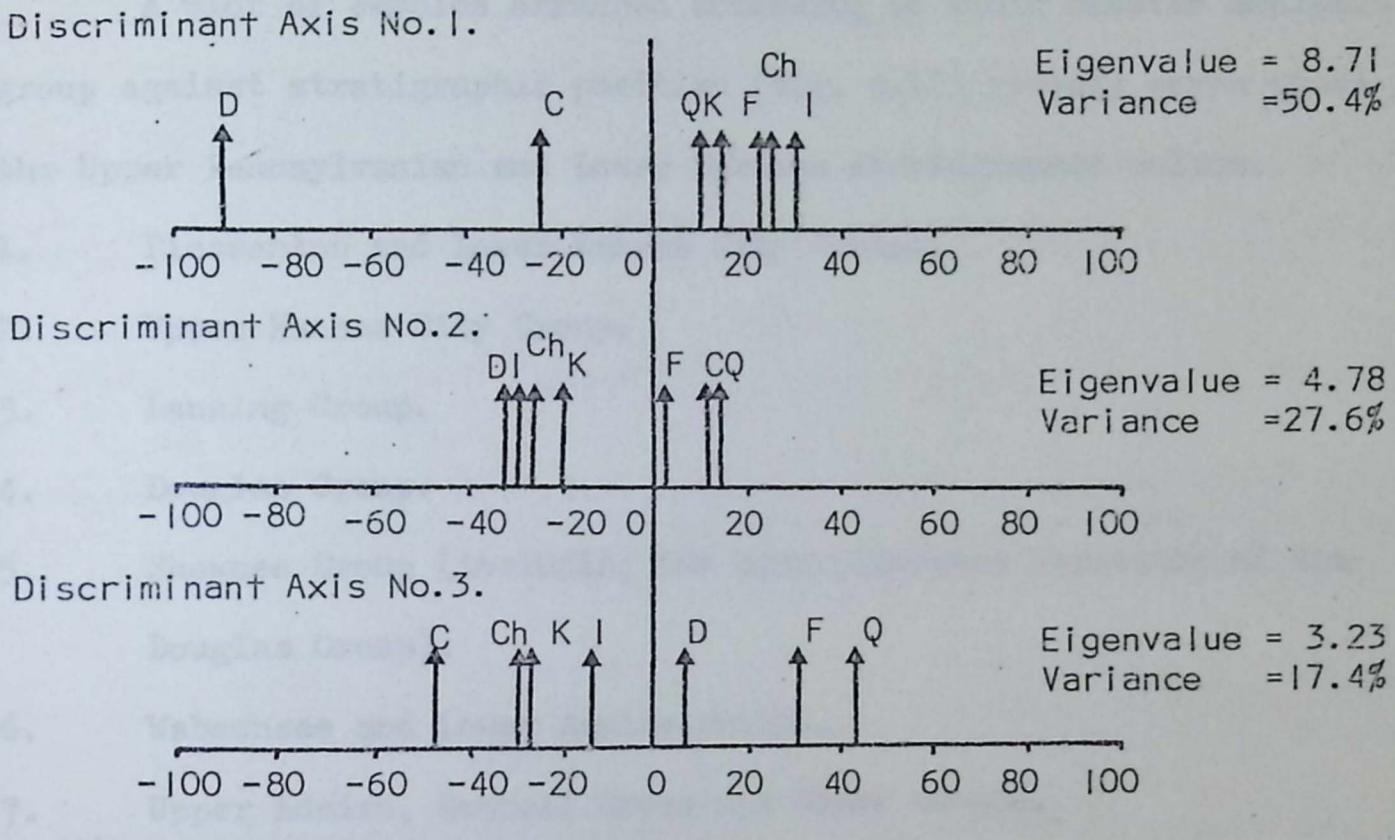

Fig. 3.16. Loadings of variables on significant discriminant axes (i.e. eigenvalue > 1.0)
D = Dolomite, C = Calcite, Q = Quartz, K = Kaolinite, F = Feldspar, Ch = Chlorite, I = Illite.

indicate that samples 281, 298, 270, 256, 79, 41, 136, 197 should be attached to group E while sample 20 is more naturally associated with group A. On reallocation we can conclude that the seven groups established are now mineralogically distinct.

A plot of samples arranged according to their cluster analysis group against stratigraphic position (Fig. 3.17) reveals seven zones in the Upper Pennsylvanian and Lower Permian stratigraphic column.

1. Pleasanton and Lower Kansas City Groups.
2. Upper Kansas City Group.
3. Lansing Group.
4. Douglas Group.
5. Shawnee Group (including the Upper Lawrence Formation of the Douglas Group).
6. Wabaunsee and Lower Admire Groups.
7. Upper Admire, Council Grove and Chase Groups.

Each division is characterised by differing mineralogical and sedimentological conditions. The Pleasanton and Lower Kansas City Groups, Lansing Group and Shawnee Group zones show an alternation of calcite + (normally associated with limestones) and quartz - rich shales (predominantly clusters B, E and A) indicating oscillating calcareous and non-calcareous environments. The non-calcareous sediments could have been derived from either the lowlands to the north and east of Kansas or from the Ouachita orogenic belt to the south. Source areas for the shales may be distinguished by comparing their geochemical and mineralogical results (see Chapter 7). On the other hand, the calcareous sediments were deposited at a time of predominantly limestone deposition and could represent either normal marine shales or the equivalent of limestone insoluble residues. Again such differences will be discussed in Chapter 7.

The Douglas and Wabaunsee Groups are dominated by shales that have

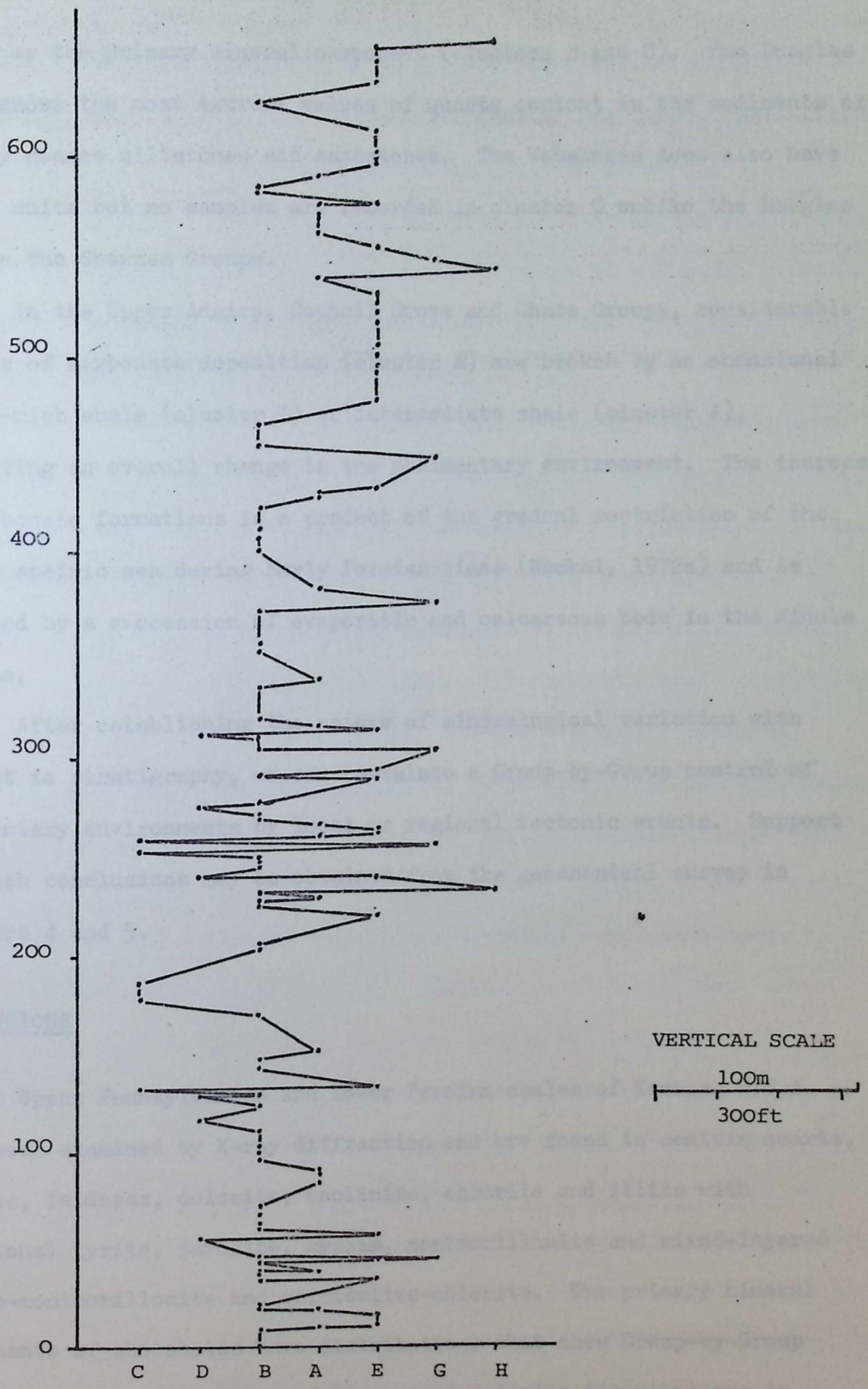

Fig. 3.17 Stratigraphic distribution of samples arranged on a horizontal scale according to their cluster analysis class (Fig. 3.12). The order of classes along the horizontal scale is arbitrary but may be interpreted as calcareous classes on the right and non-calcareous on the left. For a comparable stratigraphic column see Fig. 3.4.

quartz as the primary mineral component (clusters B and C). The Douglas Group shows the most extreme values of quartz content as the sediments are largely coarse siltstones and sandstones. The Wabaunsee does also have coarse units but no samples are recorded in cluster C unlike the Douglas or even the Shawnee Groups.

In the Upper Admire, Council Grove and Chase Groups, considerable periods of carbonate deposition (cluster E) are broken by an occasional quartz-rich shale (cluster B) or intermediate shale (cluster A), indicating an overall change in the sedimentary environment. The increase in carbonate formations is a product of the gradual restriction of the Kansas epeiric sea during Early Permian times (Heckel, 1972a) and is followed by a succession of evaporitic and calcareous beds in the Middle Permian.

After establishing the nature of mineralogical variation with respect to stratigraphy, we can postulate a Group-by-Group control of sedimentary environments by local or regional tectonic events. Support for such conclusions may be obtained from the geochemical survey in Chapters 4 and 5.

CONCLUSIONS

Upper Pennsylvanian and Lower Permian shales of Kansas, U.S.A. have been examined by X-ray diffraction and are found to contain quartz, calcite, feldspar, dolomite, kaolinite, chlorite and illite with occasional pyrite, jarosite, gypsum, montmorillonite and mixed-layered illite-montmorillonite and vermiculite-chlorite. The primary mineral components of the shales have distributions that show Group-by-Group variation. Quartz, calcite, feldspar and dolomite distributions in particular are affected by changing sedimentary and tectonic environments.

Plotting mineral components against depth, a number of stratigraphic zones can be detected. These are a Pleasanton-Kansas City-Lansing unit,

a Douglas Group zone, a Shawnee unit, a Wabaunsee unit and an Admire Council Grove-Chase unit. Statistical analysis of the quartz stratigraphic distribution emphasises these relationships but also reveals 30 ft. (9.3 m), 70 ft. (21.7 m), and higher interval patterns in the quartz data. This may indicate that the mineralogical conditions of the Upper Pennsylvanian and Lower Permian are repetitive, but it must be noted that none of the other main components show similar patterns.

A multivariate classification analysis of the mineralogical data also supports the zonation of the Upper Pennsylvanian and Lower Permian stratigraphy and provides further information on the variation within the zones. Slight modification to the original stratigraphic divisions is required following a principal components-cluster analysis-discriminant analysis study of the mineralogical data. The zones are now: Pleasanton-Lower Kansas City; Upper Kansas City; Lansing; Douglas; Shawnee (including the Upper Lawrence Formation); Wabaunsee-Lower Admire; Upper Admire-Council Grove-Chase. Of these, the Pleasanton-Upper Kansas City, Lansing and Shawnee all show alternations between calcareous and quartz-rich shales possibly representing cycles in sedimentary conditions. Calcareous shales abound in the Upper Admire-Council Grove-Chase zone whereas the opposite is true in the Upper Kansas City, Douglas and Wabaunsee zones where quartz shales and siltstones predominate.

Three principal components describe the mineralogical variation of the Upper Pennsylvanian and Lower Permian shales. Firstly, a clastic versus carbonate deposition component reflects the association of quartz, feldspar and the clay minerals in some shales and calcite or dolomite in others. The occurrence of coarse clastic deposits such as the Douglas Group are described by the detrital versus non-detrital second component and the final component essentially reflects the secondary nature of dolomite in the shales.

CHAPTER FOUR

EMISSION SPECTROSCOPY AND THE GEOCHEMISTRY OF SOME KANSAS SHALES

INTRODUCTION

The distribution of minerals in Upper Pennsylvanian and Lower Permian shales of Kansas has outlined stratigraphic zones characterised by changing sedimentary and tectonic conditions (Chapter 3). Confirmation and clarification of the depositional environments can be obtained by studying the geochemistry of the same rocks.

The geochemistry of sediments is normally determined using X-ray fluorescence (XRF) or occasionally wet chemical methods although exploration geochemists have in the past sacrificed the accuracy and sensitivity of XRF for the quantity of output obtained using emission spectroscopy. However, Davenport (1970) and Celenk (1972) have studied the problems associated with the emission spectroscopic analysis of rocks, stream sediments and ore samples and developed an efficient technique capable of handling many samples and producing results with an acceptable level of accuracy. A number of sedimentary rock analyses have subsequently been performed on the ARL 2900B direct reading spectrometer in the Geology Department at Leicester University and the results have proved most successful (Celenk, 1972; Monteleone, 1972; Turner, 1973). Availability also played an important role in the choice of technique for geochemical analysis. As Leicester University has no XRF facility, the determination of major oxide and minor element content of 127 shale samples from the Upper Pennsylvanian and Lower Permian of Kansas, U.S.A. could only be performed using emission spectroscopy.

Numerous studies of sedimentary rocks found throughout the world have been conducted to assess the geochemical evolution of sediments throughout geologic time (Reimer, 1971, 1972; Van Moort, 1972, 1973). The geochemical data obtained in this thesis and by Ebens and Connor (1972) in a geochemical survey of Missouri, was therefore compared with that quoted in the literature, to evaluate the influence worldwide geochemical trends

have had on the evolution of Upper Pennsylvanian and Lower Permian shales in Kansas, the regional geochemical variation between Kansas and Missouri sediments and finally, the stratigraphic and geochemical variation found in Kansas shales.

SPECTROSCOPIC ANALYSIS

The theory and practical details of emission spectroscopic analysis are discussed by Ahrens and Taylor (1961) and Price (1969) and specific problems encountered with the spectrometer at Leicester are covered in Davenport (1970) and Celenk (1972). However, it is appropriate to include a brief summary of the technique as emission spectroscopy is relatively unknown in the sedimentological literature.

Electrons in elements subjected to a strong electrical discharge, can become excited to a higher energy state. On reverting to a ground state (lower energy state) the electrons give off energy in the form of light of a constant wavelength. As each element has its own characteristic wavelength, the light may be used to identify the element and from the intensity of the spectral line produced, the quantity of the element present can be calculated.

A rock sample excited by an electrical discharge emits light which is broken down into its component wavelengths by a prism or a diffraction grating. The intensity of each wavelength determines the quantity of each element present by comparison with standards of known composition. Measurement of the spectral lines is made electronically using a spectrometer.

Description of the Spectrometer

Analysis was performed on an ARL 2900B direct reading emission spectrometer with a D.C. arc source unit. The spectral lines for the elements sought, are isolated from the remainder of the spectrum by passing

the light produced from the excitation of a sample over a grating and receiving the resulting lines through a set of secondary slits. The intensities of the lines are measured electronically by photomultiplier tubes and their output is stored in a series of capacitors. A digital voltimeter reads the charge on the capacitors and a peripheral electric typewriter is used to obtain a printed copy of the readout. The optical characteristics of the spectrometer are given in Table 4.1 and details of the spectral lines are presented in Table 4.2.

Sample Preparation

As a result of orientation surveys performed by Celenk (1972), the following procedure was adopted for the geochemical analysis of sedimentary rocks. Samples were ground to pass through a 150 mesh seive and preheated to 600°C recording the percentage weight loss. 100 mg. of each sample was mixed with 150 mg. of buffer (a mixture of 1 part NaF to 3 parts magicoal carbon powder), placed in a polystyrene vial containing a leucite ball and homogenized in a "Wig-L-Bug" mixer for one minute. The resulting mixture was then packed into a predrilled graphite electrode and heated by a Bunsen burner prior to arcing. During the arcing procedure, the filled electrode was used as an anode and a smooth, square-ended, graphite counter electrode was used as a cathode.

Calibration Standards

A set of synthetic bases, U.S. Geological Survey international standard rocks and British Chemical Standards were analysed for major and minor elements. The results determined the accuracy of the analytical method.

Mixtures of synthetic bases were prepared from "Specpure" Johnson and Matthey oxides, homogenized and then fused in a muffle furnace at 950°C

TABLE 4.1 Optical Characteristics of the Spectrometer (after Celenk, 1972)

Spectrometer	ARL 2900B Direct Reading
Excitation	D.C. arc
Cathode	Ringsdorf R.W. 403 graphite rod (6.15 mm in diameter) with a square faced end
Anode	As above but with a crater of 2.91 mm diameter and 5 mm in depth
Arc Gap	3 mm
Current	13-15 amp
Dispersion (Å/mm)	7 (1st order)
Integration times	45 and 100 seconds.

TABLE 4.2 Characteristics of the Spectral Lines (after Celenk, 1972)

ELEMENT	SPECTRAL LINE (Å)	SLIT WIDTH	REMARKS
Al	2378.4	75	
Ca	3158.9	150	
Fe	2739.6	150	
K	4044.0	150	
Mg	2790.8 x2	75	u/v filter
Si	2435.2 x2	75	u/v filter
Mn	2933.0 x2	75	u/v filter
Ag	3382.9	75	
Ba	4554.0	50	glass
Be	3130.4 x2	50	u/v filter
Bi	3067.7 x2	50	u/v filter
Co	3453.5 x2	50	u/v filter
Cr	4254.4	50	glass
Cu	3274.5	75	
Ga	2943.6	75	
Ge	3039.1	75	
Li	6103.0	50	glass
Mo	3170.3 x2	50	u/v filter
Ni	3414.7 x2	50	u/v filter
Pb	2833.1 x2	50	u/v filter
Sn	2840.0	50	
Sr	4607.3	50	glass
V	4379.2	75	glass
Zn(i)	4810.5	75	glass
Zn(ii)	2138.6	50	
Zr	3392.0 x2	50	u/v filter
Background	2008.6	150	

for three hours. The fused samples were ground and mixed with carefully weighed amounts of "Spec-Mix" (a mixture of 1.28% of each of the 49 element oxides), producing standards with 1000 ppm of all 49 element oxides. Stepwise dilution led to the preparation of further standards with 500, 250, 100, 50, 10 and 0 ppm concentrations.

USGS and British Chemical Standards were used for calibration of major element oxides in the rock samples. Precise minor element values have not been recorded for these standards but a range of values is provided by the USGS and other organisations for comparative studies. With minor elements of values greater than 1000 ppm, care must be exercised as the synthetic bases may not be able to match the extremes in concentrations and the analytical results may be erroneous. However, using correction procedures (Celenk, 1972), extrapolation to higher concentrations can produce meaningful results.

Sensitivity, Precision and Accuracy of the Procedure

Sensitivity of a method is defined as three times the standard deviation obtained by the repeated analysis of a sample containing zero ppm concentrations of the elements under examination (Cameron and Harton, 1967) and is practically the lowest possible concentration at which a particular trace element may be reliably detected. For the minor elements this value is less than 10 ppm except in the case of Zn (11 ppm) where although two wavelengths were recorded, only one proved sensitive enough for normal analysis.

Precision of the analytical technique is expressed in terms of a coefficient of variation and indicates the reproducibility of the results. It is calculated using the equation: $P(\%) = (2 \times \text{standard deviation} \times 100)/\text{mean}$, and is found to be better than 20% for all elements.

By comparing the results obtained from this procedure with those

calculated by Flanagan (1969), Celenk (1972) evaluated the accuracy of the method and concluded that the method was reasonably consistent, especially when the wide range of values quoted by Flanagan is taken into account.

Details of the precision and sensitivity for the method are presented in Table 4.3. Accuracies are calculated from data provided by Celenk (1972) and are reported in Table 4.4 (data were only available for MnO, Ba, Co, Cr, Cu, Ga, Li, Ni, Pb, Sr, V, Zn, Zr).

RESULTS OF THE SPECTROSCOPIC ANALYSIS

127 samples of Upper Pennsylvanian and Lower Permian shales from Kansas were analysed using the previously described procedures. The results and analysed standards are presented in Tables 4.5 and 4.6. However, the following points should be borne in mind when examining Table 4.5. The results for Cd in the standards show anomalously high readings, those for Mo and Zn read slightly higher than normal and the Fe, SiO_2 and Zr lines give low readings. Some care therefore, must be taken in interpreting the results. It must also be remembered that the extrapolation procedure may over-estimate any unusually high readings. Consequently, the value of 114% SiO_2 in sample 121 must be regarded "sceptically". More realistic estimates for the few extreme major oxide values can be obtained from the mineralogical data.

Summary statistics for all the major and minor elements are presented in Table 4.7. Two extra parameters are included in the table, firstly, the percentage weight loss on ignition (Heat Loss) and secondly an Mn/Fe ratio suitable for comparison with the Mn/Fe ratio calculated from electron spin resonance studies of the same shales (Chapter 6). The ratio is determined using the following equation: Mn/Fe = MnO (%) x 100.0/Fe oxides (%).

Of the major oxides, Al_2O_3, Fe oxides and SiO_2 show lower mean

TABLE 4.3 Precision and sensitivity of the spectroscopic technique

	Al_2O_3	CaO	Fe	K_2O	MgO	SiO_2	MnO	Ba	Be	Bi	Co	Cr	Cu	Ga
Precision (%)	8.8	8.6	10.9	17.7	13.5	8.0	6.1	12.5	6.2	8.6	9.8	15.1	9.6	3.8
Sensitivity (ppm)							8	2	1	1	2	8	6	1

	Ge	Li	Mo	Ni	Pb	Sn	Sr	V	Zn(i)	Zn(ii)	Zr
Precision (%)	10.0	5.6	15.2	10.9	15.6	17.5	9.0	11.8	9.0	14.1	18.0
Sensitivity (ppm)	1	2	6	9	8	4	1	3	24	11	8

TABLE 4.4 Accuracy of the spectroscopic technique

A comparison of results obtained by Flanagan (1969) and Celenk (1972) for rock standards GSP-1, AGV-1 and PCC-1.

Standard Rock		MnO	Ba	Co	Cr	Cu	Ga	Li	Ni	Pb	Sr	V	Zn	Zr	RESULTS BY
GSP-1	RANGE	260-	855-	<3-	5-	15-	12-	-	3-	14-	148-	38-	54-	323-	Flanagan
		450	2000	22	18	54	35		25	80	400	67	340	685	1969
	MEAN	326	1360	8	13	35	19	36	11	52	247	52	143	544	
GSP-1	RANGE	205-	1029-	2-	B.D.-	23-	16-	9-	B.D.-	44-	168-	16-	23-	256-	Celenk
		297	1576	15	14	45	25	39	8	80	362	114	143	745	1972
	MEAN	261	1308	8	5	34	21	20	2	66	263	52	67	436	
AGV-1	RANGE	640-	1047-	10-	8-	52-	14-	-	11-	18-	348-	70-	64-	186-	Flanagan
		870	2700	30-	45	83	24		27	48	1050	171	304	315	1969
	MEAN	728	1410	16	13	64	18	12	18	35	657	121	112	227	
AGV-1	RANGE	423-	900-	2-	B.D.-	48-	14-	B.D.-	B.D.-	18-	458-	46-	66-	129-	Celenk
		759	1431	20	11	78	22	17	18	53	858	272	141	342	1972
	MEAN	592	1134	0	4	65	19	6	6	37	618	83	101	194	
PCC-1	RANGE	610-	-	80-	1840-	5-	-	-	1750-	-	-	21-	24-	-	Flanagan
		1430		330	4780	6			3400			55	100		1969
	MEAN	889	7	112	3090	10	12	0	2430	13	<1	31	53	0	
PCC-1	RANGE	623-	B.D.-	88-	1830-	B.D.-	B.D.-	B.D.-	1528-	B.D.-	B.D.-	8-	22-	B.D.-	Celenk
		1126	13	173	3181	7	4	4	2950	21	2	34	128	24	1972
	MEAN	851	2	91	2169	7	1	0	1898	5	0	23	85	9	

N.B. B.D. = Below detection limit

Kansas Geological Survey

Open File Report 1975-01

Missing Page 73

TABLE 4.6 Results of the analysed standard (major oxides)

Sample	Al_2O_3(%)	CaO(%)	Total Fe Oxides(%)	K_2O(%)	MgO(%)	SiO_2(%)	MnO (ppm)
T1	16.0	5.1	5.6	1.3	1.7	63.0	700-940
Analysed Sample	16.0	4.0	5.3	1.0	1.2	61.0	740
GSP	15.0	2.0	4.3	5.5	1.0	67.0	200-453
Analysed Sample	14.0	1.9	3.5	5.6	0.4	58.0	252
AGV	17.0	5.0	6.8	2.9	1.5	59.0	700-900
Analysed Sample	15.0	4.2	5.2	2.7	0.9	53.0	643
BCR	13.6	7.0	13.5	1.7	3.3	55.0	1700
Analysed Sample	14.0	6.1	8.4	1.6	2.7	51.0	>1229
PCC	0.8	0.5	8.5	0.01	44.0	42.0	600-1400
Analysed Sample	0.0	0.1	12.5	0.40	43.7	43.0	846
G-1	14.0	1.4	1.7	5.5	0.4	72.0	180-350
Analysed Sample	14.0	1.0	1.0	4.7	0.2	61.0	196
G-2	15.0	2.0	2.8	4.5	0.8	69.0	300
Analysed Sample	14.0	1.6	1.7	3.3	0.3	59.0	239
W-1	15.0	10.7	10.0	0.6	6.6	52.0	1700
Analysed Sample	13.0	8.7	9.1	0.4	4.9	48.0	1193
DTS	0.6	0.2	8.9	0.02	50.0	41.0	1200
Analysed Sample	0.0	0.0	14.0	0.0	60.0	39.0	910
Trends			Low Reading			Low	
Comments			PCC and DTS have interference from MgO				

TABLE 4.6 (continued) Results of analysed standards (minor elements ppm)

Sample	Ag	Ba	Be	Bi	Cd	Co	Cr	Cu	Ga
T-1	<1	560-800	1	<10	<20	10-20	17-35	30-55	17-25
Analysed Sample	17	505	5	1	28	17	18	50	24
GSP	<1	1000-1800	<2	<.5	<2	8	13	15-54	12-35
Analysed Sample	0	1098	4	0	17	8	10	29	26
AGV	<1	1000-1700	<4	<1	<2	16	8-20	52-83	14-24
Analysed Sample	0	976	6	1	31	17	8	54	26
BCR	<1	500-1230	3	<5	<2	36	8-45	7-33	22
Analysed Sample	0	526	10	4	14	38	8	16	26
PCC	<1	7	0-3	<5	<2	90-300	1840-4780	5-16	4-22
Analysed Sample	0	7	4	2	0	149	2048	6	3
G-1	<1	1100-1270	3	3	0	<10-5	22	8-20	18
Analysed Sample	0	886	5	0	25	6	20	8	25
G-2	< 1	1500-2300	<3-3	<1	<2	2-8	5-12	<2-17	16-31
Analysed Sample	0	1415	6	0	19	3	6	7	24
W-1	<1	150-220	<3-3	-	<1	50	120	110	13-30
Analysed Sample	0	130	6	3	9	53	121	414	23
DTS	<1	0-6	<4	<1	<2	100-200	2840-5560	<2-15	3-21
Analysed Sample	0	0	4	2	0	167	2480	4	3
Trends						High			
Comments		Low readings at high levels				Not satis-factory			

TABLE 4.6 (continued)

Sample	Ge	Li	Mo	Ni	Pb	Sn
T-1	<10	8	2.5	2-32	14-50	29-50
Analysed Sample	2	11	34	19	33	27
GSP	<1	25-47	1-26	3-25	14-80	<10-15
Analysed Sample	0	24	3	24	59	0
AGV	1	9-15	2-5.5	11-27	18-48	<10-6
Analysed Sample	2	9	30	27	42	0
BCR	<2-2	10-19	<3-7	3-30	5-35	<10-10
Analysed Sample	4	18	54	19	24	0
PCC	< .5	< 2-17	< 1-6.5	1750-3400	<4-27	< 20-3
Analysed Sample	3	0	14	1903	23	31
G-1	1	17-25	4-14	1-21	21-58	1-9
Analysed Sample	0	15	28	12	59	0
G-2	<1	25-63	<1-2	2-14	15-43	<5-2
Analysed Sample	0	22	5	9	30	0
W-1	<1-2	8-15	<1-1.0	51-110	5-20	2
Analysed Sample	5	22	43	88	1	2
DTS	< 1	< 2-27	< 1-8	1770-3300	< 4-28	<20-4
Analysed Sample	3	0	18	1915	19	15
Trends			High			
Comments			Not a satis-factory line			

TABLE 4.6 (continued)

Sample	Sr	V	Zn	Zr
T-1	315-500	65-120	160-220	120-230
Analysed Sample	365	165	343	134
GSP	148-400	38-67	34-340	333-687
Analysed Sample	246	97	219	614
AGV	348-1050	70-171	64-304	180-315
Analysed Sample	596	176	200	118
BCR	244-525	120-700	94-278	144-275
Analysed Sample	292	542	256	112
PCC	< 1	21-55	24-100	<10
Analysed Sample	0	98	100	0
G-1	200-286	10-21	25-48	101-220
Analysed Sample	262	110	168	157
G-2	235-680	26-60	42-138	250-400
Analysed Sample	482	92	195	231
W-1	180-210	213-300	42-95	85-120
Analysed Sample	190	286	194	53
DTS	< 2	6-52	22-140	<10
Analysed Sample	0	42	150	0
Trends		High	High	Low
Comments		generally at low concen-trations		slightly

TABLE 4.7 Summary statistics for major oxides and minor elements

Element \ Statistic	Mean	Standard Deviation	Median	Minimum	Maximum	
Al_2O_3	14.16	3.57	15.40	4.10	20.20	PERCENT
CaO	8.44	8.94	4.60	0.10	38.00	PERCENT
Fe Oxides	4.72	1.34	4.70	1.80	10.30	PERCENT
K_2O	2.73	0.82	2.80	0.10	4.90	PERCENT
MgO	3.13	3.14	2.30	0.30	26.80	PERCENT
SiO_2	55.29	15.88	58.90	14.60	114.00	PERCENT
Mn/Fe	1.04	0.92	0.70	0.10	5.60	
MnO	462.42	477.73	330.00	65.00	3297.00	
Ag	1.25	4.76	0.00	0.00	46.00	
Ba	345.69	178.86	347.00	92.00	1594.00	
Be	5.15	1.94	5.00	2.00	12.00	
Bi	1.46	1.58	1.00	0.00	8.00	
Cd	29.87	25.74	23.00	0.00	168.00	P.P.M.
Co	39.98	25.33	35.00	7.00	224.00	P.P.M.
Cr	139.81	188.38	95.00	35.00	1428.00	
Cu	28.70	26.04	23.00	2.00	140.00	
Ga	18.94	5.97	20.00	3.00	32.00	
Ge	1.94	2.25	1.00	0.00	14.00	
Li	54.09	29.32	47.00	6.00	169.00	
Mo	28.32	73.53	7.00	0.00	713.00	
Ni	78.52	86.32	53.00	14.00	661.00	
Pb	27.72	43.71	15.00	2.00	356.00	
Sn	0.76	2.78	0.00	0.00	20.00	
Sr	286.28	283.32	190.00	21.00	1844.00	
V	197.91	402.46	114.00	19.00	3607.00	
Zn	207.90	179.07	182.00	0.00	909.00	
Zr	213.28	107.02	189.00	17.00	730.00	
Heat Loss	6.73	4.18	-	0.50	29.90	Percent

values than the "average shale" (Clarke, 1924) and MgO and CaO show higher values (Table 4.8). The results do, however, compare favourably with Clarke's average Mesozoic and Cenozoic shale (Clarke, 1924) indicating that there is a greater percentage of carbonates present than in other Palaeozoic shales. Similarly, of the minor elements and oxides, MnO, Ba, Cu, and Sr give lower values than reported for the "average shale" and Cd, Co, Mo, V, Zn and Zr show higher means.

Ag, Be, Bi, Ge, and Sn are only recorded in minor quantities in samples and therefore appear to have little influence on geochemical variation in the Upper Pennsylvanian and Lower Permian shales. Of the remaining elements and oxides, many show considerable numerical variation with standard deviations of the same order as the means. In terms of the elements, this indicates a lognormal distribution but as no statistical guidelines are available to determine whether the observed frequencies (Fig. 4.1) are lognormal or not, only raw data is used in further operations. Subsequently, Link and Koch (1975) have applied lognormal theory to pseudolognormal distributions and have shown that positive or negative bias or a combination of the two, can occur.

STRATIGRAPHIC VARIATION IN THE GEOCHEMISTRY

The variation of major oxides (Figs. 4.2 and 4.3) indicates both lithological and stratigraphical control of Upper Pennsylvanian and Lower Permian shales. SiO_2, in particular, is distributed in zones that correspond to those established from mineralogical variation in the same shales. The Pleasanton, Kansas City and Lansing Groups form a zone of highly variable SiO_2 values (from 35 to 70%) whereas the succeeding Douglas Group shows consistently high values (up to 90%). The Shawnee and Wabaunsee Groups show similarities to the Pleasanton-Kansas City-Lansing and Douglas zones respectively although the Shawnee has greater variability of values (20 to

TABLE 4.8 Distribution of major oxides (%) and minor elements (ppm) in shales

	Average Shale	Palaeozoic Shales	Mesozoic and Cenozoic Shales	Average Shale	Average Clay and Shale	Pennsylvanian Black Shales	Shelf and Eugeosynclinal Black Shales	Tacket Formation Black Shales	Platform Black Shales	Average Shale	Average Black Shale
Al_2O_3	15.4	16.5	13.8		16.7						
CaO	3.1	1.4	6.0		2.2						
Fe Oxides	6.5	6.9	5.7		6.5						
K_2O	3.2	3.6	2.3		3.6						
MgO	2.4	2.3	2.3		2.6						
SiO_2	58.1	60.2	55.4		58.9						
MnO				-		-	850.0	100.0	460.0	6700.0	150.0
Ag				0.1		-	0.1	2.0	3.7	0.9	1.0
Ba				-		250.0	580.0	200.0	270.0	800.0	300.0
Be				3.0		1.8	3.0	1.0	1.7	7.0	1.0
Bi				0.1		-	-	-	-	-	-
Cd				0.3		-	-	-	-	-	-
Co				20.0		7.3	19.0	7.0	19.0	12.0	10.0
Cr				100.0		290.0	90.0	500.0	260.0	160.0	100.0
Cu				57.0		70.0	45.0	100.0	130.0	38.0	70.0

TABLE 4.8 (Continued)

Ga			19.0	16.0	19.0	15.0	35.0	40.0	20.0
Ge			2.0	-	1.6	-	-	-	-
Li			60.0	-	66.0	-	-	-	-
Mo			2.0	17.0	2.6	15.0	8.9	0.7	10.0
Ni			95.0	110.0	68.0	150.0	100.0	21.0	50.0
Pb			20.0	41.0	20.0	30.0	46.0	20.0	20.0
Sn			6.0	-	-	-	-	-	-
Sr			450.0	220.0	300.0	200.0	330.0	299.0	200.0
V			130.0	260.0	130.0	500.0	220.0	130.0	150.0
Zn			80.0	-	95.0	200.0	500.0	80.0	300.0
Zr			200.0	51.0	160.0	30.0	63.0	200.0	70.0
Reference	1	2	3	4	5	6	7	8	9	10	11

REFERENCES

1. Clarke, 1924.
2. Clarke, 1924.
3. Clarke, 1924.
4. Vinogradov, 1962.
5. Wedepohl, 1967.
6. Vine, 1969.
7. Turekian and Wedepohl, 1961 with addition by Vine, 1966.
8. Vine, Tourtelot and Keith, 1969.
9. Vine and Tourtelot, 1969, 1970.
10. Green, 1959.
11. Vine and Tourtelot, 1970.

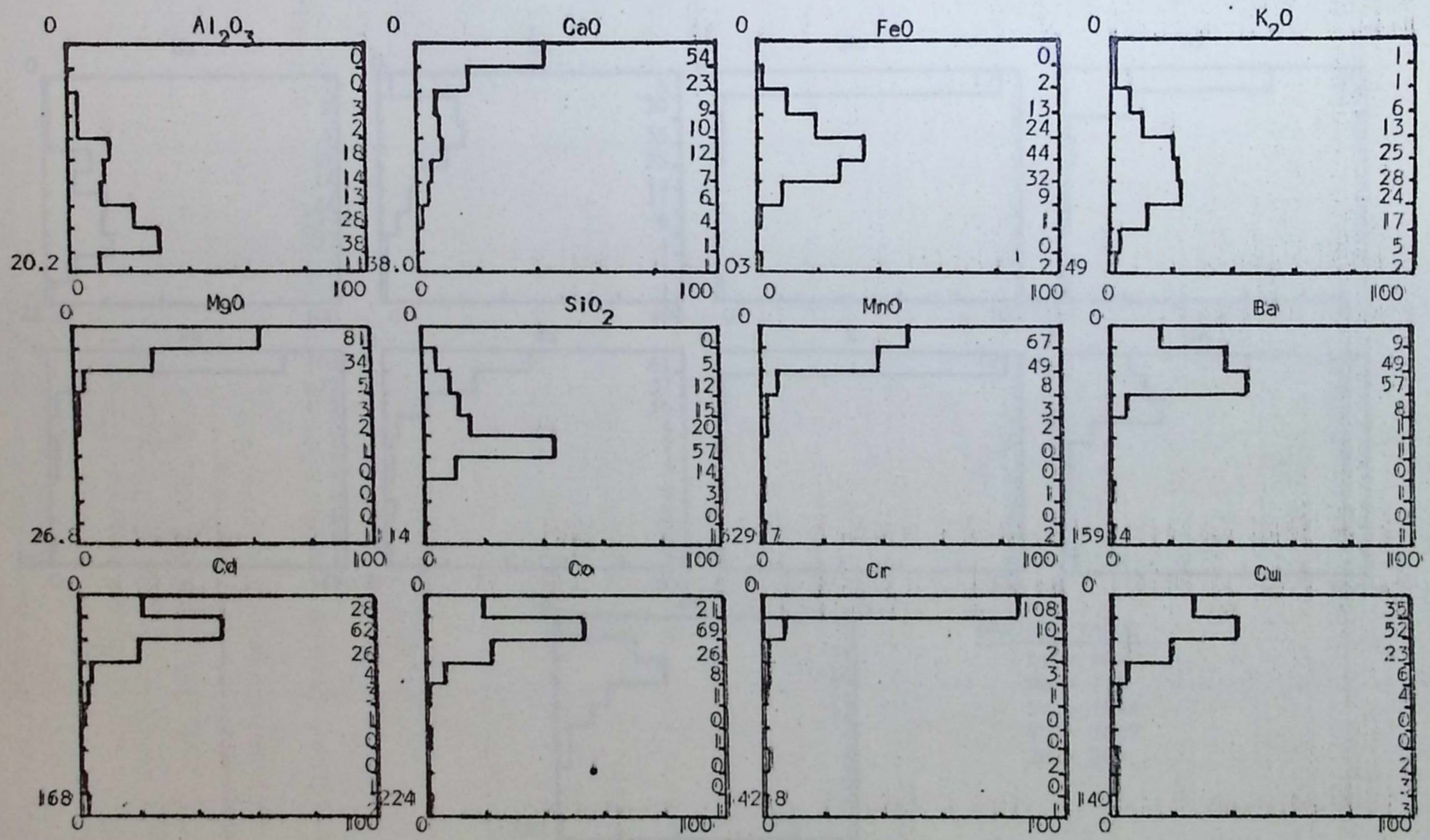

Fig. 4.1 Histograms showing the variation and distribution of major oxides and minor elements in Upper Pennsylvanian and Lower Permian shales. From Al_2O_3 to SiO_2, measurements are in % and from MnO to Zr in ppm. Scales are 0 to maximum value in 10 divisions (vertical). On the right of each histogram are the total numbers of samples contributing to each class.

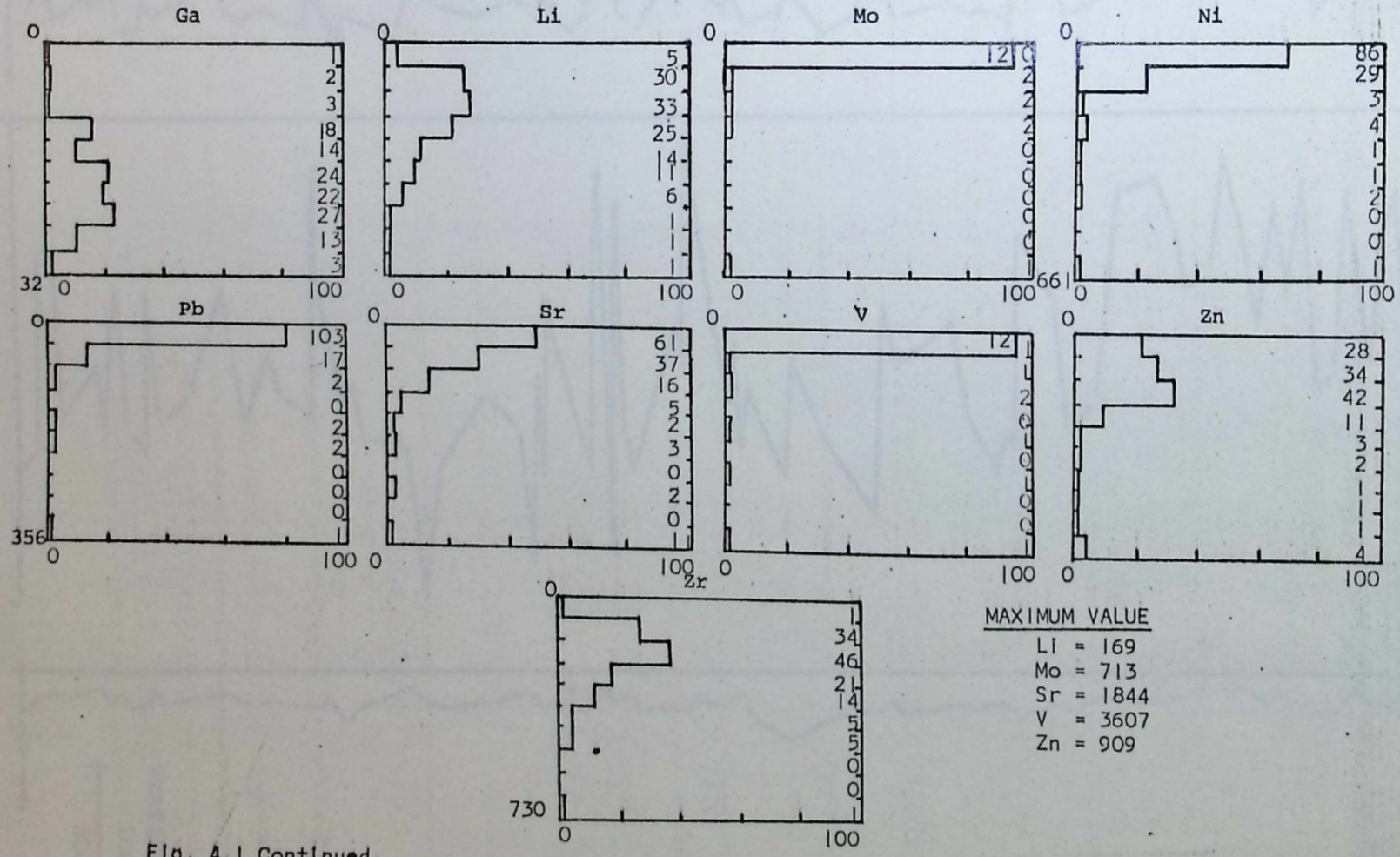

Fig. 4.1 Continued.

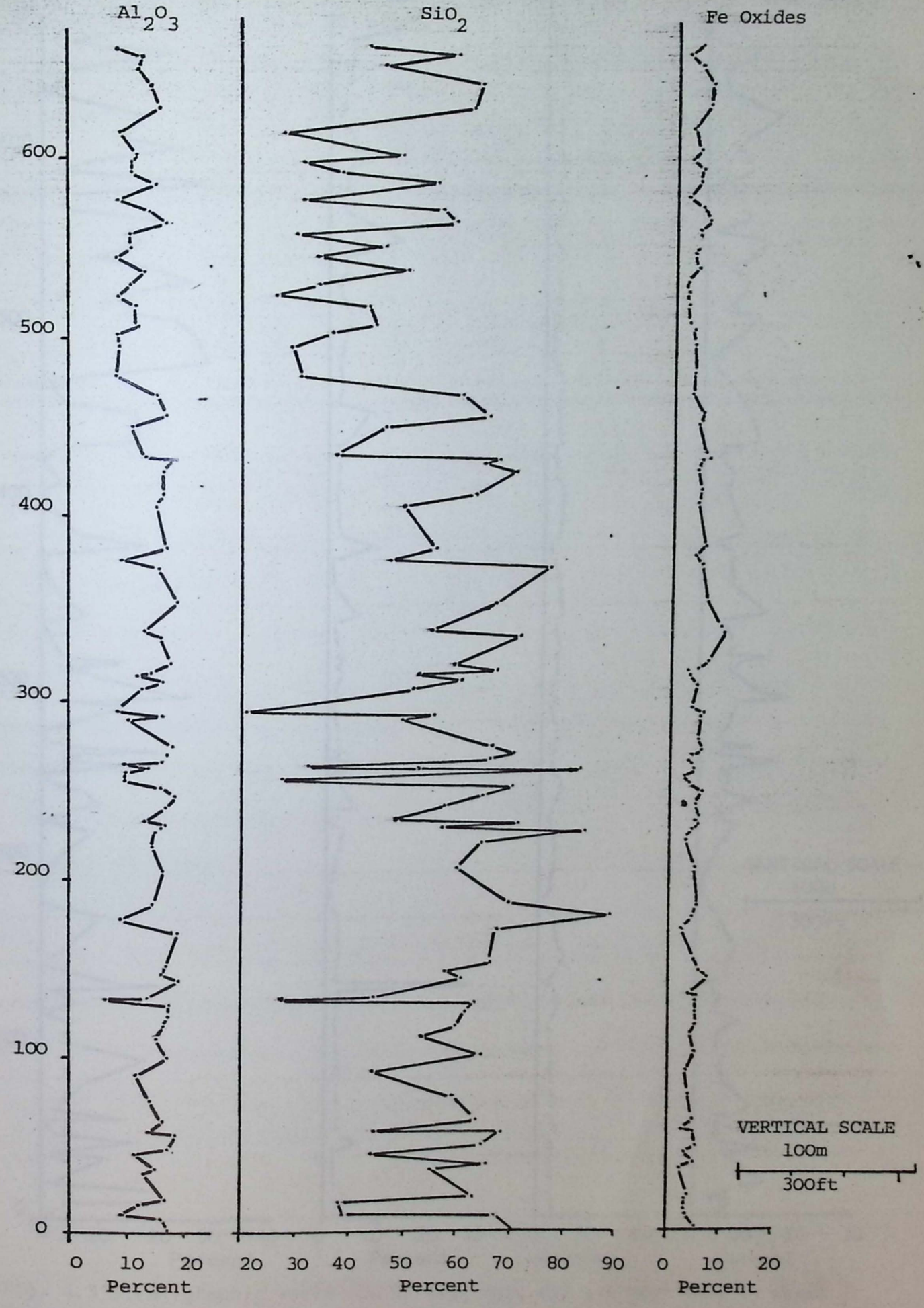

Fig. 4.2 Stratigraphic variation of Al_2O_3, SiO_2 and Fe oxides. For a comparable stratigraphic column see Fig. 3.5.

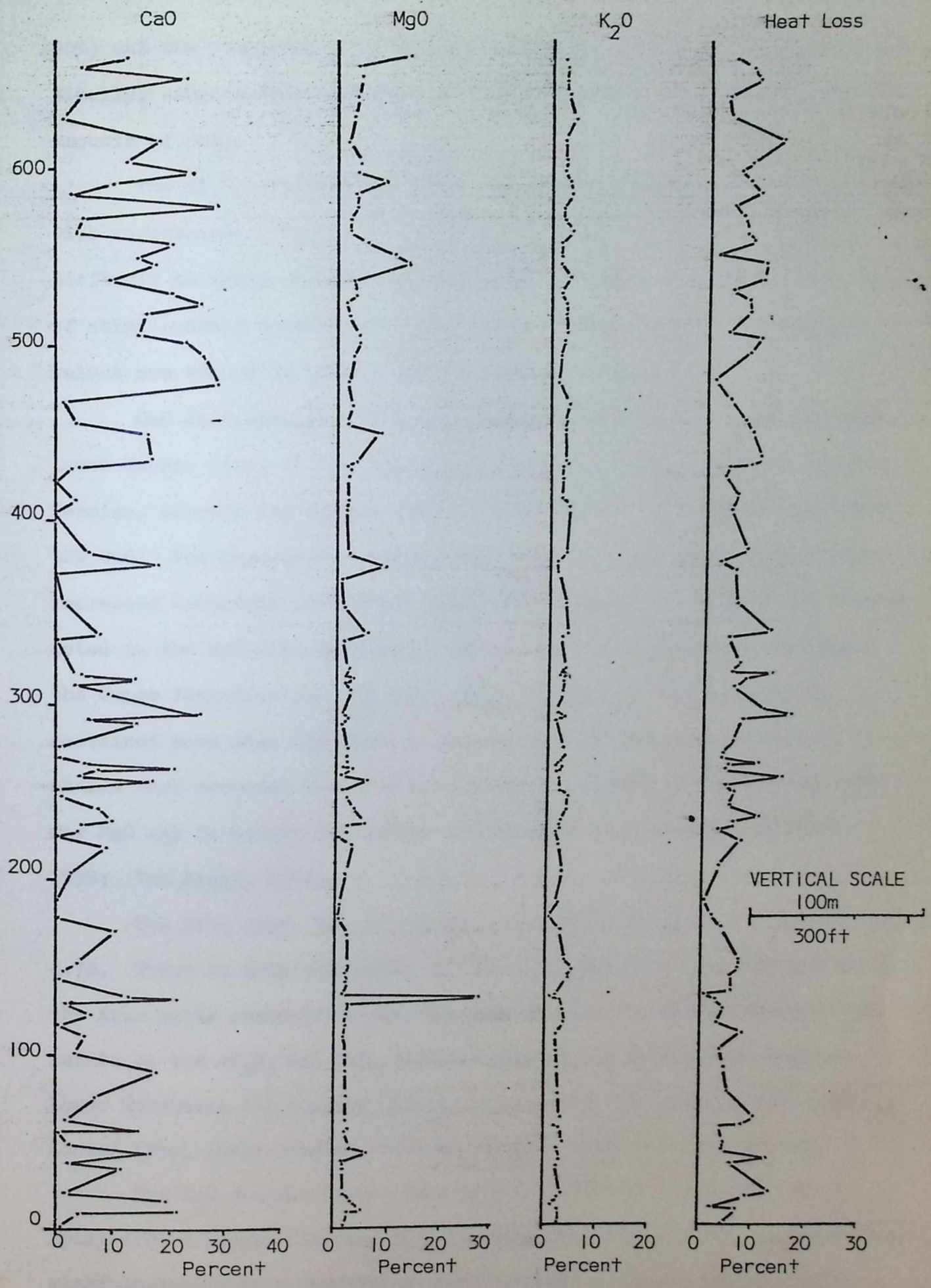

Fig. 4.3 Stratigraphic variation of CaO, MgO, K_2O and heat loss in Upper Pennsylvanian and Lower Permian shales. For a comparable stratigraphic column see Fig 3.5.

90%) and the Wabaunsee does not show such intense SiO_2 development. Finally, samples from the Permian Groups all contain relatively small amounts of SiO_2.

The Al_2O_3 distribution (Fig. 4.2) shows similarity to the SiO_2 graph with corresponding highs and lows. However, zoning the distribution is difficult as sample values only vary from 6 to 20%. The sole indication of stratigraphic control occurs in the Lower Permian where the Al_2O_3 values are around 5% lower than in the Pennsylvanian.

CaO is distributed with high values (0-40%) in the Pleasanton and Lower Kansas City, in the Lansing, in the Shawnee and also in the Lower Permian, whereas few samples from the intervening zones have greater than 10% CaO. The increase in CaO and MgO in the Permian is comparable with increased carbonate production recorded in Chapter 3. No zones are however noted in the MgO distribution as the increase is only gradual throughout the Upper Pennsylvanian and Lower Permian deposits. Only one sample contained more than 15% which is surprising as several dolomite-rich shales were detected by X-ray diffraction. However, an alternative site for MgO may be within the lattice of chlorite clay minerals (Eckhardt, 1958; Van Moort, 1972).

The iron oxide content varies from 1.8% to 10.3% with a mean of 4.7%. There is some similarity to both Al_2O_3 and SiO_2 distributions as the iron oxide curve (Fig. 4.2) has high and low values that equate with points on the Al_2O_3 and SiO_2 curves. Highs occur in the Upper Douglas, Lower Wabaunsee and Lansing Groups, whereas lows are found in the Lower Kansas City, Lower Douglas, Shawnee, Council Grove and Chase Groups.

The K_2O content ranges from 0.5% to 4.9% with a mean of 2.7%. Apart from a slight decrease in K_2O during the Lower Permian, corresponding mineralogically to a decrease in illite content (Weaver, 1967), little information can be gained from the stratigraphic variation in K_2O values.

MnO (measured in ppm) rarely exceeds 0.1% in Upper Pennsylvanian and

Lower Permian shales. Allowing, therefore, for differences of scale, the MnO (Fig. 4.4) content appears to be closely associated with the carbonate fraction of the shales. For example, the Lansing, Shawnee, Wabaunsee and Admire Groups contain beds that are rich in MnO, CaO and calcite. However, the association is not maintained in the Kansas City, Council Grove and Chase Groups. The concentration of Mn in shales may be related to an increase of Mn^{2+} ions (substituting for Ca^{2+} in calcite) in the reducing conditions (Bencini and Turi, 1974) developed at the end of the Pennsylvanian. Alternatively, the low MnO content of some calcareous shales may reflect differences in the original mineralogy of the sediments. Aragonite forms in shallow water environments (Cloud, 1962) with minor Mn substitution for Ca (Thompson, 1972). Calcite, however, predominates in deep water carbonate sediments and normally contains abundant Mn (Thompson, 1972). Therefore, the Lansing, Shawnee, Wabaunsee and Admire Groups contain shales that may represent either times of deep water sedimentation or highly reducing conditions. The Council Grove, Chase and Kansas City Groups, on the other hand, contain shales that were deposited in periods of shallow water sedimentation or less reducing conditions. Diagenetic processes, particularly dolomitization do not appear to have seriously modified the original Mn content.

Silver (Ag) is found in low concentrations in all samples (a maximum of 46 ppm) and provides negligible information for establishing the geochemical conditions prevailing during the Upper Pennsylvanian and Lower Permian. This variable, therefore, warrants no further comment. Beryllium (Be), bismuth (Bi) and germanium (Ge) are also found in minor quantities, probably as sulphides (Bi) (Goldschmidt, 1954) or within clay mineral lattices (Be and Ge) (Wedepohl, 1969, 1970).

Ba normally occurs as a substitute for Ca^{2+} in calcareous deposits. However, evidence for any such association is difficult to find in the Upper Pennsylvanian or Lower Permian shales. The distribution of barium

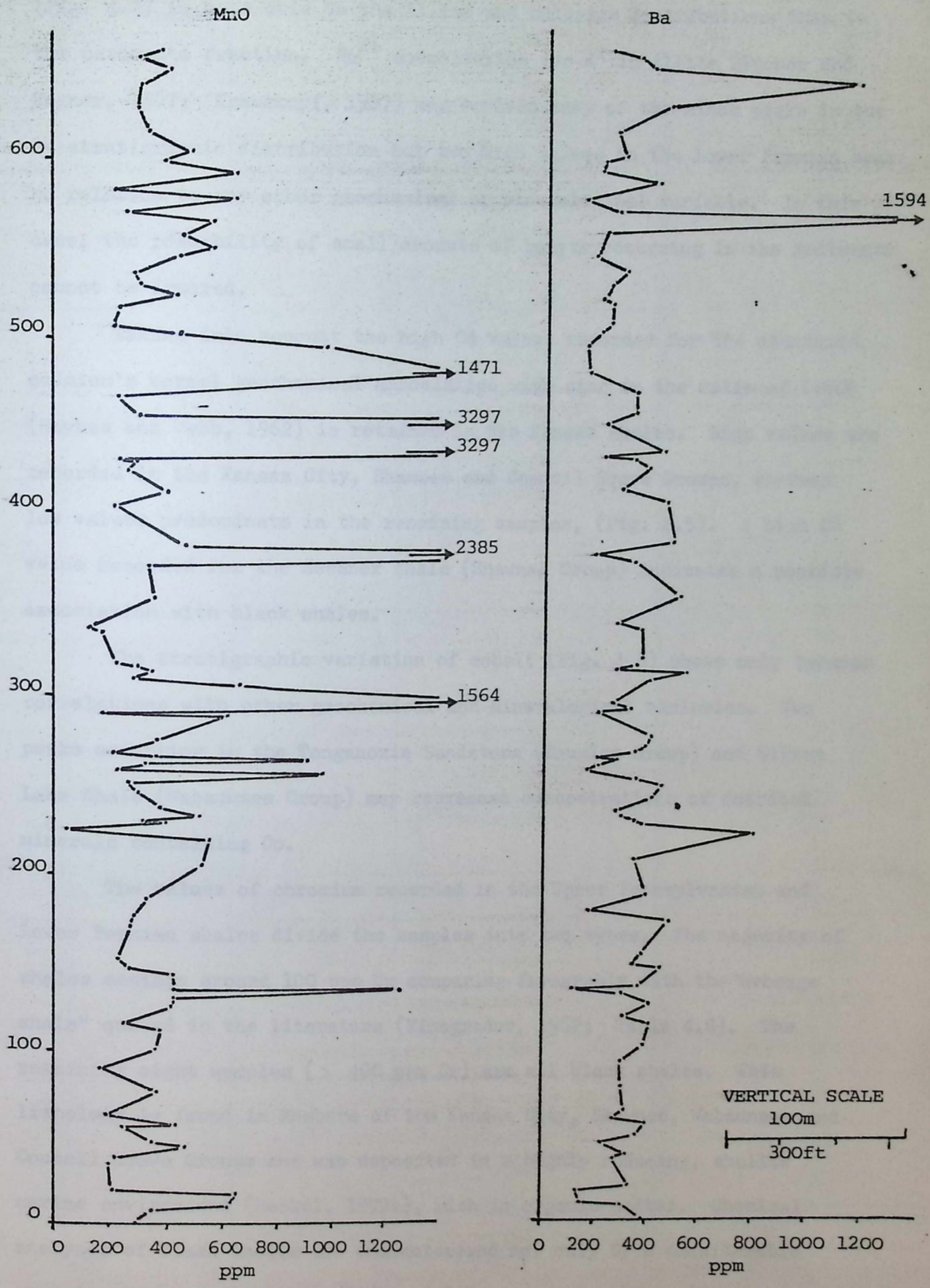

Fig.4.4 Stratigraphic variation in MnO and Ba in Upper Pennsylvanian and Lower Permian shales. For a stratigraphic column see Fig.3.5.

(Fig. 4.4) is more akin to the illite and chlorite distributions than to the carbonate fraction. Ba^{2+} substitution for K^{+} in illite (Fenner and Hagner, 1967; Krauskopf, 1967) may explain many of the minor peaks in the Ba stratigraphic distribution but two high values in the Lower Permian bear no relation to any other geochemical or mineralogical variable. In this case, the possibility of small amounts of baryte occurring in the sediments cannot be ignored.

Taking into account the high Cd values recorded for the standards, cadmium's normal geochemical association with zinc in the ratio of 1:500 (Hawkes and Webb, 1962) is retained in the Kansas shales. High values are recorded in the Kansas City, Shawnee and Council Grove Groups, whereas low values predominate in the remaining samples, (Fig. 4.5). A high Cd value recorded for the Heebner shale (Shawnee Group) indicates a possible association with black shales.

The stratigraphic variation of cobalt (Fig. 4.5) shows only tenuous correlations with other geochemical and mineralogical variables. Two peaks occurring in the Tonganoxie Sandstone (Douglas Group) and Silver Lake Shale (Wabaunsee Group) may represent concentrations of detrital minerals containing Co.

The values of chromium recorded in the Upper Pennsylvanian and Lower Permian shales divide the samples into two types. The majority of shales contain around 100 ppm Cr comparing favourably with the "average shale" quoted in the literature (Vinogradov, 1962; Table 4.8). The remaining eight samples (> 400 ppm Cr) are all black shales. This lithology is found in Members of the Kansas City, Shawnee, Wabaunsee and Council Grove Groups and was deposited in a highly reducing, shallow marine environment (Heckel, 1972a), rich in organic matter. Chemical analyses of black shales are characterised not only by a considerable organic carbon content but also by sulphur present as FeS_2 (Vine and Tourtelot, 1970). Minor elements such as V, Mo, Cu, Ni, Pb, Zn and Cr are

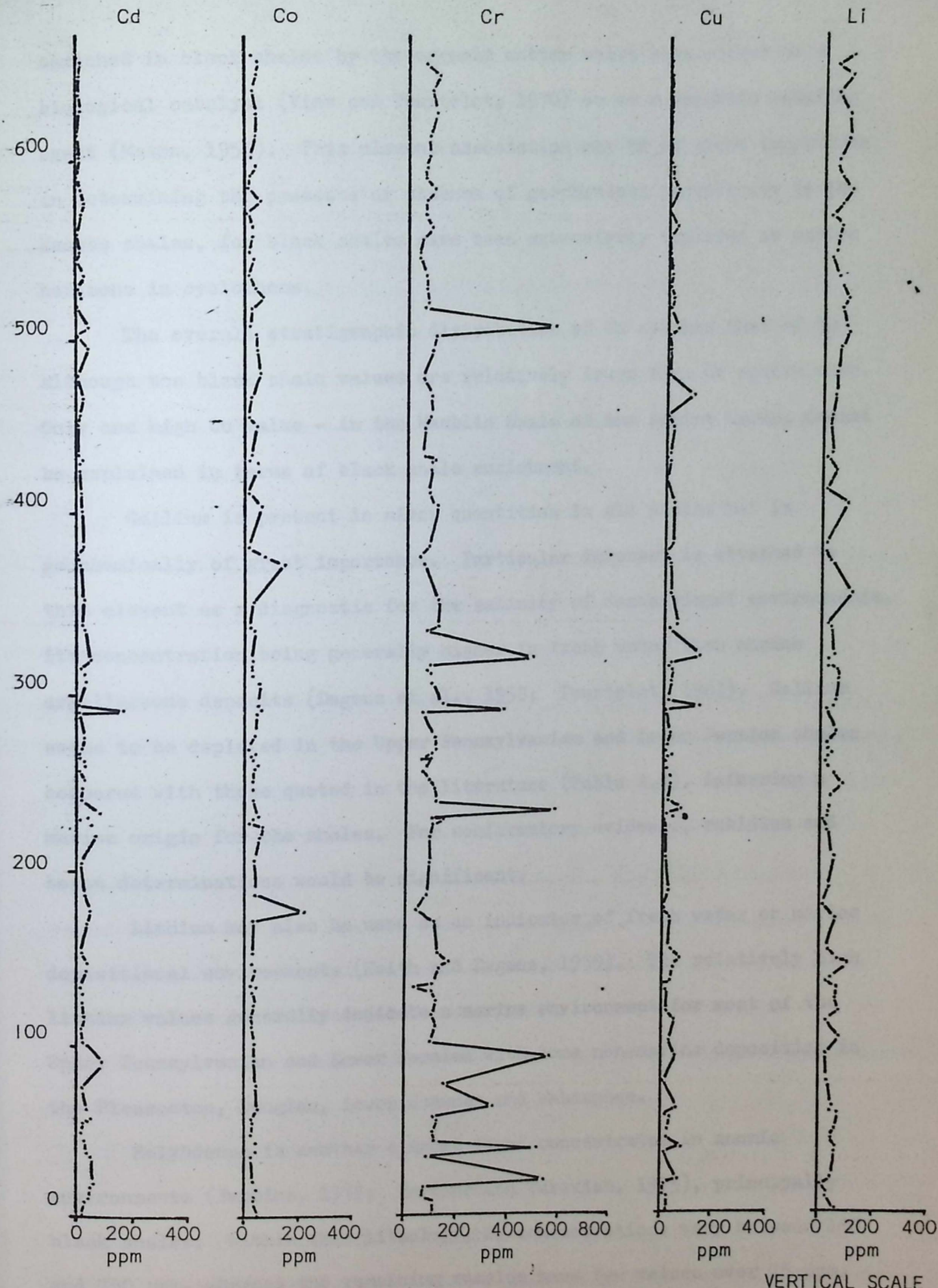

Fig. 4.5 Stratigraphic variation of Cd, Co, Cr, Cu and Li in Upper Pennsylvanian and Lower Permian shales. For a comparable stratigraphic column see Fig. 3.5

enriched in black shales by the organic matter which acts either as a biological catalyst (Vine and Tourtelot, 1970) or as a sulphide reducing agent (Mason, 1958). This element association may be of great importance in determining the presence or absence of geochemical periodicity in the Kansas shales, for black shales have been extensively employed as marker horizons in cyclothems.

The overall stratigraphic distribution of Cu matches that of Cr although the black shale values are relatively lower than Cr equivalents. Only one high Cu value - in the Hamblin Shale of the Admire Group, cannot be explained in terms of black shale enrichment.

Gallium is present in minor quantities in all shales but is geochemically of great importance. Particular interest is attached to this element as a diagnostic for the salinity of depositional environments, its concentration being generally higher in fresh water than marine argillaceous deposits (Degens et al., 1958; Tourtelot, 1964). Gallium seems to be depleted in the Upper Pennsylvanian and Lower Permian shales compared with those quoted in the literature (Table 4.8), inferring a marine origin for the shales. For confirmatory evidence, rubidium and boron determinations would be significant.

Lithium may also be used as an indicator of fresh water or marine depositional environments (Keith and Degens, 1959). The relatively high lithium values generally indicate a marine environment for most of the Upper Pennsylvanian and Lower Permian with some non-marine deposition in the Pleasanton, Douglas, Lower Shawnee and Wabaunsee.

Molybdenum is another element found concentrated in anoxic environments (Bertine, 1972; Bertine and Turekian, 1973), principally black shales. Within this lithology, Mo concentrations vary between 150 and 750 ppm, whereas the remaining samples have few values over 75 ppm. The Mo distribution has peaks in the Pleasanton, Shawnee (in which the Heebner Shale is prominent), Wabaunsee and Lower Permian Groups. In the

case of the Lower Permian Groups, there seems to have been a general rise in the Mo concentration from negligible amounts in the Upper Wabaunsee to between 30 and 100 ppm for most Permian sediments (Fig. 4.6).

Nickel values are also arranged according to the development of black shales and show close correspondence to the Cr, Cu, Mo, Pb and Zn distributions. The majority of samples have values in the range 0 to 100 ppm (Fig. 4.6), whereas those samples associated with black shales have values ranging from 100 to 700 ppm.

Lead (Pb) shows a similar distribution (Fig. 4.6) to Ni with only minor differences in the Wabaunsee Group samples. Here, two peaks in the Poney Creek Shale and Silver Lake Shale, correspond to similar peaks in the Mo distribution (Fig. 4.6) and may be connected with pyrite or organic residues (Wedepohl, 1974). Enriched shales have Pb values that range from 100 to 400 ppm (high for black shales (Wedepohl, 1974)), whereas other samples all contain less than 100 ppm Pb.

Strontium, like most other trace elements, has a bimodal distribution (Fig. 4.1), with many shale samples lying in the range 50-300 ppm and a few in the range 300-1900 ppm. Of the samples from the upper range, most are calcareous shales from the Kansas City, Shawnee, Upper Wabaunsee and Council Grove Groups. The strontium distribution (Fig. 4.6) appears to be associated with the carbonate fraction and may be controlled by salinity and basinal depth (Veizer and Demovic, 1974). The higher values, coinciding with high carbonate content, may therefore, indicate 'hypersaline' or deep water conditions. This evidence is in agreement with the MnO interpretation of the Shawnee, Upper Wabaunsee and Admire Groups, but shows discrepancies in the Kansas City and Lower Wabaunsee Groups. The latter case may be explained in terms of low carbonate content but the Kansas City values seem contradictory. Therefore, before the implications of carbonate geochemistry can be extensively applied to calcareous shales, further experimentation and analysis are required. Meanwhile, it can be

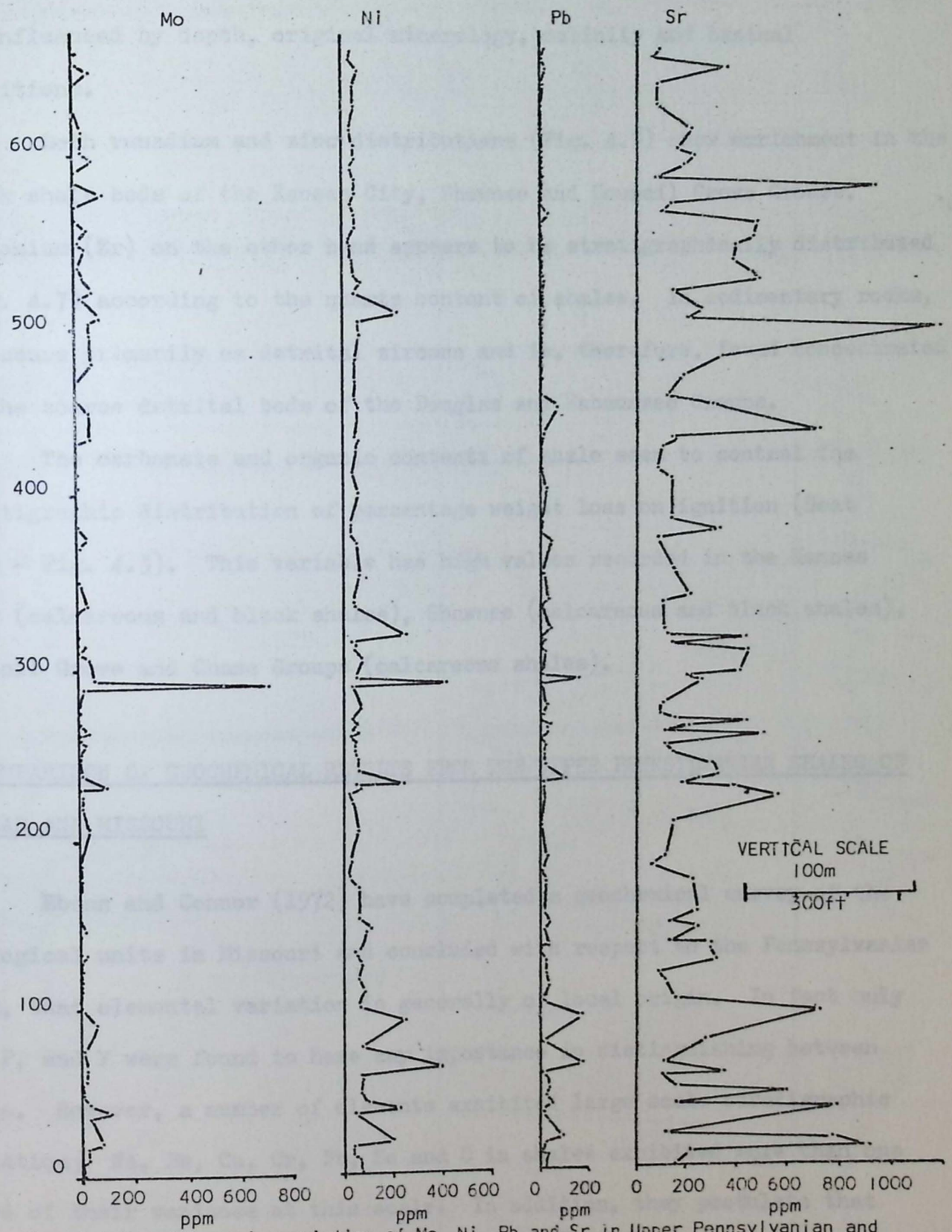

Fig. 4.6 Stratigraphic variation of Mo, Ni, Pb and Sr in Upper Pennsylvanian and Lower Permian shales. For a comparable stratigraphic column, see Fig. 3.5.

stated that there appears to be a close correlation between MnO, Sr and the carbonate fraction and that the MnO and Sr content of the shales may be influenced by depth, original mineralogy, salinity and basinal conditions.

Both vanadium and zinc distributions (Fig. 4.7) show enrichment in the black shale beds of the Kansas City, Shawnee and Council Grove Groups. Zirconium (Zr) on the other hand appears to be stratigraphically distributed (Fig. 4.7) according to the quartz content of shales. In sedimentary rocks, Zr occurs primarily as detrital zircons and is, therefore, found concentrated in the coarse detrital beds of the Douglas and Wabaunsee Groups.

The carbonate and organic contents of shale seem to control the stratigraphic distribution of percentage weight loss on ignition (Heat Loss - Fig. 4.3). This variable has high values recorded in the Kansas City (calcareous and black shales), Shawnee (calcareous and black shales), Council Grove and Chase Groups (calcareous shales).

A COMPARISON OF GEOCHEMICAL RESULTS FROM THE UPPER PENNSYLVANIAN SHALES OF KANSAS AND MISSOURI

Ebens and Connor (1972) have completed a geochemical survey of the geological units in Missouri and concluded with respect to the Pennsylvanian beds, that elemental variation is generally of local origin. In fact only Na, P, and Y were found to have any importance in distinguishing between areas. However, a number of elements exhibited large scale stratigraphic variation; Na, Be, Ca, Cr, Pb, Se and C in shales exhibited more than one third of their variance at this scale. In addition, they postulate that such variation reflects environmental differences between the limestone- and coal-bearing deposits. As a result, the base of the Kansas City Group is thought to mark a natural subdivision between the upper limestone-bearing deposits and the lower coal-bearing deposits.

Although the majority of beds under examination in this thesis fall

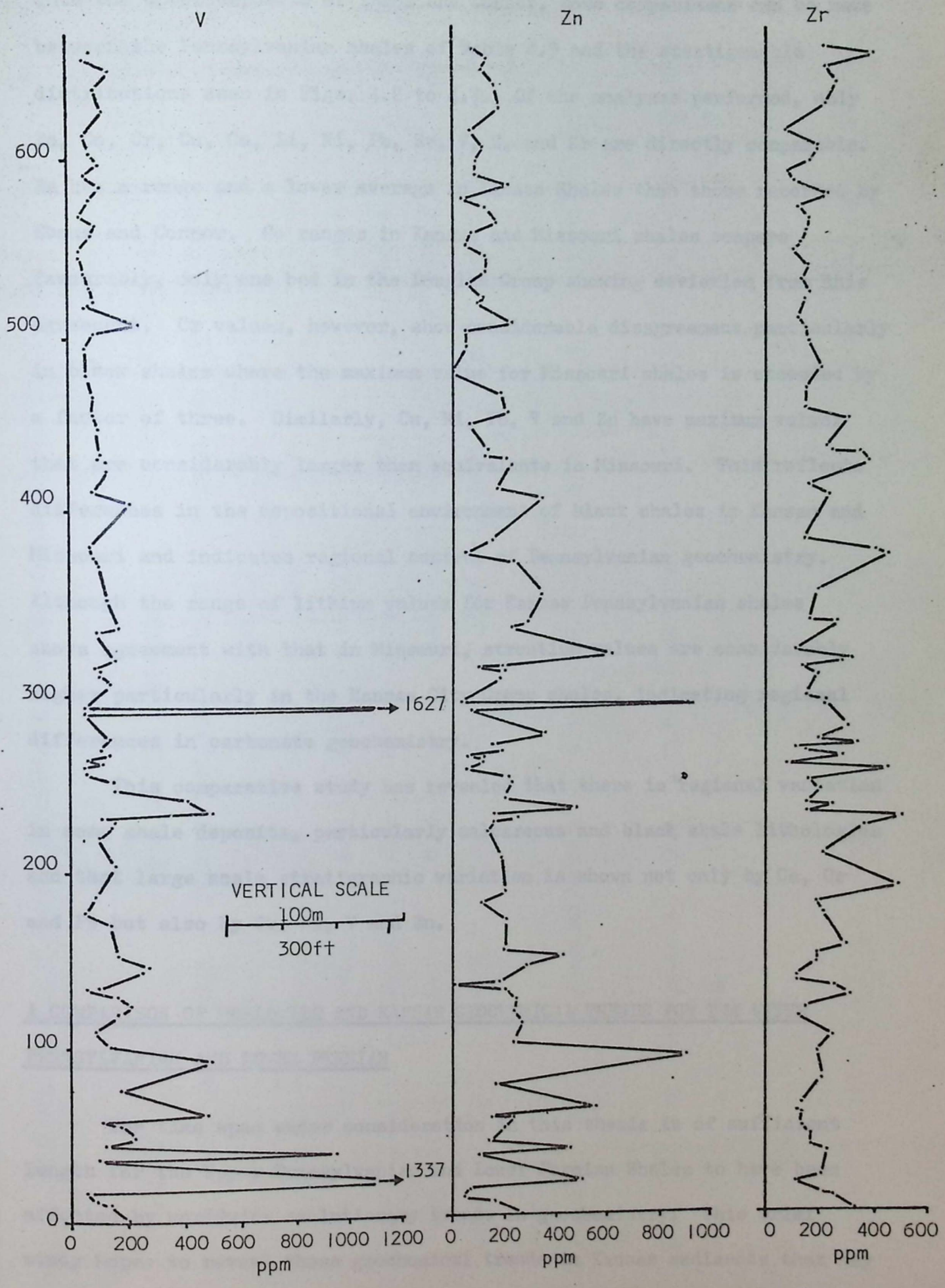

Fig. 4.7 Stratigraphic variation of V, Zn and Zr in Upper Pennsylvanian and Lower Permian shales of Kansas. For a comparable stratigraphic column, see Fig. 3.5.

into the upper deposits of Ebens and Connor, some comparisons can be made between the Pennsylvanian shales of Table 4.9 and the stratigraphic distributions seen in Figs. 4.2 to 4.7. Of the analyses performed, only Ba, Co, Cr, Cu, Ga, Li, Ni, Pb, Sr, V, Z, and Zr are directly comparable. Ba has a range and a lower average in Kansas Shales than those recorded by Ebens and Connor. Co ranges in Kansas and Missouri shales compare favourably, only one bed in the Douglas Group showing deviation from this agreement. Cr values, however, show considerable disagreement particularly in black shales where the maximum value for Missouri shales is exceeded by a factor of three. Similarly, Cu, Ni, Pb, V and Zn have maximum values that are considerably larger than equivalents in Missouri. This reflects differences in the depositional environment of black shales in Kansas and Missouri and indicates regional control of Pennsylvanian geochemistry. Although the range of lithium values for Kansas Pennsylvanian shales shows agreement with that in Missouri, strontium values are considerably higher particularly in the Kansas City Group shales, indicating regional differences in carbonate geochemistry.

This comparative study has revealed that there is regional variation in some shale deposits, particularly calcareous and black shale lithologies and that large scale stratigraphic variation is shown not only by Ca, Cr and Pb but also by Cu, Ni, V and Zn.

A COMPARISON OF WORLDWIDE AND KANSAS GEOCHEMICAL TRENDS FOR THE UPPER PENNSYLVANIAN AND LOWER PERMIAN

The time span under consideration in this thesis is of sufficient length for the Upper Pennsylvanian and Lower Permian Shales to have been affected by worldwide evolutionary trends in geochemistry. This brief study hopes to reveal those geochemical trends in Kansas sediments that may have been altered or accentuated by worldwide geochemical evolution.

TABLE 4.9 Statistical Summary of Element Concentrations in Pennsylvanian Deposits of Missouri
(Data from Ebens and Connor, 1972)

	PENNSYLVANIAN SHALES			PENNSYLVANIAN LIMESTONES			PENNSYLVANIAN SANDSTONES			ANALYTICAL TECHNIQUE
	AVERAGE	VARIATION	RANGE	AVERAGE	VARIATION	RANGE	AVERAGE	VARIATION	RANGE	
Al	8.5	1.2	5.5-13.0	0.58	2.0	0.15-2.2	3.0	2.3	0.57-16.0	XRF
Ca	0.75	4.2	0.04-13.0	30.0	1.4	15.0-60.0	0.35	7.9	0.01-22.0	XRF
Fe	3.8	1.5	1.7-8.5	0.96	2.5	0.16-6.0	1.9	2.1	0.45-8.1	XRF
K	2.7	1.3	1.6-4.5	0.17	2.5	0.03-1.1	0.66	2.8	0.08-5.2	XRF
Mg	0.95	1.5	0.45-2.0	0.67	4.1	0.04-11.0	0.21	4.3	0.01-3.9	AA
Si	27.0	1.2	20.0-35.0	2.9	3.0	0.33-26.0	34.0	1.6	13.0-90.0	XRF
Mn/Fe	-	-	-	-	-	-	-	-	-	-
MnO	170.0	2.0	44.0-660.0	830.0	2.4	150.0-4700.0	300.0	4.6	14.0-6300.0	SPECTROGRAPHIC
Ag	-	-	-	-	-	-	-	-	-	-
Ba	430.0	1.5	200.0-950.0	44.0	3.0	49.0-400.0	170.0	2.2	36.0-810.0	SPECTROGRAPHIC
Be	1.7	1.4	0.80-3.4	< 1.0	-	-	< 1.0	-	-	-
Bi	-	-	-	-	-	-	-	-	-	-
Cd	-	-	-	-	-	-	-	-	-	-
Co	12.0	1.7	4.2-33.0	< 3.0	-	-	7.2	2.7	0.98-53.0	SPECTROGRAPHIC

TABLE 4.9 (Continued)

Cr	95.0	1.3	60.0-150.0	16.0	2.1	3.7-71.0	33.0	2.3	6.5-170.0	SPECTROGRAPHIC
Cu	23.0	26.0	3.4-160.0	3.5	2.1	0.77-16.0	8.4	2.5	1.3-54.0	SPECTROGRAPHIC
Ga	30.0	1.5	14.0-63.0	<5.0	-	-	11.0	2.1	2.5-44.0	SPECTROGRAPHIC
Ge	-	-	-	-	-	-	-	-	-	-
Li	79.0	1.5	36.0-170.0	<5.0	-	-	17.0	2.3	3.2-88.0	AA
Mo	-	-	-	-	-	-	-	-	-	-
Ni	38.0	1.5	17.0-86.0	5.1	1.9	1.4-18.0	19.0	2.9	2.3-150.0	SPECTROGRAPHIC
Pb	17.0	1.9	4.7-64.0	<10.0	-	-	17.0	2.0	4.3-69.0	SPECTROGRAPHIC
Sn	-	-	-	-	-	-	-	-	-	-
Sr	200.0	1.7	73.0-540.0	990.0	3.9	67.0-15,000.0	95.0	4.2	5.4-1700.0	SPECTROGRAPHIC
V	140.0	1.4	77.0-260.0	16.0	2.3	3.0-81.0	38.0	2.2	7.5-190.0	SPECTROGRAPHIC
Zn	82.0	1.5	38.0-180.0	24.0	2.3	4.4-130.0	33.0	3.0	3.8-290.0	AA
Zr	110.0	1.5	53.0-250.0	16.0	2.3	3.0-81.0	170.0	2.3	33.0-900.0	SPECTROGRAPHIC

N.B. Al to Si values in percent, MnO to Zr in ppm.

Van Moort (1973) studied magnesium and calcium contents of sediments and noted a decrease of magnesium and an increase of calcium from older to younger sediments. This was explained respectively, in terms of a redistribution due to diagenetic and metamorphic processes and a continuous leaching from older sediments. These trends manifest themselves in an increased CaO/MgO ratio during the Upper Palaeozoic and Mesozoic (Ronov, 1972, Fig. 6). In comparison, Kansas shales show an increase in the CaO/MgO ratio from 1.89 to 3.26 (calculated from linear regression analysis of the major oxide data) and a rise in both MgO and CaO content from the Upper Pennsylvanian to the Lower Permian (Fig. 4.3).

Ronov and Migdisov (1971) have produced graphs indicating that younger sediments have lower Al_2O_3 and Fe oxide values than older sediments. Both these trends are noted in the geochemistry of the Upper Pennsylvanian and Lower Permian (Fig. 4.8) shales although in the case of Fe oxide, there is only a marginal decrease. Similarly, the lower K_2O values in the Permian compared with the Pennsylvanian closely match the trends documented by Ronov (1972) and Van Moort (1972).

It would therefore seem possible that the major oxide variation recorded in Kansas shales is influenced by both worldwide evolutionary trends in the earth's geochemistry and by local tectonic and sedimentological conditions. These factors may have additionally influenced the trace element distributions, particularly those closely associated with major oxides. Sr content, for example, has been shown to decrease in rocks during the Pennsylvanian and Permian (Reimer, 1972), although no evidence for this conclusion can be found in the Kansas shale data. Alternatively, the geochemical trends noted in Fig. 4.8 may reflect a gradual restriction of the Pennsylvanian epeiric sea and formation, in the Permian, of a calcareous and later, an evaporitic sedimentary environment.

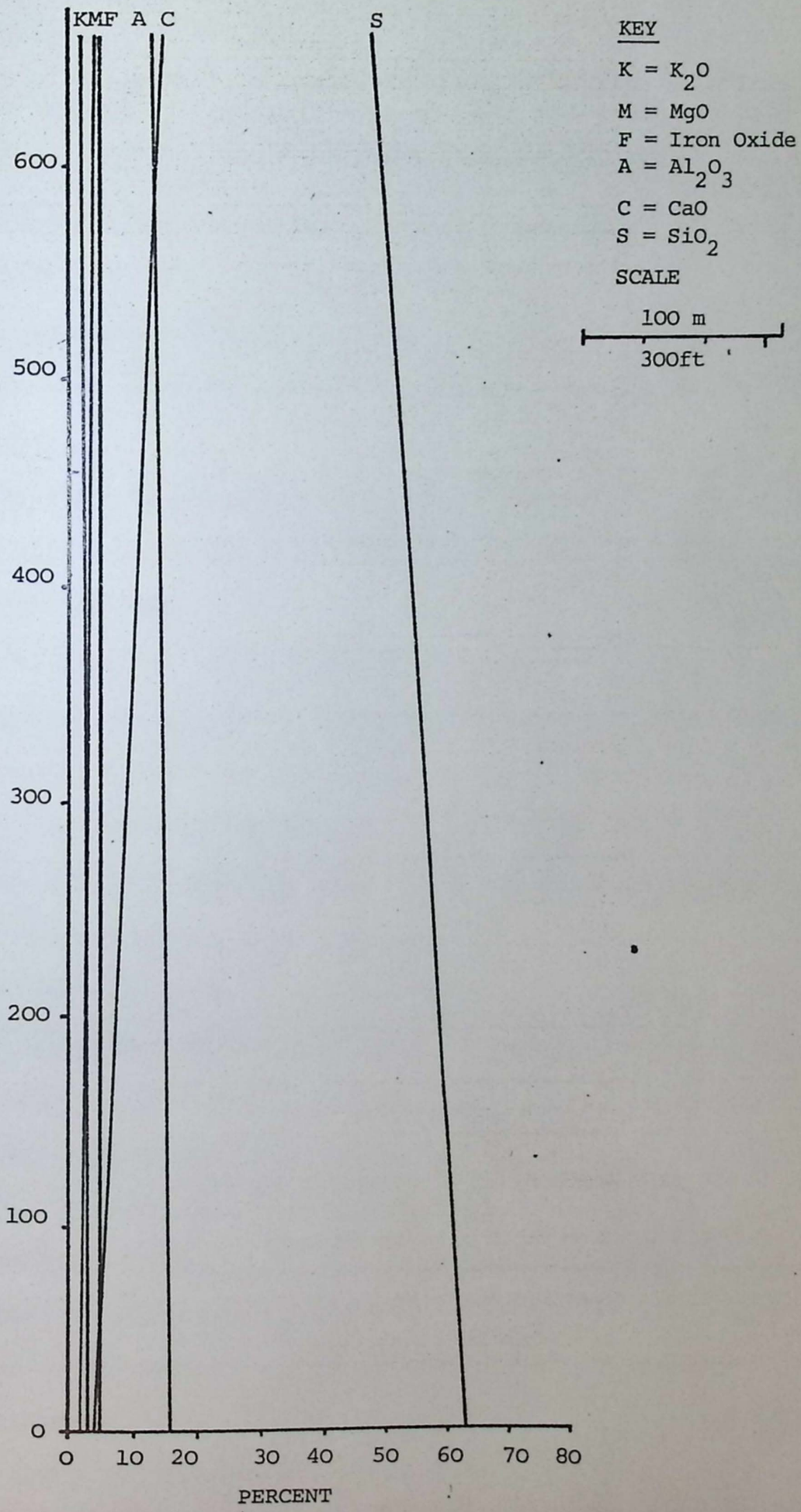

Fig. 4.8 Geochemical trends of major oxides through the Upper Pennsylvanian and Lower Permian shales of Kansas, U.S.A. A comparable stratigraphic column can be found in Fig.3.5.

CONCLUSIONS

127 samples of Upper Pennsylvanian and Lower Permian shales were analysed for major oxides and minor elements using an ARL 2900B direct reading emission spectrometer. From the results, it has been shown that the distributions of SiO_2, Al_2O_3, CaO, MgO, MnO, Co, Cr, Cu, Mo, Ni, Pb, Sr, V, Zn and Zr are stratigraphically controlled and that the values of Ag, Be, Bi, and Ge are so low that no stratigraphic relationships can be distinguished.

The major oxides present a similar stratigraphic zonation to that displayed by the mineralogical variables, i.e. The Pleasanton, Kansas City and Lansing beds form one natural division of the stratigraphy and the Douglas, Shawnee, Wabaunsee and Lower Permian Groups, further divisions. CaO and MgO have high values in the Pleasanton, Kansas City, Lansing and Shawnee Groups, whereas the Douglas and Wabaunsee Groups are rich in SiO_2 and Al_2O_3. In the Lower Permian Groups, CaO and MgO form the major geochemical components. Fe oxide and K_2O distributions are relatively stable throughout the Lower Permian and Upper Pennsylvanian.

The minor elements on the other hand, reveal a totally different pattern of stratigraphic control. MnO, for example, has a distribution that may reflect differences in the original carbonate mineralogy or the depositional environment of the sediments. High values are recorded in the Lansing, Shawnee, Wabaunsee and Admire Groups. Similarly, Sr, another geochemical facies indicator, has peaks in the Council Grove, Shawnee Chase and Pleasanton Groups that may reflect original mineralogical differences in the carbonate content of the sediments and changes in the depth or salinity of the depositional environment. Ga and Li are enriched in marine sediments relative to fresh water and indicate that parts of the Douglas and Wabaunsee were deposited in a restricted marine or non-marine environment. However, the inference drawn from all four distributions is

that a complex interrelationship between salinity, depth and original mineralogy exists in Kansas shales that cannot be unravelled by simply examining individual geochemical variables. Further information may be gained by a multivariate statistical analysis of the geochemical data (Chapter 5).

Another distinguishing feature of the minor element geochemical data, is the association of Cd, Cr, Cu, Mo, Ni, Pb, V and Zn with the occurrence of black shales. This has been extensively documented in the literature and arises from the chemical activity of organic residues in a reducing environment.

A third factor influencing the geochemical variation of the Upper Pennsylvanian and Lower Permian shales is elucidated by the distribution of zirconium. As this element is predominantly found in the detrital mineral zircon, the stratigraphic regions rich in Zr probably represent periods of detrital deposition. This conclusion is supported by the distributions of quartz, feldspar and Co which have peaks in the Douglas and Wabaunsee Groups.

A comparison of geochemical results obtained in this thesis and by Ebens and Connor in a survey of Missouri (1972), has shown that the geochemical variation in the calcareous and black shale deposits, particularly Ca, Cr, Cu, Pb, Ni, Sr, V, and Zn, is regionally controlled. Variables that had equivalent ranges of results in both Kansas and Missouri deposits, included Ba, Co and Zr.

A number of published reports on the worldwide geochemical evolution of CaO, MgO, K_2O, Al_2O_3 and Fe oxides, indicate that the distribution of major oxides in Kansas shales form a geochemical association that match worldwide trends during the Upper Pennsylvanian and Lower Permian. However, a negative correlation was noted between evolutionary trend of Sr in shales (Reimer, 1972) and that reported in this thesis.

The factors that may affect the geochemical variation in the Upper Pennsylvanian and Lower Permian shales are, therefore, worldwide geochemical evolution, particularly in the major oxides, regional events such as the distribution of Ca, Cr, Cu, Pb, Ni, Sr, V and Zn and lastly a three-fold stratigraphic control of trace elements and major oxides. In the latter case, the associations of variables noted are a carbonate fraction containing CaO, MgO, Sr, MnO and possibly Ba, Ga, Li and K_2O, a black shale fraction including Cd, Cr, Cu, Mo, Ni, Pb, Zn and V and lastly a detrital fraction, SiO_2, Al_2O_3, Zr with possibly Co and Fe oxides.

CHAPTER FIVE

STATISTICAL ANALYSIS OF GEOCHEMICAL DATA FROM THE UPPER PENNSYLVANIAN AND LOWER PERMIAN SHALES OF KANSAS, U.S.A.

INTRODUCTION

In Chapter 3, statistical analysis was applied to mineralogical data from the Upper Pennsylvanian and Lower Permian shales of Kansas and an increased understanding of those factors affecting the mineralogical content of the shales resulted. The aim of this chapter is to apply the same techniques to the geochemical results presented in Chapter 4 and to elucidate the geochemical evolution of the shales.

Emission spectroscopic results obtained in Chapter 4 indicate that several geochemical associations within Kansas shales exist; firstly, a carbonate fraction consisting of MnO, Sr, CaO with possibly Ga, Li and K_2O; secondly, a black shale fraction including Cd, Cr, Cu, Mo, Ni, Pb, Zn and V and finally a detrital association of SiO_2, Al_2O_3, Zr and possibly Co and Fe oxides. These associations were, however, inferred from a visual examination of the geochemical distribution of each oxide or element and must, therefore, be considered hypothetical.

As mentioned in Chapter 3, it is most unlikely that individual variables such as SiO_2 concentration in shales will control the geochemical evolution of the shales. However, associations of variables may reflect natural stratigraphic controls in the geochemistry of the Upper Pennsylvanian and Lower Permian shales. Multivariate statistical analysis of the geochemical data may elucidate any association of variables and redefine those factors that affect the geochemistry of the shales. Univariate statistical analysis of variable distributions (Chapter 3) have indicated mineralogical oscillations in the shales. Application of these techniques to the geochemical data may highlight periodic elements in the geochemistry of Upper Pennsylvanian and Lower Permian shales.

UNIVARIATE ANALYSIS OF GEOCHEMICAL DATA

A number of major oxide and minor element stratigraphic distributions visually examined in Chapter 4, appeared to contain geochemical oscillations.

A statistical clarification and verification of the repetitions was performed by Fourier analysis (see Appendix 1). Firstly, however, each variable was transformed using linear interpolation (Davis, 1973) from an irregularly spaced data sequence to an equal-spaced sequence, having data points at ten ft. intervals. After increasing the data sequence to 218 points, the geochemical variables were analysed by linear regression to check how equal spacing the data may have affected the geochemical distribution. No variable, however, assumed a greatly increased goodness-of-fit or correlation coefficient. This enabled the investigator to submit the equal-spaced data points to the Fourier analysis program knowing that any cycles detected would be representative of the original data. To obviate any problems associated with extraneous noise in the data, an 11-term smoothing equation was also applied to the equal-spaced data and the output submitted to the Fourier program.

The first variable studied was SiO_2 and as expected, the raw power spectrum closely matched the quartz spectrum recorded in Chapter 3. Peaks are recognised at the 3rd, 7th, 14th, 19th, 22nd, 26th and 33rd harmonics of which the 7th and 14th harmonic peaks are retained in the power spectrum of the smoothed data. The repetitive elements with intervals of 70 and 140 ft. probably represent the geochemical cycles detected in Chapter 4, whereas the small peaks retained in the region of the 30th harmonic possibly indicate a Group-by-Group cycle in the geochemistry as witnessed by the large scale stratigraphic zones observed in Chapters 3 and 4.

The CaO stratigraphic distribution has a raw power spectrum with peaks at the 4th, 7th, 9th, 13th, 15th, 17th, 19th, 21st, 27th, 31st and 33rd harmonics. After smoothing the equal-spaced data, peaks at the 5th, 7th, 9th and 13th harmonics are produced. A 70 ft. interval cycle is prominent in this data possibly indicating a cycle in carbonate deposition.

Both the K_2O and Fe oxide distribution contain a 7th harmonic peak

in their raw power spectra, although in the case of Fe oxides, this shifts to the 6th harmonic after smoothing. Similarly, Al_2O_3 and MgO have 6th harmonic peaks. Another close agreement between the power spectra of SiO_2, CaO, MgO and Al_2O_3, is the occurrence of a peak at the 12th, 13th or 14th harmonics. However, only SiO_2 records a peak around the 30th harmonic.

It seems possible, therefore, to distinguish short-term repetitions in the major oxide geochemistry corresponding to the 70 ft. cycles in the mineralogy of the Kansas shales. This is probably a reflection of the lithological cycles distinguished by Moore (1936). A 300 ft. cycle distinguished in SiO_2 may represent the Group-by-Group stratigraphic variation noted in previous chapters.

A few minor element distributions were also submitted to these procedures in an attempt to detect periodicity in the shales. MnO, Ba, Cd, Co, Cr, Ga, Li, Mo and Ni distributions were considered representative of the minor element variation detected in the Kansas shales and most likely to contain repetitive elements. In MnO, Ba, Cr, Ni, Mo, Cu and Ga distributions, the 70 ft. cycle was again dominant and in Cr, Ni, Mo and Cu, a 130 ft. cycle was also recognised. The only apparent anomaly in this study was Li which had power spectrum peaks at the 5th, 9th and 12th harmonics. A number of elements also had peaks at harmonics between 25 and 30 but no consistency was noted. It appears therefore that the peaks at the 7th and 13th harmonics are the only common features amongst the minor elements. The heat loss variable was also analysed and produced peaks at 7th and 13th harmonics.

The correspondence of results obtained from the major oxides and minor elements seems to support the hypothesis that there are geochemical cycles of 70 ft. and 130 ft. intervals. It also appears probable that the minor element geochemical cycles detected in Cr, Cu, Mo and Ni are related to the periodic occurrence of black shales. As Moore (1936) has continuously employed black shales as distinctive marker horizons in

Upper Pennsylvanian cyclothems and megacyclothems, it may be inferred that the geochemical cycles (and mineralogical as these also indicate 70 ft. cycles) are related to Moore's lithological cyclothems.

GEOCHEMICAL CORRELATIONS

Correlations between the geochemical variables are shown in Table 5.1. All variables have been included in the matrix, as parameters such as Ag, Be, Bi and Ge that seemed at first glance unimportant (Chapter 4), may prove to be of significance in a multivariate analysis.

Al_2O_3 has strong positive correlations with SiO_2, K_2O, Ba, Ga and Zn, reflecting geochemical associations in feldspar (SiO_2) and clay mineral lattices (K_2O, Ba, Ga, Zn). Negative correlations with CaO, MgO, Mn/Fe ratio, MnO, Bi, Ge, Sn and Sr are attributed to the lack of Al_2O_3 in carbonate environments. CaO shows a positive relationship to Mn/Fe, MnO, Bi, Ge, Sn and Sr, all of which are commonly associated with carbonates, and negative correlations with SiO_2, Al_2O_3, K_2O, Fe oxides, Ba, Ga, and Zn. As noted above, Fe oxides has positive correlations with Al_2O_3, K_2O, Ba, and Ga and negative with CaO. K_2O shows a similar set of correlations to the Fe oxides indicating a geochemical association in clay minerals or potash feldspar. MgO, is positively correlated with CaO reflecting an association in dolomitic shales, and negatively correlated with SiO_2 as quartz contains little MgO.

Considering the minor oxides and elements, a number of variable relationships indicated in Chapter 4 are clarified by the correlation coefficient matrix. The association of Cd, Cr, Cu, Be, Ni, Mo, Pb, V and Zn distributions is supported by high positive correlations between all the elements. There is also a strong connection between the minor elements MnO, Bi, Ge, Sn and Sr of the carbonate fraction. Be, Ga, Li, Cu and Zn form a tenuous association that probably relates to substitution

TABLE 5.1 Correlation coefficient matrix of geochemical variables; $r_{95} = \pm .15$, $r_{99} = \pm .20$, $r_{99.9} = \pm .27$

	Al_2O_3	CaO	Fe oxides	K_2O	MgO	SiO_2	Mn/Fe	MnO	Ag	Ba	Be	Bi	Cd	Co	Cr	Cu	Ga	Ge	Li	Mo	Ni	Pb	Sn	Sr	V	Zn	Zr	Heat Loss
Al_2O_3	1.00																											
CaO	-.81	1.00																										
Fe oxides	.47	-.38	1.00																									
K_2O	.67	-.42	.44	1.00																								
MgO	-.42	.38	.03	-.21	1.00																							
SiO_2	.61	-.87	.18	.14	-.45	1.00																						
Mn/Fe	-.59	.68	-.19	-.41	.33	-.55	1.00																					
MnO	-.39	.47	.10	-.26	.33	-.43	.92	100																				
Ag	-.18	-.01	-.20	-.25	-.08	.09	.01	-.05	1.00																			
Ba	.54	-.44	.40	.42	-.22	.35	-.29	-.14	-.15	1.00																		
Be	.08	.12	.11	.25	.02	-.21	.16	.16	.13	.02	1.00																	
Bi	-.53	.69	.02	-.09	.14	-.70	.48	.37	.07	-.29	.49	1.00																
Cd	.15	-.16	-.02	.05	-.20	.22	-.24	-.23	.28	.03	.44	.04	1.00															
Co	-.25	.07	-.18	-.42	-.10	.15	.20	.11	.56	-.13	.00	.11	.12	1.00														
Cr	.19	-.18	.00	.16	-.12	.14	-.24	-.20	.37	.04	.47	.01	.67	-.02	1.00													
Cu	.30	-.26	.20	.33	-.17	.12	-.26	-.19	.19	.11	.53	.07	.60	-.05	.74	1.00												
Ga	.82	-.72	.55	.80	-.40	.44	-.57	-.37	-.18	.47	.18	-.30	.12	-.31	.18	.38	1.00											
Ge	-.54	.73	-.07	-.13	.09	-.68	.53	.38	.04	-.25	.41	.93	-.06	.15	-.12	-.08	-.33	1.00										
Li	.12	.08	.24	.37	-.05	-.24	-.09	-.09	-.14	.17	.16	.33	-.17	-.09	-.03	.07	.30	.37	1.00									
Mo	-.16	.22	-.08	-.06	.01	-.19	.10	.04	.23	-.13	.54	.36	.60	.16	.48	.53	-.10	.26	.04	1.00								
Ni	.20	-.15	.06	.21	-.11	.08	-.19	-.15	.22	.02	.46	.03	.61	.12	.75	.76	.23	-.07	.03	.53	1.00							
Pb	.24	-.14	.06	.13	-.10	.08	-.14	-.08	.21	.02	.44	.04	.59	.13	.68	.68	.15	-.08	-.09	.45	.89	1.00						
Sn	-.47	.52	-.18	-.18	.18	-.50	.37	.22	.07	-.25	.29	.71	-.08	.14	-.10	-.09	-.32	.77	.30	.19	-.08	-.08	1.00					
Sr	-.50	.71	-.27	-.26	.17	-.59	.46	.32	-.02	-.33	.13	.52	.17	.04	-.12	-.18	-.45	.57	-.01	.14	-.09	-.09	.42	1.00				
V	.17	-.19	.03	.12	-.11	.15	-.19	-.16	.39	.04	.54	.05	.62	.01	.87	.69	.18	-.08	-.01	.62	.63	.62	-.08	-.13	1.00			
Zn	.43	-.46	.27	.36	-.26	.33	-.43	-.32	.17	.20	.46	-.13	.67	.01	.76	.79	.48	-.26	.05	.44	.83	.77	-.25	-.30	.67	1.00		
Zr	.11	-.28	-.09	-.25	-.22	.53	-.02	.00	-.13	.13	-.17	-.29	.04	.33	-.14	-.21	-.07	-.22	-.26	-.07	-.16	-.11	-.18	-.18	-.09	-.04	1.00	
Heat Loss	-.04	.10	.10	.13	-.06	-.21	-.04	.02	.24	-.05	.36	.28	.34	-.16	.56	.52	.04	.12	.02	.48	.46	.48	.07	.10	.67	.38	-.36	1.00

in clay mineral lattices. Ag, however, has no apparent affinities to any of these groups of minor elements but shows a high correlation with Co indicating a possible connection with the detrital fraction. The heat loss variable shows a high correlation with the Cd, Cr, Cu, Be, Ni, Mo, Pb, V and Zn association indicating that samples enriched in these elements also contain the most volatile materials.

The associations of geochemical variables elucidated by the correlation coefficient matrix are therefore:

1. an Al_2O_3, SiO_2, Zr and possibly Co and Ag combination as a detrital fraction,
2. a CaO, MgO, MnO, Mn/Fe, Bi, Ge, Sn and Sr association representing a carbonate fraction,
3. a Cd, Cr, Cu, Be, Mo, Ni, Pb, V, Zn and heat loss geochemical fraction common to black shales,
4. a K_2O, Fe oxides, Ga, Li, and possibly Cu and Zn association forming substitutes in clay mineral lattices.

MULTIVARIATE STATISTICAL ANALYSIS OF GEOCHEMICAL DATA

In order to further clarify the relationships between major oxides, minor elements, and inter-element associations and to establish the stratigraphic variation in geochemistry, the following standard statistical techniques - principal components analysis, Q-mode cluster analysis and multiple discriminant analysis were applied to the geochemical data. Details of the theoretical and computational aspects of these techniques can be found in Appendix 1.

R-mode principal components analysis of the data produced six significant components (eigenvalue > 1.0) which together account for 77% of the total variance, each component explaining more than 4% of the data variance (Table 5.2). Loadings of the variables on the components

TABLE 5.2 Eigenvalues of the principal components extracted

Component	Eigenvalue	% Variance	Cumulative % variance
1	7.9	29.2	29.2
2	5.7	21.3	50.5
3	3.1	11.3	61.8
4	1.6	6.0	67.8
5	1.5	5.6	73.4
6	1.1	4.1	77.5

TABLE 5.3 Correlations between promax oblique axes

PROMAX FACTORS

	1	2	3	4	5	6
1	1.00					
2	0.05	1.00				
3	0.20	0.21	1.00			
4	0.19	-0.07	0.01	1.00		
5	0.33	0.17	0.22	-0.01	1.00	
6	-0.01	-0.16	0.18	-0.19	0.01	1.00

are shown in Fig. 5.1 and a most complicated picture emerges. Since in geochemical investigations the components are not always independent (orthogonal), further insight into the geochemistry of the shales can be gained by performing varimax and oblique promax rotations of the six component axes. By this method, the variables influential on each axis are illuminated (Fig. 5.2) and the geochemical controls of sediment evolution, outlined.

In Chapter 3, the results of varimax and promax rotations were found to complicate the exposition of principal components loadings. However, in the multivariate analysis of geochemical data, the techniques aided interpretation. Fig. 5.3 illustrates the promax loadings and Table 5.3 presents the correlation between the rotated oblique axes. The following explanation for the components can therefore be proposed:

Component 1:-

The very high loadings of CaO, MgO, MnO and Sr suggest that this component should be designated the carbonate component. The elements Ge, Bi, Sn and Sr all show their highest loadings on the component but evidently also play dual or triple roles by showing significant loadings on other factors. The positive loadings of these elements and oxides are opposed by high negative loadings on SiO_2 and Al_2O_3 clearly indicating a detrital phase antipathetically related to a carbonate fraction.

Component 2:-

The elements Ni, Pb, Cd, Cu, V, Zn, Cr, Mo and Be dominate this component and have low values in all samples from black shales. In contrast, the opposing elements Zr, Al_2O_3 and SiO_2 have moderate positive loadings on the principal components but are removed by the effect of rotation. Therefore, component 2 is referred to as the black shale component and reflects changes in the conditions under which the shales

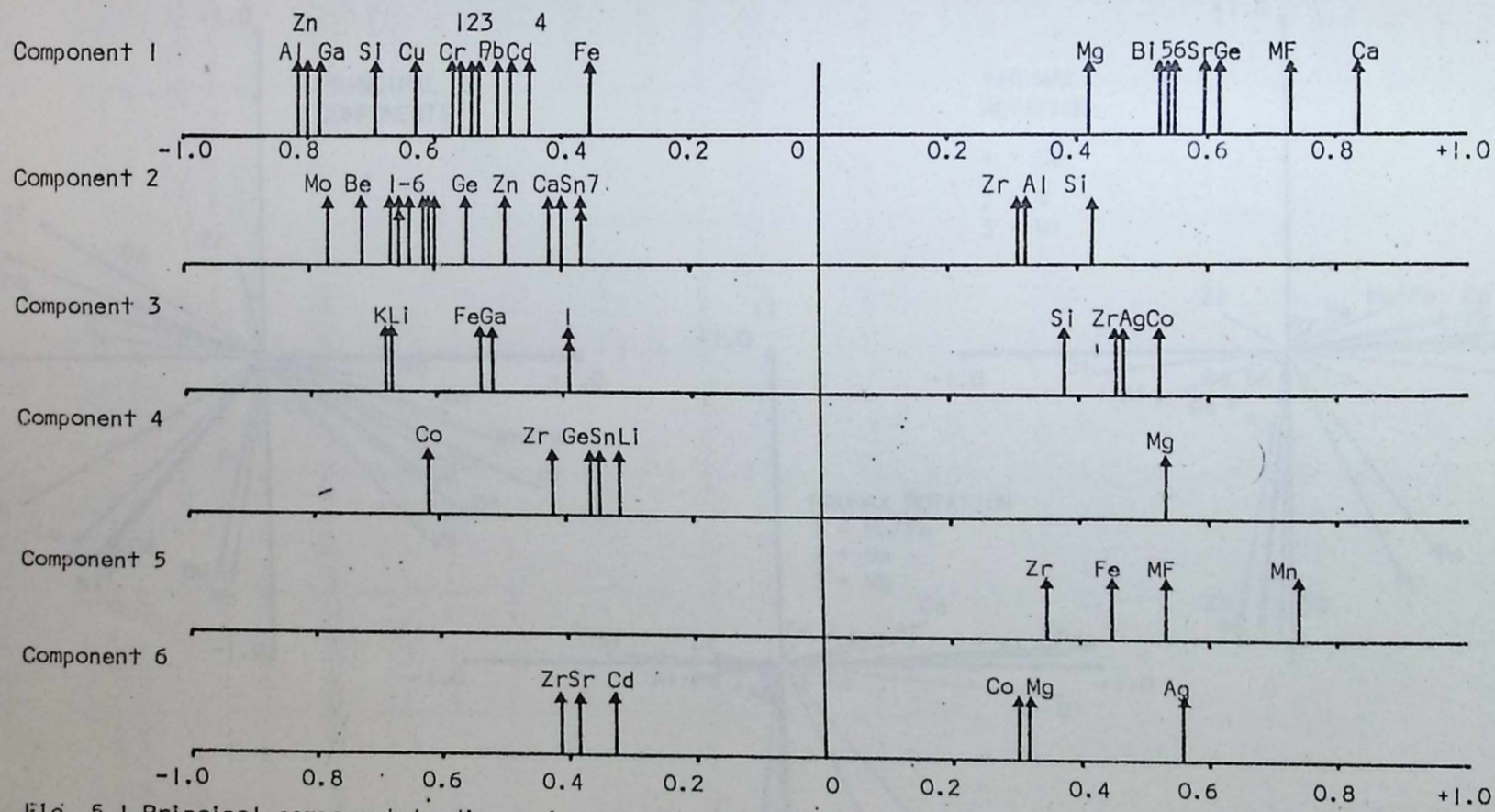

Fig. 5.1 Principal component loadings of geochemical variables. Only loadings greater than $\pm$ 0.30 are included.

KEY

On all Components:-
Al = Al_2O_3
Ca = CaO
Fe = Fe oxides
K = K_2O
Mg = MgO
Si = SiO_2
MF = Mn/Fe
Mn = MnO

On component 1:-
1 = Ni
2 = K
3 = V
4 = Bi
5 = Sn
6 = Mn

On component 2:-
1 = Ni
2 = Cr and V
3 = Pb
4 = Bi
5 = Cu
6 = Cd
7 = Sr and Ag

On component 3:-
1 = Bi and Ge

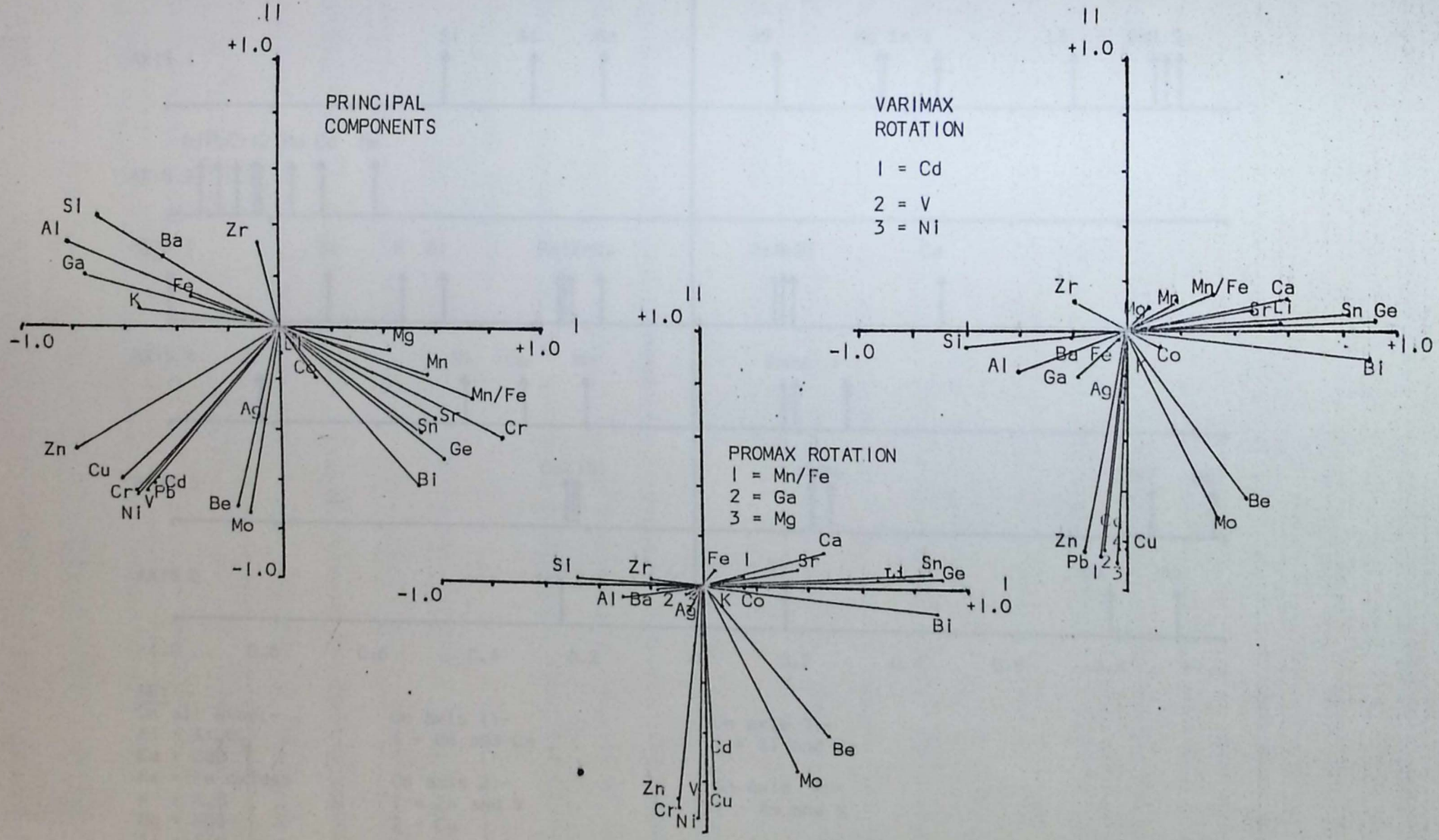

Fig. 5.2 Loadings of variables on the first two axes of a principal components analysis, varimax rotation and promax oblique rotation. In the latter case the axes are not orthogonal (correlation = 0.05) but for simplicity, are drawn so.

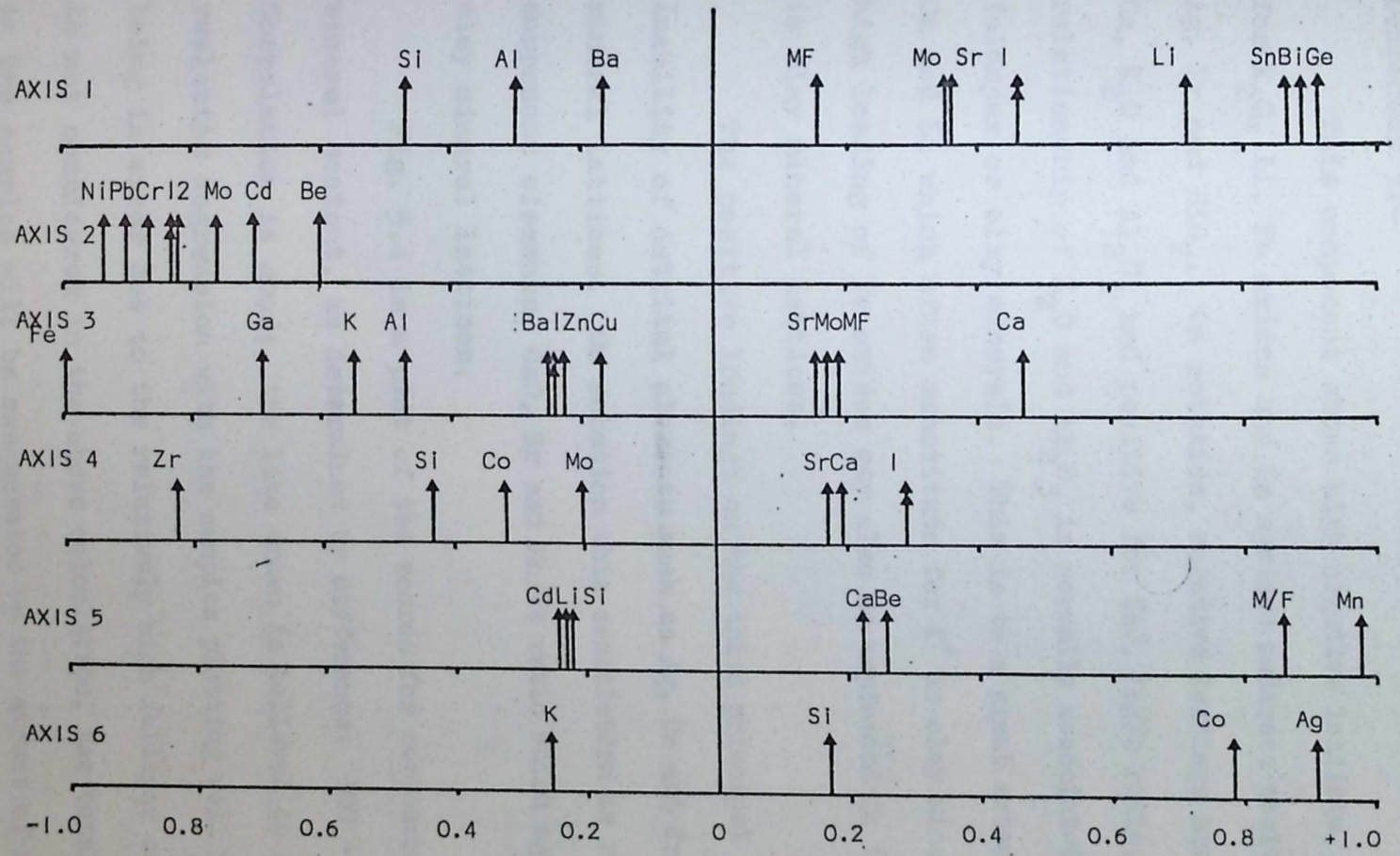

KEY

On all axes:-
Al = Al_2O_3
Ca = CaO
Fe = Fe oxides
K = K_2O
Mg = MgO
Si = SiO_2
MF = Mn/Fe
Mn = MnO

On axis 1:-
1 = Be and Ca

On axis 2:-
1 = Zn and V
2 = Cu

On axis 3:-
1 = Si and Be

On Axis 4:-
1 = Ag and K

Fig. 5.3 Oblique promax axis loadings. Loadings less than $\pm$ 0.15 are not illustrated.

were deposited. As black shales are normally developed under reducing conditions, the component may also represent an oxidation-reduction contrast or "Eh component".

Component 3:-

This component shows high negative loadings, in order of magnitude, for K_2O, Li, Fe oxides and Ga against moderate positive loadings for Co, Ag, Zr and SiO_2. On rotation, negative loadings are recorded for Fe oxides, Ga, K_2O and Al_2O_3 and positive for CaO, Mn/Fe ratio, Mo and Sr. The close relationship of K_2O and Al_2O_3 is normally associated with potassium feldspar or clay minerals. This is to a great extent substantiated by the Ga and Li which often substitute for K^+ in clay minerals. The additional high loading of Fe oxides may also be explained in terms of substitution in clay mineral lattices.

The positive loadings on the third principal component reflect the inability of detrital elements such as Ag, Co and Zr to substitute in clay mineral lattices. On rotation this association is replaced by the carbonate component elements, CaO, Sr and Mn/Fe ratio which again rarely combine in clay mineral lattices.

Fig. 5.4 is a plot of the scores for component 3 against total clay mineral content, as determined by difference: 100 - (quartz + carbonate)%. Correlation is good; the line drawn is believed to represent the most realistic regression with the samples plotting well to the right of it being in error due to the relatively high feldspar content. Since feldspar is not considered in the above calculation, the total clay mineral content in the samples will be exaggerated by the amount of feldspar. It is noticeable from Fig. 5.4 and predictable from the calculation method that the error in samples with a high clay mineral content is small (< 10%), is about 10% at a 40% clay content and can increase to about 15% in low clay samples.

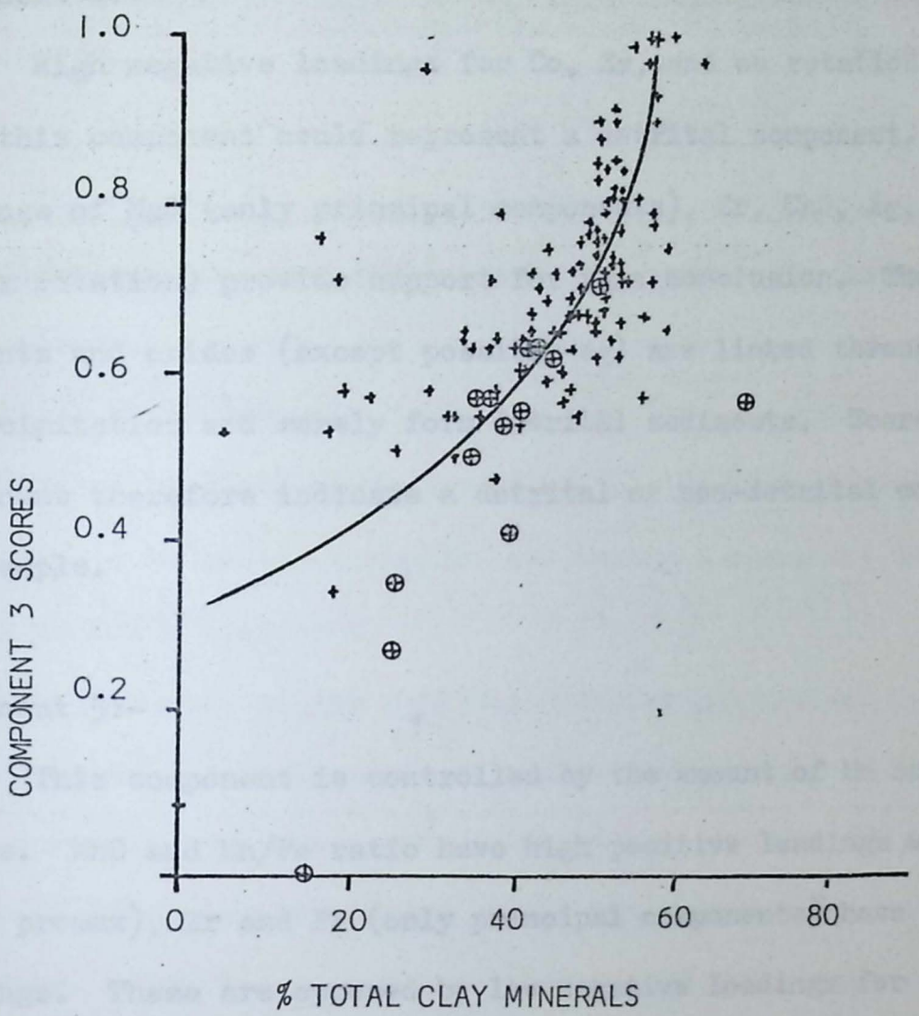

Fig. 5.4 Component 3 scores against percentage total clay

Component 4:-

High negative loadings for Co, Zr, and on rotation SiO_2, indicate that this component could represent a detrital component. High positive loadings of MgO (only principal components), Sr, CaO, Ag, and K_2O (only promax rotation) provide support for this conclusion. The positive loaded elements and oxides (except possibly Ag) are linked through the process of coprecipitation and rarely form detrital sediments. Scores for this component therefore indicate a detrital or non-detrital composition for the sample.

Component 5:-

This component is controlled by the amount of Mn occurring in the shales. MnO and Mn/Fe ratio have high positive loadings whereas Ca, Be (only promax), Zr and Fe (only principal components) have low positive loadings. These are opposed by low negative loadings for Cd, Li, and SiO_2.

As Mn^{2+} substitutes extensively for Ca in carbonates, the correlation (Table 5.3) of 0.33 between promax factors 1 and 5 is not unexpected. Although MnO also occurs in sediments as oxides with a general pyrite structure, the negative loading for SiO_2 precludes a detrital mineral association. This component is therefore termed the "manganese component" and is closely related to the "carbonate component".

Component 6:-

The elements and oxides controlling component 6 show a bipolar distribution with positive loadings recorded for Ag, and Co and negative loadings for Zr, K_2O, Al_2O_3, Ga, Sr, and Cd. This component reflects the occasional high values recorded by the Ag and Co variables in sandstones and siltstones and is consequently negatively correlated with promax factor 4. However, as both these variables are generally accorded negligible values in Kansas shales, the majority of scores on component 6

occur between 0.3 and 0.5, with occasional high Co and Ag values producing high scores.

Therefore, the geochemical relationships developed in the Upper Pennsylvanian and Lower Permian shales are found to consist of six associations. Firstly, the geochemical evolution of the shales is influenced by a carbonate component, and then successively decreasing in significance, a black shale component, a clay mineral component, a detrital component, a manganese component and lastly a component that can only be termed an Ag/Co component.

Having defined the controls over the geochemical development of Kansas shales, it is possible to examine the stratigraphic effects of these controls by studying the relationships between the samples. The scores of Kansas shale samples on the six significant components were, therefore, submitted to a Q-mode cluster analysis program. The dendrogram produced is shown in Fig. 5.5 and the samples seen to fall into a number of natural groups. Although most of the samples appear to be closely associated, a maximum of ten groups or clusters can be distinguished.

Before examining the stratigraphic distribution of these clusters, it is necessary to confirm that the ten groups are discrete and not simply a product of the clustering method. The procedure adopted as a test was described in Chapter 3 and is based on the multiple discriminant analysis program of Mather (1969). By this method, variation between clusters is maximized to produce two discriminant axes, accounting for 70.9% of the sample variance (Fig. 5.6). As the diamonds in Fig. 5.6 represent the means of each cluster $\pm$ 1 standard deviation on each axis, it can be seen that clusters A, B, C, E and G are indistinguishable and can be merged. Similarly, group J only consists of two samples and can be merged for convenience with group H. Group I, on the other hand, is found to be unique and represents black shales with high scores on component 2. A

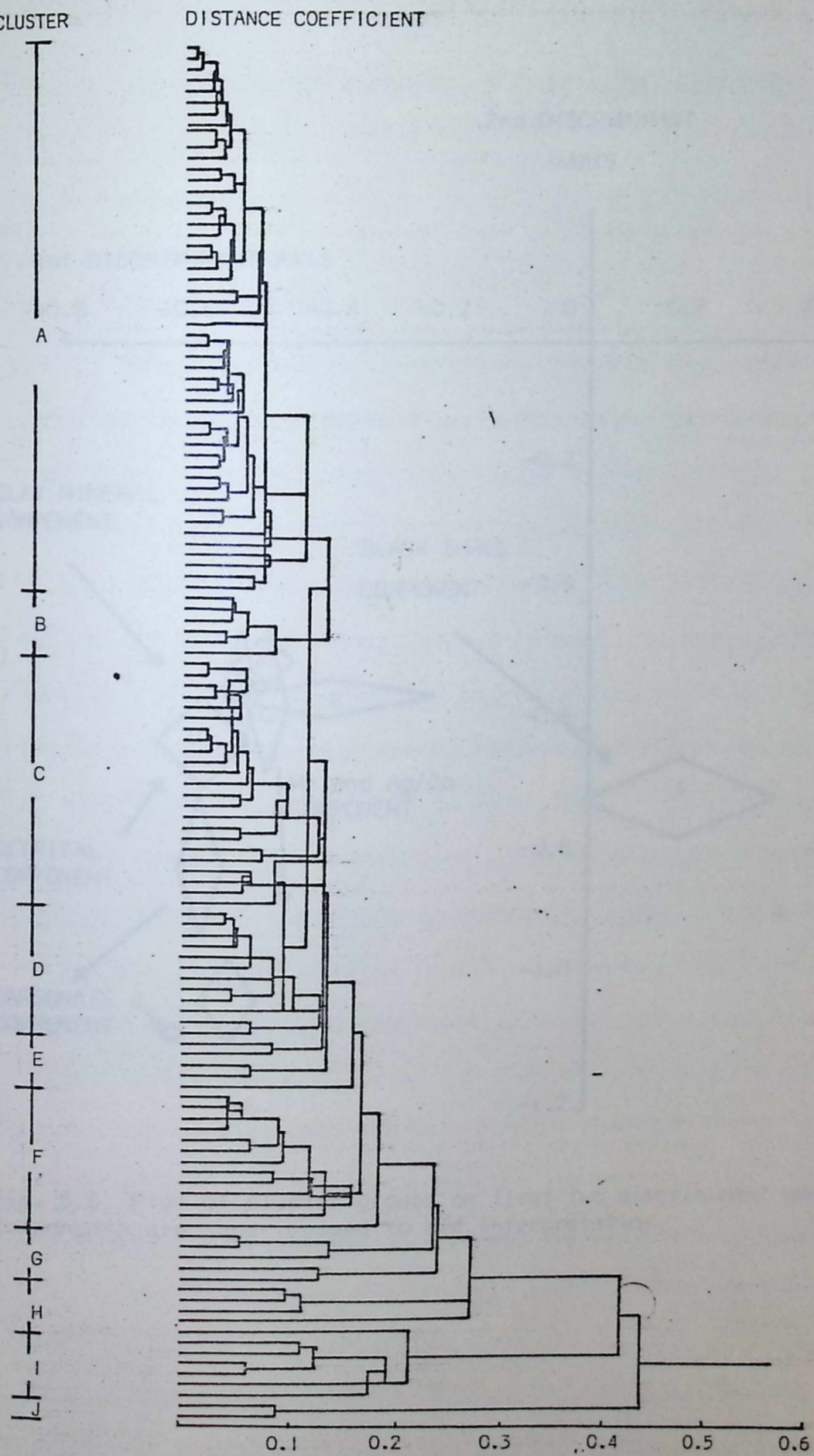

Fig. 5.5 Dendrogram of Upper Pennsylvanian and Lower Permian geochemical data. Clusters produced are outlined on the left of the diagram.

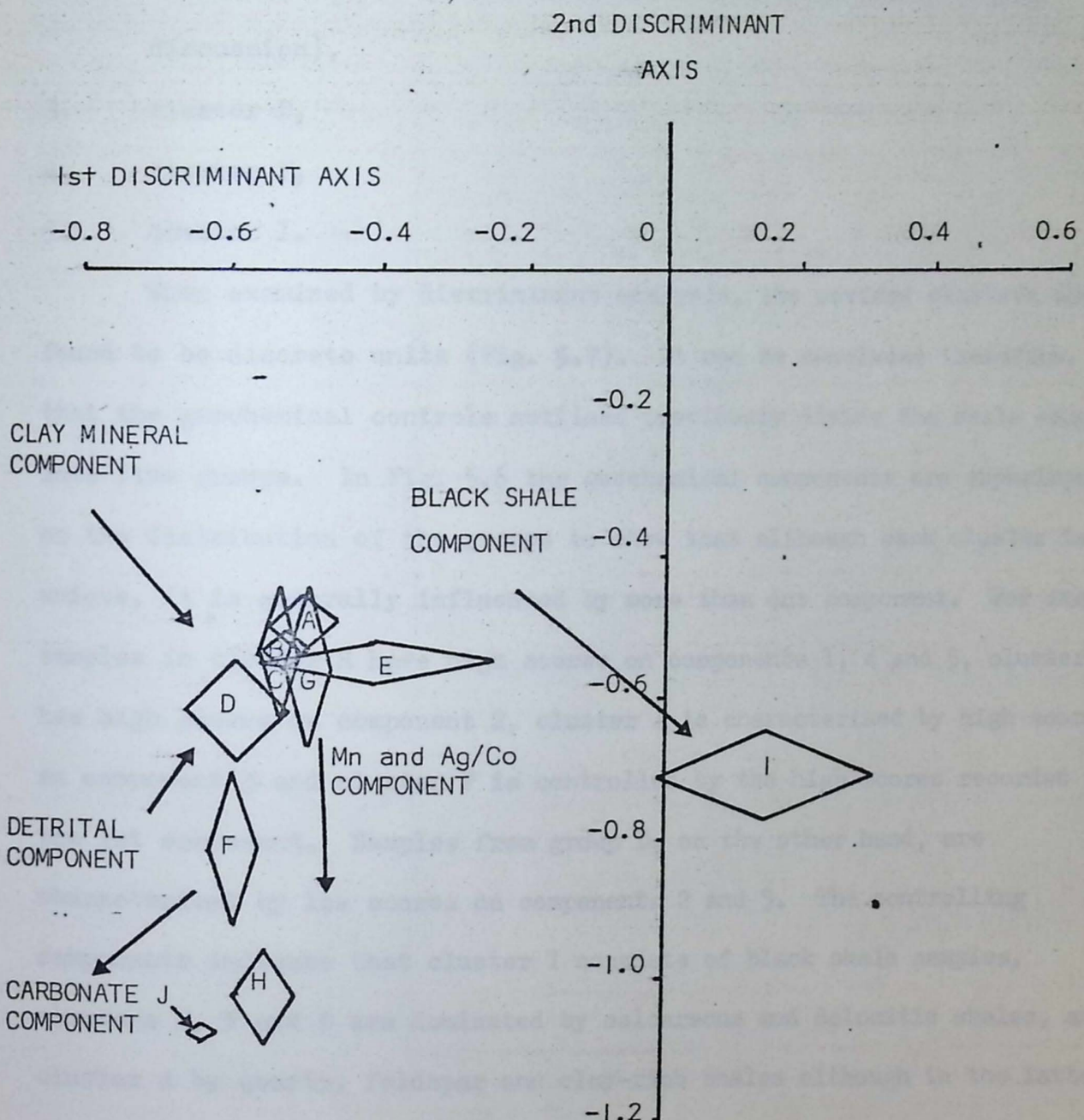

Fig. 5.6 Plot of cluster groups on first two discriminant axes. Controlling components are superimposed to aid interpretation.

more realistic arrangement of the dendrogram samples is therefore:

1. clusters A, B, C, E and G (referred to henceforth as cluster A),
2. clusters H and J (referred to as cluster H in the succeeding discussion),
3. cluster D,
4. cluster F,
5. cluster I.

When examined by discriminant analysis, the revised clusters are found to be discrete units (Fig. 5.7). It can be concluded therefore, that the geochemical controls outlined previously divide the shale samples into five groups. In Fig. 5.6 the geochemical components are superimposed on the distribution of the groups to show that although each cluster is unique, it is generally influenced by more than one component. For example, samples in cluster H have high scores on components 1, 4 and 5, cluster I has high scores on component 2, cluster A is characterised by high scores on component 3 and cluster F is controlled by the high scores recorded on the 1st component. Samples from group D, on the other hand, are characterised by low scores on components 2 and 5. The controlling components indicate that cluster I consists of black shale samples, clusters H, F and D are dominated by calcareous and dolomitic shales, and cluster A by quartz, feldspar and clay-rich shales although in the latter case, some overlap into the calcareous regime does occur. These findings are supported by a comparison between the distribution of shale samples in the X-ray diffraction and geochemical classifications (Table 5.4).

The distribution of the shale samples according to their cluster is shown in Fig. 5.8 and reveals a five-fold division of the stratigraphic column. The lowest division consists of the Pleasanton and Lower Kansas City Group beds and contains samples that fall into all five clusters; the majority of samples belonging to cluster A, four to cluster I and one from each of the remaining clusters. Samples from cluster I occur at

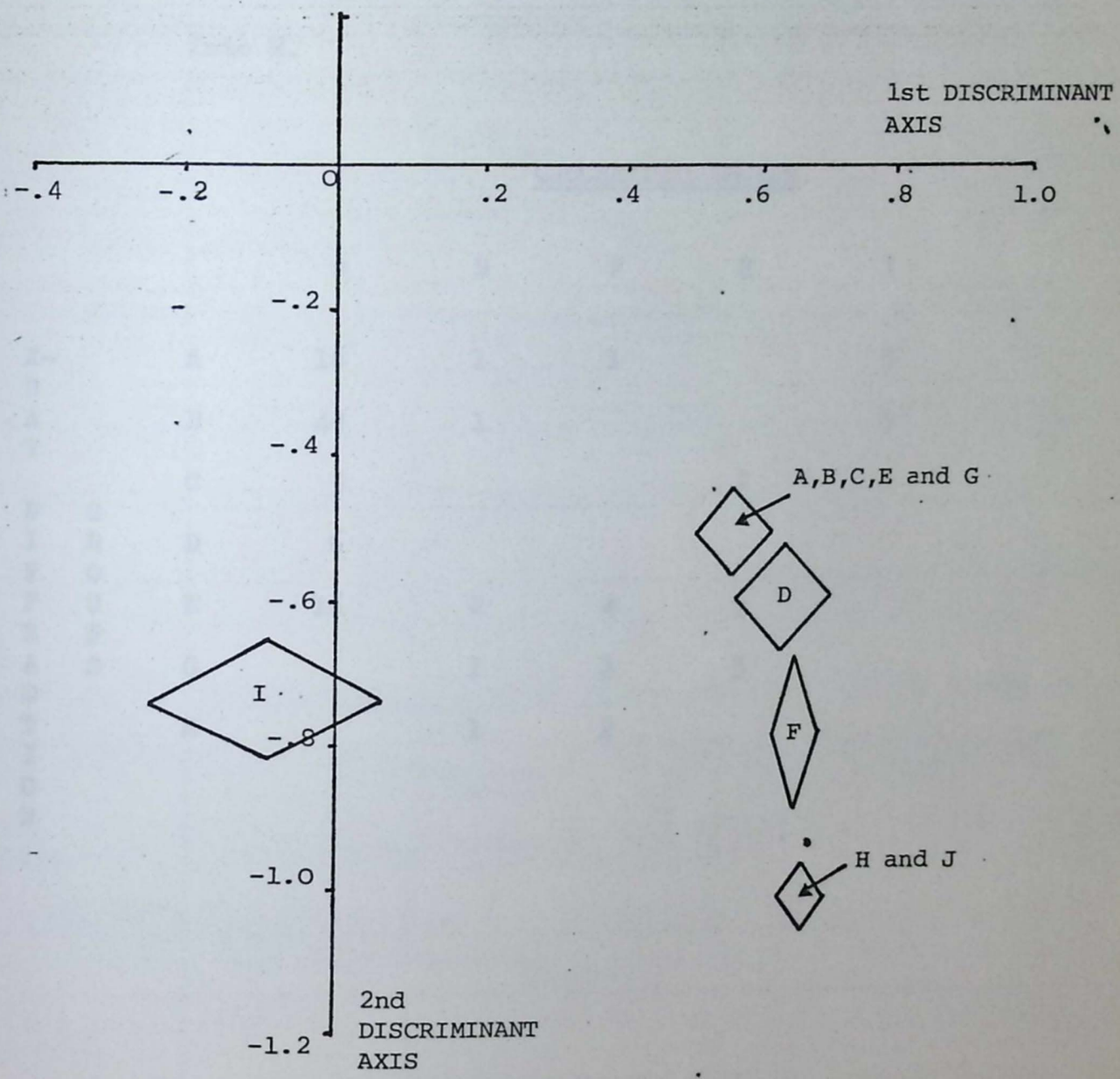

Fig. 5.7 A plot of revised clusters against first two discriminant axes. Diamonds represent mean of each cluster $\pm$ 1 standard deviation on each axis.

TABLE 5.4 Distribution of shale samples in the X-ray diffraction and geochemical classifications, indicating, for example, that of the samples in geochemical cluster F, 4 were classified into X-ray diffraction cluster E, 1 into G, 1 into A and 2 into H.

		GEOCHEMICAL GROUPS				
		A	D	F	H	I
X-RAY DIFFRACTION GROUPS	A	16	1	1		3
	B	48	1			3
	C	3			2	
	D	6				
	E	16	8	4	5	
	G		1	1	5	
	H		1	2		

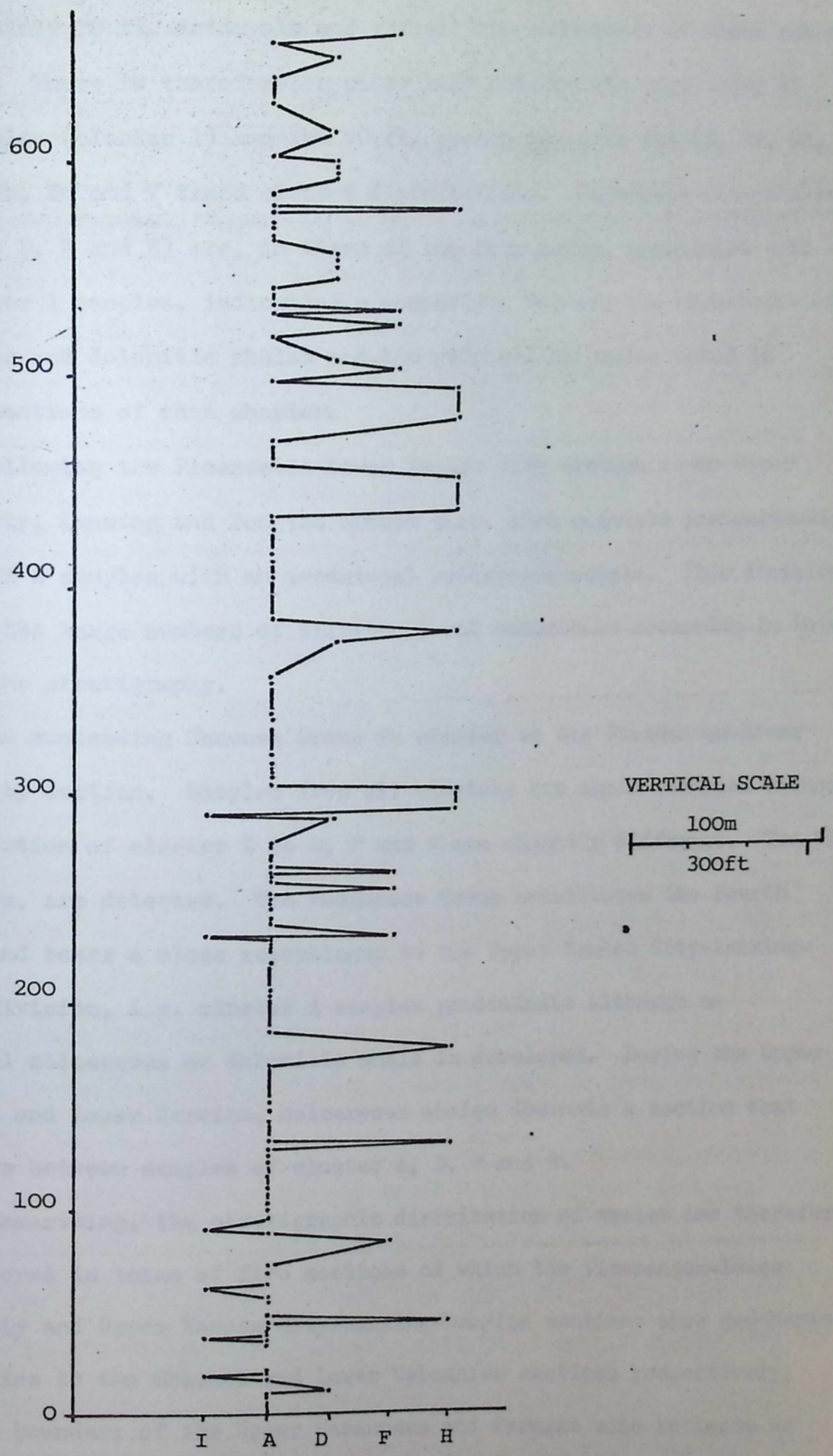

Fig. 5.8 Stratigraphic distribution of shale samples arranged according to the cluster analysis groups. The horizontal scale is arbitrary.

approximately 70 ft. intervals and reflect the occurrence of black shale deposits. There is therefore, a close link between the regularity of black shales (cluster I) and the 70 ft. cycles noted in the Cd, Cr, Cu, Mo, Ni, Pb, Zn and V trace element distributions. Carbonate-rich shales (clusters D, F and H) are, in three of the four cases, associated with the cluster I samples, indicating a connection between the occurrence of calcareous and dolomitic shales and the geochemical cycles noted in earlier sections of this chapter.

Following the Pleasanton-Lower Kansas City section is an Upper Kansas City, Lansing and Douglas Groups zone, that consists predominantly of cluster A samples with an occasional calcareous sample. This division reflects the large numbers of siltstones and sandstones occurring in this part of the stratigraphy.

The succeeding Shawnee Group is similar to the Pleasanton-Lower Kansas City section. Samples from all clusters are again recorded although the proportion of cluster I to D, F and H are slightly different. Two 70 ft. cycles, are detected. The Wabaunsee Group constitutes the fourth section and bears a close resemblance to the Upper Kansas City-Lansing-Douglas division, i.e. cluster A samples predominate although an occasional calcareous or dolomitic shale is developed. During the Upper Wabaunsee and Lower Permian, calcareous shales dominate a section that alternates between samples of cluster A, D, F and H.

Summarising, the stratigraphic distribution of shales can therefore be considered in terms of five sections of which the Pleasanton-Lower Kansas City and Upper Kansas City-Lansing-Douglas sections show geochemical similarities to the Shawnee and Lower Wabaunsee sections respectively. The lower boundary of the Upper Wabaunsee and Permian zone reflects an important change in environmental conditions from the generally clastic deposition of the Upper Pennsylvanian to the carbonate-dominated sedimentation in the Permian. The Pleasanton, Lower Kansas City and Shawnee Groups also

show evidence for geochemical cycle at 70 ft. intervals.

CONCLUSIONS

The geochemical evolution of the Upper Pennsylvanian and Lower Permian shales of Kansas has been elucidated by univariate and multivariate statistical techniques. Fourier analysis of equal-spaced geochemical data has consistently revealed cycles with an interval of 70 ft. in the stratigraphic distribution of the major oxides and minor elements, SiO_2, CaO, K_2O, Fe oxides, MnO, Ba, Cr, Ni, Mo and Cu. A comparison of geochemical and mineralogical evidence indicates that the cycles are noted in both data sets and that the cycle may be a reflection of cyclic changes in sedimentary conditions.

Close elemental associations in the geochemical data were noted by a visual inspection in Chapter 4. Statistical support for these conclusions has been found in the correlation coefficient matrix for the geochemical data. Elements and oxides are found to split into four associations that can be related to mineralogical and lithological parameters - a detrital fraction containing Al_2O_3, SiO_2, Zr, Co and Ag, a carbonate fraction containing CaO, MgO, MnO, Mn/Fe, Bi, Ge, Sn and Sr, a clay mineral fraction with K_2O, Fe oxides, Ga, Li, Cu and Zn and a black shale association of Cd, Cr, Cu, Be, Mo, Ni, Pb, V, Zn and heat loss.

A principal components analysis of the geochemical data clarifies these relationships and details the controlling influences in the geochemical evolution of Kansas shales. Six significant components are extracted from the data and are interpreted as a carbonate component, a black shale component, a clay mineral component, a detrital component, a manganese component and lastly an Ag/Co component. Each component represents associations of elements and oxides that describe an important source of variation in the geochemistry of the Upper Pennsylvanian and Lower Permian shales.

Besides determining the controls in the geochemical development of Kansas shales, it has also been possible to determine the stratigraphic effects these components have on the geochemistry of Kansas shales. A cluster analysis and multiple discriminant analysis of the geochemical data has produced a classification of shale samples into five groups that are geochemically distinct. Each group is uniquely defined by the influences each of the components has on the group.

The distribution of these sample groups delineates five stratigraphic zones that are geochemically distinct. The stratigraphic differences in shale geochemistry can be attributed to changes in the sedimentary environment. In the Pleasanton and Lower Kansas City Groups, alternations of calcareous, black and quartz-rich shales indicate four sedimentary cycles of 70 ft. intervals separated by quartz-rich shales. The succeeding Upper Kansas City-Lansing-Douglas zone contains samples that have high scores on the detrital component indicating an influx of detrital material from the Upper Kansas City to Shawnee Groups. Comparable conditions to Pleasanton-Lower Kansas City and Upper Kansas City-Lansing-Douglas zones were repeated in the Shawnee and Lower Wabaunsee respectively, although only two cycles were indicated in the Shawnee. The Upper Wabaunsee, Admire, Council Grove and Chase Groups are enriched in calcareous and dolomitic shales unlike the preceding generally quartz-rich shales. The change to calcareous sediments marks a significant boundary in the Upper Pennsylvanian and Lower Permian stratigraphy and is probably linked to the closure of the Kansas epeiric sea (Heckel, 1972a).

CHAPTER SIX

ELECTRON SPIN RESONANCE STUDIES OF UPPER PENNSYLVANIAN AND LOWER PERMIAN SHALES OF KANSAS, U.S.A.

INTRODUCTION

Conventional microscopic techniques are known to be generally inappropriate for the study and classification of shales because their constituent particles are smaller than the resolving power of an optical microscope. As a result, instrumental techniques such as X-ray diffraction (Chapter 2) and emission spectroscopy (Chapter 4) were employed to determine the mineralogical and geochemical composition of the Upper Pennsylvanian and Lower Permian shales and to classify samples on the basis of such analyses. However, questions concerning the environment of deposition of some shales have been raised by geochemical variables such as Mn and Sr (Chapter 4). This chapter hopes therefore to clarify these inconsistencies and to verify the conclusions drawn about the geochemistry of the shales.

The geochemical distributions of Mn and Sr in Upper Pennsylvanian and Lower Permian shales indicate apparently contradictory sedimentary conditions in the Kansas City and Wabaunsee Groups. The evidence for this conclusion rests on differences in the geochemical situation of each element. Mn, for example, may occur in association with carbonates or clay minerals. However, it is possible using a spectroscopic technique known as electron spin resonance (ESR) to differentiate the structural settings of ions such as Mn^{2+} and clarify the environmental problem. The shale spectra generated for this study can serve a second function, to provide supplementary evidence on the geochemical and mineralogical classifications developed previously.

ESR is relatively unknown in the geological sciences even though it has been applied quite extensively in the fields of determinative mineralogy (Marfunin, 1964), lunar mineralogy and petrology (Weeks, 1972, 1973), terrestrial silicates and carbonates (Ghose, 1968; Wildeman, 1970), crystallographic analysis (Low, 1968) and geological age dating (Morency et al., 1970). Therefore, a detailed list of applications is presented in Appendix 2 and a brief theoretical description is expounded in this chapter.

Although primarily a chemical technique for the study of paramagnetic ions in crystals, ESR is used as an instrumental tool in geology for the detection of certain ionic species in minerals and rocks and analysing the structural position these ions occupy within minerals. It is particularly applicable to ions in the transition group ($3d^n$), the palladium group ($4d^n$), the platinum group ($5d^n$), the rare earth group ($4f^n$) and the actinides group ($5f^n$). In comparison with other instrumental techniques, it is inaccurate (20% optimum precision) as a quantitative technique but is exceptionally sensitive as a qualitative technique (10^{-5} to 10^{-12} moles). ESR also possesses three other important characteristics; less than 0.5 gm of the sample (solid, liquid or powder) is required for analysis, the technique is non-destructive and sample analysis can be completed within 30 minutes. Consequently, as ESR has no functional equivalent in the instrumental techniques currently employed in the analysis of shales, the simplicity and speed of analysis suggest that the technique may be a useful supplement to standard procedures.

THEORY

Different types of chemical compounds can be distinguished according to their behaviour when placed in a magnetic field.

Firstly, diamagnetic substances are less permeable to magnetic lines of force than is a vacuum and tend to move from the strong to the weak part of the magnetic field. The phenomena of diamagnetism is found in all chemical substances and is caused by the interaction of an external magnetic field with the magnetic field produced by the movement of electrons in filled atomic orbitals.

Alternatively, paramagnetic substances show the opposite behaviour, that is they move from the weak to the strong part of the magnetic field

as they are more permeable to magnetic lines of force than is a vacuum. This arises when an atom, ion or molecule possesses one or more unpaired electrons. As the diamagnetism of a substance is generally weak, it is usually masked by the paramagnetic effects.

When a magnetic field is applied to a substance, ESR, a technique for detecting paramagnetism, can be used to study ions especially Co^{2+}, Ni^{2+}, Fe^{2+}, Mn^{2+}, Ti^{3+}, Cr^{3+}, V^{2+}, and Cu^{2+}, all of which are characterised by the presence of one or more unpaired electrons.

In theory, since a charged spinning unpaired electron possesses a magnetic moment, it can be aligned parallel or antiparallel to an externally applied magnetic field. This gives rise to two energy states (Fig. 6.1) - a stable low energy state representing electrons parallel to the field and an unstable high energy state representing those antiparallel to the field. If radiation in the microwave region is applied to the sample, electrons in the low energy state can absorb energy and thus become excited to the high energy state (provided the energy of each quantum equals the difference in energy between the electron states, i.e.

$$Lv = \Delta E = g\beta H_o$$

where L = Plancks quantum of action and v = frequency of radiation).

Provided equilibrium is not seriously disturbed, there will be a net absorption of radiation due to the larger population of unpaired electrons in the lower energy level (Boltzmann's law). To maintain steady state conditions, various relaxation processes allow the electrons to lose energy and return to the ground state. These electrons can then be re-excited to the upper energy level producing a continuous movement between the two energy levels - the resonance condition. The net absorption of energy for a sample with unpaired electrons is registered by the ESR equipment as a single line.

Although this simple situation allows an investigator to prove the

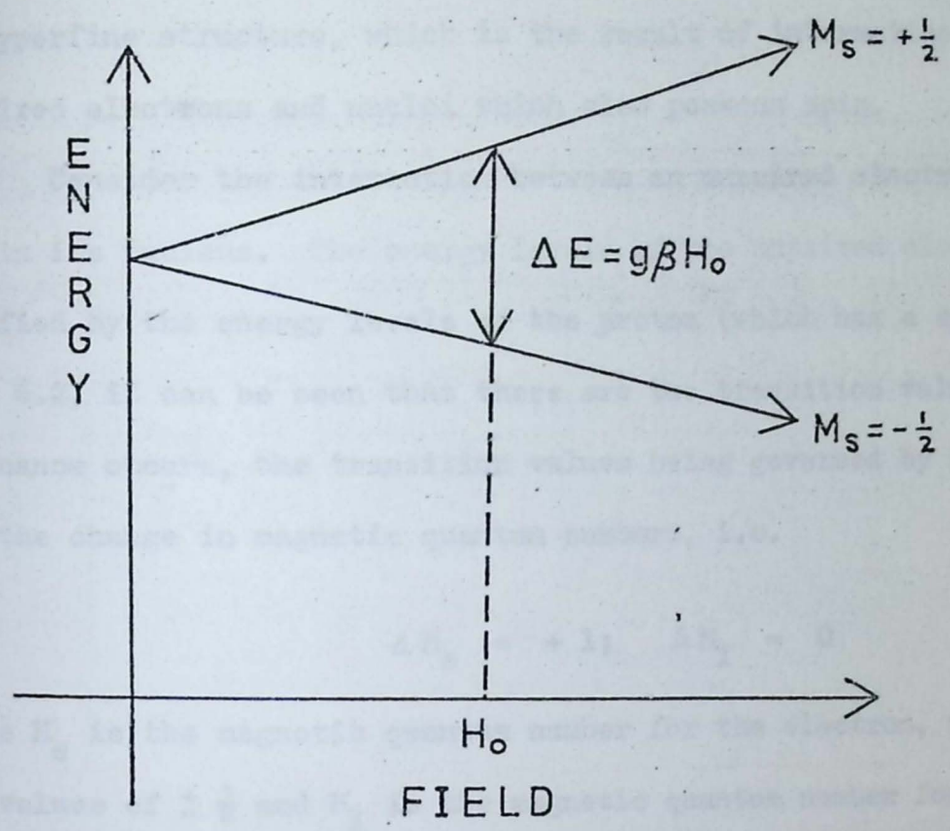

Fig. 6·1. Energy levels for an unpaired electron in a magnetic field (M_s is the magnetic quantum number which takes the value $\pm \frac{1}{2}$, β is the Bohr magneton the unit of magnetic moment, g is the spectroscopic splitting factor which is the ratio of magnetic moment to the angular momentum possessed by the electron, H_o is a particular value of a magnetic field H and E is the difference between two energy levels.)

presence of unpaired electrons in a sample, the success of ESR in solving geochemical and mineralogical problems stems mainly from the occurrence of hyperfine structure, which is the result of interaction between unpaired electrons and nuclei which also possess spin.

Consider the interaction between an unpaired electron and a proton within its nucleus. The energy levels of the unpaired electron will be modified by the energy levels of the proton (which has a spin of $\frac{1}{2}$). In Fig. 6.2, it can be seen that there are two transition values for which resonance occurs, the transition values being governed by selection rules for the change in magnetic quantum numbers, i.e.

$$\Delta M_S = +1; \quad \Delta M_I = 0$$

where M_S is the magnetic quantum number for the electron, which can take the values of $\pm \frac{1}{2}$ and M_I is the magnetic quantum number for the nucleus, which is $\pm \frac{1}{2}$ for the proton. These selection rules imply that, in this situation, as the magnetic field is varied, there are two values of the magnetic field for which resonance takes place and consequently two hyperfine lines are observed (Fig. 6.3).

Similarly, when an electron interacts with two equivalent protons (i.e. the protons have equal symmetry in the radical), the four levels in Fig. 6.2 will be split by a second proton interaction to give two sets of three levels, the central level being double degenerate (Fig. 6.4). For an interaction with three equivalent protons, the spectrum recorded consists of four hyperfine lines with relative intensities 1:3:3:1, and for an interaction with four protons, five hyperfine lines with relative intensities of 1:4:6:4:1. In general, with n equivalent protons, a hyperfine spectrum of n + 1 equally spaced lines is obtained with a distribution of relative line intensities given by the binomial coefficients ${}^{n}C_{m}$ where m equals 0,1,2,....,n.

Non-equivalent protons complicate the hyperfine structure.

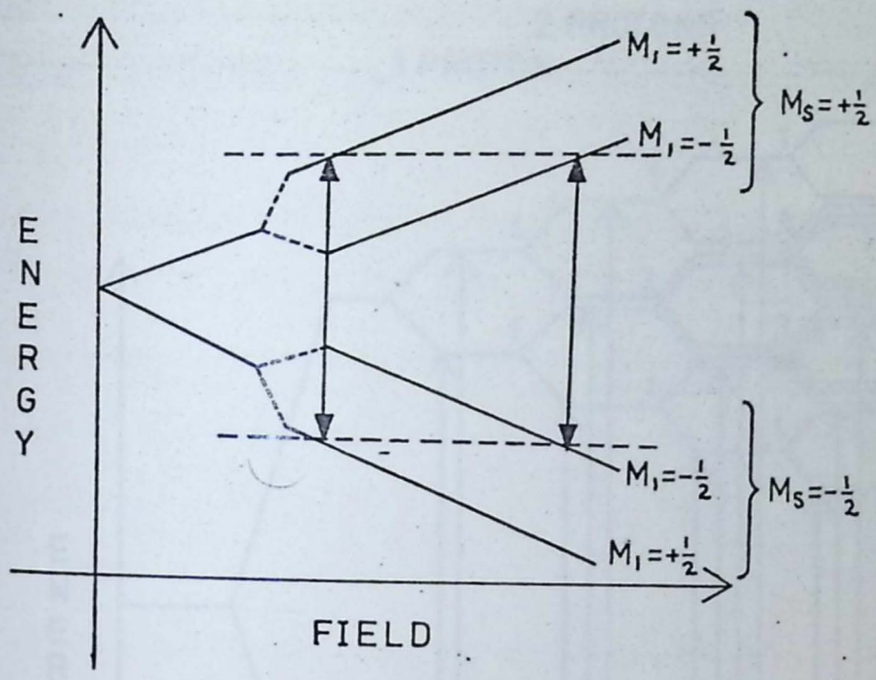

Fig. 6·2. Energy levels for an unpaired electron interacting with a proton in a magnetic field. The allowed resonance condition transitions are indicated by arrows.

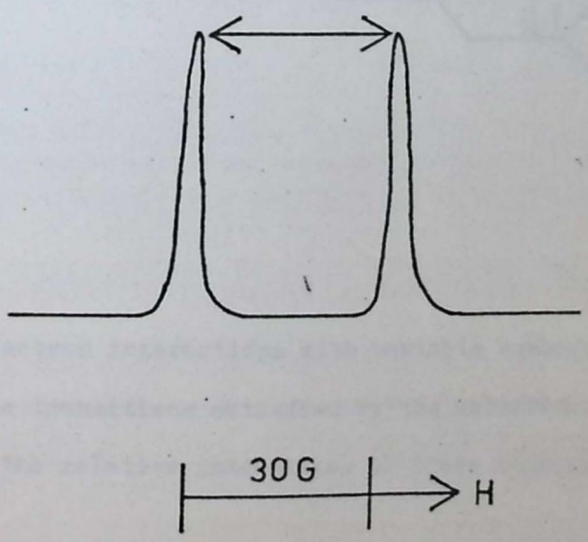

Fig. 6·3. Hyperfine structure observed when one electron interacts with one proton. The separation between the peaks is termed the hyperfine splitting constant which for protons of free radicals are in the range 0 - 30 gauss.

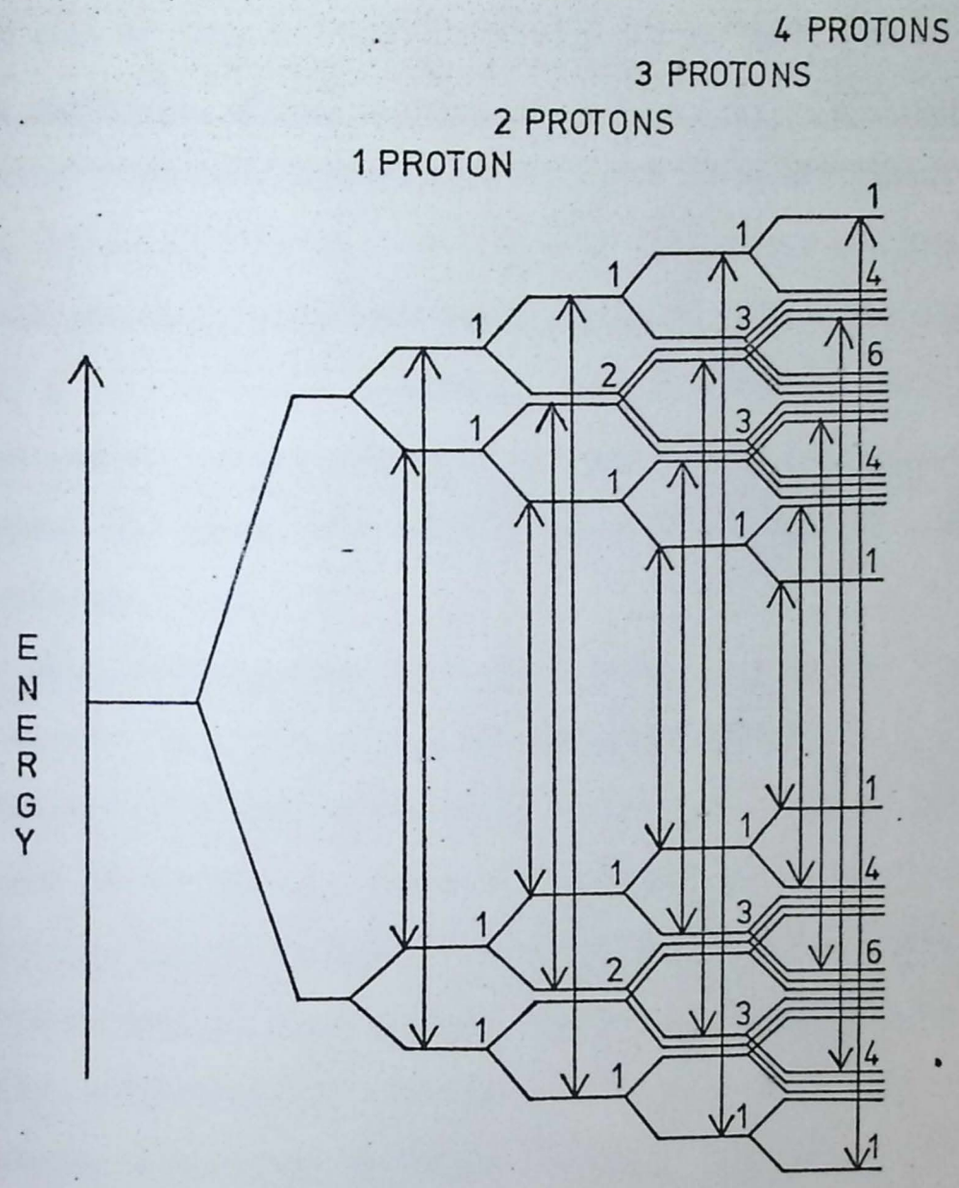

Fig. 6·4. Electron interactions with variable numbers of equivalent protons and the resonance transitions satisfied by the selection rules. This figure also illustrates the relative intensities of these transitions.

Considering two sets of non-equivalent protons m and n, in a radical, the proton set m will produce (m + 1) energy sublevels of the two energy levels seen in Fig. 6.4 and the proton set n will produce (n + 1) energy sublevels, giving a total of (m + 1) x (n + 1) energy sublevels associated with each orientation of the unpaired electron in the magnetic field. There will be (m + 1) x (n + 1) transitions satisfying the electron resonance selection rules and hence a hyperfine spectrum of (m + 1) x (n + 1) lines is obtained with an intensity distribution related to each group. If the splitting constants are of the same order of magnitude, the groups will overlap and some care will be needed to differentiate them.

Other magnetic nuclei besides protons can produce hyperfine structure. For a nucleus with a spin quantum number I, there are 2I + 1 possible orientations of a nuclear magnetic moment in the magnetic field and hence there are 2I + 1 energy sublevels associated with each of the two orientations of the unpaired electron in the field. There are 2I + 1 transitions between these groups, obeying the selection rules giving a hyperfine spectrum of 2I + 1 equally spaced and equally intense lines. This can be illustrated by the Mn^{2+} radical. Manganese with a nuclear spin of 5/2, shows six hyperfine lines with a hyperfine splitting of the order of 80 gauss (Figs. 6.5 and 6.6).

The other interaction that is sometimes important in ESR is the so-called fine structure. Two electrons in the same paramagnetic unit, for example, behave as though they have a spin of 1 and the energy level diagram now looks like Fig. 6.7. With the application of a crystal electric field and a magnetic field, the energy level diagram changes (Fig. 6.8), and in this situation we can observe two resonance lines. Extending this idea to a system of 5 electrons and an effective spin S of 5/2, a crystal electric field and a magnetic field will split the six fold degenerate level into the spectrum consisting of six lines.

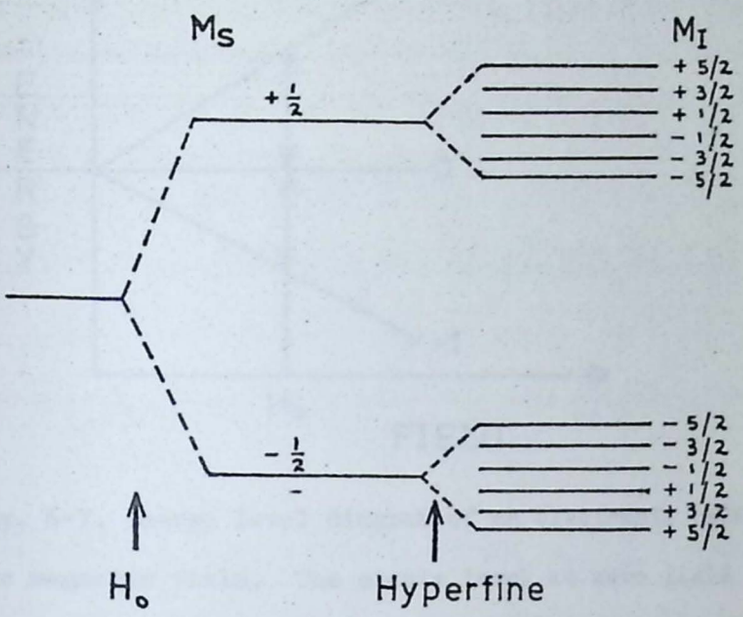

Fig. 6·5. Energy level diagram of an electron with hyperfine interactions produced by a nuclear spin of 5/2.

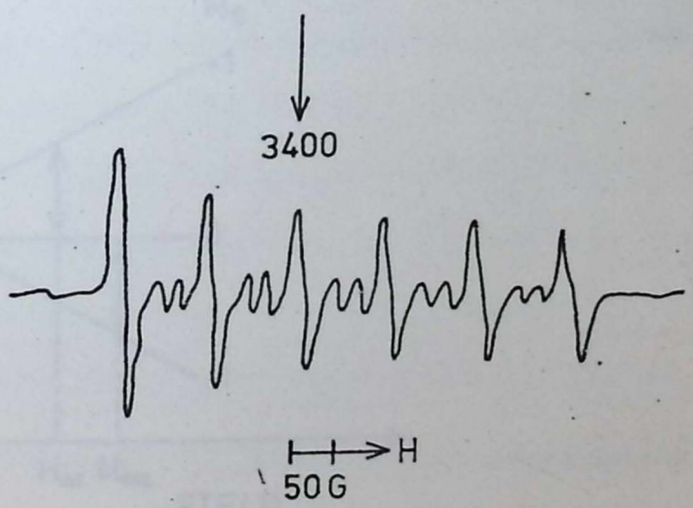

Fig. 6·6. ESR spectrum of Mn^{2+} in a sample of calcite, $CaCO_3$.

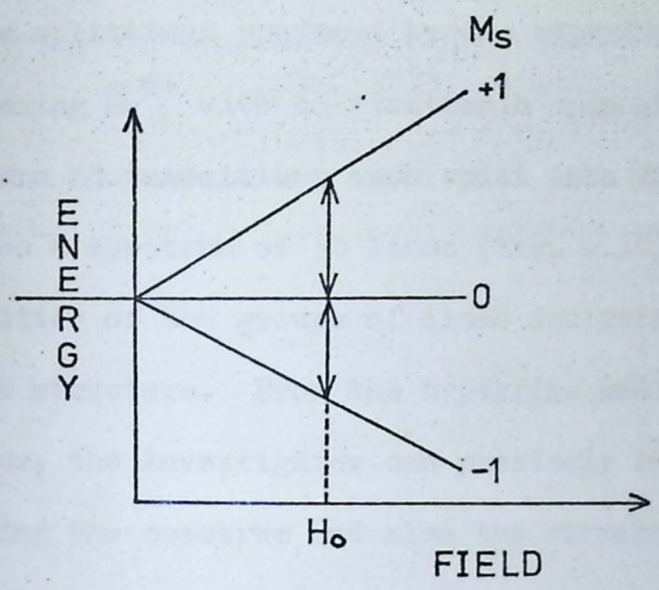

Fig. 6·7. Energy level diagram of an electronic spin (S = 1) as a function of the magnetic field. The simple level at zero field is three-fold degenerate but is split into three levels by the magnetic field. In this case, the angle between the +1 and 0 lines is exactly the same as between the 0 and -1 lines and only one transition will be observed.

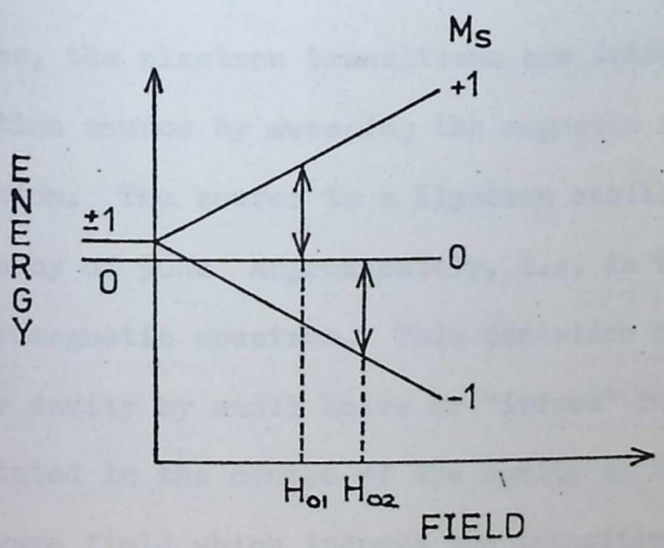

Fig. 6·8. Energy level diagram of an electronic spin (S = 1) with a zero-splitting field as a function of the magnetic field. Two transitions will be observed in this situation (at H_{01} and H_{02} field values).

Fig. 6.9 illustrates how the splitting produced by a crystal field and the splittings produced by the hyperfine interaction combine. Considering Mn^{2+} with an electronic spin of 5/2 and a nuclear spin of 5/2, there are 2S transitions each split into 2I + 1 hyperfine lines which produces a spectrum of 30 lines (Fig. 6.10). The differences in the intensities of the groups of lines indicate which is hyperfine and which is fine structure. From the hyperfine and fine structure detail of the spectrum, the investigator can precisely identify the paramagnetic ion producing the spectrum and also the structural and crystallographic setting of the ion.

The spectra are produced on an ESR spectrometer, the essentials of which are shown in Fig. 6.11. The basic requirements are a source of electromagnetic radiation, a sample cell and a detector to measure the absorption of radiation by the sample.

In ESR because of the difficulty of constructing variable microwave sources, the electron transitions are detected with a monochromatic radiation source by sweeping the magnetic field through the resonance condition. The source is a Klystron oscillator producing radiation with a frequency of 9GHz approximately, i.e. in the microwave region of the electromagnetic spectrum. This radiation is coupled in and out of the sample cavity by small holes or "irises" in the end walls. The sample is orientated in the centre of the cavity so that the magnetic vector of the microwave field which induces the transitions between energy levels, is perpendicular to the main magnetic field H. Changes in the microwave power level of the cavity are monitored by the crystal detector, amplified and observed on an oscilloscope or retained in permanent form with a pen recorder.

In the process of searching for a resonance signal, the magnetic field is linearly increased and when the field reaches the critical value satisfying the resonance condition:

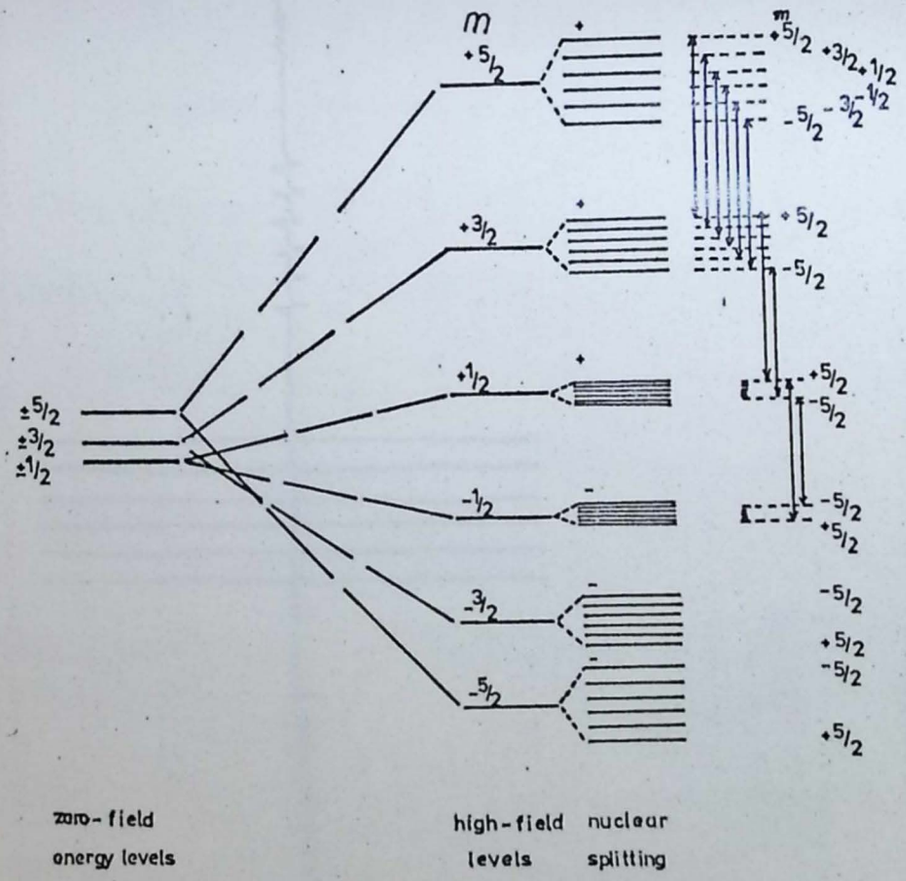

Fig. 6.9 Energy level diagram for the high-spin Mn^{2+} ion, showing the electronic levels in zero and in strong magnetic field, together with the splitting due to the nuclear spin. Some of the typical transitions are indicated by arrows.

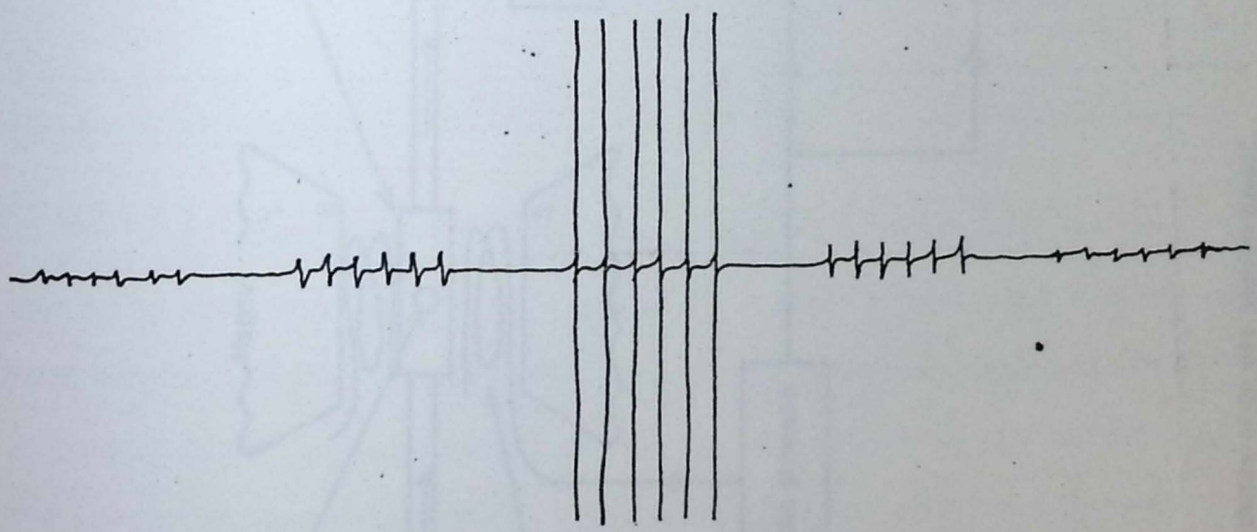

Fig. 6·10. ESR absorption spectrum of an ion with an electronic spin (S = S/2) and a nuclear spin (I = S/2).

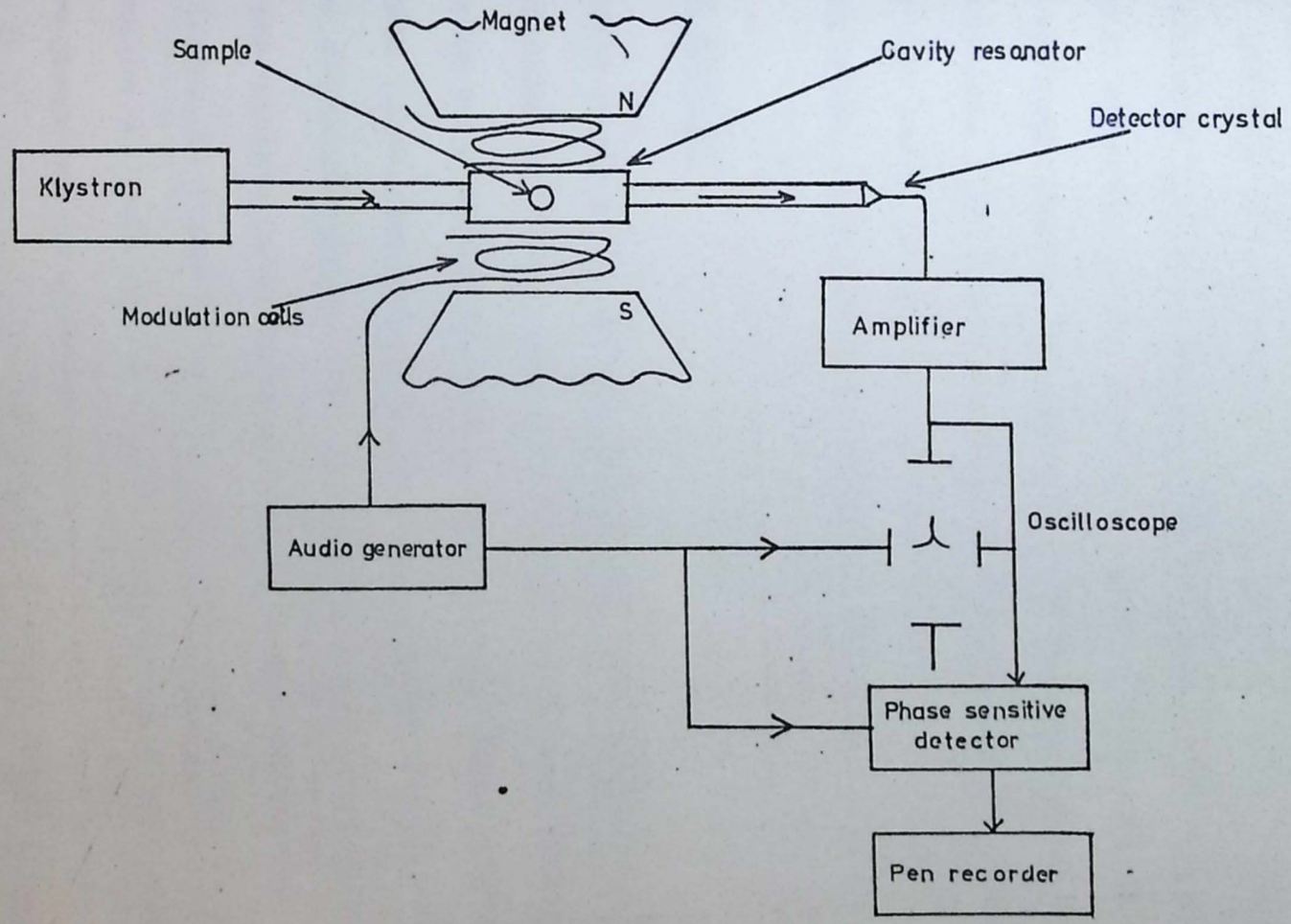

Fig. 6.11. The essential elements of an esr spectrometer.

$$h\nu = g\beta H_o$$

power is absorbed by the sample and a change in crystal current at the detector is monitored.

Sensitivity is enhanced by mounting Helmholtz coils around the cavity and superimposing a sinusoidal modulation (oscillator frequency approximately 100 Hz), on the slowly varying magnetic field. Provided the modulation amplitude is small compared with the width of the absorption line, the signal detected by the microwave detector is proportional to the slope of the spectral line as the magnetic field is swept through the resonance condition. The signal observed in ESR is the first derivative of the absorption curve rather than the true line shape as normally analysed using other spectroscopic techniques (Fig. 6.12).

PROCEDURE AND RESULTS

52 finely powdered (less than 60 microns) shale samples from the Upper Pennsylvanian and Lower Permian of Eastern Kansas were studied at room temperature on a Varian E-3 X-band spectrometer. Samples were placed in borate glass tubes, positioned in the sample chamber and analysed by the procedure described above. The samples were chosen to represent the geochemical and mineralogical range of the shales examined by X-ray diffraction (Chapters 2 and 3) and emission spectroscopy (Chapters 4 and 5). A list of samples analysed can be found in Table 6.1 and their stratigraphic positions are presented in Appendix 6.

Figs. 6.13, 6.14 and 6.15 illustrate the types of spectra detected. The ESR signals can readily be assigned to the paramagnetic ions Mn^{2+} and Fe^{3+}, together with 4 discrete features in the region of free spin ($g = 2.0023$). The Mn^{2+} spectra are of two types corresponding to Mn^{2+} in a symmetric Ca-site as found in calcite (Fig. 6.6) and to Mn^{2+} in an asymmetric Mg-site as found in dolomite (Fig. 6.16). These two types of

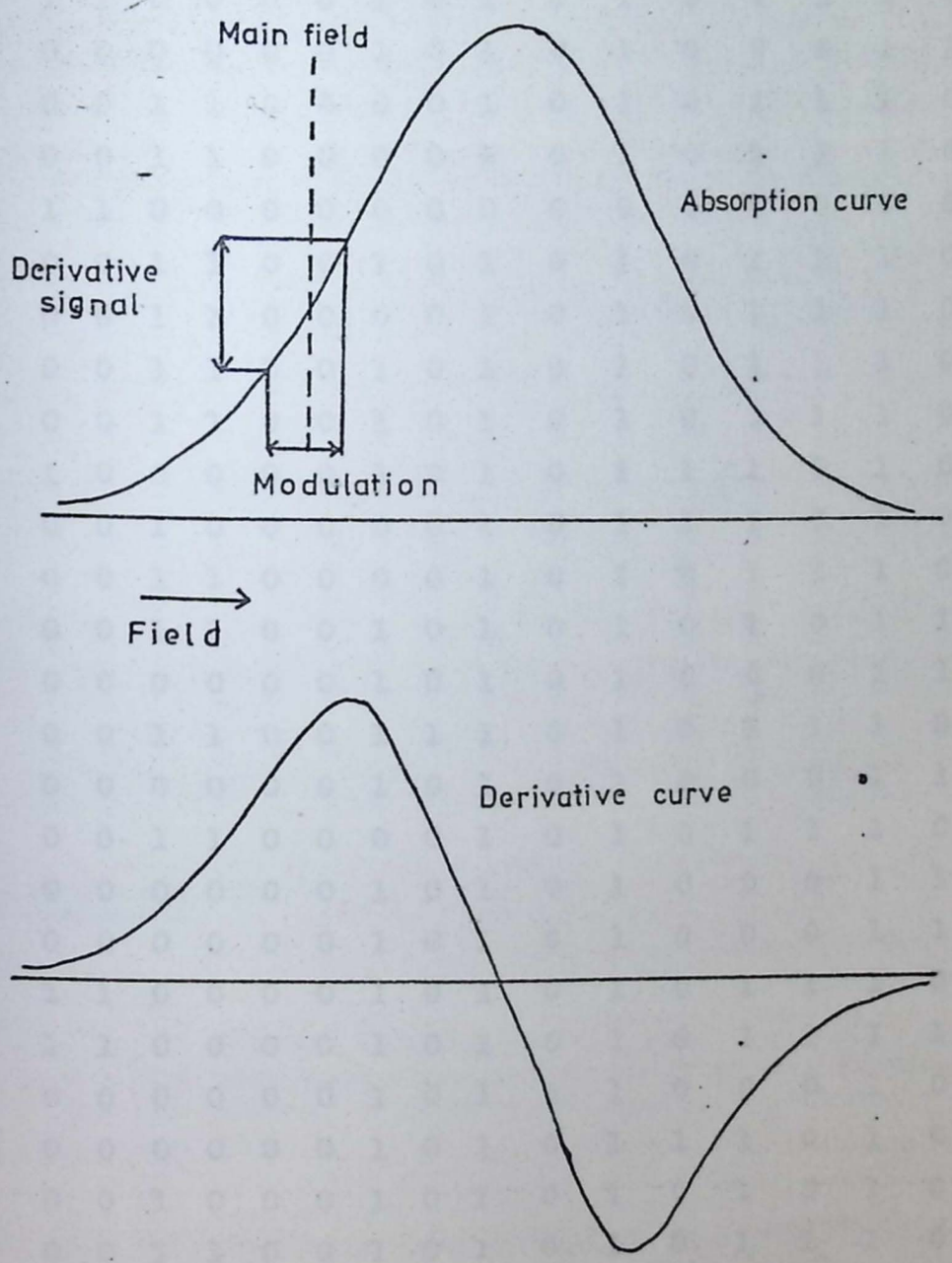

Fig. 6.12. An esr absorption curve and its first derivative which is obtained by field modulation and phase sensitive detection of the signal at the modulation frequency.

TABLE 6.1 Coded values of spectral characteristics based on presence or absence of a character and the intensity of that character relative to other characters.

SAMPLE	VARIABLE																REMARKS
	1	2	3	4	5	6	7	8	9	10	11	12	13	14	15	16	
213	1	1	0	0	0	0	1	0	1	0	1	0	1	1	1	0	
290	0	0	0	0	0	0	1	0	1	0	1	0	0	0	1	1	
94	0	0	1	1	0	0	0	0	1	0	1	0	1	1	1	0	
36	0	0	1	1	0	0	0	0	1	0	1	0	1	1	1	0	
500	1	1	0	0	0	0	0	0	0	0	0	0	0	0	0	0	—Pure calcite included as a standard
135	0	0	1	1	0	0	1	0	1	0	1	0	1	1	1	0	
105	0	0	1	1	0	0	0	0	1	0	1	0	1	1	1	0	
208	0	0	1	1	0	0	1	0	1	0	1	0	1	1	1	0	
109	0	0	1	1	0	0	1	0	1	0	1	0	1	1	1	0	
272	1	0	0	0	0	0	1	0	1	0	1	1	1	0	1	0	
69	0	0	1	0	0	0	0	0	1	0	1	1	1	0	1	0	
209	0	0	1	1	0	0	0	0	1	0	1	0	1	1	1	0	
163	0	0	1	1	0	0	1	0	1	0	1	0	1	0	1	1	
161	0	0	0	0	0	0	1	0	1	0	1	0	0	0	1	1	
186	0	0	1	1	0	0	1	1	1	0	1	0	1	1	1	0	
81	0	0	0	0	0	0	1	0	1	0	1	0	0	0	1	1	
262	0	0	1	1	0	0	0	0	1	0	1	0	1	1	1	0	
173	0	0	0	0	0	0	1	0	1	0	1	0	0	0	1	1	
244	0	0	0	0	0	0	1	0	1	0	1	0	0	0	1	1	
235	1	1	0	0	0	0	1	0	1	0	1	0	1	1	1	0	
243	1	1	0	0	0	0	1	0	1	0	1	0	1	1	1	1	
125	0	0	0	0	0	0	1	0	1	0	1	0	0	0	1	0	
16	0	0	0	0	0	0	1	0	1	0	1	1	1	0	1	0	
82	0	0	1	0	0	0	1	0	1	0	1	0	1	0	1	0	
110	0	0	1	1	0	0	1	0	1	0	1	0	1	1	1	0	
46	1	0	0	0	0	0	0	0	1	0	1	0	1	0	1	0	
168	0	0	0	0	0	0	0	0	1	0	1	1	1	0	1	0	
633	0	0	0	0	1	1	0	0	0	0	0	0	0	0	0	0	—Pure dolomite included as a standard
122	0	0	1	1	0	0	1	0	1	0	1	0	1	1	1	0	
300	0	0	0	0	1	1	0	0	1	0	1	0	0	0	1	0	
28	0	0	0	0	0	0	1	0	1	0	1	1	1	0	1	1	
200	0	0	0	0	1	1	1	1	1	0	1	0	1	1	1	1	
238	0	0	1	1	0	0	1	1	1	0	1	0	1	1	1	0	
298	0	0	0	0	1	1	1	0	1	0	1	0	0	0	1	1	

TABLE 6.1 (continued)

SAMPLE	VARIABLE															
	1	2	3	4	5	6	7	8	9	10	11	12	13	14	15	16
251	0	0	1	1	0	0	0	0	1	0	1	0	1	1	1	0
48	0	0	1	1	0	0	1	0	1	0	1	0	1	1	1	1
221	0	0	1	1	0	0	1	1	1	0	1	0	1	1	1	0
187	0	0	1	1	0	0	1	1	1	0	1	0	1	1	1	0
137	0	0	1	1	0	0	0	0	1	0	1	0	1	1	1	0
5	0	0	0	0	0	0	0	0	1	0	1	1	1	0	1	0
24	0	0	0	0	0	0	1	0	1	0	1	1	1	0	1	0
234	0	0	1	1	0	0	1	0	1	0	1	0	1	1	1	0
155	0	0	0	0	0	0	1	0	1	0	1	1	1	0	1	0
184	0	0	0	0	0	0	0	0	1	0	1	0	0	0	1	0
70	0	0	1	1	0	0	1	0	1	0	1	1	1	0	1	0
160	0	0	1	1	0	0	1	0	1	0	1	0	1	1	1	0
20	0	0	1	1	0	0	1	0	1	0	1	0	1	1	1	1
194	0	0	1	1	0	0	1	0	1	0	1	0	1	0	1	1
43	1	0	0	0	0	0	0	0	0	0	1	1	0	0	1	0
249	0	0	0	0	1	1	0	0	1	0	1	0	1	0	1	0
27	1	1	0	0	0	0	0	0	1	0	1	0	1	1	1	0
281	0	0	1	1	0	0	1	0	1	0	1	0	1	1	1	1
23	0	0	1	1	0	0	0	0	1	0	1	1	1	1	1	0

KEY TO TABLE 6.1

For code 1:-

Variable 1 = MnA present (MnA is the Mn^{2+} species found in calcite lattices).
2 = MnA peak much greater than the free spin feature peaks.
3 = MnB present (MnB is a Mn^{2+} species intermediate between MnA and MnC).
4 = MnB peak much greater than the free spin feature peaks.
5 = MnC present (MnC is the Mn^{2+} species found in dolomite lattices).
6 = MnC peak much greater than the free spin feature peaks.
7 = Fe^{3+} present.
8 = Fe^{3+} peak greater than the Mn^{2+} peak.
9 = Free spin species A present.
10 = Free spin species A peak relatively greater than the other free spin feature peaks.
11 = Free spin species B present.
12 = Free spin species B peak relatively greater than the other free spin feature peaks.
13 = Free spin species C present.
14 = Free spin species C peak relatively greater than the other free spin feature peaks.
15 = Free spin species D present.
16 = Free spin species D peak relatively greater than the other free spin feature peaks.

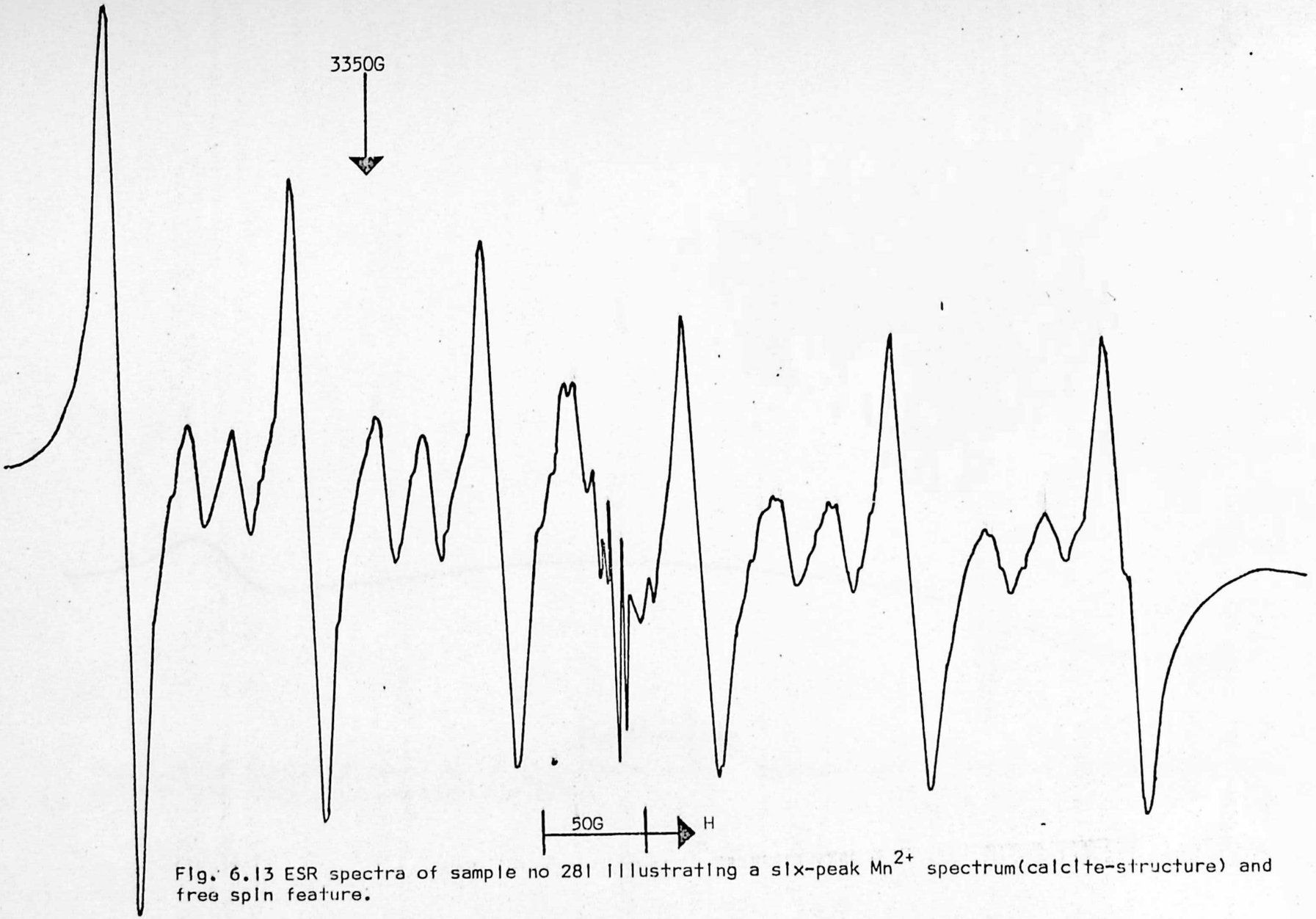

Fig. 6.13 ESR spectra of sample no 281 illustrating a six-peak Mn^{2+} spectrum(calcite-structure) and free spin feature.

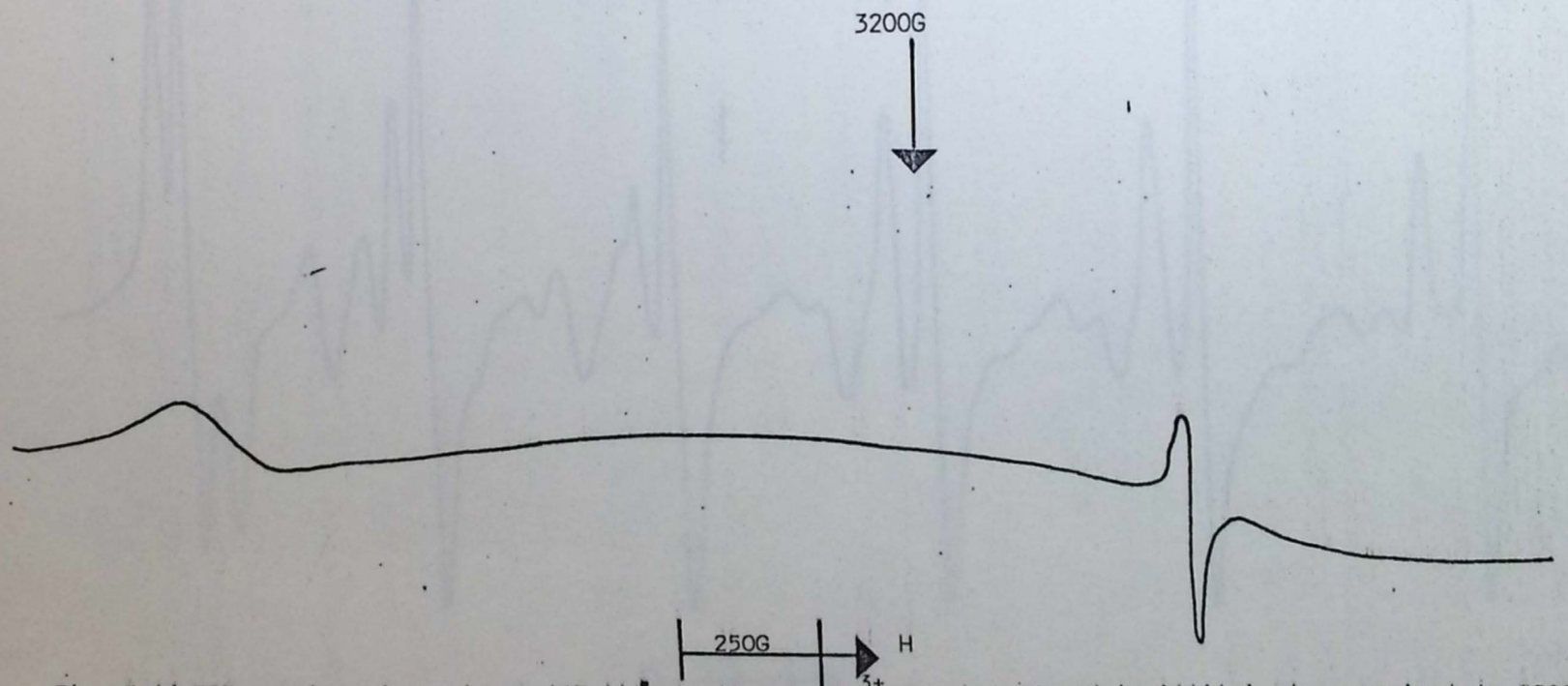

Fig. 6.14 ESR spectra of sample no 125 illustrating an Fe^{3+} spectrum(found in illite) at approximately 2000G and free spin features at approximately 3400G.

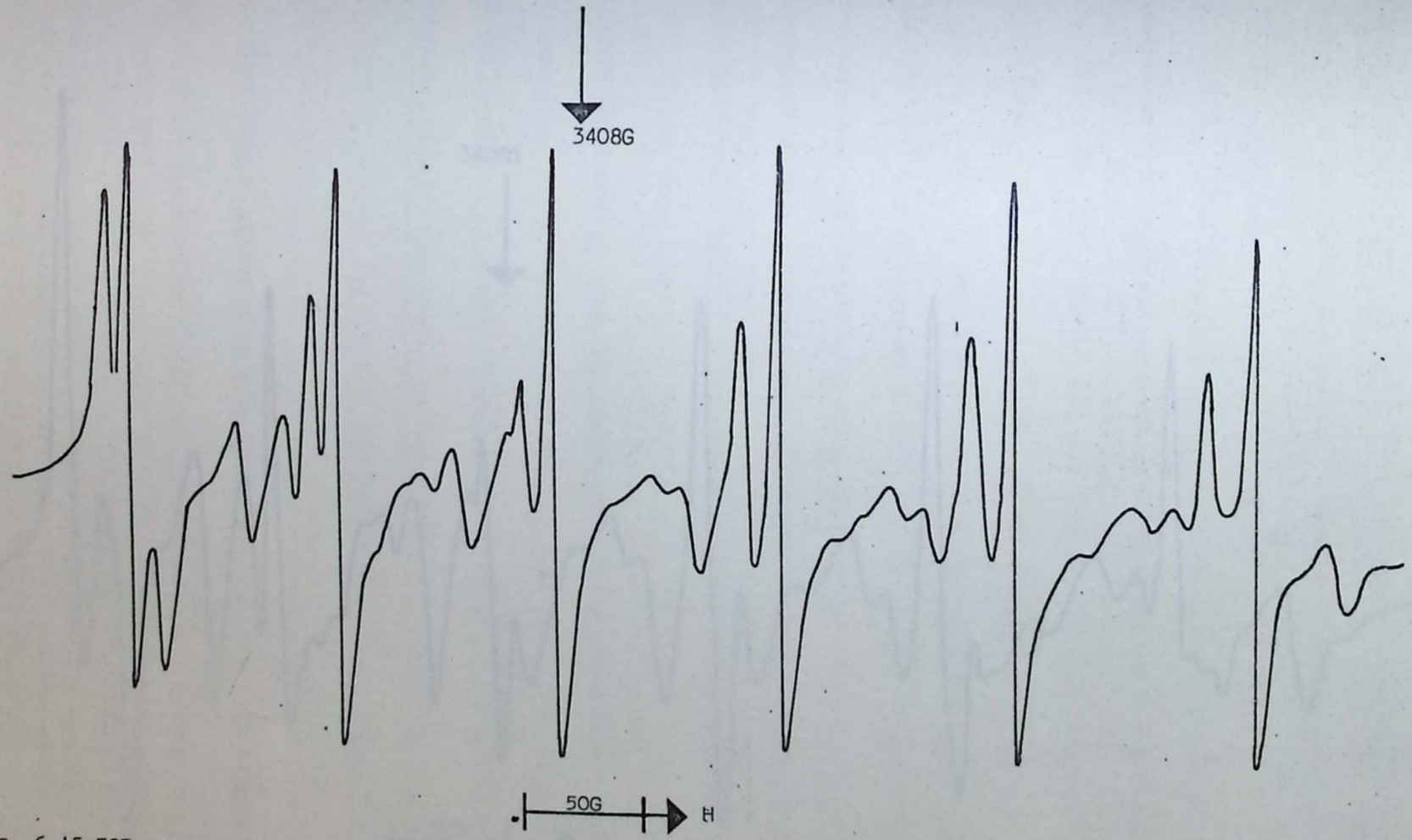

Fig. 6.15 ESR spectra of sample no 300 illustrating a six-peak Mn^{2+} spectrum(dolomite structure).

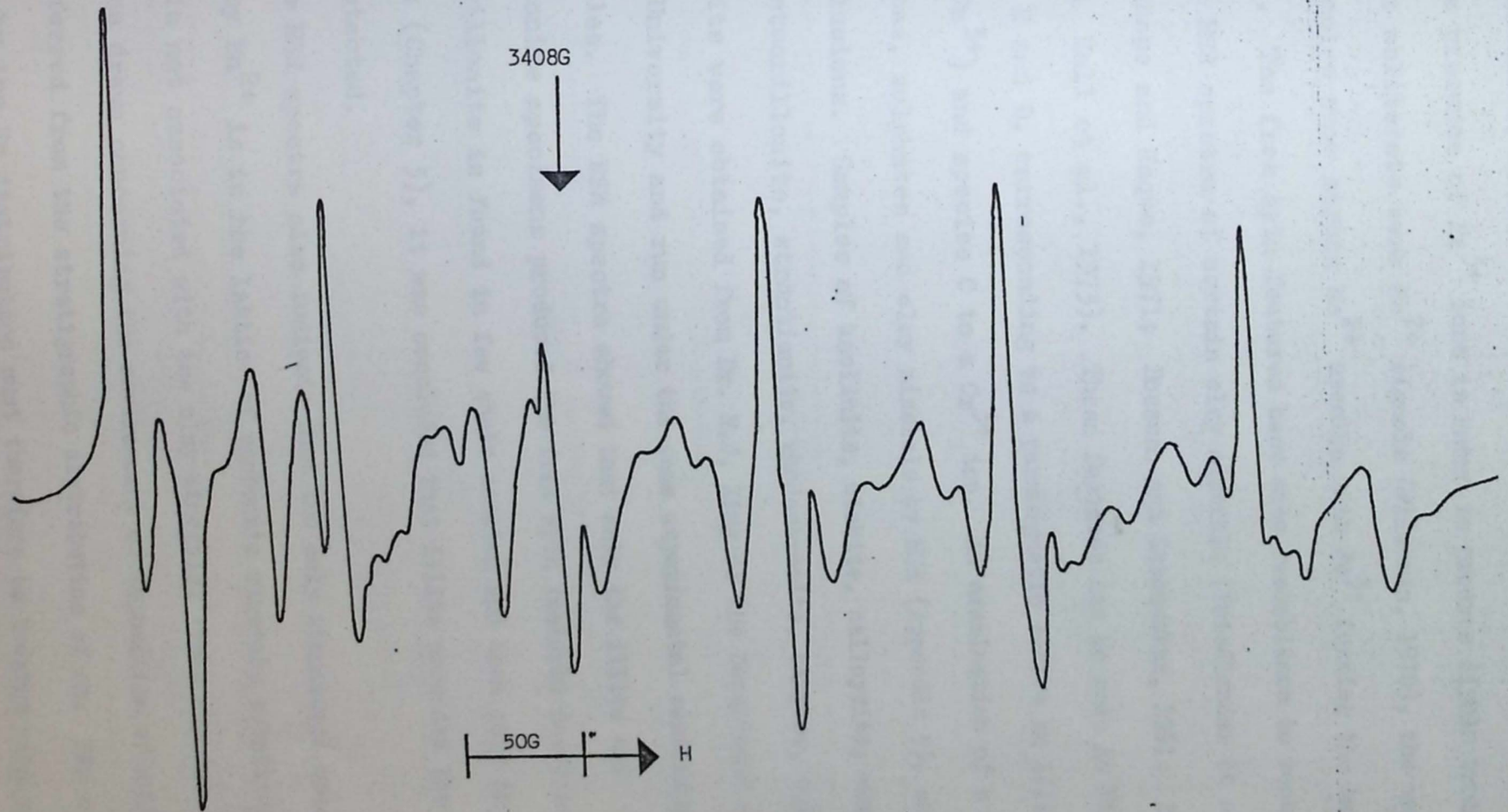

Fig. 6.16 ESR spectrum of Mn^{2+} in dolomite.

spectra are well documented in the literature (Ghosh et al., 1970; Schindler and Ghose, 1970; Wilderman, 1970; Low and Zeire, 1972). Although the presence of Fe^{3+} ions is known to produce dipole broadening effects that obliterate weak Mn^{2+} signals (Wildeman, 1970), the majority of shale samples show strong Mn^{2+} spectra with Fe^{3+} forming the background (Fig. 6.17). The free spin features bear some resemblance to room temperature ESR spectra of certain clay minerals (Friedlander et al., 1963; Wauchope and Haque, 1971; Boesman and Schoemaker, 1961; Angel and Hall, 1972; Hall et al., 1973). These features can be seen in Fig. 6.18, species A, B and D, corresponding to a paramagnetic centre in illite (probably Fe^{3+}) and species C to a Cr^{3+} ion. An examination of a variety of carbonates, sulphates and clay minerals by ESR (Appendix 5), supported these conclusions. Samples of kaolinite, dickite, halloysite, vermiculite, illite, montmorillonite, strontionite, rhodochrosite, barytes, celestine and anhydrite were obtained from Dr. R.J. King of the Department of Geology, Leicester University and run under the same experimental conditions as the shale samples. The ESR spectra showed that only the illite and montmorillonite specimens produced the free spin features described above. As montmorillonite is found in few shale samples and then only in minor quantities (Chapter 3), it was concluded that illite provided the free spin spectra detected.

The ESR spectra also indicate that the only structural sets occupied by Mn^{2+} is in the lattice of carbonate minerals substituting for Ca^{2+} and is not associated with the clay minerals. This supports the conclusions drawn concerning the environment of deposition of calcareous shales inferred from the stratigraphic distribution of Mn. The conditions indicated by the Sr distribution must therefore be treated with scepticism.

The remainder of this chapter concentrates on a statistical analysis of the ESR spectra and a verification of the geochemical and mineralogical classifications previously developed. For such a study, the uncertain

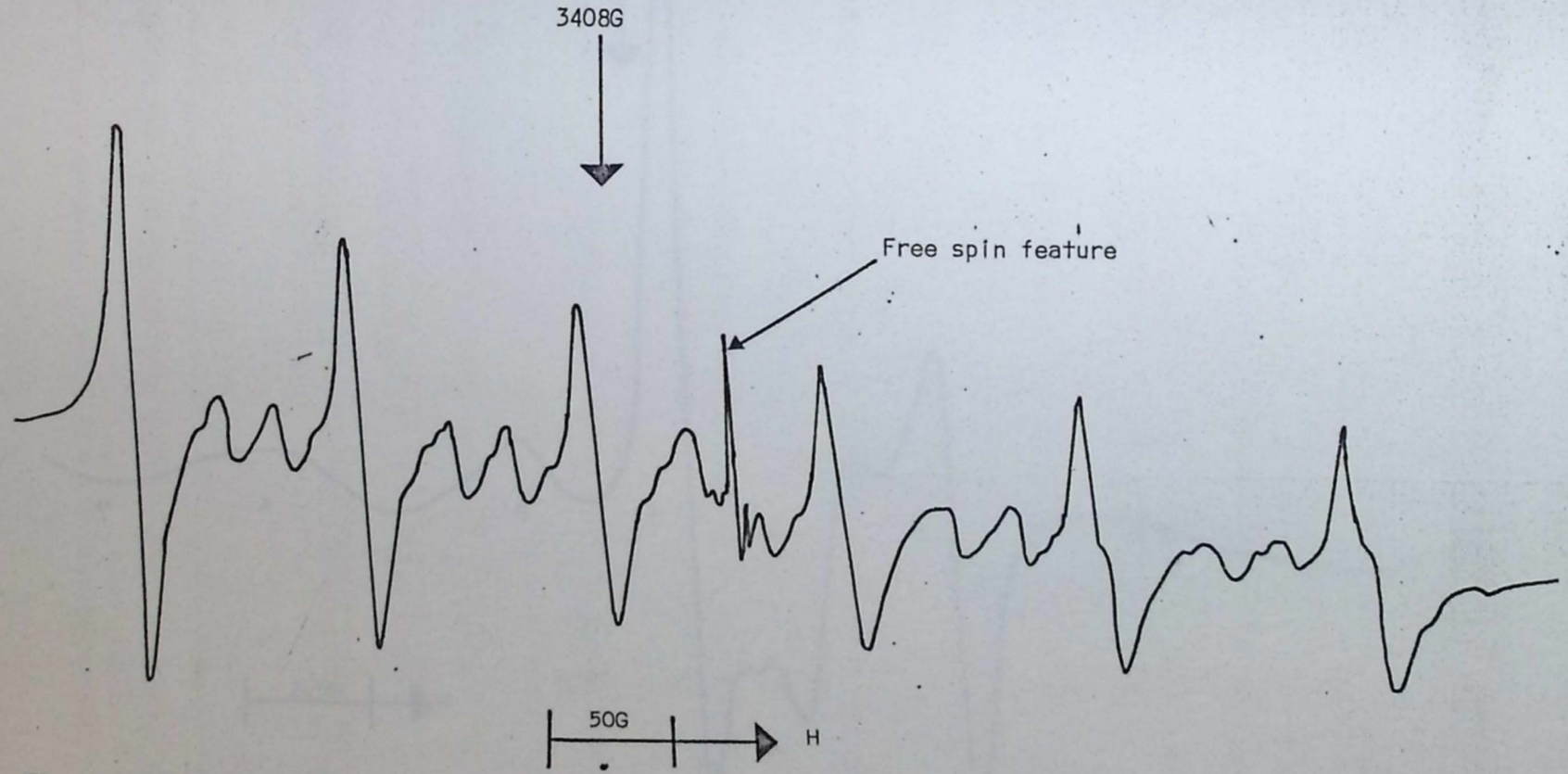

Fig. 6.17 ESR spectra of sample no 238 illustrating a Mn^{2+} spectrum (calcite structure) and free spin feature with a background Fe^{3+} spectrum manifested in the gradual downwards drift of the Mn^{2+} spectrum towards the higher field values.

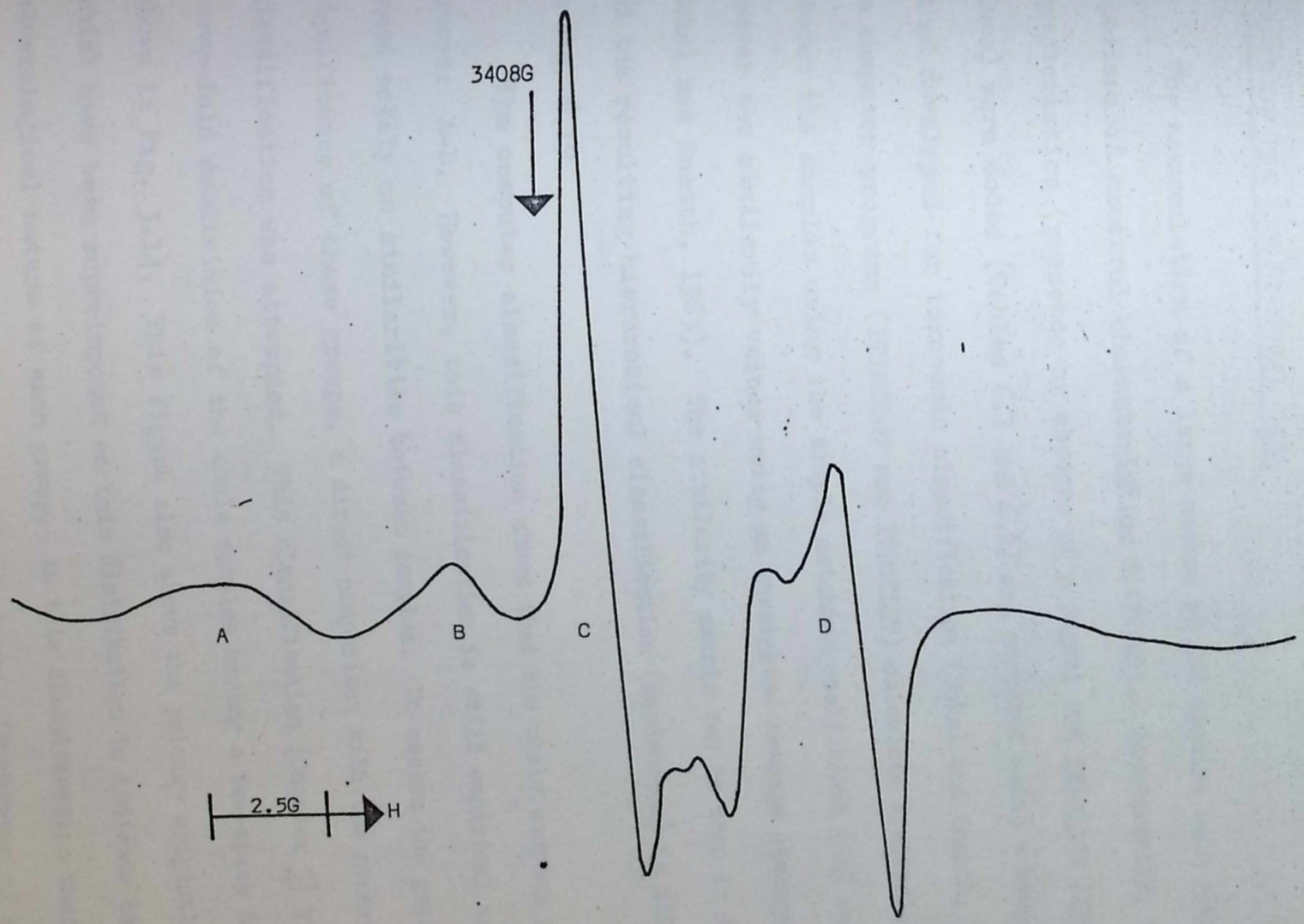

Fig. 6.18 Free spin feature in the ESR spectra of sample no. 86. See text for explanation of diagram.

nature of the species causing ESR absorptions is not a major obstacle as precise identification of each species is unnecessary for classification purposes.

ANALYSIS OF THE ESR SPECTRAL DATA

The accumulation of a large number of ESR spectra made visual comparison of spectral characteristics difficult. Consequently, these characteristics (presence or absence of a signal and relative intensity values) were coded (Tables 6.1 and 6.2) and compared using a computer method developed for taxonomic classification (Sokal and Sneath, 1963). The computer programs (ITBNTOMT and ITBNCLST) calculate similarities between the samples using the simple matching coefficient (SM) and then cluster the similarity values using an unweighted average linkage method (Sokal and Sneath, 1963). The similarity matrix can be seen in Table 6.3 and the resulting hierarchical classification (dendrogram) is illustrated in Fig. 6.19.

The computer classification shows that the shale samples form four groups: A-D. However, this classification is still empirical as it is based solely on similarities between samples. To assess the geological significance of these groups, a direct comparison with the mineralogical classification was attempted. This classification (Chapter 3) yielded a seven-fold subdivision of the shale samples having a two-space distribution shown in Fig. 3.14. This figure also shows the primary original variables which have been superimposed on this distribution to indicate the mineralogical nature of each group. In this classification therefore, the geological significance of each group is known. Comparison of shale samples contained in ESR groups A-D with their position in the mineralogical groups A-H is summarised in Table 6.4. This Table combined with Fig. 3.14 indicates the geological nature of the four ESR groups. As group C

TABLE 6.2 Summary statistics of the binary characters describing ESR spectra of shale samples (Key for the characters can be found in Table 6.1)

CHARACTER	TOTALS		PERCENTAGE	
	ABSENT (0)	PRESENT (1)	ABSENT (0)	PRESENT (1)
1	45	9	83.3	16.7
2	48	6	88.9	11.1
3	27	27	50.0	50.0
4	29	25	53.7	46.3
5	49	5	90.7	9.3
6	49	5	90.7	9.3
7	19	35	35.2	64.8
8	48	6	88.9	11.1
9	3	51	5.6	94.4
10	54	0	100.0	0.0
11	2	52	3.7	96.3
12	43	11	79.6	20.4
13	12	42	22.2	77.8
14	26	28	48.1	51.9
15	2	52	3.7	96.3
16	39	15	72.2	27.8

TABLE 6.3 Similarity matrix, entries in range 0 to 9.

SAMPLE NO.	MATRIX
213	9
235	99
272	999
243	9989
27	99889
290	666769
161	6667699
81	66676999
173	666769999
244	6667699999
125	77666999999
184	666678888899
298	5556588888879
157	77686888887669
28	6667688888887799
69	6655666666785789
168	666677777778868899
5	6666777777888899
16	77666888888886898999
24	776668888888689899999
155	7766688888888689899999
46	887787777788687888889
94	6666766666675568776667
36	66667666666755687766679
105	666676666667556877666799
209	6666766666675568776667999
262	66667566666755687766679999
251	666676666667556877666799999
137	6666766666675568776667999999
135	77666666667656676677769999999
208	776666666676566766777699999999
109	7766666666765667667776999999999
110	77666666667656676677769999999999
122	776666666676566766777699999999999
234	7766666666765667667776999999999999
160	77666666667656676677769999999999999
186	667666666666556666666688888899999999
238	6676666666665566666666888888899999999
227	66766666666655666666668888888999999999
187	667666666666556666666688888889999999999
23	665565555566466888777699999988888888889
163	66565888887667876677768888888888888888879
194	665658888876678766777688888888888888888799
48	666767777766667666666688888889999999888886999
20	6667677777666676666666888888899999998888899999
281	66676777776666766666668888888999999988888999999
82	776668888888678888888888888888888888888887888889
70	665556666676578888888688888888888888888888888889
633	333345555566634555555544444443333333333333333339
300	555567777788856677666766666665555555555555555569
249	665566666678866788777866666666666666555566655576799
200	666656666665866555666555555556666666666656666655679
500	665365555566454555555644444443333333333333333335375529
43	66556666667857678877785555555555555544446554466666379

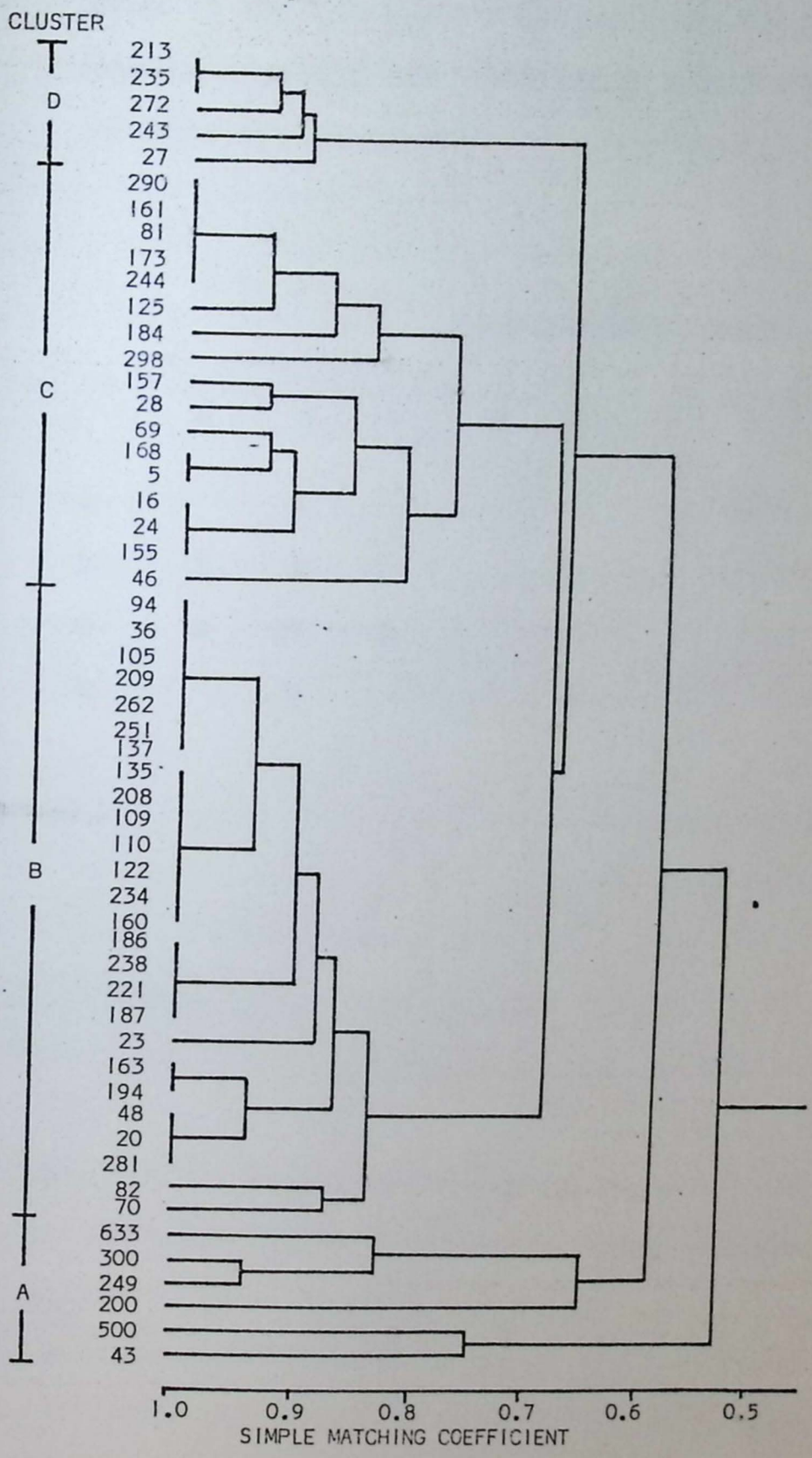

Fig. 6.19 Dendrogram of ESR data calculated using an unweighted average linkage algorithm. Clusters produced are indicated on the left.

TABLE 6.4 A comparison of the position of samples in ESR GROUPS A-D with their position within the mineralogical classification (e.g. of the 5 samples constituting group D in the ESR classification, 4 were classified in group E of the X-ray diffraction classification and 1 in group B).

		X-RAY DIFFRACTION GROUPS							
		A	B	C	D	E	G	H	Standards
ESR GROUPS	A		2					2	2
	B	7	4			13	2		
	C	2	13	1		1			
	D		1			4			

consists predominantly of shales within the mineralogical groups A, B and C, and examining Fig. 3.14, it is apparent that mineralogical groups A, B and C have high quartz values. Group C samples therefore, must be predominantly quartz rich. Similarly, ESR group A samples are predominantly dolomitic and groups B and D samples are high in calcite. The distinction between groups B and D arises from different site symmetries for Mn^{2+} in these shales.

As the mineralogical classification is, obviously, based on mineralogical data, the groups derived from this analysis must represent geologically meaningful subdivisions of the shale sample collection. As the ESR and mineralogical groups correspond, it is also probable that the parameters controlling these groups are equivalent. This assumption is supported by a plot of the samples in the four ESR groups against stratigraphical position (Fig. 6.20) which is very similar to equivalents for the mineralogical and geochemical classifications and indicates major breaks just below the base of the Permian, at the Wabaunsee-Shawnee boundary, at the top of the Douglas and the base of the Lansing, producing a five-fold division of the stratigraphical column. The Pleasanton and Kansas City (Lower and Middle) Groups are characterized by alternations of samples from all four clusters. The Upper Kansas City, Lansing and Lower Douglas Groups only contain samples of group C indicating clastic deposition throughout this period. The succeeding Upper Douglas and the Shawnee Groups consist of group B and occasionally group C samples, reflecting the general calcareous nature of the sediments. Samples in the Lower Wabaunsee Group region are also exclusively from clusters B and C. However, they are developed in different proportions to the Shawnee indicating a higher detrital content for the beds. The Permian and Upper Wabaunsee shale samples fall into all four categories with A, D and B predominating. Here is further support for the hypothesis that the Permian/Pennsylvanian boundary marks a change in sedimentological conditions from the clastic

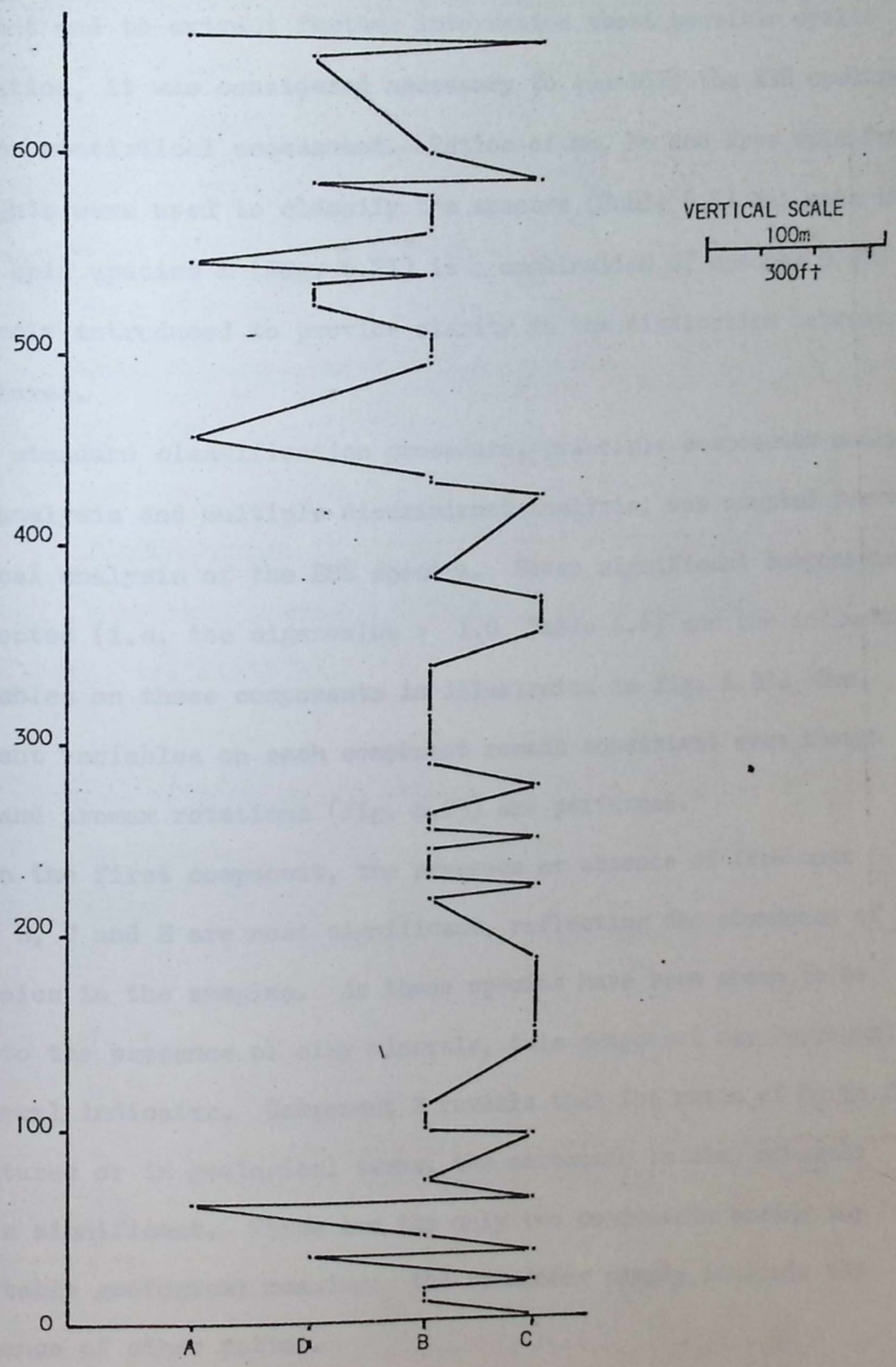

Fig. 6.20 A plot of the stratigraphic position of shale samples against their ESR cluster. The horizontal scale is arbitrary but may give some indication of increasing carbonate content to the left. For a comparable stratigraphic column see Fig. 3.5.

deposition of the Upper Pennsylvanian to the carbonate-evaporite deposits of the Permian era.

Oscillations in the ESR properties of stratigraphic units were visible in the Shawnee and Wabaunsee. However, the variation was not significant and to extract further information about possible cyclic sedimentation, it was considered necessary to quantify the ESR spectra and repeat the statistical assessment. Ratios of Mn, Fe and free spin feature peak heights were used to classify the spectra (Table 6.5) but note that the free spin species E (Fig. 6.21) is a combination of species B and C and was only introduced to provide clarity in the distinction between free spin features.

A standard classification procedure, principle components analysis, cluster analysis and multiple discriminant analysis, was adopted for the statistical analysis of the ESR spectra. Seven significant components were detected (i.e. the eigenvalue > 1.0 Table 6.6) and the influence of the variables on these components is illustrated in Fig. 6.22. The significant variables on each component remain consistent even though varimax and promax rotations (Fig. 6.23) are performed.

On the first component, the presence or absence of free spin features B, C and E are most significant, reflecting the abundance of free spin species in the samples. As these species have been shown to be related to the presence of clay minerals, this component may represent a clay mineral indicator. Component 2 reveals that the ratio of Mn to free spin features or in geological terms, the carbonate to clay minerals ratio, is significant. These are the only two components having any interpretable geological meaning; the remainder simply indicate the significance of other ratios.

The component scores of the samples on these seven components are clustered using a distance coefficient producing a dendrogram in which a maximum of ten groups can be detected (Fig. 6.24). Group discreteness is

TABLE 6.5 Presence/absence and ratio variables used to classify ESR spectra.

For Code 1:-

Variable 1. MnA present.

2. MnB present.

3. MnC present.

4. Fe^{3+} present.

5. Free spin species A present.

6. Free spin species B present.

7. Free spin species C present.

18. Free spin species E present.

19. Free spin species E peak greater than other free spin feature peaks.

20. Free spin species E develops a subsidiary peak.

Alternatives coded 0.

Numerical values of peak height ratios.

Variable 8. Mn peak height/free spin species A peak height.

9. Mn/B

10. Mn/C

11. Mn/D

12. Mn/E

13. A/D

14. B/D

15. C/D

16. E/D

17. Mn/Fe^{3+}

21. A/C

22. B/C

23. A/B

N.B. Free spin species D is present in all samples.

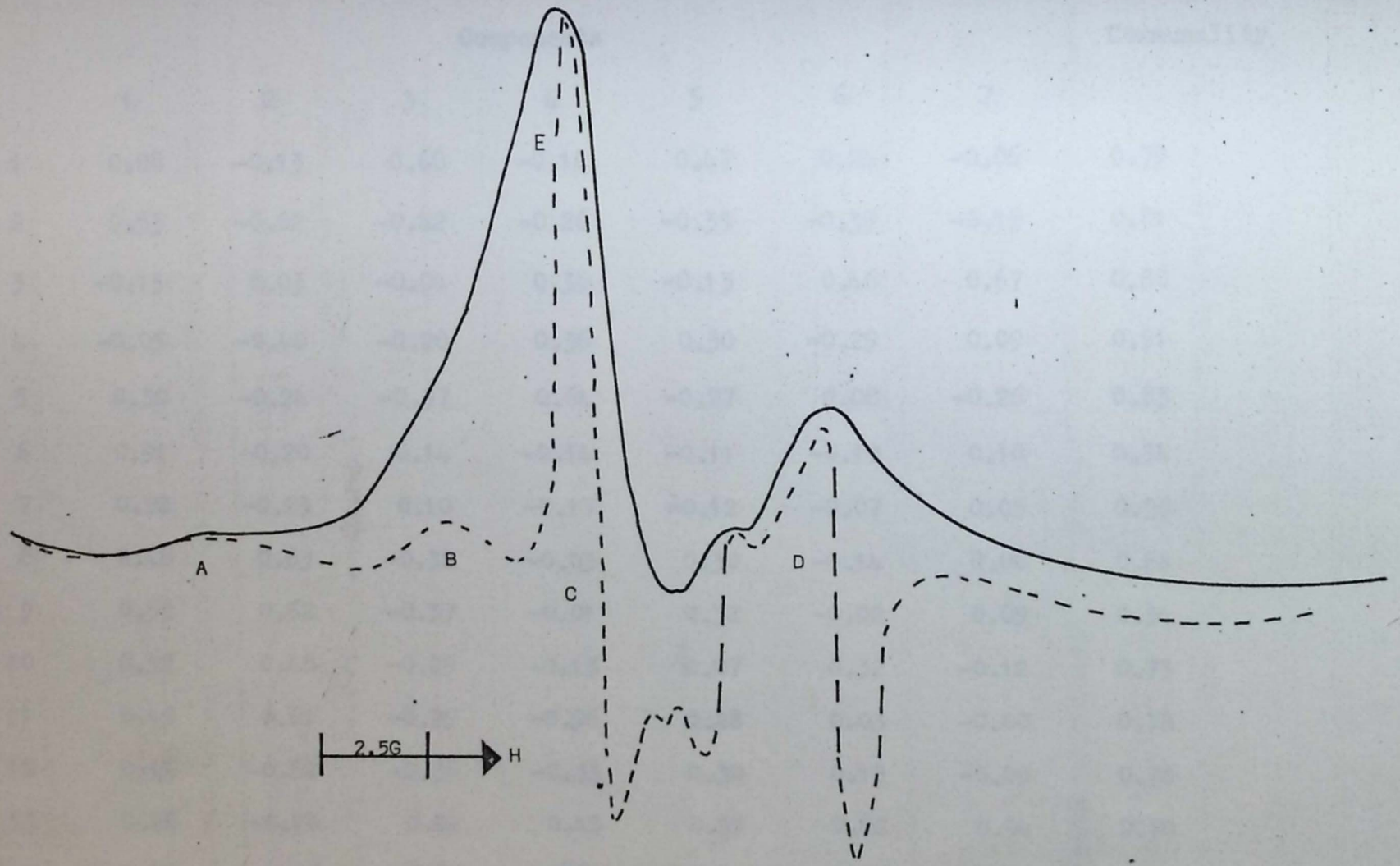

Fig. 6.21 Free spin feature E is interpreted as a combination of features B and C. A normal spectrum (dotted lines) is included to illustrate the similarities between the spectra.

TABLE 6.6 Principal components loadings for ESR spectral data

VARIABLE	Components							Communality
	1	2	3	4	5	6	7	
1	0.08	-0.13	0.68	-0.14	0.47	0.24	-0.06	0.79
2	0.53	-0.02	-0.42	-0.26	-0.35	-0.39	-0.15	0.81
3	-0.15	0.03	-0.04	0.30	-0.13	0.46	0.67	0.80
4	-0.05	-0.40	-0.20	0.36	0.30	-0.29	0.09	0.51
5	0.30	-0.24	-0.37	0.64	-0.27	0.08	-0.26	0.83
6	0.91	-0.20	0.14	-0.14	-0.11	-0.10	0.10	0.94
7	0.92	-0.23	0.10	-0.17	-0.12	-0.07	0.05	0.96
8	0.48	0.63	-0.32	-0.03	0.30	-0.14	0.06	0.84
9	0.55	0.62	-0.37	-0.01	0.32	-0.02	0.09	0.94
10	0.52	0.48	-0.29	-0.13	0.07	0.32	-0.12	0.73
11	0.49	0.61	-0.29	-0.06	0.28	0.03	-0.00	0.78
12	0.14	-0.62	-0.35	-0.33	0.30	0.15	-0.09	0.76
13	0.28	-0.28	0.02	0.45	0.59	0.02	0.04	0.70
14	0.52	-0.06	0.57	0.20	0.22	0.08	-0.32	0.80
15	0.53	0.17	0.18	0.34	0.36	-0.30	0.13	0.70

TABLE 6.6 (continued)

		Components							Communality
		1	2	3	4	5	6	7	
VARIABLE	16	-0.51	0.30	0.31	-0.58	0.25	-0.13	0.16	0.89
	17	0.41	0.32	-0.05	-0.13	-0.16	0.62	-0.13	0.71
	18	-0.77	-0.24	-0.37	-0.09	0.31	0.15	-0.09	0.92
	19	-0.69	0.26	0.04	-0.22	0.11	-0.16	-0.23	0.69
	20	-0.26	-0.36	-0.54	-0.07	0.32	0.22	-0.32	0.74
	21	0.62	-0.55	-0.16	-0.37	0.09	0.00	0.12	0.87
	22	0.73	-0.22	0.41	-0.11	-0.09	0.13	-0.22	0.83
	23	0.33	-0.56	-0.24	-0.34	0.10	0.01	0.37	0.75
Eigenvalue		6.34	3.32	2.51	1.93	1.75	1.28	1.12	

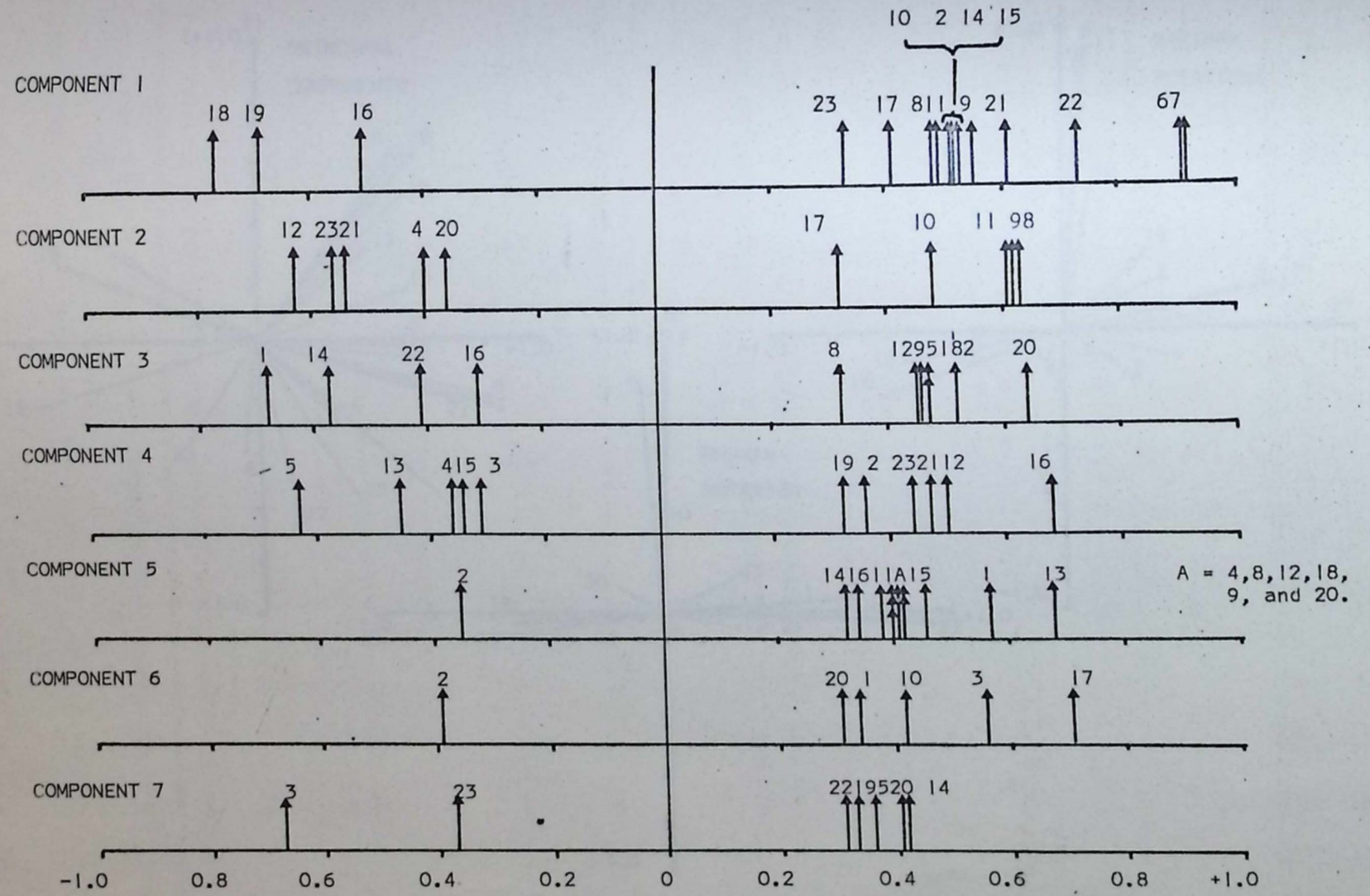

Fig. 6.22 Principal component loadings of ESR variables. For explanation of variable numbers, see Table 6.5. Only loadings > ± 0.3 are illustrated.

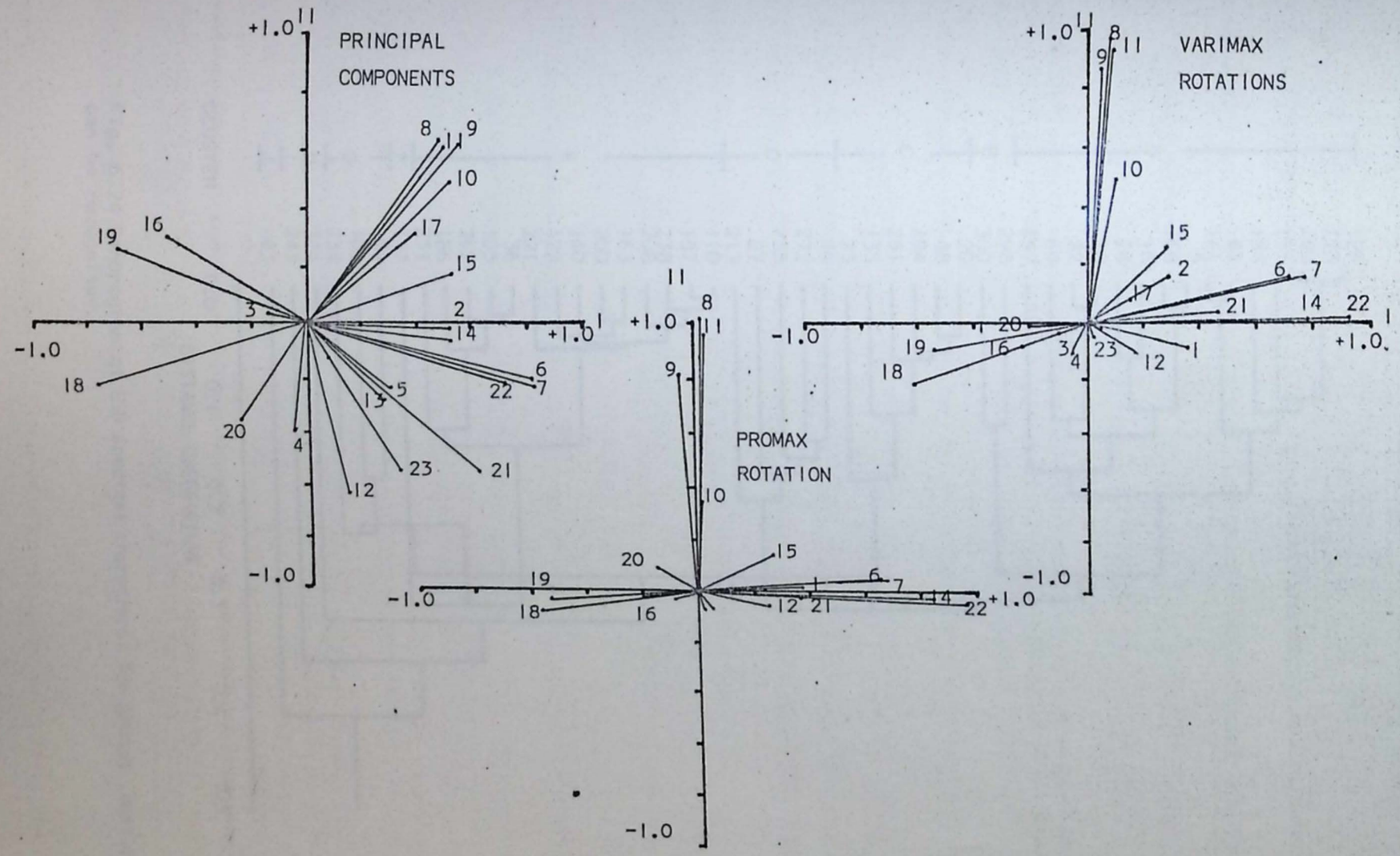

Fig. 6.23 Principal component, varimax rotation, and promax rotation plots of the ESR variables listed in Table 6.5. Note that Promax axes I and II are not orthogonal (Correlation = 0.19) but for simplicity are drawn so.

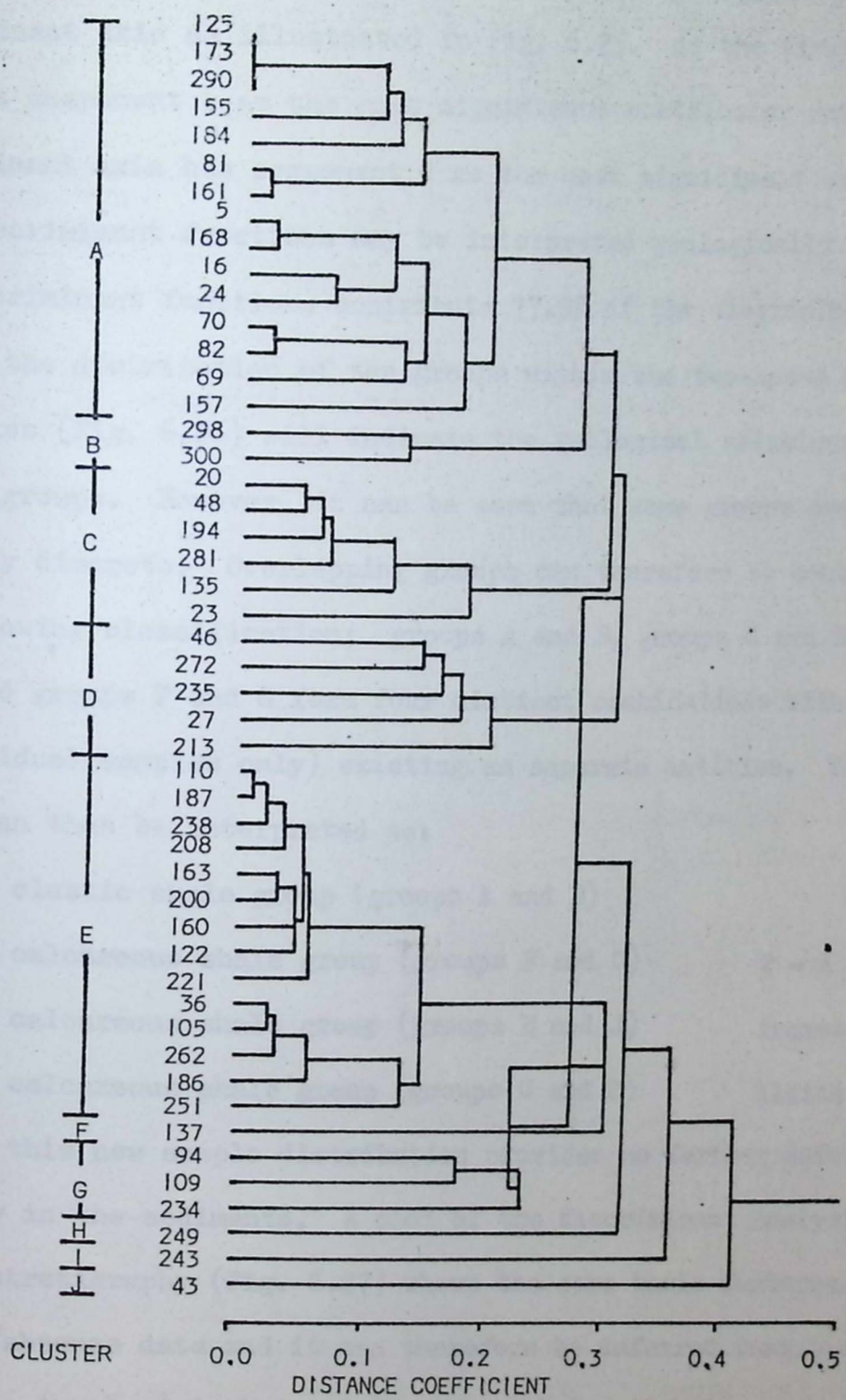

Fig. 6.24 Dendrogram of ESR spectral characters. Ten groups labelled A to J can be recognised.

tested by performing a multiple discriminant analysis on the component scores of samples in groups A-H. Six significant discriminant axes are postulated with the relative contribution of each component to each discriminant axis as illustrated in Fig. 6.25. As the first discriminant axis has component 1 as the most significant contributor and the second discriminant axis has component 2 as the most significant contributor, both discriminant functions may be interpreted geologically and as these two discriminant functions contribute 77.9% of the discriminating power, a plot of the distribution of the groups within the two-space defined by these axes (Fig. 6.26) will indicate the geological relationships between the ten groups. However, it can be seen that some groups overlap and are not truly discrete. Overlapping groups can therefore be combined to form the following classification; groups A and B, groups C and D, groups E and J and groups F and G form four distinct combinations with groups I and H (individual samples only) existing as separate entities. These shale groups can then be interpreted as:

1. A clastic shale group (groups A and B)
2. a calcareous shale group (groups F and G) 2 - 4 with an
3. a calcareous shale group (groups E and J) increasing carbonate-
4. a calcareous shale group (groups C and D) illite ratio

However, this new sample distribution provides no further information on cyclicity in the sediments. A plot of the discriminant analysis groups against stratigraphy (Fig. 6.27) shows the same basic features as the presence/absence data and it can therefore be inferred that the underlying principles involved in this study must apply as much to a numerical characterization of the ESR spectra as to simple presence/absence data.

CONCLUSIONS

Although electron spin resonance has been employed widely in geological fields (see Appendix 2), the technique has been mainly applied

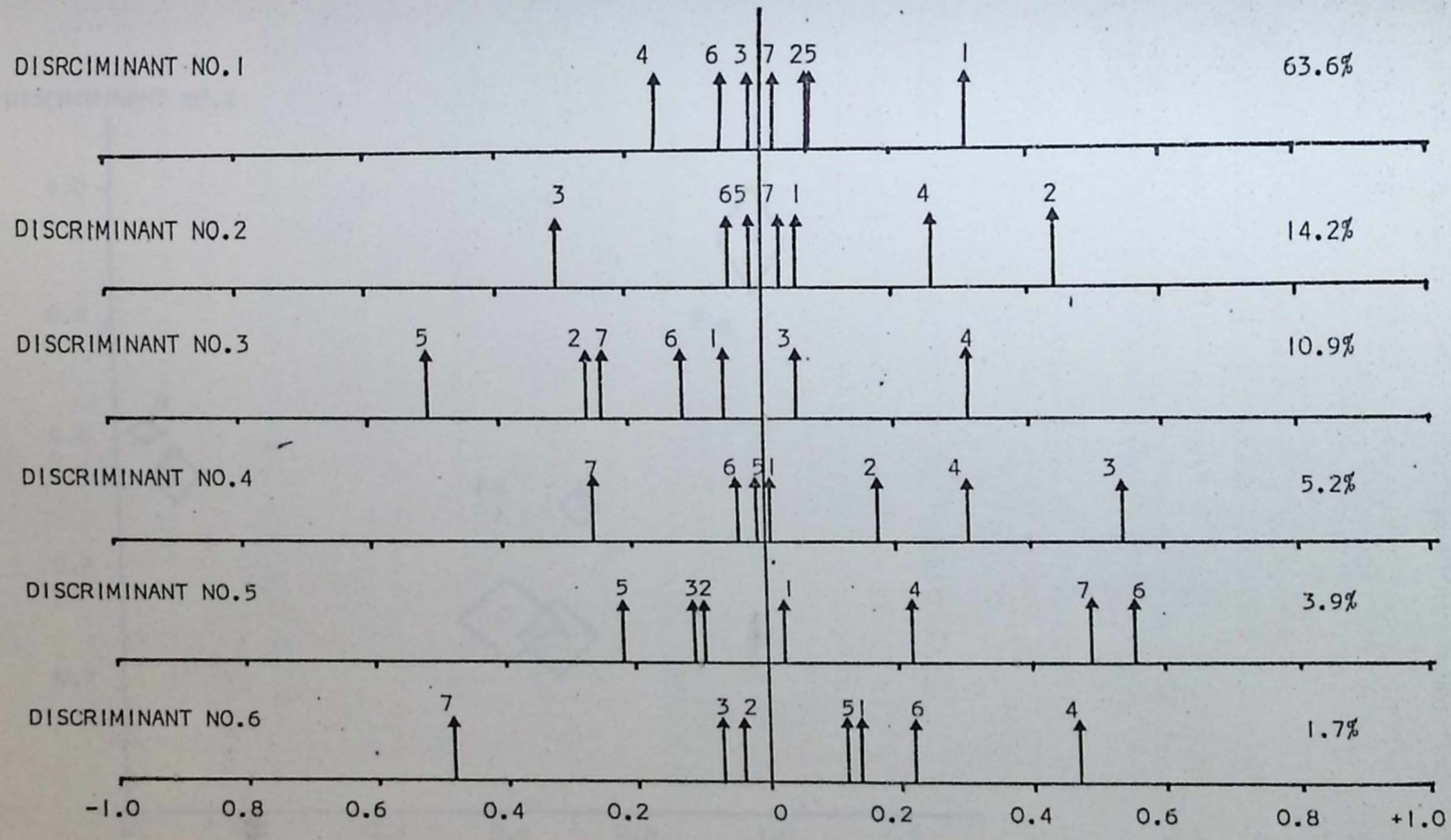

Fig. 6.25 Graphic plot of relative contribution of each variable (component) to each discriminant axis. Percentage of discriminating power contained in each function is presented on the right.

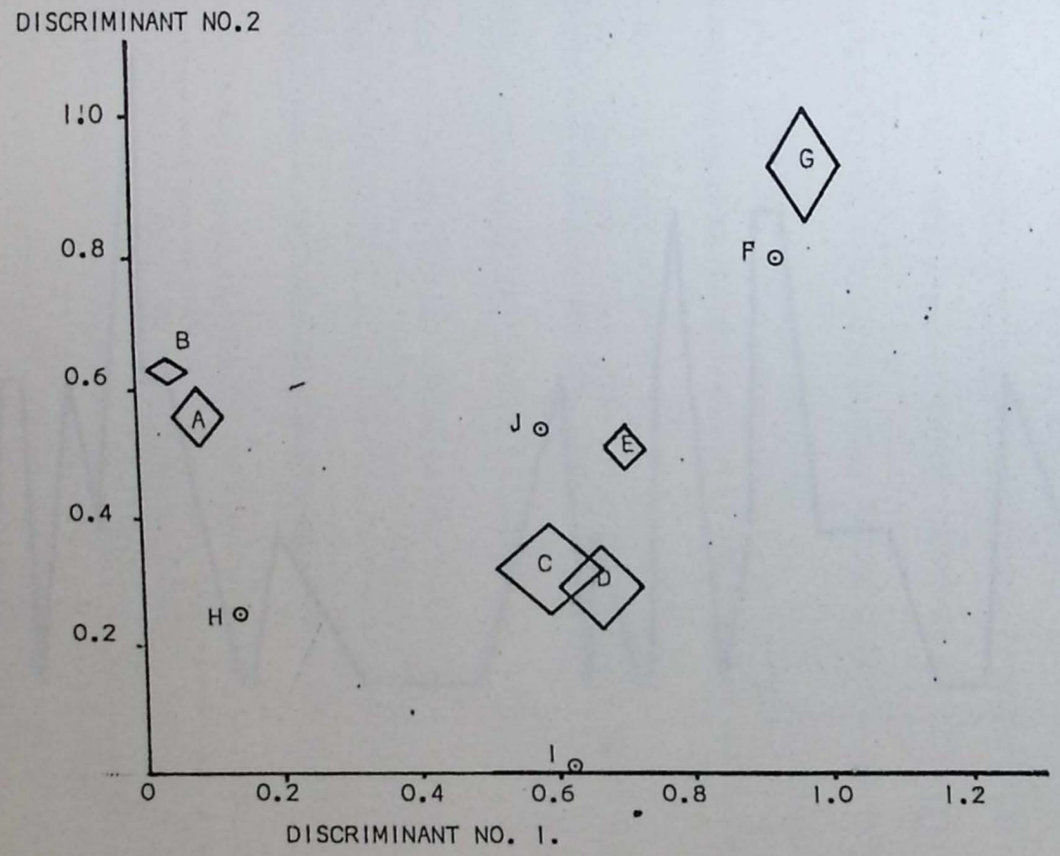

Fig. 6.26 Graphic plot of ten groups distingulshed by principle components and cluster analysis. The diamonds represent the mean of each group $\pm$ one standard deviation on each discriminant axis. Single points represent a group containing only one sample.

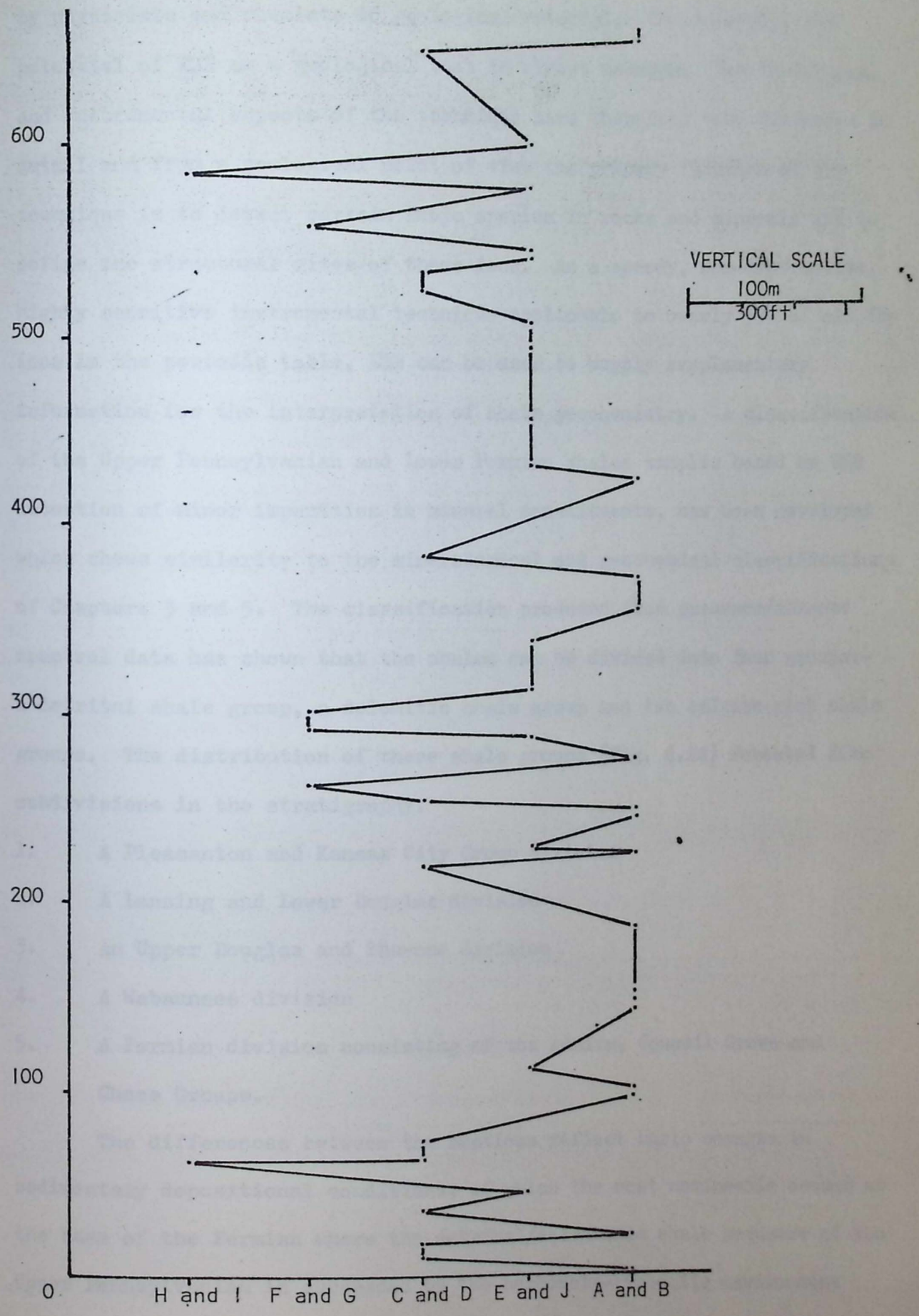

Fig. 6.27 Stratigraphic distribution of shale samples arranged according to their cluster analysis group. The horizontal scale is arbitrary.

by physicists and chemists to geological material. Consequently, the potential of ESR as a geological tool is almost unknown. The theoretical and instrumental aspects of the technique have therefore been discussed in detail and from a geological point of view the primary function of the technique is to detect certain ionic species in rocks and minerals and to define the structural sites of these ions. As a speedy, non-destructive, highly sensitive instrumental technique applicable to nearly 50% of all the ions in the periodic table, ESR can be used to supply supplementary information for the interpretation of shale geochemistry. A classification of the Upper Pennsylvanian and Lower Permian shales samples based on ESR detection of minor impurities in mineral constituents, has been developed which shows similarity to the mineralogical and geochemical classifications of Chapters 3 and 5. The classification produced from presence/absence spectral data has shown that the shales can be divided into four groups:- a detrital shale group, a dolomitic shale group and two calcite-rich shale groups. The distribution of these shale groups (Fig. 6.24) revealed five subdivisions in the stratigraphy.

1. A Pleasanton and Kansas City Group division
2. A Lansing and Lower Douglas division
3. An Upper Douglas and Shawnee division
4. A Wabaunsee division
5. A Permian division consisting of the Admire, Council Grove and Chase Groups.

The differences between the sections reflect basic changes in sedimentary depositional conditions, of which the most noticeable occurs at the base of the Permian where the detrital/calcareous shale sequence of the Upper Pennsylvanian is succeeded by the carbonate-evaporite environment of the Permian. The numerical characterization and analysis of spectral data has provided similar results to the presence/absence data.

Finally, ESR spectra of Upper Pennsylvanian and lower Permian shales

have indicated that Mn^{2+} is associated with carbonate minerals rather than clay minerals. This supports conclusions drawn in Chapter 4 concerning the environment of deposition of calcareous shales, namely that the Shawnee, Upper Wabaunsee and Admire Groups probably represent periods of deep water sedimentation and the Kansas City Group, a period of shallow water deposition.

CHAPTER SEVEN

A MULTIVARIATE STATISTICAL ANALYSIS OF GEOCHEMICAL AND MINERALOGICAL DATA FROM THE UPPER PENNSYLVANIAN AND LOWER PERMIAN SHALES OF KANSAS, U.S.A.

INTRODUCTION

Statistical analysis of mineralogical data from the Upper Pennsylvanian and Lower Permian shales has revealed mineralogical associations that mapped against depth indicate a number of stratigraphic zones (Chapter 2). Similarly, analysis of geochemical results from the same shales has produced a number of geochemical associations that also indicate stratigraphic zones (Chapters 4 and 5). However, these mineralogical and geochemical zones do not coincide throughout the stratigraphic column. It is therefore to clarify the stratigraphic divisions and also the relationships between geochemical and mineralogical variables, that a statistical analysis of the combined mineralogical and geochemical data was performed. A useful biproduct of the analysis will be an increased understanding of the relationship between mineralogical and geochemical cycles noted in Upper Pennsylvanian and Lower Permian shales.

The statistical procedures adopted were those applied in previous chapters - cluster analysis, principal components analysis and multiple discriminant analysis, and are described in Appendix 1.

CORRELATIONS

The initial step in the multivariate analysis procedure is the calculation of a correlation matrix between all geochemical and mineralogical variables. The correlations between individual geochemical variables can be found in Table 5.1 and for mineralogical variables in Table 3.5. The correlations between mineralogical and geochemical variables are given in Table 7.1 and a number of inferred relationships are confirmed.

Al_2O_3 shows high correlations with quartz, feldspar and the clay minerals reflecting concentrations of Al_2O_3 in feldspar and the clay minerals. Similarly, SiO_2 has high correlations with the silicate minerals. CaO on the other hand, has high correlations with the carbonate minerals,

TABLE 7.1 Correlations between geochemical and mineralogical variables

PA = Peak Area; PH = Peak Height, $r_{95} = \pm 0.15$, $r_{99} = \pm 0.20$, $r_{99.9} = \pm 0.27$.

	QUARTZ PA	CALCITE PA	FELDSPAR PA	DOLOMITE PA	KAOLINITE PH	ILLITE PH	CHLORITE PH
Al_2O_3%	0.30	-0.65	0.29	-0.36	0.48	0.70	0.67
CaO%	-0.67	0.85	-0.35	0.27	-0.44	-0.67	-0.60
*Fe%	-0.02	-0.42	0.10	-0.03	0.33	0.39	0.27
K_2O%	-0.18	-0.31	0.04	-0.24	0.29	0.48	0.45
MgO%	-0.38	0.06	0.26	0.59	-0.27	-0.34	-0.29
SiO_2%	0.85	-0.73	0.30	-0.31	0.31	0.48	0.43
Mn/Fe	-0.38	0.53	-0.19	0.31	-0.32	-0.42	-0.46
MnO ppm	-0.32	0.31	-0.10	0.31	-0.22	-0.27	-0.32
Ag ppm	0.16	0.00	-0.05	-0.03	-0.16	-0.21	-0.21
Ba ppm	0.20	-0.36	0.13	-0.17	0.19	0.34	0.35
Be ppm	-0.23	0.03	0.02	0.01	0.05	0.03	0.08
Bi ppm	-0.54	0.57	-0.30	0.13	-0.23	-0.38	-0.42
Cd ppm	0.21	-0.21	0.06	-0.12	0.02	0.06	-0.01
Co ppm	0.29	0.06	0.01	-0.04	-0.03	-0.07	-0.26
Cr ppm	0.04	-0.16	0.01	-0.08	-0.04	0.02	0.04
Cu ppm	0.01	-0.23	0.03	-0.14	0.08	0.14	0.16
Ga ppm	0.13	-0.56	0.18	-0.35	0.51	0.71	0.69
Ge ppm	-0.51	0.63	-0.30	0.08	-0.22	-0.37	-0.42
Li ppm	-0.36	0.12	-0.19	-0.07	0.22	0.23	0.27
Mo ppm	-0.13	0.16	-0.13	0.01	-0.13	-0.19	-0.24
Ni ppm	-0.05	-0.15	0.03	-0.09	-0.00	0.08	0.05
Pb ppm	-0.01	-0.17	0.03	-0.04	-0.02	0.05	0.01
Sn ppm	-0.13	0.28	-0.22	0.35	-0.24	-0.31	-0.33
Sr ppm	-0.43	0.54	-0.28	0.20	-0.31	-0.41	-0.43
V ppm	0.07	-0.16	0.01	-0.07	-0.01	0.02	0.00
Zn ppm	0.17	-0.44	0.14	-0.21	0.21	0.34	0.28
Zr ppm	0.65	-0.24	0.27	-0.14	0.09	0.16	-0.07
*WL%	-0.26	0.12	-0.24	0.06	-0.19	-0.23	-0.13

* Fe% = Total Fe oxides %; WL% = Percentage weight loss on ignition (= Heat Loss in previous chapters)%

calcite and dolomite. MgO is correlated with dolomite and feldspar as both minerals contain Mg. K_2O and Fe oxides are correlated with the clay minerals and are most likely found in the lattices either as primary constituents or as substituting ions.

MnO and Mn/Fe are correlated with calcite and dolomite reflecting the association of Mn with carbonates. Ba on the other hand, is correlated with illite and chlorite, an indication of possible substitution in the two minerals. Bi is positively associated with the carbonate minerals as are Ge, Sn and Sr. Co and Zr form an association with quartz and feldspar as both are often deposited as detrital elements. Gallium has a high correlation with each of the clay minerals. The remaining elements, Ag, Be, Cd, Cr, Cu, Li, Mo, Ni, Pb, V and Zn have no significant correlations.

PRINCIPAL COMPONENTS ANALYSIS

Using the correlation table described above, an R-mode principal components analysis produced nine significant components which together account for 79.9% of the total variance in the data set (Table 7.2). Loadings of the variables on the components are shown in Fig. 7.1 and a familiar pattern emerges.

Component 1:-

The high loadings of CaO, calcite, Ge, Sr, Bi, Sn, MnO, Mn/Fe and dolomite suggest that this component should be designated a carbonate component. The positive loadings of these elements, oxides and minerals are opposed by high negative loadings of Al_2O_3, Ga, SiO_2, illite, chlorite, Zn, quartz and K_2O, clearly indicating a detrital phase antipathetically related to a carbonate fraction.

This component shows a close correspondence to the first geochemical component determined in Chapter 5 and it will be apparent when the

TABLE 7.2 Eigenvalues of the components extracted (i.e. eigenvalues > 1.0).

COMPONENT	EIGENVALUE	CUMULATIVE VARIANCE (%)
1	9.91	28.3
2	6.09	45.7
3	3.67	56.2
4	2.03	62.0
5	1.72	66.9
6	1.26	70.5
7	1.14	73.8
8	1.12	77.0
9	1.02	79.9

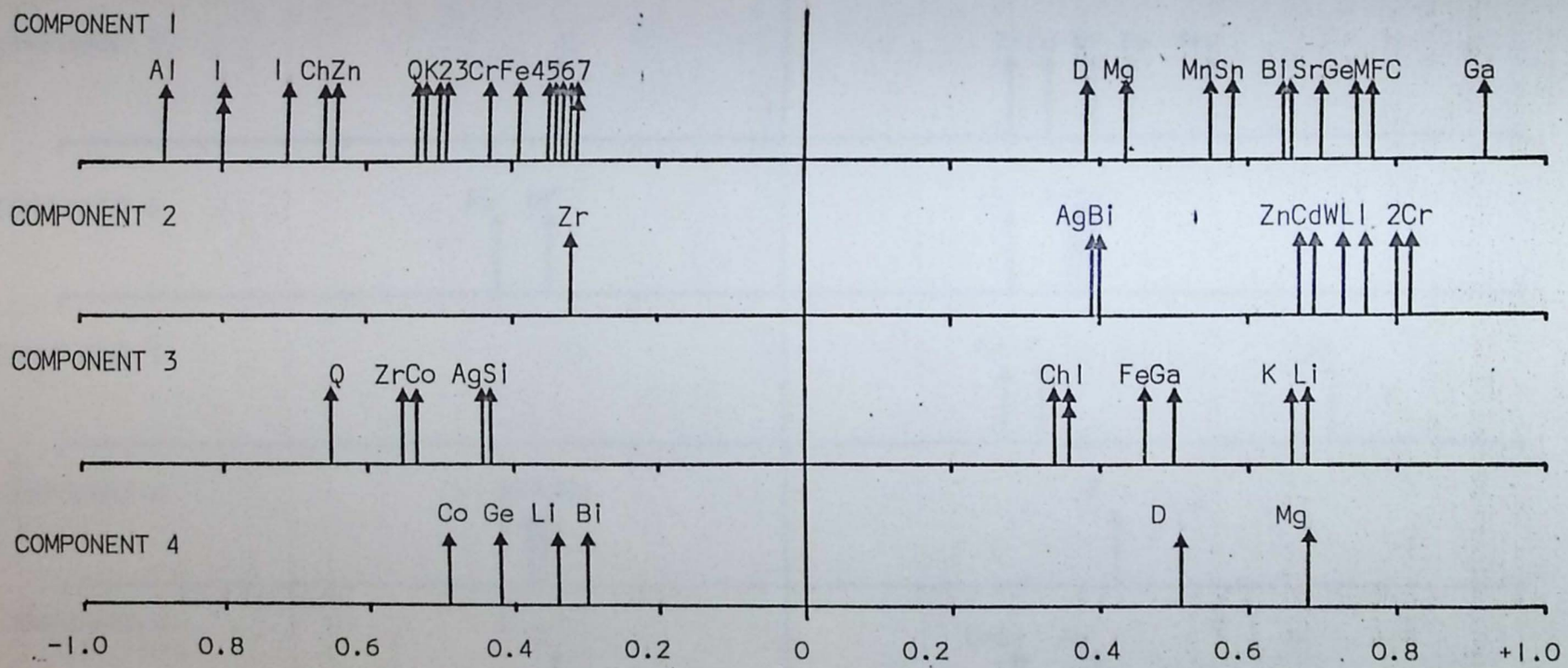

KEY

For all components:-

Same as previous figs. in Chapters 3 and 5, except

K = K_2O; Ka = Kaolinite; WL = Weight Loss

COMPONENT 1:-

1 = Ga and Si
2 = Ka
3 = Ba
4 = Cr
5 = Ni
6 = F
7 = V
8 = Cd and Pb

COMPONENT 2:-

1 = Cu, Mo and Pb
2 = Ni and V

COMPONENT 3:-

1 = Ge and Bi

Fig. 7.1 Loadings of variables on significant components. Only loadings > $\pm$ 0.30 are included.

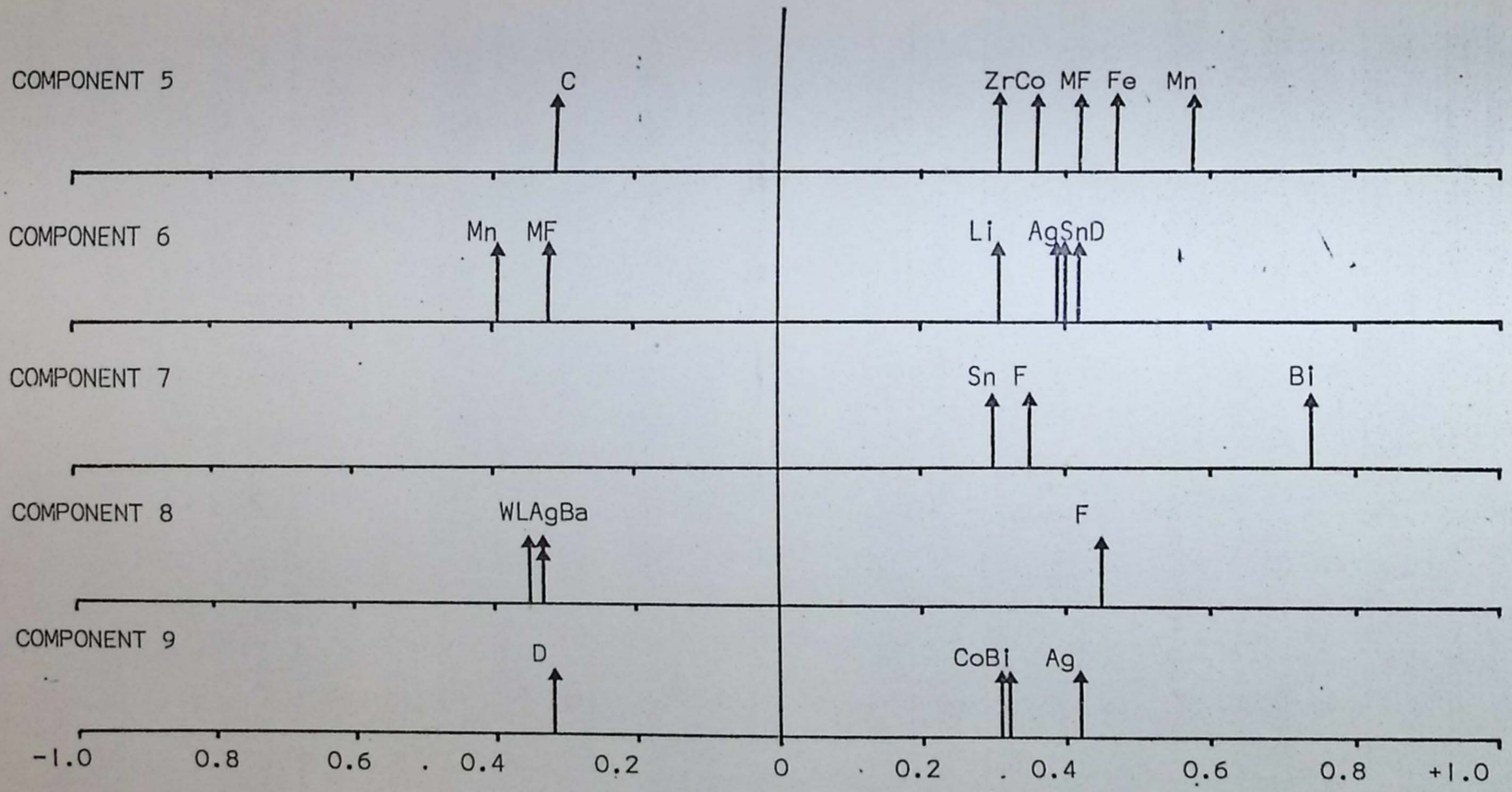

Fig. 7.1 Continued.

other components are discussed, that the geochemical variables control most of the components.

Following the procedures established in Chapters 3 and 5 a promax rotation of the principal components was performed. However, the algorithm employed in this program (Appendix 1) recreates the component axes and in doing so only eight components were developed. Components 1 to 6 matched the R-mode principal components of Fig. 7.1 but the other two differed slightly. Consequently, only the first six promax rotated axes are illustrated in Fig. 7.2.

The carbonate/detrital fraction antipathy is also noted in the promax rotation. Stratigraphic variation in component scores (Fig. 7.3) indicates that the Pleasanton, Lower Kansas City, Lansing, Shawnee, Chase, Council Grove and Admire Groups have a predominance of calcareous shales, whereas the intervening beds are generally detrital in nature.

Component 2:-

This component has high positive loadings for Cr, Cu, Mo, Pb, Ni, V, Cd, Zn, Be and weight loss representing an enrichment of trace elements in the reducing conditions of organic-rich black shales. Component scores are high in the Kansas City Group and Shawnee Group black shales (Fig. 7.3) and low for all other deposits.

Component 3:-

This component has positive Li, K_2O, Ga, Fe oxides loadings opposed by quartz, Zr, Co, Ag, and SiO_2. K_2O in the form of K^+, and Ga are normally found as ions within clay mineral lattices. Similarly, Fe oxides and Li are characteristic of clay minerals. The negative loadings of detrital components add support to the notion that this axis is essentially a clay mineral component. On rotation, the clay minerals are positively loaded with Al_2O_3 and Ga whereas negative loadings are recorded for Co,

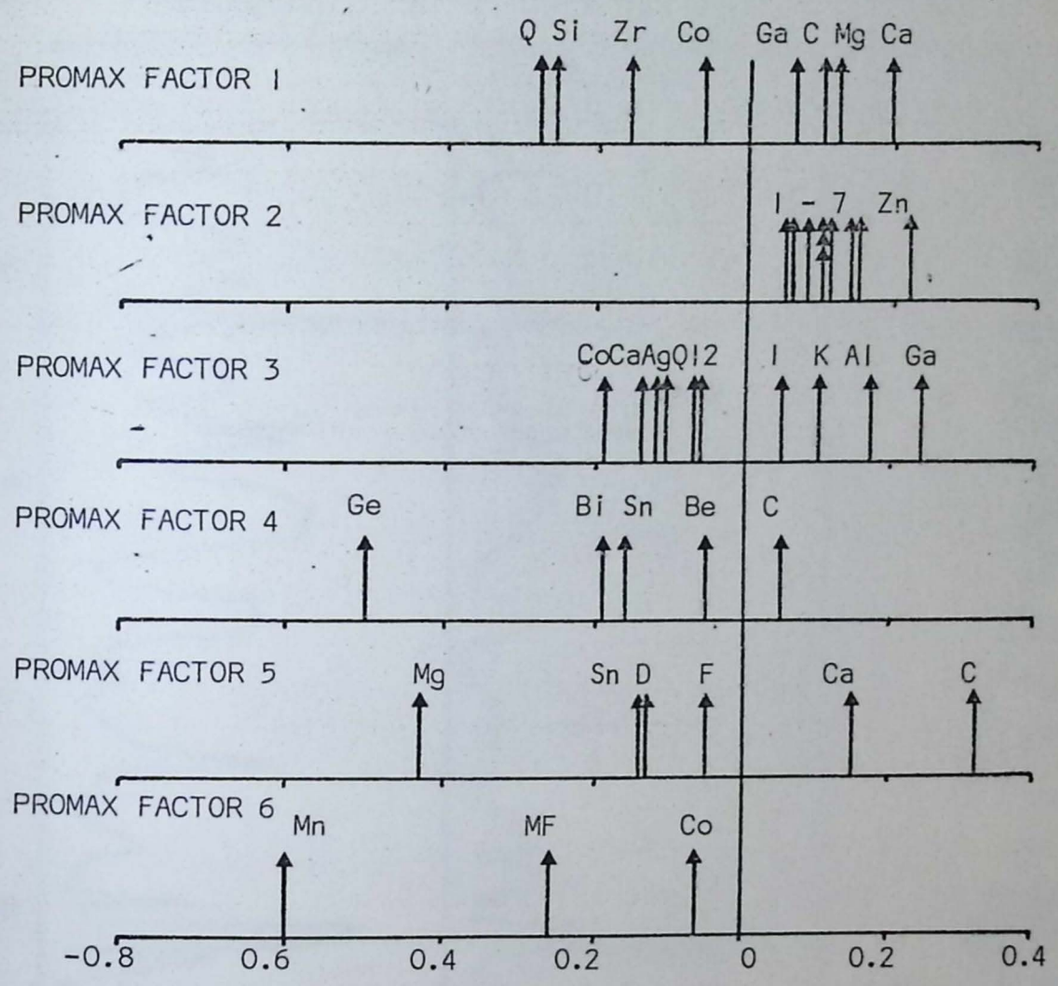

KEY

For all components:-
The same as previous figs. in Chapters 3 and 5 except
K= K_2O; Ka = Kaolinite;
WL = Weight Loss

For Component 2:-
1 = WL
2 = Mo
3 = Be
4 = Co,Cu and Pb
5 = V
6 = Cr
7 = Ni

For component 3:-
1 = Mg
2 = MF

Fig. 7.2 Loadings on promax axes. Only those loadings $\geq \pm$ 0.5 are indicated.

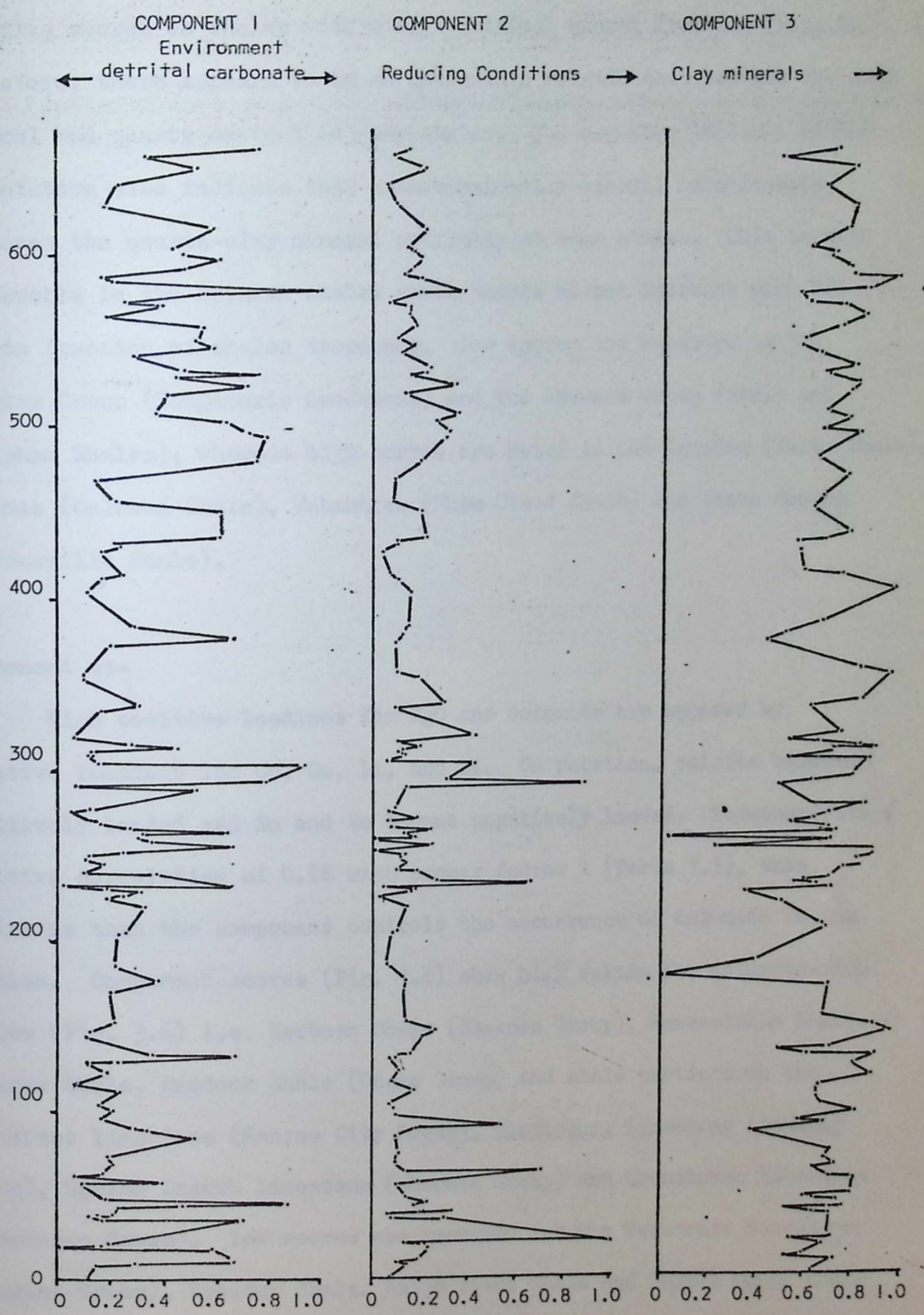

Fig. 7.3 Stratigraphic variation in component scores for components 1, 2 and 3.

CaO, Ag and quartz. Component scores, shown in Fig. 7.3 indicate high positive scores on shales with high clay mineral content (Fig. 3.7) and negative scores on shales with a high detrital quartz fraction (Fig. 3.5). Therefore, there appears to be an antipathic relationship between the clay mineral and quartz content in many shales. The negative loadings of CaO on rotation also indicate that a carbonate-clay mineral relationship replaces the quartz-clay mineral antipathy in some shales. This is most noticeable in the Permian shales where scores do not increase when the quartz fraction of shales decreases. Low scores are recorded in the Douglas Group (Tonganoxie Sandstone) and the Shawnee Group (Stull and Doniphan Shales), whereas high scores are noted in the Lansing (Vilas Shale), Shawnee (Calhoun Shale), Wabaunsee (White Cloud Shale) and Chase Groups (Havensville Shale).

Component 4:-

High positive loadings for MgO and dolomite are opposed by negative loadings for Co, Ge, Li, and Bi. On rotation, calcite becomes positively loaded and Sn and Be become negatively loaded. Together with a positive correlation of 0.18 with promax factor 1 (Table 7.3), this indicates that the component controls the occurrence of dolomite in the samples. Component scores (Fig. 7.4) show high values for dolomite-rich shales (Fig. 3.6) i.e. Heebner Shale (Shawnee Group), Havensville Shale, Stearns Shale, Paddock Shale (Chase Group) and shale partings in the Winterset limestone (Kansas City Group), Plattsburg Limestone (Lansing Group), Spring Branch Limestone (Shawnee Group) and Grandhaven Limestone (Wabaunsee Group). Low scores are recorded for the Tonanoxie Sandstone (Douglas Group), Speiser Shale, Salem Point Shale and Hughes Creek Shale (Council Grove Group) samples with low MgO and dolomite values.

TABLE 7.3 Correlations between promax factors

	PROMAX FACTORS					
	1	2	3	4	5	6
1	1.00					
2	-0.01	1.00				
3	-0.12	-0.11	1.00			
4	0.18	0.06	-0.03	1.00		
5	-0.11	-0.02	-0.01	-0.19	1.00	
6	0.08	-0.06	-0.20	-0.05	0.06	1.00

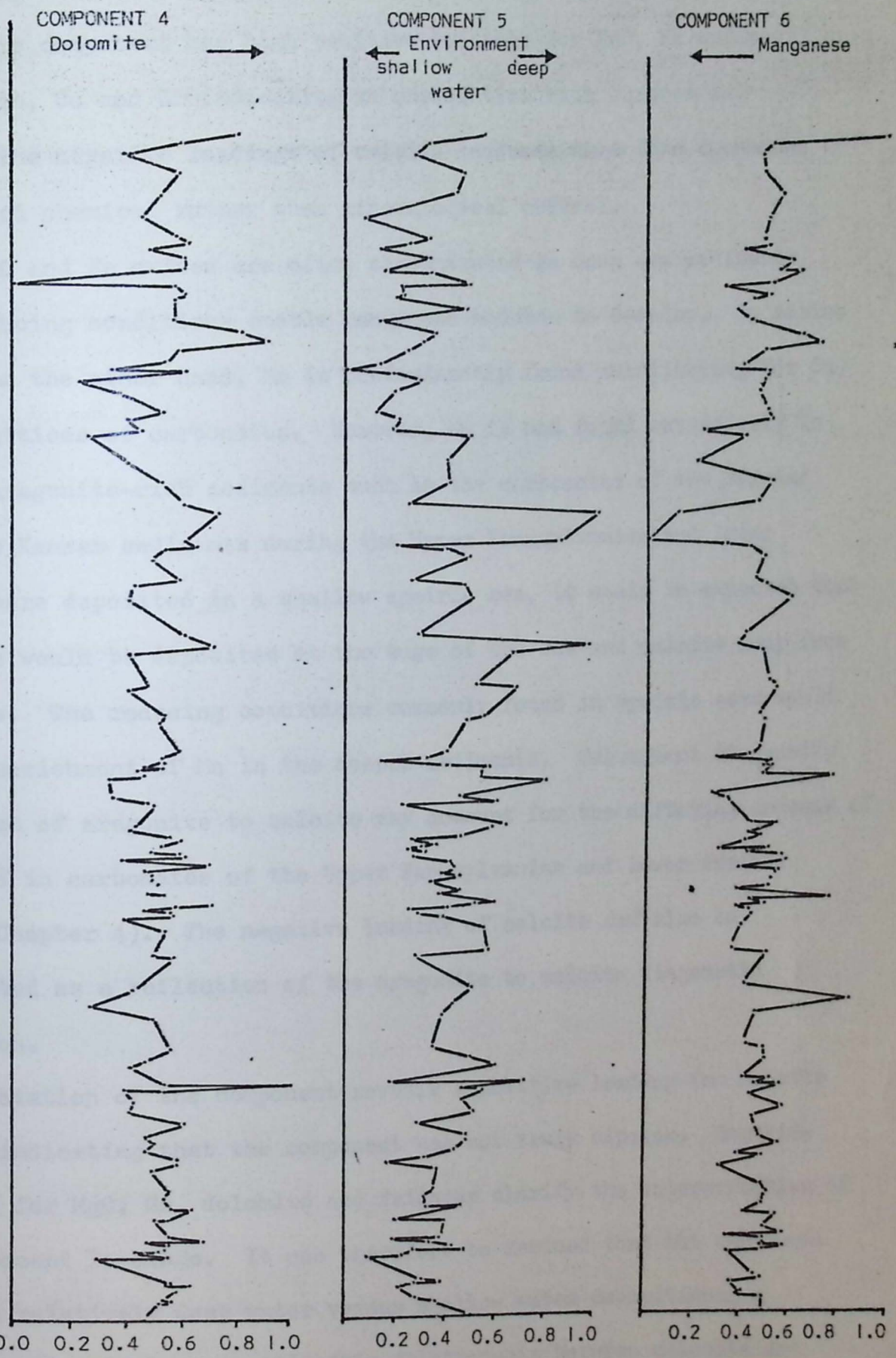

Fig. 7.4 Stratigraphic variation of component scores for components 4, 5 and 6.

Component 5:-

This component has high positive loadings for MnO, Fe oxides, Mn/Fe ratio, Co and Zr indicating an association with carbonates. However, the negative loadings of calcite indicate that this component may reflect chemical rather than mineralogical control.

MnO and Fe oxides are often concentrated in deep sea sediments where reducing conditions enable manganese nodules to develop. In marine waters, on the other hand, Mn is predominantly found substituting for Ca in the lattices of carbonates. However, Mn is not found extensively in shallow aragonite-rich sediments such as the carbonates of the Persian Gulf. As Kansas sediments during the Upper Pennsylvanian and Lower Permian were deposited in a shallow epeiric sea, it would be expected that aragonite would be deposited at the edge of the sea and calcite away from the shore. The reducing conditions commonly found in epeiric seas would aid the enrichment of Mn in the deeper sediments. Subsequent diagenetic alteration of aragonite to calcite may account for the differing amounts of MnO found in carbonates of the Upper Pennsylvanian and Lower Permian shales (Chapter 4). The negative loading of calcite can also be interpreted as a reflection of the aragonite to calcite diagenetic alteration.

Rotation of the component reveals a positive loading for calcite and CaO indicating that the component was not truly bipolar. Negative loadings for MgO, Sn, dolomite and feldspar clarify the interpretation of the component loadings. It can therefore be assumed that the component reflects relatively deep water versus shallow water depositional environments and also an antipathic relationship between dolomite and calcite. It may similarly reflect nearness to shoreline, as deep water sediments are normally found furthest from the coast.

Component scores suggest that long periods of shallow water sedimentation alternate with deeper water sedimentation. Superimposed

upon this oscillation are short time-scale fluctuations. The component scores generally increase from the Pleasanton to a peak in the Lansing Group, decrease through the Douglas to the centre of the Shawnee, rise again to the middle of the Wabaunsee, decrease through the Council Grove Group and finally begin to rise again through the Chase Group. Therefore, there are apparently three long-term oscillations in the depth of deposition for the Upper Pennsylvanian and Lower Permian shales. The highest scores are recorded in the Plattsburg Limestone, Calhoun Shale, Friedrich Shale, Silver Lake Shale and Pony Creek Shale whereas the Galesburg Shale, Neva Limestone and Oketo Shale have the Lowest scores.

Component 6:-

High positive loadings of dolomite, Sn, Ag and Li are opposed by negative loadings for MnO and Mn/Fe ratio. On rotation, the high positive loadings disappear but the MnO and Mn/Fe negative loadings are accentuated. Additionally, Co develops a high negative loading. The component can, therefore, be interpreted as a "manganese component".

Components 7, 8 and 9:-

Component 7 is controlled by the unusual combination of Bi, feldspar and Sn for which no explanation can be offered. Similarly, components 8 and 9 are uninterpretable. Examining Table 7.2, it is apparent that these components only account for 10% of the total data variance and are therefore relatively unimportant in controlling the mineralogical and geochemical evolution of Kansas shales. They probably account for occasional extreme conditions - both experimental and original environmental conditions.

Mineralogical and geochemical variation in Upper Pennsylvanian and Lower Permian shales can therefore be described by nine components of which

only six are interpretable. Scores of individual samples on the components subdivide the stratigraphic section into a number of zones. However, these zones are not consistent across all components and may in some cases be contradictory.

CLUSTER ANALYSIS AND DISCRIMINANT ANALYSIS

Another approach to the same problem can be followed using Q-mode cluster analysis, a technique that examines relationships between samples rather than variables. Using the scores on the nine components calculated above, similarity coefficients between samples are determined. A hierarchical classification (dendrogram) is developed from the similarity matrix (Fig. 7.5) and produces a ten-fold division of the samples. It can be seen that almost $\frac{2}{3}$ of the shale samples fall into one group and only one other group contains more than five samples. It is unlikely that the remaining samples form eight natural groups and a number are probably products of the clustering method. Therefore, following the procedure established in previous chapters, the scores of the samples on the nine significant components were analysed by multiple discriminant analysis to check the discreteness of the groups. Four discriminant axes were found to account for 86.9% of the data variation (Table 7.4) and the resulting distributions appear in Fig. 7.6 and 7.7. It can be seen that these axes successfully distinguish groups F, J and I, but all other groups suffer some degree of overlap. It is therefore apparent that some of the clusters are not unique and require some modification.

Along the first, second and third axes, groups C, B and H overlap and are only distinguishable by small differences in the manganese and dolomite content. Similarly, clusters A, G and E are found to be inseparable on all but the fourth discriminant axis. Simplifying the sample classification, these groups can be merged together to form six

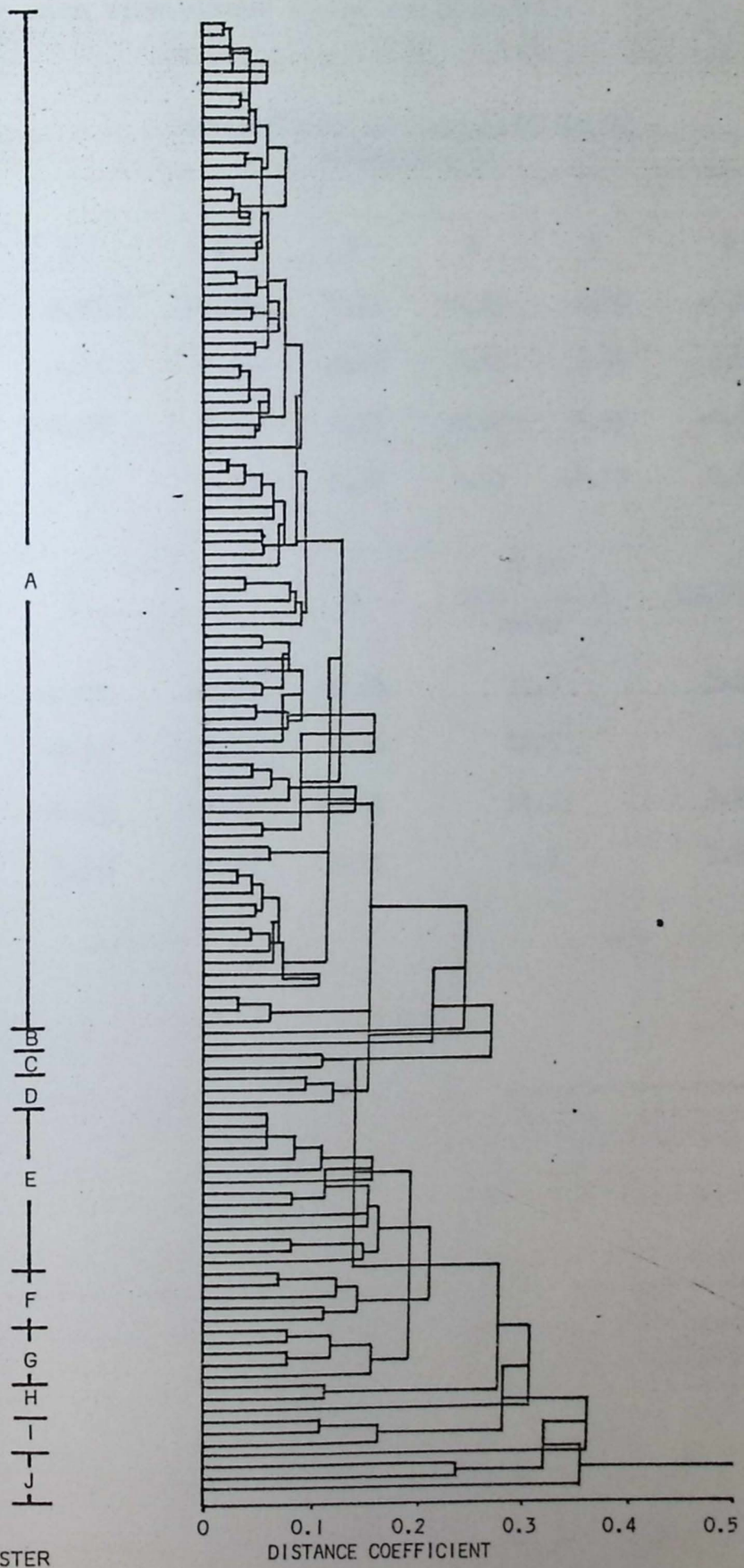

Fig. 7.5 Dendrogram of Upper Pennsylvanian and Lower Permian shales based on geochemical and mineralogical data. Cluster produced are outline on the left of the diagram.

TABLE 7.4 Discriminant analysis results (only discriminant axes with eigenvalues > 1.0 are included).

DISCRIMINANT No.	CONTRIBUTION OF EACH VARIABLE TO DISCRIMINANTS					
	1	2	3	4	5	6
1	0.28	-0.70	0.44	0.09	0.20	-0.06
2	0.88	0.31	-0.49	0.23	0.79	0.28
3	-0.29	0.31	0.27	0.44	0.39	-0.58
4	-0.09	0.05	0.32	0.52	-0.13	0.68

	7	8	9	% OF DISCRIMINANT POWER	EIGENVALUE
1	-0.54	-0.24	-0.30	37.9	5.28
2	0.10	-0.01	0.20	22.5	3.14
3	-0.23	-0.46	-0.01	14.7	2.05
4	0.23	-0.37	0.12	11.3	1.57

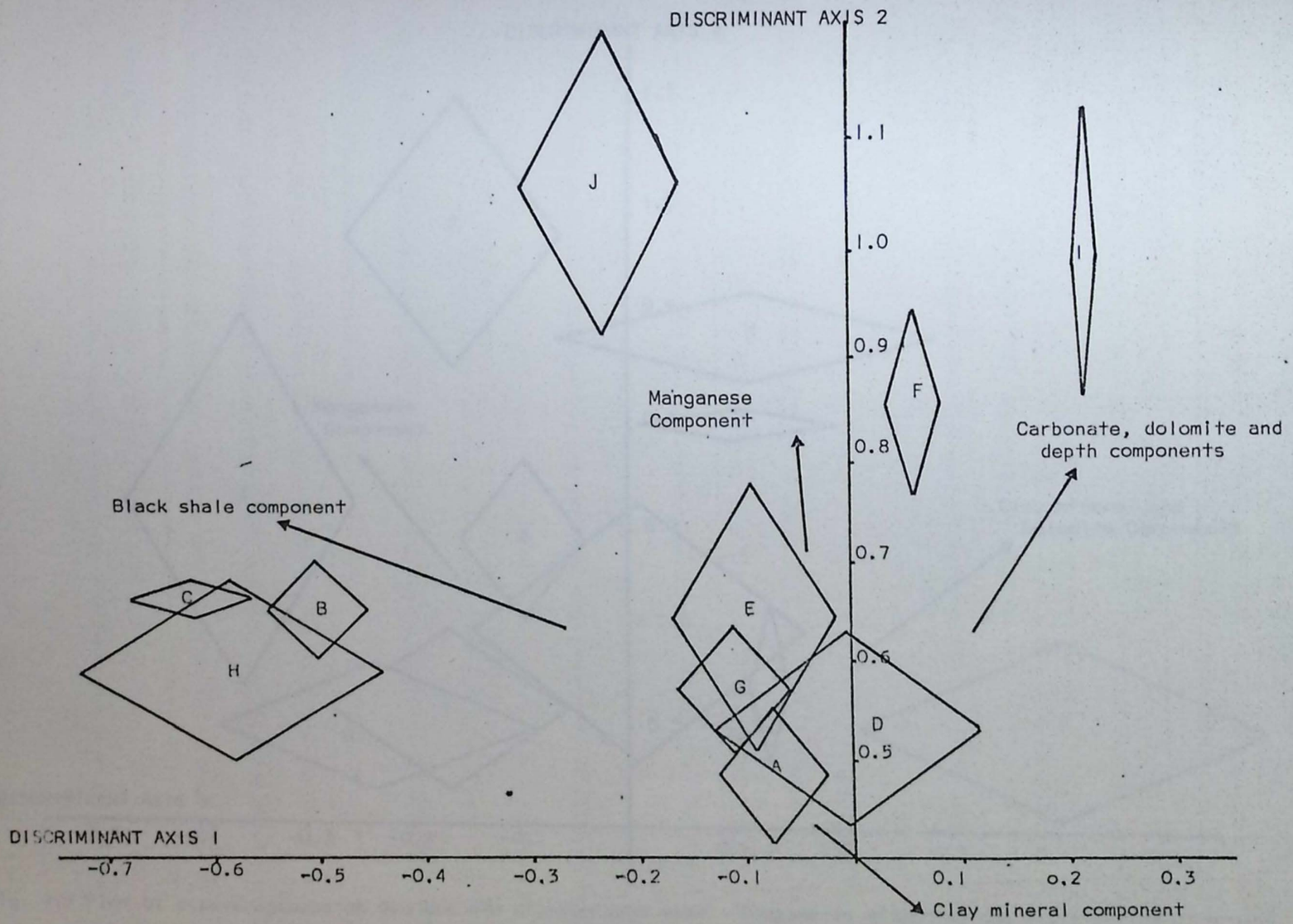

Fig. 7.6 Plot of ten cluster groups on first two discriminant axes. The components controlling the distribution are superimposed to aid interpretation.

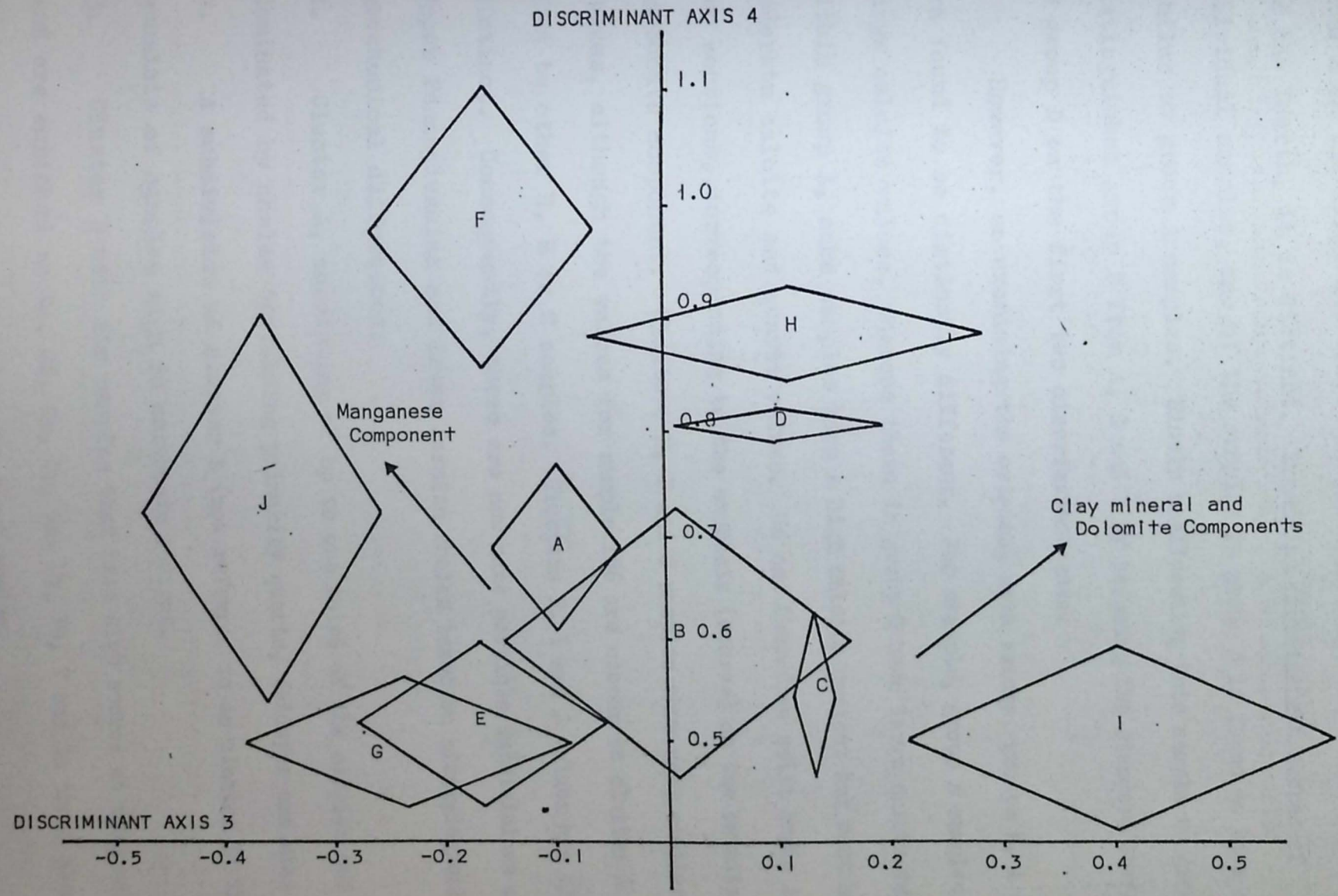

Fig. 7.7 Plot of cluster groups on 3rd and 4th discriminant asex. Components affecting the distribution of groups are superimposed to aid interpretation.

distinct clusters.

In the case of group D, we can see that it overlaps clusters A, G and E on the first and second discriminant axes but that on the third and the fourth, it is distinct. Examining discriminant scores of individual samples, one of the samples in group D is found to have scores similar to group A samples. Simply reallocating this sample to group A distinguishes group D from A, G and E by reducing the standard deviation of group D on the first two discriminant axes.

However, on examining the original data values, groups E, A and G are found to be distinctly different. For example, group E samples have large calcite values, whereas those in group G have large quartz values. Within group A, some samples have a high calcite content but most have moderate calcite and quartz values. We can therefore split group A into two sections, corresponding to the emphasis (scores) on the detrital/carbonate component. Clusters H, B and C samples show very similar data values, although the values for sample 186 are closer to cluster A samples than to other H, B or C samples. Clusters F, I and J values are also distinct. Consequently, there are now nine possible subdivisions of the Upper Pennsylvanian and Lower Permian shales based on mineralogical and geochemical differences:

1. Cluster A, consisting of up to one third of the samples and dominated by shales containing primarily quartz, feldspar and clay minerals.
2. A subdivision of cluster A (now referred to as cluster X) that consists of samples high in carbonate content.
3. Cluster B with six samples that have high scores on component two and are enriched in Be, Cd, Cr, Cu, Mo, Ni, Pb, V and Zn trace elements. Lithologically these samples are black shales.
4. Cluster D, containing only two samples, closely associated with cluster A.
5. Cluster E consists of samples with very high concentrations of calcite.

6. Cluster F, contains those shales with a high dolomite content.

7. Cluster G, contains samples with high quartz content, mainly sandstones and siltstones.

8 and 9. Two clusters, I and J, with a total of 7 extreme samples from all of the previous groups. The significance of these last groups is in doubt.

A stratigraphic plot of the distribution of samples from the nine groups is illustrated in Fig. 7.8 and a similar pattern to both mineralogical and geochemical distributions is revealed (Table 7.5, Figs. 3.17 and 5.8). A zonation of the stratigraphy is again in evidence and can be related to the factors controlling the mineralogy and geochemistry of the shales. The Pleasanton and Lower Kansas City Groups are characterized by a regular alternation of calcareous shales, (cluster E samples, black shales (B) and shales containing primarily quartz, feldspar and clay minerals (A). This three component shale cycle is repeated four times at approximately 70 ft. intervals from the Tacket Formation to the Iola Limestone. Between each shale cycle, a series of cluster A samples occur. Occasionally, a carbonate shale also develops.

The succeeding Upper Kansas City, Lansing and Douglas Groups contain predominantly samples from clusters A and G. The detrital fraction of beds in this zone is large and noticeably in the Douglas Group, manifests itself in the development of a number of siltstones and sandstones. Shales in these beds are also very rich in quartz, feldspar, zircons and detrital cobalt (as noted in the high negative scores on component 1). One calcareous bed noted in the Hickory Creek Shale, may represent a partially developed three component shale cycle.

A zone defined by the boundaries of the Shawnee Group contains an irregular collection of samples. Two black shale samples are found in the Heebner and Larsh and Burroak Shales but do not form integral parts of cycles as in the Pleasanton and Lower Kansas City zone. In this section,

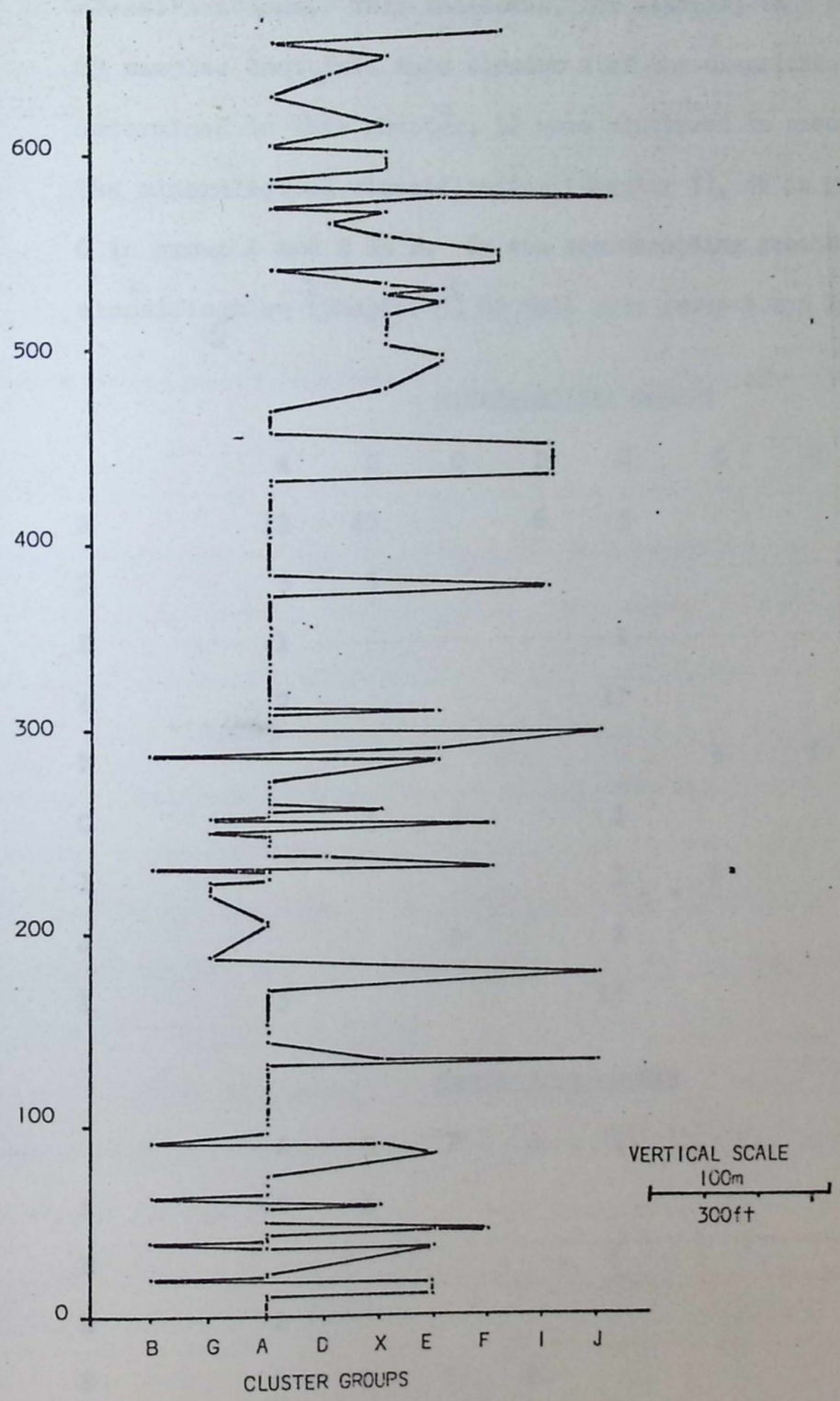

Fig. 7.8 Stratigraphic distribution of samples arranged in cluster order, Horizontal scale in arbitrary but may represent a detrital to carbonate sequence from G to F.

TABLE 7.5 Distribution of shale samples within the mineralogical, geochemical and combined mineralogical and geochemical classifications. This indicates, for example, that of the 69 samples that fell into cluster A of the classification determined in this chapter, 12 were clustered in group A of the mineralogical classification (Chapter 3), 48 in group B, 6 in group D and 4 in E. In the corresponding geochemical classification (Chapter 5) 68 fell into group A and 1 into D.

		MINERALOGICAL GROUPS						
		A	B	C	D	E	G	H
MINERALOGICAL AND GEOCHEMICAL GROUPS	A	12	48		6	3		
	B	3	3					
	D	1				1		
	E	2				11		
	F						3	3
	G		1	3		1		
	I					1	2	
	J			2		2		
	X	3				15		

		GEOCHEMICAL GROUPS				
		A	D	F	H	I
	A	68	1			
	B					6
	D	2				
	E	6	2	3	2	
	F		2	3	1	
	G	5				
	I				2	
	J				4	
	X	8	7	2	1	

no regular pattern appears, possibly as it contains samples from eight of the nine clusters. Nevertheless, some inferences can be made from the sample distribution. In the Shawnee, thick shale Formations separate four limestone Formations containing interleaved thin shales (a black shale after the second limestone bed (Moore, 1949) is the most distinctive). The majority of samples from the thick shales, known as cutside shales, are classified in clusters A and G but a few occur in cluster J. The shales within the limestone formations, inside shales, have a certain irregularity. The first shale is normally from cluster A, although one G sample was noted, the second is generally from cluster B, the black shale cluster and the third, where developed, is usually from cluster A. However, calcareous shales replace the second and third shales on occasions. The Lower and Middle Wabaunsee Group consists almost entirely of cluster A samples and is quite similar to the Upper Kansas City, Lansing and Douglas zone but without the thick sequences of siltstones and sandstones. Only one sample, from the Silver Lake Shale, is calcareous.

Finally, a zone of alternating calcareous and detrital shales encompasses the Upper Wabaunsee, Admire, Council Grove and Chase Groups. Generally, these samples are much richer in both calcite and dolomite than the Pennsylvanian indicating a distinct change in the sedimentary environment. The Pennsylvanian/Permian boundary is therefore thought to mark a change from the beds essentially dominated by the detrital fraction to those with a high carbonate content.

The subdivisions of the Pennsylvanian stratigraphy, tentatively represent two periods of oscillating environments. The conditions prevalent in the Pleasanton and Kansas City zone, seem to recur in the Shawnee and similarly those developed in the Upper Kansas City, Lansing and Douglas zone are repeated in the Wabaunsee. As these "periods" are roughly equivalent in thickness and possibly time, it is suggested that they represent a cycle of cycles.

CONCLUSIONS

Mineralogical and geochemical data analysed in previous chapters have been combined and studied using multivariate statistical techniques. The variation found throughout the Upper Pennsylvanian and Lower Permian shales of Kansas can be explained in terms of nine components. Firstly, accounting for 28% of the data variance, is a component that describes the differences between carbonate and detrital fractions of shale samples. Subsequent components describe variations in sediment reducing conditions, clay mineral content, dolomite content, depth of deposition and manganese content. Three components remained uninterpreted.

Scores of samples on the first six components in particular, indicate that the stratigraphic section can be divided into a number of zones characterized by differing geochemical and mineralogical conditions. A statistical analysis of the zonation (using Q-mode cluster analysis and multiple discriminant analysis) was performed on the component scores. Ten natural groups of samples were revealed that were subsequently pruned down to nine. The distribution of samples from these groups indicated a five-fold division of the stratigraphical section under examination:

1. Pleasanton and Lower Kansas City Groups,
2. Upper Kansas City, Lansing and Douglas Groups,
3. Shawnee Group,
4. Lower and Middle Wabaunsee Group and
5. Upper Wabaunsee, Admire, Council Grove and Chase Groups.

Zones 1 and 3 consist of regular alternations of calcareous, black organic and quartz-rich shales. Occurring at approximately 70 ft. intervals, these cycles bear a close resemblance to the oscillations identified in the Kansas City Group beds by Davis and Cocke (1972). Using a method known as substitutability analysis, the stratigraphic section

containing seventeen distinct lithologies was found to possess a two state oscillation, limestone - inside shale, perturbated by occasional outside shales or black shales. Inside shales are comparable to the calcareous shales (clusters X and E) of this chapter. Similarly, quartz-rich shales, siltstones and sandstones (clusters A and G) roughly correspond to outside shales. The black organic shales in both cases are directly equivalent. However, the quartz shales may also develop as inside shales and therefore the cycles defined in this chapter do not directly match the oscillatory patterns recognised by Davis and Cocke (1972), and Schwarzacher (1969). There also seems to be dissimilarity between the cycles recognised in this chapter and those identified by Moore (1936, 1949), and Merriam (1963). Nevertheless, simple three component shale cycles have been recognised in both zones 1 and 3.

Zones 2 and 4 are characterized by quartz-rich shales, siltstones and sandstones with occasional calcareous shale. No evidence for cyclic variation in the geochemistry or mineralogy of these beds is apparent. These zones do however oscillate with zones 1 and 3 and form the only manifestation of large-scale cycles found in Kansas deposits.

The last recognisable zone, 5, consists of a two-state oscillation from calcite or dolomitic-rich shales to quartz-rich shales. This zone is dominated by calcareous beds and reflects a basic change in environmental conditions from a detrital dominated shale regime in the Pennsylvanian to carbonate deposition in the Lower Permian.

CHAPTER EIGHT

PETROLOGY OF UPPER PENNSYLVANIAN AND LOWER PERMIAN SHALES FROM KANSAS, U.S.A.

INTRODUCTION

A classification of Upper Pennsylvanian and Lower Permian shales has produced nine groups of samples that can be distinguished on mineralogy and geochemistry (Chapter 7). As a laboratory exercise, this has its merits, but to be of practical benefit, it is also necessary to relate this classification to the sedimentary deposits observed in the field. It was with this aim in mind that a number of samples, analysed by X-ray diffraction, emission spectroscopy and electron spin resonance, were thin-sectioned and petrologically examined. This chapter presents a brief description of the facies distinguished and the implications for environments of deposition.

Following the recent work of Gipson (1965), Odom (1967), Gillott (1969, 1970) and O'Brien (1970) on the environmental significance of shale fabrics, select samples were examined using a scanning electron microscope to aid the interpretation of fine-grained sedimentary rock fabrics and to determine the depositional conditions under which the rocks were developed. A microscopic fabric analysis technique, developed by Brewer (1964) for the study of soils, was also applied with the general view of elucidating depositional environments.

LABORATORY PREPARATION

250 thin sections of selected shales were prepared at the Central Petrographic Section Services of Dallas, Texas, by a process of vacuum-impregnation in epoxy and cutting in kerosene. Some wedge-shaped sections were prepared for examination of shale fabrics. Photomicrographs of representative slides are included with discussions of specific rock types.

Several scanning electron microscope sample mounts were prepared by breaking roughly square chips off from the original shales. Samples of 3 cubic mm approximately, were cemented onto aluminium stubs leaving a

freshly fractured surface face up. A fine platinum coating was then vacuum sprayed over each sample to alleviate conductivity problems. The samples were then examined using a Cambridge scanning electron microscope belonging to the Geology Department at Leicester University. Electron photomicrographs of shale samples are included in the following sections.

SHALE PETROLOGY

Four principal facies were recognised in Upper Pennsylvanian and Lower Permian clastic deposits. These include a black shale that is considered the most distinctive of all Kansas deposits, a calcareous, grey shale facies that with the black shale facies constitute a group of sediments known as inside shales (Davis and Cocke, 1972), and a sandstone and siltstone facies that together with a thick, brown clay-shale facies form outside shales. Minor facies such as a red and purple shales and shale partings in limestone beds, are also recognised. Aspects of each facies apparent in hand specimens or thin sections are discussed in the following sections.

Black Shale Facies

Shales belonging to this facies are typically black, carbonaceous, fissile and thin-bedded, containing numerous phosphorite laminae and scattered elliptic phosphorite nodules (Fig. 8.1a, b). Fossils commonly recognised in black shales include fish spines, conodonts, orbiculoid brachiopods, and thin shelled pectinid clams, although radiolaria, sponge spines, cephalopods and sharks' teeth have been found (Fig. 8.1c, d). Macerated plant fragments are also common.

This facies, although normally represented only by a few metres of sediments, is laterally persistent from Iowa to Southern Kansas (Moore, 1964). Further south, the black shales grade into thicker sections of

Fig. 8.1 (A) Hushpuckney Shale (sample No. 24) showing small elliptic phosphorite nodules and thin phosphorite laminae in a black, clay mineral matrix. The nodules lie parallel to the laminations of the shale. Scale matches that of the following photomicrograph.

(B) Stark Shale (sample No. 31) showing occasional phosphorite nodules in a dense clay matrix. A few quartz grains can be detected on the thinner edge of the slide. Scale = 2 mm.

(C) Munsie Creek Shale (sample No. 55) contains large elliptic phosphorite nodules (up to 4 cms. in length). Within the nodules a number of radiolaria are preserved. Scale = 0.5 mm.

(D) Within the same nodules, spicules are concentrated in large numbers. The irregular black patches are thought to be organic material. Scale = 0.5 mm.

(E) An electron photomicrograph of a Stark Shale (sample No. 7) fabric, showing flat plate-like clay minerals lying parallel to the planes of fissility. The clay mineral plates occur in groups or domains. Scale = 0 = 0.14 mm.

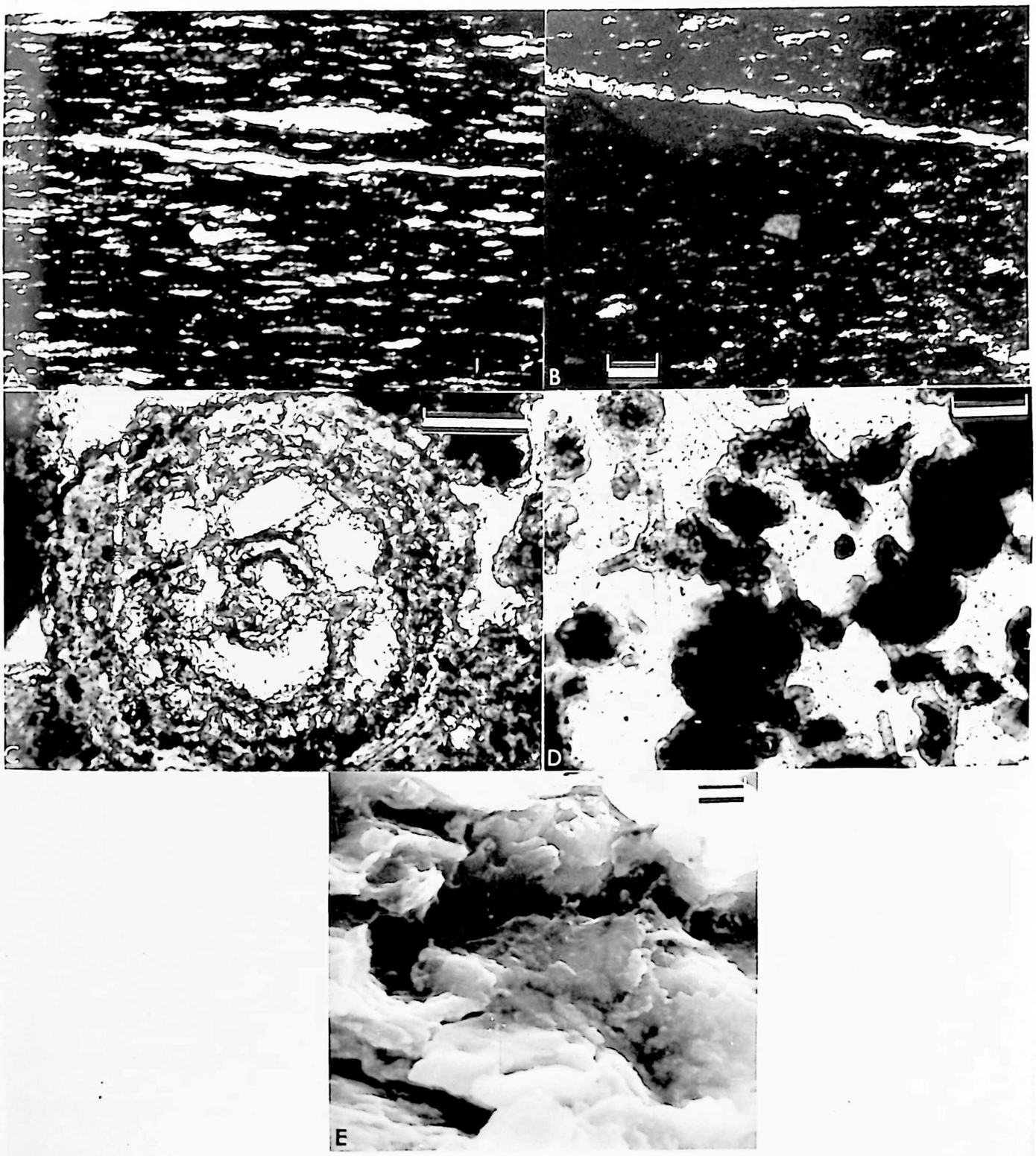
A
B
C
D
E

light coloured shales that contain normal marine fossils such as brachiopods, gastropods, echinoderms, corals and bryozoans (Evans, 1967, 1968; Heckel, 1972a). This, in turn, grades into the nonmarine deltaic clastics of Oklahoma (Wanless et al., 1970). In Iowa and Nebraska, a facies change to a fully marine section is often suggested by the reappearance of light coloured marine shales below the black shale facies.

Evans (1967) and Heckel (1972a) have established that the undisturbed nature of even stratification manifest in the primary phosphorite laminae preclude the former existence of either a root system of attached vegetation or an unpreserved burrowing or bottom feeding fauna. The presence of detrital material of only the finest sizes (primarily quartz grains scattered throughout the black shales) combined with the abundance of thin phosphorite laminae indicating long term cessation of detrital sedimentation (Bromley, 1967; Heckel, 1972), suggest that the areas of black shale development represent nearly currentless, sediment starved regions where slow deposition occurs. The fully marine extensions of black shales in Iowa and Southern Kansas indicate that black shales are probably marine deposits resulting from slow sedimentation.

The conditions responsible for the formation of black shales have been reviewed by Heckel (1972a) who concluded that in respect of the Heebner black Shale (Shawnee Group), stagnation of the sea was the most likely cause. Evans (1967) has suggested that stagnation could have been caused by a submarine barrier, resulting from sedimentation across the mouth of the Mid-Continent sea. Alternatively, the barrier may have developed as a topographical high associated with the continuation of the Ouachita foldbelt.

The Kansas epeiric sea during the deposition of black shales, may be viewed most reasonably as a broad saucer-shaped basin in which circulation has ceased over most of the bottom and into which only the finest suspended detritus was spread by currents. The aerated surface

waters contained a fauna of nektonic fish and conodont organisms along with epiplanktonic brachiopods and pectinids (Heckel, 1972a). On the edges of the basin, deltaic detrital sediments built the sea bottom up above the level of stagnation into aerated waters where benthonic life could be supported (Wanless et al., 1970).

Geochemically, the presence of organic matter in black shale environments encourages the development of reducing conditions in which the trace elements Cd, Cr, Mo, Ni, Pb, V and Zn are enriched. The organic matter also causes the dispersion of clay mineral particles by neutralization of surface charges (Moore, 1972) and gives rise, on compaction, to the fissility of black shales. Scanning electron micrographs of black shales (O'Brien, 1968; Fig. 3.1e) indicate that clay particles occur in parallel "domains" and that planes of fissility correspond to zones of organic material (Odom, 1967). High fissility also indicates an abiotic environment of deposition (Byers, 1974).

In thin section, black shales contain abundant phosphorite bands and nodules in a black, organic-rich matrix. The phosphorite laminae rarely exceed 1 mm in thickness but may extend up to several cms. in length. Phosphorite nodules also vary considerably in size and often contain fossils such as radiolaria and spicules (Fig. 8.10). Both laminae and nodules lie along planes of fissility. In the intervening black matrix, little detail can be distinguished except a few small quartz grains. In Brewer's micromorphological classification of sedimentary facies (Brewer, 1964, 1972; Bullock and Mackney, 1970; Burnham, 1970), the fabric of black shales is generally argillasepic unistrial, i.e. they consist primarily of clay minerals that exhibit preferred parallel orientation, which gives specimens as a whole a unidirectional striated extinction pattern.

Although samples of this facies are mineralogically indistinguishable from other fine-grained shale groups (Chapter 3), they are geochemically

distinct, i.e. they all fall into one cluster in Chapters 5 and 7. This facies is, therefore, a unique constituent of Kansas sediments supporting the level of importance as marker units currently placed on these shales by the Geological Survey of Kansas.

Summarizing therefore, the black shale facies is inferred as a marine deposit resulting from slow deposition in an oxygen-depleted sea. Parts of the Heebner Shale, Muncie Creek Shale, Eudore Shale, Larsh and Burroak Shale, Hushpuckney Shale and Stark Shale are typical of this facies.

Sandstone and Siltstone Facies

The sandstone and siltstone facies is found irregularly throughout the Upper Pennsylvanian clastic deposits but is almost unknown in the Lower Permian. It consists primarily of yellow to brown, arkosic greywackes and yellow/brown to grey, laminated siltstones that possess all the features of deltaic clastics. In outcrops, the sandstones are generally massively bedded with occasional irregular laminations (outlining particles or organic matter) and cross-bedding (Fig. 8.2a). The physical extent of these sandstone bodies, documented by Sanders (1959) and Wanless et al., (1963, 1970), indicate that they represent basal deltaic channel deposits. The laminated siltstones, on the other hand, show graded bedding and flow structures such as load casts and microslumps, and probably represent delta-front deposits.

Massive channel sandstones are found in the Noxie Sandstone Member (Horne, 1965) of the Kansas City Group, in the Tonganoxie Sandstone (Fig. 8.2b) and Ireland Sandstone Members of the Douglas Group (Bower, 1961), in the Pillsbury Shale, Root Shale and Wood Siding Formation of the Wabaunsee Group and finally in the Towle Shale Member of the Admire Group. Most are sinuous bodies that extend over NE Kansas and/or SE Kansas and N. Oklahoma and contain sediments derived from the Ozark Dome of Missouri and the Ouachita tectonic belt of Oklahoma and Arkansas respectively.

Fig. 8.2 (A) A section of the Tonganoxie Sandstone (samples 294, 295) showing several beds of massive sandstone with occasional irregular laminations. Beds are approximately 2-3 ft. thick.

(B) In the same outcrop as (A), cross-bedded sandstones are also in evidence.

(C) In thin section, sample 294 consists of moderately sorted, subangular to angular quartz grains, plagioclase feldspar and zircon grains in a matrix of clay minerals. Scale = 0.1 mm.

(D) A Doniphan Shale sample (No. 121) typifies many sandstones in the Upper Pennsylvanian, with heamatite coating on the subangular quartz grains. Scale = 0.05 mm.

(E) Frequently, quartz grains in the sandstones (sample No. 85) contain fluid and solid inclusions. One of the fluid inclusions in the central quartz grain also appears to contain a gas bubble. Scale = 0.05 mm.

(F) A photomicrograph of a Stull Shale sample (No. 85) showing numerous angular to sub-angular quartz grains in a matrix of mica and clay minerals. In the centre, one relatively fresh albite-twinned plagioclase grain is preserved. Scale = 0.1 mm.

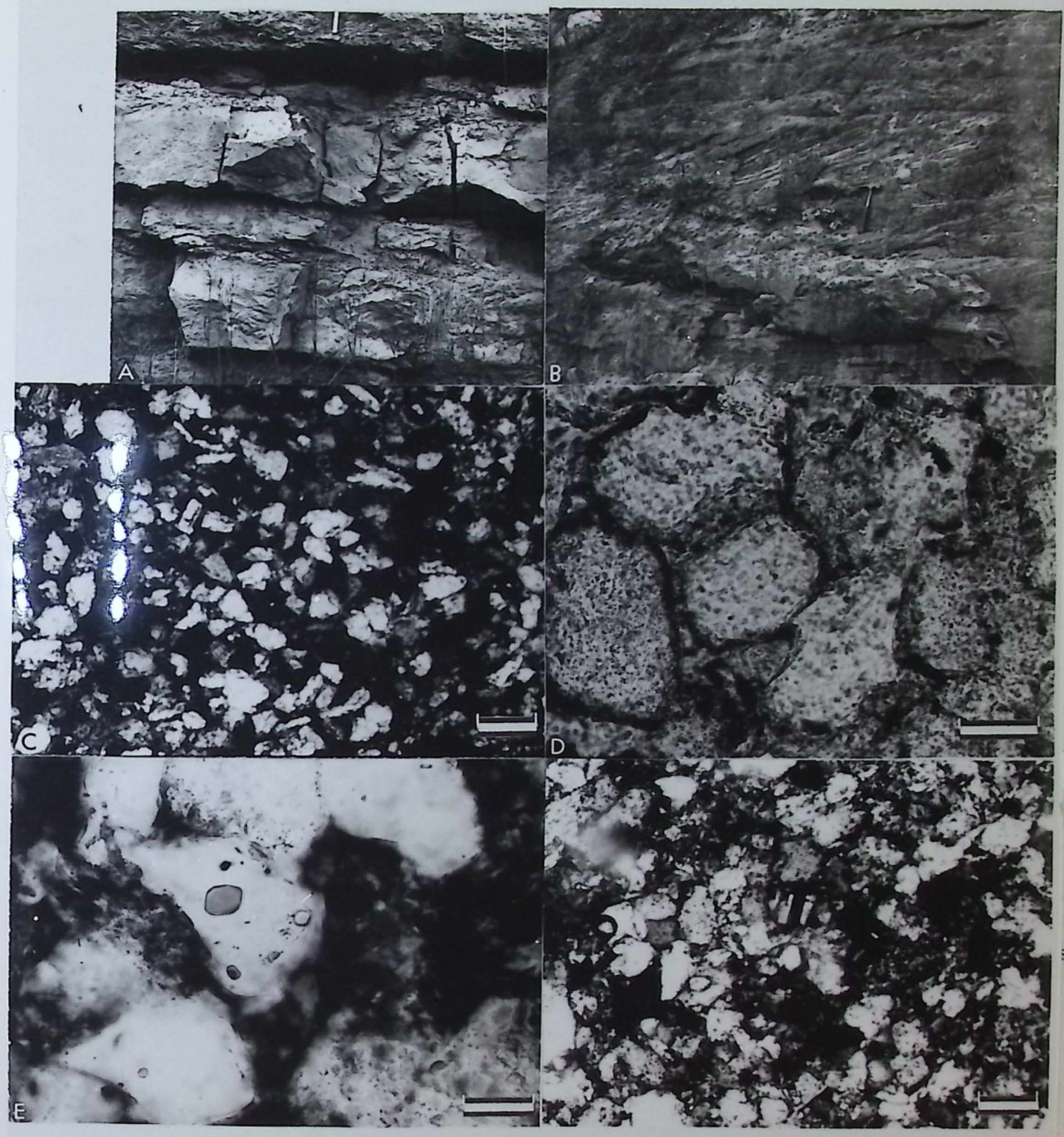
A
B
C
D
E

Channel deposits pass laterally into deltaic fine sands and siltstones (Wanless et al., 1970) characterized by uneven cross-lamination and reworking.

In thin section, the sandstones appear to be poorly to moderately sorted with numerous angular and subangular rock fragments, hematite and clay mineral coated quartz grains (Fig. 8.2d, e, f) and occasional fresh to slightly weathered, albite-twinned plagioclase (Fig. 8.2e), microcline, orthoclase and zircon grains in a clay mineral matrix (Fig. 8.2c). Samples vary in texture from immature sandstone to arkosic greywackes. Fragments of shale, igneous rocks, quartzite, undulous quartz, chert and organic material may be seen.

Laminated siltstones are found primarily in the beds separating the limestone Formations, designated by Schwarzacher (1967, 1969) as outside shales, e.g. Kanwaka, Tecumseh and Calhoun Shales of the Wabaunsee Group. In hand specimen and thin section, samples consist of alternating yellow-brown siltstones or silty shales and darker, fine-grained, slightly more carbonaceous shales (Fig. 8.3c). Graded beds and fining upwards cycles are common. Although contacts at the base of each siltstone band are sharp indicating a brief diastem, boundaries are often quite wavy, load casts are frequently present (Fig. 8.3a, b) and some small slumps are visible. The siltstone bands contain moderately sorted subangular quartz grains with occasional mica flakes, plagioclase feldspars, rock fragments and carbonaceous material. In contrast the finer bands are made primarily of mica and clay minerals with irregular amounts of fine silt size quartz grains. In both layers, however, it is apparent that the mica flakes lie parallel to the laminae (Fig. 8.2c), giving the siltstones an argillasepic, insepic or silasepic unistrial fabric (Fig. 8.3d, e; Brewer, 1964).

The zones of laminated siltstones closely resemble the regular layered structures recognised by Moore and Scrutton (1957) in modern

prodelta deposits in bays and along the coast of the Gulf of Mexico. Formation of these deposits apparently result from rapid deposition with little reworking of sediments. Fossil criteria (Heckel, 1972a) also indicate a restricted marine environment undergoing rapid sedimentation and subject to high turbidity and fluctuating salinity for much of these, thick, poorly fossiliferous Pennsylvanian Shales. A few siltstones and silt shales characterized by uneven laminations, ripple cross laminations and extensive reworking, are identified by Wanless et al., (1970) as also belonging to a deltaic facies.

This facies, therefore, represents a deltaic sequence consisting of channel sandstones, delta sands and siltstones and delta-front silts and shales which correspond to the deltaic units described by Wanless et al., (1970) for the Mid-Continent, U.S.A.

Calcareous, Grey Shale Facies

Thin beds separating limestones in limestone Formations are known as inside shales (Schwarzacher, 1969) and consist primarily of fossiliferous, grey, green and brown, blocky, calcareous shales. Most samples from this facies are massive or rubbly, but a few are laminated and fine-grained in texture.

This facies is thought to be a fully marine phase of deposition as it contains a characteristic marine fauna. Moore (1964) identified a number of ecosystems in these sediments of which the Derbyia, Rhombopora, Neochonetes and Derbyia-Neochonetes assemblages are most distinctive. Derbyia and other salinity-tolerant brachiopods and clams characterize the ecosystem found, for example, in the Speiser Shale of the Council Grove Group. Hattin (1957) interpreted the environment of deposition as belonging to an offshore zone of near normal salinity in which weak turbulence resulted from wave activity. Disseminated calcium carbonate was judged to be derived from shell disintegration. The Rhombopora

Fig. 8.3 (A) A siltstone band in the Heamader Shale (sample No. 75) shows regular alternations of silty shales (light area) and fine-grained slightly carbonaceous shales (darker zones). In many cases, load casts are developed, particularly where concentrations of silt grains develop. In this example, the pressure of the overlying silt has forced the softer, darker shale up into the silt band. Scale = 0.5 mm.

(B) A load cast, developed in the Severey Shale (sample No. 162), shows how silt grains are concentrated at the base of the structure. Note also how the organic matter forms a layer around the base of the cast. Scale = 0.5 mm.

(C) Alternating carbonaceous and silty shale bands predominate in most siltstones including the White Cloud Shale (sample No. 173). Note the wavy nature of the banding. Scale = 1 mm.

(D) The fabric of siltstones are typically argillasepic unistrial i.e. all the clay minerals and mica flakes are aligned, producing a unidirection extinction pattern. Sample No. 16. Scale = 0.2 mm.

(E) An electron photomicrograph of sample No. 16 shows the regular plate-like distribution of clay minerals. Occasional quartz grains interrupt this pattern. Scale = 0.015 mm.

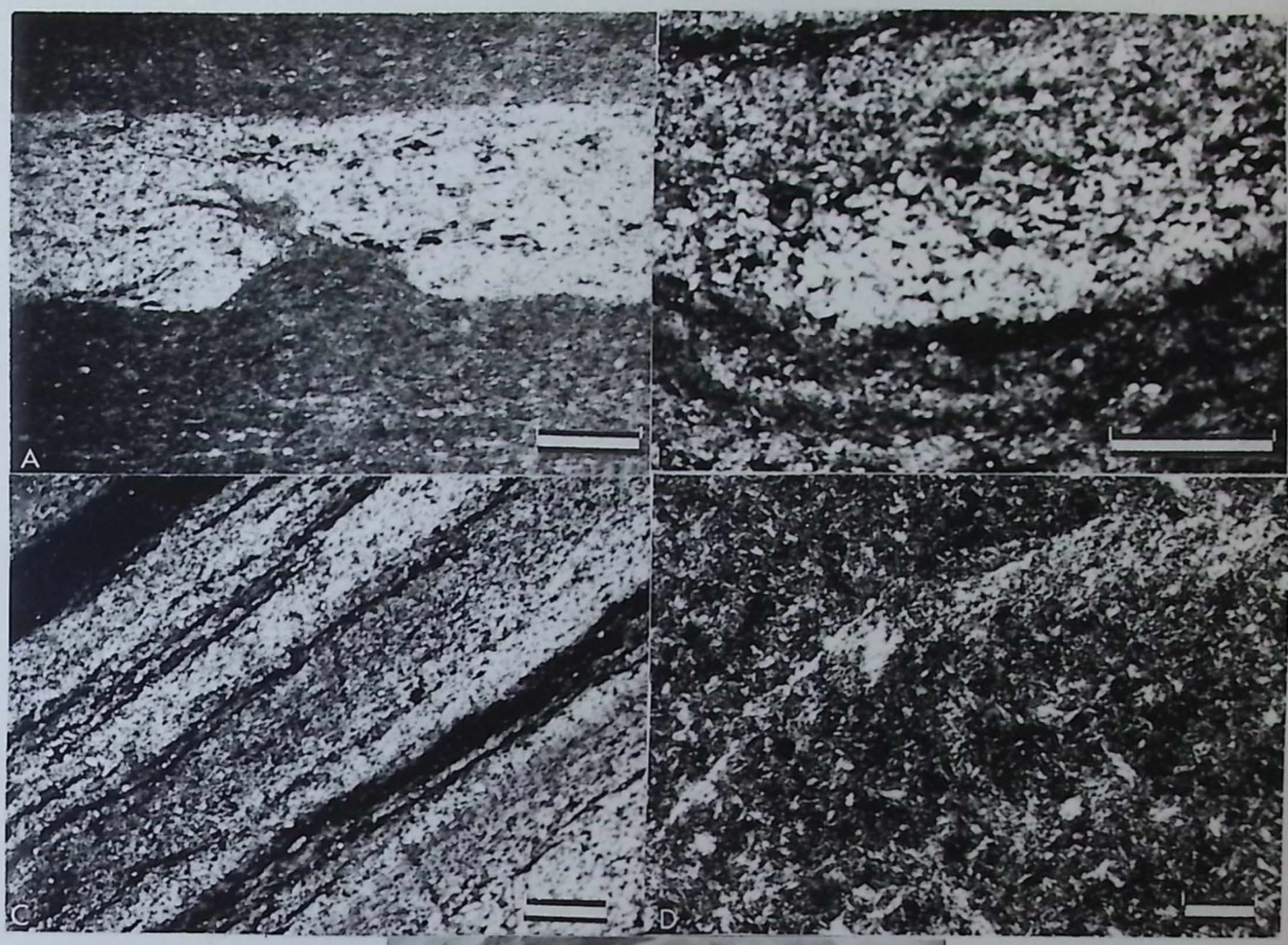
A
B
C
D

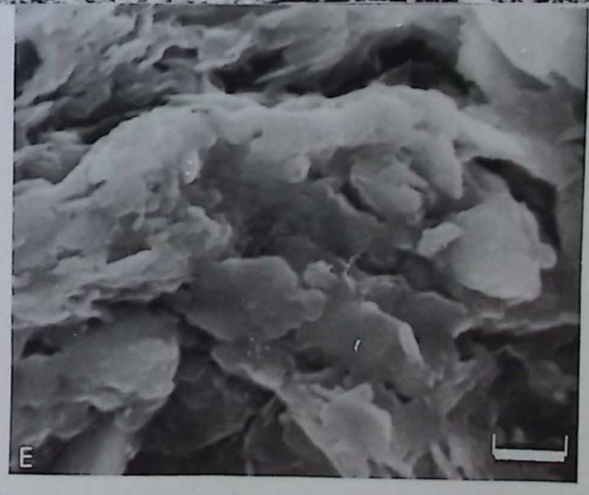
E

assemblage is identified in the initial parts of several marine sequences e.g. the Doniphan Shale of the Wabaunsee Group, and is characterized by abundant ramose bryozoans such as Rhombopora and Batostomella. The lowest marine shaley deposits of some limestone Formations contain abundant chonetoid brachiopods particularly Neochonetes. This ecosystem, exemplified by a Neochonetes assemblage in the Snyderville Shale of the Shawnee Group, has a shallow water habitat where a mud bottom bordered the shore (Moore, 1964). Finally, Moore (1964) and Imbrie, Laporte and Merriam (1964) distinguished an ecological community, typified in the Florena Shale (Council Grove Group), that corresponds to the Snyderville assemblage in Neochonetes and Derbyia content but also contains abundant fusilinids such as Schwagerina. The assemblage is, therefore, thought to have developed in the middle or regressive part of a cyclothem.

Although four fossil assemblages can be distinguished in this facies, it is most difficult to subdivide the facies on lithological evidence. However, from Moore's ecological survey, we can conclude that this facies generally represents open marine and shallow-water conditions.

In thin section, samples vary from slightly-silty, laminated, brown shales to highly calcareous, fossiliferous, marine, grey shales although the majority are calcareous, fine-grained, light grey or brown, coarsely-laminated shales. The presence of laminae in shales reflects the absence of burrowing organisms in the substrate and indicate deposition in an environment free from tidal or current movements. Off-shore marine deposition is inferred by the occurrence of brachiopods such as Derbyia and thin shelled bivalves. However, in the calcareous shales there is evidence for both near-shore and off-shore environments. In samples that are listed as dolomitic shales in the mineralogical classification, dolomite crystals are developed extensively suggesting a diagenetic alteration of some sediments. Fig. 8.4a-d illustrates the variety of sediments and textures associated with this facies.

Fig. 8.4 (A) A sample of the Oketo Shale (No. 265) contains numerous fossils such as fusilinids (outlined by organic matter), bryozoans and clam fragments, in a fine-grained calcite matrix. Scale = 0.25 mm.

(B) A fossiliferous sample of the Queen Hill Shale (No. 136) Punctate brachiopods, lamellibranch fragments and the fusilinids are found in abundance. Apart from an occasional quartz grain, the matrix is a grey micrite. Scale ; 0.5 mm.

(C) A Grant Shale sample (No. 272) illustrates the type of fabric developed in a shale containing few fossils. Numerous small calcite crystals can be seen within matrix of organic matter, clay minerals and the occasional quartz grain. Scale = 0.1 mm.

(D) Another fabric developed in a calcareous shale - Galesburg Shale (No. 27), contains far more organic matter and clay minerals. The beginning of mica alignment can be seen on the right of the sample. Scale = 0.1 mm.

(E) Red shales have many types of fabrics but the two most commonly recognised are illustrated in this and the following photo micrograph. Numerous well sorted quartz grains are surrounded by a stained, fine-grained matrix of clay minerals and calcite. Sample No. 270. Scale = 0.1 mm.

(F) This fabric contains reworked stained pellets surrounded by a fine-grained calcite matrix. Calcite overgrowths on the pellets are developed. Sample No. 256. Scale = 0.5 mm.

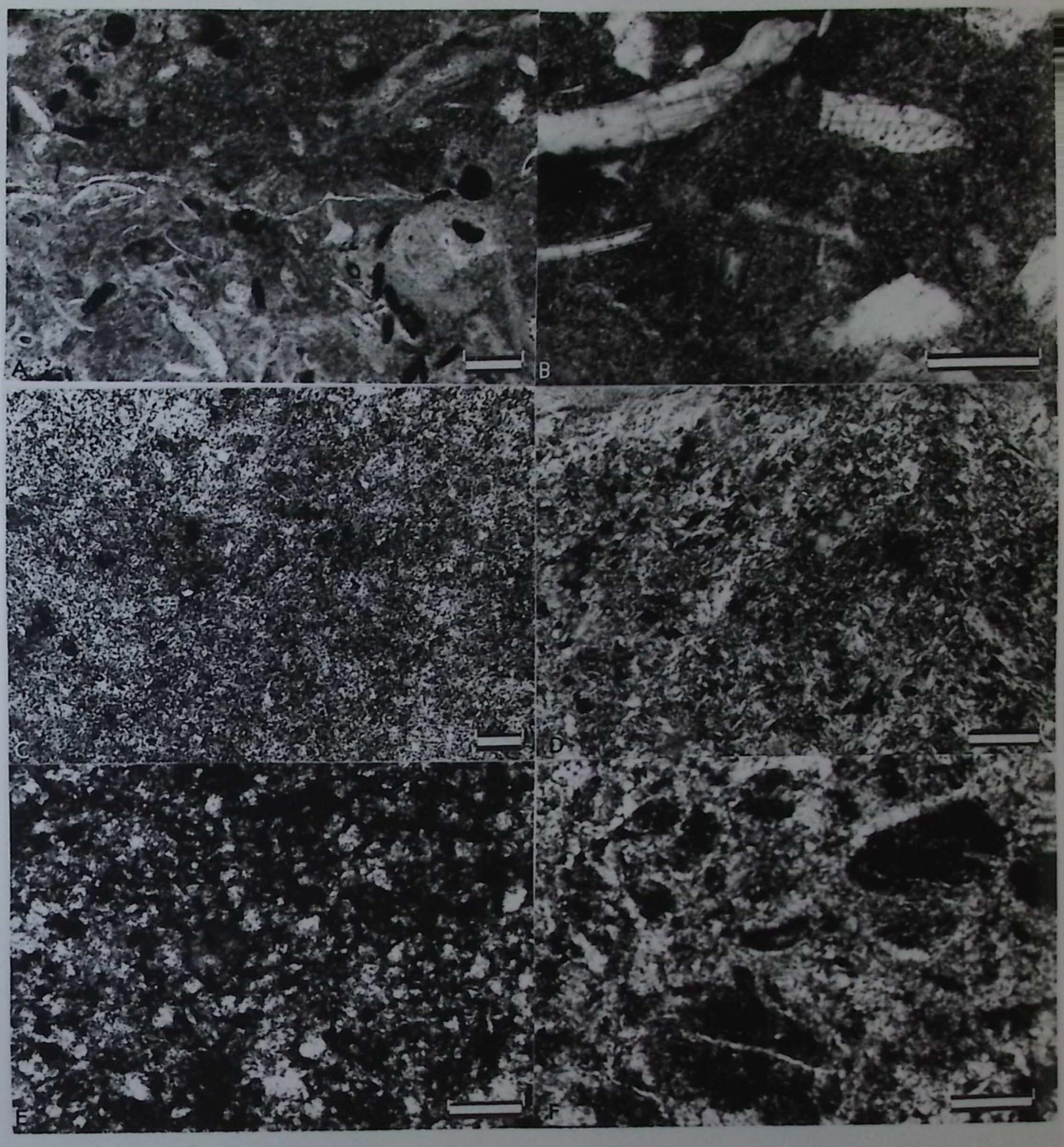
A
B
C
D
E
F

Red and Purple Shale Facies

This facies is characterized by red, green and purple mottled, calcareous shales and is only found in Lower Permian beds. Although only a few samples belonged to this facies, their characteristic colours make it a distinctive facies in the field and a brief description is therefore included here.

In hand specimen, samples are mottled red, green or purple, hard, blocky, calcareous shales and contained no fossils. The facies is found within outside shales (thick grey shales separating limestone Formations) and rarely thickens to more than 3 m. in any one bed. Furthermore, this facies shows rapid lateral variations.

Thin sections (Fig. 8.4e, f) reveal the presence of many fine, silt-size quartz particles within a matrix of stained, fine-grained calcite and clay minerals. Some samples appear to contain reworked pellets and sediments. Colour variation recorded in the shales is a reflection of the iron and/or organic content. Red colours arise from the presence of ferric oxide in the essential absence of organic material whereas green shales are probably deposited with some organic material that reduces the red ferric ion to the ferrous state (Elias, 1937). The stratigraphic association of green shales immediately above and below red shales indicate this to be true. Wells (1950) found small amounts of organic material in Eskridge red shales which he interpreted as an indication of deposition on land or in the tidal zone. Green shales were thought to be of shallow marine origin. However, red deposits are now known to form in a variety of climates and depositional environments (Broecker, 1974; Walker, 1974) from deep sea clays to moist tropical soils. It can therefore be implied that as red beds are not good palaeoenvironmental indicators (Berner, 1971), Wells interpretation is open to doubt. Unfortunately, until some viable alternative is proposed, this hypothesis has to be retained.

Mineralogically samples from this facies are all carbonates and consequently fall into group E of the mineralogical classification. However, their trace element geochemistries vary so considerably that samples fall into clusters X, A and D of the combined mineralogical and geochemical classification. Nevertheless, there is some uniformity in the major oxide content of the shales; for example, consistently high Fe oxide and CaO content.

This facies represents therefore, a locally important field unit but at the same time, is indistinguishable from other calcareous shales in terms of mineralogy and geochemistry. It would seem appropriate therefore, to consider this facies as a minor variation of the calcareous shale facies described previously.

SHALE PARTINGS IN LIMESTONES

A number of limestone units exhibit distinct layering in which the limestone beds are separated by thin shale partings. Although the thin shale studied by Troell (1969) was used as an internal stratigraphic datum, normally on exposure, the partings weather back into the outcrop face and thus receive little attention. They frequently contain corals and encrusting bryozoans that require clear water, relatively slow deposition and a firm substrate (Heckel, 1972a). These ecological considerations and the areal extent of each thin parting indicates that the shales result not from a rapid influx of clastics but rather from a long term cessation of carbonate deposition with very slow accumulation of suspended detritus.

In thin section, partings from the Winterset Limestone (Kansas City Group) and Beil Limestone are laminated calcareous brown to grey shales with abundant fragments of brachiopods, fusilinids, corals and organic matter (Fig. 8.5a, b).

Fig. 8.5 (A) A shale parting in the Winterset Limestone (sample No. 35) is calcareous, fine-grained and laminated with a few fossils. Scale = 0.4 mm.

(B) A Beil Limestone sample (No. 137) illustrates the fabric of shale partings. They are typically fine-grained, calcareous, grey or brown with occasional quartz grains. Scale = 0.1 mm.

(C) A sample from the Chanute Shale (No. 48) is representative of the clayey-shale facies. In this thin section, most are fine-grained, brown to grey, rather silty shales with scattered fossils. Scale = 0.1 mm.

(D) Another laminated silty shale showing gravitational bands. Scale = 0.05 mm.

(E) A typical exposure of the clayey-shale facies in a roadcut near Kansas City. Samples (69 to 71) of the Lane Shale were obtained from this site.

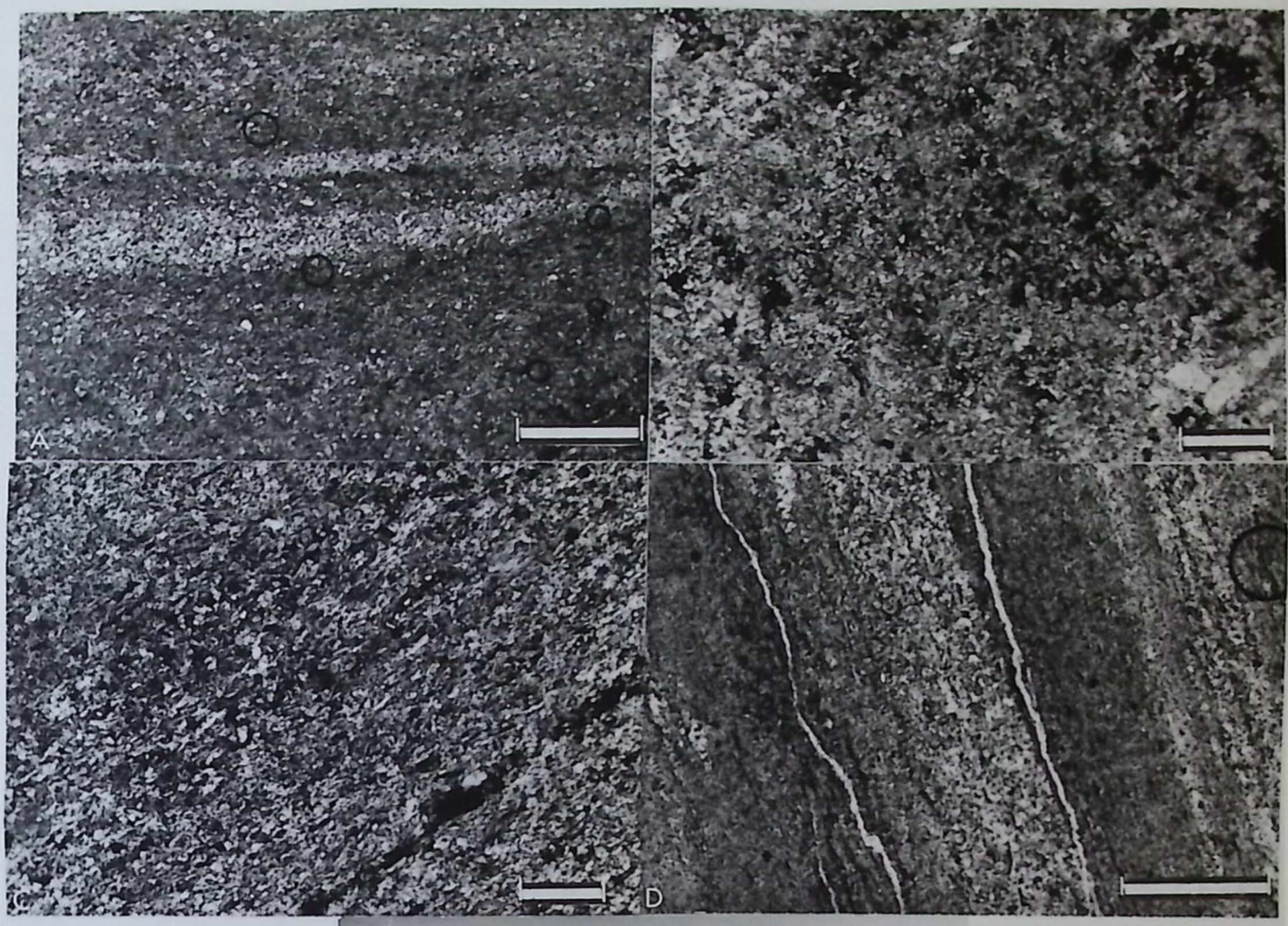

E

BROWN, SOFT, CLAYEY SHALE FACIES

Thick fine-grained, soft shale bands occur in many outside shales constituting a poorly fossiliferous, near-shore, marine sedimentary deposit. This facies generally displays a monotonous sequence of olive-grey to brown, slightly silty shales with thin zones of laminated siltstones occasionally carrying plant fragments.

Early work recognised both non-marine and marine environments in the outside shales (Moore, 1929). Later, however, identification of the consistent position of outside shale Formations between definitely marine limestone sequences, the general barrenness of the shales and the occurrence (even though local) of non-marine lithologies caused them to be considered as wholly or predominantly non-marine deposits (Moore, 1936), a concept that persists today.

However, recent investigations by Heckel (1972a) and Heckel and Baesemann (1975) have revealed the presence of fossils scattered throughout a number of outside shales, particularly in the Kansas City and Lansing Groups. Most of the fossils recovered are conodonts and small, thin-shelled pelecypods and gastropods, suggesting shallow-water or relatively rapid deposition or both. Shales of this facies are often found in association with deltaic sandstone and siltstones which necessarily place much of the facies in the near-shore shallow marine regime. Wanless et al., (1970) have therefore equated these deposits with prodeltaic marine muds and bottomset deltaic beds.

In thin-section, samples from this facies are revealed as fine-grained brown to grey, occasionally silty shales containing a few isolated fossils and organic material (Fig. 8.5c, d, e). Texturally, these shales are generally argillasepic and moderately to weakly unistrial (Brewer, 1964) although an occasional inundulic or insepic fabric was noted, indicating a lack of disruptive influences such as burrowing animals, tidal or current section and confirming the environmental interpretations placed

on this facies.

CONCLUSIONS

Clastic sedimentary deposits from the Upper Pennsylvanian and Lower Permian of Kansas, can be grouped into six facies representing differing environmental conditions.

The most distinctive of these facies is a black, laminated shale that is used as a marker horizon in cyclothems (Moore, 1950). Developed in the deepest parts of a shallow-water epeiric sea, it contains a sparse epiplanktonic fauna indicating anoxic bottom waters. Closely associated with this facies (as inside shales) are sediments that fall into the calcareous grey shale facies. These shales are deposited primarily in open marine, shallow water conditions and are characterized by abundant brachiopods, bivalves, fusilinids and bryozoans.

Inside shales separate limestone units within limestone Formations whereas outside shales are intercalated between the Formations. Two facies can be differentiated in the outside shales, a sandstone and siltstone facies and a brown, soft, clay-shale facies. Both represent environments of deposition characteristic of deltaic sedimentation. Firstly, the sandstone and siltstone facies consists of channel sandstones, laminated prodelta siltstones and deltaic sands and siltstones (terminology of Wanless et al., (1970)). Source of the detrital material is primarily from the Ouachita fold belt although subsiding deltas are developed on the lowlying land area to the north of the Forest City Basin. A minor source may originate in the Ozark dome of Missouri (Wanless et al., 1970). The brown, clay-shale facies can be equated to delta bottomsets and prodelta marine clays (Wanless et al., 1970).

A number of shale partings occurring in limestones constitute the fifth facies. Although geochemically and mineralogically indistinguishable

from other calcareous shales, they form a unique sedimentological facies. From ecological and lithological considerations, it is inferred that each thin parting developed in near-diastemic conditions.

A minor facies recognised in Lower Permian deposits is a red and purple shale lithology. It is interpreted as a product of near-shore or even tidal environments.

The interrelations between these facies are illustrated by a schematic diagram (Fig. 8.6) of a hypothetical Pennsylvanian section. It can be seen that there is an alternation of limestones and marine calcareous and black shales (inside shales) perturbated by thick, deltaic deposits (outside shales). Within each limestone, thin shale partings may occur. In the Lower Permian, all shale units become more calcareous and in places, red and purple shales may develop within outside shale units.

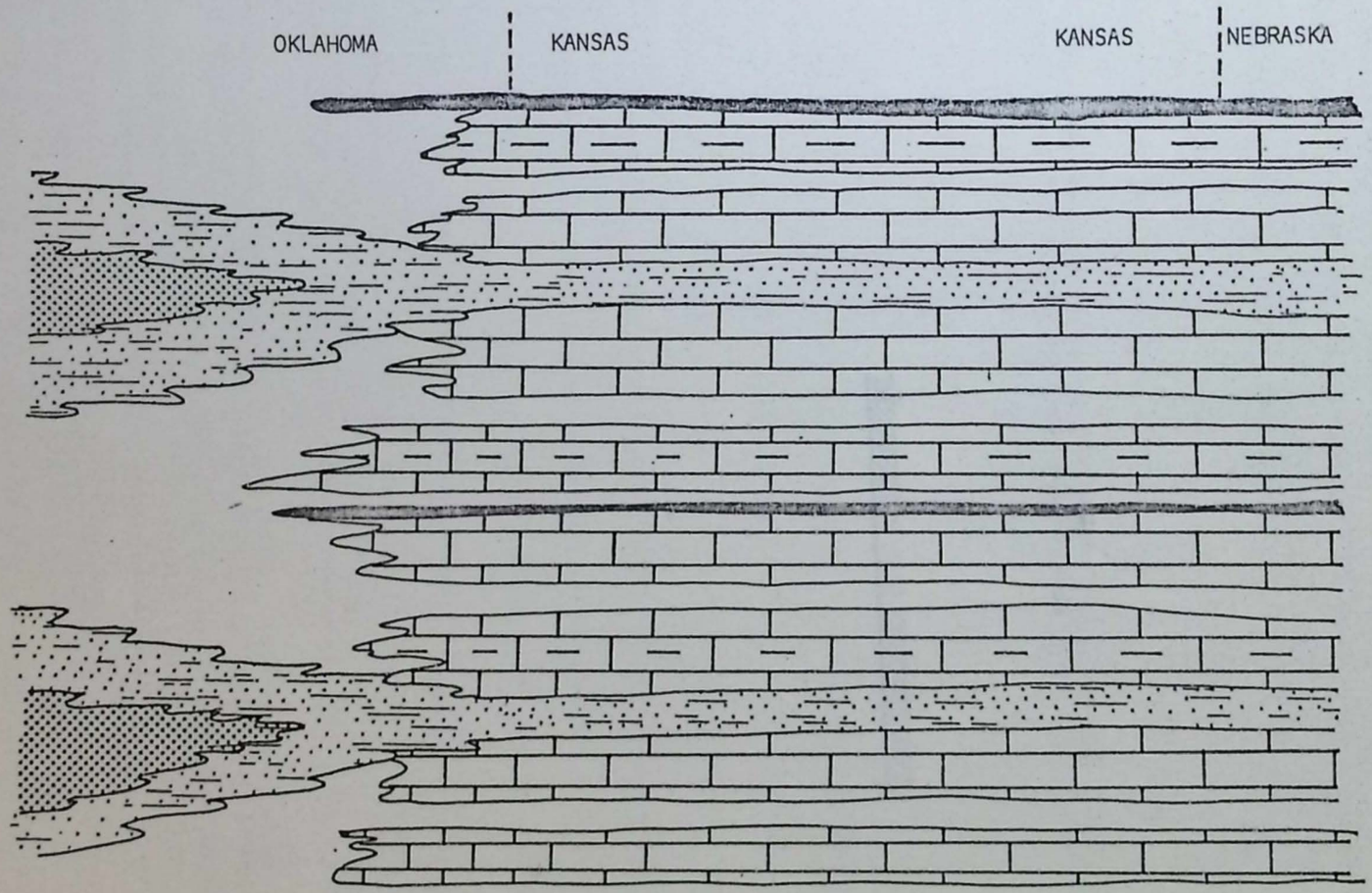

KEY

- Black shale facies
- Limestone
- Shale parting in limestone
- Delta front sands & silts
- Bottomset & prodelta shales
- Calcareous marine shales

Fig. 8.6 A schematic section illustrating facies relationships in Upper Pennsylvanian and Lower Permian shales of Kansas.

DISCUSSION AND CONCLUSIONS

GEOCHEMISTRY, MINERALOGY AND PETROLOGY

In this final section, the results obtained during the research project will be discussed, assessed in the light of the original aims and recommendations for future studies made.

Previous workers have interpreted the Upper Pennsylvanian and Lower Permian sedimentary succession of Kansas in terms of ten lithologies that form an oscillatory stratigraphic pattern (Moore, 1950, 1964; Duff, Hallam and Walton, 1967; Weller, 1958, 1960). However, only seven are lithologically distinct (Moore, 1950) and later analysis has reduced this to five (Pearn, 1964). For field use, Schwarzacher (1967, 1969) reduced this still further to four and finally, Davis and Cocke (1972) concluded that the only observable pattern was a two state limestone - inside shale oscillation, perturbated by occasional outside shales or black shales. In an attempt to clarify this confusing situation, a detailed geochemical, mineralogical and petrological study of the Upper Pennsylvanian and Lower Permian shales of Kansas was made and the variations observed were related to the stratigraphic and tectonic setting of Kansas, during this period. The limestones were, however, omitted from the study as an extensive coverage of these beds is already available (Haglund, 1967; Wilson and Heckel, 1971; Heckel, 1972a, b, 1974; Baesemann, 1973).

In this thesis, Kansas shales were found to consist of six major facies (based on the combined data, see chapters 7 and 8), each corresponding to a separate depositional environment.

1) A sandstone and siltstone facies corresponding to deltaic sands and siltstones with a source in the Ouachita Mountains of Oklahoma and Arkansas and occasionally, the lowlands of Iowa, Nebraska and Missouri. This facies contains abundant quartz, feldspar, and detrital zircons and is, therefore, enriched in SiO_2, Al_2O_3, and Zr.

2) A clayey shale facies corresponding to prodeltaic marine muds which is the seaward extension of the previous facies. The shales are therefore rich in quartz and feldspar and have an increased clay mineral content. Ga, Li and K_2O may also be enriched in these shales.

3) A black shale facies that is a product of a restricted marine environment (Heckel, 1972a). The regular stagnation of bottom waters, leading to development of reducing conditions in the sediments, may be caused by tectonic uplifts of a barrier at the mouth of the epeiric sea. These shales are enriched in the trace elements Cd, Cr, Cu, Be, Mo, Ni, Pb, V, Zn by the chemical action of organic matter.

4) A calcareous grey shale facies that represents open marine, shallow water deposits which are characterised by abundant brachiopods, bivalves, fusilinids and bryozoans. These shales have high calcite, CaO, MnO, Sr, Sn, Ge, and Bi content.

5) A shale partings in limestones facies is equated to diastemic conditions but is mineralogically and geochemically similar to the calcareous facies.

6) A facies of minor importance is a red and purple shale facies that occurs in certain sections of Lower Permian shales and possibly represents a calcareous equivalent of facies 2.

These facies equate to the lithologic divisions noted by Schwarzacher (1969), Davis and Cocke (1972) and Heckel and Baesmann (1975). By combining facies 1 and 2, a group of deltaic shales is obtained that occur primarily in the thick shale Formations separating limestone Formations (outside shales). In Chapter 1, it was conjectured that the appearance of these deposits may be related to tectonic uplifts of the Ouachita foldbelt resulting from cyclic movement along subduction zones (Bott and Deans, 1973). Facies 3 and 4 generally occur as shale Members separating individual limestone beds in a limestone Formation (inside

shales). The black shales are normally located above the second limestone bed. Facies 5 (equivalent to inside shales) and 6 (equivalent to outside shales), however, are only of minor importance as they represent a small number of shale samples.

Stratigraphically, these facies were found to be distributed in a number of zones.

1) In the Pleasanton, Kansas City and Lansing Groups, there are regular alternations of limestones and inside shales separated into Formations by thick beds of deltaic outside shales.

2) The succeeding Douglas Group, however, appears to contain only outside shales.

3) The Shawnee Group, reverts to the limestone - inside shale alternation with outside shales separating limestone Formations.

4) The Upper Pennsylvanian culminates in the Wabaunsee Group with outside shales and occasional limestones.

5) In the Admire, Council Grove and Chase Groups of the Lower Permian, a general increase in the carbonate content of all rocks is manifest in the development of calcareous outside shales (red and purple shale facies) separating the alternations of inside shales and limestones. Towards the top of this division evaporites are developed, although the geochemical data showed no evidence for increasing salinity.

A number of different oscillatory patterns can be detected in these deposits. Firstly, in the Pleasanton, Kansas City, Lansing,

Shawnee and Lower Permian Groups, a succession of alternating inside shales and limestones constitutes a limestone Formation. The limestone Formations are separated by outside shales, thereby outlining a set of sedimentary deposits approximately equivalent, in thickness, to a cyclothem (Moore, 1950). However, there is no firm evidence for such cycles in the stratigraphic distribution of the facies. The only corroborative support is obtained from the statistical analysis of mineral and element distributions. Fourier analysis of the stratigraphic distribution of quartz, SiO_2, Al_2O_3, CaO, MnO, Ba, Cr, Ni, Mo, Cu and Ga indicate the presence of 70 foot cycles in the shales. This agrees with the thickness attributed to cyclothems by Moore (1950) although no evidence for the lithological complexity of cycles presented by Moore (1950) can be found. It is, therefore, suggested that the 70 foot cycles recognised in this thesis match the mathematically derived oscillations noted by Schwarzacher (1969) and Davis and Cocke (1972) and are possibly manifestations of a simplified "ideal" cyclothem. It can also be inferred that, in terms of detecting cyclicity, Fourier analysis is a more appropriate and sensitive tool than multivariate analysis. Dunn (1974) also recognised this potential.

In the intervening Douglas and Wabaunsee Groups, no evidence for cycles was noted. The beds are primarily deltaic clastics and may represent the products of important tectonic events in the orogenic belts to the South. The Douglas and Wabaunsee Groups are also recognised by Moore (1964) and Schwarzacher (1969) as distinct zones although they distinguish poorly developed or incomplete cyclothems in the Formations.

The stratigraphic zones 1 to 4, therefore, form an alternation

of cyclothem bearing and non-cyclothem bearing deposits, i.e. the Pleasanton, Kansas City, and Lansing Groups contain cyclothems whereas the succeeding Douglas Group does not contain cycles and similarly the Shawnee Group contains cycles and the Wabaunsee does not. The oscillation of stratigraphic zones may represent a large scale cyclic development, possibly related to tectonism. These cycles roughly correspond to hypercyclothems (Merriam, 1963) but have been described in detail only in this project.

The cyclic development of outside shales and black shales has been accounted for by orogenic events in the Ouachita foldbelt. Major tectonic periods may also account for the differences between zones containing cyclothems and those without. Although the basic cause of the oscillation remains unknown, several tectonic controls have been proposed:

a) varying rates of subsidence allowing transgressions and regressions (Matthews, 1974);

b) repeated eustatic changes in sea level and variation in clastic influx, controlled by climatic changes (Wanless and Shepard, 1936);

c) diastropic uplift and subsidence of source area (Weller, 1956).

In the light of modern theories of global tectonics and sea-floor spreading, it would seem likely that a combination of controls such as a and c may provide the answer.

A multivariate statistical analysis elucidated the geochemical and mineralogical evolution of the Upper Pennsylvanian and Lower Permian shales and indicated that the stratigraphical variation in the mineralogical and geochemical data is controlled by nine components - a carbonate component, a black shale component, a clay mineral component, a dolomite

component, a shallow versus deep water environment component, a manganese component and three uninterpretable components. These carbonate and black shale factors may be related to the orogenic controls of outside and inside shales and, similarly, the manganese component is related to marine conditions of the inside shales. The dolomite component indicates that diagenetic activity has affected the shales particularly in the Lower Permian.

In conclusion, therefore, the research conducted for this thesis has shown that the concept of a ten-component "ideal" cycle envisaged by Moore (1936) is not supported by mineralogical, geochemical or petrological data from the Upper Pennsylvanian and Lower Permian shales of Kansas. However, a simplification of the clastic classification to three components - calcareous marine shales, restricted marine black shales and finally, deltaic and prodeltaic shales, sandstones and siltstones, suggests cycles at approximately 70 ft. intervals in the Pleasanton, Kansas City, Lansing and Shawnee Groups. This classification matches the mathematically-derived lithological divisions observed in the Kansas City Group by Davis and Cocke (1972). The calcareous shales of this thesis equate to inside shales and similarly deltaic shales to outside shales. Black shales are in both cases equivalent.

However, a major criticism of this research project is recognised in the extensive interpretations and conclusions made from such a small data set. In retrospect, a more satisfactory data set could have been obtained by sampling at a fixed interval within the clastic deposits. It would also have been more appropriate to have chosen a smaller section, for example the Shawnee and Wabaunsee Groups, and

to have analysed both the limestones and shales. The sampling interval should be related to the oscillatory patterns noted in this thesis, i.e. less than 70 foot.

A further criticism of this project has been the relatively subjective decision to sample on a bed by bed basis. In retrospect, it would have been more desirable to have sampled extensively within beds (on a fixed interval scale) and also along the strike of the beds producing another level of replication and information for the project.

The accuracy of the data, particularly the geochemical data, can also be questioned suggesting that the conclusions drawn about the stratigraphic variation in the elemental data may be affected by experimental error. The technique applied, emission spectroscopy, should therefore be used to determine the geochemical variation of the shales and a more precise technique such as X-ray fluorescence should be used to quantitatively analyse the shales.

This combination of errors and subjective decisions has made the identification of cycles in Kansas shales difficult. It is recognised that the conclusions drawn in this thesis do not provide any new information on the nature or origins of the cyclothems in Kansas; nevertheless it can be inferred that Moore's "ideal" cyclothem is not developed in the stratigraphic section examined but that a simplified cycle may be. The procedure adopted for the analysis of cyclic sequences may be strengthened by employing Markov chain analysis (Schwarzacher, 1967, 1969) on the data. This would be particularly appropriate for fixed interval data from a reduced stratigraphic section.

Diagenesis and weathering may play important roles in the mineralogical and geochemical variation of the shales. However, these aspects

were not examined in detail and the conclusions should be viewed in the light of this omission. As the significance of these effects is at present unknown, the secondary alteration of Kansas shales should be examined particularly in the Lower Permian where dolomites are developed, and related to the geochemical variation noted in this thesis.

In conclusion, future projects on this stratigraphic section should concentrate on a smaller section of the Upper Pennsylvanian, possibly the Shawnee and Wabaunsee Groups, and combine both fixed interval vertical as well as lateral sampling of clastic and non-clastic beds. The problems of diagenesis and weathering should be examined by comparing the outcrop data with the numberous bore-hole cores available at the Kansas Geological Survey. Fourier analysis of geochemical and mineralogical variables has proved a powerful statistical technique for the detection of cyclic variation and should be applied to the analysis of any future data of this type. Markov chain analysis should also be pursued. A number of projects could be developed out of the geochemical variation noted in these shales, particularly the elements in the carbonate fraction. The work of Veizer and Demovic (1974) and Bencini and Turi (1974) on environmental interpretation of trace element distributions in limestones could be applied successfully to calcareous shales as suggested by the geochemical analysis in Chapters 4 and 7.

The textural analysis of shales by the scanning electron microscope and micromorphological techniques is also suggested as

a future development from the facies analysis performed in Chapter 8.

INSTRUMENTAL TECHNIQUES AND PROCEDURES

Fine-grained sedimentary rocks are renowned for difficulties of light microscope analysis. It is, therefore, a common procedure to supplement the petrological examination of shales and clays by instrumental techniques such as X-ray diffraction, atomic absorption and X-ray fluorescence. However, not all these techniques were practically available to the researcher and in order to study the geochemistry of shales, emission spectroscopy and electron spin resonance were introduced into the repertoire of instrumental techniques.

X-ray diffraction is available in most science departments and is frequently applied to the determination of sediment mineralogy. It is particularly useful for the study of shales, whose fine-grained nature normally precludes light microscope mineralogical analysis. However, in X-ray diffraction, experimental results are often highly variable; consequently, numerous sample preparation techniques and conditions have been developed, for the quantitative assessment of mineralogy. A statistical analysis of errors in quantitative X-ray diffraction analysis of fine-grained sediments enabled the researcher to establish standardized sample preparation procedures and analytical conditions which minimized

the controllable errors.

Results of this analysis show that the commonly used smear technique (Gibbs, 1965) is superior for distinguishing between shales on the basis of quantitative assessment of mineral content. However, practical considerations make this technique inapplicable for large experiments. The next most effective methods are the pressed pellet technique (Hildago,and Renton, 1970) and the mounting of samples onto membrane filters (Appendix 5). Both methods are rapid and subject to minimal operator variation.

Using either of these two methods, a combination standards technique produced calibration charts for the major mineral constituents of the Upper Pennsylvanian and Lower Permian shales. Extremely high linear correlations for the three standard regression curves indicate that the expected error of estimates made within the range of the standards will be small, less than 6% at a maximum. This technique is particularly applicable where pure minerals identical to sediment components can be obtained but has the disadvantage that standards, for minerals with variable composition such as clay minerals are still difficult to construct. Research into this aspect of quantitative X-ray diffraction could be beneficial to sedimentary petrologists.

Geochemical analysis of the same shales was performed on a direct reading emission spectrometer using standardized sample preparation and analytical procedures (Celenk, 1972). Emission spectroscopy was used in preference to X-ray fluorescence or atomic absorption for a number of reasons: availability of instruments, speed and ease of sample preparation, small weight of sample required and relatively sensitive and precise results (Table Concl. 1). It is, with hindsight however, considered more appropriate to use this technique as a "quick look" method of assessing which trace elements are enriched in the sediments and then using a more accurate technique such as X-ray fluorescence for determining the precise

TABLE CONCL. 1 A comparison of instrumental techniques employed in this thesis and in other geological applications

	X-RAY DIFFRACTION	X-RAY FLUORESCENCE	EMISSION SPECTROSCOPY	ATOMIC ABSORPTION	ELECTRON SPIN RESONANCE
PRINCIPAL APPLICATION (Mj = Major oxides, Tr = Trace elements, M = Minerals)	M	Mj, Tr	Tr	Mj, Tr (alkali metals)	Tr (ionic species)
SENSITIVITY	1 to 5%	0.007 - 0.1%	1ppm to 24ppm	0.01ppm to 10.0ppm	10^{-5} to 10^{-12} moles
PRECISION (OPTIMUM)	1 - 5%	0.5 - 5%	3 - 18%	1%	20%
PREPARATION AND ANALYSIS TIME (S=slow; M=moderate; F = fast)	M	MF	F	M	F
WEIGHT OF SAMPLE OR VOLUME REQUIRED & TYPE OF SAMPLE ACCEPTED	0.05gm. POWDER	200mgm. POWDER PELLET	10mgm. POWDER	2mls. LIQUID	0.2cm.^{3} SOLID, LIQUID OR POWDER
COMMENTS AND REFERENCES	Chapter 2, Clay minerals are quantitatively difficult	Smales and Wager (1960). 80 elements can be analysed. See also Hutchinson (1974)	Celenk, (1972) Mo, V, Zn have poor sensitivities	Browning (1969). Sensitivity poor for Hg, Ti, Si, Pt, Sn and Ge	Whiffen (1968). Useful for Mn, Fe, Cu, Co. Non-destructive

quantities present in samples. Nevertheless, it has proved a sufficiently accurate technique in the context of this thesis and it is envisaged that further research on sediments using this advanced instrumental technique, will be pursued in future.

In order to determine the structural sites that certain trace elements occupy in sedimentary rocks and consequently their environmental situation, a spectroscopic technique used extensively in chemistry but almost unknown in geology, electron spin resonance, was applied to the Upper Pennsylvanian and Lower Permian shales. A comprehensive bibliography (Appendix 2) for the technique is therefore presented and its characteristics are summarised in Table Concl. 1. The ionic species of Mn, Fe, Cu and Co proved particularly suitable for examination by ESR. It is extremely sensitive, requiring only a small amount of sample in liquid, solid or powder form, and produces results quickly and cheaply. One other feature worth mentioning is the non-destructive nature of the technique, of great importance when dealing with small amounts of material. Of the disadvantages, the most striking is that quantitative procedures have not been developed to the precise level of X-ray fluorescence, for example. However, the advantages are thought to far outweigh the disadvantages and may encourage the adoption of this chemical technique as a standard analytical procedure for geochemists. It is certainly an area where considerable fruitful research could be conducted.

APPENDIX ONE

THEORETICAL AND COMPUTATIONAL ASPECTS OF THE STATISTICS AND DATA ANALYSIS TECHNIQUES EMPLOYED IN THE ANALYSIS OF GEOCHEMICAL AND MINERALOGICAL DATA FROM THE UPPER PENNSYLVANIAN AND LOWER PERMIAN SHALES OF KANSAS, U.S.A.

INTRODUCTION

The analysis of large arrays of geochemical and mineralogical data is normally performed by computer using a variety of univariate and multivariate statistical techniques. This appendix gives a brief summary of the theoretical and computational aspects of these statistics and a discussion of problems associated with their use in the context of this thesis.

1. ELEMENTARY STATISTICS

a) Arithmetic Mean

The mean is another word for the arithmetic average and is defined as the sum of all observations (X_i) divided by the number of observations (n).

$$\bar{X} = \frac{\sum_{i=1}^{n} X_i}{n}$$

This statistic is of fundamental importance in the calculation of other parameters (standard deviation, skewness, etc.).

b) Median

The median is the value midway in the frequency distribution. This is a useful measure of central tendency in such cases where occurrences of even a few high or low values seriously distort the impression of the distribution given by the mean. In an unsymmetric distribution, the median as a typical value is a more suitable measure than the mean. On the other hand, in spite of the distribution shape, the mean always communicates the same thing, the point about which the sum of deviations is zero.

c) Mode

A mode is a value which occurs with more frequency than neighbouring values. However, as the mean and median provide greater information on

central tendency, this statistic was not used as extensively.

d) Variance and Standard Deviation

The following equation measures the spread or dispersion about the mean (variance).

$$\text{Variance } (s^2) = \frac{\sum_{i=1}^{n} (X_i - \bar{X})^2}{n - 1}$$

The square root of the variance is the standard deviation (s). A small s value indicates that observations are clustered tightly around a central value. Conversely, a large standard deviation indicates that values are scattered widely about the mean and the tendency for central clustering is weak. In the same manner as the arithmetic mean, this statistic is most appropriately applied to a normal distribution.

e) Maximum and Minimum

These give an indication of the total range of values encountered.

f) Covariance

Computational procedures used to calculate the variance of a single property, can be extended to calculate a measure of the mutual variability in a pair of properties. This measure, termed the covariance, is the joint variance of two variables about a common mean and can be calculated using the standard equation (Davis, 1973):

$$\text{CoV}_{jk} = \frac{\sum_{i=1}^{n} (X_{ij} - \bar{X}_j)(X_{ik} - \bar{X}_k)}{n - 1}$$

Young and Cramer (1971) have proposed an alternative algorithm for this computation and Mather (1973) has discussed its application.

g) Correlation Coefficient

In order to assess the interrelationship between variables in a manner not influenced by measured units, the correlation coefficient, r,

is used. Correlation is the ratio of the covariance of two variables, j and k, to the product of their standard deviations:

$$r_{jk} = \frac{CoV_{jk}}{s_j s_k} = \frac{\sum_{i=1}^{n} (X_{ij} - \bar{X}_j)(X_{ik} - \bar{X}_k)}{(n-1)s_j s_k}$$

As covariance may equal but not exceed the product of the standard deviations of its variables, correlation ranges from +1 (perfect positive linear correlation) to -1 (perfect negative linear correlation) with 0.0 representing the lack of any linear correlation. Problems caused by sampling a population (Griffiths, 1969) can be overcome by testing the correlation coefficient against a t-distribution using the relationship:

$$t = \frac{r\sqrt{(n-2)}}{\sqrt{(1-r^2)}}$$

with n - 2 degrees of freedom at the 95% significance level.
Both the correlation coefficient and/or the variance/covariance matrix are used as the basis of many multivariate statistical techniques in classification studies (see: Classification procedures).

2. ANALYSIS OF VARIANCE (ANOVA)

Where two or more sets of data are to be compared, the analysis-of-variance procedure is appropriate; it is one of the most versatile tools at the disposal of geologists. It is, however, necessary to decide before starting any experiment, what the goals are and which design is most suitable for their achievment. The types of experimental design in geological use have been extensively discussed by Drumbein and Graybill (1965) and Griffiths (1969) and, therefore, only the experimental design and analysis of variance used in this thesis will be considered here.

a) One-way ANOVA

In this analysis, a linear model is used which states that the value of any observation (i) in a "treatment" group is composed of a simple sum:

$$X_{ij} = \mu + \alpha_j + \epsilon_{i(j)}$$

where μ is the mean of the j "treatment" populations, the effect α_j is associated with the particular "treatment" j and $\epsilon_{i(j)}$ is the random error term. The complete ANOVA table for a one-way design in shown in Table A1.1.

b) Two-way ANOVA

In this experimental design, there are two different sets of "treatments" which require analysing. Each observation X_{ij} may be expressed as:

$$X_{ij} = \mu + \alpha_i + \beta_j + (\alpha\beta_{ij} + \epsilon_{ij})$$

where α_i, β_j are the main effects of the two sets of treatments, $\alpha\beta_{ij}$ is the interaction and ϵ_{ij} is the error term.

c) Two-way ANOVA with Replicates

In many geological problems, it is necessary to assess the effects of α_i separately from β_j. This can only be achieved in a two-way ANOVA when $\alpha\beta_{ij}$ is zero. In practice, it is advisable to determine whether this requirement is fulfilled and so a separate estimate of the contribution of $\alpha\beta_{ij}$ is necessary, together with an appropriate error term to test the hypothesis $\alpha\beta_{ij} = 0$. More than one observation of each treatment (replicate) in the two-way classification is therefore taken. The structure of the experiment now becomes:

$$X_{ijk} = \mu + \alpha_i + \beta_j + \alpha\beta_{ij} + (\delta_{k(ij)} + \epsilon_{(ijk)})$$

where each observation X_{ijk} contains an estimate of the true mean μ,

plus a contribution α_i from the first main effect, plus a contribution β_j from the second main effect plus a contribution $\alpha\beta_{ij}$ from the inconsistency of α_i across β_j plus variation from replication $\delta_{k(ij)}$ and variation from all other sources $\epsilon_{(ijk)}$. The structure of the experiment can be seen in Fig. 2.1 and the complete ANOVA is set out in Table 2.1. The significance of the mean squares can be assessed using an F-test or variance ratio. Three assumptions are, however, necessary for the analysis of ANOVA results by F-test:

1) the observations X_{ijk} are random variables,

2) the variables are the sums of the component variables α_i and β_j, i.e. $\Sigma\alpha_i = \Sigma\beta_j = \Sigma\alpha_i\beta_j = 0$ and

3) the random variables are distributed with the variances σ_α^2, σ_β^2 and σ_ϵ^2, and all covariances are zero.

This implies no interaction between the variables, but using the ANOVA tests described above, any interactions that may exist can be assessed and their significance tested.

3. LINEAR REGRESSION

In geological studies, it is often important to detect overall trends in a data set, e.g. the trend of quartz content in a set of shale samples from a borehole. This trend can be represented by a line of best fit calculated by the method of least squares:

$$Y_i = \hat{\alpha} + \hat{\beta} X_i + \epsilon_i$$

where ϵ_i is a measure of "error" or the amount by which Y_i departs from the line for all Y_i at a given X_i. $\hat{\alpha}$ and $\hat{\beta}$ are estimates for the best fitting straight line to the observed points where α and β represent the intercept of the line on the Y axis and the slope of the line, respectively. The line of "best fit", is defined as that line which minimizes ϵ_i^2 and is calculated using the following expressions:

TABLE A1.1 ANOVA Table for One-Way Design

Source of variation	Sums of squares	Degrees of freedom	Mean square	F-test
Among samples	SS_A	$m - 1$	MS_A	
Within samples	SS_W	$N - m$	MS_W	$\frac{MS_A}{MS_W}$
Total variation	SS_T	$N - 1$		

$$\hat{\beta} = \frac{\sum_{i=1}^{n} X_i Y_i - \left(\sum_{i=1}^{n} X_i \sum_{i=1}^{n} Y_i\right)/n}{\sum_{i=1}^{n} X_i^2 - \left(\sum_{i=1}^{n} X_i^2\right)/n}$$

$$\hat{\alpha} = \frac{\sum_{i=1}^{n} Y_i}{n} - \frac{\hat{\beta} \sum_{i=1}^{n} X_i}{n} = \bar{Y} - \hat{\beta}\bar{X}$$

The minimizing function for the previous equations is:

$$\sum_{i=1}^{n} (\hat{Y}_i - Y_i)^2 = \text{minimum}$$

where $\hat{Y}_i$ is the estimated value of Y_i for specific values of X_i. We can define three terms which express variation of the dependent variable Y.

1) Total sums of squares

$$SS_T = \sum_{i=1}^{n} Y_i^2 - \frac{\left(\sum_{i=1}^{n} Y_i\right)^2}{n} = \sum_{i=1}^{n} (Y_i - \bar{\bar{Y}})^2$$

2) Sums of squares due to regression

$$SS_R = \sum_{i=1}^{n} \hat{Y}_i^2 - \frac{\left(\sum_{i=1}^{n} \hat{Y}_i\right)^2}{n} = \sum_{i=1}^{n} (\hat{Y}_i - \bar{\bar{Y}})^2$$

3) Sums of squares due to deviations

$$SS_D = SS_T - SS_R$$

The variance statistics for the linear regression (Table A1.2) can be used to test the significance of the line. Another useful statistic, the goodness of fit of the line to the points, can be defined by:

$$R^2 = \frac{SS_R}{SS_T}$$

If the line fits the data well, the ratio will be near unity. When the ratio is very low, the regression model is inappropriate for the data set and a higher order polynomial regression model is required for the

TABLE A1.2 ANOVA for Simple Linear Regression (after Davis, 1973, Table 8.8)

Source of variation	Sums of squares	Degrees of freedom	Mean squares	F-test
Linear regression	SS_R	1	MS_R	
Deviation	SS_D	n - 2	MS_D	$\frac{MS_R}{MS_D}$
Total variation	SS_T	n - 1		

detection of trends in the data.

In this thesis, only the linear model was used for determining overall trends as it was not necessary to have a satisfactory goodness-of-fit ratio. Deviations from the trend were analysed by other techniques including fourier analysis.

4. EQUISPACING AND INTERPOLATION OF DATA POINTS

It is necessary for time-trend analysis and fourier series analysis to input a series of regularly spaced data points. The nature of the sampling program used in this thesis, however, prohibited regularly spaced sample collection from the stratigraphical column. A series of equally spaced data points were therefore calculated from the variably spaced data points using linear interpolation, a technique described in detail by Davis (1973).

5. TIME-TREND ANALYSIS

One objective of this thesis has been to detect periodic elements in geochemical and mineralogical data. A method of highlighting these oscillations is by filtering the data. If the observations are considered as two parts, an underlying long-term signal or meaningful pattern of variation and a superimposed noise or random variation, an enhancement of the periodic signal can be most effectively achieved by reducing the variance of the original sequence using a simple moving average function. This dampens the short-term noise and gives a clearer view of the underlying signal. Although smoothing the data produces a shift of peaks and troughs in the smoothed curve, allowance can be made in the overall interpretation of the curves.

Whittaker and Robinson (1929) have proposed a number of smoothing equations suitable for time-trend analysis. Several moving averages were used in this thesis and revealed important repetitions in the geochemical

and mineralogical data. Summary statistics for this type of analysis are seen in Table A1.3.

Examples of the use of this technique in geology can be found in Fox and Brown (1965), Fox (1967), Merriam (1967), Harbough and Merriam (1968) and Davis (1973). The mathematics of time-trend analysis are discussed by Vistelius (1961) and Fox (1964).

6. FOURIER SERIES ANALYSIS

Having unmasked the underlying signal by smoothing the raw data, it was necessary to establish whether this signal or even the raw data had any cyclic or repetitive elements. The dominant periodic component can be calculated using the Fourier series:

$$Y_i = \sum_{n=1}^{\infty} \left(\alpha_n \cos \frac{2n\pi X_i}{\lambda} + \beta_n \sin \frac{2n\pi X_i}{\lambda} \right)$$

i.e. the amplitude Y_i at the point X_i is determined by the sum of the amplitudes of the component sine and cosine waves at a distance X_i from the origin of the series.

In geology, Fourier series has been used on a variety of stratigraphical, sedimentological, geophysical and X-ray diffraction data (Preston and Henderson, 1964; Harbough and Merriam, 1968; Davis, 1973; and Dunn, 1974).

7. EFFECT OF CLOSURE

It must be noted that the geochemical and mineralogical data created in this thesis with the exception of ESR data, form closed data arrays i.e. the variables add up to a constant sum, 100%. The closure of a data array is known to produce induced correlations (Vistelius and Sarmanov, 1961; Krumbein and Graybill, 1965; Chayes and Kruskall, 1966

TABLE A1.3

Variance of the original data array, variance of the smoothed array and approximate percentage of sums of squares accounted for by smoothing.

For original data

$$SS_o = \sum_{i=1}^{n} Y_i^2 - \frac{(\sum_{i=1}^{n} Y_i)^2}{n}$$

$$SS_o^* = \sum_{i=1}^{n} Y_i^2 - \frac{(\sum_{i=1}^{n^*} Y_i)^2}{n}$$

For smoothed data

$$SS_S = \sum_{i=1}^{n^*} \hat{Y}_i^2 - \frac{(\sum_{i=1}^{n^*} \hat{Y}_i)^2}{n^*}$$

For deviation

$$SS_D = \frac{\sum_{i=1}^{n^*} (Y_i - \hat{Y}_i)^2}{n^*}$$

Approximate percentage of sums of squares

$$\frac{SS_S}{SS_O^*} \cdot 100\%$$

Where n is the number of data points in the original sequence and n^* is the number of data points in the smoothed sequence.

and Chayes, 1971). For example, in a three component system, there will always be two negative and one positive correlations whatever the variances.

Methods of assessing the effects of closure have been proposed by Vistelius and Sarmanov (1961) who suggested that all values in a major oxide analysis should be divided by the oxygen content and Chayes and Kruskal (1966) and Chayes (1971) who suggest the use of Niggli Variation diagrams in overcoming closure within ternary arrays. However, these methods have been critically examined by Saha et al., (1974) and found to be only applicable in modal analysis when the number of variables is high, the sample size is large (greater than 30) and there is no negative element in the variance vector of the corresponding open variables (Chayes and Kruskal, 1966). As this was not the case in this thesis, it was considered more appropriate to assess the effects of closure at the interpretation stage rather than in the data analysis.

8. CLASSIFICATION PROCEDURES

The procedures used in sections 9-11 are all multivariate classification techniques designed to place "similar objects into an unknown number of distinct groups, with the objects in each category being more similar to each other than to the objects in all other categories" (Parks, 1966, p. 703). A variety of techniques have been used for classification purposes (Sokal and Sneath, 1963; Ward, 1963; McCammon, 1966, Parks, 1966; Oxnard, 1969; Howarth, 1971, 1973; Davis, 1973 and David et al., 1974) but in this thesis emphasis is placed on principal components analysis, cluster analysis and multiple discriminant analysis.

9. PRINCIPAL COMPONENTS ANALYSIS

This technique, developed by psychologists in the 1930's and

1940's, has become a standard geological procedure in the past decade. The theoretical details of principal components analysis (PCA) are presented in Cooley and Lohnes (1961), Cattell (1965), Harman (1967, Mather (1969) and Davis (1973), with a coverage of modern developments by Mather (1973). Numerous examples of geological applications can be found in Krumbein (1957), Imbrie and Purdy (1962), Imbrie (1963), Krumbein and Imbrie (1963), Imbrie and Newall (1964), Imbrie and Van Andel (1964), Manson and Imbrie (1964), Harbaugh and Demirmen (1964), McCammon (1966, 1969), Miesch et al. (1966), Webb and Briggs (1966), Griffiths (1966), Klovan (1966, 1968), Nichols et al. (1966), Garrett and Nichol (1969), Khaleelee (1969), Davis (1970), Henley (1970), Howarth (1970), Obial (1970), Celenk (1972), Drapeau (1973), Rao et al. (1973), Size (1973), Till and Colley (1973), Saager and Sinclair (1974), Symons and De Meuter (1974) and Waitr and Stenzel (1974).

The purpose of principal components analysis is to evaluate the structure of a variance-covariance or correlation-coefficient matrix (a standardized variance-covariance matrix) of a multivariate data collection. The structure of the data can be thought of either as a series of vectors in multi-dimensional space, representing the variance and covariance of each variable, or in the form of an mxm variance-covariance matrix (m equals the number of variables). The vectors or elements of the matrix can be regarded as defining points lying on an m-dimensional ellipsoid. The eigenvectors of the matrix yield the principal axes of the ellipsoid and the eigenvalues represent the length of these axes. Because a variance-covariance matrix is always symmetrical, these m eigenvectors will be orthogonal. Thus, the method of components analysis essentially involves the rotation of co-ordinate axes to a new frame of reference in the total variable space - an orthogonal transformation wherein each of the m original variables is described in terms of m new principal components.

The total variance of the data set can be defined as the sum of

the individual variances. Similarly, the principal axes also represent the total variance of the data set (Davis, 1973), and each accounts for an amount of the total variance equal to the eigenvalue divided by the trace of the matrix (the diagonal of the variance-covariance matrix). The elements of the eigenvectors called loadings (Table A1.4) are coefficients of the linear equation which the eigenvector defines.

Examining the raw data, it may be imperative that the data set is reduced to a smaller number of variables. This may be required as redundancy is a common feature of geological data. A reduction can be achieved by discarding either original variables (reducing the total variance by the sum of the variances for the discarded variables) or converting our observations to scores (described subsequently) on the principal axes and discarding the insignificant components. As it inevitably happens that at least one of the principal axes will be more efficient (in terms of accounting for total variance) than any of the original variables (i.e. eigenvalue > 1.0) we can assume, therefore, that any component with an eigenvalue > 1.0 is significant - a relationship known as Kaiser's Criterion (Childs, 1970). Another method advocated by Cattell (1966) and known as the Scree test, is the plotting of eigenvalues in descending numerical order and noting any major break in the plot indicative of falling significance. Both methods were used in this thesis to determine which components to discard, the 'break' method being particularly effective where a large number of components with eigenvalues greater than 1.0 were extracted.

When several variables are highly loaded on these significant components, geological interpretation is often difficult. In order to simplify interpretation the component axes may be rotated, retaining their orthogonality, to new axes where component loadings are maximized. In this thesis, rotation is carried out by the 'varimax' method (Harman, 1967), that finds a best fit position for the axes. Oblique or promax rotation

TABLE A1.4 Component loadings matrix showing the relationship between communality and eigenvalue.

		COMPONENTS							
		1	2	3	4	5	...	n	Communality
VARIABLES or SAMPLES	1	X_{11}	X_{12}	X_{13}	X_{14}	X_{15}	...	X_{1n}	$\sum_{j=1}^{n} (X_{1j})^2$
	2	X_{21}	X_{22}	X_{23}	X_{24}	X_{25}	...	X_{2n}	$\sum_{j=1}^{n} (X_{2j})^2$
	3	X_{31}	X_{32}	X_{33}	X_{34}	X_{35}	...	X_{3n}	$\sum_{j=1}^{n} (X_{3j})^2$
	4	X_{41}	X_{42}	X_{43}	X_{44}	X_{45}	...	X_{4n}	$\sum_{j=1}^{n} (X_{4j})^2$
	5	X_{51}	X_{52}	X_{53}	X_{54}	X_{55}	...	X_{5n}	$\sum_{j=1}^{n} (X_{5j})^2$
		.	.	.	.	.	...	.	.
		.	.	.	.	.	...	.	.
	n	X_{n1}	X_{n2}	X_{n3}	X_{n4}	X_{n5}	...	X_{nn}	$\sum_{j=1}^{n} (X_{nj})^2$
Eigenvalue		$\sum_{i=1}^{n} (X_{i1})^2$	$\sum_{i=1}^{n} (X_{i2})^2$	$\sum_{i=1}^{n} (X_{i3})^2$	$\sum_{i=1}^{n} (X_{i4})^2$	$\sum_{i=1}^{n} (X_{i5})^2$	...	$\sum_{i=1}^{n} (X_{in})^2$	$\sum_{j=1}^{n} \sum_{i=1}^{n} (X_{ij})^2$

TOTAL VARIANCE OF DATA

(Imbrie and Purdy, 1962) is also used to aid interpretation of the components. However, the rotated axes are no longer orthogonal but oblique with respect to each other. In practice, rotation resulted in slight accentuation and clarification of the components, but these benefits were offset by problems of interpretation. Similar results were obtained by Khaleelee (1969).

Criteria for assessing the significance of component loadings have been proposed by:

1) Griffiths (1966), who suggested examining the statistical tables for a cut-off value which is significantly above the 5% probability level. Component loadings less than this value are considered to be insignificant. However, with a large number of samples, the cut-off level nears zero and the method becomes meaningless.

2) Child (1970), who estimated that component loadings greater than 0.3 (absolute) are significant, i.e. loadings representing at least 10% of the communality.

3) Henley (1970), who determined the level of significance using the empirical relationship,

$$r_{sig} = \frac{\pm 2.5}{n^{0.5}}$$

for which large numbers of samples or variables give values similar to the usual 95% significance level of the correlation coefficient.

In this thesis, Child's rule of thumb method was used most extensively. The Sphericity test proposed by Bartlett (1950, 1951a, 1951b) and described by Hope (1968) has been extensively applied, but principally in the social sciences.

As mentioned previously, the interpretation of the variance-covariance matrix eigenvalues is aided by converting the observations to scores and discarding the irrelevant axes. Component scores are simply the projections of each original observation onto the principal axes.

Geometrically, calculation of the first of these component scores is equivalent to projection of the observations in m-space onto the best-fitting line given by the first eigenvector. It is customary to standardize the component scores so that their variance becomes one.

Fruchter (1954), Child (1970) and Davis (1973) all drew attention to various limitations of the technique of principal components analysis. Within the context of this thesis the most important are:

1) The number of samples must be large and those belonging to different populations should not be pooled when the correlation matrix is computed, since components may be obscured when pooling takes place.

2) Distributions should not be excessively skewed or multi-modal.

3) Oblique solutions introduce greater subjectivity into a process already arbitrary.

The first two of these limitations were difficult to adhere to in this thesis and thus care must be taken when considering the investigators interpretations.

Summarising, therefore, principal components analysis is a standard statistical technique used in this thesis as an orthogonalizing procedure to obtain independent variables (redundancy is removed).

10. CLUSTER ANALYSIS

Cluster analysis is used primarily as a means of classifying variables and/or samples (R and Q-mode respectively). However, it differs from principal components analysis in that it displays these relationships in the form of a hierarchical dendritic network (dendrogram).

The technique is extensively used in the biological sciences (Sokal and Sneath, 1963 and Cole, 1969) and has been applied to geological problems by Purdy (1963), Howd (1964), Kaesler and McElroy (1966), Parks (1966, 1970), McCammon (1968), Rhodes (1969), Obial (1970), Celenk (1972),

Collyer and Merriam (1973) and Joyce (1973). Theoretical aspects are covered by Krumbein and Graybill (1965), Harbaugh and Merriam (1968), Tryon and Bailey (1970) and Davis (1973).

Cluster analysis is a two-fold process involving:

1) preparation of a similarity matrix representing relationships between every pair of samples or variables. A number of similarity coefficients are available in geology (Cubitt, 1970; Sepkoski, 1974) but considering the variety of data types recorded in this thesis (ppm, percent, peak area, etc.) it was necessary to choose a similarity coefficient independent of measured units - the correlation coefficient. However, where measurement units were consistent, a distance coefficient was employed.

2) searching the similarity matrix for the variables or samples with the largest similarity coefficient. This pair by pair comparison of samples or variables results in a two-dimensional representation of the relationships known as a dendrogram.

The dendrogram consists of a number of clusters which are normally separated through the subjective choice of a similarity level by the investigator. This often produces clusters that are not discrete. However, the choice of similarity level has not proved as severe a limitation to interpreting the dendrogram as the algorithm producing the hierarchical classification. This process involves a reduction of an n-dimensional space to a two-dimensional space, and consequently, induces some distortion in the basic variable/sample relationships which will then be accentuated by the subjective choice of similarity level. Furthermore, in the dendrogram, relationships between individual members of one cluster and another are poorly defined (Boyce, 1968). McCammon and Wenninger (1970) have attempted to solve these problems by depicting both within-cluster similarity and between-cluster similarity in a modified dendrogram. However, the use of discriminant analysis (see next section) proved to be

more suitable in the context of this thesis.

Therefore, cluster analysis still remains a powerful tool for the representation of generalised group relationships and it has a distinct advantage in the ease of interpretation.

In this thesis, Q-mode cluster analysis was used to classify samples into groups by one of two processes. The procedure described previously was used to generate a dendrogram provided there was less than 50 samples (due to limitations on computer store). When the analysis involved more than 50 samples, the following distance procedure was adopted:

1) computation of a Q-mode similarity matrix from the component scores (the scores are automatically calculated studying the variable relationships, see principal components analysis).

2) clustering by an agglomerative, polythetic, unweighted pair group algorithm (Sokal and Sneath, 1963). With only the highest similarity coefficients stored, the procedure iteratively removes a pair of samples with the highest similarity, recalculates all relationships using averages for these samples and places the next highest similarity coefficient in the store.

3) production of a dendrogram.

However, the latter procedure (an adaptation of an algorithm developed by Parks (1966)) is subject to annoying reversals in the dendrograms caused by the pair-group method of clustering.

11. DISCRIMINANT ANALYSIS

Discriminant analysis differs from other classification techniques in that it requires some a priori knowledge of the number of groups and samples within a group. In the context of this thesis, discriminant analysis is used to test the discreteness of sample groups distinguished by

cluster analysis.

It is one of the most widely used statistical techniques in the Earth sciences and also one of the most powerful tools of the numerical analyst. Although developed by Fisher (1936, 1938) for anthropology, discriminant analysis has been discussed extensively in the literature (Kendall, 1957; Cooley and Lohnes, 1962; Krumbein and Graybill, 1965; Davis and Sampson, 1966; Griffiths, 1966; Harbaugh and Merriam, 1968; McCammon, 1969; Mather, 1969; Koch and Link, 1971; and Davis, 1973) and examples of geological applications are numerous (Griffiths, 1957, 1964, 1966; Wood, 1961; Potter et al., 1963; Sahu, 1964; Chayes and Velde, 1965; Jizba, 1966; Sevon, 1966; Cameron, 1969; Connor, 1969; Wignall, 1969; Howarth, 1971, 1971, 1972, 1973, 1973, 1973; Pearce and Cann, 1971; Celenk, 1972; Haynes, 1972; Hawkins and Rasmussen, 1973).

The principles of discriminant analysis are most simply described by considering the following situation. Fig. A1.1 shows two groups A and B which cannot be separated by a linear function in (X-Y) measured space. The purpose of discriminant analysis is to establish a linear function (e.g. J - J') which will separate groups A and B and maximize their differences. By extending this problem to n-dimensional space, a set of discriminant functions is obtained by determining the (n - 1)-dimensional planes that effectively separate the clusters of points representing the groups. The functions are determined by maximizing the ratios of the between-groups (A) to within-groups (W) pooled sums of squares and cross-products matrices, A/W or $W^{-1}A$. In this thesis, groups of multiple observations distinguished by cluster analysis, a process that distorts an n-dimensional relationship into 2 dimensions (the dendrogram), have been examined by discriminant analysis for discreteness. In fact, given two or more groups of samples, it has been possible using discriminant analysis,

1) to decide whether or not to reject the null hypothesis that each group of samples are discrete units,

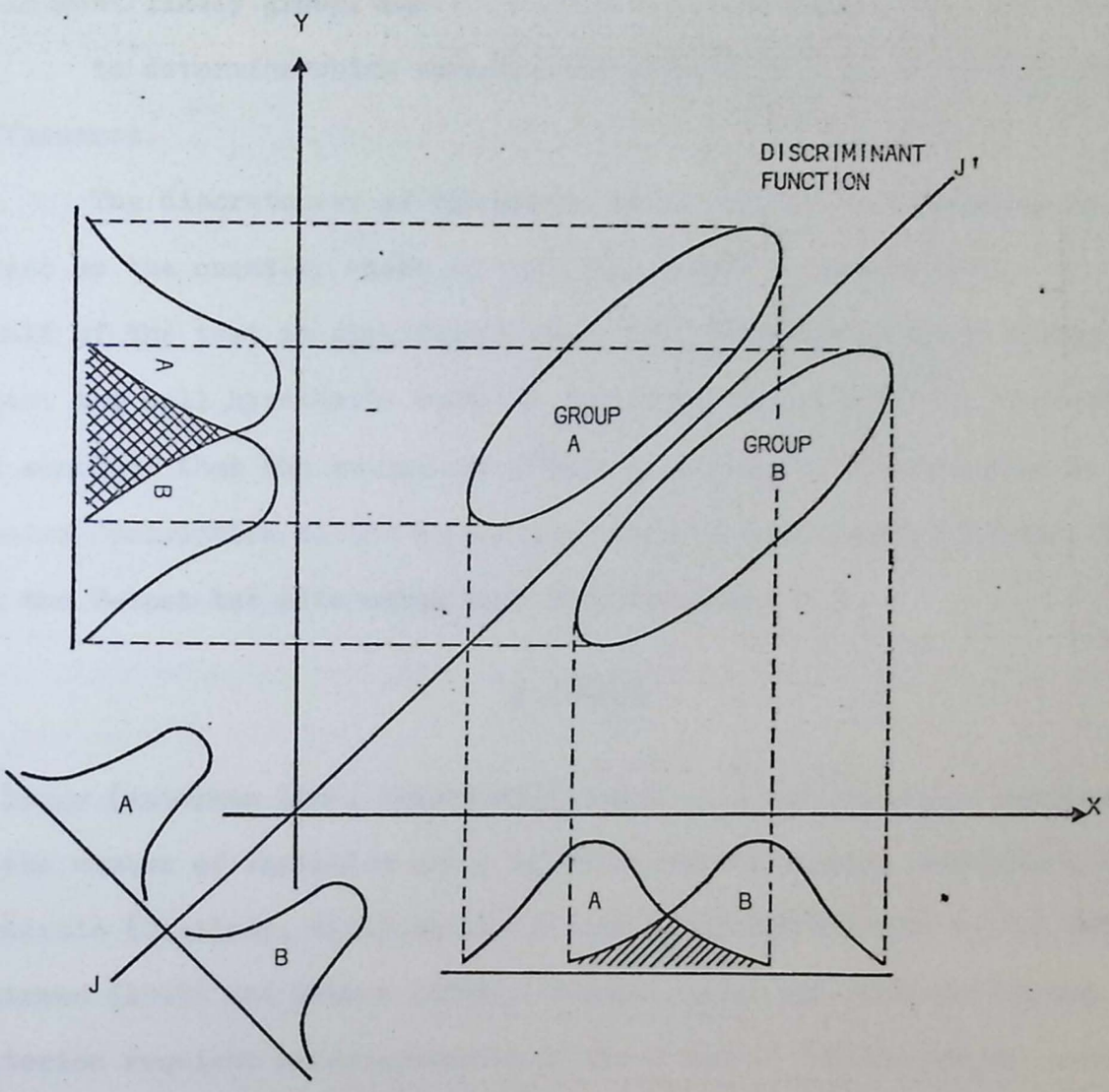

Fig. AI.1 Geometric representation of two groups of samples, A and B, which cannot be separated by a linear function in XY space but can be separated by a linear function J - J' in a redefined space. Their distinctness can be measured by calculating the distance between their bivariate mean. This concept can be extended to multivariate populations.

2) to calculate a set of linear functions which has the valuable property of maximizing between-group differences,

3) to use the set of functions to assign unidentified samples to their most likely group, and

4) to determine which variables contribute most to the inter-group differences.

The discreteness of the groups can be tested by performing an F-test on the quantity known as the Wilks Lambda criterion (Λ). If the result of the test is significant at a given probability level we may reject the null hypothesis that all groups are drawn from one population and conclude that the groups are discrete. Mather (1969) provides a concise description of the calculation of the Wilks Lambda criterion (Λ) and the F-test but also notes that when the ratio

$$N - \frac{m + g}{2}$$

is large (Anderson 1966, Mather 1969) where N is the number of samples, m is the number of variables and g is the number of groups, Bartlett's V-statistic (Bartlett, 1941) should be used as an alternative to the F-test. Demirmen (1969) and Mather (1969), however, point out that use of the criterion requires non-singularity of the W matrix (within-groups sums of squares and cross products matrix) which in turn requires $m \leqslant N - g$. When $m \geqslant N - g$, orthonormalization (Demirmen, 1969) can be used to reduce the number of variables before performing classification analysis. Celenk (1972) also noted that although the Λ criterion estimates the overall discreteness of the groups, it cannot give an accurate assessment of how different one group is from another nor which groups overlap. Extensive use of the Λ criterion in this thesis supports this conclusion. Consideration of Demirmen's alternatives to the basic Λ criterion (Demirmen, 1969) is suggested before further use of this procedure is made.

Discriminant analysis produces as many discriminant functions as

the number of original variables. Furthermore, the discriminant functions are mutually orthogonal and their 'strength' or importance is measured by the numerical values of the $W^{-1}A$ eigenvalues. As only a maximum of p of the original m discriminant axes are required to separate its groups (Mather, 1969), Rao and Slater (1949) and Rao (1952) suggest a method of selecting these p discriminant functions based on the null hypothesis that the discriminating power (a quantity based on the eigenvalues and calculated for each discriminant) of the linear discriminant functions is due to chance. The results are tested against chi-square and the null hypothesis accepted if the results are less than the tested value. Alternatively, Cooley and Lohnes (1962) suggest that discriminant functions accounting for 80-90% of the discriminating power could be selected for later interpretation. In practical terms, one is inclined to use as small a number of discriminants as possible, sacrificing increased power for greater ease in working with a small number of discriminants (2 or 3).

Discriminant analysis also has the ability to classify unknown samples into established groups (Celenk, 1972). The statistic used, the standard discriminant score distance (SDSD) is calculated in the following manner. Initially, a quantity known as a discriminant score (DS_{ij}) is estimated for each of the unknowns,

$$DS_{ij} = \sum_{k=1}^{m} C_{ik}X_k$$

where C_{ik} is the i^{th} eigenvector of the k^{th} discriminant function, X_k is the value of the k^{th} variable on the individual and m is the number of variables. These are simply the projection of data points onto an axis defined by the eigenvector which represents the line connecting the multivariate centres of the groups being discriminated (Davis, 1973). From this value, we can determine the standard discriminant score distance (Celenk, 1972) of the unknown with respect to the nearest established groups. For example, two groups A and B with mean discriminant scores of

MDS_A and MDS_B are selected for the "parenthood" of the unknown sample (u). Then the standardized discriminant scores distance for both groups are calculated from the following equations:

For A,

$$SDSD = | DS_u - MDS_A | / \sigma_A$$

and for B,

$$SDSD = | DS_u - MDS_B | / \sigma_B$$

the smaller score being indicative of the group most likely to be the parent. However, this procedure proved to miscalculate some samples when the following situation arose. Considering two groups, one with a large variance and small number of samples and the other with a large number of samples and small variance, the investigator observed that an unknown individual spaced equally between the two groups, would be classified into the first group. The computational operation emphasises differences in variance rather than physical size of the groups and in this case, the group with the larger variance will attract the unknown. A weighting factor related to the number of samples in each group might ease the problem.

In alternative discriminant analysis algorithms (Wignall, 1969; Howarth, 1971) a priori probabilities are taken into account to minimize miscalculations. Probability density functions for each group in the classification forms the basis of their approach. Fisher's Z function (Hays, 1973; Hayes and Winkler, 1971) although not used in this thesis, was tested as an alternative to discriminant analysis within the limitations of the thesis data set. However, the function requires an initial assumption that all samples are drawn from a bivariate normal population. As this is often very questionable, the test then requires the use of a large number of samples, an obvious disadvantage with this data set. However, for large sample studies it may prove a valuable addition to discriminant analysis.

Basic assumptions about the input data set required by discriminant analysis are defined by Davis (1973):

1) the observations in each group are randomly chosen,

2) the probability of an unknown observation belonging to any group is equal,

3) variables are normally distributed within each group,

4) the variance-covariance matrices of the groups are equal in size,

5) none of the observations used to calculate the function were misclassified and

6) all variables are independent.

Of these, 2-4 are the most difficult to justify. Fortunately, the function is not seriously affected by limited departures from normality.

The basic limitations of the method are:

1) dependent variables should not purposefully be included,

2) overlap of groups may lead to poor evaluation of results and the investigator may be forced to pool excessively overlapping groups, and

3) the Wilks Lambda test of significance has proved to be ineffectual in most situations.

Bearing in mind the assumptions and limitations of the technique, a discriminant algorithm developed by Mather (1969) and Celenk (1972) was extensively employed in this thesis.

12. STATISTICAL COMPUTATION

This section presents a summary of the computer programs developed for the analysis of geochemical and mineralogical data using statistical methods described previously. The majority of programs are adaptations of previously published programs or programs already available within the Geology Department and Computer Laboratory program library of Leicester University. However, a number of programs were developed by the author and

listings are available.

Limited Computer capabilities restricted the use of large array programs (e.g. Q-mode cluster analysis) and brief details of computer facilities at Leicester would be beneficial here. The University has an Elliot 4130 computer (replaced in 1975 by a Cyber 72 computer) with 64 x 1024 24-bit words of 2 second core and 32 x 1024 24-bit words of 6 second core. Input can be in the form of cards, magnetic tapes, paper tapes and from discs. Magnetic tapes, paper tape, discs, lineprinter and plotter are available for output. All programs and data were initially prepared on an IBM 29 card punch using EBCDIC card code and read through a card reader (400 cards/min.) to be filed on disc (transference rates effectively prohibited great use of magnetic tapes). All subsequent work was performed by taking data and programs from storage disc and analysing the data in working space on a system disc. Results were normally generated on lineprinter paper (300 lines/min.) or paper tape (110 characters/sec. 5/8 tracks), although some results were retained on disc for further manipulation. A digital incremental plotter was used to output dendrograms and univariate statistical plots on line. Further details of the computer hardware, software and services can be found in the ICL 4100 Computer System Technical Information booklet and in the Leicester University Computer Laboratory Users Manual.

The computer programs developed for the thesis are briefly described in Table A1.5 and listings of the programs are lodged with Dr. Khan of the Geology Department, University of Leicester.

TABLE A1.5 Computer Programs used in this thesis

NAME	AUTHOR(S)	FUNCTION	LANGUAGE
1. ELEST	J.M. CUBITT	Computes elementary statistics i.e. mean, standard deviation, histograms, etc.	FORTRAN IV
2. CLUSR	PARKS (1966) adapted by O. CELENK & J.M. CUBITT	Computes correlation coefficients of a normalized n x m data matrix, performs a principal components analysis, computes component scores and a Q-mode similarity matrix using distance function. Clustering by an unweighted pair group method, produces a lineprinter dendrogram.	FORTRAN IV
3. DISCRIMF	P.MATHER (1969) adapted by O. CELENK (1972), & J.M. CUBITT	Used to discriminate groups of samples, assigned on an a priori level from the previous program. Classifies unknown samples. Expanded to take over 100 samples.	FORTRAN IV
4. STERO	J.M. CUBITT & O. CELENK	Program to plot stereopairs of X, Y, Z data	FORTRAN IV
5. MSTAT	J.M. CUBITT	Program to calculate Fisher's Z statistic.	FORTRAN IV

TABLE A1.5 (continued)

	NAME	AUTHOR(S)	FUNCTION	LANGUAGE
6.	VARID package	J.M. CUBITT - Subroutines from J.C.DAVIS (1973)	Programs to compute linear regressions, smoothing of data, fourier analysis and equal spacing of data. Produces plots on a line-printer and X-Y plotter.	FORTRAN IV
7.	STATPAK package	Birmingham Educ. Dept.(University) adapted by Leicester Univ. Computer Laboratory	A series of programs to calculate correlation coefficients, principal components analysis, varimax, and promax rotations, factor scores.	FORTRAN IV
8.	COVAR	J.C.DAVIS (1973) adapted by J.M. CUBITT	Computes variance/ covariance matrix of n x m data matrix.	FORTRAN IV
9.	CLUSTR	J.C.DAVIS (1973) adapted by J.M. CUBITT	Computes a Q-mode cluster analysis. Weighted pair group method is used with either correlation or distance coefficients.	FORTRAN IV
10.	ANOVA	J.C. DAVIS	Two way analysis of variance.	FORTRAN IV
11.	FACTO	IBM Scientific subroutines	Factor analysis and varimax rotation.	FORTRAN IV

TABLE A1.5 (continued)

	NAME	AUTHOR(S)	FUNCTION	LANGUAGE
12.		Unknown origin	Plots a dendrogram on X-Y plotter using paper tape output from CLUSR	ALGOL
13.	ITBNTOMT AND ITBNCLST	M.J. SACKIN (Mrc Unit) Leicester University	Calculates similarities coefficients on presence/ absence data using a simple-matching coefficient and performs a cluster analysis using both unweighted average and single linkage methods.	ALGOL

APPENDIX TWO

A BIBLIOGRAPHY OF ELECTRON SPIN RESONANCE APPLICATIONS IN THE EARTH SCIENCES

INTRODUCTION

Electron spin resonance (ESR) is a spectroscopic technique developed by chemists to detect paramagnetism. In the Earth sciences this technique has been applied extensively in the fields of lunar mineralogy and petrology, the mineralogy of terrestrial silicates and carbonates, and in the study of coal and related organic material. Using ESR, it has been possible to study the distribution of radicals in these natural and synthetic materials as the radicals, normally transition metal ions, free radicals and other energy centres, all produce paramagnetism (due to the magnetic moments of unpaired electrons, etc.). Details of the theory behind ESR can be found in two textbooks:

1. Spectroscopy. D.R. Browning. 1969. McGraw-Hill, London.
2. Spectroscopy. D.H. Whiffen. 1968. Longmans, London.

For the Earth Scientist, ESR has many advantages over other spectroscopic techniques including speed of sample preparation, production of graphic results and simplicity of operation. Consequently, ESR has great potential as a standard analytical technique for mineralogists, geochemists and petrologists.

This bibliography was designed to bring to the attention of these Earth Scientists, the extensive literature on the subject and to reveal the range of applications within the Earth Sciences.

The bibliography contains over 500 references published during the past 25 years, in alphbetic order of author. Source material was obtained from Chemical Abstracts, Mineralogical Abstracts and the Science Citation Index, although a number of references were found in leading papers. All references are consistent with Geosystems' established referencing system and all journal titles are abbreviated according to the "International List of Word Title Abbreviations".

A typical reference would thus be:

133:625	3 figure number used for cross-referencing in a subject index.
BROWN, TA and SMITH, JC,	Author(s)
An ESR study of Mn^{2+} in calcite.	Title of paper
J.Chem.Phys. (44/2) 70 p1926-1031.	Journal (Vol.No./Part No.) Year. Inclusive pages

or:

425	Subject index cross-reference number
SMITH, CV,	Author
Electron Spin Resonance of Coals	Title of paper
In: JONES, M.A. /Ed./:	Editor of book
Chemistry of coals. 1969	Title of book and year of publication
p 143-p 146. Pergammon, Oxford, U.K.	Inclusive pages, Publisher.

As this bibliography is to be published by Geosystems in Geocom Bulletin, each reference is preceded by a series of three figure numbers that refer to sections of a subject index. Using Geosystems computer retrieval programs, recompilation of the bibliography either in subject or author index order can then be performed. The subject index consists of the following sections - Paramagnetic centres, Petrology, Colour and defect centres, Organic substances, Mineral groups, Minerals and Miscellaneous.

AUTHOR INDEX

425

ALQUIE, AM, LEGRAND, AP, UEBERSFELD, J, CHAUVIN, R and CHICHE, P,

EPR study of pure vitrinite carbonized at various temperatures.

Carbon (10/4) 72 p401-407.

120:790

ANDERSON, JC and DONOVAN, B,

Internal ferromagnetic resonance in magnetite.

Proc. Phys. Soc. (75/1) 60 p149-151.

400:870

ANDERSON, JH and WEIL, JA,

Paramagnetic resonance of colour centres in germanium-doped quartz.

J. Chem. Phys. (31/2) 59 p427-434.

100:765

ANGEL, BR and HALL, PL,

Electron spin resonance studies of kaolins.

Proc. Int. Clay Conf. /Madrid/ Reprints (1) 72 p71-84.

100:680

ANGEL, BR and SMITH, MJA,

Reduction of electron-spin resonance linewidths in synthetic diamond.

J. Phys. D - Appl. Phys. (11/3) 68 p373-374.

138:680

ANGEL, BR, SMITH, MJA and CHARETTE, JJ,

Correlation between nitrogen impurity content and crystal habit of synthetic diamond.

Nature (218/5148) 68 p1246-1247.

116:153:895

ANTIPIN, AA, KATYSHEV, AN, KURKIN, IN and SHEKUN, LYa,

Paramagnetic resonance and spin-lattice relaxation of Er^{3+} and Tb^{3+} ions in the crystal lattice of $CaWO_4$.

Sov. Phys. Solid-State (10/2) 68 p468-474.

107:625

ANTIPIN, AA, VINOKUROV, VM and ZARIPOV, MM,

EPR of Co^{2+} in calcite. [Translated from:

Fiz. Tverd. Tela (6) 64 p2178].

Sov. Phys. Solid-State (6/7) 68 p1718.

400:880

ARKHANGEL'SKII, GE, MORGENSHTERN, ZL and NUESTUEV, VB,

Colour centres in ruby crystals.

Phys. Status Solidi (22/1) 67 p289-295.

400:880

ARKHANGEL'SKII, GE, MORGENSHTERN, ZL and NUESTUEV, VB,

Effect of light on a coloured ruby.

In: Specktrosk. Krist., Mater. Simp., 2nd. 1967 1970 p273-280.

400:880

ARKHANGEL'SKII, GE, MORGENSHTERN, ZL and NUESTUEV, VB,

Colour centres in ruby crystals.

Izv. Akad. Nauk SSSR. Ser. Fiz. (32/1) 69 p2-5.

112:400:880

ARKHANGEL'SKII, GE, MORGENSHTERN, ZL and NUESTUEV, VB,

Effect of colour centres on the Cr^{3+} spectrum of ruby.

Phys. Status Solidi (36/2) 69 p451-457.

210:

ASHFORD, NA and JARKE, FH,

Electron paramagnetic resonance (EPR) investigation of limestones and their calcines and their correlation with reactivity with acid glasses.

U.S. Nat. Tech. Inf. Serv., PB Rep. No. 211504, 1972, 78pp.

440

ATHERTON, NM, CRANWELL, PA, FLOYD, AJ and HAWORTH, RD,

Humic acid, i. ESR study of humic acids.

Tetrahedron (23/4) 67 p1653-1667.

112:925

ATSARKIN, VA,

Paramagnetic resonance of the Cr^{+++} ion in spinel.

Zh. Eksp. Teor. Fiz. (43) 62 p839-840.

122:810

ATSARKIN, VA and FRANTSEASON, AV,

Fe^{3+} paramagnetic resonance in natrolite.

Fiz. Tverd. Tela (9/11) 69 p3352-3353.

122:125:625

ATSARKIN, VA, LUSHNIKOV, VG and SOVOKINA, LP,

Electron paramagnetic resonance of Gd and Fe trivalent ions in synthetic calcite.

Fiz. Tverd. Tela (7/8) 65 p2367-2369.

425

AUSTEN, DEG, INGRAN, DJE, GIVEN, PH, BINDER, CR and HILL, LW,

Electron spin resonance of pure macerals.

Adv. Chem. Ser. (55) 60 p344-359.

140:515

BAGDASAROV, KhS, BERSHOV, LV, MARTIROSYAN, VC and MEILMAN, ML,

State of molybdenum impurity in yttrium - aluminium garnet.

Phys. Status Solidi B (46/2) 71 p745-751.

118:125:133:715

BAKER, JM, BLEANEY, B and HAYES, W,

Paramagnetic resonance of S - state ions in calcium fluoride.

Proc. R. Soc. Ser. A (247/1249) 58 p141-152.

100:715

BAKER, JM, HAYES, W and JONES, DA,

Paramagnetic resonance of impurities in CaF_2.

Proc. Phys. Soc. (73/6) 59 p942-945.

100:540

BARRY, TI,

Exploring the role of impurities in non-metallic materials by Electron paramagnetic resonance.

J. Mater. Sci. (4/6) 69 p485-498.

100:560

BARRY, TI, McNAMARA, P and MOORE, WJ,

Paramagnetic resonance and optical properties of amethyst.

J. Chem. Phys. (42/7) 65 p2599-2606.

100:560

BARRY, TI and MOORE, WJ,

Amethyst: optical properties and paramagnetic resonance.

Science (144/3616) 64 p289-290.

112:555

BARRY, WR and TROUP, GJ,

EPR of Cr^{3+} in alexandrite.

Phys. Status Solidi (35/2) 69 p861-864.

122:650

BARRY, WR and TROUP, GJ,

EPR of Fe^{3+} ions in chrysoberyl.

Phys. Status Solidi (38/1) 70 p229-234.

154:660

BATES, CA, BENTLEY, JP, JONES, BF and MOORE, WS,

Lattice - ion interactions of Ti^{3+} in corundum. III Analysis of the electron paramagnetic resonance line shape.

J. Phys. C Solid State Phys. (3/3) 70 p570-578.

455

BELLA, F,

Application of ESR to geological dating.

Rend. Soc. Ital. Miner. Petrol. (27/2) 71 p259-261.

132:805

BELOUSOV, AM and GRANKOV, AG,

EPR spectrum of manganese in muscovite.

Izv. Leningr. Elektrotekh. Inst. (No. 110) 72 p18-20.

515:925

BELOV, VF,

Magnetic properties of some ferrite garnets and spinels.

Tr. Mosk. Inst. Neftekhim. Gaz. Prom. (No. 58) 65 p101-104.

154:605

BERSHOV, LV,

EPR of titanium (III) ion in beryls.

Zh. Strukt. Khim. (10/1) 69 p141-142.

148:540

BERSHOV, LV,

EPR spectra and electronic structure of some phosphorous containing radical ions.

Teor. Eksp. Khim. (6/3) 70 p397-402.

114:670

BERSHOV, LV and MARFUNIN, AS,

Electron paramagnetic resonance of Cu^{2+} in danburite. [Translated from: Geokhim. (1965/10) 65 p1259-1260].

Geochem. Int. (2/5) 65 p921-923.

410:540

BERSHOV, LV and MARFUNIN, AS,

Electron spin resonance of electron-hole centres in minerals. [Translated from: Dokl. Akad. Nauk SSSR (173/2) 67 p410-412].

Dokl. Acad. Sci. USSR, Earth Sci. Sect. (173/2) 67 p91-93.

133:595

BERSHOV, LV, MARFUNIN, AS and MINEEVA, RM,

Electron paramagnetic resonance of Mn^{2+} in apophyllite. [Translated from: Dokl. Akad. Nauk SSSR (164/5) 65 p1141-1142].

Dokl. Acad. Sci. USSR, Earth Sci. Sect. (164/5) 65 p132-135.

133:963

BERSHOV, LV, MARFUNIN, AS and MINEEVA, RM,

Electron paramagnetic resonance of Mn^{2+} in tremolite. [Translated from: Geokhim. (1966/4) 66 p464-466].

Geochem. Int. (3/2) 66 p352-355.

135:895

BERSHOV, LV, MARFUNIN, AS and MINEEVA, RM

Electron paramagnetic resonance of tetrahedral complex, $(MnF_4)^{2-}$ in scheelite. [Translated from: Zh. Eksp. Teor. Fiz. (49) 65 p743-746.]

410:670:675

BERSHOV, LV and MARTIROSYAN, VO,

Point defects in the borosilicates, danburite and datolite.

Kristallogr. (14/5) 69 p946-948.

410:580

BERSHOV, LV, MARTIROSYAN, VO, MARFUNIN, AS and SPERANSKII, AV,

Yttrium - stabilized electron-hole centres in anhydrite.

Phys. Status Solidi B (44/2) 71 p505-512.

135:950

BERSHOV, LV and MINEEVA, RM,

Electron paramagnetic resonance of bivalent manganese in talc.

Radiospecktrosk. Tverd. Tela (1967) 67 p308-310.

100:626

BERSHOV, LV, MINEEVA, RM and TARASCHAN, AN,

EPR and luminescence in calcium carbonate crystals containing ions with the configuration d^9.

Teor. Eksp. Khim (6/3) 70 p395-397.

400:625

BERSHOV, LV, SAMOILOVICH, MI, LUSHNIKOV, VG and ANDRUSENKO, NI,

On the nature of pink coloured calcite.

Zap. Vses. Min. Obshch. (97/3) 68 p357-368.

400:585:645:900

BERSHOV, LV, SAMOILOVICH, MI and MARTIROSYAN, VO,

EPR at colour centres in aragonite ($CaCO_3$), cerusite ($PbCO_3$) and siderite ($FeCO_3$).

Zh. Strukt. Khim. (9/5) 68 p905-907.

133:675

BERSHOV, LV, VINOKUROV, VM, ZARIPOV, MM, KROPATOV, VS and STEPANOV, VG,

Paramagnetic resonance of Mn^{2+} ions in natural crystals of datolite.

/Translated from: Geokhim. (1966/1) 66 p122-123/.

Geochem. Intn. (3/1) 66 p76-77.

120:790

BICKFORD Jr, LR,

Ferromagnetic resonance absorption in mangetite.

Phys. Rev. (76/1) 49 p137-138.

120:790

BICKFORD Jr, LR,

Ferromagnetic resonance absorption in magnetite single crystals.

Phys. Rev. (78/4) 50 p449-457.

100:540

BILDUKEVICH, AL, VINOKUROV, VM, ZARIPOV, MM, POLSKII, YuE, STEPANOV, VG and SHEKUN, Lya,

Paramagnetic resonance in some minerals.

In: Paramagnitin. Rezonans. Sub. Kazan, Kazan Univ., USSR. 1960 p7-11.

100:575

BILDUKEVICH, AL, VINOKUROV, VM, ZARIPOV, MM, POLSKII, YuE, STEPANOV, VG, CHIRKIN, GK and SHEKUN, LYa,

Electron paramagnetic resonance in andalusite.

Zh. Eksp. Teor. Fiz. (39/6) 60 p1548-1541.

200:420

BINDER, GR,

Electron ppm resonance. Its application to the study of thermal and natural histories of organic sediments.

Dis. Abstr. B (27/3) 66 p796-797.

100:875

BISHOP, TIP, FARACH, HA and POOLE, CP,

EPR and optical studies of rhodochrosite.

Bull. Am. Phys. Soc. (15/11) 70 p1307.

122:765

BOESMAN, E and SCHOEMAKER, D,

Resonance paramagnetique de l'ion Fe^{3+} dans la kaolinite.

C.R. Hebd. Seances Acad. Sci. (252/13) 61 p1931-1933.

122:890

BOGLE, GS and SYMMONS, HF,

Paramagnetic resonance of Fe^{3+} in sapphires at low temperatures.

Proc. Phys. Soc. (73/3) 59 p531-533.

122:890

BOGLE, GS and SYMMONS, HF,

On the exactness of the spin hamiltonian description of Fe^{3+} in sapphires.

Proc. Phys. Soc. (79/3) 62 p468-473.

425:440

BRATASHEVSKII, YuA, GAIDAROV, OI, GORDIENKO, SA and OVCHARENKO, FD,

Complexing of humic acids extracted from brown coals.

Agroken. Talajtan (20/1-2) 71 p31-35.

400:880

BROSSEL, J and MARGERIE, J,

Fine structure in the green absorption band of pink ruby as observed by magnetic resonance technique.

In: Paramagnetic Resonance, Proc. Int. Conf., 1st., Jerusalem 1962.

(2) 63 p535-549.

100:605

BROWN, LC and WILLIAMS, D,

Magnetic resonance spectra of beryl crystals.

Phys. Rev. (95/4) 58 p1110.

435

BROWN, TH, GUTOWSKY, HS and Van HOLDE, KE,

Electron spin resonance and colloidal properties of crude oil.

J. Chem. Eng. Data (5) 60 p181-182.

112:925

BRUN, E, HAFNER, St, LOEWGER, H and WALDNER, F,

Zur paramagnetischen resonanz von Cr^{3+} in spinell ($MgAl_2O_4$).

Helv. Phys. Acta (33/9) 60 p966-968.

100:610

BULKA, GR, VEDENIN, SV, VINOKUROV, VM, ZAKHARCHENCHO, TA, NIZAMUTDINOV, NM and TUKHVATULLIN, RS,

Electron paramagnetic resonance of ionic impurities and proto magnetic resonance of water in astrakanite.

Kristallogr. (16/1) 71 p138-145.

132:590:905

BURNEY, SP,

The allowed and forbidden transitions in the paramagnetic resonance of manganese ion in trigonal sites in apatite and smithsonite.

Aust. J. Phys. (17/4) 64 p537-542.

122:600

BURNEY, SP and TROUP, GJ,

Paramagnetic resonance of Fe^{3+} in benitoite.

Br. J. Appl. Phys. (16/3) 65 p315-318.

200:420

BYLYNA, EA, RODIONOVA, KF, CHUTKERASHVILI, SO, CHETVERIKOVA, OP and PENTINA, TYu,

Electron paramagnetic resonance in narrow fractions of organic substances from sedimentary rocks.

Tr., Vses Nauchno. Issled. Geologarazved. Neft. Inst. (68) 69 p171-182.

515

CAGAN, V,

Crystal orientation of garnet single crystals by magnetic resonance.

Arch. Sci. (13) 60 p319-324.

122:885

CARTER, DL and OKAYA, A,

Electron paramagnetic resonance of Fe^{3+} in TiO_2 (rutile).

Phys. Rev. (118/6) 60 p1485-1490.

425

CASTLE Jr, JG,

Magnetic resonance properties of raw cokes.

Phys. Rev. (98/5) 55 p1564.

141:885

CHANG, TeTse,

Electron spin resonance of Mo^{5+} in rutile.

Phys. Rev. (136A/5) 64 p1413-1416.

425

CHAUVIN, R, CHICHE, P, QUINTEN, MF and UEBERSFELD, J,

Electron paramagnetic resonance of a coal and its rapid pyrolysis tars.

C.R. Hebd. Seances Acad. Sci., Ser. C, Sci. Chim. (262/22) 67 p1212-1215.

360

CHATELAIN, A, KLINE, D, KOLOPUS, JL and WEEKS, RA,

Electron and nuclear magnetic resonance of 3 chondritic meteorites.

J. Geophys. Res. (75/29) 70 p5681-5692.

350:465:523

CHATELAIN, A, KOLOPUS, JL and WEEKS, RA,

Paramagnetic resonance spectra of simulated lunar rocks and other silicate rocks - a review.

Trans. Am. Geophys. Union (50/4) 69 p215.

360:830

CHATELAIN, A, KOLOPUS, JL and WEEKS, RA,

EPR spectra of olivine and tektites - effects of thermal treatments.

Abstr. pap. Am. Chem. Soc. 1969 pNu05.

360:725

CHATELAIN, A and WEEKS, RA,

EPR study of Mn^{2+} ordering in Mg_2SiO_4.

Bull. Am. Phys. Soc. (15/3) 70 p249.

360:725

CHATELAIN, A and WEEKS, RA,

Electron paramagnetic resonance study of ordered Mn^{2+} in magnesium silicate.

J. Chem. Phys. (52/11) 70 p5682-5687.

400:565:870

CHENTSOVA, LG, TSINOBER, LI and SAMOILOVICH, MI,

Quartz of amethyst colour.

Kristallogr. (11/2) 66 p236-244.

200:420

CHUTKERASHVILI, SE,

Electron paramagnetic resonance of organic substance scattered in sedimentary rocks.

In: Nov. Metody Ann. Yad. Geofiz. Geochem. 1970 p249-300.

132:915

CLERJAUD, B, MARTI, C and VISOCEKAS, R,

Electron paramagnetic resonance of zinc sulphide/manganese: forbidden lines $\Delta_M = 2$; $\Delta_m = 0, \pm 1$.

C.R. Hebd. Seances Acad. Sci., Ser. B, Sci. Phys. (266/15) 68 p1030-1033.

122:132:625

CONSTANTINE, JG,

Paramagnetic resonance absorption spectra of bivalent manganese and trivalent iron in calcite.

U.S. Gov. Res. Dev. Rep. (40/3) 65 p98.

122:870

COOK, AR and MATARRESE, LM,

Zero field EPR of ferric ion in quartz.

J. Chem. Phys. (50/6) 69 p2361-2364.

400:715

COUILLARD, B and ROCH, J,

Electron paramagnetic resonance study of a colour centre, obtained by ultraviolet radiation of a fluorite single crystal.

C.R. Hebd. Seances Acad. Sci., Ser. B, Sci. Phys. (268/7) 69 p568-570.

132:795

DANILOV, AG and MANCOGIAN, A,

Electron spin resonance of Mn^{2+} impurities in monticellite.

Can. J. Phys. (47/8) 69 p839-846.

100:958

DATARS, WR and CALVO, C,

Electron spin resonance of thortveitite.

J. Chem. Phys. (47/9) 67 p3224-3227.

134:870

DAVIES, JJ, SMITH, SRP and WERTZ, JE,

Electron paramagnetic resonance of trivalent manganese ions at tetragonal and octahedral sites in MgO.

Phys. Rev. (178/2) 69 p608-612.

154:870

DAVIES, JJ and WERTZ, JE,

The EPR spectrum of trivalent titanium in orthorhombic symmetry in MgO.

J. Phys. Chem. Solids (31/11) 70 p2489-2494.

460

DAVISON, PS,

Electron spin resonance and related subjects; literature sources of spectra and information.

Spectrosc. Mol. (15/167) 66 p14-15.

425

DE WOLF, E, VAN ITTERBEEK, A and VAN GERVEN, L,

Paramagnetic electron resonance in coal and germanium.

Bull. Inst. Int. Froid. Annexe (1956) 56 p125-132.

133:620

DECLERCK, C and TOUSSAINT, J,

EPR of Mn^{++} in brucite.

Bull. Soc. R. Sci. Liege (35/5-6) 66 p364-368.

122:660

DEIGON, MF, CEIFMAM, JN and GLINCHUK, MD,

Broadening of Fe^{3+} EPR lines in corundum by crystal lattice defects.

Fiz. Tverd. Tela (11/12) 69 p3514-3517.

122:961

DENISON, AB, ENSIGN, TC and SIMS, LJ,

Electron paramagnetic resonance of Fe^{3+} in natural topaz.

Phys. Lett. A (24/8) 67 p405-407.

100:680

DENNING, RM and POINDEXTER, EH,

Crystallographic implications of EPR in neutron-irradiated diamond.

Am. Miner. (49/3-4) 64 p277-285.

465

DEPIREUX, J,

Electron and nuclear magnetic resonances.

In: BACQ, ZM, [illegible],

Pergamon, Oxford, U.K. Fundam. Biochem. Pharmacol. 1971, p13-19.

420:470

DEPIREUX, J, DUCHESNE, J and VAN DER KAA, JM,

Electron paramagnetic resonance in vegetable fossils.

J. Chim. Phys. (56) 59 p810-812.

100:965

DIAZ, J, FARACH, HA and POOLE, CPJ,

An electron spin resonance and optical study of turquoise.

Am. Miner. (56/5-6) 71 p773-781.

100:410:961

DICKINSON, AC and MOORE, WJ,

Paramagnetic resonance of metal ions and defect centres in topaz.

J. Phys. Chem. (71/2) 67 p231-240.

100:705

DMITRIEVA, LV,

Impurity centres in a eucryptite single crystal studied by radicspectroscopic methods.

Yad. Magn. Rezonans (1969/3) 69 p43-48.

100:705:930

DMITRIEVA, LV, ZONN, ZN and SHAKHDINAROV, GM,

NMR and EPR spectra of eucryptite and spodumene.

Fiz. Tverd. Tela (12/1) 70 p42-45.

100:625

DOYLE, LR,

The electron spin resonance (EPR) absorption of two solid-state paramagnetic centres I Frozen tetramethyl ammonium solutions, II Crestmore blue calcite.

U.S. A.E.C., UCRL 9602, 1961, 55 pp.

200:420

DUCHESNE, J,

Nuclear quadrupole resonance in irradiated organic crystals and in a semiconductor: electron spin resonance in carbonaceous rocks.

U.S. Dep. Commer., Off. Tech. Serv., PB Rep. 147, 112 1960, 32 pp.

100:360:420

DUCHESNE, J, CORNIL, P, READ, M and DELTOUR-LITT, C,

Etude comparee des effects de saturation des raies de resonance paramagnetique electronique de la meteorite Mighei et des charbon.

C.R. Hebd. Seances Acad. Sci. (260/10) 65 p2879-2881.

122:360

DUCHESNE, J and DEPIREUX, J,

Ferromagnetism in meteorites.

Nature (182/4640) 58 p931.

350

DUCHESNE, J, DEPIREUX, J, GERARD, A, GRADMJEAU, F and READ, M,

A study by electron paramagnetic resonance and Mössbauer spectroscopy of some lunar samples collected by Apollo 12.

Bull. Acad. R. Belg. Cl. Sci. (56/8) 70 p768.

425:435:470

DUCHESNE, J, DEPIREUX, J and VAN DER KAA, JM,

Electron paramagnetic resonance in plant fossils, coals and crude oils.

In: Proc. 4th Int. Meet. Mol. Spectrosc., Bologna 1959 (3) 62 p1217-1219.

100:360

DUCHESNE, J, DEPIREUX, J and LITT, C,

Concerning the nature of free radicals in the cold Bokkeveld meteorite.

/Translated from: C.R. Hebd. Seances Acad. Sci. (259/11) 65 p1891-1893/.

Geochem. Int. (2/5) 65 p1022-1024.

109:625

DUGAS, J and BACQUET, G,

Paramagnetic resonance of the carbonate ion in X-irradiated natural calcite.

Proc. Colloq. AMPERE /1966/ (14) 67 p775-776.

100:740

DUPREE, R, FORWOOD, CJ and SMITH, MJA,

Conduction electron spin resonance in small particles of gold.

Phys. Status Solidi (24/2) 67 p525-530.

120:605

DVIR, M and LOW, W,

Paramagnetic resonance and optical spectrum of iron in beryl.

Phys. Rev. (119/5) 60 p1587-1591.

105:625

EACHUS, RS and SYMONS, MCR,

Oxide and oxyanions of the non-metals. IX Electron spin resonance study of the $ClCO_3^{2-}$ radical anion.

J. Chem. Soc. A (1968/10) 68 p2433-2437.

103:626

EACHUS, RS and SYMONS, MCR,

Oxides and oxyanions of the non-metals. X The BO_3^{2-} impurity centre in irradiated calcium carbonate.

J. Chem. Soc. A (1968/10) 68 p2438-2441.

100:905

EGOTSEVA, LI, PRODAN, EA and PAVLYUCHENKO, MM,

Thermal decomposition of smithsonite studied by spectroscopic methods.

Zh. Prikl. Spektrosk. (16/2) 72 p373-375.

425

ETIENNE, A and UEBERSFELD, J,

Paramagnetic resonance of coals.

J. Chim. Phys. (51) 54 p328.

400:890

FERGUSON, J and FIELDING, PE,

Origins of colour in natural sapphires.

Aust. J. Chem. (7/25) 72 p1371-1385.

100:885

FREDERIKSE, HPR,

Recent studies on rutile (TiO_2).

J. Appl. Phys. (32/10 suppl) 61 p2211-2215.

114:840

FRIEBEL, C and REINEN, D,

ESR studies on the Jahn-Teller effect of cupric ions in oxidic perovskites.

Z. Naturforsch. A (24/10) 69 p1518-1525.

100:505

FRIEDLANDER, HZ, SALDICK, J and FRINK, CR,

Electron spin resonance spectra in various clay minerals.

Nature (199/4888) 63 p61-62.

112:635

FROM, WH,

Electron paramagnetic resonance of Cr^{3+} in SnO_2.

Phys. Rev. (131/3) 63 p961-963.

122:865

FUJINURA, T and TORIZUKA, Y,

Ferromagnetic resonance absorption in a pyrrhotite single crystal.

J. Phys. Soc. Japan. (11) 56 p327.

100:540

FUJIWARA, S,

Developments in analytical chemistry.

Kagaku no. Ryoiki (15/7) 61 p487-493.

132:625

FUJIWARA, S,

Investigation of trace impurities in solids by electron paramagnetic resonance. Distribution of manganese in calcium carbonate.

Anal. Chem. (36/12) 64 p2259-2261.

100:465:540

FUJIWARA, S, and SAGITANI, Y,

Application of radio-frequency spectroscopy to mineralogy.

Kobut Sugaku Zasshi (8/2) 66 p69-83.

122:570

GAINON, D and LACROIX, R,

Electron paramagnetic resonance of Fe^{3+} ion in anatase.

Proc. Phys. Soc. (79/3) 62 p658-659.

122:510

GAITE, JM and MICHOULIER, J,

Application de la resonance paramagnetique electronique de l'ion Fe^{3+} a l'etude de la structure des feldspaths.

Bull. Soc. Fr. Miner. Cristallogr. (93/3) 70 p341-356.

425

GALKIN, AA and KICHIGAN, DA,

The paramagnetic resonance in coals of the Donetz Basin.

Khim. Tekhnol. Topl. Masel (3/7) 58 p8-14.

132:590

GARBER, PR, NIKITINA, ET, SOTNIKOV, VI and SHCHERBAKOVA, MYa,

Character of luminescence and paramagnetic properties of manganese ions in accessory apatite.

In: KLYAROVSKII, VM, Issled. Strukt, Osob. Miner. Sovrem. Fiz. - Khim. Metod. "Nauka", Sib. Otd., Novosibirsk, SSSR. 1970 p95-103.

122:660

GARIFULLINA, RL, ZARIPOV, MM and STEPANOV, VG,

Study of an exchange coupled pair of Fe^{3+} ions in corundum by electron paramagnetic resonance. [Translated from:

Fiz. Tverd. Tela (12/1) 70 p55-58].

Sov. Phys. Solid State (12/1) 70 p43-45.

425

GARIF'YANOV, NS and AKSEL'ROD, MM,

Magnetic resonance in some coals.

Khim. Tekhnol. Topl. Masel (4/3) 59 p64-68.

420:425

GARIF'YANOV, NS and KOSYREV, BM,

Paramagnetic resonance of anthracite and other carbonaceous substances.

/Translated from: Zh. Eksp. Teor. Fiz. (30) 56 p272-276/.

Sov. Phys. JETP (3/2) 56 p255-258.

100:425

GARIF'YANOV, NS and KOZYREV, BM,

/Formation of/ free radicals during baking of Angren coal.

Khim. Tekhnol. Topl. Masel (1957/2) 57 p29-32.

350:510

GARLICK, GFJ, LAMB, W, STEIGMANN, GA and GEAKE, JE,

Thermoluminescence of lunar samples and terrestrial plagioclases.

In: Proc. 2nd Lunar Sci. Conf., Geochim. Cosmochim. Acta Suppl. 2, (3) 71 p2227-2283.

350

GEAKE, JE, DOLLFUS, A, GARLICK, GFJ, LAMB, W, WALKER, G, STEIGMANN, GA and TITULAER, C,

Luminescence, electron paramagnetic resonance and optical properties of lunar material.

Science (167/3918) 70 p717-719.

350

GEAKE, JE, DOLLFUS, A, GARLICK, GFJ, LAMB, W, WALKER, G, STEIGMANN, GA and TITULAER, C,

Luminescence, electron paramagnetic resonance and optical properties of lunar material from Apollo II.

In: Proc. of the Apollo II Lunar Sci. Conf., Geochim. Cosmochim. Acta Suppl. 1, (3) 70 p2127-2147.

160:885

GERRITSEN, HJ and LEWIS, HR,

Paramagnetic resonance of V^{4+} in TiO_2.

Phys. Rev. (119/3) 60 p1010-1012.

146:147:885

GERRITSEN, HJ and SABISKY, ES,

Paramagnetic resonance of Ni^{2+} and Ni^{3+} in TiO_2.

Phys. Rev. (125/6) 62 p1853-1859.

134:885

GERRITSEN, HJ and SABISKY, ES,

Paramagnetic resonance of trivalent manganese in rutile (TiO_2).

Phys. Rev. (132/4) 63 p1507-1512.

112:880

GEUSIC, JE,

Paramagnetic fine structure spectrum of Cr^{+++} in a single ruby crystal.

Phys. Rev. (102/5) 56 p1252-1253.

112:695

GEUSIC, JE, PETER, M and SCHULZ-FU-BOIS, EO,

Paramagnetic resonance spectrum of Cr^{3+} in emerald.

Bell. Syst. Tech. J. (38/1) 59 p291-296.

465:523

GHOSE, S,

Application of electron paramagnetic resonance in silicate minerals.

In: Resonance Spectroscopy in minerals, AGI short course lecture notes, Am. Geol. Inst. Washington D.C. 1969, pp. G1-G15.

133:685

GHOSE, S and SCHINDLER, P,

Determination of the distribution of trace amounts of Mn^{2+} in diopsides by electronpparamagnetic resonance.

In: Pyroxenes & Amphiboles: Crystal chemistry and phase petrology. Miner. Soc. Am., Spec. Pap. No. 2, 1969, p51-58.

133:685

GHOSE, S, SCHINDLER, P and HAFNER, S,

Mn^{2+} distribution in diopsides by electron spin resonance.

Trans. Am. Geophys. Union (49/1) 68 p340.

122:133:158:990

GHOSE, S and TSANG, T,

Ordering of V^{2+}, Mn^{2+} and Fe^{3+} ions in zoisite, $Ca_2Al_3Si_3O_{12}(OH)$.

Science (171/3969) 71 p374-376.

133:465:626

GHOSH, PK, SAMADDAR, M, SINHA, SC, TIWARI, TS and BANERJI, AC,

Geological applications of ESR spectrometry: Mn^{2+} ions in calcium carbonate minerals.

Technology (7/4) 70 p276-280.

133:590

GILINSKAYA, LG and SHCHERBAKOVA, MYa,

Mn^{2+} electron paramagnetic resonance in natural apatite, $Ca_5(PO_4)_3F$.

Zh. Strukt. Khim. (11/6) 70 p1017-1022.

133:590

GILINSKYA, LG and SHCHERBAKOVA, MYa,

Electron spin resonance of Mn^{2+} in hydroxyl - containing apatites.

/Translated from: Dokl. Akad. Nauk SSSR (195/3) 70 p686-688/.

Dokl. Acad. Sci. USSR, Earth Sci. Sect. (195/3) 70 p125-127.

133:590

GILINSKAYA, LG and SHCHERBAKOVA, MYa,

Peculiarities in Mn^{2+} entering an apatite structure as revealed by EPR studies.

In: Magnetic Resonance and Relat. Phenomena. Proc. Congr. AMPERE, /1970/ (16) 71 p755-758.

133:860

GILINSKAYA, LG, SHCHERBAKOVA, MYa and BAKAKIN, VV,

Temperature induced changes in the electron paramagnetic spectrum of Mn^{2+} in pyromorphite, $PB_5(PO4)_3Cl$. /Translated from:

Fiz. Tverd. Tela (11/8) 69 p2263-2267./

Sov. Phys. Solid State (11/8) 70 p1827-1831.

100:590

GILINSKAYA, LG, SHCHERBAKOVA, MYa and ZAMNIN, YN,

Carbon in the structure of apatite according to electron paramagnetic resonance data.

Sov. Phys. Crystallogr. (15/6) 70 p1016. Translated from:

Kristallogr. (15/6) 70 p1164-1167.

133:963

GOLDING, RM, NEWMAN, RH, RAE, AD and TENNANT, WC,

Single crystal ESR study of Mn^{2+} in natural tremolite.

J. Chem. Phys. (57/5) 72 p1912-1918.

100:755

GOLUBOVA, GA, GRIGOREVA, TN, NAKALAEVA, IV and SHCHERBAKOVA, MYa,

Use of Infra-red spectroscopy, X-ray diffraction analysis, and EPR to study hisingerite.

In: Primen. Mol. Spektrosk. Khim., Sb. Dokl. Sib. Soveshch., 3rd, Krasnoyarsk, USSR, 1964, p263-266.

760

GOODENOUGH, JB and STICKLER, JJ,

Theory of the magnetic properties of the ilmenites.

Phys. Rev. (164/2) 67 p768-778.

127:605

GRECHUSHNIKOV, EN, KORYAGIN, VF, NOVOZHILOV, AI and SAMOILOVICH, MI,

Electron paramagnetic resonance of atomic hydrogen in beryl.

Radiospecktrosk. Tverd, Tela (1967) 67 p316-317.

100:680:870

GRIFFITH, JHE, OWEN, J and WERTZ, IM,

Magnetic resonance in irradiated diamond and quartz.

In: Defects in crystalline solids. Rept. Bristol Conf., London Phys. Soc. 1954.

120:350

GRISCOM, DL and MARQUARDT, CL,

Electron spin resonance studies of iron phases in lunar glasses and simulated lunar glasses (abstract).

In: WATKINS, C, /Ed/. LUNAR SCIENCE III. Lunar Sci. Inst. Contrib. No. 88 1972, p341-343.

350

GRISCOM, DL and MARQUARDT, CL,

Evidence of lunar oxidation processes: Electron spin resonance spectra of lunar materials and simulated lunar materials.

In: Proc. 3rd Lunar Sci. Conf., Geochim. Cosmochim. Acta Suppl. 3 (3) 72 p2397-2415.

160:665

GRUNIN, VS,

EPR of V^{4+} in cristobalite.

Fiz. Tverd. Tela (12/8) 70 p2234-2238.

122:665:870

GRUNIN, VS and PAVLOVA, GA,

EPR of Fe^{3+} in cristobalite and quartz glass.

Fiz. Tverd. Tela (13/3) 71 p772-775.

340:435

GUBERGRITS, MYa, BRODSKAYA, EKh, KUIV, KA and PAALME, L,

Changes in the chemical structure of Kugersite oil shale during thermal decomposition.

Goryuch. Slants. (1961/4) 61 p75-89.

340:435

GUBERGRITS, MYa, POLOK, LS, BRODSKAYA, EKh, KUIV, KA and EMIN, YuB,

The electron paramagnetic spectra of Baltic oil shale.

Dokl. Akad. Nauk SSSR (136) 61 p824-827.

100:435

GUTOWSKY, HS, ROGER RAY, B, RUTLEDGE, RL and UNTERBERGER, RR,

Carbonaceous free radicals in crude petroleum..

J. Chem. Phys. (28/4) 58 p744-745.

127:715

HALL, JL and SCHUMACHER, RT,

Electron spin resonance of hydrogen atoms in CaF_2.

Phys. Rev. (127/6) 62 p1892-1912.

245

HALL, PL, ANGEL, BR and BRAVEN, J,

Electron spin resonance and related studies of lignite and ball clay.

J. Chem. Geol. (in press).

132

HALL, TPP, HAYES, W and WILLIAMS, FFB,

Paramagnetic resonance of manganese.

Proc. Phys. Soc. 78/2) 61 p883-894.

350

HAMEKAN, D and MILLER, DJ,

Clean lunar rock surfaces: unpaired electron density and absorptive capacity for oxygen.

In: Proc. 2nd Lunar Sci. Conf., Geochim. Cosmochim. Acta Suppl. 2 (3) 1971 p2529-2541.

156:570

HAUSER, C and CONRAD, P,

Evidence for EPR of a complex $(TiO)^{3+}$ in the crystal of TiO_2, anatase.

Chem. Phys. Lett. (5/4) 70 p226-228.

100:885

HASIGUTI, RR, IGUCHI, E and TAKAHASHI, S,

Electron paramagnetic resonance in slightly reduced rutile.

In: Proc. 9th Int. Conf. Phys. Semicond. (2) 68 p1142-1146.

122:655

HEDGECOCK, NE and CHAKRAVARTTY, SC,

Electron spin resonance of Fe^{3+} in cordierite.

Can. J. Phys. (44/11) 66 p2749-2755.

475

HEISE, JJ,

Application of electron spin resonance spectroscopy to oceanographic samples.

Mar. Sci. Instrum. (1968/4) 68 p25-35.

100:895

HEMPSTEAD, CF and BOWERS, KD,

Paramagnetic resonance of impurities in $CaWO_4$. 1. Two S-state ions.

Phys. Rev. (118/1) 60 p131-134.

120:790

HIRONE, T, WATANABE, H, MIZUNO, J and TSUYA, N,

Ferromagnetic resonance absorption in magnetite single crystals at 9400 and 4560 megacycles.

Sci. Repts. Res. Insts. Tohoku Univ., Ser. A. (2) 50 p774-779.

122:510

HOCHLI, U,

Electron spin resonance of Fe^{3+} in feldspar.

Proc. Colloq. AMPERE /1963/ (12) 64 p191-197.

133:625

HODGES, JA, MARSHALL, SA, McMILLAN, JA and SERWAY, RA,

Superhyperfine interaction due to ^{13}C in the ESR absorption spectrum of Mn^{2+} in single crystal calcite.

J. Chem. Phys. (49/6) 68 p2857-2858.

122:575

HOLUJ, F,

Paramagnetic resonance absorption spectrum of trivalent iron in a single crystal of andalusite.

Can. J. Phys. (43/4) 65 p762-767.

132:930

HOLUJ, F,

EPR of manganese ions in spodumene. I. Natural crystals.

Can. J. Phys. (46/14) 68 p287-302.

148:850

HOLUJ, F,

Phosphorous centres in phenacite.

J. Chem. Phys. (54/3) 71 p1430-1431.

133:930

HOLUJ, F and MANOOGIAN, A,

EPR of Mn^{2+} in spodumene. 2. Heated crystals.

Can. J. Phys. (46/4) 68 p303-306.

122:961

HOLUJ, F and QUICK, SM,

ESR spectrum of Fe^{3+} [trivalent iron ion] in topaz. II. Hyperfine structure.

Can. J. Phys. (46/9) 68 p1087-1099.

100:540

HOLUJ, F and QUICK, SM,

Hyperfine structure in the effective spin formation of ^6S state ions in crystals.

Phys. Lett. A (25/8) 68 p591-592.

122:575

HOLUJ, F, THYER, JR and HEDGECOCK, NE,

ESR spectra of Fe^{3+} in single crystals of andalusite.

Can. J. Phys. (44/3) 66 p509-523.

122:570

HORN, JM,

EPR of substitutional and charge compensated Fe^{3+} in anatase TiO_2 and its temperature dependence.

Diss. Abst. Int. B (32/10) 72 p5997.

122:570

HORN, M and SCHMERDTFEGER, CF,

Reinterpretation and temperature dependence of EPR in TiO_2: Fe^{3+} anatase.

Solid State Commun. (8/21) 70 p1741-1743.

122:570

HORN, M and SCHMERDTFEGER, CF,

EPR of substitutional and charge compensated Fe^{3+} in anatase (TiO_2).

J. Phys. Chem. Solids (32/11) 71 p2529-2538.

132:935

HOWLING, DH,

Crystal field axes of manganese sites in single crystal willemite.

J. Magn. Resonance (1/3) 69 p339-355.

110:625

HUGHES, RC and SOOS, ZG,

EPR of CO_2 - defects in calcite: motional and non-secular contributions.

J. Chem. Phys. (52/12) 70 p6302-6310.

133:626

HURD, FK, SACHS, M and HERSHBERGER, WD,

Paramagnetic resonance absorption of Mn^{++} single crystals of $CaCO_3$.

Phys. Rev. (93/3) 54 p373-380.

122:560:870

HUTTON, DR,

Paramagnetic resonance of Fe^{3+} in amethyst and citrine quartz.

Phys. Lett. (12/4) 64 p310-311.

122:550

HUTTON, DR, LE MARSHALL, J and TROUP, GJ,

Paramagnetic resonance of Fe^{3+} in adamite.

Phys. Status Solidi A (14/2) 72 pK147-K158.

112:770

HUTTON, DR and TROUP, GJ,

Paramagnetic resonance of Cr^{3+} in kyanite.

Br. J. Appl. Phys. (15/3) 64 p275-280.

125:985

HUTTON, DR and TROUP, GJ,

Paramagnetic resonance of Gd^{3+} in zircon.

Br. J. Appl. Phys. (15/4) 64 p405-407.

100:560:870

HUTTON, DR and TROUP, GJ,

Paramagnetic resonance centres in amethyst and citrine quartz.

Nature (211/5049) 66 p621.

100:990

HUTTON, DR, TROUP, GJ and STEWART, GA,

Paramagnetic ions in zoisite.

Science (174/4015) 71 p1259.

435

IL'YASOV, AV, GARIF'YANOV, NS and RYZHMANOV, YM,

The electron paramagnetic resonance of some crude oils and their heavy residues.

Khim. Tekhnol. Topl. Masel (6/1) 61 p28-31.

420

INGRAM, DJE, TAPLEY, JG, JACKSON, R, BOND, RL and MURNAGHAM, AR,

Paramagnetic resonance in carbonaceous solids.

Nature (174/4434) 54 p797-798.

425

INOUYE, K,

An X-ray diffraction line observed in acid-treated carbonized coals and paramagnetic absorption.

Bull. Chem. Soc. Japan (29/5) 56 p644-645.

410:870

IOFFE, VA and YANCHEVSKAYA, IS,

Structural defects in quartz.

Izv. Akad. Nauk. SSSR, Neorg. Mater. (1/12) 65 p2093-2099.

100:680

IOFFE, VA and YANCHEVSKAYA, IS,

Thermoluminescence and electron paramagnetic resonance of irradiated diamond.

Opt. Spektrosk. (23/3) 67 p494-496.

122:845

JA, YH,

Anisotropic broadening of the line width of the electron paramagnetic resonance spectrum of Fe^{3+} in petalite $LiAlSi_4O_{10}$.

Aust. J. Phys. (23/3) 70 p445-448.

100:962

JA, YH,

$g = 4.3$ isotropic EPR line in tourmaline.

J. Chem. Phys. (57/7) 72 p3020-3023.

100:895

KAPITONOV, MD, SHCHERBAKOVA, MYa and SOLUTSER, VP,

Electron paramagnetic resonance of scheelite from the Balkansk deposit, Southern Urals.

Geokhim. (1972/2) 72 p205-211.

100:870

KATS, A,

Absorption spectra of silica glass and quartz crystals containing contaminations by germanium.

Verres Refract. (12) 58 p191-205.

100:885

KAZANSKII, VB, NIKITINA, OV, PARIISKII, GB and KISELEV, VF,

Electron paramagnetic resonance /EPR/ study of the radical form of absorption of molecular oxygen in reduced titanium oxide.

Dokl. Akad. Nauk SSSR (151/2) 63 p369-372.

132:915

KELLER, SP, GELLES, IL and SMITH, WV,

Paramagnetic resonance absorption in Mn-activated hexagonal ZnS.

Phys. Rev. (110/4) 58 p850-855.

100:625

KEMP, JC,

Electron spin resonance in neutron-irradiated calcite.

J. Chem. Phys. (35/4) 60 p1269-1270.

100:625

KEMP, JC,

Further notes on the magnetic centres in neutron-irradiated calcite.

J. Chem. Phys. (35/1) 61 p377-378.

120:805:855

KEMP, RC,

Orthorhombic iron centres in muscovite and phlogopite.

J. Phys. C Solid State Phys. (4/1) 71 pL11-L13.

122:855

KEMP, RC,

Electron spin resonance of Fe^{3+} in phlogopite.

J. Phys. C Solid State Phys. (5/24) 72 p3566-3572.

154:570

KIBLER, MR and KODRATOFF, Y,

Paramagnetic study of the EPR spectra of titanium (III) in anatase.

J. Chim. Phys. (69/6) 72 p905-908.

425

KICHIGAIN, DA, KOBACHEV, VP and CHERKINA, EA,

Saturation of electronic paramagnetic resonance in natural coals.

Ukr. Fiz. Zh. (9/12) 64 p1323-1330.

133:610

KIGGINS, B and MANOOGIAN, A,

Electron spin resonance of Mn^{2+} impurities in blodite.

Can. J. Phys. (49/2A) 71 p3174-3179.

133:625

KIKUCHI, C,

Doublet structure in paramagnetic absorption spectra of Mn^{++} in calcite.

Phys. Rev. (100/4) 55 p1245.

133:625

KIKUCHI, C and MATARRESE, LM,

Paramagnetic resonance absorption of ions with spin $5/2$: Mn^{++} in calcite.

J. Chem. Phys. (33/2) 60 p601-606.

100:880

KIRKBY, CJ and THORP, JS,

Analyses of the EPR spectrum of ruby using variance techniques.

J. Appl. Phys. (38/4) 67 p1985-1986.

100:680

KLINGSPORN, PE, BELL, MD and LEIVO, WJ,

Analyses of an electron spin resonance spectrum in natural diamonds.

J. Appl. Phys. (41/7) 70 p2977-2980.

100:680

KLYUEV, YuA, NEPSHA, VI, DUDENKOV, YuA, ZVONKOV, SD and ZUBKOV, VM,

Absorption spectra of various types of diamonds.

Dokl. Akad. Nauk SSSR (203/5) 72 p1054-1057.

120:925

KOJIMA, Y,

The g-factor of ferromagnetic spinels.

Sci. Repts. Res. Insts Tohoku Univ., Ser. A (6) 54 p614-622.

150:955

KOLOPUS, JL, FINCH, CB and ABRAHAM, MM,

ESR of Pb^{3+} centres in ThO_2.

Phys. Rev. B (2/6) 70 p2040-2045.

122:840

KOLOPUS, JL and HOLROYD, LV,

Higher order transitions in EPE spectrums of Fe^{3+} in MgO.

Phys. Status Solidi (8/3) 65 p711-717.

125:159

KOLOPUS, JL, HOLROYD, LV and MANN, KE,

EPR spectra of Cd^{3+} and V^{3+} in SrO.

Phys. Status Solidi (9/2) 65 pK95-K101.

350

KOLOPUS, JL, KLINE, D, CHATELAIN, DA and WEEKS, RA,

Magnetic resonance properties of lunar samples: mostly Apollo 12.

In: Proc. 2nd Lunar Sci. Conf., Geochim. Cosmochim. Acta Suppl. 2 (3)

71 p2501-2514.

122:840

KOLOPUS, JL, LEWIS, JT and UNRUH, WP,

EBR studies of Fe^{3+} in $KMgF_3$.

Bull. Am. Phys. Soc. (15/3) 70 p248.

350

KOLOPUS, JL and WEEKS, RA,

Magnetic resonance studies of lunar material.

J. Met. (21/3) 69 pA77.

425:430:440

KOMISSAROV, ID and LOGINOV, LF,

Electron paramagnetism of humic acids extracted from peat and oxidized coals.

In: KOVALEV, RV [Ed]: Dokl. Sib. Pochvored "Nauka" Sib. Otd.,

Novosibirsk, USSR. 1968 p149-158.

100:870

KONOV, IL and NOVOZHILOV, AI,

Electron paramagnetic resonance in irradiated natural quartz single crystals

(arcumpolar Urals). [Translated from: Geokhim. (1968/11) 1968 p1409-1411].

Geochem. Intn. (5/6) 68 p1152-1155.

154:660

KORNILENKO, LS and PROKHOROV, AM,

Electron paramagnetic resonance (EPR) of the Ti^{3+} ion in corundum.

Zh. Eksp. Teor. Fiz. (38) 60 p1651-1652.

118:540

LACROIX, R and RYTER, C,

Paramagnetic resonance of bivalent europium. Second order effect on hyperfine structure.

Arch. Sci. (10) 57 p132-135.

100:425

LADNER, WR and WHEATLEY, R,

Electron spin resonance measurements on the free radicals in coals and chars.

Br. Coal Util. Res. Assoc., Mon. Bull. (297) 65 p201-231.

133:590:625:925

LAZUKIN, VN and TERENT'EVSKII, AN,

Forbidden electron paramagnetic resonance spectrum of Mn^{2+} in the lattices of calcite, spinel and apatite.

Vest. Mosk. Univ., Fiz. Astron. (22/6) 71 p105-108.

100:540

LAZUKIN, VN, TERENT'EVSKII, AN and OZHEREL'EV, BV,

Origin of forbidden spectra in electron paramagnetic resonance.

Zh. Eksp. Teor. Fiz. (55/5) 68 p1612-1618.

120:400:560

LEHMANN, G,

Iron colour centres as the cause of amethyst colour.

Z. Naturforsch. A (22/12) 67 p2080-2085.

120:400:870

LEHMANN, G,

Structure of yellow iron centres in quartz.

Phys. Status Solidi B (40/1) 71 pK65-K67.

120:870

LEHMANN, G and MOORE, WJ,

Optical and paramagnetic properties of iron centres in quarts.

J. Chem. Phys. (445) 66 p1741-1745.

400:560:870

LEHMANN, G and MOORE, WJ,

Colour centres in amethyst quartz.

Sci. (152/3725) 66 p1061-1062.

152:840

LEWIS, JT, ABRAHAM, MM, KOLOPUS, JL and FINCH, CB,

EPR of rare-earth impurity ions in $KMgF_3$.

Bull. Am. Phys. Soc. (163) 71 p360.

410:840

LEWIS, JT, KOLOPUS, JL and SONDER, E,

A study of trapped hole centres in $KMgF_3$.

Bull. Am. Phys. Soc. (155) 70 p425.

425

LOSEV, BI and BYLYNA, EA,

Paramagnetic resonance in coal.

Dokl. Akad. Nauk SSSR (125) 59 p814-816.

425:470

LOSEV, BI and BYLYNA, EA,

Paramagnetic resonance of fossil coals.

Zh. Prikl. Khim. (32) 59 p2359-2361.

112:835

LOW, W,

Paramagnetic resonance and optical absorption spectra of Cr^{3+} in H_2O.

Phys. Rev. (105/3) 57 p801-805.

132:715:835

LOW, W,

Paramagnetic resonance spectrum of manganese in cubic MgO and CaF_2.

Phys. Rev. (105/3) 57 p793-800.

125:715

LOW, W,

Paramagnetic resonance spectrum of trivalent gadolinium in the cubic field of calcium fluoride.

Phys. Rev. (109/2) 58 p265-271.

100:465:540

LOW, W,

Electron spin resonance - a tool in mineralogy and geology.

Adv. Electron. Electron. Phys. (24) 68 p51-108.

100:465:515:840:885:925

LOW, W and OFFENBACHER, EL,

Electron spin resonance of magnetic ions in complex oxides. Review of ESR results in rutile, perovskites, spinels and garnet structures.

Solid State Phys. (17) 65 p135-216.

132:660

LOW, W and SUSS, JT,

Paramagnetic resonance spectra of manganese in corundum.

Phys. Rev. (119/1) 60 p132-133.

133:596

LOW, W and ZEIRE, S,

ESR spectra of Mn^{2+} in heat-treated aragonite.

Am. Miner. (57/7-8) 72 p1115-1125.

100:850

LOZYKOWSKI, H and HOLUJ, F,

Luminescence in phenacite.

J. Chem. Phys. (51/6) 69 p2315-2321.

410:850

LOZYKOWSKI, H, WILSON, RG and HOLUJ, F,

EPR study of the hole-centres in phenacite.

J. Chem. Phys. (51/6) 69 p2309-2315.

133:500

LUPEI, V and URSU, I,

Intensity of EPR spectral lines of Mn^{2+} in trigonal carbonates.

In: RUVKIND, AI, /Ed/: Paramagn. Rezonans. 1944-1969. Vses. Yubileinaya Konf. 1969 p117-120.

133:625

LUPEI, V, LUPEI, A and URSU, I,

Further ESR studies of forbidden hyperfine transitions of Mn^{2+} in calcite.

Phys. Rev. B (6/11) 72 p4125-4131.

410:815:870

LYSAKOV, VS, SAKHKU, TE, SEREBRENNIKOV, AI and SOLNTSEV, VP,

The nature of trapping and luminescence centres in quartz and nepheline.

Dokl. Akad. Nauk SSSR (186/1) 69 p177-180.

100:870

LYSAKOV, VS, SEREBRENNIKOV, AI and SOLNTSEV, VP,

Centres and spectra of thermally stimulated luminescence in natural quartz crystals.

Zh. Prikl. Spectrosk. (11/4) 69 p757-760.

430

MAL, SS, DMITRIEVA, LP, PLOTKINA, YuN, PANKRATOV, NS, SOROKINA, NF and FALYUSHIN, PL,

Use of an EPR method during a study of the self-heating of peat.

Dokl. Akad. Nauk Belorussk. SSR (14/12) 70 p1096-1099.

350

MANATT, SL, ELLEMAN, DD, VAUGHAN, RW, CHAN, SI, TSAY, FD and HUNTRESS Jr., WT,

Magnetic resonance studies of lunar samples.

Science (167/3918) 70 p709-711.

350

MANATT, SL, ELLEMAN, DD, VAUGHAN, RW, CHAN, SI, TSAY, FD and HUNTRESS Jr., WT,

Magnetic resonance studies of lunar samples.

In: Proc. Apollo 11 Lunar Sci. Conf. Geochim. Cosmochim. Acta Suppl. 1 (3) p2321-2323.

112:660

MANENKOV, AA and FEDOROV, VB,

Width and slope of Cr^{+++} ion paramagnetic resonance (EPR) spectral lines in corundum single crystals.

Zh. Eksp. Teor. Fiz. (38) 60 p1042-1046.

112:122:885

MANENKOV, AA, MILYAEV, VA and PROKHOROV, AM,

Cr^{+++} and Fe^{+++} relaxation times in rutile single crystals.

Fiz. Tverd. Tela (4) 62 p388-391.

112:660

MANENKOV, AA and PROKHOROV, AM,

Hyperfine structure of the paramagnetic resonance spectrum of $(Chromium\text{-}53)^{3+}$ in alumina. /Translated from: Zh. Eksp. Teor. Fiz. (31) 56 p346-347/.

Sov. Phys. JETP (4/2) 57 p286-289.

112:660

MANENKOV, AA and PROKHOROV, AM,

Spin-lattice relaxation in chromium-corundum.

Zh. Eksp. Teor. Fiz. (38) 60 p729-733.

133:625

MANKOVITZ, J and LOW, W,

Forbidden transitions ($\Delta_m = \pm 1$) in paramagnetic resonance absorption of Mn^{2+} in calcite.

Phys. Rev. B (2/1) 70 p28-32.

133:963

MANOOGIAN, A,

Electron spin resonance of Mn^{2+} in tremolite.

Can. J. Phys. (46/2) 68 p129-133.

133:963

MANOOGIAN, A,

Intensity of allowed and forbidden electron spin resonance lines of Mn^{2+} in tremolite.

Can. J. Phys. (49/9) 68 p1029-1033.

122:930

MANOOGIAN, A, HOLUJ, F and CARSWELL, JW,

Electron spin resonance of Fe^{3+} in single crystals of spodumene.

Can. J. Phys. (43/12) 65 p2262-2275.

133:802

MANOOGIAN, A and HSU, Y,

Electron spin resonance of Mn^{2+} impurities in morinite.

Can. J. Phys. (47/17) 69 p1869-1875.

133:820

MANOOGIAN, A and WIGGINS, B,

Electron spin resonance of Mn^{2+} impurities in newberyite.

Am. Miner. (57/1-2) 72 p52-62.

100:465:540

MARFUNIN, AS,

Radiospectroscopy in minerals.

Geol. J. (4/2) 65 p361-390.

100:465:540

MARFUNIN, AS and BERSHOV, LV,

Application of electron paramagnetic resonance to mineralogy.

Itogi. Nauki: Ser. Geokhim. Miner. Pet. 1964 (64).

100:510

MARFUNIN, AS and BERSHOV, LV,

Paramagnetic centres in feldspars and their possible crystallochemical and petrological significance.

Dokl. Akad. Nauk SSSR (193/2) 70 p412-414.

121:510

MARFUNIN, AS, BERSHOV, LV, MEILMAN, ML and MICHOULIER, J,

Paramagnetic resonance for ferric ion in some feldspars.

Schweiz. Miner. Petrogr. Mitt. (47/1) 67 p13-20.

133:161:595:895:920:963

MARFUNIN, AS, BERSHOV, LV and MINEEVA, RM,

La resonance paramagnetique electronique de l'ion Vo^{2+} dans le sphere et l'apophyllite et de l'ion Mn^{2+} dans la tremolite, l'apophyllite et la scheelite.

Bull. Soc. Fr. Miner. Crystallogr. (89/2) 66 p177-183.

100:625

MARSHALL, SA,

Investigation of narrow-line paramagnetic resonance absorption spectrum of calcite.

NASA Access. No. N64-18031, Rept. No. AD 433680 1964 (64).

100:625

MARSHALL, SA,

Narrow-line absorptions in single crystal calcite.

NASA Access. No. N65-36267, Rept. No. AD 619963 1965 (65).

122:625

MARSHALL, SA, HODGES, JA and SERWAY, RA,

Evidence for an isotropic shift in the electron spin resonance absorption spectrum of Fe^{3+} in calcite.

Phys. Rev. A (133/5) 64 p1427-1431.

110:124:625

MARSHALL, SA and McMILLAN, JA,

Electron spin resonance absorption spectrum of CO_2^- molecule ions associated with F^- in single crystal calcite.

J. Chem. Phys. (49/11) 68 p4887-4890.

145:890

MARSHALL, SA and REINBERG, AR,

Paramagnetic resonance absorption of nickel in sapphire.

J. Appl. Phys. (31/5) 60 p3365-3375.

122:625

MARSHALL, SA and REINBERG, AR,

Paramagnetic resonance absorption spectrum of trivalent iron in single crystal calcite.

Phys. Rev. (132/1) 63 p134-142.

122:625

MARSHALL, SA and REINBERG, AR,

Paramagnetic resonance absorption spectrum of trivalent iron in calcite.

Bull. Am. Phys. Soc., Ser. II (8) 63 p24-32.

125:625

MARSHALL, SA and SERWAY, RA,

Electron spin resonance absorption spectrum of trivalent gadolinium in single-crystal calcite.

Phys. Rev. (171/2) 68 p345-349.

101:625

MARSHALL, SA and SERWAY, RA,

Electron spin resonance absorption spectrum of AsO_2^{2-} molecule in γ-irradiated single crystal calcite.

J. Chem. Phys. (50/1) 69 p435-439.

133:625

MATARRESE, LM,

Comments on the EPR of Mn^{++} in calcite.

J. Chem. Phys. (34/1) 61 p336.

133:915

MATARRESE, LM and KIKUCHI, C,

Paramagnetic resonance absorption of Mn^{++} in single crystals of zincblende.

Phys. Chem. Solids (1/2) 56 p117-127.

100:640

MATSUZAKI, T, SETAKA, M, GROMOV, VV and KWAN, T,

Stable paramagnetic species in natural strontium sulphate crystals.

Bull. Chem. Soc. Japan (45/9) 72 p2773-2775.

100:985

MATUMURA, O and KOGA, H,

Magnetic resonance in irradiated zircon.

J. Phys. Soc. Japan (18/Suppl.2) 63 p312. Crystal lattice defects Conf., Kyoto 1962.

100:757

MATYASH, IV, POL'SHIN, EV and KALINICHENKO, AM,

Investigation of the effect of thermal treatment on hydromica by radiospectroscopy.

Geokhim. (1969/7) 69 p840-845.

100:505

MDIVNISHVILI, OM, URIDIYA, LYa and CHIKVAIDZE, EG,

New methods for the study of active centres in clay minerals.

Tr. Kavk. Inst. Miner. Syr'ya (1971/9) 71 p325-328.

133:530

MICHOULIER, J and DUCROS, P,

Electron paramagnetic resonance of Mn^{++} in the random crystalline field of a zeolite.

Proc. Colloq. AMPERE [1963] (12) 64 p215-222.

133:725

MICHOULIER, J, GAITE, JM and MAFFEO, B,

Electron paramagnetic resonance of Mn^{2+} ion in a fosterite monocrystal.

C.R. Hebd. Seances Acad. Sci., Ser. B, Sci. Phys. (269/12) 69 p535-538.

122:685

MICHOULIER, J, GAITE, JM and MAFFEO, B,

Electron paramagnetic resonance of Fe^{3+} ion in a diopside monocrystal.

C.R. Hebd. Seances Acad. Sci., Ser. B, Sci. Phys. (269/13) 69 p578-581.

150:625

MINEEVA, RM and BERSHOV, LV,

Hyperfine interaction of Fe^{3+} in calcite.

[Translated from: Fiz. Tverd. Tela (11/3) 69 p803-804].

Sov. Phys. Solid-State (11/3) 69 p653-654.

107:155:885

MIYAKO, Y,

Substitutional Co^{2+} ions combined with the interstitial Ti^{4+} in rutile.

J. Phys. Soc. Japan (31/6) 71 pl732-1737.

455

MORENCY, M, EMOND, PL and VON BITTER, TH,

Dating conodonts using electron spin resonance: a possible technique.

Bull. Kans. Geol. Surv. (199/1) 69 pl7-19.

420:425

MROZOWSKI, S and WOBSCHALL, D,

Electron spin resonance (EPR) in chars of some carbonaceous materials.

J. Chim. Phys. (57) 60 p915-925.

133:626

McCONNELL, HM,

Paramagnetic resonance absorption of Mn^{++} in single crystals of $CaCO_3$.

J. Chem. Phys. (24/4) 56 p904-905.

110:625

McMILLAN, JA and MARSHALL, SA,

Motional effects on the electron spin resonance absorption spectrum of CO_2^- molecule ions in single crystal calcite.

J. Chem. Phys. (48/1) 68 p467-471.

100:870

McMORRIS, DW,

ESR detection of fossil alpha damage in quartz.

Nature (226/5241) 70 p146-148.

450

McMORRIS, DW,

Trapped-electron dating studies: ESR studies.

Nature (222/5196) 69 p870-881.

McMORRIS, DW,

Impurity colour centres in quartz and trapped electron dating: Electron spin resonance, therroluminescence studies.

J. Geophys. Res. (76/32) 71 p7875-7887.

133:626

NARAYANA, PA,

Angular variation of intensities of forbidden lines in Mn^{2+} doped calcium carbonate in parallel and perpendicular configurations.

J. Chem. Phys. (55/9) 71 p4283-4286.

435

NICOLAU, C, PASCARU, I and RASHEEV, S,

Electron spin resonance investigation on some Rumanium crude oils.

Rev. Phys. Acad. Rep. Pop. Roum. (7) 62 p361-365.

133:530

NICULA, A, URSU, I and NISTOV, SV,

Forbidden transitions in the ESR (electron spin resonance) spectrum of Mn^{++} in zeolites.

Rev. Roum. Phys. (10/2) 65 p229-237.

100:590

NIKITINA, Ye I, SOTNIKOV, VI and SHCHERBAKOVA, MYa,

The evolution of accessory apatite on the basis of EPR data.

Geol. Geofiz. (1969/4) 69 p136-140.

100:530

NISTOV, SV,

Study of zeolites by magnetic resonance.

Rev. Roum. Chem. (19/2) 68 p117-119.

100:750

NIZAMUTDINOV, NM, VEDENIN, SV, ZANHARCHENKO, TA and VINOKUROV, VM,

Nuclear and electron paramagnetic resonance in herderite. [Translated from: Geokhim. (1971/3) 71 p361-365].

Geochem. Int. (8/2) 71 p305.

160:775

NIZAMUTDINOV, NM and VINOKUROV, VM,

Electron paramagnetic resonance of V^{4+} ions in lazulite.

Geochem. Int. (6/1) 69 p69-71.

133:630

NOVOZHILOV, AZ and SAMOILOVICH, MI,

Hyperfine structure in the EPR spectrum of Mn^{2+} in cancrinite.

Tr. Vses. Nauchno-Issled. Inst. Miner. Syr'ya (1969/10) 69 p131-133.

100:720

NOVOZHILOV, AI, SAMOILOVICH, MI and ANIKIN, IN,

EPR in fluorphlogopite.

Izv. Akad. Nauk SSSR, Neorg. Mater. (7/7) 71 p1282-1283.

410:518:720:945

NOVOZHILOV, AI, SAMOILOVICH, MI, ANIKIN, IN and SERGEYEV-BOBR, AA,

Structural defects in crystals of synthetic mica (fluorphlogopite and taeniolite). Studies by electron paramagnetic resonance method.

Zh. Strukt. Khim. (12/4) 71 p617.

410:945

NOVOZHILOV, AI, SAMOILOVICH, MI, ANIKIN, IN and SERGEYEV-BOBR, AA,

Electron paramagnetic resonance of hole-type centres in taeniolite with boron admixture.

Zh. Neorg. Khim. (16/3) 71 p874-876.

120:132:157:720

NOVOZHILOV, AI, SAMOILOVICH, MI, ANIKIN, IN and SERGEYEV-BOBR, AA,

Vanadium, iron and manganese paramagnetic impurities in synthetic fluorphlogopite crystals.

Izv. Akad. Nauk SSSR, Neorg. Mater. (6/1) 70 p108-112.

100:850

NOVOZHILOV, AI, SAMOILOVICH, MI and KARACHKOVSKAYA, AN,

Electron paramagnetic resonance in irradiated phenakite Be_2SiO_4.

Zh. Strukt. Khim. (11/3) 70 p428-432.

400:630

NOVOZHILOV, AI, SAMOILOVICH, MI, MIKUL'SKAYA, EK and PARUSHNIKOVA, LI,

Nature of the blue colouration in canorinite crystals.

Zap. Vses. Min. Obshch. (95/6) 66 p736-738.

100:870

NOVOZHILOV, AI, SAMOILOVICH, MI and TSINOBER, LI,

Short lived paramagnetic centres in quartz with Ge additions.

Zh. Strukt. Khim. (5/4) 64 p630-631.

100:962

NOVOZHILOV, AI, VOSKRESENSKAYA, IL and SAMOILOVICH, MI,

Electron paramagnetic resonance study of tourmalines.

Sov. Phys. Crystallogr. (14/3) 69 p416-418.

400:870

O'BRIEN, MCM,

The structure of the colour centre in smoky quartz.

Proc. R. Soc., Ser. A - Math. Phys. Sci. (231/1186) 55 p404-414.

100:680:870

O'BRIEN, MCM and PRYCE, MHL,

Paramagnetic resonance in irradiated diamond and quartz: Interpretation.

In: Defects in crystalline solids, Rept. Bristol Conf., London Phys. Soc. 1954.

425

OHUCHI, H, SHIOTANI, N and SOHMA, J,

ESR studies of virgin coals.

Fuel (48/2) 69 p187-190.

154:870

OKADA, M, RINNEBERG, H, WEIL, JA and WRIGHT, PM,

EPR of Ti^{3+} centres in α-quartz.

Chem. Phys. Lett. (11/3) 71 p275-276.

100:790

OKAMURA, T and TORIZUKA, Y,

Microwave resonance absorption in magnetite at low temperature.

Sci. Repts. Res. Insts. Tohoku Univ., Ser. A (3) 51 p214-218.

133:590

OKUDO, Y,

Electron spin resonance spectra of bivalent manganese ions in natural apatite single crystals.

J. Phys. Soc. Japan (18/6) 63 p916.

114:133:800

PAFONOV, MM, SIL'CHENKO, NA, TARASEVICH, Yu I, TELICHKUN, VP and BRATASHEVSKII, Yu A,

State of Cu^{2+} and Mn^{2+} exchange cations in montmorillonite saturated by acetonitrile and pyridine studied by EPR.

Ukr. Khim. Zh. (37/7) 71 p672-674.

121:540

PARKS, GA and AKHTAR, J,

Magnetic moment of Fe^{2+} in paramagnetic minerals.

Am. Miner. (53/3-4) 68 p406-416.

133:590

PARODI, JA,

An electron paramagnetic resonance study of the chemistry of Mn^{++} during the formation of fluorapatite.

J. Electrochem. Soc. (114/4) 67 p370-377.

132:620

PIECZONKA, WA, PETCH, HE and McLAY, AB,

An electron spin resonance study of Mn impurity in brucite.

Can. J. Phys. (39) 61 p145-157.

133:590

PIPER, WW,

Crystal field environment of divalent manganese in calcium halophosphate.

In: Proc. Int. Conf. Lumin. /1969/ 1970 p669-677.

400:590

PIPER, WW, KRAVITZ, LC and SWANK, RK,

Axial symmetric paramagnetic colour centres in fluorapatite.

Phys. Rev. A (136/6) 65 p1802-1814.

250:400:970

POVARENNYKH, AS, PLATONOV, AN and BELICHENKO, VP,

Mineralogy of Ilimaussaq.19. Colour of Ussingite from the Ilimaussaq (South Greenland) and Lovozero (Kola Peninsula) alkaline intrusions.

Bull. Geol. Soc. Den. (20/1) 70, p20-26.

410:885

PURCELL, T and WEEKS, RA,

Paramagnetic resonance of structural defects in rutile.

Bull. Am. Phys. Soc. (13/1) 68 p71.

410:885

PURCELL, T and WEEKS, RA,

Paramagnetic defects in TiO_2 produced by radiation.

J. Chem. Phys. (54/7) 71 p2800-2810.

114:700

RAOULT, G and DUCLAUX, AM,

Electron paramagnetic resonance (EPR) of Cu^{++} ($CuSO_4$) diluted in epsomite ($MgSO_4$).

Arch. Sci. (13/Spec. No.) 61 p199-204.

145:660

RAOULT, G, DUCLAUX, AM and CHENON, MF,

Electron paramagnetic resonance of nickel ion in a single crystal of alumina.

Proc. Colloq. AMPERE /1962/ (11) 63 p456-460.

114:652

RAPP, J, KALLO, D and MIKHEIKIN, ID,

EPR study of the coordination state of Cu^{2+} ions in natural clinoptilolites.

Kinet. Katal. (13/5) 72 p1344-1346.

107:660

RAY, DK,

Covalent band theory for cobalt salts and analysis of Co^{++} paramagnetic resonance spectrum in corundum.

Fiz. Tverd. Tela (3) 61 p2223-2239.

425

REICOFSKY, HL, STARK, JM and FRIEDEL, RA,

EPR g-values of coals.

Chem. Ind. (1967/13) 67 p1327-1328.

425

REICOFSKY, HL, STARK, JM and FRIEDEL, RA,

Electron spin resonance in American coals.

Anal. Chem. (40/11) 68 p1699-1704.

425:440

REX, RW,

Electron paramagnetic resonance (EPR) studies of stable free radicals in lignins and humic coals.

Nature (188/4757)60 p1185-1186.

100:710

RICHARDSON, JT,

ESR studies of cationic oxidation sites in faujasite.

J. Catal. (9/2) 67 p172-177.

133:715

RICHARDSON, RJ,

Electron spin resonance of Mn^{2+} in BaF_2, SrF_2, CdF_2 and CaF_2.

Phys. Rev. B (6/3) 72 p1065-1066.

112:680

RIMAI, L, STATZ, H, WEBER, MJ and deMARS, GA,

Paramagnetic resonance of exchange-coupled Cr^{3+} pairs in ruby.

Phys. Rev. Lett. (4/3) 60 p125-128.

121:615

ROSTWOROWSKI, JA, HOHL, M and SCHWERDTFEGER, CF,

EPR of substitutional iron (II) in titanium dioxide (brookite).

J. Phys. Chem. Solids (34/2) 73 p231-234.

120:745

RUDASHEVSKII, EC and SIAL'NIKOVA, TA,

Antiferromagnetic resonance in haematite.

Zh. Eksp. Teor. Fiz. (47/3) 69 p886-891.

114:800

RUPERT, JP,

Electron spin resonance spectra of interlamellar copper (II)-amine complexes on montmorillonite.

J. Phys. Chem. (77/6) 73 p784-789.

118:125

RYTER, C,

Paramagnetic resonance in the 10,000 megacycle per sec. band of europium and gadolinium in a cubic crystalline field.

Helv. Phys. Acta (30/5) 57 p353-373.

400:985

SAHADDAR, M and GHOSH, PK,

Origin of colouration in zircon crystals.

Technology (6/1) 69 p42-44.

175:540

SAMOILOVICH, MI,

An ESR study of sulphur-bearing radical ions in minerals.

/Translated from: Geokhim. (1971/4) 71 p477-485/.

Geochem. Int. (8/2) 71 p306.

100:625

SAMOILOVICH, MI and ANDRUSENKO, NI,

A paramagnetic centre in calcite.

Zh. Strukt. Khim. (8/6) 67 p1093-1094.

145:680

SAMOILOVICH, MI, BEZRUKOV, GN and BUTUZOV, V,

Electron paramagnetic resonance of Ni in synthetic diamonds.

/Translated from: Zh. Eksp. Teor. Fiz., Pis. Red. (14/10) 71 p551-553/.

JETP Lett. (41/10) 71 p379-381.

400:625

SAMOILOVICH, MI and LUCHNIKOV, VG,

Nature of the yellow colouring in calcite.

Zap. Vses. Min. Obshch. (98/4) 69 p492-495.

122:961

SAMOILOVICH, MI, MEIL'MAN, ML and NOVOZHILOV, AI,

Electron paramagnetic resonance of Fe^{3+} in topaz.

Tr. Vses. Nauchno-Issled. Inst. Mineral. Syr'ya (1970/12) 70 p121-124.

100:985

SAMOILOVICH, MI, NOVOZHILOV, AI and BARSANOV, GP,

Electron paramagnetic resonance in irradiated zircons containing various elements.

/Translated from: Geokhim. (1968/4) 68 p494-495/.

Geochem. Int. (5/2) 68 p420.

100:640

SAMOILOVICH, MI, NOVOZHILOV, AI, BEZNOV, LV and ANDRUSENKO, NI,

EPR in irradiated strontium sulphate single crystals.

Radiokhim. (10/4) 68 p506-507.

120:400:605

SAMOILOVICH, MI, TSINOBER, LI, DUNIN-BARKOVSKII, RL,

The nature of the colour of beryl containing an iron impurity.

Kristallogr. (16/1) 71 p186-189.

400:870

SAMOILOVICH, MI, TSINOBER, LI and KLADZHI, IP,

Coloured synthetic quartz crystals.

Dokl. Akad. Nauk SSSR (184/1) 67 p91-93.

400:870

SAMOILOVICH, MI, TSINOBER, LI and KREISKOP, VN,

The smoky colour of natural quartz-morion crystals.

Kristallogr. (15/3) 70 p519-522.

157:435

SARACENO, AJ, FANALE, JP and GOGGESHALL, ND,

An electron paramagnetic resonance investigation of vanadium in petroleum oils.

Anal. Chem. (33/4) 61 p500-503.

425

SARKAR, GN, MUKHERJI, A, CHATTERJEE, RN and GHOSH, US,

Investigations on the paramagnetic resonance in coal with a transmission type electron paramagnetic resonance spectrometer.

Indian J. Phys. (33) 59 p117-122.

133:690:785

SCHINDLER, P and GHOSE, S,

Electron paramagnetic resonance of Mn^{2+} in dolomite, $CaMg(CO_3)$ and magnesite, $MgCO_3$, and Mn^{2+} distribution in dolomites.

Trans. Am. Geophys. Union. (50/4) 69 p357.

133:690:785

SCHINDLER, P and GHOSE, S,

Electron paramagnetic resonance of Mn^{2+} in dolomite and magnesite and Mn^{2+} distribution in dolomites.

Am. Miner. (55/11-12) 70 p1889-1896.

410:870

SCHNADT, R and SCHNEIDER, J,

Electronic structure of a trapped-hole centre in smoky quartz.

Phys. Kondens. Mater. (11/1) 70 p19-42.

133:980

SCHNEIDER, J and SIRCAR, SR,

Paramagnetische resonanz von Mn^{2+} ionen in synthetischen und natürlichen Zno-cristallen (I).

Z. Naturf. (17A/7) 62 p570-577.

100:880:890

SCHULZ-DUBOIS, EO,

Paramagnetic spectra of substituted sapphires I. ruby.

Bell. System Tech. J. (38) 59 p271-290.

360:420

SCHULZ, KF and MACLEOD ELOFSON, R,

Electron spin resonance studies of organic matter in the Orgueil meteorite.

Geochim. Cosmochim. Acta (29/3) 65 p157-160.

154:745

SEARLE, C/ and WANG, ST,

Magnetic resonance properties of pure and titanium-doped hematite.

J. Appl. Phys. (39/2) 68 p1025-1026.

100:590

SEGALL, B, LUDWIG, G/, WOODBURY, KH and JOHNSON, PD,

Electron spin resonance of a centre in calcium fluorophosphate.

Phys. Rev. (128/1) 62 p76-79.

235

SERGANOVA, GK and RAFIKOV, SR,

Structure and properties of Baltic amber.

Zh. Prikl. Khim. (38/8) 65 p1813-1818.

133:626

SERWAY, RA,

Temperature-dependent spin-Hamiltonian parameters of Mn^{2+} in trigonal sites of calcium carbonate.

Phys. Rev. B (3/3) 71 p608-615.

109:625

SERWAY, RA and MARSHALL, SA,

Electron spin resonance absorption spectrum of orthorhombic CO_3^{--} molecule-ions in irradiated single crystal calcite.

J. Chem. Phys. (47/2) 67 p868-869.

148:410:625

SERWAY, RA, MARSHALL, SA, McMILLAN, JA, MARSHALL, RL and OLISEN, WD,

Electron spin resonance absorption spectra of hole-type centres associated with phosphorous in irradiated single crystal calcite.

J. Chem. Phys. (51/11) 69 p4978-4982.

100:590

SHCHERBAKOVA, MYa,

Study of natural apatite by electron paramagnetic resonance.

Radiospektrosk. Tverd. Tela (1967) 67 p337-340.

100:590

SHCHERBAKOVA, MYa, GILINSKAYA, LG and GOLOVIKOV, AA,

Paramagnetic centres in apatite.

/Translated from: Kristallogr. (13/2) 68 p353-356/.

Sov. Phys. Crystallogr. (13/2) 68 p289.

100:465:540

SHCHERBAKOVA, MYa and GILINSKAYA, LG,

Study of minerals by paramagnetic radiospectroscopy.

Geol. Geofiz. (1964/8) 64 p57-65.

148:590

SHCHERBAKOVA, MYa, GILINSKAYA, LG and ZHIDOMIROV, GM,

Paramagnetic defect centres of PO_3^{2-} in apatite.

In: BRODSKII, AI, /Ed/: Str. Mol. Kvantovaya Khim. "Naukova Dumka", Kiev, USSR 1920 p69-76.

100:590

SHCHERBAKOVA, MYa, GOLOVIKOV, AA, GILINSKAYA, LG and VASIL'EVA, ZV,

Study of apatite of various geneses by the electron paramagnetic resonance method.

In: KLYAROVSKII, VI, /Ed/: Issled. Strukt. Osob. Miner. Sovrem. Fiz.-Khim. Metod. "Nauka", Sib. Otd., Novosibirsk, USSR 1970 p91-94.

100:635

SHCHERBAKOVA, MYa, PURVINSKII, OF and GILINSKAYA, IG,

Electron paramagnetic resonance study of natural cassiterite.

In: KLYAROVSKII, VM /Ed/: Issled. Strukt. Osob. Miner. Sovrem. Fiz-Khim. Metod. "Nauka", Sib. Otd. Novosibirsk, USSR 1970 p104-107.

122:133:795

SHCHERBAKOVA, MYa, SHIPILOV, LD, SINYAKOV, VI and ISTOMIN, VE,

Electron paramagnetic resonance study of Mn^{++} and Fe^{+++} in the structure of monticellite.

Zh. Strukt. Khim. (9/6) 68 p984-989.

100:680

SHCHERBAKOVA, MYa, SOBOLEVA, EV and NADOLINNYI, VA,

Electron spin resonance low-symmetry impurity centres in diamond.

Dokl. Akad. Nauk SSSR (204/4) 72 p851-854.

138:680

SHCHERBAKOVA, MYa, SOBOLEVA, EV, SAMSONENKO, ND and AKSENOV, VK,

Electron paramagnetic resonance of ionized nitrogen pairs in diamonds.

/Translated from: Fiz. Tverd. Tela (11/5) 69 p1364-1367/.

Sov. Phys. Solid-State (11/5) 69 p1104-1106.

138:680

SCHASTNEV, PV and SEMENOV, A,

Electron paramagnetic resonance of nitrogen-aluminium pairs in diamonds.

/Translated from: Fiz. Tverd. Tela (13/2) 71 p341-346/.

Sov. Phys. Solid-State (13/2) 71 p281-285.

125:895

SHCHERBAKOVA, MYa, SOLNTSEV, VP, ANDRIEVSKII, VYa and NIKITINA, VI,

Paramagnetic resonance of orthorhombic complexes of gadolinium (III) in scheelite.

In: Radiatsion. Defekt. Tverd. Tela, Sb. 2nd. 1967 1970 p236-239.

130:150:153:176:895

SHEKUN, LYa,

Magnetic properties of Pb^{3+}, Tb^{3+}, Ho^{3+} and Tm^{3+} in scheelite structures.

Fiz. Tverd. Tela (8/10) 66 p2929-2933.

122:133:780

SHUSKUS, AJ,

Electron spin resonance of Fe^{3+} and Mn^{2+} in single crystals of CaO.

Phys. Rev. (127/5) 62 p1529-1531.

100:835

SIBLEY, WA, KOLOPUS, JL and MALLARD, WC,

A study of the effect of deformation on the ESR, luminescence and absorption of MgO single crystals.

Phys. Status Solidi (31/1) 69 p223-231.

100:425

SIDOROV, AA and ANUFRIENKO, VF,

Electron paramagnetic resonance study of free radicals in natural coals and semicokes.

Izv. Sib. Otd. Akad. Nauk SSSR, Ser. Khim. Nauk (1966/1) 66 p155-158.

125:715

SIERRO, J and LACROIX, R,

Paramagnetic resonance in fluorite of the Gd^{+++} ion subject to a tetragonal crystalline field.

C.R. Hebd. Seances Acad. Sci. (250/15) 60 p2686-2687.

112:885

SIERRO, J, LACROIX, R and MULLER, KA,

Hyperfine structure of the magnetic resonance spectrum of chromium in rutile.

Helv. Phys. Acta (32/4) 59 p266-280.

112:885

SIERRO, J, MULLER, KA and LACROIX, R,

Paramagnetic resonance of chromium in a monocrystal of rutile.

Arch. Sci. (12) 59 p122-123.

114:765

SIL'CHENKO, VA, PAPCHOV, MN, TARASEVICH, Yul, MATYASH, IV and SUYUNOVA, ZE,

Electron paramagnetic resonance of Cu^{2+} exchange cations in kaolinite.

Ukr. Khim. Zh. (37/12) 71 p1238-1241.

100:870

SILSBEE, RH,

Electron spin resonance in neutron-irradiated quartz.

J. Appl. Phys. (32/8) 61 p1459-1462.

420

SINGER, LS,

Review of electron spin resonance on carbonaceous materials.

In: Proc. Conf. Carbon. 5th. Univ. Park. Penna (2) 63 p37-64.

120:925

SMETANA, Z,

Relaxation and resonance line width of ferromagnetic spinels.

Cesk. Cas. Fys. (18/2) 68 p191-206.

425

SMIDT, J,

Electron spin resonance of coals: saturation effect.

Nature (181/4603) 58 p176.

425

SMIDT, J,

The second moment and width of the resonance curves of coals (vitrinites).

Arch. Sci. (11/Spec. No.) 58 p180-184.

425

SCHIDT, J and VAN KREVELAN, DW,

Electron spin resonance in vitrains during carbonization in vacuo.

Chim. Ind. (82) 59 p487-493.

425

SCHIDT, J and VAN KREVELAN, DW,

Chemical structure and properties of coal. XXIII Electron spin resonance of vitrains.

Fuel (38) 59 p355-368.

680

SMITH, MJA,

A physicists view of diamond.

J. Gemmology (11) 69 p327-331.

100:680

SMITH, MJA and ANGEL, BR,

Some electron spin resonance properties of heat treated synthetic diamond.

Philos. Mag. (15/136) 67 p783-796.

100:680

SMITH, WV, GELLES, IL and SOROKIN, PP,

Electron spin resonance of acceptor states in diamond.

Phys. Rev. Lett. (2/2) 59 p39-40.

138:680

SMITH, WV, SOROKIN, PP, GELLES, IL and LASHER, GJ,

Electron spin resonance of nitrogen donors in diamond.

Phys. Rev. (115/6) 59 p1546-1552.

133:915

SMOL'KOV, NA, PETROPAVLOV, MV and KULAGIN, EG,

Electron paramagnetic resonance of Mn^{2+} in natural sphalerite, β-zinc blende.

In: BLYUMENFEL'D, LA /Ed/: Radiospektrosk. Kvantovokhim. Metody. Strukt. Issled. "Nauka", Moscow, USSR 1967 p145-146.

425

SOMA, J,

ESR of coal.

Nenryo Kyokaishi (48/505) 69 p274-285.

166:895

SOLNTSEV, VP and SHCHERBAKOVA, NYa,

W^{5+} electron paramagnetic resonance in scheelite.

Zh. Strukt. Khim. (12/3) 71 p397-402.

154:870:985

SOLNTSEV, VP and SHCHERBAKOVA, NYa,

Electron paramagnetic resonance of Ti^{3+} in α-quartz and zircon.

Zh. Strukt. Khim. (13/5) 72 p924-927.

125:895

SOLNTSEV, VP, SHCHERBAKOVA, NYa and SOTNIKOV, VI,

Electron paramagnetic resonance of gadollinium (III) in natural scheelite.

Geol. Geofiz. (1969/2) 69 p125-127.

480

SOLOZHENKIN, PM,

Study of some problems of flotation theory by electron paramagnetic resonance.

Fiziko-Tekh. Probl. Razrab. Polezn. Iskop. (1968/2) 68 p72-79.

100:985

SOLOZHENKIN, PM and PACHADZHANOV, DN,

Some data on the EPR spectra of zircons.

/Translated from: Geokhim. (1967/7) 67 p874-876/.

Geochem. Int. (4/4) 67 p716.

480

SOLOZHENKIN, PM and ZHITOMIRSKII, AN,

Use of magnetic radio spectroscopy (electron paramagnetic resonance) in studying some problems of flotation theory.

Tsvet. Met. (39/9) 60 p8-9.

100:480:640

SOLOZHENKIN, PM, ZHITOMIRSKII, AN, POPOV, LZ, KOPITSYA, NI and POROSHIN, KT,

Paramagnetic centres of celestine as influencing its flotation properties.

Dokl. Akad. Nauk SSSR (181/6) 60 p1440.

133:895

SOTNIKOV, VI, NIKITINA, YeI, SHCHERBAKOVA, MYa and SOLNTSEV, VF,

On the possibility of utilization of Mn^{2+} EPR spectra in scheelites as criteria for determining their origin.

Geol. Geofiz. (1969/1) 69 p126-131.

112:132:925

STAHL-BRADA, R and LOW, W,

Paramagnetic resonance spectra of Cr and Mn in the spinel structure.

Phys. Rev. (116/3) 59 p561-564.

120:735

STANKOWSKI, J, WOLSKI, W and KLINASZYNSKI, B,

EPR investigations of the anti-ferromagnetic-paramagnetic phase transitions in goethite.

Bull. Acad. Pol. Sci., Ser. Sci. Math., Astron. Phys. (15/12) 67 p875-879.

440

STEELINK, C and TOLLIN, G,

Stable free radicals in soil humic acids.

Biochim. Biophys. Acta (59/1) 62 p25-34.

132:925

STOMBLER, MP, FARACH, HA and POOLE, CP,

Electron spin resonance study of manganese substituted spinel.

Phys. Rev. B (6/1) 72 p40-45.

100:680

SURMA, M and FURDYNA, JK,

Electron paramagnetic resonance in natural semiconducting diamond and artificial aluminium-doped diamonds.

Poznan. Tow. Przyj. Nark. Pr. Kom. Mat.-Przyr. (1969/5) 69 p121-141.

122:890

SYMONS, HF and EOGLE, GS,

Exactness of the spin-hamiltonian description of Fe^{+++} in sapphire.

Proc. Phys. Soc. (79) 62 p468-472.

100:680

SZENDREI, T,

Electron spin resonance of spin S=1 states in irradiated diamond.

Solid State Commun. (9/4) 71 p313-314.

100:765

TADZHIEV, FKh, ERMOLENKO, GM and KRIVOVYAZ, IM,

Physiochemical processes on firing cationic forms of kaolin as studied by using electronic paramagnetic resonance spectra.I Dehydration and beginning of exagenous effects.

Tr. Tashk. Politekh. Inst. (1963/22) 63 p204-215.

100:230

TAKEMOTO, S and SHINODA, S,

Microwave resonance absorption by iron sands.

Bull. Shimane Univ. (1954/4) 54, p22-29.

133:780

TANIMOTO, DH and KEMP, JC,

Forbidden hyperfine transitions in the electron spin resonance of Mn^{2+} in CaO and SrO crystals.

J. Phys. Chem. Solids (27/5) 66 p887-891.

122:961

THYER, JR, QUICK, SM and HOLUJ, F,

ESR spectrum of Fe^{3+} in topaz.

Can. J. Phys. (45/11) 67 p3597-3610.

114:122:133:915

TITLE, RS,

Electron paramagnetic resonance spectra of Cr^{3+}, Mn^{++} and Fe^{3+} in cubic ZnS.

Phys. Rev. (131/2) 63 p623-627.

133:915

TONSCAINT, J and DECLERCK, C,

Electron spin resonance spectrum of Mn^{2+} in (zinc) blende.

Bull. Soc. R. Sci. Liege (35/1-2) 66 p87-92.

425

TOYODA, S,

Application of ESR to coal study.

Nenryo Kyokaishi (49/523) 70 p803-915.

425

TOYODA, S and HONDA, H,

Two components of electron spin resonance in Yuban coal.

Nenyro Kyokaishi (44/462) 65 p697-704.

425

TOYODA, S, SUGAWARA, S and HONDA, H,

Chemical structure and properties of heat treated coal in the early state of carbonization. V Electron spin resonance of coal.

Nenyro Kyokaishi (45/476) 66 p876-883.

122:770

TROUP, GJ and HUTTON, DR,

Paramagnetic resonance of Fe^{3+} in kyanite.

Br. J. Appl. Phys. (15/12) 64 p1493-1499.

122:133:158:159:990

TSANG, T and GHOSE, S,

Electron paramagnetic resonance of V^{2+}, Mn^{2+}, Fe^{3+} and optical spectra of V^{3+} in blue zoisite $Ca_2 Al_3 Si_3 O_{12} (OH)$.

J. Chem. Phys. (54/3) 71 p856-862.

100:990

TSANG, T and GHOSE, S,

Ordering of transition metal ions in zoisite.

Trans. Am. Geophys. Union (52/4) 71 p331.

350

TSAY, FD, CHAN, SI and HAMATT, SL,

Magnetic resonance studies of Apollo 11 and Apollo 12 samples. In:

Proc. 2nd Lunar Sci. Conf. Geochim. Cosmochim. Suppl. 2 (3) 71 p2515-2528.

120:350

TSAY, FD, CHAN, SI and MANATT, SL,

Ferromagnetic resonance of lunar samples.

Geochim. Cosmochim. Acta (35/9) 71 p865-875.

350

TSAY, FD, CHAN, SI and MANATT, SL,

Electron paramagnetic resonance of radiation damage in a lunar rock.

Nature Phys. Sci. (237/77) 72 p121-122.

132:625

TSAY, FD, MANATT, SL and CHAN, SI,

Electron spin resonance of manganous ions in frozen methanol solution.

Chem. Phys. Lett. (17/2) 72 p223-226.

120:350

TSAY, FD, MANATT, SL and CHAN, SI,

Magnetic phases in lunar fines: metallic Fe or ferric oxides.

Geochim. Cosmochim. Acta (37/5) 73 p1201-1211.

400:560:870

TSINOBER, LI,

Some properties of the smoky and amethyst colourization of synthetic quartz crystals.

Tr. Vses. Soveshch. Radiats. Khim. (60) 62 p677-682.

400:870

TSINOBER, LI, SMOILOVICH, MI, GORDIENKO, LA and CHENTSOVA, LG,

Anomalous pleochroism of synthetic quartz crystals having smoky colour.

Kristallogr. (12/1) 67 p65-69.

425

TYUTYUNNIKOV, YuB, RODIONOV, IS and SENTSOVA, LG,

Nature of EPR signals from coal.

Khim. Tverd. Topl. (1973/1) 73 p140-141.

425

TYUTYUNNIKOV, YuB, SINESEROVA, LG and ROMODANOV, IS,

Use of electron paramagnetic resonance to study coals and processes for their thermal treatment.

Khim. Tverd. Topl. (1967/15) 67 p61-68.

100:425

UEBERSFELD, J,

Free radicals in coals and charcoals and their interaction with external media.

J. Chim. Phys. (56) 59, p805-809.

425

UEBERSFELD, J,

Paramagnetic resonance of coals and carbons.

Ind. Chim. Belge, Suppl. (1) 59 p413-415.

100:425

UEBERSFELD, J and ERB, E,

Paramagnetic resonance of charcoal. Detection of free radicals unstable in air.

J. Phys. Radium (16/4) 55 p340.

425

UEBERSFELD, J, ETIENNE, A and COMBRISSON, J,

Paramagnetic resonance, a new property of coal-like materials.

Nature (174/4430) 54 p614.

112:530

URUSHADZE, MV and TSITSISHVILI, GV,

EPR spectra of chromium-containing zeolite.

Kinet. Katal. (11/4) 70 p1080-1081.

235

URBANSKI, T, BEREK, S and MALINOWSKI, S,

Analytical data of Polish amber from Baltic Sea.

Bull. Acad. Pol. Sci., Ser. Sci. Chim. (19/4) 71 p227-229.

133:625

URSU, I, LUPEI, A and LUPEI, V,

Effect of neutron irradiation of the EPR spectrum of Mn^{2+} ions in calcite.

In: RIVKIND, AI /Ed/: Paramagn. Razonans. 1944-1969, Vses. Yubileinaya Konf. 1969 p143-145. "Nauka", Moscow, USSR.

133:625

URSU, I and LUPEI, V,

Electron spin resonance of manganese (II) ion in calcite.

Proc. Colloq. AMPERE /1965/ (14) 66 p303-304.

133:625

URSU, I, LUPEI, V and LUPEI, A,

Forbidden hyperfine transitions in the electron spin resonance spectra of manganese (II) in calcite.

Rev. Roum. Phys. (11/9-10) 66 p875-883.

133:530

URSU, I and NICULA, A,

Electron spin resonance (ESR) of the Mn (II) ion in zeolites.

Rev. Roum. Phys. (9/4) 64 p343-350.

116:985

VALISHEV, RM, VINOKUROV, VM, ZARIPOV, MM and STAPANOV, VG,

Electron paramagnetic resonance of Er^{3+} ions in zircon $ZrSiO_4$ crystals.

Geochem. Int. (2/5) 65 p925. Translated from:- Geokhim. (1965/10)65 p1265.

425

VAN GERVEN, L, VAN ITTERBEEK and DE WOLF, E,

Résonance paramagnétique électronique dans du charbon du "Donetz".

J. Phys. Radium (17/2) 56 p140-142.

133:540

VAN VIERINGEN, JS,

Paramagnetic resonance of divalent manganese incorporated in various lattices.

Disc. Farad. Soc. (19) 55 p118-126.

400:870

VAN VIERINGEN, JS, HAVEN, Y and KATS, A,

Paramagnetic resonance of colour centres in α -quartz containing germanium.

Proc. Colloq. AMPERE /1962/ (11) 63 p403-408.

425

VASIL'EVA, IM, ANUFRIENKO, VF and SHULYAEV, AA,

New findings on the structure of the EPR spectra of coals and cokes.

Kinet. Katal. (12/5) 71 p1310-1314.

425

VASIL'EVA, IM, BOCHKAREVA, KZ, SHIRYAEVA, KM, SHKLYAEV, AA and ANUFRIENKO, VF,

EPR studies of fusains.

Khim. Tverd. Topl. (1972/2) 72 p48-55.

425

VASIL'EVA, IM, RYABCHENKO, SN and BOCHKAREVA, KI,

EPR study of weathered coals.

Khim. Tverd. Topl. (1971/5) 71 p129-131.

120:785

VASIL'EVA, IM and SHCHERBAKOVA, MYa,

Ferromagnetic resonance of magnetites from rhythmic aggregates of various origin.

Mater. Genet. Eksp. Miner. (1972/7) 72 p79-85.

132:177:590

VINNIKOV, AP, GARKUSHA, VA and GUGEL, EM,

Distribution of manganese and antimony in calcium chloro- and fluorapatite.

Izv. Akad. Nauk SSSR, Ser. Fiz. (35/7) 71 p1501-1504.

132:590

VINNIKOV, AP and GUGEL, EM,

Effect of exchange on manganese luminescence in calcium chlor- and fluorapatite.

Sb. Nauch. Tr., Vses. Nauchno-Issled. Inst. Lyumiroforov Osobo Chist. Veshchestv. (1971/6) 71 p23-28.

100:350

VINOGRADOV, AP, VDOVYKIN, GP and MAROV, IN,

Free radicals in the Mighei meteorite.

/Translated from: Geokhim. (1964/5) 64 p395-398/.

Geochem. Int. (1/3) 64 p395-397.

120:132:540

VINOKUROV, VM,

Electron paramagnetic resonance data on isomorphism in manganese and iron ions in certain minerals.

/Translated from: Geokhim. (1966/10) 66 p1247-1254/.

Geochem. Int. (3/5) 66 p996-1002.

100:465:540

VINOKUROV, VM,

Electron paramagnetic resonance spectroscopy and isomorphism in minerals.

In: VINOGRADOV, AP /Ed/: Probl. Izomorfnykh Zameshchenii At. Krist.

"Nauka", Moscow, USSR 1972 p172-181.

170:172:985

VINOKUROV, VM, GAINULLINA, IM, ERGAKOVA, LA, NIZAMUTDINOV, NM and SUSLINA, AN,

Zr^{4+} — Y^{3+} isomorphism and features of accompanying charge compensation

in zircon crystals.

Kristallogr. (16/2) 71 p318-323.

122:260:985

VINOKUROV, VM, GAINULLINA, IM, NIZAMUTDINOV, NM and KVASNOBAEV, AA,

Distribution pattern of Fe^{3+} impurity ions in zircon single crystals from

Mir pipe kimberlites.

Geokhim. (1972/11) 72 p1402-1405.

133:605

VINOKUROV, VM, KROPOTOV, VS and STEPANOV, VG,

Investigation of occurrence of Mn^{2+} in beryl by the EPR method.

/Translated from: Geokhim. (1965/1) 65 p104.

Geochem. Int. (2/6) 65 p71-72.

107:133:935

VINOKUROV, VM, NIZAMUTDINOV, MM and TUKHVATULLIN, RS,

EPR of Mn^{2+} and Co^{2+} in struvite.

In: VINOKUROV, VM /Ed/: Fiz. Miner. Issl. Kazan. Univ., Kazan, USSR 1969

p13-19.

100:660

VINOKUROV, VM, NIZAMUTDINOV, MM and TUKHVATULLIN, RS,

EPR study of isomorphism in schtrakmite crystals.

In: VINOKUROV, VM /Ed/: Fiz. Miner. Issl. Kazan Univ., Kazan, USSR 1969 p3-12.

133

VINOKUROV, VI and STEFANOV, VG,

Mn^{2+} electron paramagnetic resonance in SrF_2 single crystals.

Fiz. Tverd. Tela (6/2) 64 p380-381.

125:895

VINOKUROV, VI and STEFANOV, VG,

Magnitude of initial splittings of gadolinium ions in crystals of scheelite series. /Translated from: Fiz. Tverd. Tela (9/4) 67 p1081-1084/.

Sov. Phys. Solid State (9/4) 67 p844-846.

133:825

VINOKUROV, VI and TUKHVATULLIN, RS,

Electron paramagnetic resonance of Mn^{2+} ions in northupite.

/Translated from: Geokhim. (1968/2) 68 p243-244/.

Geochem. Int. (5/1) 68 p194-195.

133:935

VINOKUROV, VI and TUKHVATULLIN, RS,

Electron paramagnetic resonance of Mn^{2+} ions in struvite.

/Translated from: Geokhim. (1968/4) 68 p496-497/.

Geochem. Int. (5/2) 68 p423.

400:590

VINOKUROV, VI and ZARIPOV, MM,

On the blue colour of apatites.

Dokl. Akad. Nauk SSSR (136) 61 p61-62.

133:655

Electron paramagnetic resonance (EPR) on Mn^{2+} in cordierite.

/Translated from: Geokhim. (1965/12) 65 p1486-1487/

Geochem. Int. (3/5) 65 p1086.

112:575

VINOKUROV, VM, ZARIPOV, MM, POLSKII, YuE, STEPANOV, VG, CHIRKIN, GK and SHEKUN, LYa,

Paramagnetic resonance of Cr^{3+} in andalusite.

Fiz. Tverd. Tela (3/8) 62 p646-649.

121:575

VINOKUROV, VM, ZARIPOV, MM, POLSKII, YuE, STEPANOV, VG, CHIRKIN, GK and SHEKUN, LYa,

A study of the peculiarities of isomorphism of ferric ions in andalusite by the method of paramagnetic resonance.

Kristallogr. (7/2) 62 p318-320.

125:715

VINOKUROV, VM, ZARIPOV, MM, POLSKII, YuE, STEPANOV, VG, CHIRKIN, GK and SHEKUN, LYa,

Electron paramagnetic resonance of Gd^{3+} in CaF_2.

Fiz. Tverd. Tela (4) 62 p2238-2242.

125:715

VINOKUROV, VM, ZARIPOV, MM, POLSKII, YuE, STEPANOV, VG, CHIRKIN, GK and SHEKUN, LYa,

Electron paramagnetic resonance of Gd^{3+} in CaF_2.

Fiz. Tverd. Tela (5/2) 63 p599-604.

125:715

VINOKUROV, VM, ZARIPOV, MM, POLSKII, YuE, STEPANOV, VG, CHIRKIN, GK and SHEKUN, LYa,

Electron paramagnetic resonance of Gd^{3+} in CaF_2.

Fiz. Tverd. Tela (5/10) 63 p2902-2907.

118:125:143:715:985

VINOKUROV, VM, ZARIPOV, MM, POLSKII, YuE, STEPANOV, VG, CHIRKIN, GK and SHEKUN, LYa,

Electron paramagnetic resonance determination of small amounts of Gu^{2+}, Gd^{2+} and Nb^{4+} and their isomorphism in fluorite and zircon.

/Translated from: Geokhim. (1963/11) 63 p1002-1007/.

Geochem. (1963/11) 63 p1041-1046.

133:690:785

VINOKUROV, VM, ZARIPOV, MM and STEPANOV, VG,

Paramagnetic resonance of Mn^{2+} in dolomite and magnesite.

Zh. Eksp. Teor. Fiz. (39) 60 p1552-1553.

132:500

VINOKUROV, VM, ZARIPOV, MM and STEPANOV, VG,

A study of some Mn-bearing carbonates by EPR.

Kristallogr. (6/1) 61 p104-108.

133:685

VINOKUROV, VM, ZARIPOV, MM and STEPANOV, VG,

Electron paramagnetic resonance (EPR) of Mn^{2+} in diopside crystals.

Fiz. Tverd. Tela (6/4) 64 p1130-1137.

133:730

VINOKUROV, VM, ZARIPOV, MM and STEPANOV, VG,

Electron paramagnetic resonance of Mn^{2+} ions in gaylussite.

/Translated from: Geokhim. (1964/12) 64 p1318-1319/.

Geochem. Int. (1/6) 64 p1179-1180.

133:590

VINOKUROV, VM, ZARIPOV, MM and STEPANOV, VG,

Electron paramagnetic resonance of Mn^{2+} in apatite.

Fiz. Tverd. Tela (6/4) 64 p1125-1129.

143:985

VINOKUROV, VM, ZARIPOV, MM, STEPANOV, VG, CHIRKIN, GK and SHEKUN, LYa,
Paramagnetic resonance of Nb^{4+} ions in zircon single crystals.
Fiz. Tverd. Tela (5/7) 63 p2034-2035.

122:600

VINOKUROV, VM, ZARIPOV, MM, STEPANOV, VG, CHIRKIN, GK and SHEKUN, LYa,
The electron paramagnetic resonance (EPR) of iron (III) in benitoite.
Zh. Strukt. Khim. (5/1) 64 p49-52.

100:650

VINOKUROV, VM, ZARIPOV, MM, STEPANOV, VG, POLSKII, YuE, CHIRKIN, GK and SHEKUN, LYa,
Electron paramagnetic resonance in natural chrysoberyl.
Fiz. Tverd. Tela (3/8) 61 p2475-2479.

100:890

VINOKUROV, VM, ZARIPOV, MM and VAFAEV, MR,
Fine structure of electron paramagnetic resonance spectrum in natural sapphire.
Zh. Eksp. Teor. Fiz. (37) 59 p302-304.

425

VOELKEL, G, WANDEWIG, S and WIDSCH, W,
Electron paramagnetic resonance as a method for investigation of the structure of coal.
Freib. Forschungsh. A (360) 66 p17-38.

133:625

WAIT, DF,

Hydrostatic pressure dependence of the paramagnetic resonance of an S-state ion in a non-cubic lattice. Mn^{2+} in calcite.

Phys. Rev. (132/2) 63 p601-607.

133:625

WAKABAYASHI, J,

Three-level maser materials: a survey of possible materials.

NASA Doc. N63-20413, 1962, 112 pp.

122:625

WAKABAYASHI, J,

Paramagnetic resonance spectrum of Fe^{3+} in calcite.

J. Chem. Phys. (38/8) 63 p1910-1912.

133:925

WALDNER, F,

Mn^{2+} spektrum paramagnetischer elecktronenresonanz (EPR) in einen natürlichen $MgAl_2O_4$ spinell.

Helv. Phys. Acta (35/7-8) 62 p756-764.

122:980

WALSH Jr., WM and RUPP, LW,

Paramagnetic resonance of trivalent Fe^{57} in zinc oxide.

Phys. Rev. (126/3) 62 p952-955.

100:505

WAUCHOPE, RD and HAGUE, R,

ESR in clay minerals.

Nature Phys. Sci. (233/42) 71 p141-142.

410:870

WEAVER, HE and SCHINDLER, P,

Electron paramagnetic resonance defects in quartz crystals.

Naturwiss. (51/4) 64 p81-82.

109:870

WEEKS, RA,

Paramagnetic spectra of E_2^1 centres in crystalline quartz.

Phys. Rev. (130/2) 63 p570-576.

100:870

WEEKS, RA,

Paramagnetic resonance and optical absorption in gamma-ray irradiated alpha-quartz: The Al centre.

J. Am. Ceram. Soc. (53/4) 70 p176-179.

122:133:154:510

WEEKS, RA,

Paramagnetic resonance spectra of Ti^{3+}, Fe^{3+} and Mn^{2+} in lunar plagioclases.

Trans. Am. Geophys. Union (53/4) 72 p551.

350

WEEKS, RA,

Magnetic phases in lunar material and their electron magnetic resonance spectra: Apollo 14.

In: Proc. 3rd Lunar Sci. Conf., Geochim. Cosmochim. Acta Suppl. 3 (3) 72 p2503-2517.

127:870

WEEKS, RA and ABRAHAM, M,

Electron spin resonance of irradiated quartz: atomic hydrogen.

J. Chem. Phys. (42/1) 65 p68-71.

350

WEEKS, RA, CHATELAIN, A, KOLOPUS, JL, KLINE, D and CASTLE, JG,
Magnetic resonance properties of some lunar material.
Science (167/3918) 70 p704-707.

350

WEEKS, RA and KOLOPUS, JL,
Magnetic resonance studies of lunar material.
Abst. papers Am. Chem. Soc. Apr. 1969 pMu03.

350

WEEKS, RA, KOLOPUS, JL, CHATELAIN, A and KLINE, D,
Magnetic and electrical properties of lunar materials.
Am. Ceram. Soc. (49/4) 70 p485.

350

WEEKS, RA, KOLOPUS, JL and KLINE, D,
Magnetic phases in lunar material and their electron paramagnetic resonance spectra: Apollo 14.
In: WATKINS, C, /Ed/: Lunar Science III. Lunar Sci. Contrib. No. 88 1972 p791-793.

120:132:350

WEEKS, RA, KOLOPUS, JL, KLINE, D and CHATELAIN, A,
Apollo 11 lunar material. Nuclear magnetic resonance of ^{27}Al and electron resonance of Fe and Mn.
In: Proc. Apollo 11 Lunar Sci. Conf., Geochim. Cosmochim. Acta Suppl. 1 (3) 70 p2467-2490.

154:885

WEEKS, RA and PURCELL, T,
Electron spin resonance of irradiation-produced defects in TiO_2 - interstitial Ti^{3+}.
Bull. Am. Phys. Soc. (13/3) 68, p435.

150:870

WEEKS, RA and SONDER, E,

Relations between magnetic susceptibility, electron spin resonance (ESR) and optical absorption of the E_1 centre in fixed silica.

In: Param. Reson. Proc. Int. Conf., 1st, Jerusalem 1962 (2) 63 p869.

150:870

WEIL, JA and ANDERSON, JA,

Electron spin resonance (EPR) of radiation-produced defects in doped quartz.

USAEC Rept. TID-15542, 1962, 4 pp.

410:835

WERTZ, J, AUXINS, P, GRIFFITHS, JHE and ORTON, JW,

Spin resonance studies of defects in magnesium oxide.

Disc. Farad. Soc. (28) 59 p136-141.

410:835

WERTZ, J, ORTON, J and AUZINS, P,

Spin resonance of point defects in magnesium oxide.

J. Appl. Phys. (33/1) 62 p322-328.

425

WHITAKER, A,

The ultimate structure of coal.

J. Inst. Fuels (28) 55 p218-223.

400:625

WIERSEMA, A,

Experiments on colour centres in Crestmore blue calcite.

USAEC Rept. UCRL-9494, 1960 33 pp.

133:690

WILDEMAN, TR,

The distribution of Mn^{2+} in dolomite by electron paramagnetic resonance.

Amer. Geophys. Union (50/4) 69 p357.

133:500

WILDEMAN, TR,

The distribution of Mn^{2+} in some carbonates by electron paramagnetic resonance.

Chem. Geol. (5/3) 70 p167-177.

435

WILLIAMS, RD,

Magnetic resonance and microwaves in the petroleum industry.

In: Am. Chem. Soc., Div. Pet. Chem., Symp. No. 32 1955 p85-102.

154:400:870

WRIGHT, FM, WEIL, JA, BUCH, T and ANDERSON, JH,

Titanium colour centres in rose quartz.

Nature (197/4864) 63 p246-248.

120:154:885

YAMAKA, E and BAILES, RG,

Paramagnetic resonance of iron group elements in rutile. I. The Ti^{47} and Ti^{49} hfs interaction.

Phys. Rev. A (135/1) 64 p144-148.

122:510

YARRINGTON, I.I,

Electron paramagnetic resonance study of Fe^{3+} in orthoclase.

Diss. Abs. Int. B (32/2) 70 p880.

425

YOKOZAWA, Y, MIYASHITA, I, KUGO, M and HIGBI, K,

Paramagnetic resonance absorption of coals and coal extracts.

Bull. Chem. Soc. Japan (28/7) 55 p536.

425

ZABRAMNYI, DT, NASRITDINOV, S and POMEMONOSTSEVA, OI,

Methods for studying the molecular structure of coals and humic acids.

Uzb. Khim. Zh. (16/3) 72 p65-66.

100:625

ZAITOV, MM,

The effect of uniaxial pressure on the EPR spectrum of ions in calcite.

Fiz. Tverd. Tela (9/2) 67 p453-456.

114:725

ZAMOTRINSKAYA, EA, BRYSHEV, EK and SHAULER, AS,

Copper EPR in fosterite ceramics.

Izv. Vyssh. Ucheb. Zaved. Fiz. (10/3) 67 p16-21.

133:540

ZARIPOV, MM, MANTAZIN, ShF and STEPANOV, VG,

Calculation of the paramagnetic resonance of Mn^{++}.

Opt. Spektrosk. (14/3) 63 p421-422.

154:720

ZARIPOV, MM, NOVOSHILOV, AI, SAMOILOVICH, MI, SURGUZEV-BORT, AA and

STEPANOV, VG,

EPR of Ti^{3+} ions in synthetic fluorphlogopite.

/Translated from: Geokhim. (1967/3) 67 p276-377/.

Geochem. Int. (4/2) 67 p331-332.

100:880

ZARIPOV, MM and SHAKONIN, YuYa,

Paramagnetic resonance in synthetic ruby.

Zh. Eksp. Teor. Fiz. (30) 56 p291-295.

100:605

ZARIPOV, MM and SHAMONIN, YuYa,

Paramagnetic electron resonance in natural beryls.

Izv. Akad. Nauk SSSR, Ser. Fiz. (20) 56 p1224-1225.

455

ZELLER, EJ, LEVY, PM and MATTERN, PL,

Geologic dating by electron spin resonance.

USAEC Rept. BNL-11080 1967 13p.

100:870

ZIL'BERSHTEIN, KhI, IOFFE, VA and FEDEROV, YuF,

Electron paramagnetic resonance in irradiated quartz single crystals with aluminium impurities.

Kristallogr. (10/5) 65 p727-731.

107:660

ZVEREV, GM and PETELINA, NG,

Electron paramagnetic resonance of Co^{++} ions in corundum.

Zh. Eksp. Teor. Fiz. (42) 62 p1186-1190.

112:660

ZVEREV, GM and PROKHOROV, AM,

Fine and hyperfine structure of the paramagnetic resonance spectrum of the chromic ion in corundum.

Zh. Eksp. Teor. Fiz. (34) 58 p513-514.

159:660

ZVEREV, GM and PROKHOROV, AM,

Electron paramagnetic resonance of the vanadium^{+++} ions in corundum.

Zh. Eksp. Teor. Fiz. (34) 58 p1023-1024.

107:660

ZVEREV, GM and PROKHOROV, AM,

Electron paramagnetic resonance of Cobalt (II) ions in corundum.

Zh. Eksp. Teor. Fiz. (36) 59 p647-648.

159:660

ZVEREV, GM and PROKHOROV, AM,

Spectrum of the electronic paramagnetic resonance of V^{+++} in corundum.

Zh. Eksp. Teor. Fiz. (38) 60 p449-454.

107:660

ZVEREV, GM and PROKHOROV, AM,

Paramagnetic resonance and spin lattice relaxation of the Co^{++} ion in corundum.

Zh. Eksp. Teor. Fiz. (39) 60 p57-63.

159:660

ZVEREV, GM and PROKHOROV, AM,

The electron paramagnetic resonance of the V^{+++} ion in corundum.

Zh. Eksp. Teor. Fiz. (40) 61 p1016-1018.

SUBJECT INDEX

Paramagnetic centres

MINERALS 540-990

Minerals (unspecified)	540	Datolite	675
Adamite	550	Diamond	680
Alexandrite	555	Diopside	685
Amethyst	560	Dolomite	690
Amklygorite	565	Emerald	695
Anatase	570	Epsomite	700
Andalusite	575	Eucryptite	705
Anhydrite	580	Faujasite	710
Apatite	590	Fluorite	715
Apophyllite	595	Fluorphlogopite	720
Aragonite	596	Fosterite	725
Benetoite	600	Gaylussite	730
Beryl	605	Goethite	735
Blodite	610	Gold	740
Brookite	615	Hematite	745
Brucite	620	Herderite	750
Calcite	625	Hissingerite.	755
Calcium Carbonate (unspecified)	626	Illite	757
Cancrinite	630	Ilmenite	760
Cassiterite	635	Kaolinite	765
Celestine	640	Kyanite	770
Cerussite	645	Lazurite	775
Chrysoberyl	650	Lime	780
Clinoptilolite	652	Magnesite	785
Cordierite	655	Magnetite	790
Corundum	660	Monticellite	795
Cristobalite	665	Montmorillonite	800
Danburite	670	Morinite	802

Muscovite	805	Taeniolite	945
Natrolite	810	Talc	950
Nepheline	815	Thorianite	955
Newberyite	820	Thortveitite	960
Northupite	825	Topaz	961
Olivine	830	Tourmaline	962
Periclase	835	Tremolite	963
Perovskite	840	Tourquoise	965
Petallite	845	Ussingite	970
Phenakite	850	Willemite	975
Phlogopite	855	Zincite	980
Pyrromorphite	860	Zircon	985
Pyrrhotine	865	Zoisite	990
Quartz	870		
Rhodochrosite	875		
Ruby	880		
Rutile	885		
Sapphire	890		
Scheelite	895		
Siderite	900		
Smithsonite	905		
Sodalite	910		
Sphalerite	915		
Sphene	920		
Spinel	925		
Spodumene	930		
Struvite	935		
Sylvine	940		

APPENDIX THREE

STEREOGRAMS IN GEOLOGY

The need for a quick, inexpensive and meaningful method of representing three-dimensional data has been apparent in many scientific fields. This need can be fulfilled by the use of stereograms.

In this technique, left and right stereo images are prepared using simple geometric principles and when placed in a stereo viewer, a three-dimensional model can be visualised. Stereograms have been applied in biometry, e.g. forestry studies (Fraser and Kovats, 1966) and numerical taxonomy (Rohlf, 1968), but has had little use in geology (with the exception of palaeontology (Kaesler, 1970; Raup, 1970), palaeoecology (Kaesler and Taylor, 1970) and aerial photography).

Data collected in a geological study often consists of measurements on a number of variables. Normally such data is illustrated as two-dimensional plots of one variable against another. However, it is often simpler and more advantageous to describe the relationship between any three of the variables. In the past restrictions on the illustration of three-dimensional data had been due to the laborious and time-consuming construction of models and stereograms. The use of computers and high speed plotters reduces this time considerably and enables one to apply stereograms in many three-variable problems.

Geological data can for the convenience of this appendix be divided into areal and non-areal data. Geochemical prospecting data as a suitable example of areal data can be easily illustrated using stereograms - the co-ordinates of the sample point constituting two of the stereogram variables and any metal values, the third. An example of non-areal data described by stereograms is factor scores on the first three axes in a principle components analysis.

This appendix describes the basic details of stereogram preparation and interpretation. Possible application of the technique to the illustration of various geological data is also described.

METHOD

One of the most effective ways of displaying the dimensionality of real or imaginary objects has been the construction of small scale three-dimensional models. The difficulty exercised and the time consumed on such models are readily appreciated. A realistic alternative is provided by stereograms.

The basis of this technique lies in the ability of the human brain to visualise a three-dimensional object by viewing the object from two separate points, corresponding to the eye positions. The principle is illustrated in Figure A3.1, in which the eyes are positioned at E_R and E_L, separated by a distance $(r_x - l_x)$ and at a height h_e from the X-Y plane. When a point such as $H(X',Y',Z')$, a distance h_p above the X-Y plane, is viewed with the left eye, an image will apparently form at $H_L(X_L,Y_L,Z_L)$. Similarly, viewed with the right eye, another image will appear at $H_R(X_R,Y_R,Z_R)$. Since the human brain successfully fuses the two images obtained to form a point (H) in space, one only needs to prepare two diagrams (a stereo pair or stereogram) corresponding to the right and left eye viewing positions for the brain to 'visualise' any object, real or imaginary.

Some people can see the three-dimensional image without recourse to optical aids. However, most people require the use of a lens or mirror stereoscope.

COMPUTATION

The computation and the geometric basis for the preparation of left and right stereo images are very simple. As previously noted, left stereo image of a point $H(X',Y',Z')$ will form at $H_L(X_L,Y_L,Z_L)$. In order to calculate this image, we need to determine the co-ordinates (X_L,Y_L and Z_L) of H_L. This is achieved by considering the geometric properties of similar triangles.

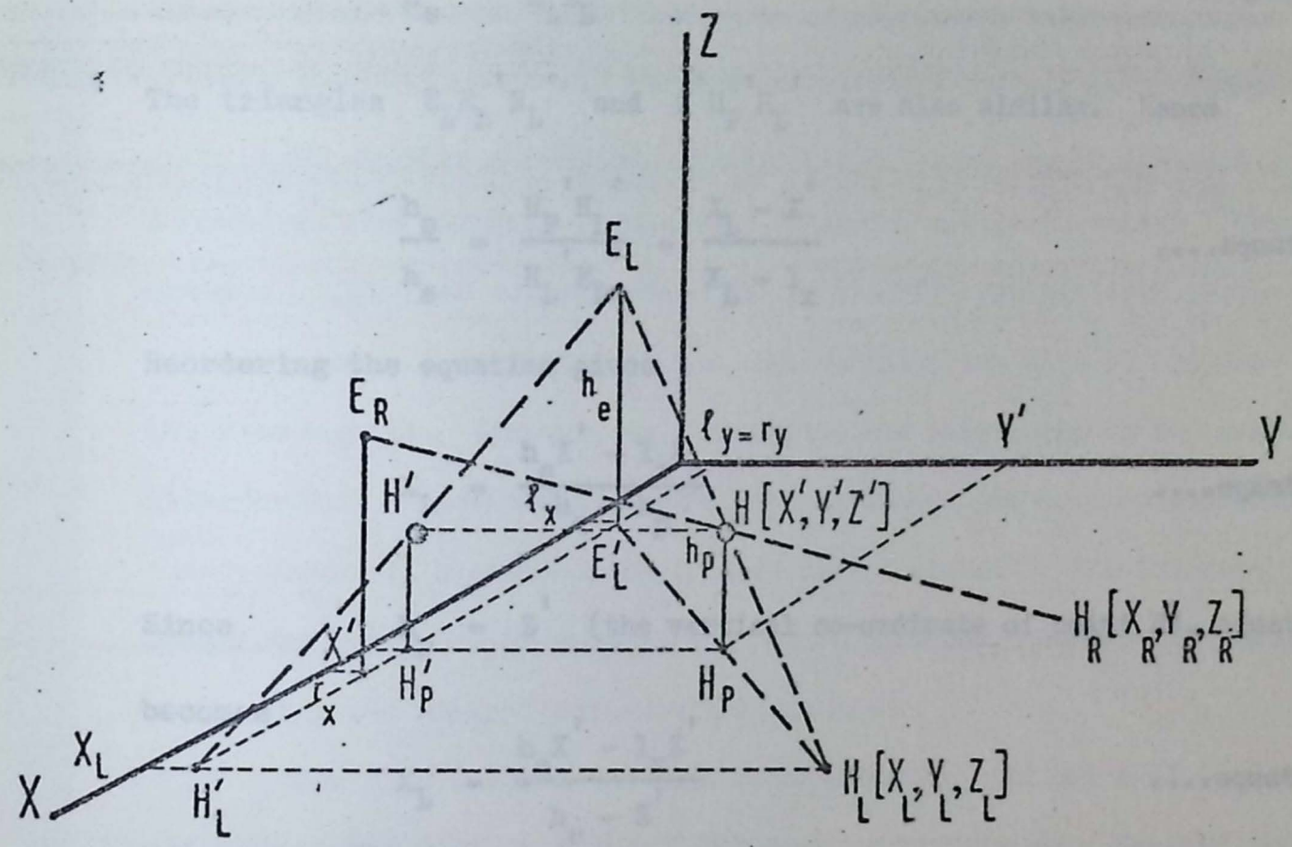

Fig. A3.1 Principles of stereogram computation.

The triangles $E_L E_L' H_L$ and $H H_P H_L$ are similar triangles such that

$$\frac{h_p}{h_e} = \frac{H_P H_L}{H_L E_L} \qquad \text{....equation 1}$$

The triangles $E_L E_L' H_L'$ and $H' H_P' H_L'$ are also similar. Hence

$$\frac{h_p}{h_e} = \frac{H_P' H_L'}{H_L' E_L'} = \frac{X_L - X'}{X_L - l_x} \qquad \text{....equation 2}$$

Reordering the equation gives

$$X_L = \frac{h_e X' - l_x h_p}{h_e - h_p} \qquad \text{....equation 3}$$

Since $h_p = Z'$ (the vertical co-ordinate of point H), equation 3 becomes

$$X_L = \frac{h_e X' - l_x Z'}{h_e - Z'} \qquad \text{....equation 4}$$

Similarly,

$$Y_L = \frac{h_e Y' - l_y Z'}{h_e - Z'}$$

By the same means, the co-ordinates of the right stereo image are given by

$$X_R = \frac{h_e X' - r_x Z'}{}$$

$$Y_R = \frac{h_e Y' - r_y Z'}{h_e - Z'}$$

To achieve the most desirable three-dimensional effect, it is advisable to range-transform the values on each axis. Since some geological data is log-normally distributed (e.g. geochemical data), it may also be useful to logarithmically transform the values on the axis representing the dependent variable.

AREAL DATA

Stereograms are ideally suited to the illustration of geochemical data. Using this technique, spatial distributions of stream sediment sample points can be viewed and areas of high metal values examined without resorting to trend surface analysis and contouring programs.

For example Figure A3.2 represents a map of log-transformed lead concentrations obtained by analysis of stream sediment samples. The areas of high lead concentration can be clearly distinguished in the North-eastern region. Estimates of the concentration can also be obtained from the stereograms. However, as stereograms are only designed to provide illustration of quantitative data, the estimates can only be relative.

However, a combination of this highly effective illustrative technique and a simple sample site map can provide considerable information concerning the mineralisation within an area.

From Figure A3.2, the high metal concentration and a line of cut-off associated with it in the North-east part of the area suggest the presence of mineralisation which can be confirmed by a more detailed survey.

Stereograms have also been used to distinguish mineralised and barren sample sites from the Pirejman area of South-east Turkey. Figure A3.3 shows the scores of stream sediment samples on the first discriminant axis in a multivariate discriminant analysis of geochemical stream sediment data plotted against site co-ordinates. A sample site map (Figure D.53 in Celenk, 1972) can be used in conjunction with the stereogram to reveal areas of mineralisation. As the first discriminant axis was interpreted as a mineralisation/non-mineralisation axis (Celenk, 1972), a mineralised area in the centre and along the lower edge of the stereogram can be distinguished as having generally higher scores than along the top edge.

Stereograms could be used to map folded and faulted beds. Figure A3.4 illustrates a diapiric structure noted from borehole and outcrop

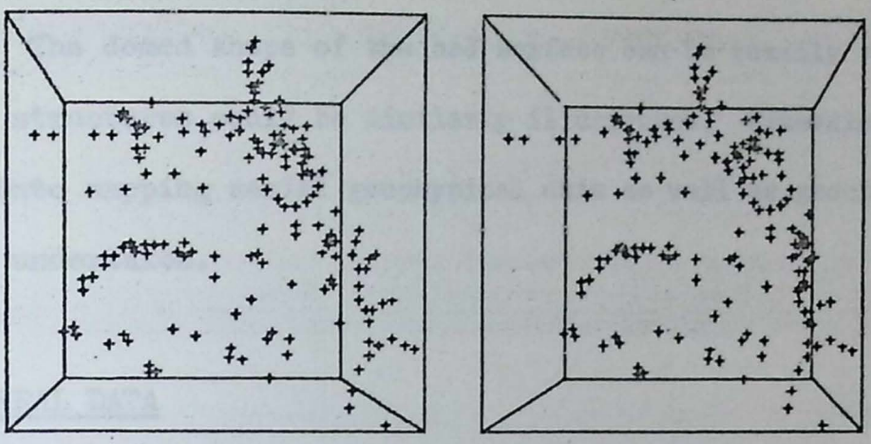

Fig. A3.2 Lead concentrations in stream sediments. A lead mineralised area occurs in the NE corner.

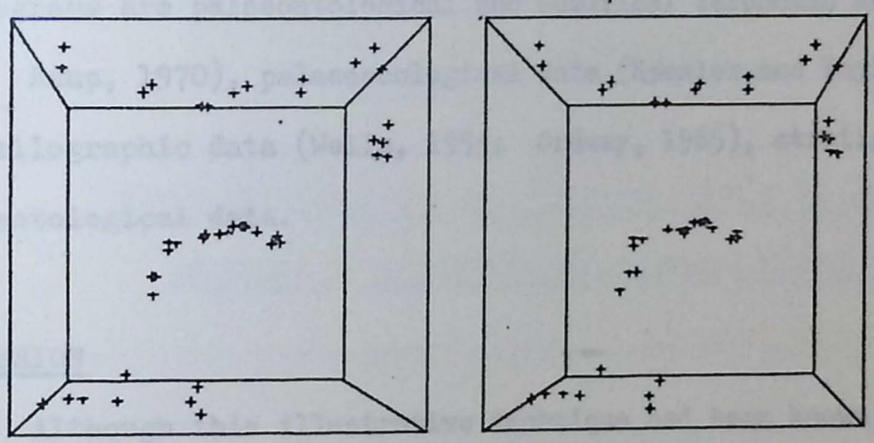

Fig. A3.3 Discriminant scores of stream sediment samples plotted against site co-ordinates.

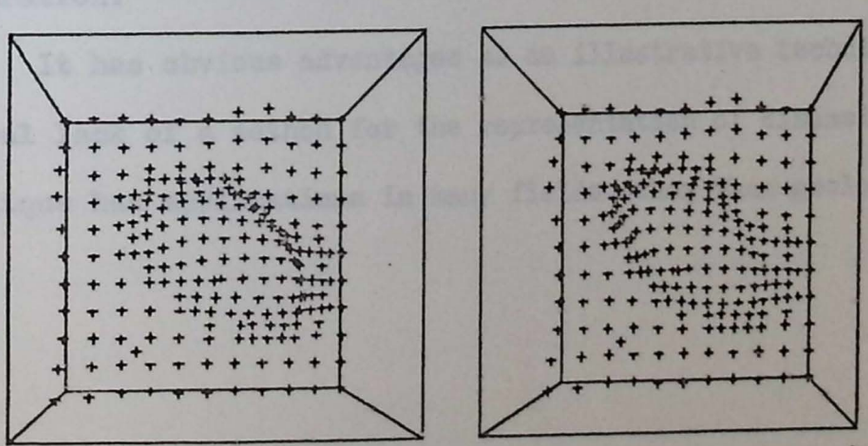

Fig. A3.4 Diapiric structures.

data. The domed shape of the bed surface can be readily visualised and other structures could be similarly illustrated. Extensions of this work into mapping aerial geophysical data as well as geochemical data are being undertaken.

NON-AREAL DATA

It has been mentioned previously that a typical non-areal data situation could be the illustration of multivariate statistical data (Fraser and Kovats, 1966).

Other types of non-areal data suitable for illustration by stereograms are palaeontological and numerical taxonomic data (Kaesler, 1970; Raup, 1970), palaeoecological data (Kaesler and Taylor, 1970), crystallographic data (Wells, 1954; Ordway, 1965), stratigraphical and sedimentological data.

CONCLUSION

Although this illustrative technique had been known for some time, the laborious construction of the stereograms has prevented its application to geological problems. However, using a computer, it is now possible to plot stereograms of geochemical data with minimal data preparation.

It has obvious advantages as an illustrative technique and with the general lack of a method for the representation of dimensional data, the technique has applications in many fields other than geology.

APPENDIX FOUR

THE PREPARATION OF SHALE SPECIMENS FOR X-RAY DIFFRACTION ANALYSIS BY A SUCTION-ONTO-MEMBRANE FILTER METHOD

One major requirement of quantitative X-ray diffraction analysis of shale mineralogy is a simple, accurate and reproducible method of sample preparation. However, problems arise firstly, with the tendency of the clay minerals to assume preferred orientations which cannot be accurately reproduced from sample to sample and secondly, with the segregation of mineral phases during the settling stage. Quantitative determination of mineral percentages in shales by X-ray diffraction must avoid both these problems, and a number of techniques for producing randomly orientated samples have been proposed, e.g. Hughes and Bohor's (1970) spray drying technique, a method employing polyester foam sheeting (Thomson, Duthie and Wilson, 1972) and others by Brindley and Kurtossy (1961), Jonas and Kuykendall (1966), Martin (1966) and Niskanen (1964). However, all these techniques were developed specifically for clay mineral studies and few are suitable for the analysis of shale samples.

A method has been developed for the quantitative mineralogical analysis of shales by X-ray diffraction using Millipore filter equipment and membrane filters (Millipore equipment is manufactured by Millipore Filter Corporation, Bedford, Massachusetts, U.S.A.). The method has proved simple and quick to operate and the accuracy and reproducibility are very high in comparison with alternative techniques (Chapter 2). This technique has been successfully applied in a study of Upper Pennsylvanian and Lower Permian shales of Kansas, U.S.A.

SAMPLE PREPARATION

Approximately 0.05 gm of ground shale sample (less than 60 microns) is placed in a small beaker and 20 ml of distilled water added by pipette. The materials are then agitated by sonic probe and the disaggregated shale/water mixture is placed in a Millipore filter funnel (Figure A4.1). Vacuum pressure applied to the membrane filter sucks all the liquid through the filter in 20-30 seconds preventing orientation and segregation

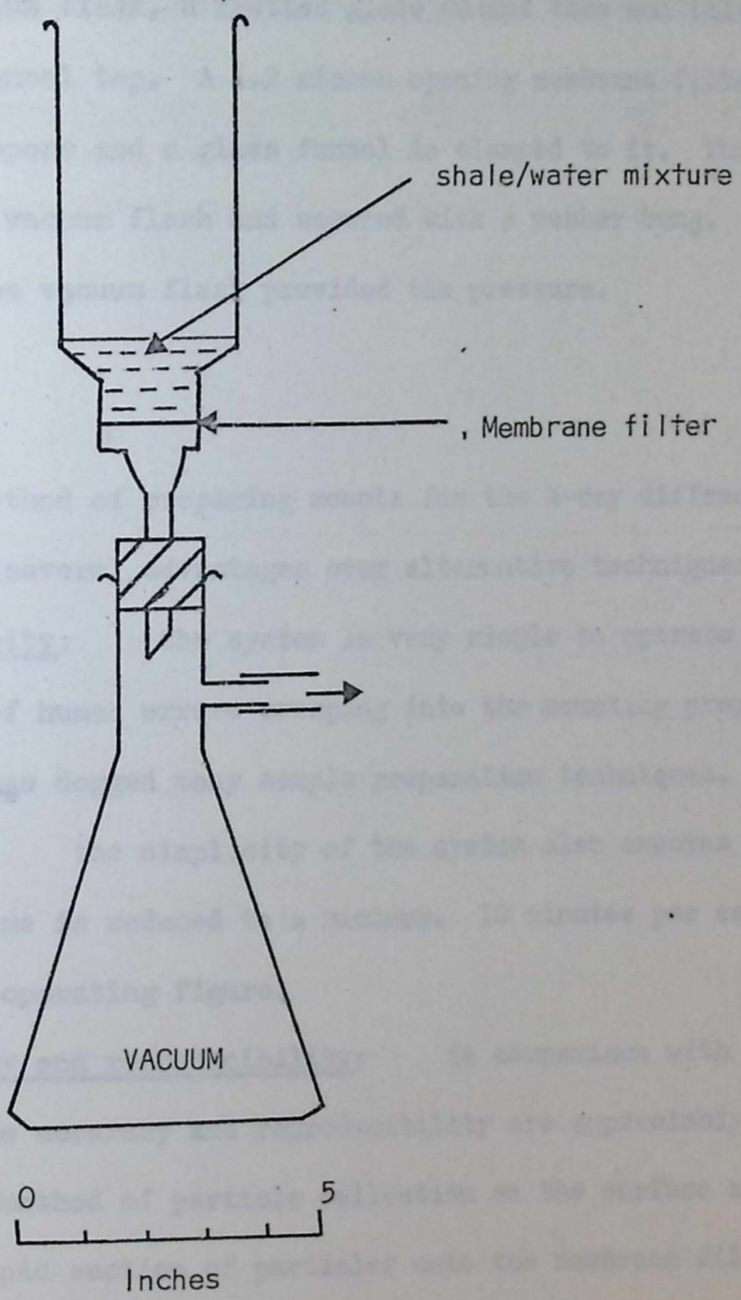

Fig. A4.1. Millipore filter Apparatus

of minerals. The filter paper is removed from the apparatus, and taped onto a microscope slide. After drying for a few minutes, the slide-mounted filter paper can be examined by X-ray diffraction.

The Millipore filter apparatus (Figure A4.1) consists of four parts - a vacuum flask, a fretted glass funnel base and filter support, a clamp and a funnel top. A 1.2 micron opening membrane filter is placed on the filter support and a glass funnel is clamped to it. The base is then placed in the vacuum flask and secured with a rubber bung. A water pump attached to the vacuum flask provided the pressure.

DISCUSSION

This method of preparing mounts for the X-ray diffraction analysis of shales has several advantages over alternative techniques.

1. Simplicity: the system is very simple to operate and prevents the majority of human errors creeping into the mounting preparation, a failure that has dogged many sample preparation techniques.

2. Speed: the simplicity of the system also ensures that the preparation time is reduced to a minimum. 10 minutes per sample seems to be an optimum operating figure.

3. Accuracy and reproducibility: in comparison with standard techniques, the accuracy and reproducibility are appreciably higher. This is due to the method of particle collection on the surface of the filter paper. The rapid suction of particles onto the membrane filter obviates preferential settling and orientation. Any preponderance of non-flaky minerals in the shales will also aid the random orientation of mineral grains.

The technique was found to be suitable for large numbers of shale samples and has been successfully applied to the mineralogical analysis of the Upper Pennsylvanian and Lower Permian shales of Kansas, U.S.A. This technique has only one disadvantage when applied to these shales - no

detailed high temperature analysis of clay minerals may be undertaken due to the nature of the mount. In this case, an alternative technique, i.e. ground dry sample moulded into a pellet using a high pressure press (Hildago and Renton, 1970), may prove to be a suitable substitute. However, the value of the method lies in its speed, accuracy, simplicity and reproducibility and as such provides a "quick look" technique for the mineralogical analysis of shales.

APPENDIX FIVE

ELECTRON SPIN RESONANCE SPECTRA OF SELECTED CARBONATES, SULPHATES AND CLAY MINERALS

This study was conducted to establish the nature of free spin features in shale ESR spectra (Chapter 6).

A number of common carbonate, sulphate and clay minerals were chosen to represent possible constituent minerals of the Upper Pennsylvanian and Lower Permian shales of Kansas, U.S.A. Table A5.1 contains a list of these minerals, provided by Dr. R.J. King of the Geology Department, University of Leicester, with their standard chemical formulae and localities.

Small pieces of mineral were ground with a pestle and mortar and analysed on a Varian E-3 X-band Spectrometer using the procedure described in Chapter 6. The majority of these minerals have never been examined by ESR previously and it is hoped that the spectra recorded in this appendix (Figures A5.1 to A5.15) will serve as reference spectra for future experimental studies on individual minerals in a similar manner to the service provided to organic chemists by the ESR spectra recorded in Bielski and Gebicki (1967).

The spectra have brief descriptions as figure captions but it was beyond the scope of this thesis to perform experimental work to confirm these assertions. The descriptions must therefore be considered to be suggestions rather than fact. The figures include where necessary, references to other experimental ESR spectra on minerals.

TABLE A5.1 COMMON MINERALS REPRESENTING POSSIBLE CONSTITUENTS OF UPPER PENNSYLVANIAN AND LOWER PERMIAN SHALES OF KANSAS

	MINERAL NAME	CHEMICAL FORMULA	MINERAL LOCALITY
1.	Strontianite	$SrCO_3$	Whitesmith Mine, Strontian, Argyllshire, U.K.
2.	Rhodochrosite	$MnCO_3$	Emma Mine, Butte, Montana, U.S.A.
3.	Chalybite	$2(FeCO_3)$	Ivigtut, Greenland.
4.	Barytes	$BaSO_4$	Silverband Mine, Knock, Westmoorland, U.K.
5.	Celestine	$SrSO_4$	Yate, Gloucestershire, U.K.
6.	Anhydrite	$CaSO_4$	Billingham, Durham, U.K.
7.	Kaolinite	$Al_4Si_4O_{10}(OH)_8$	St. Austell, Cornwall, U.K.
8.	Dickite	$Al_4Si_4O_{10}(OH)_8$	San Juanito, Chichuahua, Mexico.
9.	Halloysite	$Al_4Si_4O_{10}(OH)_8$	Wagon Wheel Gap, Colorado, U.S.A.
10.	Vermiculite	$Mg_3Si_4O_{10}(OH)_2.xH_2O$	Ampandrandar, Madagascar.
11.	Chlorite (Pennine)	$Mg_5Al(AlSi_3O_{10})(OH)_8$	Traversella, Piedmont, Italy.
12.	Illite	$KAl_2(AlSi_3O_{10})(OH)_2$	Morris, Illinois, U.S.A.
13.	Montmorillonite	$Al_2Si_4O_{10}(OH)_2.xH_2O$	Clay Spur, Wyoming, U.S.A.

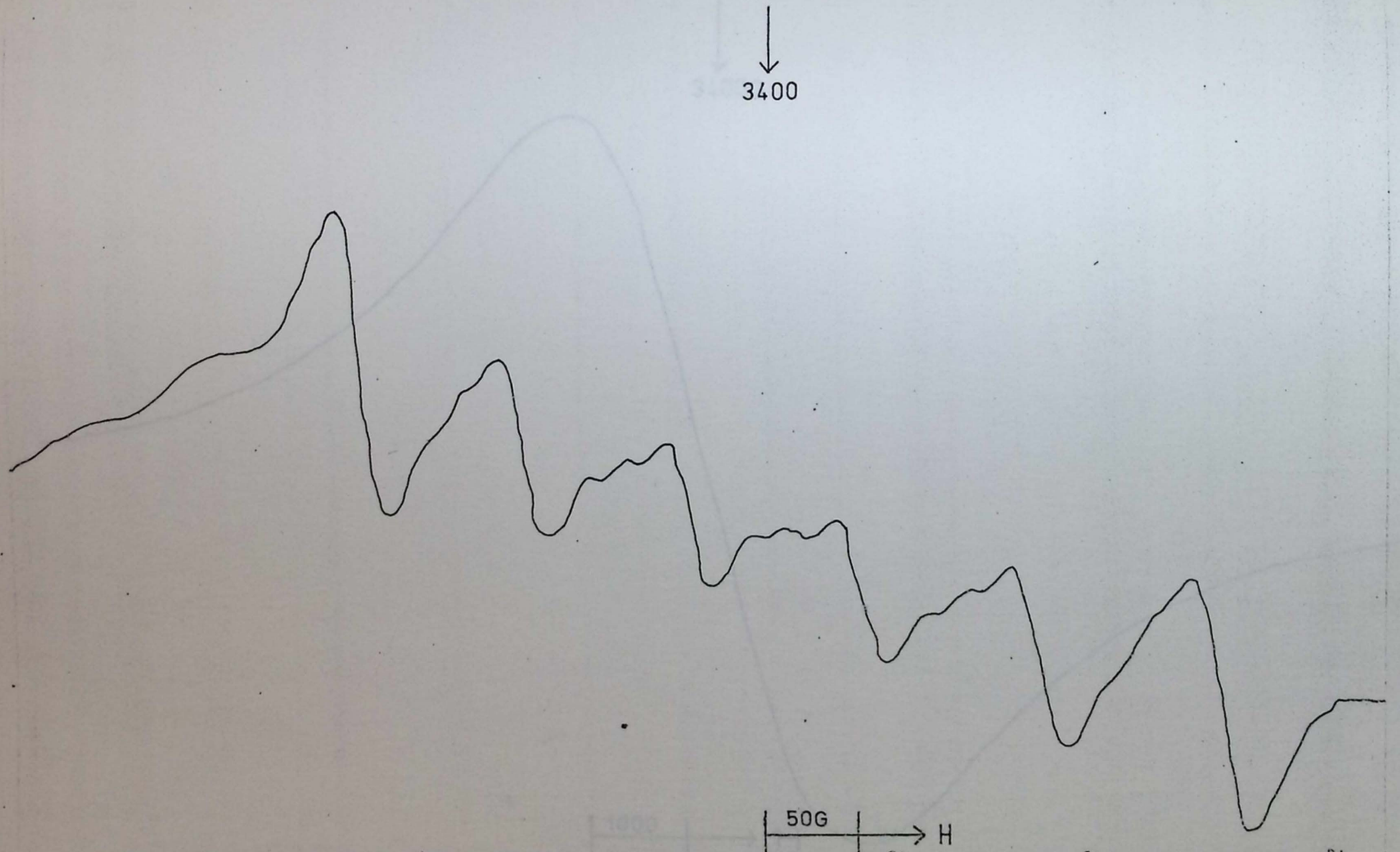

Fig. A5.1, A room temperature ESR spectra of strontianite showing typical Mn^{2+} features. The Mn^{2+} is substituting for Sr^{2+} in the $Sr^{2+}CO_3^{2-}$ lattice. The hyperfine splitting is 100G approximately.

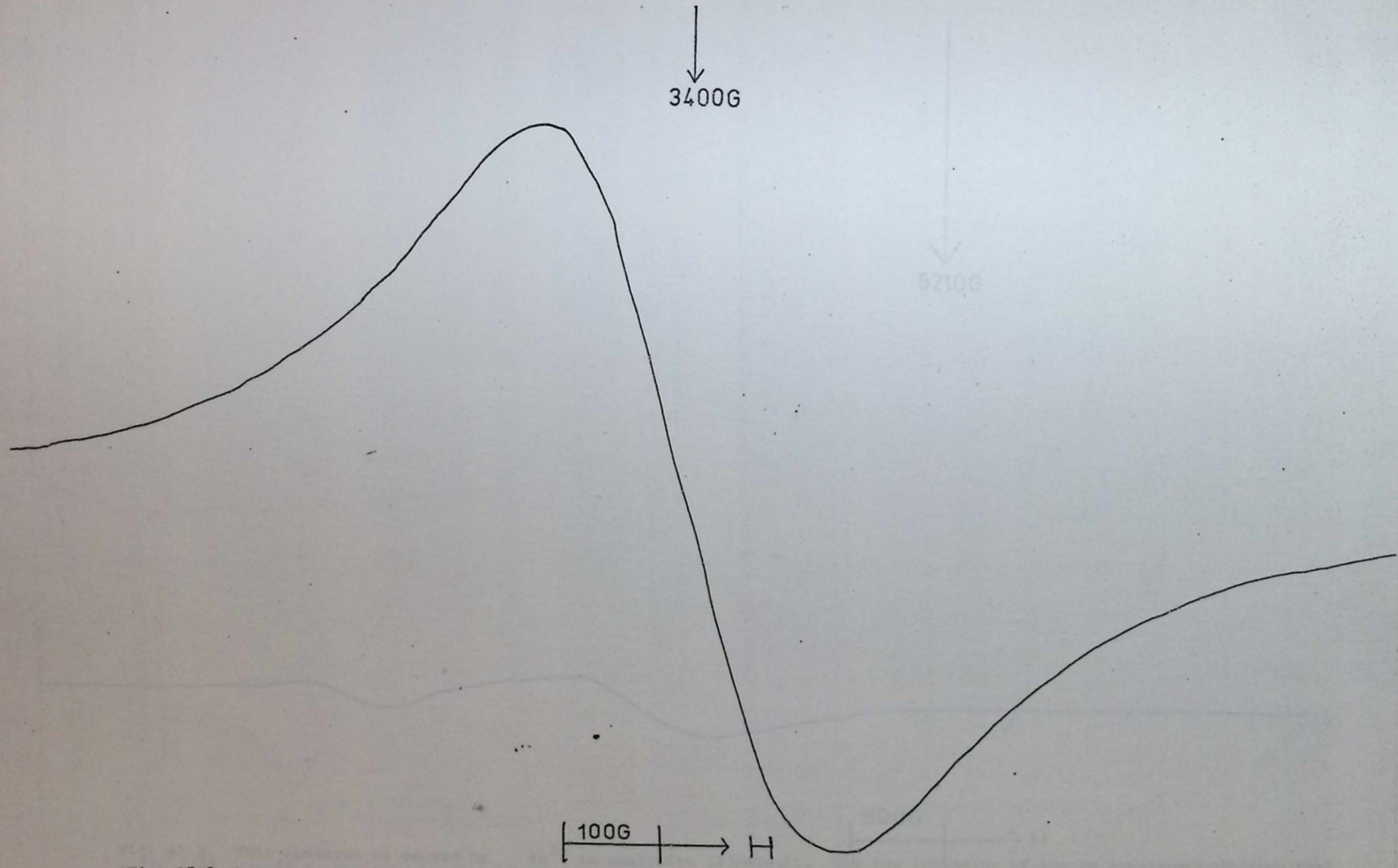

Fig. A5.2. A room temperature spectra of rhodochrosite.

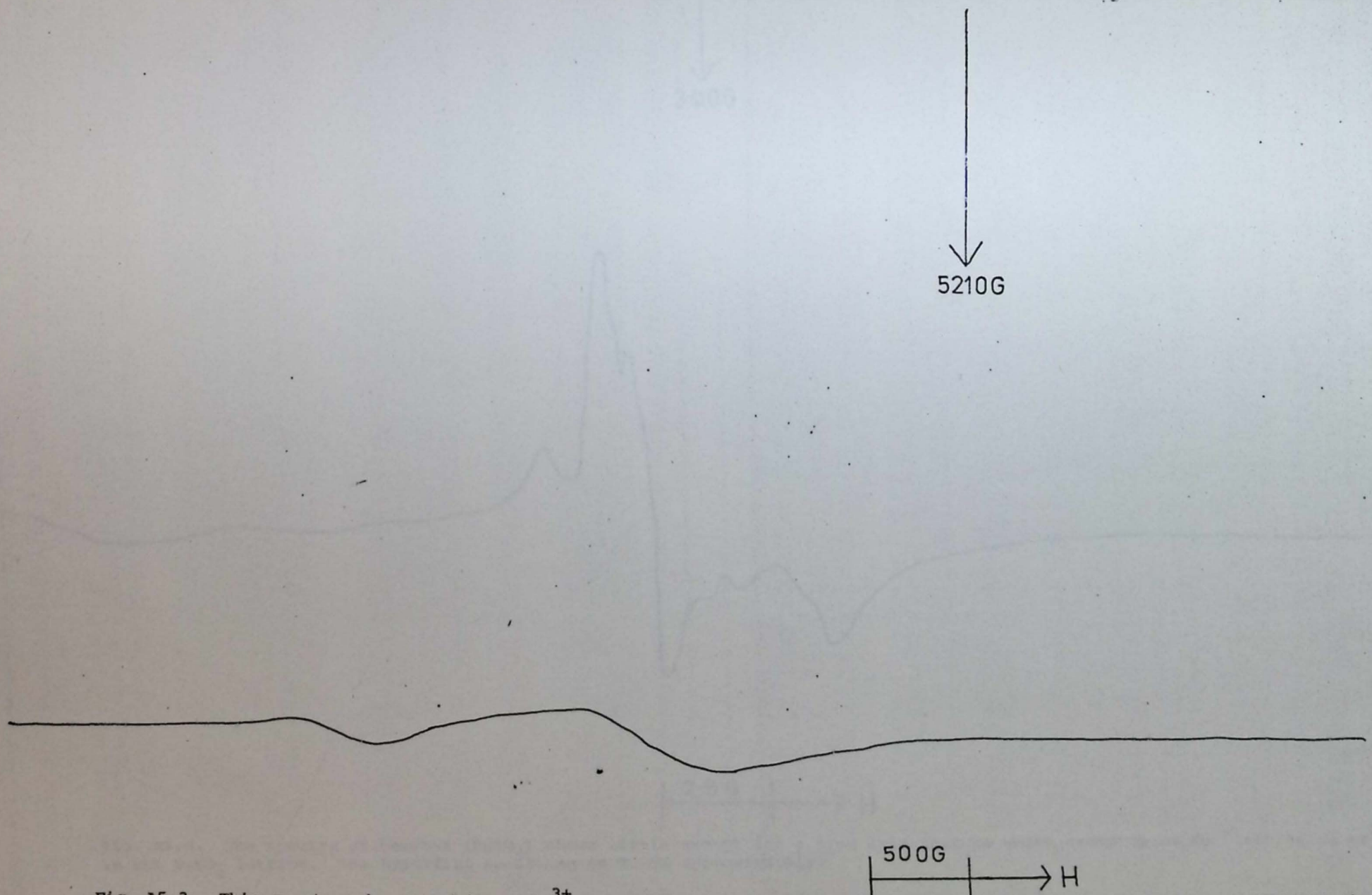

Fig. A5.3. This spectrum is caused by Fe^{3+} in chalybite ($2(FeCO_3)$). The low intensity of the Fe spectrum indicates that $Fe^{2+} \gg Fe^{3+}$, (Fe^{2+} is not detectable by ESR).

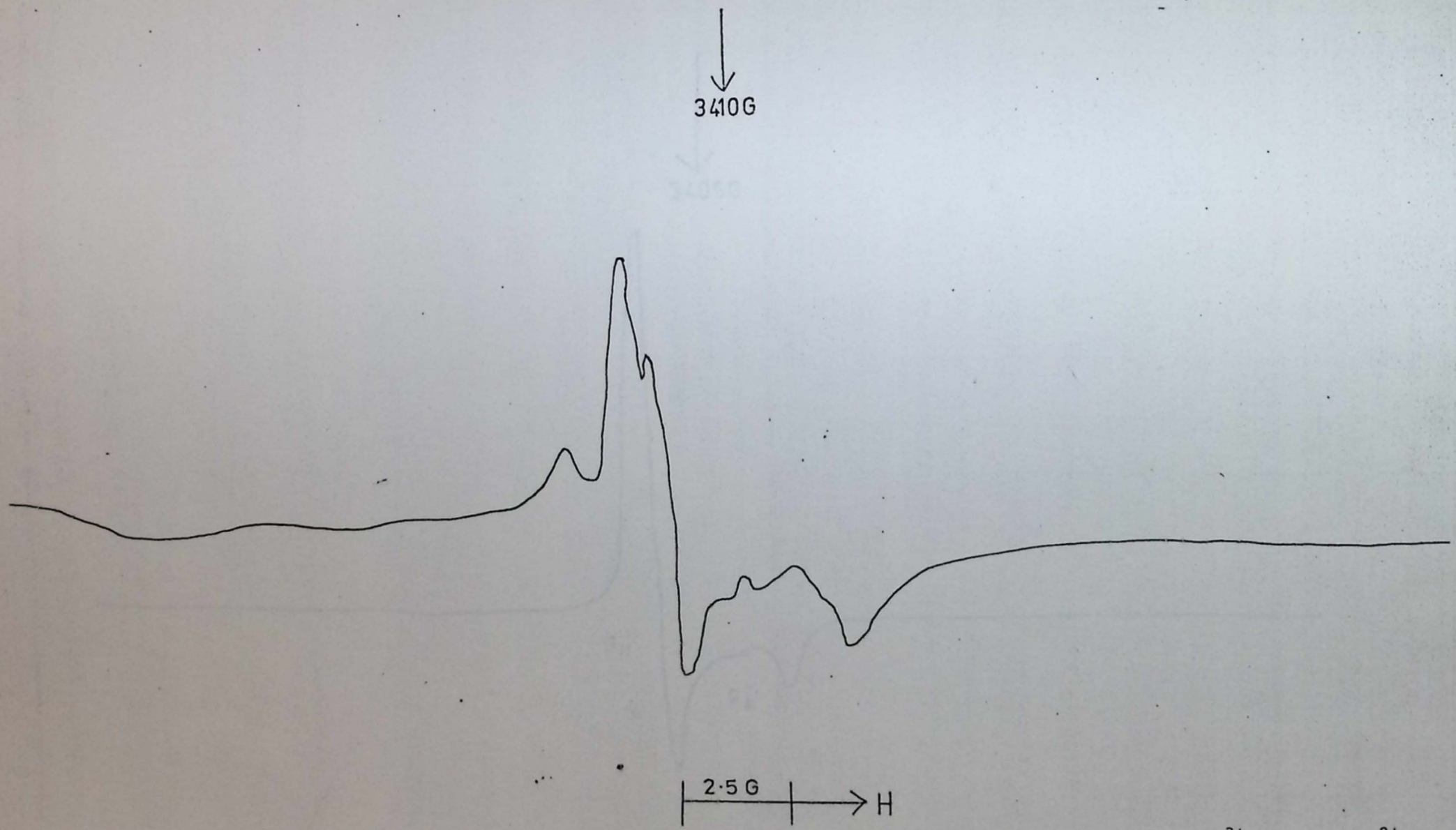

Fig. A5.4. The spectra of barytes ($BaSO_4$) shows little except for a free spin feature which seems to be Fe^{3+} replacing Ba^{2+} in the $BaSO_4$ lattice. The hyperfine splitting is 1.25G approximately.

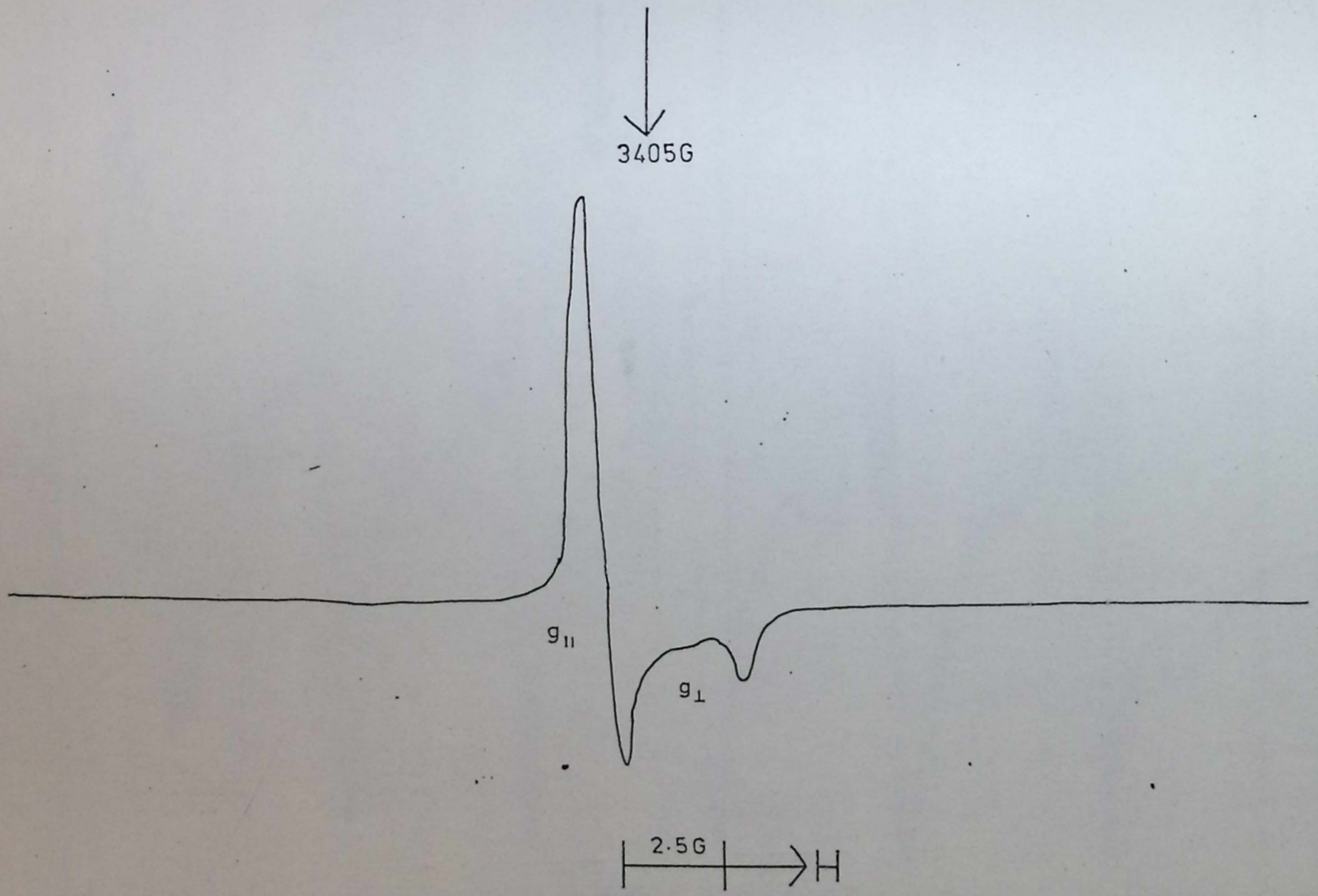

Fig. A5.5 Celestine ($SrSO_4$) unlike strontianite ($SrCO_3$) shows no Mn^{2+} but does exhibit free spin features, the origin of which are unknown. Fe^{3+} may be a contributor to this spectrum. The hyperfine splitting of this feature is 3.75G.

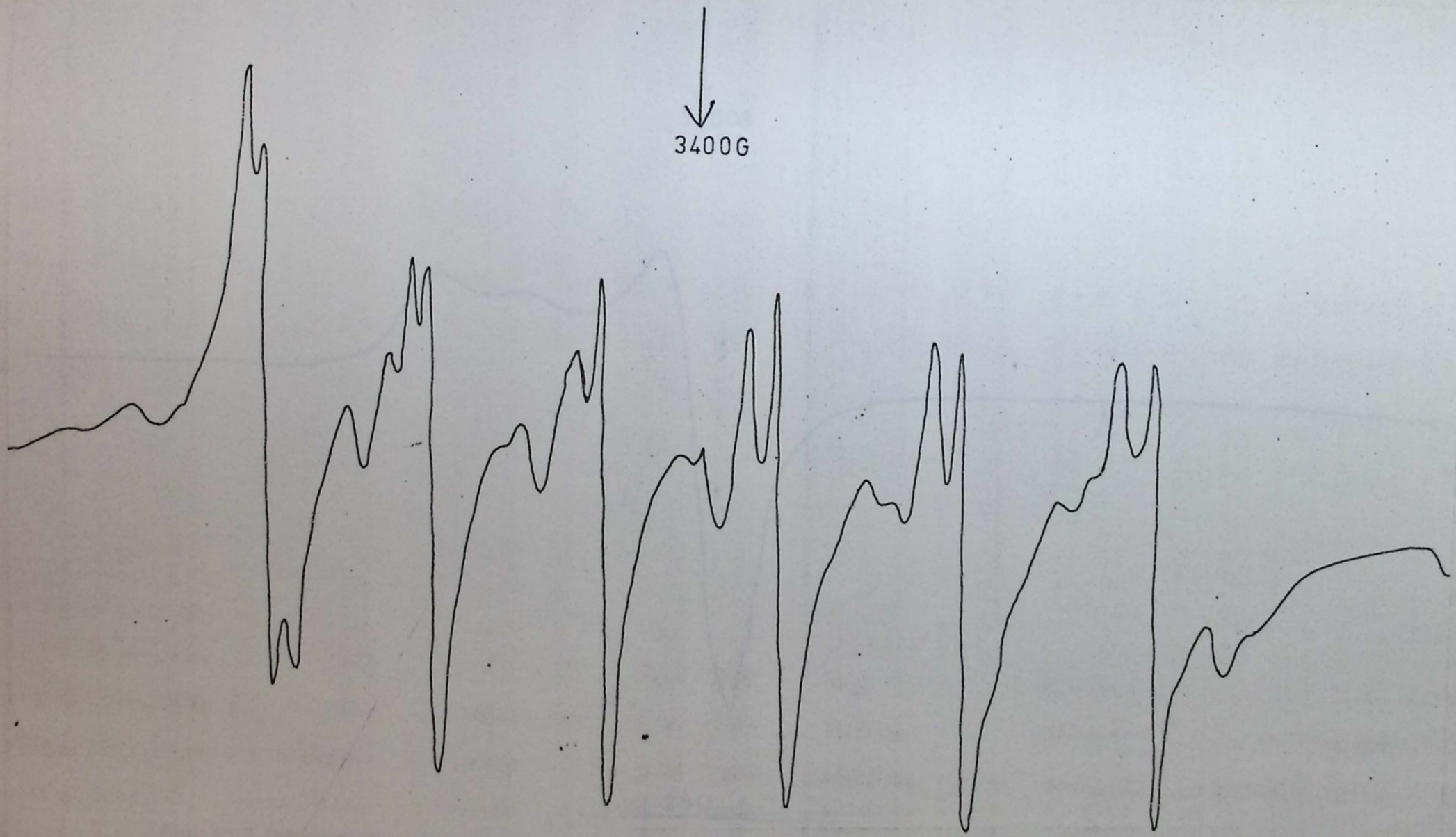

Fig.A5.6 Mn^{2+} is found in anhydrite ($4(CaSO_4)$ substituting for Ca^{2+} in the $CaSO_4$ tetrahedron. A free spin feature was detected but the low peak intensity prevented accurate determination of its origin

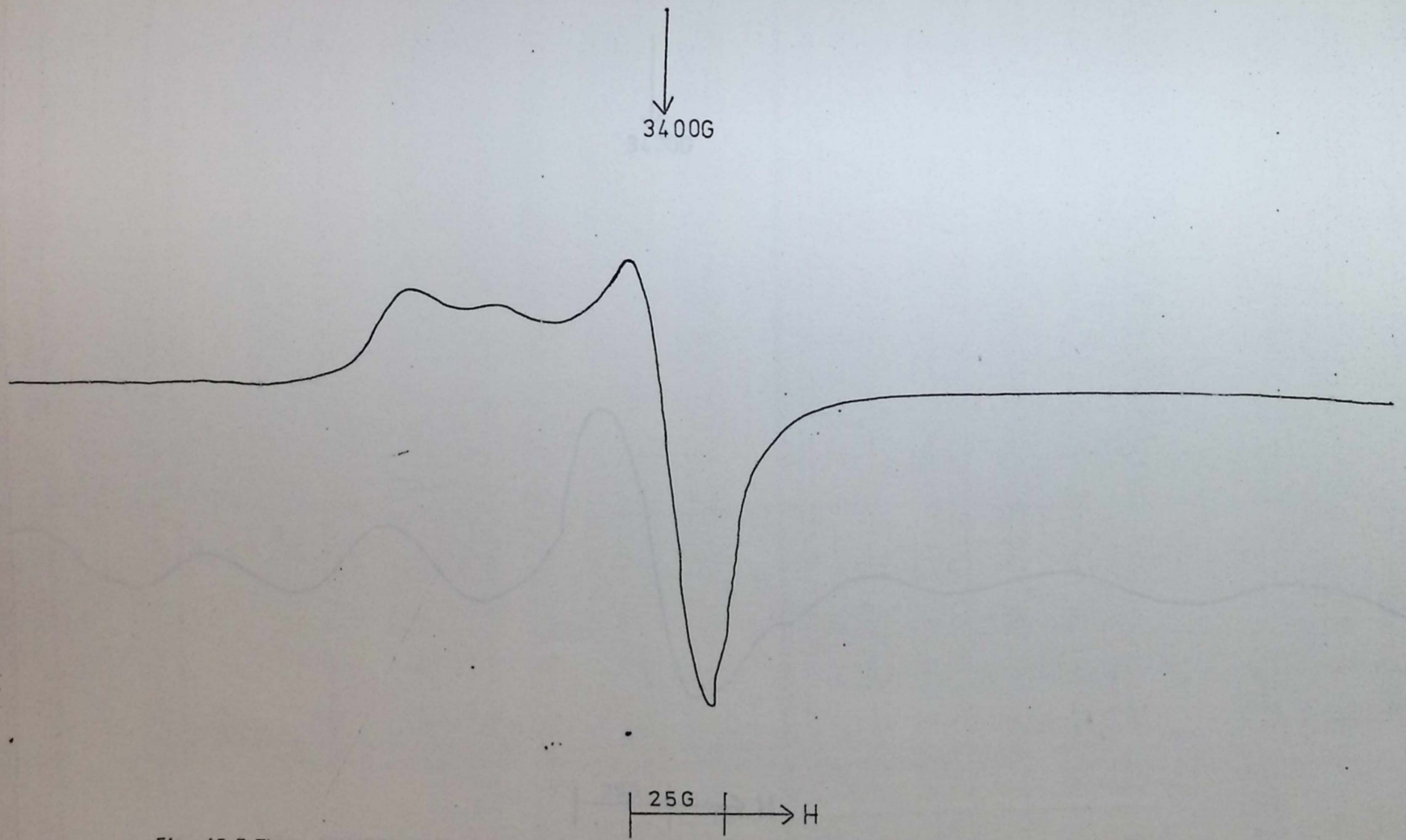

Fig. A5.7. The asymmetric double peak of kaolinite is identical to that reported by Friedlander et al. (1963), Wauchope and Hague (1971) and Angel and Hall (1973). Angel and Hall have suggested that this may be caused by a tetrahedrally co-ordinated Fe^{3+} ion whereas Wauchope and Haque have identified it as an oxygen species.

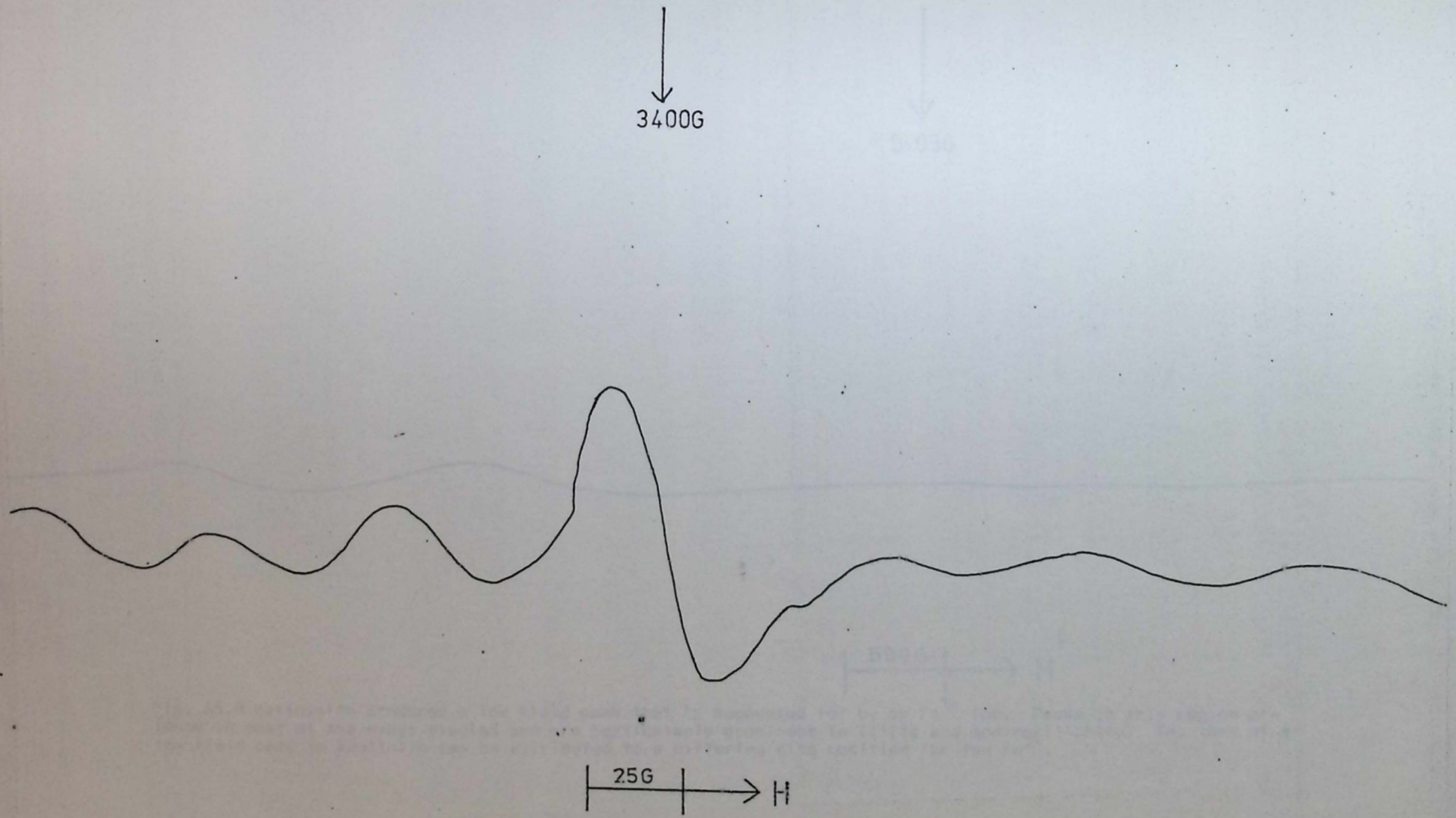

Fig. A5.8 The dicklte spectrum shows an asymmetrical peak distribution with a central peak surrounded by six less intense peaks. Its origins are entirely unknown at present.

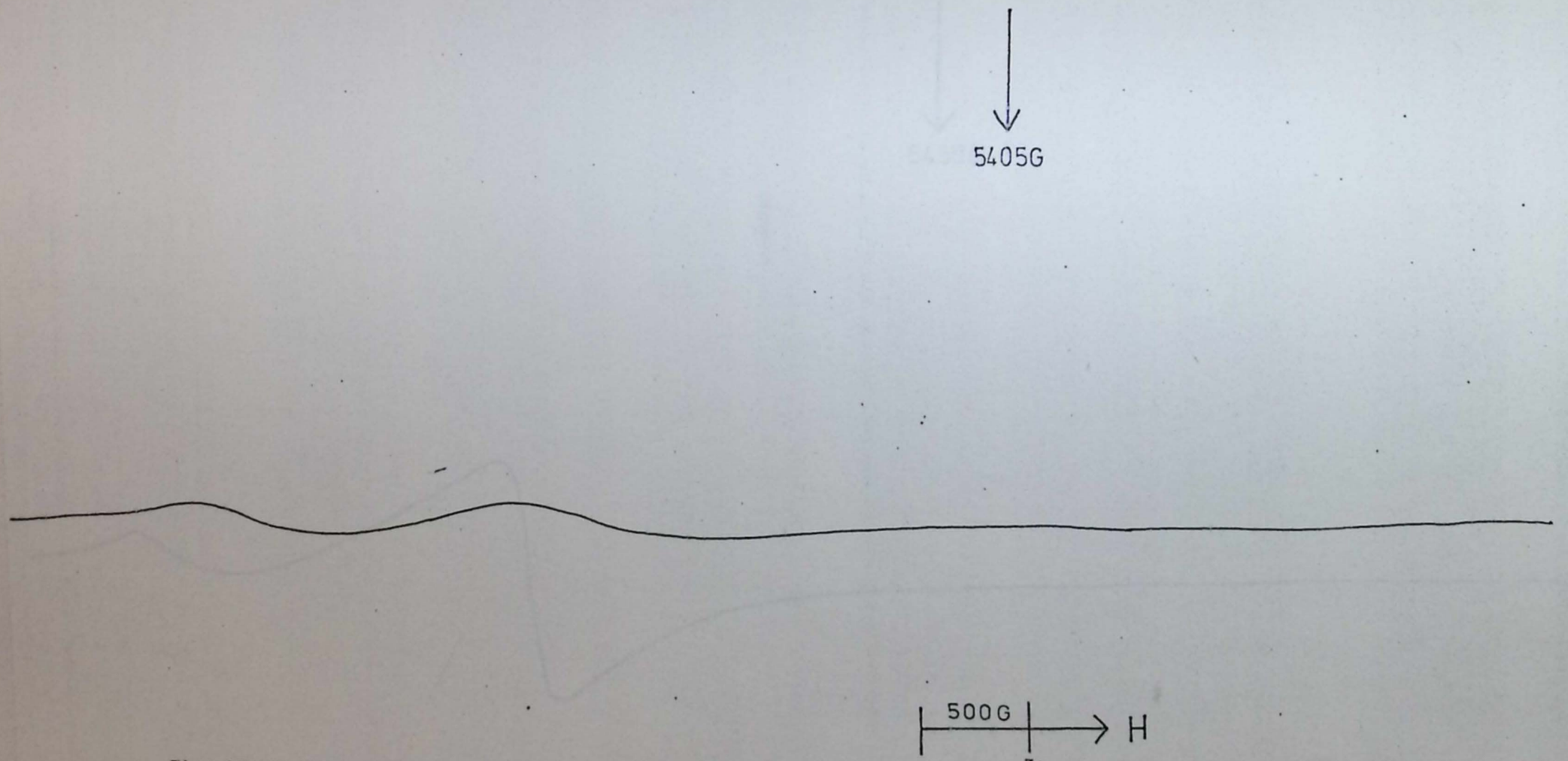

Fig. A5.9 Halloysite produced a low field peak that is accounted for by an Fe^{3+} ion. Peaks in this region are found in most of the clays studied and are particularly prominent in illite and montmorillonite. The lack of a low field peak in kaolinite can be attributed to a differing site position for the Fe^{3+}.

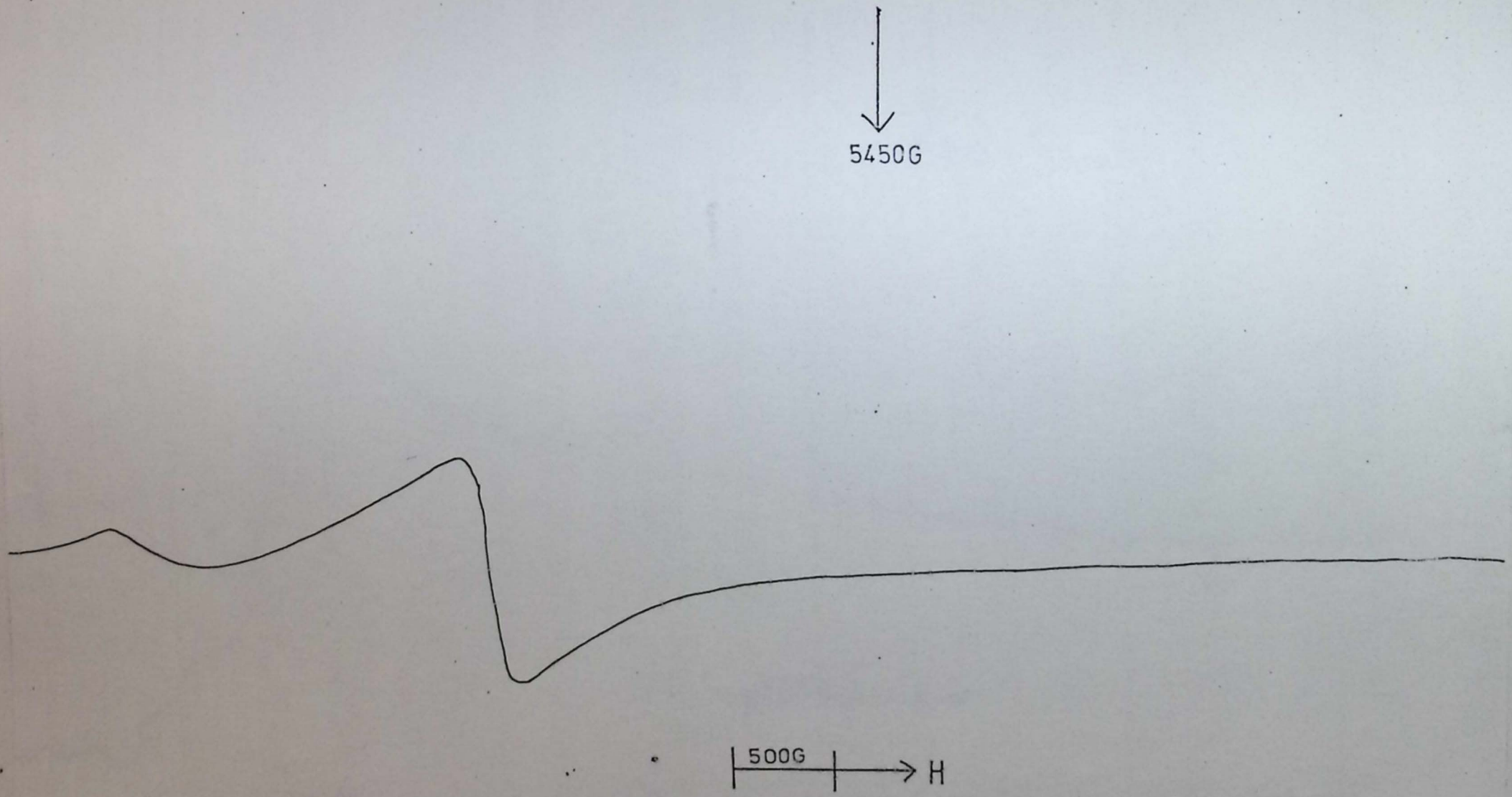

Fig. A5.10 Vermiculite shows peaks at both 3400G and 1600G approximately. Again Fe^{2+} possibly in 2 differing sites, accounts for the peak positions.

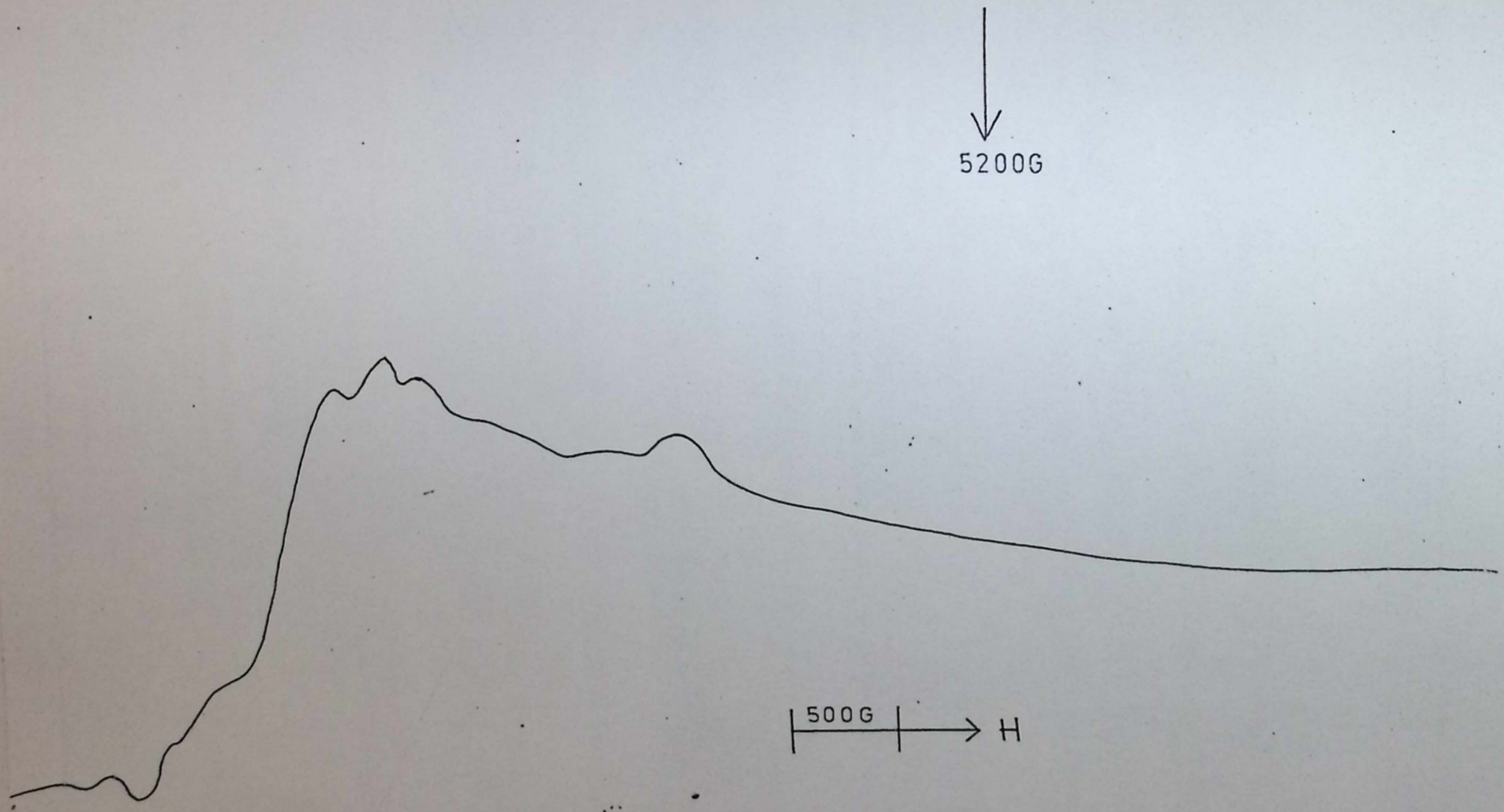

Fig. A5.11 A most complex and unusual spectrum was produced by chlorite. This spectrum will require further study to determine the exact nature of the paramagnetic species.

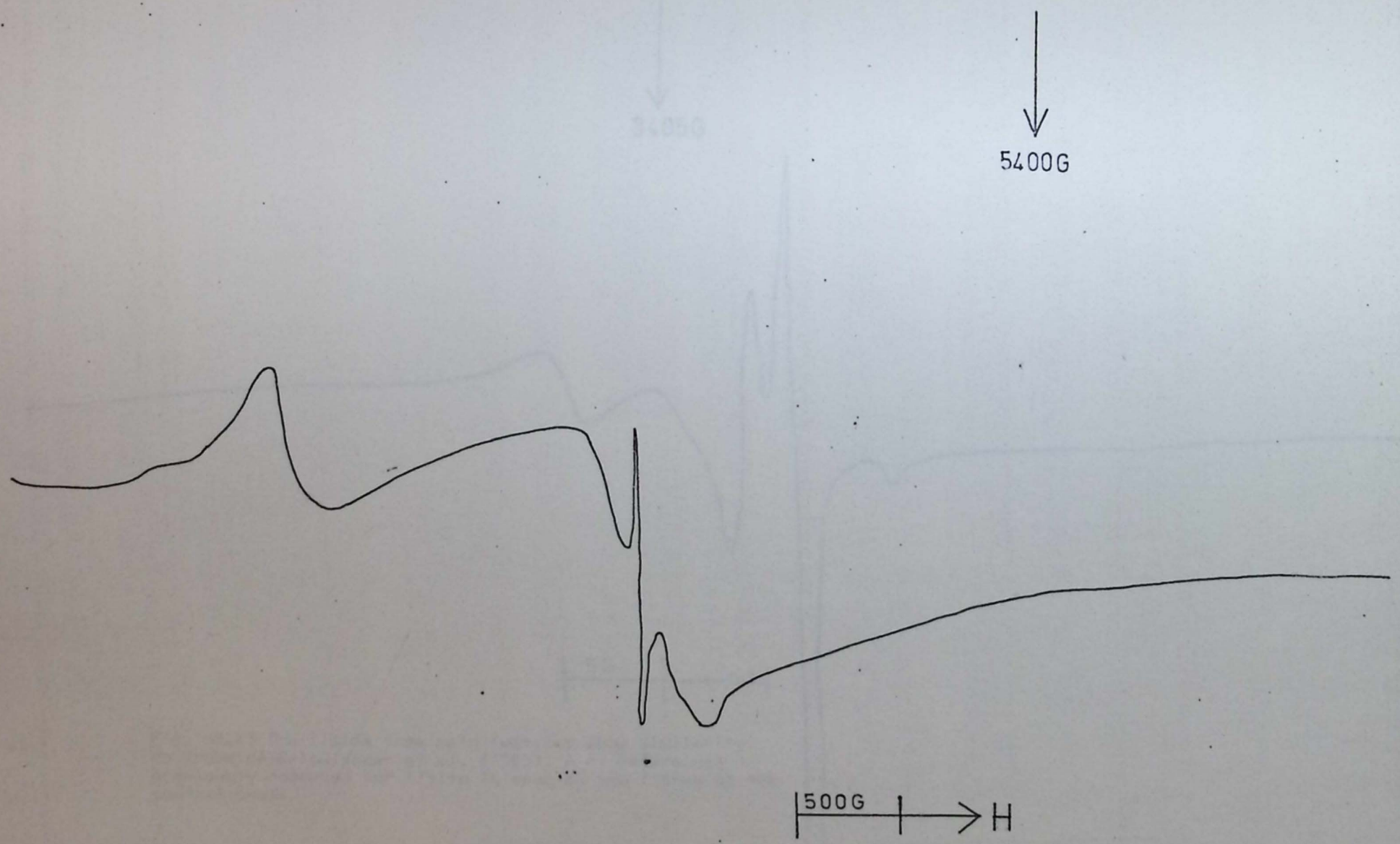

Fig. A5.12 This spectrum of illite shows 2 Fe^{2+} peaks previously identified and a set of free spin features (Fig.A5.13). The Fe^{2+} peaks are seen at 3400g and 1600G with the free spin features ar 3100G.

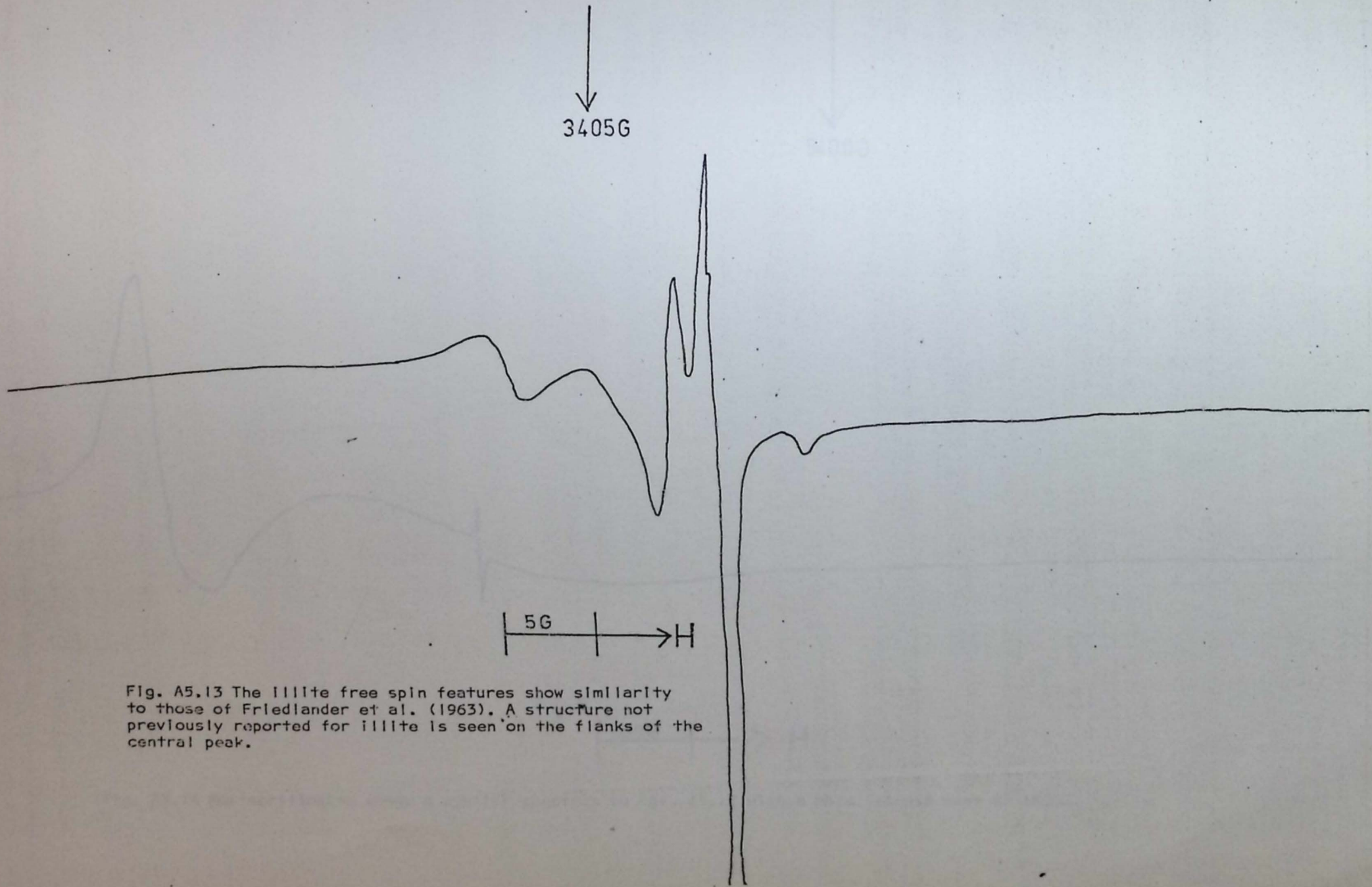

Fig. A5.13 The illite free spin features show similarity to those of Friedlander et al. (1963). A structure not previously reported for illite is seen on the flanks of the central peak.

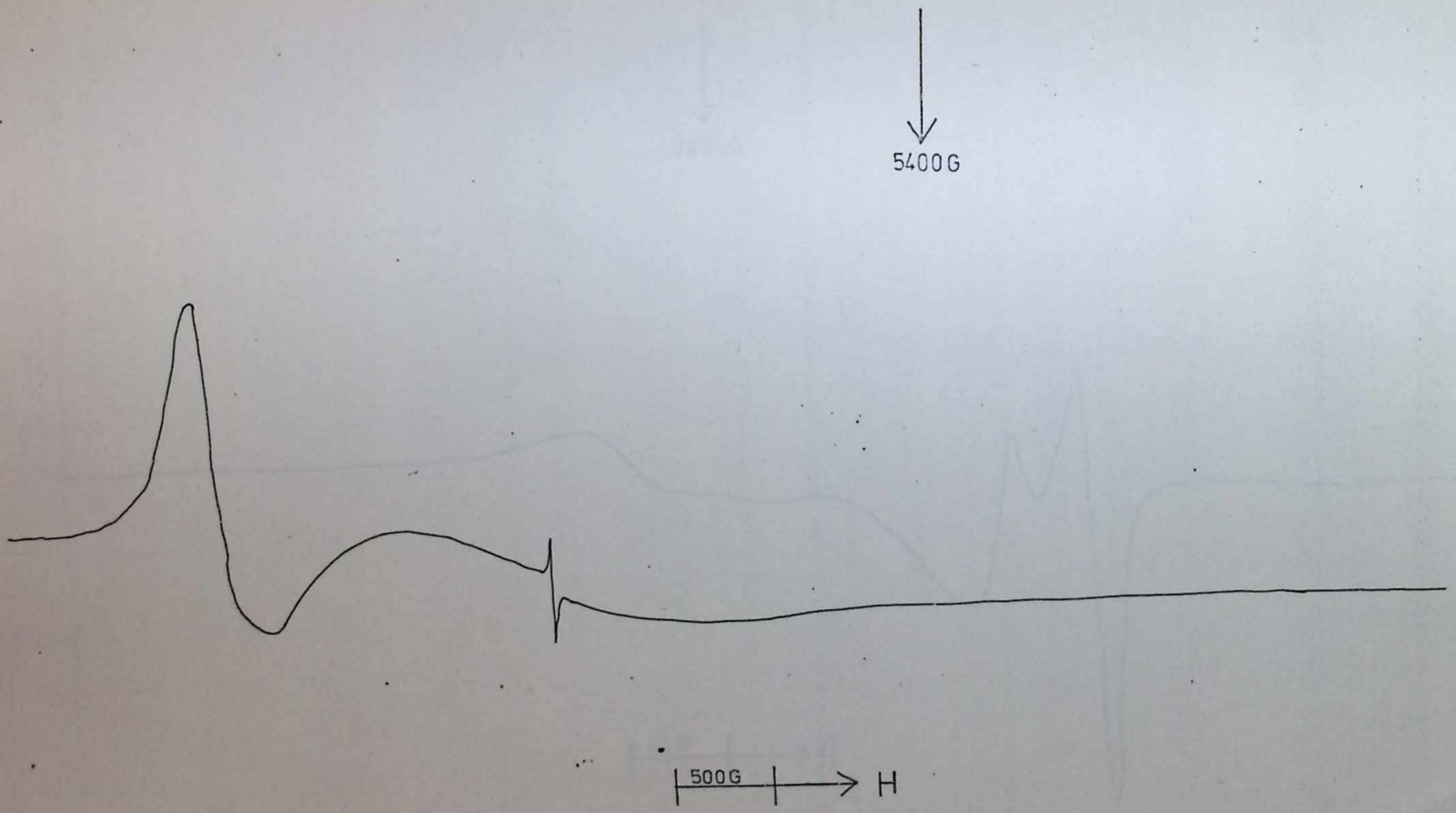

Fig. A5.14 Montmorillonite shows a similar spectrum to Fgl. A5.12 with a more intense peak at 1600G.

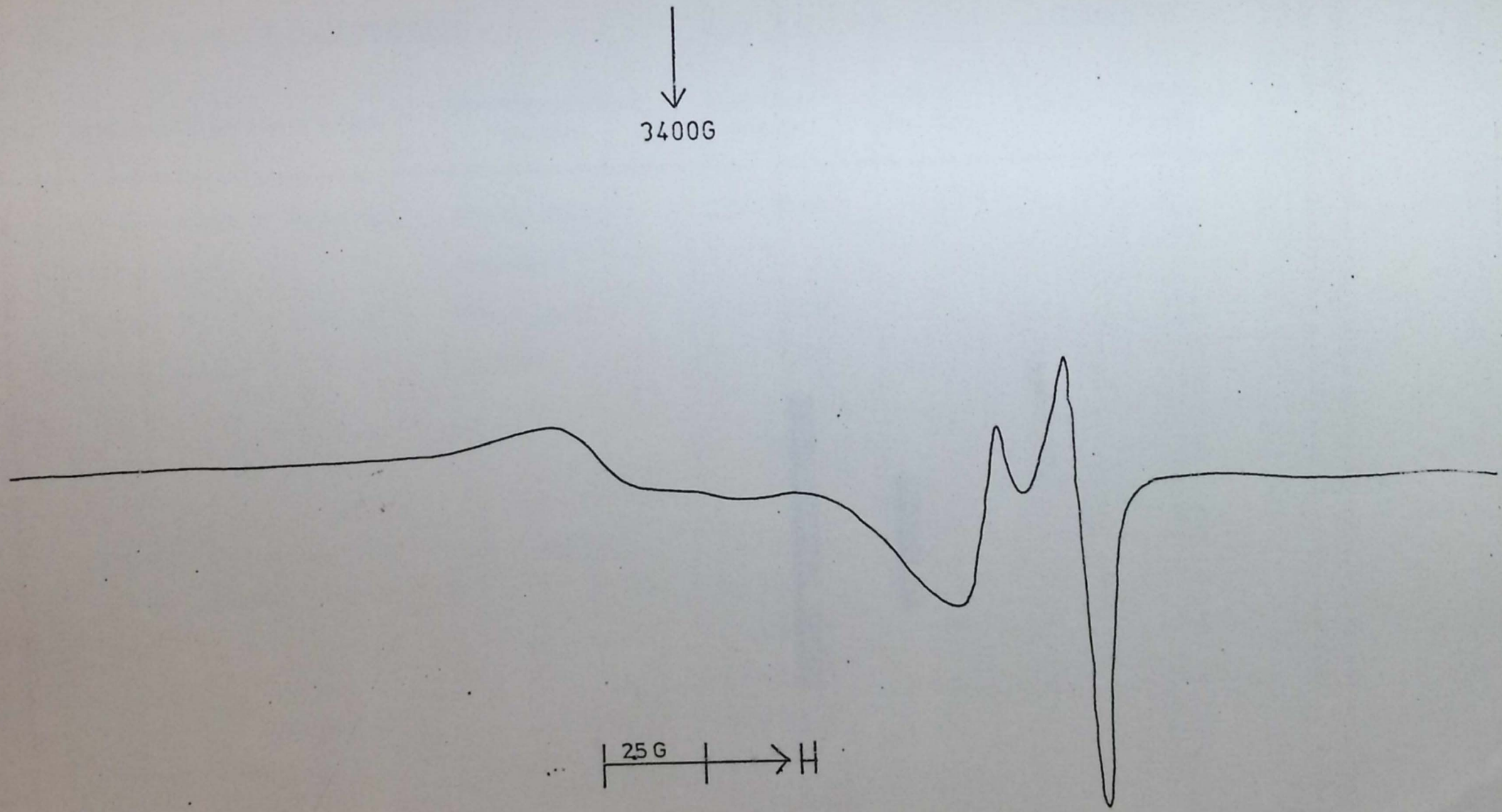

Fig. A5.15 The montmorillonite free spin features are very similar to those of illite (Fig. A5.13) and to those reported by Freidlander (1973) and Wauchope and Haque (1971), reflecting a common structural site for the radical. The most likely solution is a Fe^{2+} substitution for Al^{3+} in montmorillonite, illite and kaolinite.

APPENDIX SIX

SAMPLE COLLECTING STATIONS

	SAMPLE SITE			ANALYSIS			
Sample	Sample Collection Station	Stratigraphical Position	Township/ Range	Thin Section	X.R.D.	Emiss. Spec.	E.S.R.
1	K96 Route out of Neodesha, Wilson County	Spring Hill Limestone	T30S R15E				
2	Highway 75, Near Altoona, Wilson County	Vilas Shale	T29S R16E				
3	"	"	"		1	1	
4	"	"	"				
5	"	"	"		1	1	1
7	Highway 59, 3 Miles west of Stark, Neosho county	Stark Shale	SE corner SE SE Sect. 15,T27S R20E		1	1	
10	Intersection Highways, 52/31/59 W of Kincaid, Anderson County	Lane Bonner Springs Shale	T22S R20E, S line, SE, SE,Sect.35	1			
11	"	"	"	1			
12	"	"	"		1	1	

13	½ ml. S. of Intersection 52/31/59 on highway 52/59, Anderson County	Lane Bonner Springs Shale	W line NE, NE, Sect.2 T23S R20E				
14	"	"	"				
15	"	Hickory Creek Shale	"		1	1	
16	Route 52, 2-3 miles SW of Mound City, Linn County	Tacket Formation	SW Corner, NESE, Sect. 23 T22S R23E	2	1	1	1
17	"	"	"	2			
18	"	"	"	2			
19	"	Mound City Shale	"	2	1	1	
20	"	"	"		1	1	1
21	"	Sniabar Limestone	"		1	1	

22	Route 52, 2-3 miles SW of Mound City, Linn County	Ladore Shale	T22S R23E SW Corner, NESE, Sect. 23	2			
23	"	"	"	1	1	1	1
24	"	Hushpuckney Shale	"	2	1	1	1
25	"	"	"		1	1	
26	"	"	"		1	1	
27	Coldstorage plant on Inland Drive, Nr. Kansas City, Johnson County	Galesburg Shale	T12S R23-24E	2	1	1	1
28	"	"	"		1	1	1
29	"	Stark Shale	"				
30	"	"	"	2			
31	"	"	"	2	1	1	
32	"	"	"	2	1	1	
33	"	Winterset Limestone	"				

34	Coldstorage plant on Inland Drive,Nr. Kansas City, Johnson County	Winterset Limestone	T12S R23-24E		1	1	
35	"	"	"	2	1	1	
36	"	"	"	2	1	1	1
37	"	"	"	2			
38	"	Fontana Shale	"		1	1	
39	"	Wea Shale	"	2			
40	"	"	"		1	1	
41	"	Westerville Limestone	"		1	1	
42	¼ mile from Cold Storage Plant on Inland Drive, towards Kansas City, Johnson County	Quivera Shale	T12S R23-24E	2			
43	"	"	"	2	1	1	1
44	"	"	"	2			
45	"	"	"	2			
46	"	"	"		1	1	1

47	¼ mile from Cold Storage Plant on Inland Drive, towards Kansas City, Johnson County	Chanute Shale	T12S R23-24E	2	1	1	
48	"	"	"	2	1	1	1
49	"	"	"				
50	"	"	"		1	1	
51	"	Munsie Creek Shale	"				
51C	"	"	"	2			
52	"	"	"				
53	"	"	"		1	1	
54	Highway 10, 2½ mls. E of Zarah, Johnson County	Chanute Shale	N side SE NE Sect.14 T12S R23E	2	1	1	
55	"	Munsie Creek Shale	"	2			
56	"	"	"	2			

57	Highway 10, 3 mls. E of Zarah, Johnson County	Island Creek Shale	N side SE NE Sect.14 T12S R23E				
58	"	"	"	2			
59	"	Farley Limestone	"				
60	"	"	"	2			
61A	"	"	"		1	1	
61B	"	Bonner Springs Shale	S side NE NE Sect.13 T12S R23E				
62	"	"	"				
63	"	"	"		1	1	
64	"	"	"				
65	"	Plattsburg Limestone	"				
66	"	"	"	2	1	1	
67	"	"	"		1	1	
69	K32, E of intersection with K7, Wyandotte County	Lane Shale	W side SE SE Sect.28 T11S R23E	1	1	1	1

70	K32, E of intersection with K7, Wyandotte County	Lane Shale	W side SE SE Sect.28 T11S R23E	2	1	1	1
71	"	"	"		1	1	
72	Highway 10, 3 mls. E of Zarah, Johnson County	Bonner Springs Shale	E side NE NE Sect.13 T12S R23E	2			
73	Kerford Quarry, 1 ml. S of Atchinson on Highway 7, Atchinson County	Heumader Shale	Centre SW SE Sect. 7 T6S R21E	1			
74	"	"	"	2			
75	"	"	"	3			
76	"	"	"				
77	"	"	"	2			
78	"	"	"				
79	"	"	"		1	1	
80	"	Jackson Park Shale	"		1	1	

81	5½ mls. E of Doniphan, Atchinson County	Stull Shale	Centre SW SE Sect. 7 T6S R21E		1	1	1
82	"	Jackson Park Shale	"		1	1	1
83	"	Stull Shale	"	1			
84	"	"	"	2			
85	"	"	"	1	1	1	
86	5½ mls. E of Doniphan, Atchinson County	"	T5S R20E				
87	"	Spring Branch Limestone	"				
88	"	"	"				
89	"	Doniphan Shale	"				
90	"	"	"				
91	"	"	"	2			
92	"	Queen Hill Shale	"	1			
93	"	"	"				

94	Quarry, 4 mls. NE of Lancaster, Atchinson County	Calhoun Shale	NW SW Sect. 11 T5S R19E	1	1	1	1
95	"	"	"	2			
96	"	"	"	2	1	1	
97	"	"	"	2	1	1	
97B	Road alongside quarry, 4 mls. NE of Lancaster, Atchinson County	Turner Creek Shale	NW SW Sect. 11 T5S R19E		1	1	
98	"	Jones Point Shale	"				
99	"	"	"				
100	"	Iowa Point Shale	"				
101	"	"	"		1	1	
102	"	Tecumseh Shale	"	2			
103	"	"	"	2			
104	"	"	"	1			

105	Roadside 4 mls. NE of Lancaster, Atchinson County	Oskaloose Shale	Centre of S side SW sect. 10 T5S R19E	2	1	1	1
106	"	"	"	1			
107	"	Larsh & Burroak Shale	"		1	1	
108	"	"	"				
109	Roadside 4½ mls. NE of Lancaster, Atchinson County	Ervine Creek Limestone	Centre of E half, NE, Sect. 11 T5S R19E		1	1	1
110	Quarry SE of Burlington, Coffey County	Snyderville Shale	Centre NW NW Sect.31 T21S R16E		1	1	1
111	Intersection of Highways 75/57, Coffey County	"	SW Corner SW SW Sect. 35 T22S R15E	2			
112	"	"	"		1	1	

113	Intersection of Highways 75/57, Coffey County	Snyderville Shale	SW Corner SW SW Sect. 35 T22S R15E	2		
114	"	"	"	2		
115	"	"	"			
116	100 yds. N of intersection of 75/57 Coffey County	Toronto Limestone	W side SW SW Sect.35 T22S R15E		1	1
117	Intersection of Highways 75/57, Coffey County	Snyderville Shale	SW Corner SW SW Sect. 35 T22S R19E			
118	"	"	"			
119	2½ mls. NE of Gridley, Coffey County	King Hill Shale	West Line SW NW Sect. 14 T22S R14E			
120	"	Beil Limestone	"			

121	3 mls. NE of Gridley, Coffey County	Doniphan Shale	E line NE Sect. 24, T22S R14E	2	1	1	
122	Quarry 9½ mls. W of Burlington, Coffey County	Jones Point Shale	Centre NE NW Sect.30 T21S R14E		1	1	1
124	Highway 70, 3½ mls. E of Big Springs, Douglas County	Snyderville Shale	NW corner Sect. 21 T125S R18E				
125	"	Lawrence Shale	"		1	1	1
126	"	Snyderville Shale	"				
127	"	"	"	1			
128	"	Heebner Shale	"	3	1	1	
129	"	"	"				
130	"	"	"		1	1	
131	"	"	"				
132	"	Heumader Shale	"	1			

133	Highway 70, 5 mls. W of Lawrence, Douglas County	Spring Branch Limestone	NW NW Sect. 19 T12S R19E	1			
134	"	"	"	1			
135	"	"	"	1	1	1	1
136	Highway 70, 5½ mls. W of Lawrence, Douglas County	Queen Hill Shale	NE NE Sect. 24 T12S R18E	1	1	1	
137	"	Beil Limestone	"	1	1	1	1
138	Highway 70, 5 mls. W of Lawrence, Douglas County	Doniphan Shale	NW NW Sect. 19 T12S R19E		1	1	
139	Highway 70, 7½ mls. W of Lawrence, Douglas County	Oskaloosa Shale	NE NW Sect. 22 T12S R18E	1			
140	"	"	"	2			
141	"	"	"	1			
142	"	Larsh and Burroak Shale	"				

143A	Highway 70, 4 mls. E of Topeka, Shawnee County	Larsh and Burroak Shale	SE NE Sect. 8 T12S R17E			
143B	Highway 70/40 intersection in Topeka, Shawnee County	Iowa Point Shale	Centre NW SE Sect.4 T12S R16E			
144	"	Calhoun Shale	"	3	1	1
145	"	"	"	2		
146	"	Jones Point Shale	"	2		
148	Highway 24, ½ ml. W of intersection with Highway 4, Shawnee County	Holt Shale	S of Centre Sect. 14 T11S R16E		1	1
149	Roadside 7 mls. W of Lawrence, Douglas County	King Hill Shale	S line SW SW Sect.13 T12S R18E	2	1	1
150	"	Avoca Limestone	"	1	1	1

151	Lecompton Quarry, Douglas County	Heumader Shale	Centre SW SW Sect.35 T11S R18E	2	1	1	
152	Highway 7, 3½ mls. N of Atchinson, Atchinson County	Tecumseh Shale	W side SW SW Sect.12 T5S R20E		1	1	
153	"	"	"	2	1	1	
154	"	"	"				
155	"	"	"		1	1	1
156	Highway 70, 1 ml. W of Bonner Springs, Wyandotte County	Eudora Shale	Centre Sect. 18 T11S R23E				
157	"	"	"	1	1	1	1
158	"	Rock Lake Shale	"				
159	Highway 70, 7/10 ml. E of Kansas City Toll Booth, Wyandotte County	Quindaro Shale	E line NE SE Sect.9 T11S R24E	1			
160	"	"	"		1	1	1

161	Highway 70, 1 ml. W of Bonner Springs, Wyandotte County	Rock Lake Shale	Centre Sect. 18 T11S R23E		1	1	1
162	Highway 470, S. Topeka, Shawnee County	Severey Shale	Centre S side NW Sect. 19 T12S R16E	2	1	1	
163	"	Aardo Shale	"	1			
164	"	"	"				
165	"	"	"	2			
166	"	"	"	2			
167	Highway 470, 4½ mls. SW of Topeka, Shawnee County	Silver Lake Shale	SE NE SE Sect. 4 T13S R15E	1			
168	"	"	"	1	1	1	1
169	"	Cedar Vale Shale	"				
170	"	"	"	1	1		

171	Highway 470, 5½ mls. SW of Topeka, Shawnee County	White Cloud Shale	SE NE SW Sect. 9 T13S R15E	1	1	1	
172	"	"	"	2			
173	"	"	"	2	1	1	1
174	Highway 470, 2 mls. SW of Auburn, Shawnee County	Harveyville Shale	NE SW SW Sect. 35 T13S R14E	1			
176	Highway 470, 2½ mls. SW of Auburn, Shawnee County	Willard Shale	NE SW NE Sect. 3 T14S R14E				
177	"	"	"	2			
178	Highway 470, 2½ mls. SW of Auburn, Shawnee County	"	"	2			
179	"	"	"	2			
180	Highway 470, 3 mls. SW of Auburn, Shawnee County	"	SW SW NE Sect. 3 T14S R14E	2	1	1	
181	"	Wamego Shale	"		1	1	

182	Highway 470, 4 mls. NE of Admire Lyon County	Pillsbury Shale	SW SW NW Sect. 12, T16S R13E				
183	"	"	"	2			
184A	"	"	"	2	1	1	1
184B	"	"	"				
185	"	Dry Shale	"		1	1	
186	"	Grandhaven Limestone	"		1	1	1
187	"	Friedrich Shale	"	2	1	1	1
188	"	"	"	2			
190	"	Dry Shale	"				
191	Highway 70, 2 mls. W of Topeka, Shawnee County	Silver Lake Shale	SW NE NW Sect. 31, T11S R15E				
192	"	"	"		1	1	
193	"	Soldier Creek Shale	"				
194	"	"	"		1	1	1

195	Highway 70, 2 mls. W of Topeka, Shawnee County	Soldier Creek Shale	SW NE NW Sect. 31, T11S R15E				
196	Highway 70, 2 mls. S of Maple Hill, Wabaunsee County	Pony Creek Shale	Centre S line SW Sect. 26 T11S R12E	1			
197	"	"	"		1	1	
198	"	"	"				
199	"	Towle Shale	"				
200	"	"	"		1	1	1
201	Highway 70, 2½ mls. SW of Maple Hill, Wabaunsee County	Haxby Shale	SW SW SW Sect. 27, T11S R12E				
202	"	"	"				
203	"	"	"				
204	"	West Branch Shale	"				
205	"	"	"		1	1	

206	Highway 70, ½ ml. S of Paxico, Wabaunsee County	Hamblin Shale	SW SW SW Sect. 27, T11S R12E	1	1	
207	"	Hughes Creek Shale	SE SW SE Sect. 27, T11S R11E			
208	"	"	"	1	1	1
209	"	"	"	1	1	1
211	Highway 70, 3 mls. N of Alma, Wabaunsee County	Roca Shale	Centre W side Sect.26 T11S R10E			
212	"	Legion Shale	"	1	1	
213	"	Salem Point Shale	"	1	1	1
214	Highway 70, ½ ml. S of Paxico, Waubaunsee County	Hamblin Shale	SE SW SE Sect. 27 T11S R11E			
220	Highway 70, 3 mls. NW of Alma, Wabaunsee County	Speiser Shale	S line SE NW Sect.29 T11S R10E	1	1	1

221	Highway 70, 3 mls. NW of Alma, Wabaunsee County	Speiser Shale	S line SE NW Sect.29 T11S R10E	1	1	1	1
222	"	"	"	2	1	1	
223	"	"	"				
225	Highway 70, 3½ mls. NW of Alma, Wabaunsee County	Blue Rapids Shale	SE SE NE Sect. 30 T11S R10E				
226	"	"	"		1	1	
227	"	"	"		1	1	
228	"	"	"	2			
229	"	"	"	1			
230	Highway 70, 4 mls. NW of Alma, Wabaunsee County	Easy Creek Shale	S line SW NE Sect.30 T11S R10E	1	1	1	
231	"	"	"				
232	"	"	"				
233	"	"	"	2			
234	"	Hooser Shale	"		1	1	1

235	Highway 70, 4½ mls. NW of Alma, Wabaunsee County	Eskridge Shale	W line NE SW Sect.30 T11S R10E	1	1	1	1
236	"	"	"	2			
237	"	Neva Limestone	"	2	1	1	
238	"	Eskridge Shale	"		1	1	1
239	"	"	"				
240	"	"	"				
241	"	Neva Limestone	"				
242	"	Salem Point Shale	"				
243	Highway 70, 6½ mls. S of Zeandale, Riley County	Havensville Shale	W line NW SW Sect.28 T11S R9E		1	1	1
244	"	"	"		1	1	1
247	Highway 70, 6 mls. SE of Manhattan, Riley County	Stearns Shale	W line SW NW Sect.25 T11S R8E				
248	"	"	"	1	1	1	
249	"	Florena Shale	"		1	1	1

250	Highway 70, 1 ml. E of Manhattan Exit, Geary County	Blue Springs Shale	W line NW SW Sect.27 T11S R8E				
251	"	"	"		1	1	1
252	"	"	"				
253	"	Kinney Limestone	"	1	1	1	
254	"	Blue Springs Shale	"				
255	"	"	"				
256	"	"	"	2	1	1	
258	Highway 177, ½ ml. SE of Manhattan, Riley County	Johnson Shale	SW SW NE Sect. 20 T10S R8E				
259	"	"	"				
260	"	Bennett Shale	"	1			
261	"	Johnson Shale	"		1	1	
262	Highway 113, ½ ml. W of Manhattan, Riley County	Bennett Shale	NW SE NE Sect. 14, T10S R7E		1	1	1

263	Highway 113, 1 ml. N of Manhattan, Riley County	Neva Limestone	N line NE NW Sect. 2 T10S R7E	2			
264	"	"	"	2	1	1	
265	Highway 77, 2 mls. N of Junction City, Geary County	Oketo Shale	Centre SW NW Sect.27 T11S R5E	2	1	1	
266	"	"	"	2			
267	"	Holmesville Shale	"				
268	Highway 77, 2½ mls. N of Junction City, Geary County	"	Centre NW NW Sect.27 T11S R5E	2	1	1	
269	"	"	"	1			
270	3/10ths ml. S of Intersection of Highways 57/77, Geary County	Gage Shale	N line NW NW Sect.34 T11S R5E	2	1	1	
271	"	"	"				
272	Junction of Highway 57/77, Geary County	Grant Shale	Centre NW SW Sect.27 T11S R5E	1	1	1	1

273	Highway 70, 2 mls. E of Junction City, Geary City	Wymore Shale	Centre SE SE Sect. 5 T11S R5E		1	1	
274	"	"	"	1			
280	1½ mls. N of Baldwin, Douglas County	Wathena Shale	W line SW NW Sect.27 T14S R20E				
281	"	"	"	2	1	1	1
282	"	"	"				
283	"	Ireland Sandstone	"				
284	"	"	"		1	1	
286	2 mls. N of Baldwin, Douglas County	"	NW NW NW Sect. 27 T14S R20E	2			
287	2½ mls. N of Baldwin, Douglas County	"	W line NE SW Sect.22 T14S R20E		1	1	

288	Highway 10, 2 mls. E of Lawrence, Douglas County	Ireland Sandstone	N line NE NE Sect.10 T13S R20E				
289	"	"	"	2			
290	15th Street, Lawrence, Douglas County	Vinland Shale	N line NW NE Sect. 5 T13S R20E		1	1	1
291	"	"	"	1			
292	"	"	"				
294	Highway 7, 3 mls. N of Bonner Springs, Wyandotte County	Tonganoxie Sandstone	NE SW NW Sect. 8 T11S R23E	1	1	1	
295	"	"	"	3			
296	"	"	"				
297	1 ml. N of Chapman, Dickinson County	Weston Shale Odell Shale.	SE SW Sect. 17 T12S R4E	1	1	1	
298	"	"	"				
299	"	"	"		1	1	1

300	Intersection of Highways	Paddock	N, NE	1	1	1
	206/70, Dickinson County	Shale	Sect. 30			
			T12S R4E			

REFERENCES

Abbreviations according to the World List of Scientific Periodicals, Butterworths, and British Standard 4148, 1967 and 1970.

ABERNATHY, G.E., 1937, The Cherokee group of south-eastern Kansas: Kans. Geol. Soc. Guidebook, 11th Ann. field conf. SE Kansas NE Oklahoma 1937, 18-23.

ALEXANDER, L. and KLUG, H.P., 1948, Basic aspects of X-ray absorption in quantitative diffraction analysis of powder mixtures: Analyt. Chem., 20, 886-889.

ANDERSON, H.E., 1966, Regression, discriminant analysis and a standard notation for basic statistics: In: CATTELL, R.B. (Ed). Multivariate procedures in experimental psychology: Rand McNally, Chicago.

ANGEL, R.B. and HALL, P.L., 1972, Electron spin resonance studies of kaolins: Int. Clay Conf., Madrid, 71-86.

BAESEMANN, J.F., 1973, Missourian (Upper Pennsylvanian) conodonts of northeastern Kansas. J. Paleont., 47, 689-710.

BALL, S.M., 1964, Stratigraphy of the Douglas Group (Pennsylvanian, Virgilian) in the northern Mid-Continent Region: Unpublished Ph.D. thesis, Univ. Kansas, 490p.

BAKER, W.E., 1968, X-ray diffraction analysis of Broken Hill dusts: Proc. Australian Inst. Min. Metall., (228), 23-29.

BARTLETT, M.S., 1941, The statistical significance of canonical correlations; Biometrika, 32, 29-38.

BARTLETT, M.S., 1950, Tests of significance in factor analysis: Br. J. Statist. Psychol., 3, 77-85.

BARTLETT, M.S., 1951a, The effect of standardization on a χ^2 approximation in factor analysis: Biometrika, 38, 337-344.

BARTLETT, M.S., 1951b, A further note on tests of significance in factor analysis: Br. J. Statist. Psychol., 4, 1-2.

BENCINI, A. and TURI, A., 1974, Mn distribution in the Mesozoic carbonate rocks from Lima Valley, Northern Apennines: J. Sedim. Petrol., 44, (3), 774-782.

BENNETT, C.A. and FRANKLIN, N.L., 1954, Statistical analysis in chemistry and the chemical industry: John Wiley & Sons, New York, 724p.

BERNER, R.A., 1971, Principles of chemical sedimentology: McGraw-Hill Book Co., New York, 240p.

BERTINE, K.K., 1972, The deposition of molybdenum in anoxic waters: Mar. Chem., 1, (1), 45-53.

BERTINE, K.K. and TUREKIAN, K.K., 1973, Molybdenum in marine deposits: Geochim. Cosmochim. Acta, 37, 1415-1434.

BIELSKI, B.H. and GEBICKI, J.M., 1967, Atlas of electron spin resonance spectra: Academic Press, London, 665p.

BIFANO, F.V., CUBER, A.L. and CUFFEY, R.J., 1974, Ostracode palaeoecology in shales of the Wreford megacyclothem (Lower Permian; Kansas and Oklahoma): Okla. Geol. Notes, 34, (3), 124.

BOESMAN, E. and SCHOEMAKER, D., 1961, Resonance paramagnetique de l'ion Fe^{3+} dans la kaolinite: Hebd. Seanc. Acad. Sci., Paris. 252, 1931-1933.

BOTT, M.H.P. and DEAN, D.S., 1973, Stress diffusion from plate boundaries: Nature Phys. Sci., 243, (5406), 339-341.

BOWEN, R.L., 1974, The enigma of Late Palaeozoic orogeny in Southeastern North America: Okla. Geol. Notes, 34, (3), 123.

BOWER, R.R., 1964, Dispersal centres of sandstones in the Douglas Group (Pennsylvanian) of Kansas: Unpublished M.S. thesis, Univ. Kansas, 19p.

BOYCE, A.J., 1968, Mapping diversity: A comparative study of some numerical methods. In: COLE, A.J., (Ed). Colloq. on numerical taxonomy, Univ. St. Andrews, p.1-28.

BRANSON, C.C., 1960a, Proposed American standard of early Permian (?) rocks - a century-old controversy: Okla. Geol. Notes, 20, (9), 229-235.

BRANSON, C.C., 1960b, Carboniferous problems of the Mid-Continent area: Kans. Geol. Soc. 25th field conf. guidebook, 44-47.

BRANSON, C.C., (Ed). 1962a, Pennsylvanian System in the United States: Am. Ass. Petrol. Geol., Tulsa, Okla., U.S.A. 508p.

BRANSON, C.C., 1962b, Pennsylvanian system of the Mid-Continent: In: BRANSON, C.C. Pennsylvanian system in the United States, Am. Ass. Petrol. Geol. Tulsa, Okla., U.S.A., 431-460.

BREWER, R., 1964, Fabric and mineral analysis of soils: John Wiley & Sons, New York, 470p.

BREWER, R., 1972, The basis of interpretation of soil micromorphological data: Geoderma, 8, 81-94.

BRINDLEY, G.W., 1961, Quantitative analyses of clay mixtures: In: BROWN, C., (Ed). The X-ray identification and crystal structure of clay minerals: Miner. Soc., London, p.489-516.

BRINDLEY, G.W. and KURTOSOY, S.S., 1961, Quantitative determination of kaolinite by X-ray diffraction: Am. Miner., 46, 1205-1215.

BRISTOL, C.C., 1969, The quantitative determination of minerals in some metamorphosed volcanic rocks by X-ray powder diffraction: Can. J. Earth Sci., 5, 235-242.

BROECKER, W.S., 1974, Chemical Oceanology: Harcourt Brace Jovanovich, Inc. New York, 214p.

BROMLEY, R.G., 1967, Marine phosphorites as depth indicators: Mar. Geol., 5, 503-509.

BRONDOS, M.D., 1974, Diversity and palaeoecology of some ostracodes from the Upper Pennsylvanian of Kansas: Abs. with Programs, 6, (2), 97-98.

BROOKINGS, D.G. and CHAUDHURI, S., 1973, Comparison of potassium-argon and rubidium-strontium determinations for Eskridge and Stearns Shales (Early Permian), Eastern Kansas: Am. Ass. Petrol. Geol., 57, (3), 520-527.

BROWN, J.E., 1973, Depositional histories of sand grains from surface textures: Nature, 242, 396-398.

BROWN, S.L., 1966, General stratigraphy and depositional environment of the Elgin Sandstone in South-Central Kansas: Unpublished M.S. thesis, Univ. Kansas., 52p.

BROWN, S.L., 1967, Stratigraphy and depositional environment of the Elgin Sandstone (Pennsylvanian) in South-Central Kansas: Bull. Kans. Geol. Surv., (187), pt. 3, 9p.

BROWN, W.G., 1956, Stratigraphy of the Beil Limestone, Virgilian, of Eastern Kansas: Unpublished M.S. thesis, Univ. Kansas, 180p.

BROWNING, D.R., 1969, Spectroscopy: McGraw-Hill Book Co., Maidenhead, 183p.

BULLOCK, P. and MACKNEY, D., 1970, Micromorphology of strata in the Boyn Hill terrace deposits, Buckinghamshire: In: OSMOND, D.A. and BULLOCK, P., (Eds), Tech. Monogr. 2 , Agric. Res. Council., Soil Survey of G.B., Harpenden, Herts., 97-105.

BURNHAM, C.P., 1970, The micromorphology of argillaceous sediments: particularly calcareous clays and siltstones: In: OSMOND, D.A. and BULLOCK, P., (Eds), Tech. Monogr. 2 , Agric. Res. Council, Soil Survey of G.B., Harpenden, Herts., 83-96.

BYERS, C.W., 1974, Shale fissility: relation to bioturbation: Sedimentology, 21, 479-484.

CALVERT, S.E., 1966, Accumulation of diatomaceous silica in the sediments of the gulf of California: Bull. Geol. Soc. Am., 77, 569-596.

CAMERON, E.M., 1969, Regional geochemical study of the Slave Point carbonate, Western Canada: Can. J. Earth Sci., 6, 247-268.

CAMERON, E.M. and HORTON, A.E., 1967, Analysis of rocks using a multichannel emission spectrometer: Chem. Geol., 2, 135-145.

CARROLL, D., 1970, Clay minerals: A guide to their X-ray identification: Geol. Soc. Am. Spec. Paper, 126.

CATTELL, R.B., 1965, Factor analysis: An introduction to essentials. I: the purpose and underlying models: Biometrics, 21, 190-210: II: The role of factor analysis in research: Biometrics, 21, 405-435.

CATTELL, R.B., 1966, Handbook of multivariate experimental psychology: Rand McNally, Chicago, 174-243.

CEBULL, S.E. and KELLER, G.R., 1974, Plate tectonics and the Ouachita system in Texas, Oklahoma and Arkansas: Reply: Bull. Geol. Soc. Am., 85, 147-148.

CEBULL, S.E., KELLER, G.R., SHURBET, D.H. and RUSSELL, L.R., 1974, Transform faults as explanation for offsets in the Southern Appalachian-Ouachita Tectonic Belt: Okla. Geol. Notes, 34, (3), 123-124.

CELENK, C., 1972, Application of computer orientated statistical and mathematical techniques to the interpretation of geochemical prospecting data, with particular reference to the Pirejman area, South-East Turkey: Unpublished Ph.D. thesis, Univ. Leicester.

CHAYES, F., 1971, Ratio correlation: Univ. Chicago Press. Chicago, 99p.

CHAYES, F. and KRUSKALL, W., 1966, An approximate statistical test for correlations between proportions: J. Geol., 74, (5), pt. 2, 692-702.

CHAYES, F. and VEIDE, D., 1965, On distinguishing basaltic lavas of circumoceanic and ocean-island type by means of discriminant functions: Am. J. Sci., 263, 206-222.

CHILDS, D., 1970, The essentials of factor analysis: Holt, Rinehart & Winston, London, 107p.

CHRONIC, J., 1964, Nature and variability in Pennsylvanian sedimentary cycles in Colorado: In: MERRIAM, D.F., (Ed), Symp. cyclic sedimentation: Bull. Kans. Geol. Surv., (169), 63-68.

CLARK, G.L. and REYNOLD, D.H., 1936, Quantitative analysis of mine dusts by X-ray diffraction: Ind. Engng. Chem. Analyt. Edit. 8, 36-40.

CLARK, T.H. and STEARN, C.W., 1968, The geological evolution of North America: Ronald Press Co., New York, 2nd Edit., 570p.

CLOUD, P.E., 1962, Environment of calcium carbonate deposition west of Andros Island, Bahamas. U.S. Geol. Surv. Prof. Paper, (350), 1-138.

COLE, A.J., (Ed), 1969, Colloquium in Numerical Taxonomy: Univ. St. Andrews Press, 260p.

COLLYER, P.L. and MERRIAM, D.F., 1973, An application of cluster analysis in mineral exploration: Math. Geol., 5, (3), 213-224.

CONDRA, G.E., 1927, The stratigraphy of the Pennsylvanian System in Nebraska: Bull. Neb. Geol. Surv. (1), 2nd series, 1-291.

CONNOR, J.J., 1969, A geochemical discriminant for sandstones of Mississippian and Pennsylvanian age in Kentucky: Q.J. Colo. Sch. Mines, 64, 17-34.

COOLY, W.W. and LOHNES, R.R., 1962, Multivariate procedures for the behavioural sciences: John Wiley & Sons, New York, 211p.

CROWLEY, D.J., 1969, Algal-bank complex in Wyandotte Limestone (Late Pennsylvanian) in Eastern Kansas: Bull. Kans. Geol. Surv. (198), 58p.

CUBITT, J.M., 1970, Cluster Analysis in biofacies analysis: Unpublished B.Sc. dissertation, Univ. Leicester, 26p.

CUTTER, R.J., 1967, Bryozoan fabulipora carbonaria in Wyeford Megacyclothem (Lower Permian) of Kansas: Univ. Kans. Paleont. Contr., art. 43, (Bryazoan, art. 1), 1-96.

DAVENPORT, T.G., 1970, Geochemical studies of the bauxite deposits of the McKenzie region, Guyana: Unpublished Ph.D. thesis, Univ. Leicester.

DAVID, M., CAMPIGLIO, C. and DARLING, R., 1974, Progress in R- and Q-mode analysis: correspondence analysis and its application to the study of geological processes: Can. J. Earth Sci., 11, 131-146.

DAVIS, J.C., 1959, Reef structure in the Plattsburg and Vilas Formations (Missourian) in southeast Kansas: Compass, 36, (4), 319-335.

DAVIS, J.C., 1967, Petrology of the Mowry Shale: Unpublished Ph.D. thesis, Univ. Wyoming, 141p.

DAVIS, J.C., 1970, Information contained in sediment-size analyses: Math. Geol., 2, (2), 105-122.

DAVIS, J.C., 1973, Statistics and data analysis in Geology: John Wiley & Sons, New York, 550p.

DAVIS, J.C. and COCKE, J.M., 1972, Interpretation of complex lithologic successions by substitutability analysis: In: [illegible], D.F., (Ed), Mathematical models of sedimentary processes: Plenum Press, New York, 27-52.

DAVIS, J.C. and SAMPSON, R.J., 1966, Fortran II program for multivariate discriminant analysis using an IBM 1620 computer: Comput. Contr. 4, Kans. Geol. Surv.

DEGENS, E.J., WILLIAMS, E.G. and KEITH, M.L., 1958, Environmental studies of Carboniferous sediments Part II: Application of geochemical criteria: Bull. Am. Ass. Petrol. Geol., 42, (5), 981-997.

DEMIRMEN, F., 1969, Multivariate procedures and FORTRAN IV Program for evaluation and improvement of classifications: Comput. Contr. 31, Kans. Geol. Surv.

DEWEY, J.F. and BIRD, J.M., 1970, Mountain belts and the new global tectonics: J. Geophys. Res., 75, 2625-2647.

DOTT, R.H. and BATTEN, R.L., 1971, Evolution of the earth: McGraw-Hill Book Co., New York, 649p.

DRAPEAU, G., 1973, Factor analysis: How it copes with complex geological problems: Math. Geol., 5, (4), 361-364.

DUFF, P.McL., HALLAM, A. and WALTON, E.K., 1967, Cyclic Sedimentation: Developments in sedimentology 10, Elsevier Publ. Co., Amsterdam, 280p.

DUNN, C.E., 1974, Identification of sedimentary cycles through Fourier analysis of geochemical data: Chem. Geol., 13, 217-232.

EBENS, R.J. and CONNOR, J.J., 1972, Geochemical survey of geologic units: In: Environmental geochemistry, U.S. Geol. Surv. Denver, Colo., Open file report 1972, 6-40.

ECKHARDT, F.J., 1958, Über chlorite in sedimenten: Geol. Jb., 75, 437-474.

ELIAS, M.K., 1937, Depth of deposition of the Big Blue (Late Palaeozoic) sediments in Kansas: Bull. Geol. Soc. Am., 48, 403-432.

ELIAS, M.K., 1964, Depth of Late Palaeozoic sea in Kansas and its Megacyclic sedimentation: Bull. Kans. Geol. Surv. (169), 87-106.

ESLINGER, E.V., MAYER, L.M., DURST, T.L., HOMER, J. and SAVIN, S.M., 1973, An X-ray technique for distinguishing between detrital and secondary quartz in the fine-grained fraction of sedimentary rocks: J. Sedim. Petrol., 43, (2), 540-543.

EVANS, J.K., 1967, Depositional environment of a black shale (Heebner) in Kansas and adjacent states: Unpublished Ph.D. thesis, Rice Univ., 189p.

EVANS, J.K., 1968, Environment of deposition of a Pennsylvanian black shale (Heebner) in Kansas and adjacent states (Abs): Geol. Soc. Am. Ann. Meet., Mexico City, 92-93.

FAGERSTROM, J.A. and BURCHETT, R.R., 1972, Upper Pennsylvanian shoreline deposits from Iowa and Nebraska: their recognition, variation and significance: Bull. Geol. Soc. Am., 83, 367-388.

FENNER, P. and HAGNER, A.F., 1967, Correlation of variations in trace elements and mineralogy of the Esopus Formation, Kingston, New York, Geochim. Cosmochim. Acta, 31, 237-261.

FERM, J.C., 1973, Late Palaeozoic elastic wedges in Appalachian Province: Okla. Geol. Notes., 33, (4), 170.

FISHER, R.A., 1936, The use of multiple measurements in taxonomic problems: Ann. Eugenics, 7, 179.

FISHER, R.A., 1938, The statistical utilization of multiple measurements: Ann. Eugenics, 8, 376-386.

FLANAGAN, F.J., 1969, U.S.G.S. Standard II: First compilation of data for new U.S.G.S. rocks: Geochim. Cosmochim. Acta, 33, 81-120.

FLAWN, P.T., et al., 1961, The Ouachita System: Univ. Texas, Bur. Econ. Geol. Publ. (6120), 410p.

FOX, W.T., 1964, FORTRAN and FAP program for calculating and plotting time-trend curves using an IBM 7090 or 7094/1401 computer system: Kans. Geol. Surv. Spec. Dist. Publ. (12), 1-24.

FOX, W.T., 1967, Simulation models of time-trend curves for palaeoecological interpretation: In: [illegible], D.F., (Ed), Colloquium on time-series analysis: Comput. Contr. 18, Kans. Geol. Surv., 18-29.

FOX, W.T. and [illegible], J.A., 1965, The use of time-trend analysis environmental interpretation of limestones: J. Geol., 510-518.

FRASER, A.R. and KOVATS, M., 1966, Steroscopic models of multivariate statistical data: Biometrics, 22, 849-852.

FRIEDLAENDER, H.Z., SALDICK, J. and FRENK, C.R., 1963, Electron spin resonance spectra in various clay minerals: Nature, 199, (4888), 61-62.

FROST, J.G., 1968, Algal banks of the Dennis Limestone (Pennsylvanian) of Eastern Kansas: Unpublished Ph.D. thesis, Univ. Kansas.

FROST, J.G., 1975, Winterset algal-bank complex, Pennsylvanian, Eastern Kansas: Bull. Am. Ass. Petrol. Geol., 59, (2), 265-292.

FRUCHTER, B., 1954, Introduction to factor analysis, Van Nostrand, New York, 280p.

GALLE, O.K. and WAUGH, W.N., 1966, Compositional variance in the Plattsmouth Limestone Member (Pennsylvanian) in Kansas: Bull. Kans. Geol. Surv., (180), pt. 1, 9p.

GALLOWAY, W.E. and BROWN, Jr., L.R., 1973, Depositional systems and shelf-slope relations on cratonic basin margin, uppermost Pennsylvanian of North-Central Texas: Bull. Am. Ass. Petrol. Geol., 57, (7), 1185-1218.

GARRELS, R.M. and MacKENZIE, F.T., 1971, Evolution of sedimentary rocks: Norton, New York, 297p.

GARRETT, R.G. and NICHOL, I., 1969, Factor analysis as an aid in the interpretation of regional geochemical stream sediment data: In: CANNEY, F.C., (Ed), Int. Geochem. Expl. Symp., Q.J. Colo. Sch. Mines, 64, 245-264.

GHOSE, S., 1968, Application of electron paramagnetic resonance in silicate minerals: In: Resonance spectroscopy in mineralogy. Short course lecture notes. Am. Geol. Inst. G1-15.

GHOSH, P.K., SAHADDAR, M., SINHA, S.C., TIWARI, J.S. and BANERJI, A.C., Geological applications of ESR spectrometry. Mn^{2+} ions in calcium carbonate minerals: Technology, 7, (4), 276-280.

GIBBS, R.J., 1965, Error due to segregation in quantitative clay mineral X-ray diffraction mounting techniques: Am. Miner., 50, 741-751.

GIBBS, R.J., 1967, Quantitative X-ray diffraction analysis using clay mineral standards extracted from the samples to be analysed: Clay Miner., 7, 79-90.

GIBBS, R.J., 1968, Clay mineral mounting techniques for X-ray diffraction analysis: J. Sedim. Petrol., 38, 242-244.

GIBBS, R.J., 1969, X-ray diffraction mounts: In: CARVER, R.E., (Ed), Procedures in sedimentary petrology: John Wiley & Sons, New York, 531-54.

GILLOT, J.E., 1969, Study of the fabric of fine-grained sediments with the scanning electron microscope: J. Sedim. Petrol., 39, (1), 90-105.

GILLOTT, J.E., 1970, Fabric of Leda Clay investigated by optical, electron optical and X-ray diffraction methods: Engng. Geol., 4, (1970), 133-153.

GIPSON, M., 1965, Application of the electron microscopy to the study of particle orientation and fissility in shale: J. Sedim. Petrol., 35, (2), 408-414.

GIPSON, M., 1966, Preparation of orientated slides for X-ray analysis of clay minerals: J. Sedim. Petrol., 36, 1143.

GLICK, E.E., 1973, Palaeotectonic history of Carboniferous rocks of Arkansas: Abs. with Programs, 5, (3), 258-259.

GOODYEAR, J. and DUFFIN, W.J., 1954, The indentification and determination of plagioclase feldspars by the X-ray powder method: Min. Mag., 30, 306-326.

GORBUNOVA, Z.N., 1969, X-ray diffraction method for determining carbonates, quartz and other minerals in sediments: Lithol. Miner. Res. (2), 239-244.

GORDON, M.Jr. and STONE, C.G., 1973, Correlation of Carboniferous rocks of the Ouachita geosyncline with those of the adjacent shelf: Okla. Geol. Notes, 33, (3), 124-125.

GORDON, R.L. and HARRIS, G.W., 1956, Counter equipment for quantitative diffraction analysis of powders: Safety in Mines Res. Est. Res. Rep. B8, 1-67.

GREEN, J., 1959, Geochemical table of the elements for 1959: Bull. Geol. Soc. Am., 70, (9), 1127-1183.

GRIESSMER, A.D., 1972, Palaeoecology of the Ervine Creek Limestone (Late Pennsylvanian) in the Mid-Continent region: Okla. Geol. Notes, 32, (2), 59-60.

GRIFFIN, G.M., 1971, Interpretation of X-ray diffraction data: In: CARVER, R.E., (Ed), Procedures in sedimentary petrology: Wiley-Interscience, New York, 541-569.

GRIFFIN, C.G., 1954, A new internal standard for the quantitative X-ray analysis of shales and mine dusts: Safety in Mines Res. Est. Res. Rep. 101.

GRIFFIN, V.S. Jr., 1974, Plate tectonics and the Ouachita System in Texas, Oklahoma and Arkansas: Discussion: Bull. Geol. Soc. Am., 85, 145-146.

GRIFFITHS, J.C., 1957, Petrolgraphical investigation of the salt wash sediments: U.S.A.E.C. RME - 3151, 38p.

GRIFFITHS, J.C., 1964, Statistical approach to the study of the potential oil reservoir sandstones: Stanford Univ. Publ., Geol. Sci., 9, (2), 637-668.

GRIFFITHS, J.C., 1966, Application of discriminant functions as a classification tool in the geosciences: In: MERRIAM, D.F., (Ed), Colloquium on classification procedures: Comput. Contr., 7, Kans. Geol. Surv., 48-52.

GRIFFITHS, J.C., 1966, A genetic model for the interpretive petrology of detrital sediments: J. Geol., 74, (5), 655-672.

GRIFFITHS, J.C., 1967, Scientific method in analysis of sediments: McGraw-Hill Book Co., New York, 508p.

GRIM, R.E., 1968, Clay mineralogy: McGraw-Hill Book Co., New York, 596p.

HAGLUND, W.M., 1967, Brachiopod genus Enteletes in Pennsylvanian deposits of Kansas: Kans. Univ. Palaeont. Contr. Pap. 23, 20p.

HAKES, W.G., 1973, Trace fossils and the depositional environment of the Lawrence Shale (Upper Pennsylvanian) of Eastern Kansas: Abs. with Programs, 5, (4), 319.

HALEY, B.R. and CHARLES, G., 1973, Palaeozoic stratigraphy and depositional environments on the Ouachita Mountains, Arkansas: Abs. with Programs, 5 (3), 259-260.

HALL, B.P., 1961, Cross-bedding in sandstones and limestones of the Kansas City Group throughout Kansas: Unpublished M.S. thesis, Univ. Kansas, 33p.

HALL, P.L., ANGEL, B.R. and BRAVEN, J., 1974, Electron spin resonance and related studies of lignite and ball clay from South Devon, England: Chem. Geol., 13, (2), 97-113.

HAMBLIN, W.K., 1969, Marine palaeoncurrent directions in Limestones of the Kansas City Group (Upper Pennsylvanian) in Eastern Kansas: Bull. Kans. Geol. Surv., (194), pt. 2, 25p.

HARBAUGH, J.W., 1959, Marine bank development in Plattsburg Limestone (Pennsylvanian), Neodesha-Fredonia area, Kansas: Bull. Kans. Geol. Surv., (134), pt. 8, 289-311.

HARBAUGH, J.W., 1960, Petrology of marine bank limestones of Lansing Group (Pennsylvanian), Southern Kansas: Bull. Kans. Geol. Surv., (142), pt. 5, 189-234.

HARBAUGH, J.W., 1964, Significance of marine banks in Southeastern Kansas in interpreting cyclic Pennsylvanian sediments: In: MERRIAM, D.F., (Ed), Symposium in Cyclic sedimentation: Bull. Kans. Geol. Surv., (169), 199-203.

HARBAUGH, J.W. and DEMIRMEN, F., 1964, Application of factor analysis to petrologic variations of Americus Limestone (Lower Permian), Kansas and Oklahoma: Kans. Geol. Surv. spec. Distr. Publ. 15.

HARBAUGH, J.W. and MERRIAM, D.F., 1968, Computer applications in stratigraphic analysis: John Wiley & Sons, New York, 282p.

HARBAUGH, J.W., MERRIAM, D.F., GRAY, J.L. and JACQUOT, T.H., 1965, Field conference guide to Pennsylvanian marine banks, southeastern Kansas: In: Pennsylvanian marine banks in Southeastern Kansas: Geol. Soc. Am. Ann. Meet., Kansas City field conf. guidebook, 1-46.

HARMAN, H.H., 1960, Modern factor analysis: Univ. Chicago Press, Chicago, 469p.

HARMAN, H.H., 1967, Factor analysis: Univ. Chicago Press, 2nd Edit. 474p.

HATCHER, R.D., 1973, North American Palaeozoic foldbelt and deformation histories: A plate tectonic anomaly: Abs. with Programs, 5, (7), 656.

HATCHER, R.D., 1974, North American Palaeozoic foldbelt and deformation histories: A plate tectonic anomaly: Am. J. Sci., 274, 135-147.

HATTIN, D.E., 1957, Depositional environment of the Wreford Megacyclothem (Lower Permian) of Kansas: Bull. Kans. Geol. Surv., (124), 150p.

HAUSEN, D.M., 1973, Applications of quantitative mineralogy by X-ray diffraction to problems in mineral exploration: Q.J. Colo. Sch. Mines, 68, 61-84.

HAWKES, H.E. and WEBB, J.S., 1962, Geochemistry in Mineral Exploration: Harper & Row, New York, 415p.

HAWKINS, D.M. and RAGHUSSEN, S.E., 1973, Use of discriminant analysis for classification of strata in sedimentary successions: Math. Geol., 5, (2), 163-178.

HAYES, D.E. and RINGIS, J., 1973, Seafloor spreading in the Tasman Sea: Nature, 243, (5418), 454-458.

HAYNES, L., 1972, Empirical discriminant classification of regional stream sediment geochemistry in Devon and Cornwall, Discussion: Trans. Instn. Min. Metall., Sect. B, Appl. Earth Sci., 81, 108-109.

HAYS, W.L., 1973, Statistics for the social sciences: Holt, Rinehart & Winston, Inc., New York, 2nd Edit., 954p.

HAYS, W.L. and WINKLER, R.L., 1971, Statistics: probability: inference and decision: Holt, Rinehart & Winston Inc., New York, 937p.

HECKEL, P.H., 1972a, Recognition of ancient shallow marine environments: In: RIGBY, J.K. and HAMLIN, W.M., (Eds), Recognition of ancient sedimentary environments: Soc. Econ. Palaeont. Miner. spec. publ. (16), 226-286.

HECKEL, P.H., 1972b, Pennsylvanian stratigraphic reefs in Kansas, Some modern comparisons and implications: Geol. Rundschau, 61, (2), 584-598.

HECKEL, P.H., 1974, Carbonate buildups in the Geologic Record, A Review: In: LAPORTE, L.F., (Ed), Reefs in time and space: Soc. Econ. Palaeont. Miner., spec. publ. (18), 90-154.

HECKEL, P.H. and BAESEMANN, J.F., 1975, Environmental interpretation of conodont distribution in Upper Pennsylvanian (Missourian) Megacyclothems in Eastern Kansas: Bull. Am. Ass. Petrol. Geol., 59, (3), 486-509.

HECKEL, P.H. and COCKE, J.M., 1969, Phylloid algal-mound complexes in outcropping Upper Pennsylvanian rocks of the Mid-Continent: Bull. Am. Ass. Petrol. Geol., 53, (5), 1058-1074.

HENLEY, S., 1970, The geology and geochemistry of the Perranporth Cornwall: Unpublished Ph.D. thesis, Univ. Nottingham

HILDAGO, R.V. and RENTON, J.J., 1971, The use of pelletized samples for X-ray diffraction analysis of clay minerals in shale: W. Va. Geol. Econ. Surv., Circ. Series (12), 9p.

HILLS, J.M., 1972, Late Palaeozoic sedimentation in West Texas, Permian basin: Bull. Am. Ass. Petrol. Geol., 56, (12), 2303-2322.

HINKLEY, D.N., 1963, Variability in 'crystallinity' values among the kaolin deposits of the coastal Plain of Georgia and South Carolina: In: INGERSON (Ed), Proc. 11th Nat. Conf., Clays and Clay Miner., Pergamon Press, New York, 229-235.

HINDS, H. and GREENE, F.L., 1915, The stratigraphy of the Pennsylvanian series in Missouri: Missouri Bur. Geol. Mines, 13 (2nd series), 407p.

HOPE, K., 1968, Methods of multivariate analysis: Unibooks, Univ. London Press, London, 165p.

HORNES, J.C., 1965, Environmental study of the Bond Formation of the Illinois Basin and the Kansas City Group of the Northern and Central Mid-Continent: Unpublished M.S. thesis, Univ. Illinois, Urbana, 65p.

HOWARTH, R.J., 1970, Principle components analysis of the geochemistry and mineralogy of the Portaskaig Tillite and Kiltylanned schist (Dalradian) of Co. Donegal, Eire: Math. Geol., 2, (3), 285-302.

HOWARTH, R.J., 1971, An empirical discrimination method applied to sedimentary rock classification from major element geochemistry: Math. Geol., 3, 51-60.

HOWARTH, R.J., 1971, Empirical discriminant classification of regional stream sediment geochemistry in Devon and East Cornwall: Trans. Instn. Min. Metall., Sect. B., Appl. Earth Sci., 80, 142-149.

HOWARTH, R.J., 1972, Empirical discriminant classification of regional stream sediment geochemistry in Devon and East Cornwall. Reply to Discussion: Trans. Instn. Min. Metall., Sect. B, Appl. Earth Sci., 81, 115-119.

HOWARTH, R.J., 1973, Preliminary assessment of the non-linear mapping algorithm in a geological context: Math. Geol., 5, 39-57.

HOWARTH, R.J., 1973, The pattern recognition problem in applied geochemistry: In: Geochemical Exploration, 1972: Instn. Min. Metall., London, 259-273.

HOWARTH, R.J., 1973, FORTRAN IV Program for empirical discriminant classification of spatial data: Geocom. Bull., 6, (1-2), 1-32.

HOYD, F.H., 1964, The taxonomy program - a computer technique for classifying geologic data: In: Computers in the mineral industries, part A: Q.J. Colo. Sch. Mines, 59, 207-222.

HSU, K.J., RYAN, W.B.F. and CITA, M.B., 1973, Late Miocene dessication of the Mediterranean: Nature, 242, (5395), 240-244.

HUGHES, R., and ECHOR, B., 1971, Random clay powders prepared by spray-drying: Am. Miner., 55, (11), 1780-1786.

HUTCHINSON, C.S., 1974, Laboratory handbook of petrographic techniques: John Wiley & Sons, New York, 527p.

IMBRIE, J., 1955, Quantitative lithofacies and biofacies study of Florena Shale (Permian) of Kansas: Bull. Am. Ass. Petrol. Geol., 39, 649-670.

IMBRIE, J., 1963, Factor and vector analysis programs for analyzing geological data: Office of Naval Res., Geography Branch, Tech. Rep. (6), ONR Task No. 389-135, Contract Nonr (1228(26)), 83p.

IMBRIE, J., LAPORTE, L.F. and MERRIAM, D.F., 1959, Beattie Limestone facies and their bearing on cyclic sedimentation theory: Kans. Geol. Soc. 24th field conf. guidebook, 69-78.

IMBRIE, J., LAPORTE, L.F. and MERRIAM, D.F., 1964, Beattie Limestone facies (Lower Permian) of the Northern Mid-Continent: In: MERRIAM, D.F. (Ed), Symposium on cyclic sedimentation: Bull. Kans. Geol. Surv., (169), 219-238.

IMBRIE, J. and NEWALL, N., 1964, Approaches to palaeoecology: John Wiley & Sons, New York, 432p.

IMBRIE, J. and PURDY, E.G., 1962, Classification of modern Bahamian carbonate sediments: In: Classification of carbonate rocks, a symposium: Am. Ass. Petrol. Geol. Mem. 1, 253-272.

IMBRIE, J. and VAN ANDEL, T.H., 1964, Vector analysis of heavy mineral data: Bull. Geol. Soc. Am., 75, 1131-1155.

JACKA, A.D., 1964, Replacement of fossils by length-slow chalcedony and associated dolomitization: J. Sedim. Petrol., 44, (2), 421-427.

JEWETT, J.M., 1940, Asphalt rock in Eastern Kansas: Bull. Kans. Geol. Surv. (29), 1-23.

JEWETT, J.M., EMERGY, P.A. and HATCHER, D.A., 1965, The Pleasanton Group (Upper Pennsylvanian) in Kansas: Bull. Kans. Geol. Surv., (175), pt. 4, 11p.

JIZBA, Z.V., 1964, A contribution to the statistical theory of classification: In: PARKS, G.E., (Ed), Computers in the mineral industry: Stanford Univ. Press, 726-756.

JOHNSON, K.R. and COOK, A.C., 1973, Cyclic characteristics of sediments in the Moon Island Beach Subgroup, Newcastle Coal Measures, New South Wales: Math. Geol., 5, (1), 91-110.

JONAS, E.C. and KUYKENDALL, J.R., 1966, Preparation of montmorillonite for random powder diffraction: Clay Miner., 6, 232-235.

JOYCE, A.S., 1973, Application of cluster analysis to detection of subtle variation in a granitic intrusion: Chem. Geol., 11, 297-306.

KAESLER, R.L., 1969, Numerical taxonomy in palaeontology classification, ordination and reconstruction of phylogenies: North Am. Palaeont. Conv. Chicago, 1969, Proc. E, 84-101.

KAESLER, R.L. and McELROY, M.N., 1966, Classification of subsurface localities of the Reagan sandstone (Upper Cambrian) of central and

KAESLER, R.L. and TAYLOR, R.S., 1970, Cluster analysis and ordination in palaeoecology of Ostracoda from the Green River Formation, (Eocene, USA): In: OERTLI, H.J., (Ed), Palaeoecologies Ostracodes Pau, 1970, 153-165.

KEITH, M.L. and DEGENS, E.T., 1957, Geochemical indicators of marine and fresh water sediments: In: ABELSON, P.H., (Ed), Researches in Geochemistry: John Wiley & Sons, New York.

KELLER, G.R. and CEBULL, S.E., 1973, Plate tectonics and the Ouachita System in Texas, Oklahoma and Arkansas: Bull. Geol. Soc. Am., 83, 1659-1666.

KENDALL, M.G., 1957, A course in multivariate analysis: C. Griffin & Co., London, 185p.

KHALEELEE, J., 1969, The application of some data processing techniques in the interpretation of geochemical data: Unpublished Ph.D. thesis, Univ. London.

KINELL, C.B., 1962, Clay mineralogy of the Vilas Shale (Upper Pennsylvanian) in Wilson and Montgomery Counties: Unpublished M.S. thesis, Univ. Kansas, 35p.

KING, P.B., 1961, History of the Ouachita System: In: The Ouachita System: Texas Bur. Econ. Geol., publ. (6120).

KINTER, E.B. and DIAMOND, S., 1956, A new method for preparation and treatment of orientated-aggregate specimens of soil clays for X-ray diffraction analysis: Soil Sci., 81, 111-120.

KITTRICK, J.A., 1961, A comparison of the moving-liquid and glass-slide methods for the preparation of orientated X-ray diffraction specimens: Soil Sci., 92, 155-160.

KOVAN, J.E., 1966, The use of factor analysis in determining depositional environments from grain-size distributions: J. Sedim. Petrol., 36, (1), 115-125.

KOVAN, J.E., 1968, Selection of target areas by factor analysis: In: Proceedings of a symposium on decision making in mineral exploration, Vancouver, B.C., 1968, 19-27.

KLUG, H.P. and ALEXANDER, L.E., 1954, X-ray diffraction procedures for polycrystalline and amorphous materials: John Wiley & Sons, New York, 716p.

KOCH, G.S. and LINK, R.F., 1971, Statistical analysis of geological data, Vol. 2: John Wiley & Sons, New York, 438p.

KOSANKE, R.M., SIMON, J.A., WANLESS, H.R. and WILLMAN, H.B., 1960, Classification of Pennsylvanian strata in Illinois: Illinois Geol. Surv. Rep. Invest. (214) 84p.

KRAUSKOPF, K.B., 1967, Introduction to geochemistry: McGraw-Hill Book Co. New York, 721p.

KINSLEY, D.H. and DONAHUE, J., 1968, Environmental interpretations of sand grain surface textures by electron microscopy: Bull. Geol. Soc. Am., 72, p743-748.

KRINSLEY, D.H. and DOORNKAMP, J.C., 1973, Atlas of quartz sand grain surface textures: Cambridge Univ. Press, Cambridge, 91p.

KRUMBEIN, W.C., 1957, Comparison of percentage and ratio data in facies mapping: J. Sedim. Petrol., 27, 293-297.

KRUMBEIN, W.C. and IMBRIE, J., 1963, Stratigraphic factor maps: Bull. Am. Ass. Petrol. Geol., 47, 698-701.

KRUMBEIN, W.C. and GRAYBILL, F.A., 1965, An introduction to statistical models in geology: McGraw-Hill Book Co., New York, 475p.

LAPORTE, L.F., 1962, Palaeoecology of the Cottonwood Limestone (Permian), Northern Mid-Continent: Bull. Geol. Soc. Am., 73, 521-544.

LAPORTE, L.F. and IMBRIE, J., 1964, Phases and facies in the interpretation of cyclic deposits: In: MERRIAM, D.F., (Ed), Symposium on Cyclic Sedimentation: Bull. Kans. Geol. Surv., (169), 249-264.

LEROUX, J., LENNOX, D.H. and KAY, K., 1953, Direct quantitative X-ray analysis by diffraction-absorption technique: Analyt. Chem., 25, 740-743.

LEVY, I., 1964, Quantitative determination of quartz in rocks containing calcite by X-ray diffraction: Israel J. Chem., 2, 71-73.

LINK, R.F. and KOCH, G.S., 1975, Some consequences of applying lognormal theory to pseudolognormal distributions: Math. Geol., 7, (2), 117-128.

LOW, W., 1968, Electron spin resonance - a tool in mineralogy and geology: Adv. Electronics Electron. Phys., 24, 51-103.

LOW, W. and ZEIRI, S., 1972, ESR spectra of Mn^{2+} in heat-treated aragonite: Am. Miner., 57, 1115-1124.

LUMSDEN, D.N., LEDBETTER, M.T. and SMITH, G.T., 1973, Lithostratigraphic analysis of the Bird Spring-Callville Group and Pakoon Formation (Pennsylvanian-Lower Permian), Southern Clark County, Nevada: J. Sedim. Petrol., 43, (3), 655-671.

LUTZ-GARIHAN, A.B., 1974, The brachiopod genus Composita from the Wreford Megacyclothem (Lower Permian) in Nebraska, Kansas and Oklahoma: Okla. Geol. Notes, 34, (3), 126-127.

LUTZ-GARIHAN, A.B. and CUFFEY, R.J., 1973, Stratigraphy of the Wreford Megacyclothem (Lower Permian) in southernmost Kansas and Northern Oklahoma: Okla. Geol. Notes, 33, (3), 121-122.

McBRIDE, E.F., (Ed) 1969, Stratigraphy - sedimentary structure and origin of flysch and pre-flysch rocks of the Marathon Basin, Texas: Dallas Geol. Soc. guidebook, 104p.

McCAMMON, R.B., 1966, Principal component analysis and its application in large scale correlation studies: J. Geol., 74, (5), pt. 2, 721-733.

McCAMMON, R.B., 1968, Multiple component analysis and its application in classification of environments: Bull. Am. Ass. Petrol. Geol., 52, (11), pt. 1, 2178-2196.

McCAMMON, R.B., 1969, Aspects of classification: In: FENNER, P., (ed), An introduction to mathematical geology; Models of geologic processes: Am. Geol. Inst., R-C1-Rm-C41.

McCAMMON, R.B. and WEBMISTER, G., 1970, The dendrogram: Comput. Contr. 48, Kans. Geol. Surv.

McCRONE, A.W., 1963, Palaeoecology and biostratigraphy of the Red Eagle Cyclothem (Lower Permian) in Kansas: Bull. Kans. Geol. Surv., (164), 114p.

McKEE, E.D. and CRIEL, S.S., 1967, Palaeotectonic maps of the Permian System: U.S. Geol. Surv., Misc. Geol. Invest. Map 1-450.

McMILLAN, N.J., 1956, Petrology of the Nodaway underclay (Pennsylvanian) Kansas: Bull. Kans. Geol. Surv., (119), pt. 6, 191.

MAHER, J.C. and COLLINS, J.B., 1948, Hugoton Embayment of Anadarko Basin in Southeastern Kansas, Southeastern Colorado and Oklahoma Panhandle: Bull. Am. Ass. Petrol. Geol., 32, 813-816.

MANSON, V. and IMBRIE, J., 1964, Fortran program for factor and vector analysis of geologic data using an IBM 7090 or 7090/1401 computer system: Kans. Geol. Surv. spec. distr. publ. (13).

MARFUNIN, A.S., 1964, Radiospectroscopy of minerals: Geol. J., 4, 361-390.

MARTIN, R.T., 1966, Quantitative fabric of wet kaolinite: Clays and Clay Mineral Proc. 14th nat. conf., 271-287.

MASON, B., 1958, Principles of geochemistry: John Wiley & Sons, New York, 2nd edit., 310p.

MATHER, P.H., 1969, Analysis of some Late Pleistocene sediments from South Lancashire and relation to glacial and fluvioglacial processes: Unpublished Ph.D. thesis, Univ. Nottingham.

MATHER, P.M., 1969, Multiple discriminant analysis: Comput. Appl. Nat. Soc. Sci., (6), 17p.

MATHER, P.M., 1973, Recent advances in factor analysis: In: Multivariate analysis in geography: Working paper set (1), study group in quantitative methods, Inst. Br. Geogr., 45-47.

MATHER, P.M., 1973, The last word: Comput. Appl., 1, (2), 117.

MATTHEWS, R.K., 1974, Dynamic stratigraphy: Prentice-Hall Inc., New Jersey, 370p.

MAYERS, I.R. and WORSLEY, T.R., 1973, Statistical recognition of late Cretaceous cyclic sedimentation by means of calcareous nannofossil population studies: Palaeogeogr. Palaeoclimatol. Palaeoecol., 13, 81-90.

MERRIAM, D.F., 1963, The geological history of Kansas: Bull. Kans. Geol. Surv., (162), 317p.

MERRIAM, D.F., (ed), 1964, Symposium of cyclic sedimentation: Bull. Kans. Geol. Surv., (169), 656p.

MERRIAM, D.F., 1967, Colloquium on time-series analysis: Comput. Contr. 18, Kans. Geol. Surv.

MIESCH, A.T., CHAO, E.C.T. and CUTTITTA, F., 1966, Multivariate analysis of geochemical data on tektites: J. Geol., 74, (5), 673-691.

MITCHELL, W.A., 1960, A method for quantitative mineralogical analyses by X-ray powder diffraction: Min. Mag., 32, 492-499.

MONTELCNE, P.H., 1973, The geology of the carboniferous limestone of Leicestershire and South Derbyshire: Unpublished Ph.D. thesis, Univ. Leicester.

MOON, C.F., 1972, The microstructure of clay sediments: Earth Sci. Rev., 8, 303-321.

MOORE, D.G. and SCHUTTON, P.C., 1957, Minor internal structures of some recent unconsolidated sediments: Bull. Am. Ass. Petrol. Geol., 41, 2723-2751.

MOORE, R.C., 1929, Environment of Pennsylvanian life in North America: Bull. Am. Ass. Petrol. Geol., 13, 459-487.

MOORE, R.C., 1936, Stratigraphic classification of the Pennsylvanian rocks of Kansas: Bull. Kans. Geol. Surv., (22), 256p.

MOORE, R.C., 1949, Divisions of the Pennsylvanian system in Kansas: Bull. Kans. Geol. Surv., (83), 203p.

MOORE, R.C., 1950, Late Palaeozoic cyclic sedimentation in central United States: Int. Geol. Congr. 18th, London, 1948, Rep. 4, 5-16.

MOORE, R.C., 1957, Geological understanding of cyclic sedimentation represented by Pennsylvanian and Permian rocks of the Northern Mid-Continent region: Kans. Geol. Soc. 21st field conf. guidebook, 77-84.

MOORE, R.C., 1959, Geological understanding of cyclic sedimentation represented by Pennsylvanian and Permian rocks of the northern Mid-Continent region: In: MOORE, R.C. and MERRIAM, D.F., (Ed), Kansas Field Conf. Guidebook for Ass. Am. State Geol. Kans. Geol. Surv., Lawrence, Kansas, 46-55.

MOORE, R.C., 1964, Palaeoecological aspects of Kansas Pennsylvanian and Permian cyclothems: In: MERRIAM, D.F., (Ed), Symposium of cyclic sedimentation: Bull. Kans. Geol. Surv., (169), 287-380.

MOORE, R.C. and MERRIAM, D.F., 1959, Kansas Field Conference - 1959, Kans. Geol. Surv. guidebook, 1-55.

MOORE, R.C. and MERRIAM, D.F., 1965, Upper Pennsylvanian cyclothems in the Kansas River valley: Field guidebook for the ann. meet. Geol. Soc. Am. Ass. Soc., Kansas City, Missouri, 1965: Kans. Geol. Surv. guidebook, 21p.

MOORE, V.A. and NELSON, R.B., 1974, Effect of Cambridge-Chadron structural trend on Palaeozoic and Mesozoic thicknesses, Western Nebraska: Bull. Am. Ass. Petrol. Geol., 58, (2), 260-268.

MORENCY, M., EMOND, P.L. and VON PITTER, P.H., 1970, Dating conodonts using electron spin resonance: A possible technique: Bull. Kans. Geol. Surv., 199, (1), 17-19.

MORGAN, L.C., 1932, Central Kansas Uplift: Bull. Am. Ass. Petrol. Geol., 16, 483-484.

MORRIS, R.C., 1973, Sedimentary and tectonic history of Ouachita Mountains: Okla. Geol. Notes, 33, (4), 171.

MOSSLER, J.H., 1970, Facies and diagenesis of Swope Limestone (Upper Pennsylvanian) Southeast Kansas: Unpublished Ph.D. thesis, Univ. Iowa, 228p.

MOSSLER, J.H., 1971, Diagenesis and dolomitization of Swope Formation (Upper Pennsylvanian) Southeast Kansas: J. Sedim. Petrol., 41, 962-970.

MOSSLER, J.H., 1973, Carbonate facies of the Swope Limestone formation (Upper Pennsylvanian) Southeast Kansas: Bull. Kans. Geol. Surv., (206), pt. 1, 17p.

MUDGE, M.R., 1956, Sandstone and channels of the Upper Pennsylvanian and Lower Permian in Kansas: Bull. Am. Ass. Petrol. Geol., 44, (4), 654-678.

MUDGE, M.R. and YOCHELSON, E.L., 1962, Stratigraphy and paleontology of the uppermost Pennsylvanian and lowermost Permian rocks in Kansas: U.S. Geol. Surv. Prof. Pap. 323, 213p.

NELSON, C.S. and COCHRANE, R.H.A., 1970, A rapid X-ray method for the quantitative determination of selected minerals in fine-grained and altered rocks: Tane, 16, 151-162.

NEWTON, G.B., 1970, The Rhabdomesidae of the Wreford megacyclothem (Wolfcampian, Permian) of Nebraska, Kansas and Oklahoma: Unpub. Ph.D. thesis, Pennsylvania State Univ.

NEWTON, G.B., 1971, Rhabdomesid bryozoans of the Wreford Megacyclothem (Wolfcampian, Permian) of Nebraska, Kansas and Oklahoma: Univ Kans., Palaeont. Contr. art. 56 (Bryozoa, art. 2), 1-71.

NICHOL, I., GARRETT, R.G. and WEBB, J.S., 1966, Automatic data plotting and statistical interpretations of geochemical data: In: CAMERON, E.M., (Ed), Proc. Symp. Geochemical Prospecting, Ottawa, Dept. Mines, Tech. Surv., Geol. Surv. Can. Pap., 66-54, 195-210.

NISKANEN, E., 1964, Reduction of orientation effects in the quantitative X-ray diffraction analysis of kaolin minerals: Am. Miner., 49, 705-714.

NOBLE, W.R., 1971, A study of disorder in kaolinite: Clay Miner., 9, 71-81.

ONIAL, R.C., 1970, Multi-element geochemical studies in the southern Pennine orefield and north Leicestershire, England: Unpublished Ph.D. thesis, Univ. Leicester.

O'BRIEN, N., 1968, Electron microscope study of a black shale fabric: Naturwiss., 55, 490-491.

O'BRIEN, N., 1970, The fabric of shale - an electron-microscope study: Sedimentology, 15, 229-246.

O'CONNOR, H.G., 1963, Changes in Kansas stratigraphic nomenclature: Bull. Am. Ass. Petrol. Geol., 47, 1873-1877.

ODOM, I.E., 1967, Clay fabric and its relation to structural properties in Mid-Continent Pennsylvanian sediments: J. Sedim. Petrol., 37, (2), 610-623.

ORDWAY, F., 1965, A simple method for making steroscopic drawings: Am. Miner., 50, 1496-1498.

OXNARD, C.E., 1969, Mathematics, shape and function: Am. Sci., 57, (1), 75-96.

PARKS, J.M., 1966, Cluster analysis applied to multivariate geologic data: J. Geol., 74, (5), pt. 2, 703-715.

PARKS, J.M., 1970, Fortran IV program for Q-mode cluster analysis on distance function with printed dendrogram: Comput. Contr. 44, Kans. Geol. Surv.

PEARCE, J.A. and CANN, J.R., 1971, Ophiolite origin investigated by discriminant analysis using Ti, Zr and Y. Earth Planet Sci. Lett., 12, 339-349.

PEARN, W.C., 1964, Finding the ideal cyclothem: In: MERRIAM, D.F., (Ed), Symp. on cyclic sedimentation: Bull. Kans. Geol. Surv., (169), 399-415.

PERKINS, R.D., PERRY, T.G., and HATTIN, D.E., 1962, Some Bryzoans from the Beil Limestone member of the Lecompton Limestone, (Virgilian) of Kansas: Bull. Kans. Geol. Surv., (157), pt. 5, 25p.

POTTER, P.E., SHRINP, N.F. and WITTERS, J., 1963, Trace elements in marine and fresh water argillaceous sediments: Geochim. Cosmochim. Acta, 27, 669-694.

PRESTON, F.W. and HENDERSON, J.H., 1964, Fourier series characteristics of cyclic sediments for stratigraphic correlation: In: MERRIAM, D.F., (Ed), Symp. on cyclic sedimentation: Bull. Kans. Geol. Surv., (169), pt. 2, 415-425.

PRICE, W.J., 1969, Atomic emission spectroscopy: In: BROWNING, D.R., (Ed), Spectroscopy: McGraw-Hill Book Co., London, 125-154.

PURDY, E.G., 1963, Recent calcium carbonate facies of the Great Bahama Bank, 1. Petrography and reaction groups: J. Geol., 71, 334-355.

QUAKERNAAT, J., 1970, Direct diffractometric quantitative analyses of synthetic mineral mixtures with molybdenite as an orientation indicator: J. Sedim. Petrol., 40, 506-514.

RANKIN, A.H., 1973, Fluid inclusion studies in apatite from some East African carbonatites and ijolites: Unpublished Ph.D. thesis, Univ. Leicester.

RAO, C.P., MANN, C.J. and CAROZZI, A.V., 1973, Factor analysis testing of microfacies and interpreted environmental factors in Ste. Genevieve Limestone (Mississippian) Illinois: J. Geol., 81, (1), 65-80.

RAO, C.R., 1952, Introduction to advanced statistical methods in biometrics: John Wiley & Sons, New York.

RAO, C.R. and SLATER, P., 1949, Multivariate analysis applied to difference between Neurotic groups: Br. J. Psychol., Statist. sect., 2, 17-29.

RASCOE, B. Jr., 1962, Regional stratigraphic analysis of Pennsylvanian and Permian rocks in Western Mid-Continent, Colorado, Kansas, Oklahoma and Texas: Bull. Am. Ass. Petrol. Geol., 46, 1345-1373.

RASCOE, B. Jr., 1972, Late Mississippian Epeirogeny and the Ouachita Orogeny in the Mid-Continent: Okla. Geol. Notes, 32, (3), 99-100.

RAUP, D.M., 1969, Modelling and simulation of morphology by computer: N. Am. Palaeont. Conv. 1961, Proc. E, Chicago, 71-84.

READ, W.A., 1961, Aberrant cyclic sedimentation in the limestone coal group of the Stirling Coalfield: Trans. Edin. Geol. Soc., 18, 271-292.

READ, W.A., 1965, Shoreward facies changes and their relation to cyclic sedimentation in part of the Namurian east of Stirling, Scotland: Scot. J. Geol., 1, 69-92.

READ, W.A., 1967, Trend-surface analysis applied to problems of cyclically deposited Namurian sediments, east of Stirling, Scotland: Proc. Geol. Soc. London, (1642), 199-201.

READ, W.A., 1969, Analysis and simulation of Namurian sediments in central Scotland using a Markov - process model: Math. Geol., 1, 199-219.

READ, W.A. and DEAN, J.M., 1967, A quantitative study of a sequence of coal-bearing cycles in the Namurian of Central Scotland, 1: Sedimentology, 9, 137-156.

READ, W.A. and DEAN, J.M., 1968, A quantitative study of a sequence of coal-bearing cycles in the Namurian of Central Scotland, 2: Sedimentology, 10, 121-136.

READ, W.A. and DEAN, J.M., 1972, Principal component analysis of lithological variables from some Namurian (E_2) perallic sediments in Central Scotland: Bull. Geol. Surv. G.B., (40), 83-99.

READ, W.A. and MERRIAM, D.F., 1972, A simple quantitative technique for comparing cyclically deposited successions: In: MERRIAM, D.F., (Ed), Mathematical models of sedimentary processes: Plenum Press, New York, 203-233.

REED, E.C., 1954, Central Nebraska has possibilities: World Oil, 139, (6), 113-116.

REINER, Th., 1971, Strontium depletion in early PreCambrian sediments: N. Jb. Miner. Mh., 1971, (12), 527-541.

REIMER, Th., 1972, The evolution of the rubidium and strontium content of shales: N. Jb. Miner. Abh., 116, (2), 167-195.

REYMENT, R.A. and COLLINSON, J.D., 1971, Periodicity in Namurian sediments of Derbyshire, England, (A quantitative sedimentary analysis): Sediment. Geol., 5, 23-26.

RHODES, J.M., 1969, The application of cluster and discriminant analysis in mapping granite intrusions: Lithos, 2, 223-237.

RHOLF, F.J., 1968, Stereograms in numerical taxonomy: Syst. Zoo., 17, 246-255.

RONOV, A.B., 1972, Evolution of rock composition and geochemical processes in the sedimentary shell of the earth: Sedimentology, 19, 157-172.

RONOV, A.B. and MIGDISOV, A.A., 1971, Geochemical history of the crystalline basement and the sedimentary cover of the Russian and North American platforms: Sedimentology, 16, 137-185.

ROSE, K.E. and HARDY, R.G., 1967, Recovery of phosphate from the Cabaniss and Pleasanton shales of Kansas: Bull. Kans. Geol. Surv., (187), pt. 4, 12p.

ROSS, C.A., 1973, Pennsylvanian and Early Permian depositional history, Southeastern Arizona: Bull. Am. Ass. Petrol. Geol., 57, (5), 887-912.

ROWELL, B.F., 1973, SYMAP analysis of palaeontological data from the Doniphon shale (Pennsylvanian): Abs. with Programs, 5, (6), 507-508.

ROWETT, C.L., 1974, A modified pre-drift model based on provinciality of late Palaeozoic invertebrates of North and South America: Abs. with Programs, 6, (2), 121.

ROWETT, C.L. and WALPER, J.L., 1973, Plate tectonics and new proposed intercontinental reconstruction: Okla. Geol. Notes, 33, (2), 83-84.

RUNNELS, R.T., 1949, Preliminary report on phosphate-bearing shales in Eastern Kansas: Bull. Kans. Geol. Surv., (82), pt. 2, 37-48.

RUNNELS, R.T., SCHLEICHER, J.A. and VAN NORTWICK, H.A., 1953, Composition of some uranium-bearing phosphate nodules from Kansas shales: Bull. Kans. Geol. Surv., (102), pt. 3, 93-104.

SAAGER, R. and SINCLAIR, A.J., 1974, Factor analysis of stream sediment geochemical data from the Mount Hansen area, Yukon Territory, Canada: Miner. Deposita (Berl.), 9, 243-252.

SAHA, A.K., BHATTACHARYYA, C. and LAKSHMIPATHY, S., 1974, Some problems of interpreting the correlations between the model variables in granitic rocks: Math. Geol., 6, (3), 245-258.

SAHU, B.K., 1964, Depositional mechanisms from size analysis of clastic sediments: J. Sedim. Petrol., 34, 73-84.

SANDERS, D.T., 1959, Sandstones of the Douglas and Pedee Groups in Northeastern Kansas: Bull. Kans. Geol. Surv., (134), pt. 3, 125-159.

SCHINDLER, P. and GHOSE, S., 1970, Electron paramagnetic resonance of Mn^{2+} in dolomite and magnesite, and Mn^{2+} distribution in dolomites: Am. Miner., 55, 1889-1896.

SCHUBERT, C., 1963, An atlas of palaeogeographic maps of North America: John Wiley & Sons, New York, 177p.

SCHULTE, G.S., 1959, The Cottage Grove and Noxie Sandstones ("Layton") in South-Central Kansas: Kans. Geol. Soc. 24th field conf. guidebook, 101-106.

SCHULTZ, L.G., 1964, Quantitative interpretation of mineralogical composition from X-ray and chemical data for the Pierre Shale: U.S. Geol. Surv. Prof. Pap., 391-C, 1-31.

SCHWARZACHER, W., 1967, Some experiments to simulate the Pennsylvanian rock sequence of Kansas: In: MERRIAM, D.F., (Ed), Colloquium of time-series analysis: Comput. Contr., 18, 5-14. Kans. Geol. Surv.

SCHWARZACHER, W., 1969, The use of markov chains in the study of sedimentary cycles: Math. Geol., 1, (1), 17-39.

SCOTT, G.L., 1970, Bethany Falls Limestone (Missourian) sedimentation and diagenesis, Missouri and Kansas (Abs): Bull. Am. Ass. Petrol. Geol., 54, 879-894.

SEPKOSKI, J.J. Jr., 1974, Quantified coefficients of association and measurement of similarity: Math. Geol., 6, (2), 135-153.

SEVON, W.D., 1966, Distinction of New Zealand beach, dune and river sand by grain size characteristics: N.Z. J. Geol. Geophys., 9, 212-233.

SEYFERT, C.K. and SIRKIN, L.A., 1973, Earth history and plate tectonics: Harper & Row, New York, 504p.

SHAW, H.F., 1972, The preparation of orientated clay mineral specimens for X-ray diffraction analyses by a suction-onto-ceramic tile method: Clay Miner., 9, 349-350.

SIZE, W.B., 1973, Interpretation of factor analysis on modal data from the Red Hill syenitic complex: Math. Geol., 5, (2), 191-199.

SLOSS, L.L., DAPPLES, E.C. and KRUMBEIN, W.C., 1960, Lithofacies maps: An atlas of United States and Southern Canada: John Wiley & Sons, New York, 108p.

SMALES, A.A. and WAGER, L.R., 1960, Methods in geochemistry: Interscience Publishers Ltd., London, 464p.

SMITH, J.V., 1956, The powder pattern and lattice parameters of plagioclase feldspar, I. The soda-rich plagioclases: Min. Mag., 31, 47-68.

SMITH, J.V. and YODER, H.S., 1956, Variations in X-ray powder diffraction patterns of plagioclase feldspars: Am. Miner., 41, 632-647.

SOKAL, R.R. and SNEATH, P.H.A., 1963, Principles of numerical taxonomy: W.H. Freeman & Co., San Francisco, 359p.

SYMONS, F. and DE MEUTER, F., 1974, Foraminiferal associations of the Mid-Tertiary Edegem Sands at Terhagen, Belgium: Math. Geol., 6, (1), 1-16.

TATLOCK, D.B., 1966, Rapid model analysis of some felsic rocks from calibrated X-ray diffraction patterns: Bull. U.S. Geol. Surv., (1209), 1-41.

THOMAS, W.A., 1973, An interpretation of Ouachita - Appalachian regional structure: Abs. with Program, 5, (3), 287-288.

THOMPSON, G., 1972, A geochemical study of some lithified carbonate sediments from the deep sea: Geochim. Cosmochim. Acta, 36, 1237-1253.

THOMPSON, A.P., DUTHIE, D.M.L. and WILSON, M.J., 1972, Randomly orientated powders for quantitative X-ray determination of clay minerals: Clay Miner., 9, 345-348.

TILL, R. and COLLEY, H., 1973, Thoughts on use of principal component analysis in petrogenic problems: Math. Geol., 5, (4), 341-350.

TILL, R. and SPEARS, D.A., 1969, The determination of quartz in sedimentary rocks using an X-ray diffraction method: Clays and Clay Miner., 17, 323-327.

TOOMEY, D.F., 1964, Lateral homogeneity in a "middle limestone Member" (Leavenworth) of a Kansas Pennsylvanian Megacyclothem: Unpublished Ph.D. thesis, Rice Univ., 184p.

TOURTELOT, H.A., 1964, Minor element composition and organic carbon content of marine and non-marine shales of late Cretaceous age in the western interior of the United States: Geochim. Cosmochim. Acta, 28, 1579-1604.

TROELL, A.R., 1965, Sedimentary facies of the Toronto Limestone, lower limestone member of the Cread Megacyclothem (Virgilian) of Kansas: Unpublished Ph.D. thesis, Rice Univ., 213p.

TROELL, A.R., 1969, Depositional facies of Toronto Limestone Member (Cread Limestone, Pennsylvanian), subsurface marker unit in Kansas: Bull. Kans. Geol. Surv., (197), 29p.

TRYON, R.C. and BAILEY, D.E., 1970, Cluster analysis: McGraw-Hill Book Co., New York, 347p.

TUREKIAN, K.K. and WEDEPOHL, K.H., 1961, Distribution of the elements in some major units of the earth's crust: Bull. Geol. Soc. Am., 72, 175-192.

TURNER, P., 1973, The stratigraphy and sedimentology of the Ringerike group of Norway: Unpublished Ph.D. thesis, Univ.Leicester.

VAN MOORT, J.C., 1972, The K_2O, CaO, MgO and CO_2 contents of shales and related rocks and their implications for sedimentary evolution since the Proterozoic: Int. Geol. Congr., 24th Sect., 10 (Geochemistry), 427-439.

VAN MOORT, J.C., 1973, The magnesium and calcium contents of sediments especially pelites, as a function of age and degree of metamorphism: Chem. Geol., 12, 1-37.

VEIZER, J. and DEMOVIC, R., 1974, Strontium as a tool in facies analysis: J. Sedim. Petrol., 44,(1), 93-115.

VIELE, G.W., 1973, Structure and tectonic history of the Ouachita Mountains, Arkansas: In: DE JONES, K.A. and SCHOLTEN, R., (Ed), Gravity and tectonics: John Wiley & Sons, New York, 361-377.

VINE, J.D., 1966, Element distribution in some shelf and eugeosynclinal black shales: Bull. U.S. Geol. Surv., (1214-E), 31p.

VINE, J.D., 1969, Element distribution in some Palaeozoic black shales and associated rocks: Bull. U.S. Geol. Surv., (1214-G), 32p.

VINE, J.D. and TOURTELOT, E.B., 1969, Geochemical investigations of some black shales and associated rocks: Bull. U.S. Geol. Surv., 1314-A, 43p.

VINE, J.D. and TOURTELOT, E.B., 1970, Geochemistry of black shale deposits, a summary report: Econ. Geol., 65, (3), 253-272.

VINE, J.D., TOURTELOT, E.B. and DIETH, J.R., 1969, Element distribution in some trough and platform types of black shale and associated rocks: Bull. U.S. Geol. Surv., 1214-H, 38p.

VINOGRADOV, A.P., 1962, Srednive soder zhaniya khimicheskikh elementov v glavnkh tipakh izverzhennykh gornykh porod zemnoi kory: Geokhimiya, 1962, 560-561.

VISTELIUS, A.B., 1961, Sedimentation time-trend functions and their application for correlation of sedimentary deposits: J. Geol., 69, 703-728.

VISTELIUS, A.B. and SARMANOV, O.V., 1961, On the correlation between percentage values: Major component correlations in ferromagnesium micas: J. Geol., 69, (2), 145-153.

VON BITTER, P.H., 1973, Geographic distribution of conodont faunas in parts of the Lower Shawnee Group (Upper Pennsylvanian) of the Mid-Continent region, U.S.A: Okla. Geol. Notes, 33, (3), 121.

WAITR, I. and STRNZEL, P., 1974, Application of factor analysis to classification of engineering-geological environments: Math. Geol., 6, (1), 17-33.

WALKER, B.H., 1951, The megafauna of the Florena Shale of Southern Kansas: Unpublished M.S. thesis, Wisconsin Univ., 114p.

WALKER, T.R., 1974, Formation of Red beds in moist tropical climates: A hypothesis: Bull. Geol. Soc. Am., 85, 633-638.

WALPER, J.L. and ROWETT, C.L., 1973, Plate tectonics and origin of Carribbean Sea and Gulf of Mexico: Okla. Geol. Notes, 33, (1), 21-22.

WANLESS, H.R., 1950, Late Palaeozoic cycles of sedimentation in the United States: 18th Int. Geol. Congress, London, 1948, Rep. 4., 17-28.

WANLESS, H.R. and SHEPARD, F.P., 1936, Sea level and climatic changes related to late Palaeozoic cycles: Bull. Geol. Soc. Am., 47, 1177-1206.

WANLESS, H.R., TUBB, J.B. Jr., GEDNETZ, D.E. and WEINER, J.L., 1963, Mapping sedimentary environments of Pennsylvanian cycles: Bull. Geol. Soc. Am., 74, 437-486.

WANLESS, H.R. et al., 1970, Late Palaeozoic deltas in central and eastern United States: In: MORGAN, J.P., (Ed), Deltaic sedimentation - Modern and Ancient: Soc. Econ. Palaeont. Miner. spec. publ., (15), 215-245.

WARD, J.J., 1963, Hierarchical grouping to optimize an objective function: Am. Sta. Ass. J., 58, 236-244.

WARNER, D.J. and CUFFEY, R.J., 1973, Fistulpoacean Bryzoans of the Wreford Megacyclothem (Lower Permian) of Kansas: Univ. Kans. Palaeont. Contr. (65), 1-24.

WAUCHOPE, R.D. and HAGUE, R., 1971, ESR in clay minerals: Nature-Phys. Sci., 233, 141-142.

WEAVER, C.E., 1967, Potassium, illite and the ocean: Geochim. Cosmochim. Acta, 31, 2182-2196.

WEBB, W.M. and BRIGGS, L.I., 1966, The use of principal components analysis to screen mineralogical data: J. Geol., 74, (5), pt. 2, 716-720.

WEDEPOHL, K.H., 1967, Geochemie: de Gruyter & Co., Berlin, 220p.

WEDEPOHL, K.H., (Ed), 1969, Handbook of geochemistry, V.II-1: Springer-Verlag, Berlin.

WEDEPOHL, K.H., (Ed), 1970, Handbook of geochemistry, V.II.-2, Springer-Verlag, Berlin.

WEDEPOHL, K.H., (Ed), 1972, Handbook of geochemistry, V.II-3: Springer-Verlag, Berlin.

WEDEPOHL, K.H., (Ed), 1974, Handbook of geochemistry, V.II-4: Springer-Verlag, Berlin.

WEEKS, R.A., 1972, Magnetic phases in lunar material and their electron magnetic resonance spectra: Apollo 14: Geochim. Cosmochim. Acta, 3, 2503-2517.

WEEKS, R.A., 1973, Paramagnetic resonance spectra of Ti^{3+}, Fe^{3+} and Mn^{2+} in lunar plagioclases: J. Geophys. Res., 78, (14), 2393-2401.

WELLER, J.M., 1956, Argument for diastophic control of Late Palaeozoic cyclothems: Bull. Am. Ass. Petrol. Geol., 40, 17-50.

WELLER, J.M., 1958, Cyclothems and large sedimentary cycles of the Pennsylvanian: J. Geol., 66, 195-207.

WELLER, J.M., 1960, Stratigraphic principles and practices: Harper & Bros., New York, 725p.

WELLS, A.F., 1954, The geometric basis of crystal chemistry, Part 2: Acta Crystallogr., 7, 545-554.

WELLS, J.D., 1950, A study of the Eskridge Shale: Trans. Kans. Acad. Sci., 53, (4), 535-543.

WERNER, W.E., 1974, Petrology of the Cutler Formation (Pennsylvanian-Permian) Near Gateway, Colorado and Fisher Towers, Utah: J. Sedim. Petrol., 44, (2), 292-298.

WHIFFEN, D.H., 1968, Spectroscopy: Longmans, Green & Co., London, 205p.

WHITTAKER, E.T. and ROBINSON, G., 1929, The calculus of observations: Blackie & Sons, Glasgow, 2nd Edit., 295p.

WIGNALL, T.K., 1969, Generalized bayesian classification functions: K classes: Econ. Geol., 64, 571-574.

WILDEMAN, T.R., 1970, The distribution of Mn^{2+} in some carbonates by electron paramagnetic resonance: Chem. Geol., 5, 167-177.

WILSON, A.O. and HECKEL, P.H., 1971, Quantitative comparison of carbonate members of Shawnee Group Megacyclothems (Upper Pennsylvanian), Eastern Kansas (Abs.): 8th Intn. Sed. Cong. Heidelberg, Program with Abs., 109.

WILSON, F.W., 1957a, Barrier reefs of the Stanton Formation (Missourian) in Southeastern Kansas: Unpublished M.S. thesis, Kansas State Univ., 50p.

WILSON, F.W., 1957b, Barrier reefs of the Stanton Formation (Missourian) in Southeast Kansas: Trans. Kans. Acad. Sci., 60, (4), 429-436.

WILSON, F.W., 1962, A discussion of the origin of the reeflike limestone lenses of the Lansing Group (Upper Pennsylvanian) of Southeast Kansas: In: Geoeconomics of the Pennsylvanian marine banks in Southeast Kansas: Kans. Geol. Soc. 27th field conf. guidebook, 101-105.

WILSON, L.R., 1973, Palynological evidence for a Pennsylvanian Age assignment of the Eskridge Shale: Okla. Geol. Notes, 33, (3), 128-129.

WILSON, P.C., 1962, Pennsylvanian stratigraphy of Powder River Basin and adjoining areas: In: BRANSON, C.C., (Ed), Pennsylvanian system in the United States: Am. Ass. Petrol. Geol., Tulsa, Okla., U.S.A., 117-158.

WINCHELL, R.L., 1957, Relationship of the Lansing Group and the Tonganoxie (Stalnaker) sandstone in South-central Kansas: Bull. Kans. Geol. Surv., (127), pt. 4, 125-152.

WOOD, G.V., 1961, Discriminating between refractory and non-refractory quartzite petrography: J. Sedim. Petrol., 31, (4), 530-533.

WRIGHT, T.L., 1968, X-ray optical study of alkali feldspar: II An X-ray method for determining the composition and structural state from measurement of 2θ values for three reflections: Am. Miner., 53, 88-104.

YOUNGS, E.A. and CRAMER, E.M., 1971, Some results relevant to choice of sum and sum-of-product algorithms: Technometrics, 13, 657-665.

ZELLER, D.E., 1968, The stratigraphic succession in Kansas: Bull. Kans. Geol. Surv., (189).

ZHEMCHUZHNIKOW, Y.A., 1958, Similarities and differences between facies, facies-cyclic, and facies-tectonic methods of the study of coal measures: Izv. Acad. Sci. USSR. Geol. Ser., 1, 1-7.

PUBLISHED PAPERS

"A novel method for the study and classification of shales".
Chem. Geol. 13, 57-61.

J.M. Cubitt prepared all samples, ran the ESR spectra (with Dr. Wilkinson's aid), interpreted the results and prepared the manuscript (in conjunction with Dr. Wilkinson). Dr. Wilkinson provided the ESR technical information, helped prepare the spectra and manuscript.

Chemical Geology, 13 (1974) 57—61

A NOVEL METHOD FOR THE STUDY AND CLASSIFICATION OF SHALES

J.M. CUBITT[1] and J.G. WILKINSON[2]

[1] *Department of Geology and* [2] *Department of Chemistry, University of Leicester, Leicester (Great Britain)*

(Accepted for publication January 29, 1974)

ABSTRACT

Cubitt, J.M. and Wilkinson, J.G., 1974. A novel method for the study and classification of shales. Chem.Geol., 13: 57—61.

The electron spin resonance spectra of a range of shales, from the Upper Pennsylvanian and Lower Permian of Kansas, U.S.A., have been recorded. Cluster analysis of the spectral data produced a four-group classification of the samples. The results compare well with a classification based on X-ray diffraction results.

INTRODUCTION

The classification of fine-grained rock samples is normally based on mineralogical content or chemical composition obtained from techniques such as X-ray diffraction (X.R.D.), X-ray fluorescence (X.R.F.) and chemical analysis because conventional microscopic techniques have proved to be inappropriate. Since, in recent years, electron spin resonance (E.S.R.) has been extensively applied to mineralogy (Marfunin, 1965; Low, 1968), we decided to study a series of shale samples in order to specify the paramagnetic impurities and to provide further information on their mineralogy. As a result of this work it has been possible to classify Upper Pennsylvanian and Lower Permian shales of Kansas, U.S.A.

EXPERIMENTAL

The shale samples were finely ground in a shatterbox and then packed in 3-mm internal diameter borosilicate tubes. E.S.R. spectra were recorded at room temperature and 77°K (in a quartz insert dewar) on a Varian E-3 X-band spectrometer. Only spectra observed at room temperature were used for the computer analysis.

RESULTS AND DISCUSSION

The E.S.R. signals could readily be assigned to the paramagnetic ions Mn^{2+} and Fe^{3+}, together with four discrete features in the region of free spin (g = 2.0023). The E.S.R. spectra for Mn^{2+} and Fe^{3+} are similar to those previously reported in the literature for powdered calcite and dolomite samples (Wildeman, 1969, 1970; Ghosh et al., 1970; Schindler and Ghose, 1970; Low and Zeira, 1972). The free spin features bear some resemblance to room temperature E.S.R. spectra of certain clay minerals (Boesman and Schoemaker, 1961; Friedlander et al., 1963; Wauchope and Hague, 1971; Angel and Hall, 1972; Hall et al., 1974). A complete discussion of possible candidates for these E.S.R. spectra will be given in a subsequent paper (J.M. Cubitt and J.G. Wilkinson, to be published).

It was noted that the above E.S.R. signals were common to all the spectra but since there were many samples and characteristic signals, comparison of the spectra was difficult. Consequently, a computer program, commonly used in taxonomic classification (Sokal and Sneath, 1963), was used to compare the spectral characteristics of each sample. The computer programs available (ITBNTOMT and ITBNCLST) calculated the similarities between the samples using a simple matching coefficient, (SM), and then clustered the similarity values using both unweighted average linkage and single linkage methods (Sneath, 1966). This provides us with a hierachical clustering of the shale samples, as illustrated in Fig.1.

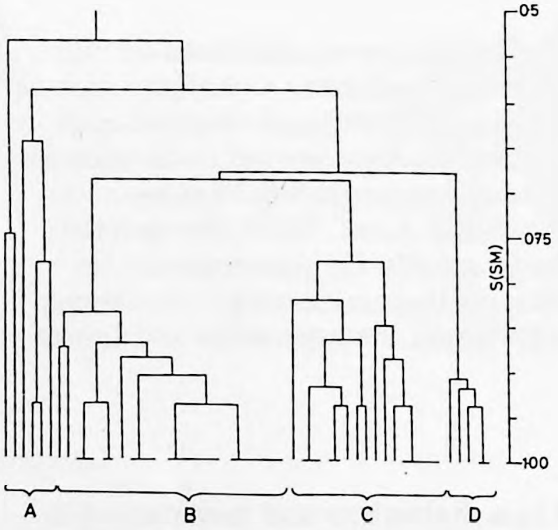

Fig.1. Dendrogram of the clusters, unweighted average linkage.

The results of the computer analysis clearly show that the shale samples lie in four distinct groups (Fig.1). These groupings correlate with a classification based on the mineralogical composition of the shales as determined by X.R.D. The shales were quantitatively analysed for seven major minerals

quartz, calcite, dolomite, feldspar, kaolinite, illite and chlorite. Computational analysis of the data by R-mode principal component analysis, cluster analysis and multiple discriminant analysis produced eight groups of samples which were spatially distributed as shown in Fig.2. The areas represented by the diamond shapes correspond to the mean of the groups ± 1 standard deviation along each discriminant axis, i.e., 67% of the samples in that group lie within the diamond. The controlling variables have been superimposed on this distribution to indicate the mineralogical nature of each group. It is then apparent that groups 1 and 4 are high in quartz content, groups 3 and 8 high in calcite, and group 7 high in dolomite. This provides a geologically meaningful explanation of the X.R.D. classification. A complete discussion of the X.R.D. studies will be presented at a later date (J.M. Cubitt, to be published).

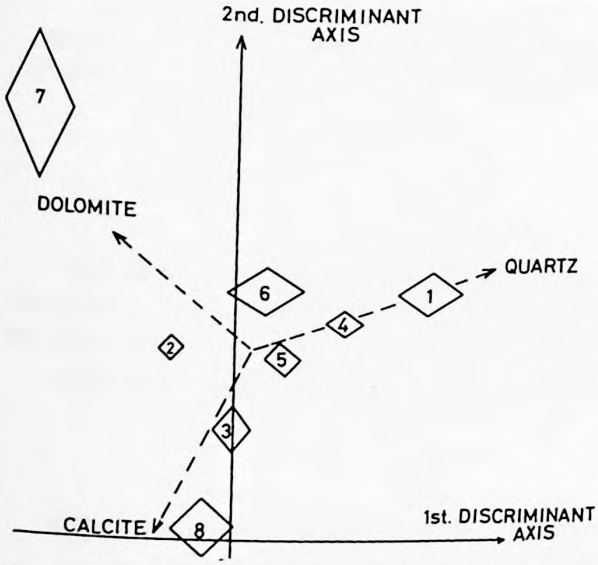

Fig.2. Spatial distribution of groupings based on X.R.D. data.

An analogous explanation for the E.S.R. classification can be invoked by simply comparing the distribution of samples within the E.S.R. groups A—D and the more accurately sub-divided X.R.D. groups 1—8. This comparison is summarised in Table I. As the geological nature of the X.R.D. groups is known a direct comparison of Fig.2 and Table I will enable the geological nature of the E.S.R. groups to be estimated. This type of comparison shows that Group A, as determined by E.S.R., corresponds to predominantly dolomitic shales with some included standards. Groups B and D are mainly calcareous shales and the fundamental distinction between the groups is due to the different site symmetries for Mn^{2+} in these shales. Quite clearly, Group C corresponds to sandy shales.

TABLE I

A comparison of the distribution of samples in E.S.R. groups A—D with X.R.D. groups 1—8*

E.S.R. group	Number of samples in each X.R.D. group								Standards and unclassified
	1	2	3	4	5	6	7	8	
A				1	1		2		2
B	2	2	6	2	5	1	1	3	2
C	9			3	2	1			2
D			2			1		2	

*It is clearly seen that of the 15 samples in E.S.R. group C, 9 lie in group 1 of the X.R.D. classification, 3 in group 4, 2 in group 5 and 1 in group 6. Since X.R.D. groups 1 and 4 are predominantly quartz-rich (see Fig.2) we can conclude that E.S.R. group C is also predominantly quartz-rich.

CONCLUSION

Since room temperature E.S.R. spectra can be recorded quite quickly (usually less than 30 min per sample), and application of the clustering techniques is straight-forward, we feel that this approach can be of significant importance in the study of shales and may have wider uses in geochemistry.

ACKNOWLEDGEMENTS

We thank Drs. J. Davis, A. Khan and D. West for their advice and assistance, M.J. Sackin, M.R.C. Microbial Systematics Unit, University of Leicester who provided the computer programs and Professor M.C.R. Symons for the use of the E.S.R. equipment.

REFERENCES

Angel, B.R. and Hall, P.L., 1972. Electron spin resonance studies of kaolins. Proc. Int. Clay Conf., Madrid, 1972, reprints, 1: 71—84.

Boesman, E. and Schoemaker, P., 1961. Resonance paramagnetique de l'ion Fe^{3+} dans la kaolinite. Compt. Rend. Acad. Sci., 252: 1931.

Friedlander, H.Z., Saldick, J. and Frink, C.R., 1963. Electron spin resonance spectra in various clay minerals. Nature, 199: 61—62.

Ghosh, P.K., Samaddar, M., Sinha, S.C., Tiwari, J.S. and Banerji, A.C., 1970. Geological applications of E.S.R. spectrometry: Mn^{2+} ions in calcium carbonate minerals. Technology, 7: 276—280.

Hall, P.L., Angel, B.R. and Braven, J., 1974. Electron spin resonance and related studies of lignite and ball clay. Chem. Geol., in press.

Low, W., 1968. Electron spin resonance — a tool in mineralogy and geology. Adv. Electr. and Electr. Phys., 24: 51—108.

Low, W. and Zeira, S., 1972. E.S.R. spectra of Mn^{3+} in heat-treated aragonite. Am. Mineral., 57: 1115—1125.

Marfunin, A.S., 1965. Radiospectroscopy of minerals. Liverp. Manch. Geol. J., 4: 361—390.

Schindler, P. and Ghose, S., 1970. Electron paramagnetic resonance of Mn^{2+} in dolomite and magnesite and Mn^{2+} distribution in dolomites. Am. Mineral., 55: 1889—1896.

Sneath, P.H.A., 1966. A comparison of different clustering methods as applied to randomly-spaced points. Class. Soc. Bull., 1: 2—18.

Sokal, R.R. and Sneath, P.H.A., 1963. Principles of Numerical Taxonomy. Freeman, San Francisco, Calif., 359 pp.

Wauchope, R.D. and Hague, R., 1971. E.S.R. in clay minerals. Nature, 233: 141—142.

Wildeman, T.R., 1969. The distribution of Mn^{2+} in dolomite by electron paramagnetic resonance. Trans. Am. Geophys. Union, 50: 357.

Wildeman, T.R., 1970. The distribution of Mn^{2+} in some carbonates by electron paramagnetic resonance. Chem. Geol., 5: 167—177.

SUMMARY STRATIGRAPHIC COLUMNS FOR INTERPRETATION OF TEXT FIGURES